Contract No:

This document was prepared in conjunction with work accomplished under Contract No. DE-AC09-08SR22470 with the U.S. Department of Energy (DOE) Office of Environmental Management (EM).

Disclaimer:

Fluidized Bed Steam Reformed Mineral Waste Form Performance Testing to Support Hanford Supplemental Low Activity Waste Immobilization Technology Selection

C.M. Jantzen, SRNL
E.M. Pierce, ORNL
C.J. Bannochie, SRNL
P.R. Burket, SRNL
A.D. Cozzi, SRNL
C.L. Crawford, SRNL
W.E. Daniel, SRNL
K.M. Fox, SRNL
C.C. Herman, SRNL
D.H. Miller, SRNL
D.M. Missimer, SRNL
C.A. Nash, SRNL
M.F. Williams, SRNL
C.F. Brown, PNNL
N. P. Qafoku, PNNL
J.J. Neeway, PNNL
M.M. Valenta, PNNL
G.A. Gill, PNNL
D.J. Swanberg, WRPS
R.A. Robbins, WRPS*
L.E. Thompson, WRPS

October 2015

SRNL-STI-2011-00387

*current affliliation International Atomic Energy Agency, Vienna, Austria

DISCLAIMER

Printed in the United States of America

Prepared for
U.S. Department of Energy

SRNL-STI-2011-00387
Revision 0

Keywords: *Hanford, Steam Reforming, LAW, WTP*

Retention: Permanent

Fluidized Bed Steam Reformed Mineral Waste Form Performance Testing to Support Hanford Supplemental Low Activity Waste Immobilization Technology Selection

C.M. Jantzen, SRNL
E.M. Pierce, ORNL
C.J. Bannochie, SRNL
P.R. Burket, SRNL
A.D. Cozzi, SRNL
C.L. Crawford, SRNL
W.E. Daniel, SRNL
K.M. Fox, SRNL
C.C. Herman, SRNL
D.H. Miller, SRNL
D.M. Missimer, SRNL
C.A. Nash, SRNL
M.F. Williams, SRNL
C.F. Brown, PNNL
N.P. Qafoku, PNNL
J.J. Neeway, PNNL
M.M. Valenta, PNNL
G.A. Gill, PNNL
D.J. Swanberg, WRPS
R.A. Robbins, WRPS*
L.E. Thompson, WRPS

*current affiliation, International Atomic Energy Agency, Vienna, Austria

October 2015

Prepared for the U.S. Department of Energy under contract number DE-AC09-08SR22470.

Savannah River National Laboratory™
OPERATED BY SAVANNAH RIVER NUCLEAR SOLUTIONS

REVIEWS AND APPROVALS

AUTHOR:

C.M. Jantzen, Engineering Process Development Date

APPROVAL:

C. C. Herman, Manager Date
SRNL Hanford Mission Programs

CUSTOMER:

David J. Swanberg, Washington River Protection Solutions, LLC Date

ACKNOWLEDGEMENTS

The benchscale testing with simulant and radioactive Hanford Tank Blends, mineral product characterization and testing, and monolith testing and characterization were funded by DOE EM-31 Technology Development & Deployment (TDD) Program Technical Task Plan WP-5.2.1-2010-001 entitled "Fluidized Bed Steam Reformer Low-Level Waste Form Qualification", Inter-Entity Work Order (IEWO) M0SRV00054 with Washington River Protection Solutions (WRPS) entitled "Fluidized Bed Steam Reforming Treatability Studies Using Savannah River Site (SRS) Low Activity Waste and Hanford Low Activity Waste Tank Samples", and IEWO M0SRV00080, "Fluidized Bed Steam Reforming Waste Form Qualification Testing Using SRS Low Activity Waste and Hanford Low Activity Waste Tank Samples". This was a multi-organizational program that included Savannah River National Laboratory (SRNL), THOR® Treatment Technologies (TTT), Pacific Northwest National Laboratory (PNNL), Oak Ridge National Laboratory (ORNL), Office of River Protection (ORP), and Washington River Protection Solutions (WRPS).

The SRNL testing of the non-radioactive pilot-scale Fluidized Bed Steam Reformer (FBSR) products made by TTT, subsequent SRNL monolith formulation and testing and studies of these products, and SRNL Waste Treatment Plant Secondary Waste (WTP-SW) radioactive campaign were funded by DOE Advanced Remediation Technologies (ART) Phase 2 Project in connection with a Work-For-Others (WFO) between SRNL and TTT.

The authors would like to thank Arlin L. Olson, Kevin E. Ryan, Brent K. Evans, J. Bradley Mason, Vishal V. Vora, and Brad Eldredge of TTT for performing the engineering scale FBSR studies on a non-radioactive Hanford Tank Blend waste and providing the FBSR bed and fines materials produced for the SRNL WFO studies supported by ART. This data was used for comparison to non-radioactive and radioactive studies performed at SRNL at the bench-scale for the same Hanford Tank Blend waste as detailed in this report. The authors would also like to thank TTT for their technical guidance and support during the execution of the radioactive work scope at SRNL.

The authors would like to thank the following SRNL personnel: Holly Hall and all the regulatory support personnel including Bill Wilson, Kerri Crawford, and Amy Blunt for all the guidance that has helped SRNL perform these treatability studies in compliance with Resource Conservation & Recovery Act (RCRA) waste handling procedures.

The SRNL researchers would like to thank Babb Attaway, who is manager of the SRNL Shielded Cell Operations (SCO) group, and the SCO technical team consisting of Carolyn Conley, Steve Beard, Lucy Beasley, Ron Blessing, Phyllis Burkhalter, Jane Howard, Monica Jenkins, Jeffery Mixon, Raenan Stanley, Rita Sullivan, and Denise Wheeler. The authors would also like to thank Vernon Bush, Michael Lee, Vickie Williams, Pat Simmons, Sherry Vissage, Ronnie Rutherford, David Best, Whitney Riley, Beverly Wall, and Kimberly Wyszynski. SRNL's Analytical Development (AD) provided $Fe^{2+}/\Sigma Fe$ measurements and digestions for chemical/radiochemical composition and mass balance activities, which was supported by Damon Click, Chuck Coleman, Dave DiPrete, Ceci DiPrete, Boyd Wiedenman, Mark Jones, Curtis Johnson, Tom White, and Rob Lascola. SRNL would also like to thank personnel from the Separations Science Program: John Scogin and Wanda Mathews for the radioactive Brunauer-Emmett-Teller – Surface Area (BET-SA) measurements and Michael Bronikowski and Michael Lee for the radioactive density measurements. Kevin Fox and Jake Amoroso of SRNL are also thanked for their role in checking all of the calculations performed by others, especially the durability release calculations.

The SRNL team thanks our manager, Connie C. Herman, for making our jobs easier and keeping us on schedule. The SRNL lead author thanks John Pareizs for reviewing the volume reduction calculations in

Appendix H. Work was performed under Contract No. DE-AC09-08SR22470 with the U.S. Department of Energy (DOE).

The work conducted at PNNL was financially supported by the United States Department of Energy, Office of Environmental Management. The authors would like to thank Cristian Iovin, Igor Kutnyakov, Jordana Wood, and Key-Young Choe for their technical guidance and support during the Toxicity Characteristic Leaching Procedure (TCLP) and Product Consistency Test (PCT) conducted at PNNL. The authors also appreciate the analytical support provided by Keith Geiszler, Steven Baum, Cristian Iovin, and David Woodbury. PNNL is operated by Battelle for the U.S. Department of Energy under Contract DE-AC06-76RL01830.

WRPS would like to thank James Duncan, Heinz Huber, John Smith, and Gene Juteau for their efforts to prepare and ship Hanford tank waste samples to SRNL for testing.

The work conducted at ORNL was financially supported by the U.S. DOE, Office of Environmental Management. ORNL is managed by UT-Battelle, LLC for the U.S. DOE under contract DE-AC05-00OR22725. The authors would like to thank Wayne Lukens (Lawrence Berkley National Laboratory; LBNL) and Jeffrey Fitts (Brookhaven National Laboratory, BNL) for their support to ORNL in conducting and analyzing the results from the X-ray absorption spectroscopy (XAS) measurements. Portions of the XAS measurements were conducted at the National Synchrotron Light Source (NSLS) at BNL, Stanford Synchrotron Radiation Lightsource (SSRL) a Directorate of Stanford Linear Accelerator Collider (SLAC) National Accelerator Laboratory, and the Advance Photon Source (APS) at Argonne National Laboratory (ANL). The NSLS is supported by the U.S. DOE, Office of Science, Office of Basic Energy Sciences, under Contract No. DE-AC02-98CH10886. SSRL is a Directorate of SLAC National Accelerator Laboratory and an Office of Science User Facility operated for the U.S. DOE Office of Science by Stanford University. The SSRL Structural Molecular Biology Program is supported by the DOE Office of Biological and Environmental Research, and by the National Institutes of Health, National Center for Research Resources, Biomedical Technology Program (P41RR001209). APS is an Office of Science User Facility operated for the U.S. DOE Office of Science by ANL, was support by the U.S. DOE under contract No. DE-AC02-06CH11357.

EXECUTIVE SUMMARY

The U.S. Department of Energy's Office of River Protection (ORP) is responsible for the retrieval, treatment, immobilization, and disposal of Hanford's tank waste. A key aspect of the River Protection Project (RPP) cleanup mission is to construct and operate the Hanford Tank Waste Treatment and Immobilization Plant (WTP). The WTP will separate the tank waste into high-level waste (HLW) and low-activity waste (LAW) fractions, both of which will subsequently be vitrified.

The projected throughput capacity of the WTP LAW Vitrification Facility is insufficient to complete the RPP mission in the time frame required by the Hanford Federal Facility Agreement and Consent Order, also known as the Tri-Party Agreement (TPA), i.e. December 31, 2047. Supplemental Treatment is likely to be required both to meet the TPA treatment requirements as well as to more cost effectively complete the tank waste treatment mission. The Supplemental Treatment chosen will immobilize that portion of the retrieved LAW that is not sent to the WTP's LAW Vitrification facility into a solidified waste form. The solidified waste will then be buried on the Hanford site in the Integrated Disposal Facility (IDF).

One of the immobilization technologies under consideration as a Supplemental Treatment for Hanford's LAW is Fluidized Bed Steam Reforming (FBSR). The FBSR technology forms a mineral waste form at moderate processing temperatures; thus retaining and atomically bonding the halides, sulfates, and technetium in the mineral phases (nepheline, sodalite, nosean, carnegieite). Additions of kaolin clay are used instead of glass formers, and the minerals formed by the FBSR technology offers (1) atomic bonding of the radionuclides and constituents of concern (COC) comparable to glass, (2) short and long-term durability comparable to glass, (3) disposal volumes comparable to glass in either granular or monolith form, and (4) higher Na_2O and SO_4^{-2} waste loadings than glass. The higher FBSR Na_2O and SO_4^{-2} waste loadings contribute to the low disposal volumes but also provide for more rapid processing of the LAW. For once through processing (no recycle), this study demonstrates that the FBSR pyrolysis process retains 83-86% of the ^{99}Tc with 98% of the ^{99}Tc in the mineral product compared to processing LAW glass under oxidizing conditions which retains a nominal 33%.[ξ]

The nepheline and carnegieite minerals that compose the granular FBSR product are the host minerals for Cs and Na, the sodalite can also host Cs and Na and provides a cage structure to host Cl, I, F, Re, Mo, ^{99}Tc, B, Be, Re, and Ge, the nosean is isostructural with sodalite and also has a cage structure that binds sulfate and sulfides to the surrounding oxygen atoms. Mixed anion-bearing sodalites (ideally $M_8[Al_6Si_6O_{24}]X_2$, where M = alkali cations and X = monovalent anion), and nosean (ideally $M_8[AlSiO_4]_6SO_4$) where X is a divalent anion, exist and mixed anion sodalites where X is partially monovalent anion and partially divalent anions are also reported in the open literature. The common attribute of the sodalite group of minerals is the flexible framework structure that can expand to enclathrate various guest anions of various sizes by cooperative changes in the Al—O—Si bond angle. It is important to note that the sodalite cages are too small to allow for the exchange of ions (i.e., ion exchange of caged anions) from the structure without the destruction of the Al—O—Si framework.

The FBSR product is granular in nature. Monolithing of the granular product can prevent dispersion during transport and/or during burial/storage. While a monolith is desirable for control of dispersion, burial site subsidence, and intruder prevention, there are other means by which this requirement can be met for a granular waste form, e.g. waste stabilization in High Integrity Containers (HIC's). The primary waste form, the granular product, was the focus of the majority of the Waste Form Qualification (WFQ) testing summarized in this document. Testing of geopolymeric monoliths is also summarized in this document but is considered supplementary data to the testing of the primary waste form, i.e. the granular

[ξ] percentage from reference 207

mineral product. Monoliths and HIC's are compared in terms of IDF disposal volumes and the relative Na_2O oxide waste loading criteria for Hanford LAW. The disposal of the granular product is shown to give the highest Na_2O oxide waste loadings compared to glass at equivalent volume reductions. Higher volume reducions can be achieved by some compaction of the granular product.

Recent FBSR processing and testing with Rassat 68 tank blended LAW made from SRS Tank 50 LAW and Hanford radioactive LAW (Tank SX-105 and AN-103) waste is summarized in this study and compared to previous radioactive and non-radioactive LAW processing and testing. This affords a "tie-back" strategy by which the radioactive FBSR mineral products and durability can be shown to be equivalent to previous non-radioactive tests performed at the bench-scale, the pilot-scale, and the engineering-scale on FBSR bed and fines products. The "tie-back" strategy provides a framework for the FBSR products from all scales to be qualified with respect to disposal at Hanford based on a 2003 Risk Assessment (RA) performed on the 2001 pilot scale FBSR product.

Radioactive bench-scale reformer (BSR) testing commenced at SRNL using SRS LAW from Tank 50 chemically shimmed to have a chemical composition like Hanford's 68 tank blended LAW known as the Rassat simulant. The Rassat simulant composition had been tested in the non-radioactive BSR, the non-radioactive pilot-scale FBSR at the Science Applications International Corporation-Science and Technology Applications Research (SAIC-STAR) facility in Idaho Falls, ID and in the THOR® Treatment Technologies LLC (TTT) Engineering-Scale Technology Demonstration (ESTD) at Hazen Research Inc. (HRI) in Denver, CO. The radioactive Rassat blend LAW waste was shimmed with Re, ^{99}Tc, ^{125}I, and ^{129}I to determine mass balance and determine if Re was a good surrogate for ^{99}Tc in an FBSR waste form. The Tank 50 waste had enough Cs that an additional shim was not necessary.

Radioactive BSR testing continued with radioactive Hanford LAW samples from tanks SX-105, AN-103, and AZ-101/AZ-102. The Hanford Tank SX-105 contained moderate concentrations of anions such as Cl and SO_4^{-2}. No shims of excess radionuclides were added; on the other hand, excess Re was added. The Hanford Tank AN-103 was a low anion, high sodium tank waste. The AZ-101/AZ-102 mixture of wastes from these two tanks was a high Cr and high anion containing waste.

During radioactive Rassat LAW testing, Re was found to be a good surrogate for ^{99}Tc in the off-gas mass balance and in durability testing. Thus, SX-105 and AN-103 non-radioactive and radioactive wastes were shimmed with Re as a surrogate for ^{99}Tc in order to provide additional supporting data. The radioactive SX-105 and AN-103 samples already contained ^{99}Tc and no additional ^{99}Tc was shimmed into the wastes. Due to funding constraints, the AZ-101/AZ-102 testing only consisted of analyzing the radioactive waste when received after shimming it with Re in preparation for the radioactive BSR campaigns, developing a recipe for a simulant, shimming the simulant with Re, performing non-radioactive BSR campaigns, and sending the product for TCLP testing.

For the radioactive Rassat LAW testing and the SX-105, 200-300 mg ^{99}Tc per kg of product along with Re was shimmed into the last 100 mL of feed processed in the BSR to facilitate X-ray Absorption Spectroscopy (XAS) studies that were performed at the National Synchrotron Light Source (NSLS) located at Brookhaven National Laboratory (BNL). A radioactive mixed Re-^{99}Tc sodalite standard was also made at SRNL to provide a phase pure standard to support the XAS studies being performed. The Re and ^{99}Tc XAS analyses were completed on (1) two non-radioactive granular FBSR products (2004 pilot-scale fines and 2008 bed-fines blend), (2) non-radioactive and radioactive samples from the Tank 50 Rassat LAW BSR campaigns, and (3) a radioactive sample from the SX-105 BSR campaigns. The BSR products spanned a REDuction/Oxidation (REDOX) potential from oxidized to reduced, and this was used to assess whether product REDOX had an impact on how much Re or ^{99}Tc was in the sodalite cage structure and whether the location of the Re/^{99}Tc made a difference in the durability response of the BSR products.

The XAS data indicated that Re always reports to the +7 state irregardless of the sample REDOX and is present in the sodalite cage. In an attempt to determine the location of Re +7 in the non-rad pilot scale samples, thin sections of the 2008 TTT/HRI sample and the module B BSR sample were prepared and analyzed at the NSLS using a combination of beamline micro-X-ray fluorescence (XRF), XANES, and micro-X-ray diffraction (XRD). The micro-X-ray fluorescence was used to identify rhenium hot spots, once identified these locations were probed using XANES to confirm the rhenium oxidation state. Finally, micro-X-ray diffraction (XRD) was used to identify the phase that contained the rhenium present in the mixed mineral FBSR and BSR matrix. The results collected from these analyses confirmed that rhenium is associated with sodalite, probably as a mixed anion phased sodalite mineral given the small distortion present in the micro-XRD pattern.

The XAS data on ^{99}Tc indicates that the +7 oxidation state in the sodalite cage is between 65-79% in the REDOX range of the FBSR operation and ~56% at REDOX ranges more reduced than normal FBSR operation. The remainder of the Tc is present as +4 in TcO_2 oxide and/or $Tc_2S(S_3)_2$: during durability testing, even long-term testing, there was no change in durability with sample REDOX, which means that the +7 fraction of the ^{99}Tc is insoluble in the sodalite cage, while the +4 fraction of the ^{99}Tc is insoluble as the oxide and/or sulfide. TcO_2 is the same reduced oxide species present in HLW waste glasses formed under slightly reducing flowsheets like the Defense Waste Processing Facility (DWPF). An Electromotive Force Series (EMF) for ^{99}Tc was developed and is presented in this study based on the XAS data.

The BSR mineral products from all the non-radioactive and radioactive campaigns (Rassat LAW blend, SX-105, and AN-103) were analyzed chemically and by x-ray diffraction (XRD) to determine the phase assemblages. Mineralogy of radioactive and simulant products from the BSR and ESTD and the 2001 (AN-107) and 2004 pilot-studies (Rassat simulant) were determined to be the same. This is because the FBSR process control strategy "MINCALC™" was used to control the chemistry of all FBSR products since 2004. MINCALC™ targets the same NAS chemistry shown to be acceptable in 2001 with AN-107 simulants, i.e. the simulant that was used for the RA, by adjusting the clay chemistry to accommodate Na, Al, and Si variations in the feed.

The FBSR process control strategy adjusts the clay content and type in order to account for alumina in the LAW waste. Therefore, alumina does not need to be removed and is not a limiting factor in FBSR product formulation. The AN-103 radioactive sample contained large concentrations of $Al(OH)_3$ precipitates that were adjusted for by the clay additive composition and the feed was processed with the precipitates, i.e. precipitates do not have to be removed before FBSR processing.

Mass balances were calculated for all radioactive and non-radioactive BSR campaigns to determine the partitioning of the elements to the off-gas and the mineral products. The significant findings of the mass balance for the radioactive campaigns are given in tabular form below:

Method	Radio-isotope	RAD B (SRS LAW)		RAD C (Hanford SX-105)		RAD D (Hanford AN-103)	
		Total %	Product %	Total %	Product %	Total %	Product %
Radiometric	^{137}Cs	124	99	Indeterminate			
	^{125}I*	84	95	Not shimmed			
	^{129}I	69-75	95	75-89	86-88	100	69
	^{99}Tc	87	88	80	98	86	98
ICP-MS	^{99}Tc	Analysis not Performed		83	98	83	98
	Re	98	98	71	98	88	98

*Signal for ^{125}I is stronger and more accurate than ^{129}I

Note that the recovery of ^{99}Tc in the mineral waste form for the radioactive campaigns, based on once through processing, were very high minimizing the need for large recycle streams to handle the emitted Tc. Data for the non-radioactive campaigns are similar and given in the body of the document. REDOX in the FBSR/BSR was determined not to impact the volatility of any species.

The FBSR products (granular and monolith) were tested by short-term and long-term (up to one year) ASTM C1285 (PCT), ANSI 16.1/ASTM C1308, and the EPA Toxicity Characteristic Leaching Procedure (TCLP). In addition, for the Rassat LAW blend Single Pass Flow Through (SPFT, ASTM 1662) and Pressure Unsaturated Flow-through (PUF) testing were performed. All of the BSR durability testing for non-radioactive and radioactive FBSR products was compared to previous testing at the pilot-scale (2001 and 2004) and engineering-scale (2008). Note that all tests with STAR-SAIC pilot-scale (2004) material and the TTT/HRI engineering scale (2008) products were performed using combined bed and filter fines mineral product solids. No impact of product REDOX on durability was noted in short and long-term PCT testing. All testing of BSR products were consistent with previous testing of SAIC/STAR pilot-scale testing and ESTD engineering-scale testing. The only impact of REDOX on durability that was noted was the Cr retention in TCLP testing. The Cr retention was determined to be controllable by the addition of additional iron oxide catalyst (IOC) since this material is also used as a denitration aid in the FBSR process. The IOC provides an insoluble Cr+3 host mineral ($FeCr_2O_4$) for Cr stabilization. A process control algorithm for IOC addition was developed and added to MINCALC™.

In order to interpret the SPFT data on “mixed anion” sodalite, pure non-radioactive standards of the end member Cl, SO_4^{-2}, I, Re sodalites were made at the SRNL as standards for the ORNL XAS and SPFT studies. A “mixed anion” Re/^{99}Tc sodalitie was also made at SRNL. These phase pure and mixed sodalite allowed the determination of how the nepheline dissolution rates differed from the sodalite dissolution rates, how the various sodalite differed in dissolution rates compared to each other, and allowed the determination of thermodynamic constants. This supported the development of rate-law parameters, all of which are needed to support Hanford Performance Assessment (PA) calculations for the

Hanford Integrated Disposal Facility (IDF). This information is included, in part, in this document but will be published more fully elsewhere.

The significant findings from the ASTM 1285 short-term and long-term durability testing, SPFT testing, and PUF testing of the granular waste form are given below:

- ASTM C1285 (Product Consistency Test) releases are below 2 g/m^2 for the constituents of concern for the FBSR granular product and the monoliths
  - Use of BET surface area to account for the surface roughness of the mineral granules demonstrates that the FBSR product leach rate is 2 orders of magnitude lower than the 2 g/m^2 target
  - Use of the geometric surface area, which ignores the surface roughness of the mineral granules compared to glass, gives an equivalent leach rate to vitreous waste forms
  - All the durability results for the non-radioactive constituents from the BSR testing and the ESTD testing are in agreement with the previous data from 2001and 2004
- Re is a good surrogate for ^{99}Tc during leaching experimentation proving that the radioactive and simulant BSR campaign products using Re and ^{99}Tc match the historic and engineering scale data that used Re only, proving the "tie back" strategy
- Long-term PCT testing (1, 3, 6, and 12 month) at 90°C by ASTM C1285 for the ESTD Rassat simulant, the BSR Rassat (radioactive and non-radioactive), and the SX-105 (radioactive) has not shown any significant change in the mineral assemblages as analyzed by XRD
  - The ESTD samples did contain small amounts of halloysite ($Al_2Si_2O_5(OH)_4$) as a reaction product which is a known reaction product of kaolin clay
    - The ESTD campaigns used ~10 wt% excess kaolin clay
    - Halloysite does not increase in amount with leaching time for the ESTD sample indicating that it is forming from a minor phase in the mineral waste form
    - Halloysite was not found in the BSR products since these campaigns contained ≤5 wt% excess kaolin and often no excess kaolin
- SPFT tests were performed on the Rassat LAW and SX-105 non-radioactive and radioactive BSR products and the ESTD Rassat LAW
  - Tests were performed at various flow rates, at 40°C, in pH 9 and in deionized water for 28 to 70 days
  - The FBSR Rassat LAW mineral products exhibit a relatively low forward dissolution rate on the order of 10^{-3} $g/(m^2d)$
    - The material made in the BSR gave slightly higher values than that made at the engineering-scale but of the same order of magnitude
    - Re and I were shown to have similar release behavior and there was similar behavior of Re and ^{99}Tc
    - Re, I, ^{99}Tc, and S all showed delayed release from the sodalite phase(s) confirming that the Si-O-Al bonds of the sodalite cage have to dissolve before these species can be released
    - The SPFT data for Si from the BSR Rassat product are two orders of magnitude lower than the data for LAWA44 glass
    - SPFT forward dissolution rates of BSR products are similar to Si releases measured on the Rassat simulant FBSR bed product made at SAIC-STAR in 2004
- The PUF test method allows for the accelerated weathering of materials, including radioactive waste forms, under hydraulically unsaturated conditions, thus mimicking the open-flow and transport properties that most likely will be present at the Hanford IDF
  - PUF tests of 1-year duration were performed on the non-radioactive Rassat LAW FBSR granular products made in the BSR and the ESTD
    - The ESTD sample was 20% bed product and 80% fines

- The experiments showed a trend of decreasing release of Na, Si, Al, and Cs as a function of time
- The elements I and Re showed a steady release throughout the year long test
- The difference in the release rates of Na, Si, Al and Cs compared to I and Re suggests that the release I and Re species from the sodalite cage occurs at a different rate compared with the dissolution of the predominant nepheline phase

o Comparisons to PUF tests of a 2.5-year duration on the 2004 SAIC-STAR pilot scale FBSR products made with the Rassat LAW simulant were in agreement with the PUF testing of the BSR and ESTD products
- The time-dependent elemental release rates were combined with geochemical modeling calculations and suggest that aluminum and sodium release is controlled by nepheline solubility, whereas silicon is being controlled by amorphous silica solubility after being released from the FBSR Na_2O-Al_2O_3-SiO_2 (NAS) matrix
- For the duration of the experiment, Re and S releases were within the experimental error of one another, suggesting their release is either from the same phase or a phase with similar stability
- The PUF data indicates that Re release from the multiphase FBSR NAS granular product is an order of magnitude lower than ^{99}Tc release [$(2.1 \pm 0.3) \times 10^{-2}$ g/(m^2d)] from LAW glass (LAW AN102)
- Geochemical calculations using PHREEQ-C on 200 day PUF data suggests the steady-state S and Re concentrations are within order of magnitude of solubility of phase pure nosean and Re-sodalite, respectively
- PUF testing and modeling suggests that Re and S are being released from a "mixed-anion" sodalite phase (likey Re and SO_4^{-2} bearing), which has a different stoichiometry in comparison to the pure mineral end-members and a thermodynamic stability that lies between the pure phase end-members, e.g. such a solid solution is already known between the Cl and SO_4^{-2} sodalite/nosean endmembers and a mixed Re/^{99}Tc sodalite made at SRNL

The chemical, phase identification, and durability test results on the granular waste form all compare favorably to the results obtained on the FBSR mineral products from the 2001 and 2004 pilot-scale testing and the 2008 ESTD testing. Test results confirm that the performance of the mineral (ceramic) waste form is affinity controlled like vitreous waste forms, oxides, and other silicate minerals, i.e. the long-term dissolution rate drop is controlled by the chemical affinity. The dissolution may be controlled by interfacial dissolution–reprecipitation mechanism as noted in the literature for other silicate minerals. The Re release appears to be controlled by solubility and the impact pH has on solubility concentration. This was seen in the ASTM C1285 (PCT) testing, the ASTM C1662 (SPFT) testing, the PUF testing presented in this document for ESTD (Rassat LAW similant) and BSR (Rassat LAW simulant and SX-105), and the same observations were made during similar testing of the 2001 and 2004 pilot-scale AN-107 and Rassat LAW testing.

Monolithing of the granular FBSR product was investigated but the monolith formulation and testing is considered supplementary. Monolithing in an inorganic geopolymer binder made from kaolin clay was found to be superior to geopolymers made from fly ash. Geopolymers were found to be the most compatible with the NAS chemisty of the FBSR product. The geolpolymer, which has a similar NAS chemistry to the FBSR product, is an amorphous macro-encapsulant and the geopolymer itself does not sequester any COCs but inhibits COCs from leaching from the FBSR mineral products.

The ASTM C1308/ANSI 16.1 was performed for up to 90 days duration. The data generated were used to compare the monolithed BSR non-radioactive waste forms to the monolithic ESTD non-radioactive waste forms made from fly ash and to BSR non-radioactive monoliths made from clay in order to

compare clay based to fly ash based geopolymer monoliths. A leach index (LI) is derived directly from immersion test results and is the negative log of the diffusivity for monolithic waste forms that release COCs via a diffusion-controlled mechanism. The LI is used as a criterion to assess whether solidified/stabilized waste will likely be acceptable for subsurface land disposal. For the Hanford IDF, the solidified waste is considered effectively treated for IDF dispoal when the LI (Re, Tc) ≥ 9 after a few days and LI(Na) ≥ 6 in 2 hours. The FBSR monoliths pass ANSI/ANS 16.1/ASTM C1308 durability testing with Re achieving a LI of ≥ 9 in 5 days and Na achieving an LI in the first few hours. The significant findings of durability testing of the monoliths are summarized below:

- All monoliths made from radioactive and non-radioactive (ESTD engineering-scale) and non-radioactive BSR "Module B," granular products maintain PCT leach rates <2 g/m^2, and perform well in ASTM C1308/ANSI 16.1 testing indicating that the binder material is not degrading the granular product durability response.
    - Clay monoliths were found to have superior durability to fly ash monoliths in ASTM C1308 and ANSI 16.1 testing.

SPFT and PUF testing was performed on the fly ash based geopolymers as was short-term and long-term ASTM C1285. The SPFT and PCT demonstrated slower releases from the monoliths than from the granular product but PUF testing revealed the opposite. The PCT testing, like the ASTM C1308/ANSI16.1 testing, revealed that the clay based geopolymers are superior to the fly ash based geopolymers. Since the SPFT and PUF tests were performed on the fly ash based geopolymers, no further conclusions should be drawn from these results.

The ASTM C39 Compressive Strength test and TCLP testing was also performed on the monoliths, and a comparison made between the monolithic radioactive and non-radioactive BSR and ESTD waste forms. All monoliths made from radioactive and non-radioactive (ESTD and BSR Rassat Law blend) pass compression testing at >500 psi but clay based monoliths performed better than fly ash based geopolymers.

TABLE OF CONTENTS

LIST OF TABLES

LIST OF FIGURES

LIST OF ABBREVIATIONS

AA	Atomic Absorption
ALARA	As Low as Reasonablly Achievable
ANL	Argonne National Laboratory
APS	Advanced Photon Source
AR	Aqua Regia dissolution
ASTM	American Society for Testing and Materials
BET-SA	Brunauer, Emmett, and Teller - Surface Area
BNL	Brookhaven National Laboratory
BSR	Bench-scale Steam Reformer
BSRG	Bench-scale Steam Reformer Granular
BSRM	Bench-scale Steam Reformer Monolith
CAA	Clean Air Act
COC	Constituents of Concern
CRR	Carbon Reduction Reformer
CSEM	Contained Scanning Electron Microscopy
DBVS	Demonstration Bulk Vitrification System
DET	Determination of Equivalent Treatment
DMR	Denitration Mineralization Reformer
DOE	Department of Energy
DQO	Data Quality Objective
DWPF	Defense Waste Processing Facility
EDS	Energy Dispersive Spectroscopy
EIS	Environmental Impact Statement
EMF	Electro-Motive Force
EPA	Environmental Protection Agency
ESTD	Engineering-scale Test Demonstration
EXAFS	Extended X-Ray Analysis Fine Structure
FBSR	Fluidized Bed Steam Reformer
FIB	Focus Ion Beam
GAC	Granular Activated Charcoal
HEPA	High Efficiency Particle Aie(filter)
HIC	High Integrity Container
HLVIT	High Level Vitrification
HLW	High Level Waste
HRI	Hazen Research Inc.
HTWOS	Hanford Tank Waste Operations Simulator
HWC	Hazardous Waste Combustor
IC	Ion Chromatography
ICP-AES	Inductively Coupled Plasma – Atomic Emission Spectroscopy
ICP-MS	Inductively Coupled Plasma – Mass Spectroscopy
IDF	Integrated Disposal Facility
IEWO	Inter-Entity Work Order

IHLW	Immobilized HLW
ILAW	Immobilized LAW
INL	Idaho National Laboratory
INTEC	Idaho Nuclear Technology & Engineering Center
inwc	inches of water column
IOC	Iron Oxide Catalyst
ISO	International Standardization Organization
IWTU	Integrated Waste Treatment Unit
KAPL	Knolles Atomic Power Laboratory
LAW	Low Activity Waste
LBNL	Lawrence Berkley National Laboratory
LDR	Land Disposal Restrictions
LDRD	Laboratory Directed Research & Development
LI	Leaching Indices
LLRW	Low Level Radioactive Waste
LLW	Low Level Waste
LNNL	Lawrence Livermore National Laboratory
LOD	Loss on Drying (at 110°C)
LOI	Loss (of weight) on Ignition (at 525°C)
LRO	Long Range Order
MACT	Maximum Achievable Control Technology
MRO	Medium Range Order
MS	Mass Spectrometer
NAR	Nozzle Atomizing Ratio
NAS	Na_2O-Al_2O_3-SiO_2
NaTPB	Sodium Tetraphenyl Borate
NQA	Nuclear Quality Assurance
NRC	Nuclear Regulatory Commission
NSLS	National Synchrotron Light Source
ORNL	Oak Ridge National Laboratory
OGC	Off-gas Cooler
OGF	Off-gas Filter
OPC	Ordinary Portland Cement
ORP	Office of River Protection
ORR	Operational Readiness Review
PA	Performance Assessment
PCT	Product Consistency Test (ASTM C1285)
PDF	Powder Diffraction File
PF	Peroxide Fusion
PGF	Process Gas Filter
PID	Pressure Indicating Device
PNNL	Pacific Northwest National Laboratory
PR	Product Receipt
PSAL	Process Science Analytic Laboratory
PSD	Particle Size Distribution

PUF	Pressure Unsaturated Flow-through
R&D	Research & Development
RA	Risk Assessment
REALM	REgression Analyses of Leaching Models
REDOX	REDuction/Oxidation
RCRA	Resource Conservation and Recovery Act
RPP	River Protection Project
SAIC-STAR	Science Applications International Corporation-Science and Technology Applications Research
SBW	Sodium Bearing Waste
SC	South Carolina
sccm	standard cubic centimeters per minute
SCO	Shielded Cells Operation
SEM	Scanning Electron Microscopy
SLAC	Stanford Linear Accelerator Colloider
SPFT	Single Pass Flow Through Test (ASTM C1662)
SR-FTIR	Synchrotron Radiation-based Infra-Red microscopy
SRNL	Savannah River National Laboratory
SRO	Short Range Order
SRS	Savannah River Site
SSRL	Stanford Synchrotron Radiation Lightsource
SST	Single Shell Tank(s)
STORM	Subsurface Transport Over Reactive Multiphases
STP	Supplementary Treatment Project
SYNROC	SYNthetic ROCk
TDD	Technology Development and Deployment
TIC	Total Inorganic Carbon
TCLP	Toxicity Characteristic Leaching Procedure
THOR®	THermal Oxidation Reduction
TEM	Transmission Electron Microscopy
TMP	Technolgy Maturation Plan
TPA	Tri-Party Agreement
TRA	Technology Readiness Assessment
TRL	Technology Readiness Level
TRU	Transuranic
TST	Transition State Theory
TTT	THOR® Treatment Technologies
US	United States
UTS	Universal Treatment Standards
VHT	Vapor Hydration Test (ASTM 1663)
VMI	Virginia Military Institute
VSL	Vitreous State Laboratory
WAPS	Waste Acceptance Product Specification
WCP	Waste Compliance Plan
WFO	Work for Others

WFQ	Waste Form Qualification
WGSR	Water Gas Shift Reactions
WIPP	Waste Isolation Pilot Plant
WIR	Waste Incidentical to Reprocessing
WRPS	Washington River Protection Solutions, LLC
WTP	Waste Treatment Plant
WTP-SW	Waste Treatment Plant-Secondary Waste
WVDP	West Valley Demonstration Project
XAFS	X-ray Absorption Fine Structure
XAS	X-Ray Absorption Spectroscopy
XANES	X-ray Absorption Near Edge Structure
XRD	X-ray Diffraction

1.0 Introduction

The Hanford Site in southeast Washington State has 56 million gallons of radioactive and chemically hazardous wastes stored in 177 underground tanks.[1] The United States (U.S.) DOE Office of River Protection (ORP) is responsible for the retrieval, treatment, immobilization, and disposal of Hanford's tank waste. A key aspect of the River Protection Project (RPP) cleanup mission is to construct and operate the Hanford Tank Waste Treatment and Immobilization Plant (WTP). Within the WTP, the pretreatment facility will receive the retrieved waste from the tank farms and separate it into two treated process streams. The pretreated high-level waste (HLW) mixture will be sent to the HLW Vitrification Facility, and the pretreated low-activity waste (LAW) stream will be sent to the LAW Vitrification Facility. The two WTP vitrification facilities will convert these process streams into glass, which is poured directly into stainless steel canisters. The immobilized HLW (IHLW) canisters will ultimately be disposed of at an offsite federal repository. The immobilized LAW (ILAW) canisters will be disposed of onsite in the Integrated Disposal Facility (IDF).

The projected throughput capacity of the WTP LAW Vitrification Facility is insufficient to complete the RPP mission in the time frame required by the Hanford Federal Facility Agreement and Consent Order, also known as the Tri-Party Agreement (TPA). Without additional LAW treatment capacity, the mission would extend beyond December 31, 2047, the Tri-Party Agreement milestone date for completing all tank waste treatment. A supplemental treatment is likely to be required to (1) meet the TPA treatment requirements and (2) to more cost effectively complete the tank waste treatment mission. The supplemental treatment technology chosen should therefore: (1) atomically bond the radionuclides and constituents of concern (COC) in a comparable manner to glass, (2) be as durable as glass during short and long-term durability testing, (3) have disposal volumes comparable to glass, and (4) be able to retain higher Na_2O and SO_4^{-2} waste loadings than glass. The higher Na_2O and SO_4^{-2} waste loadings contribute to low disposal volumes but also theoretically provide for more rapid processing of the LAW.

The Supplemental Treatment Project (STP) will design, construct, and operate the processes and facilities required to treat and immobilize LAW into a solidified waste form for that portion of the retrieved LAW that is not sent to the WTP's LAW Vitrification Facility. The solidified waste will then be disposed on the Hanford site in the IDF.

Four immobilization technologies are under consideration as part of the STP including:

- second WTP LAW vitrification;
- bulk vitrification;
- cementitious solidification (cast stone); and
- fluidized bed steam reforming (FBSR).

The FBSR mineral waste form meets all of the criteria discussed above to meet the TPS milestone and more cost effectively completes the Hanford tank waste treatment mission. The DOE has made substantial past investments in evaluating each of the proposed vitrification processes (i.e., WTP LAW and bulk vitrification) and cementitious solidification processes at Hanford. Additionally, numerous other sites within the DOE complex have examined the performance of cementitious solidification of LAW for a number of years. As of 2008, the DOE had made some but not sufficient investments in the FBSR process to produce a mineralized waste form for Hanford LAW immobilization.

Technology Readiness Levels (TRL) are used in the DOE complex to provide a common language and measurement scale to enhance communication within and between the science and technology and project/program communities.[2] In 2008, before the DOE-EM Waste Form Qualification (WFQ)

program (Section 5.0), the FBSR technology was only at a TRL of 4 as no radioactive testing of LAW had been performed at any scale (bench-scale, pilot-scale, or engineering-scale) and engineering-scale demonstrations of LAW simulants had not been completed.

The DOE-EM WFQ research and development (R&D) summarized in this document has substantially increased the TRL level of the FBSR process to a TRL of 6, which is the TRL required for a technology to enter design. With the recent process maturity of a full scale FBSR system being used at the Idaho Nuclear Technology and Engineering Center (INTEC) for acidic LAW known as Sodium Bearing Waste (SBW) (see Section 3.4), the FBSR technology has reached a TRL of 7. The INTEC facility, known as the Integrated Waste Treatment Unit (IWTU), underwent an Operational Readiness Review (ORR) and a Technology Readiness Assessment (TRA) in March 2014. When the IWTU begins radioactive operations later in 2014, the FBSR technology will have reached a TRL of 8 for LAW applications.

The STP selection process will generate a decision document for Hanford LAW, the scope of which will be to:

- clearly identify the immobilization technology options being evaluated;
- identify those immobilization technology options not evaluated and provide rationale as to why they were not further evaluated;
- rigorously evaluate each of the selected technology options using a set of defined, weighted, and measured evaluation criteria; and
- recommend to Washington River Protection Solutions LLC (WRPS) management and ORP the technology option that best meets RPP's programmatic needs.

This STP down selection process will result in a recommendation to ORP of which of the four immobilization technologies to pursue. Following approval of that decision by ORP, the STP will commence a Conceptual Design project to develop a Critical Decision package for the selected immobilization technology in accordance with DOE Order 413.3. Data from the FBSR WFQ test program will be needed to support a go / no-go evaluation of waste form performance and the determination of whether the FBSR technology should be included in the subsequent immobilization technology down select process.

1.1 Purpose and Scope

The FBSR Na_2O-Al_2O_3-SiO_2 (NAS) waste form is primarily a multiphase mineral (ceramic) waste form consisting of three minerals: nepheline, sodalites including nosean, and spinel (see Section 2.2). This document represents a synopsis of all of the R&D that has been published regarding the FBSR technology between 2001-2008 and 2008-present, with the primary focus being on the 2008-present timeframe.

Since 2008, the FBSR R&D has been primarily funded by EM-31 and driven by the need for advanced waste forms and processes as discussed in the National Research Council report **—Advice on the Department of Energy's Cleanup Technology Roadmap: Gaps and Bridges—**, Waste Processing gap number 5 (WP-5) which states that the baseline tank waste vitrification process significantly increases the volume of high-level waste to be disposed. This report comments:

> *"Waste forms that include little or no added binder. Idaho calcine is one such example. Perhaps sintered or minimally bonded sludges could be developed for Hanford and SRS. Such work would probably rely heavily on computer modeling of waste and repository characteristics to show that they could meet their disposal requirements."*

This EM31 Technology Development and Deployment (TDD) Program Document WP5.2.1-210-001, is discussed in more detail in Section 5.0, and the task plan is given in Appendix A.

This FBSR technology synopsis evaluates the potential for the FBSR NAS sodalite-bearing multiphase ceramic waste form to resist aqueous corrosion and retain key risk driving radionuclides, e.g., ^{99}Tc. This update summarizes the performance results for the FBSR waste form data obtained from a series of bench-scale steam reformer (BSR) treatability tests with Hanford radioactive LAW Tank Waste (68 tank blend, Tanks SX-105, AN-103, and AZ-101/AZ-102), and the details can be found in References 3,4, and 5. The data from these treatability tests is compared to previous non-radioactive LAW processing and testing [6 and Appendix B] at the bench-scale, pilot-scale, and engineering-scale to provide a large body of data that demonstrates how the FBSR technology satisfies the IDF disposal requirements as well as the DOE TRL criteria and should be included in the LAW Supplemental Technology downselect process.

1.2 Report Contents and Organization

The ensuing sections of this report document (1) the importance of mineral waste forms in the DOE complex and (2) the mineral phases in the NAS waste form that sequester the radionuclides and COCs (Section 2.0). Section 3.0 discusses the FBSR THermal Organic Reduction (THOR™) flowsheet, the pilot and engineering scale testing that has been performed since 2001, and the FBSR process maturity. The data discussed in Section 3.4 demonstrate that all of the waste form performance test results from 2001-2008 have been consistent, and it is the purpose of this document to show that all of the data generated between 2008-2011 are internally consistent and that the 2008-2011 data is also consistent with the data generated in the 2001-2008 time frame.

In Section 4.0, the testing required for disposal of an FBSR mineral product in IDF are discussed as well. Section 5.0 lays out the details of the WFQ test program developed in 2008-2010 and the essential elements of the EM-30 WP 5.2.1 (see Appendix A) task plan. Section 5.1 includes the rationale for the selection of the specific radioactive Hanford tank wastes and prescribes what tests are required for the FBSR supplementary technology downselect.

Section 6.0 lays out the process control strategy used by the pilot-scale and engineering-scale FBSR flowsheets compared to the design and operation of the Savannah River National Laboratory (SRNL) BSR. Section 6.0 also describes how the mineralogy of the FBSR waste form product is constistently controlled using the SRNL process control spreadsheet called "MINCALC™" that has been used on all FBSR bench-, pilot-, and engineering-scale demonstrations since 2003. Other process control strategies for REDuction/OXidation (REDOX) control, Iron Oxide Catalyst (IOC) control used for improved denitration and for the sequestration of chromium +6 in the waste as insoluble chromium +3 in the waste form, i.e. in a $FeCr_2O_4$ spinel phase are also discussed in Section 6.0.

Section 7.0 describes the SRNL BSR operation and operating conditions, while Section 8.0 documents all the treatability test results. Section 8.1 documents all of the feed and product compositions, the resulting mineralogy and REDOX of the granular FBSR waste form and includes the mass balance of various radionuclides (^{99}Tc, ^{125}I, ^{129}I, ^{137}Cs). Section 8.2 details all of the WFQ test results for the granular FBSR waste form. Each level three heading in Section 8.2 relates to a critical WFQ test element in Table 5-4: test elements are discussed in the sequence given in Table 5-4.

The granular FBSR waste form, which meets IDF durability criteria, can be disposed of in a High Integrity Container (HIC). Alternatively, Section 9.0 demonstrates that the granular FBSR waste form can be made into a monolith with a geopolymer binder so that the granular waste form is macroencapsulated in this monolith matrix. Subsections of Section 9.0 give supplementary WFQ test data but the majority of the testing was performed on preliminary geopolymer monolith formulations.

Section 10.0 discusses the relative waste loading (Na_2O content) of the granular and monolithic FBSR products compared to LAW glass and cast stone and the relative disposal volumes of the three technologies. The granular FBSR product accommodates more Na_2O than the monolithic FBSR product and more Na_2O than LAW glass at equivalent disposal volumes to glass. The disposal calculations are performed assuming no compaction of the FBSR granular product in the HIC. Even minimal compaction would provide a lower disposal volume for granular FBSR than for glass at higher Na_2O waste loadings.

Section 11.0 discusses what is known about the durability of ceramic waste forms vs. vitreous waste forms, what was learned about the leaching mechanisms from the studies summarized in this document, and what is known about nepheline and sodalite leaching from the literature and in natural geologic environments.

1.3 Quality Assurance

The overarching Task Plan for the FBSR studies supported by SRNL, PNNL, and ORNL is the DOE EM-31 TDD Program Task Plan WP-5.2.1-2010-001 (see Appendix A). This Task Plan gives the details of the individual laboratories QA plans under which the work was performed.

The task was performed in accordance with a Quality Assurance Program (QAP) that meets the Quality Assurance criteria specified in DOE O. 414.1, *Quality Assurance*, 10 CFR 830, *Nuclear Safety Management*, Subpart A, "*Quality Assurance Requirements*", paragraph 830.122 and also meets the requirements of ASME Nuclear Quality Assurance (NQA)-1-2004, *Quality Assurance Requirements for Nuclear Facility Applications* including NQA-1a-2005 and NQA-1b-2007 Addenda, or later version.

A summary of the multi-laboratory success criteria outlined in the TDD program task plan is given in Section 5.0. The list is annotated with references to different documents which contain the results of the testing.

2.0 Mineral Waste Forms

The FBSR technology forms a mineral waste form at moderate processing temperatures (700-750°C) in the presence of steam; retaining and atomically bonding the halides, sulfates, and ^{99}Tc in the mineral phases known as nepheline (nominally $NaAlSiO_4$ of hexagonal symmetry), sodalite (nominally $M_8(Al_6Si_6O_{24})X_2$, where M is an alkali cation such as Cs, K, Na, etc—and X is a monovalent anion or a monovalent or divalent oxyanion, such as Br^-, Cl^-, I^-, TcO_4^-, ReO_4^-, SO_4^{2-}, etc), nosean (nominally $Na_8[AlSiO_4]_6SO_4$ with a larger cubic sodalite structure), and carnegieite (nominally $NaAlSiO_4$ of orthorhombic symmetry). All aluminate sodalite that host Sr and Cr are known (see Table 2-1) and sodalites with a variety of Al:Si ratios are known. Sodalites also host B, Mn, Ge, Ga, Be, and S. Additions of kaolin clay to the waste form sodalite and nephelines in a similar manner to the way in which glass formers are added to waste to form a borosilicate glass. The minerals formed by the FBSR technology offers atomic bonding of the radionuclides and COCs comparable to glass at higher Na_2O and SO_4^{2-} waste loadings than glass. The higher FBSR Na_2O and SO_4^{2-} waste loadings contribute to low disposal volumes and theoretically provide for more rapid processing of the LAW.

Nepheline, sodalite, and nosean are known as the feldspathoid minerals. Feldspathoid minerals and zeolites, including the sodalite and nosean, are a large and diverse classes of minerals characterized by a crystalline framework of tetrahedral Al and Si with a three-dimensional pore system that can accommodate a variety of anions. The common theme in sodalite group minerals is the flexible framework structure that can expand to enclathrate various guest anions by cooperative changes in the Al-O-Si bond angle.[7]

The synthesis and stability of sodalite under laboratory and hydrothermal conditions have been studied extensively because of the importance of zeolite-type phases as industrial catalysts and molecular sieves. Additionally, the sodalite phases have been postulated to form in the Hanford soil at locations where the unintentional release of caustic, high ionic strength, Al-rich waste solutions that exceed 60°C have reacted with subsurface sediments that are rich in SiO_2 (quartz, feldspar, clays such as illite, kaolinite, smectite, and calcite [8,9,10]). Researchers' at Hanford had also developed and patented a process for stabilizing alkali metal iodides or aqueous solutions into alkali sodalites for applications at Hanford.[11] Hanford also investigated the sodalite for aqueous radionuclide retention as long ago as 1973.[12]

The sodalite group of minerals and nepheline have been studied by a number of investigators as a potential host media for the immobilization of defense HLW, commercial nuclear waste, and transactinide elements, such as plutonium, in multiphase ceramic waste forms.[Table 2-1 and 13,14,15,16,17,18,19,20, 21,22,23,24,25,26] For example, a glass-bonded sodalite has been considered as a host matrix for the disposal of electrorefiner wastes from sodium-bonded metallic spent nuclear fuel removed from the EBR II fast breeder reactor. [14,18,19] The glass bonded sodalite waste form captures I and Cl and is 70% sodalite and 25% borosilicate glass and ~5% oxides (PuO_2 and nepheline) and halite.[27,28] The amount of sodalite formed is a function of how much NaCl, NaI, and other sodium oxyanions are in the EBR II wastes, otherwise traces of nepheline form instead because it takes six nepheline unit cells to form a sodalite structure (see Section 6.1).

2.1 Importance of Mineral Waste Forms in the DOE Complex

The concept of immobilizing radioactive waste in either vitreous or crystalline materials is over 50 years old. In 1953, Hatch [15] of Brookhaven National Laboratory introduced the concept of immobilizing radioactive elements in an assemblage of mineral phases. The first borosilicate glass formulations were developed in the United States between 1956 and 1957 by Goldman and others at the Massachusetts Institute of Technology.[29,30,31] These researchers examined calcium-aluminosilicate porcelain glazes to which boron oxide (B_2O_3) had been added to achieve a pourable glass and minimize radionuclide volatilization. The most promising vitreous systems for future development were determined to be borosilicate based, e.g., CaO-Al_2O_3-B_2O_3-SiO_2 and Na_2O-CaO-Al_2O_3-B_2O_3-SiO_2.

Extensive R&D programs were performed on nuclear waste forms during the late 1970s and early 1980s, resulting in the examination of a wide variety of single-phase and polyphase ceramics made by a variety of high temperature processes. By this time "low leachability" had become the main criterion for waste form comparisons [32,33], and such comparisons between crystalline ceramics and glass generated considerable controversy as the crystalline ceramics were considered to be more durable than glass.[34,35] However, the high-temperature processing of these alternative waste forms frequently resulted in the formation of an intergranular glassy phase, especially when alkali-containing wastes were processed. This intergranular glass limited product stability and durability because radionuclides, such as ^{137}Cs and ^{90}Sr, were frequently incorporated into the intergranular glassy phase(s) [36,37,38,39] and were determined to leach at the same rates as those from glass waste forms.[40]

Beginning in 1978, alternative waste form studies intensified culminating in a final review [41], which recommended borosilicate glass for immobilizing HLW at the Savannah River Site (SRS) in South Carolina and West Valley in New York and also identified SYNROC/tailored ceramics as promising alternatives.[16] These high temperature ceramic waste forms were later determined to be difficult to process, more costly to implement, and not as flexible for accommodating variations in waste composition as borosilicate glass.[42,43,44,45,46,47,48,49]

Research activity on alternative waste forms was severely curtailed as a result of the 1981 decision in the United States to immobilize defense HLW in borosilicate glass and the subsequent construction of the

Defense Waste Processing Facility (DWPF) at the SRS and the West Valley Demonstration Project (WVDP) at West Valley. The R&D effort on nuclear waste forms during this period has been summarized by Lutze and Ewing [20].

More recently, interest in crystalline waste forms has undergone a resurgence due to the need to develop durable materials for the stabilization and disposal of excess plutonium from defense and civilian programs [50,51]. Additional R&D has been performed on minerals and their analogs (e.g., apatite, monazite, zirconolite, zircon and pyrochlore) [52] and SYNROC formulations [53], as well as another down-selection between glass and ceramic waste forms [54] that recommended ceramic/mineral waste forms for Pu stabilization.

Crystalline (mineal/ceramic) waste forms[f] made from clay have been studied almost continuously since 1953 [15,42]. In 1981, Roy [55] proposed low-temperature, hydrothermally processed, low-solubility phase assemblages consisting of mica, apatite, pollucite, sodalite-cancrinite, and nepheline, many of which could be made from reactions between clays (kaolin, bentonite, illite) and waste. Clay based crystalline (ceramic/mineral) waste forms made at moderate temperatures (700-750°C) were not pursued in the late 1970's and early 1980's because there was no continuous commercial technology, like FBSR, available that could process the waste/clay mixtures in a hydrothermal environment [20].

Mineral waste forms made from clays have been recently re-examined for the immobilization of high-sodium, salt supernate (LAW) at the Hanford Site in Washington; high-sodium recycle streams from tank cleaning at the Idaho National Laboratory (INL), and low-activity waste melter off-gas condensates at Hanford. These mineral waste forms are made using a moderate-temperature (700-750°C) thermal pyrolysis treatment [56,57] by adding clay to the waste to form feldspathoid mineral analogs (sodalite and nepheline) or dehyroxylated mica [58,59], depending on clay composition. These clay based mineral waste forms have a higher capacity to stabilize more Na_2O and SO_4^{2-} (higher waste loadings) than glass for Hanford LAW (see Section 10.0).

Table 2-1. Similarity of Mineral Phases in FBSR Waste Forms to HLW Waste Forms Previously Studied

Mineral Phases Formed in FBSR at ~700°C [60,61]	**Mineral Phases Formed in HLW Ceramic Waste Forms [**13,15-17,20-26**]**	**Mineral Phases in Glass Bonded Sodalite Waste Forms [18,19,27,28]**
Nosean-Sodalite $(NaAlSiO_4)_6(Na_2SO_4)$	Sodalite $(NaAlSiO_4)_6(NaMoO_4)_2$	Sodalite $(NaAlSiO_4)_6(NaI,NaCl)_2$
Nepheline $NaAlSiO_4$	Nepheline $NaAlSiO_4$	Nepheline $NaAlSiO_4$
Cubic Nepheline $NaAlSiO_4$		NaCl
Corundum Al_2O_3	Corundum Al_2O_3	PuO_2
Hematite Fe_2O_3		
Magnetite Fe_3O_4		

[f] Crystalline (ceramic or mineral) waste forms include Na-Al-Si sodium aluminosilicate (NAS) mineral/ceramics, silicate based ceramics (supercalcines[‡]), aluminate based ceramics (Tailored ceramics), and titania based ceramics (SYNthetic ROCk known as SYNROC). Crystalline waste forms leach incongruently which means that some phases leach more preferentially than others.

2.2 FBSR Mineral Waste Form Product Description

The FBSR primary waste form is a granular multiphase NAS mineral (ceramic) product, which can be containerized or monolithed for disposal. The granular NAS product is composed of the individual minerals given in Table 2-1 and these minerals will be discussed in Sections 2.2.1 to 2.2.5.

The granular NAS product contains bed products of several millimeters in diameter (Figure 2-1 and Figure 2-2), which are agglomerates of smaller particles. These particles have a rough surface topography (Figure 2-2 and Figure 2-3) and sometimes have unreacted clay cores in them (Figure 2-3a-c). The identification of the unreacted clay cores is reported in Reference 62. Process improvements have led to more complete waste/clay reactions and clay cores are no longer observed (Figure 2-3d).

Some portions of the granular NAS product are fines that get carried over into a process gas filter (PGF). The fines have a similar mineralogy and may either be admixed with the bed product as the primary waste form, or the fines can be, but usually are not, recirculated to the reformer with the bed products as "seed particles" to enhance further particle agglomeration. In this section, the mineralogy of the bed products and fines will be discussed while the mineralizing reactions in the FBSR will be discussed in Section 6.1.

Table 2-2. Substitutional Cations and Oxy-anions in Feldspathoid Mineral Structures

Nepheline – Kalsilite Structures*	Carnegieite Structures	Sodalite Structures**	Nosean Structures
$Na_xAl_ySi_zO_4$ [63] *where x=1-1.33, y and z = 0.55-1.1(H)*	$NaAlSiO_4$ high carnegieite (C) [64; PDF #11-221]	$[Na_6Al_6Si_6O_{24}](NaCl)_2$ [63,65,66]	$[Na_6Al_6Si_6O_{24}](Na_2SO_4)$ [63,67,68]
$NaAlSiO_4$ [PDF #052-1342;69] (O)[t]	$NaAlSiO_4$ low carnegieite [64; PDF #11-220 no symmetry given]	$[Na_6Al_6Si_6O_{24}](NaFl)_2$ [63]	$[Na_6Al_6Si_6O_{24}](Na_2MoO_4)$ [63,70]
$KAlSiO_4$[63]	$Na_{1.45}Al_{1.45}Si_{0.55}O_4$ [71,72]	$[Na_6Al_6Si_6O_{24}](NaI)_2$ [11,68]	$[Na_6Al_6Si_6O_{24}]((Ca,Na)SO_4)_{1\text{-}2}$ [73]
$K_{0.00}Na_{1.00}AlSiO_4$ to $K_{0.25}Na_{0.75}AlSiO_4$ solid solution [63]	$Na_{1.95}Al_{1.95}Si_{0.05}O_4$ [71,72]	$[Na_6Al_6Si_6O_{24}](NaBr)_2$ [68]	$[(Ca,Na)_6Al_6Si_6O_{24}]((Ca,Na)S,SO_4,Cl)_x$ [PDF[f] #17-749]
$(Na_2O)_{0.33}NaAlSiO_4$ [74] (C)	$Na_{1.75}Al_{175}Si_{0.25}O_4$ [71,72]	$[Na_6Al_6Si_6O_{24}](NaReO_4)_2$ [75]	
$CsAlSiO_4$ [63]	$Na_{1.65}Al_{165}Si_{0.35}O_4$ [71,72]	$[Na_6Al_6Si_6O_{24}](NaMnO_4)_2$ [76,77]	
$RbAlSiO_4$ [63]	$Na_{1.55}Al_{155}Si_{045}O_4$ [71,72]	$[NaAlSiO_4]_6(NaBO_4)_2$ [78,79]	
$(Ca_{0.5},Sr_{0.5})AlSiO_4$ [63]	$Na_{1.15}Al_{115}Si_{085}O_4$ [71,72]	$(Fe,Zn,Mn)_4[Be_3Si_3O_{12}]S$ [68]	
$(Sr,Ba)Al_2O_4$ [63]	$Na_3MgAlSi_2O_8$ [71,72]	$Sr_8[Al_{12}O_{24}](CrO_4)_2$ [80]	
$KFeSiO_4$ [63]		$Na_8[AlSiO_4]_6(SCN)_2$ [81]	
$(Na,Ca_{0.5})YSiO_4$ [76]		$Na_6Al_6Si_6O_{24}$ (Zeolite A) [82,83]	
(Na,K)$LaSiO_4$[76]		$Na_8[ABO_4]_6 \cdot X_2$, where A=Al and Ga, B=Si and Ge, and X includes Cl^-, Br^-, I^-, $(ClO_3)^-$, $(BrO_3)^-$, $(HCOO)^-$, $(MnO_4)^-$, $(SCN)^-$ and $(SeCN)^-$ [84,85]	
$(Na,K,Ca_{0.5})NdSiO_4$[76]		$Na_{7.50}Fe^{2+}_{0.05}[Si_{6.07}Al_{5.93}]O_{24}Cl_{1.99}(SO_4)_{0.01}$ (hackmanite0 [86]	

* Iron, Ti^{3+}, Mn, Mg, Ba, Li, Rb, Sr, Zr, Ga, Cu, V, and Yb all substitute in trace amounts in nepheline.[63]

** Higher valent anionic groups such as AsO_4^{3-} and CrO_4^{2-} form Na_2XO_4 groups in the cage structure where X= Cr, Se, W, P, V, and As [76]

f Powder Diffraction File

t may be low-carnegieite per original reference

Note: (C) is for cubic crystal symmetry, (H) is for hexagonal crystal symmetry, (O) is for orthorhombic crystal symmetry (see text).

Figure 2-1. Optical Microscopy of FBSR Particles From the THOR® Treatment Technologies (TTT) Pilot Scale test in 2001 at Hazen Research Inc. (HRI). The Divisions on the Ruler shown are 1mm. The surface irregularities of the agglomerates are clearly visible.

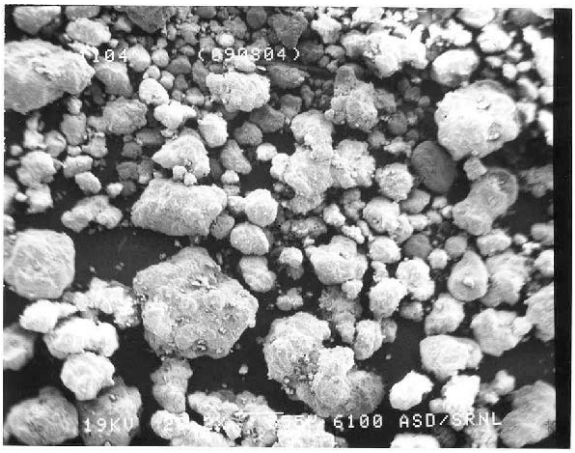

(a) 1123 Bed product from 2004 Pilot Scale Testing

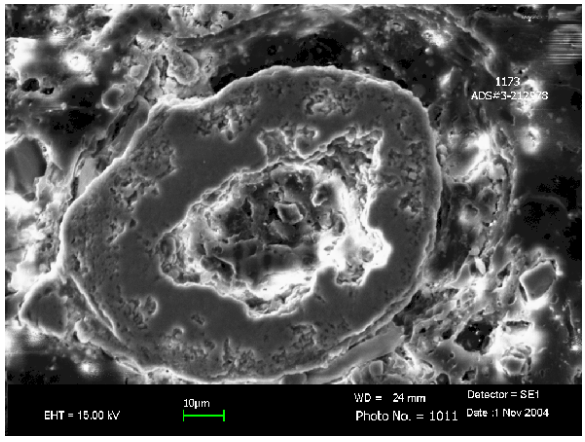

(b) 1173 Bed product (sectioned) from 2004 Pilot Scale Testing

Figure 2-2. Scanning Electron Microscopy (SEM) Photos of FBSR Bed Products Made with INL SBW at the INL Science Applications International Corporation-Science and Technology Applications Research (SAIC-STAR) facility showing the Surface Topography and Porosity in the FBSR samples.

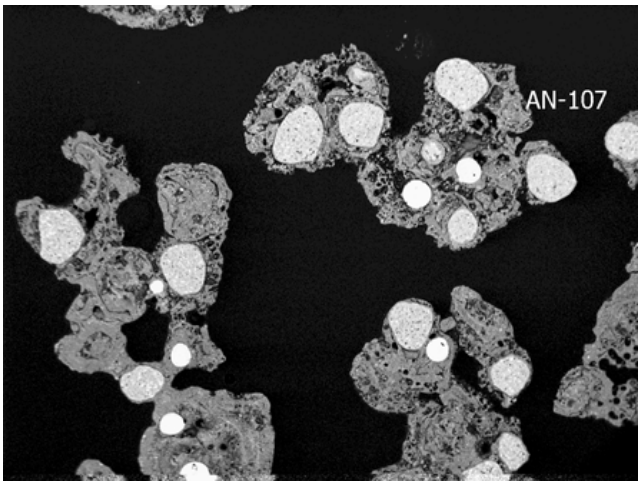

(a) AN-107 from 2001 TTT/HRI Pilot Test

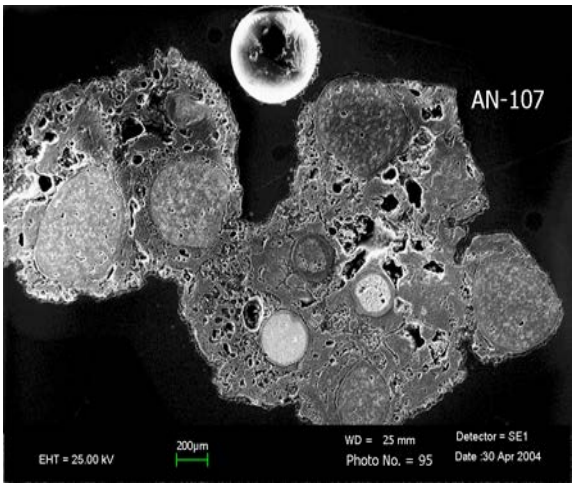

(b) AN-107 from 2001 TTT/HRI Pilot Test

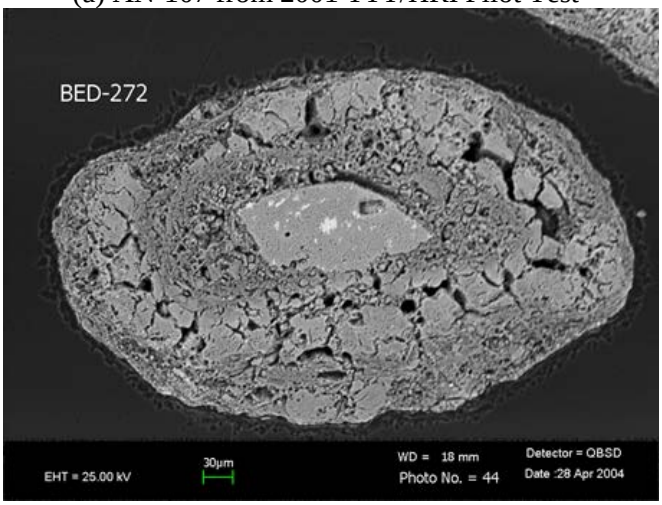

(c) Bed 272 INL SBW from 2004 Pilot Scale Testing at SAIC-STAR

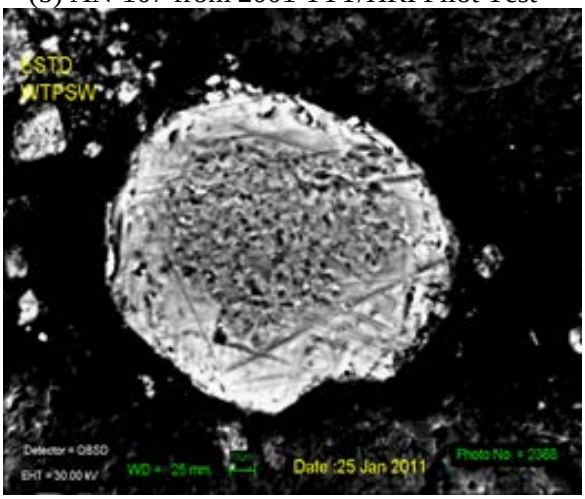

(d) Hanford WTP Secondary Waste 2008 Engineering Scale Testing by TTT/HRI

Figure 2-3. Scanning Electron Microscopy of Granules and Agglomerate FBSR products in Cross Section from the 2001 TTT/HRI pilot scale tests, the 2004 INL SAIC-STAR pilot scale tests, and the 2008 Engineering Scale Technology Demonstration (ESTD) tests.

Note that process improvements made before the ESTD testing led to better reactivity of the clay and waste and minimization of unreacted clay cores.

2.2.1 *Sodalites*

The flexibility of the sodalite structure to accommodate oxyanions is shown in Table 2-2 and demonstrates that monovalent species such as Cs^{+}, K^{+}, $Ca_{0.5}$, $Sr_{0.5}$, etc. can substitute for Na^{+} in the sodalite family of structures, while $(SO_4)^{-2}$, $(MoO_4)^{-2}$, $(AsO_4)^{-2}$, $(MnO_4)^{-1}$, and $(ReO_4)^{-1}$ and $(TcO_4)^{-1}$, can all substitute for the Cl^{-1} atoms in the sodalite structure (Figure 2-4). The cage-like structure is shown in Figure 2-5 for the Re containing sodalite showing that Re is encapsulated inside the cage like structure of the Al and Si tetrahedral. In the perrhennate sodalite, i.e. two $NaReO_4$, occupy the cage structure of the Re sodalite.[75]

For elements such as S, Mo, Re (Tc) and Mn, the oxygens in tetrahedral polyhedra around these elements provide the oxygen bonds for the tetrahedral XO_4 groups. These oxygen come from four of the six tetrahedra forming a ring along the body diagonal of the cubic unit cell.[87] In addition, I^{-}, Br^{-}, OH^{-}, and NO_3^{-2} can all substitute for the Cl^{-} atoms in the sodalite structure. The sodalite minerals are known to

accommodate Be in place of Al and S_2 in the cage structure along with Fe, Mn, and Zn (Table 2-2). Boron, beryllium, and gallium can substitute for Al in a tetrahedral polyhedra in the sodalite structures as can titanium, while germanium substitutes for Si and elements like iron and zinc substitute for Na^+ (Table 2-2).

All bonding in sodalite/nosean is ionic and the atoms are regularly arranged. This is similar to the manner of ionic bonding in glass, but more highly ordered than the atomic arrangements in glass. For example, the sodium atoms in sodalite are tetrahedrally coordinated and bound ionically to one Cl^- (or substitutes as discussed above) and bound ionically to three non-bridging oxygens from the framework $(AlO_4)^{-5}$ and $(SiO_4)^{-4}$. In glass, sodium atoms are only loosely bound in cavities between the framework $(AlO_4)^{-5}$ and $(SiO_4)^{-4}$ and loosely surrounded by 10 or 12 oxygen atoms. In addition, the structural bonding of I^-, Cl^- and TcO_4^- in oxidized glasses or TcO_2 in reduced glasses is poorly understood.[88,89,90]

The sodalites are classified [91] as "clathrasils", which are structures with large polyhedral cavities that the "windows" in the cavity are too small atomically to allow the encaged polyatomic ions and/or molecules to pass through once the structure is formed. See the structure for the Re-sodalite from reference 75. The sodalites differ from zeolites in that the zeolites have tunnels or larger polyhedral cavities interconnected by windows large enough to allow diffusion of the guest species through the crystal.[91] The sodalite cage structure usually has alternating Si and Al tetrahedra, TO_4 where T=Si or Al, with equal numbers of each that bond to form the cage. If there are more Al tetrahedra and fewer Si tetrahedra or vice versa they are all treated as solid solutions with the same cavity structures.[91] This framework is flexible and can expand to enclathrate various guest anions or oxyanions by cooperative changes in the Al-O-Si bond angle.[7] The framework can collapse via tilting and deformation of the Si and Al tetrahedral to accommodate ions of various sizes (see Table 2-3). It is important to note that these cages are too small to allow for the exchange of ions (i.e., ion exchange of caged anions) from the structure without the destruction of the Al—O—Si framework. More information about phase pure sodalite structures can be found in Reference 62, and information about mixed anion (guest-guest) sodalities where combinations of binary anions occupy the cage structure can be found in References 92 and 93, which includes projections for mixed TcO_4^- anions in a sodalite structure. Because anions can co-exist in guest-guest sodalities, the Tc sodalite cage retention values reported in Section 8.2.2 may be biased low. See additional discussion in Reference 162.

A large region of solid solution exists between sodalite ($Na_8(AlSiO_4)_6Cl_2$) and nosean $Na_8(AlSiO_4)_6SO_4$) [63,94] as shown in Figure 2-6 because the two species are isostructural. Trill, et. al [95] found a "solubility" gap in the ($Na_8(AlSiO_4)_6Cl_2$) and ($Na_8(AlSiO_4)_6I_2$) binary system between 15% and 85% of either species at synthesis temperatures of 180°C. Therefore, "mixed anion" sodalites are known, e.g. where the sodalite cage is jointly occupied by NaCl and Na_2SO_4 or NaCl and NaI. However, the only published sodalite binary phase diagram, which has been defined between two sodalite structures, is the one given in Figure 2-6. It is likely that other "mixed anion" sodalite combinations also exist but have not been rigorously studied.

Table 2-3. List of Oxidation State and Atomic Radii for Common Anions Incorporated in the Sodalite Framework

Element	Mineral Name	Oxidation State	Coordination Number	a(Å)	Space Group	Ionic Radii fom Ref. 6 (Å)	Ionic Radii from Ref. [96] (Å)
F^-	F-sodalite	-1	VI	NM	P43n	1.33	
Cl-	Cl-sodalite	-1	VI	8.8835	P43n	1.81	1.78
ClO_4^-	Cl-sodalite	-1	VI	8.8835	P43n	2.40	
SO_4^{2-}	Nosean	+6	VI	9.0932	P43n	2.30	2.37-2.57
TcO_4^-	Tc-sodalite	+7	VI	NM	P43n	2.52	
ReO_4^-	Re-sodalite	+7	VI	9.1528	P43n	2.60	
I^-	I-sodalite	-1	VI	9.0027	P43n	2.16	2.14-2.17
Br^-	Br-sodalite	-1	VI	NM	P43n	1.95	1.93
OH^-	Hydroxy-sodalite	-1	VI	8.89	P43n	1.36	1.48-1.51
NO_3^-	Nitrated-sodalite	-1	VI	8.978	P43n	2.00	

NM=Not Measured

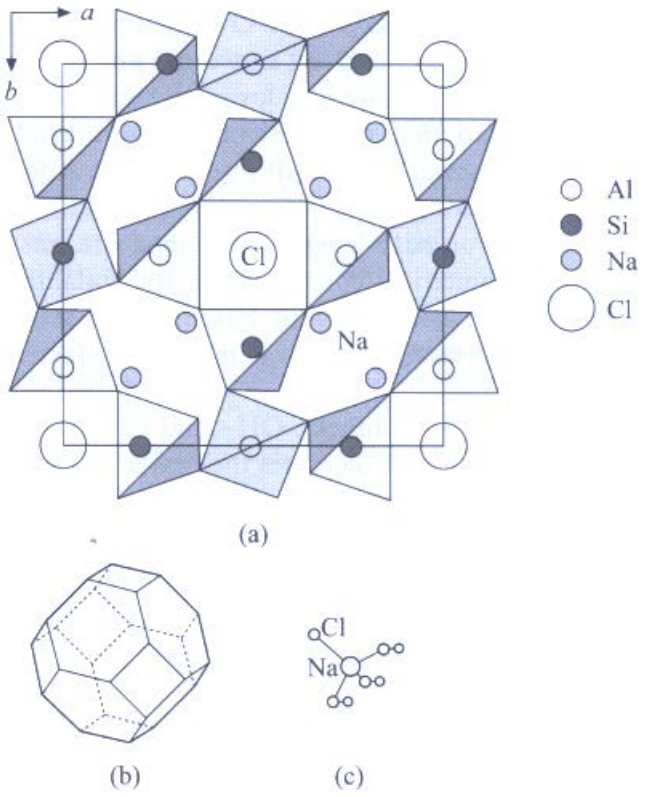

Figure 2-4. Structure of Sodalite showing (a) two-dimensional projection of the (b) three-dimensional structure and (c) the four fold ionic coordination of the Na site to the Cl^- ion and three framework oxygen bonds. [63]

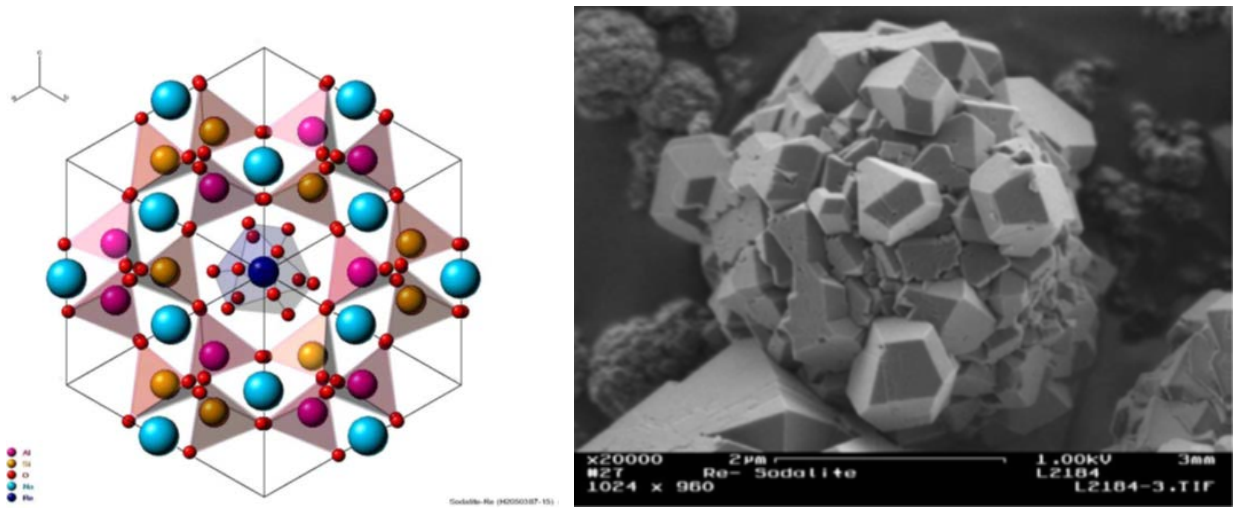

(a) (b)

Figure 2-5. Structure of a Re-sodalite (left) and a scanning electron microscope image of the same Re sodalite[75]. The dark blue atom in the center is Re in the left hand part of the figure.

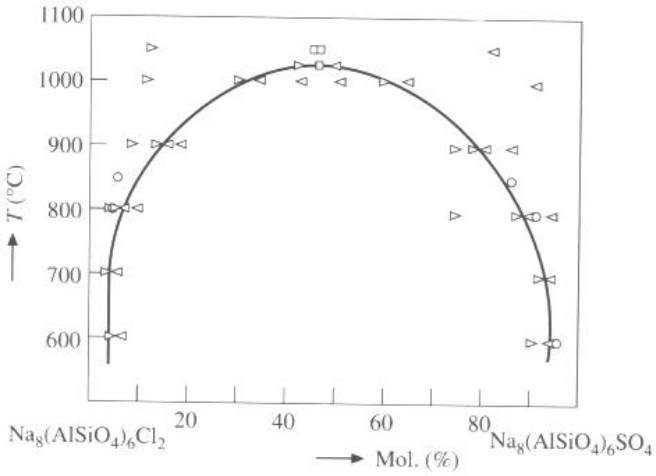

Figure 2-6. Experimentally Determined Sodalite-Nosean Solid Solution [94]

2.2.2 *Nephelines*

The nephelines are nominally $NaAlSiO_4$ or $Na_3KAl_4Si_4O_{16}$, which is 1/6 or 2/3 of the unit cell of the sodalite cage structure given as $[Na_6Al_6Si_6O_{24}]$ in Table 2-2. This is because six and four membered rings of tetrahedra, such as those in nepheline, define the cage structures in the sodalites. Thus, the aluminosilicate framework of sodalite is related to the structure of nepheline. Leaching of the nepheline framework, in terms of the degradation of the matrix elements of Al and Si should be similar to the leaching of the other sodalite minerals due to the similarity of the framework structure, $[Na_6Al_6Si_6O_{24}]$.

Nepheline is a hexagonal structured feldspathoid mineral (Table 2-2). The ring structured aluminosilicate framework of nepheline forms cavities within the framework (Figure 2-7). There are eight large coordination sites that bond Ca, K, and Cs ionically to nine framework (Al,Si tetrahedral) oxygens and six smaller coordination sites that bond Na ionically to eight framework (Al,Si tetrahedral) oxygens.[68] The larger nine-fold sites can hold large cations such as Cs, K, and Ca, while the smaller sites accommodate the Na. The K nepheline is known as kalsilite ($KAlSiO_4$). In nature, the nepheline structure is known to accommodate Fe, Ti and Mg as well.[68] Rare earth nephelines are known, e.g. $NaYSiO_4$, $Ca_{0.5}YSiO_4$, $NaLaSiO_4$, $KLaSiO_4$, $NaNdSiO_4$, $KNdSiO_4$, and $Ca_{0.5}NdSiO_4$, where the rare earth substitutes for Al in the structure.[76; Table 2-2] Many of the same alkali and alkaline earth substitutions that occur in sodalite can occur in the 8 and 9 coordinated ring sites in nepheline. As discussed in the previous section, the ring structures in nepheline are similar to the ring structures in the sodalites. Nepheline can be a host mineral for other alkali or alkaline earth elements (Cs, K, $Ca_{0.5}$) substituting for Na^+[Table 2-2]. Iron, Ti^{3+}, Mn, Mg, Ba, Li, Rb, Sr, Zr, Ga, Cu, V, and Yb all substitute in trace amounts in the nepheline lattice.[63] In addition, $BaAl_2O_4$, $SrAl_2O_4$, $(Sr,Ba)Al_2O_4$, $RbAlSiO_4$, $CsAlSiO_4$, and $KFeSiO_4$ all have nepheline/kalsilite structures with similar ring structures.[63] The structures of two of the $CsAlSiO_4$ and $RbAlSiO_4$ are given in Reference 62.

A sodium rich cubic structured nepheline with excess Na was also found in the FBSR mineralized products made with AN-107 in 2001 (Table 2-1), i.e. $(Na_2O)_{0.33}\,Na[AlSiO_4]$. This nepheline structure has large cage like voids in the structure where the Na can bond ionically to 12 framework oxygens.[74] This cage structured nepheline is not known to occur in nature, but the large cage-like voids are capable of retaining large radionuclides, especially monovalent radionuclides such as Cs. Sodium deficient nepheline structures are known (Table 2-2 and Figure 2-8) that have been found in other FBSR mineralizing campaigns for INL's alumina rich SBW. The Figure 2-8 image is important because it demonstrates that the non-stoichiometric nepheline structures sequester the alkali, including species such as Cs, in the same types of aluminosilicate rings as the stoichiometric nepheline structure shown in Figure 2-7.

During testing of the FBSR products (non-radioactive and radioactive), both the normal hexagonal nepheline and an orthorhombic nepheline were identified (Table 2-2). Upon further investigation, the crystal symmetry of the orthorhombic nepheline, the original reference [69] states that it may be a low-carnegeite phase which will be discussed in the next section (Section 2.2.3). In the References 3 and 4, which describe the BSR mineral products, this distinction is made.

It should be noted that there are broad regions of nepheline solid solutions in the Na_2O-Al_2O_3-SiO_2 system in which nepheline can form along with other NAS minerals.[98] Any deviations from stoichiometry (Al:Si of 1:1) do not affect the cage and ring structures but merely create lattice site vacancies. The use of the MINCALC™ process control strategy for FBSR production discussed in Section 6.2 ensures that the major NAS phase is nepheline/sodalite and that minor phases such as sodium silicate, sodium aluminate, and albite are minimized.

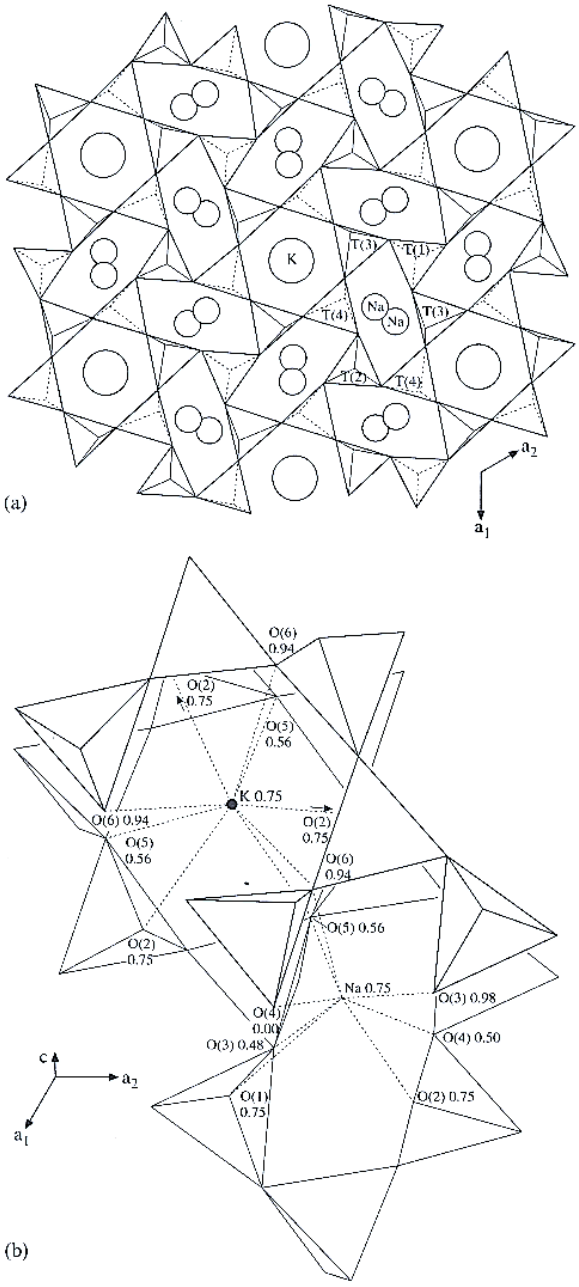

Figure 2-7. Two-dimensional representation of the structure of nepheline showing the smaller 8 oxygen sites that are occupied by Na and the larger 9 oxygen sites that are occupied by K and larger ions such as Cs and Ca. [63]

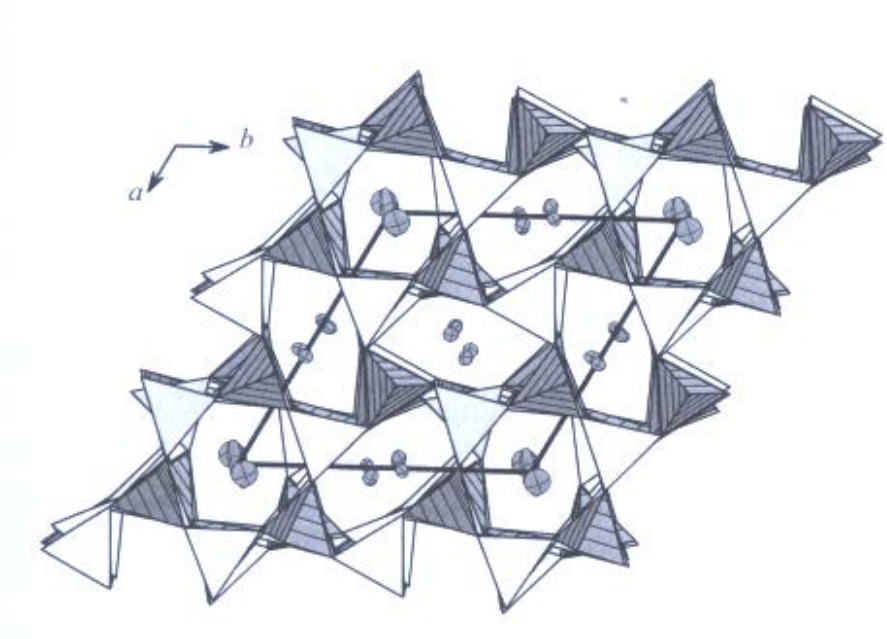

Figure 2-8. Crystal structure of monoclinic sodium deficient nepheline ($Na_{7.85}Al_{7.85}Si_{8.15}O_{32}$ showing the sixfold rings made of $(SiO_4)^{-4}$ and $(AlO_4)^{-5}$ tetrahedra. Sodium cations are bonded ionically to oxygen atoms as in stoichiometric nepheline (from reference 97).

2.2.3 *Carnegeites*

The carnegeites are also nominally $NaAlSiO_4$, the same as the nephelines. Four polymorphs of $NaAlSiO_4$ are known and most are known to crystallize from a melt.[64] Under cooling conditions, high-carnegieite forms first at temperatures above 1250°C. At 1250°C, high-carnegieite can transorm to high-nepheline, which is orthorhombic (Table 2-2). At temperatures closer to 900°C, high-nepheline transforms to low-nepheline, which is hexagonal and stable down to room temperature. High-carnegieite (cubic) can also undergo an inversion to low-carnegieite (orthorhombic) at 690°C.[64]

For FBSR applications, there is no molten phase, mixtures of $Al(OH)_3$ and sodium silicate have been found to make a hydrated nepheline gel at temperatures of ~80°C.[69] This hydrated nepheline is orthorhombic and forms orthorhombic low-carnegeite at temperatures in the range of 700-800°C, which can subsequently transform to hexagonal nepheline at ~950°C.

Low-carnegieite was identified in the 2001 FBSR pilot scale filter fines but not in the bed products. In later pilot scale testing (2004) at high nozzle-to-atomizing ratio, low-carnegieite (PDF#11-0220 in Table 2-2) and a Si-deficient carnegieite ($Na_{1.45}Al_{1.45}Si_{0.55}O_4$) was found in the bed products and filter fines. In later FBSR pilot scale testing (2008), low-carnegieite was only present as a minor phase in the bed and filter fines.[98] This is likely due to the fact that the fines do not have a long residence time in the reformer bed before they are carried over to the filter fines and have less time to convert from the orthorhombic low-carnegieite to hexagonal nepheline. In the BSR, both hexagonal and orthrhomic nephelie phases were identified as orthorhombic nepheline (PDF #052-1342). There is no disordering of the Al and Si tetrahedra, as measured by Nuclear Magnetic Resonance (NMR), in carnegeite but just a rotation of the tetrahedra that lowers the cystal symmetry of the carnegeite form of $NaAlSiO_4$.[99] Therefore, the carnegeite phase should allow the same crystallographic substitutions of alkali and alkaline earth elements as the nephelines.

2.2.4 *Corundum (Al_2O_3)*

Corundum, nominally Al_2O_3, enters the FBSR product as a startup bed material during steam reforming. It is more abundant in the first few reformer batches and is gradually replaced by the FBSR mineral product. It is inert and does not sequester any COCs.

2.2.5 *Iron Oxides (Fe_2O_3 and Fe_3O_4)*

The spinels such as Fe_3O_4 ($Fe_2^{+2}Fe^{+3}O_4$) are known to take Cr^{+3} and Ti^{+3} into their lattice in place of Fe^{+3} (
Figure 2-9), and many of the divalent transition metals like Ni^{2+}, Mn^{2+}, Zn^{2+}, Mg^{2+} into their lattice as well [99]. Spinels have both tetrahedral and octahedral coordination spheres with oxygen. The trivalent ions reside in the four-fold coordination positions and the divalent ions reside in the six-fold coordination positions. All the trivalent and divalent ions are ionically bonded to oxygen.

The Fe_3O_4 enters the FBSR product due to the addition of an IOC that is used to enhance denitration and provide a host for the hazardous Resource Conservation and Recovery Act (RCRA) metals. Some of the Fe_3O_4 based catalyst gets oxidized during the denitration reactions to Fe_2O_3 during processing which is why an IOC processing algorithm was developed to ensure adequate Fe_3O_4 was present in the product to sequester the RCRA metals.

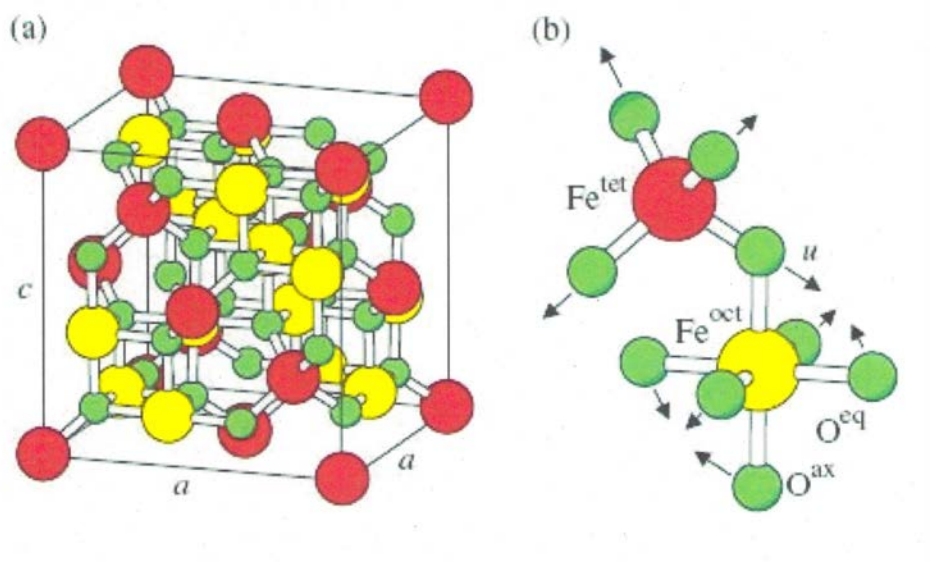

Figure 2-9. Face-centered cubic spinel structure of magnetite and an inset showing the magnification of one tetrahedron sharing an oxygen atom. Large spheres labelled by Fe^{tet} and Fe^{oct} represent iron atoms on tetrahedrally and octahedrally coordinated sublattices, respectively.[100] Chromium in +3 coordination substitues for Fe^{3+} in the Fe^{oct} sites. In order for the Cr^{+3} to leach out six Cr-O bonds would have to be broken and these ionic bonds are very strong and magnetite is very insoluble.

2.2.6 *Titanium Oxides (TiO_2)*

TiO_2 has two polymorphs, rutile and anatase. The TiO_2 is an impurity in many of the clays used to form the NAS minerals in the FBSR. While some Ti can be accommodated in nepheline and sodalite, the temperature of the FBSR process is likely not high enough to activate the refractory TiO_2 impurity and so it remains as rutile or anatase in the FBSR product.

3.0 THermal Organic Reduction (THOR®) Mineralizing FBSR Process Description

The THOR® FBSR mineralizing technology uses reformers to pyrolyze organics in the presence of a fluidization media of steam. Steam reforming, as chemical separation process, has been used for >100 years in the oil and gas industry. Mineralizing FBSR's can be externally heated or internally heated or a combination of the two heating methods. Externally heated FBSR's are normally limited to a diameter in the 6-8" range while coal or another reductant can be used to assist in the denitration reactions. Coal is also used to auto-thermally heat larger reformers (>8" diameter). Oxygen is bled in to the reformer to react with the coal and that reaction is exothermic and creates heat. FBSR flowsheets can be single reformer or dual reformer. Organics not pyrolyzed in the DMR and excess H_2 are oxidized in the second reformer as the second reformer usually runs at higher temperatures and is more oxidizing than the first reformer. A simplified THOR® dual reformer flowsheet of the steam reforming process is provided in Figure 3-1. More details regarding the flowsheet and the gaseous reactions are given in Sections 3.1 and 7.1.

In the THOR® process, waste feed, superheated steam, and co-reactants are introduced into a steam reformer vessel, known as the Denitration and Mineralization Reformer (DMR) where liquids are evaporated, organics are destroyed, and reactive chemicals in the waste feed are converted to a stable mineral product that incorporates essentially all of the radionuclides. The fluidized bed design of the steam reformer provides a large surface area for the waste to fully and efficiently react. Carbon and iron-based co-reactants are used to convert nitrates and nitrites directly to nitrogen gas in the reformer. Clay or other inorganic co-reactants are added to the waste feed or bed to convert the radionuclides, alkali/alkaline earth metals (sodium and potassium), sulfate, chloride, fluoride, rare-earths, and non-volatile heavy metals into an immobilized mineral product. The process operates safely at low pressure or a slight vacuum and at moderate temperatures (700–750°C). The DMR operates at slightly greater than atmospheric pressure and the CRR operates at a slight vacuum.

The steam reforming process destroys organic constituents. To ensure complete organic destruction, any organic intermediates being released from the DMR go to a second reformer, the Carbon Reduction Reformer (CRR) that operates at 950°C or alternatively to a thermal oxidizer. Toxic organics are converted to carbon dioxide and water vapor in the steam reformer by a combination of steam reforming and oxidizing reactions.

Off-gases from the CRR are filtered in the off-gas filter (OGF) and then passed through a High Efficiency Particle Air (HEPA) filter so that the primary emissions released from to the atmosphere from the process are carbon dioxide and water vapor (there are no liquid effluents from the process). Any fine particulate carryover from the DMR (or CRR if one is used) are caught in the Process Gas Filter (PGF) and/or Off-gas Filter (OGF). As shown in Figure 3-1, the mineralized product from the DMR along with any solids carryover from the PGF or OGF are comingled in the Product Receipt (PR) vessel for disposal.

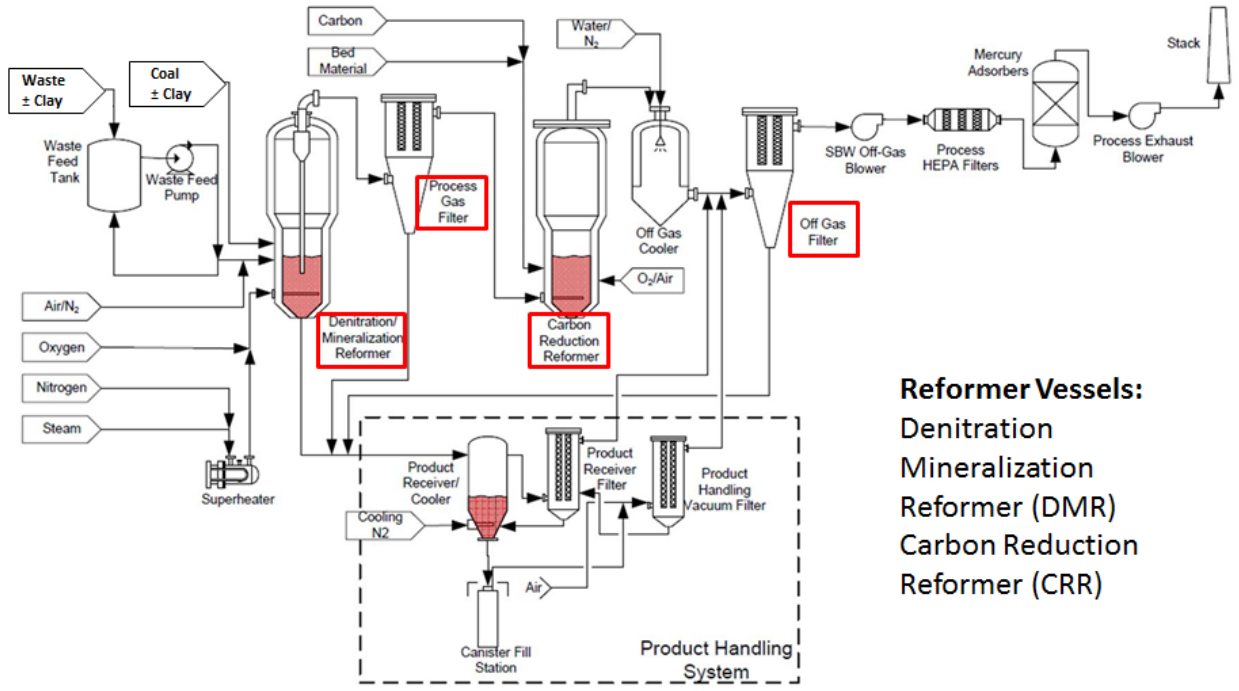

Figure 3-1. THOR® Dual Reformer Flowsheet of the Steam Reforming Process.

The reforming process is effective in pyrolizing organics and incorporates sulfur and halogens into the solid mineral product at moderate temperatures (650°C for carbonate mineralization and 700-750°C for aluminosilicate mineralization). In the FBSR, the organic compounds are pyrolyzed to CO_2 via the water gas shift reaction (WGSR), while nitrate/nitrite species are converted to N_2 through reaction with carbon and carbon reactions with superheated steam, which is the fluidizing media.[60,101,102] See reactions in Section 3.2.

The FBSR process is not combustion and is Clean Air Act (CAA) compliant. The FBSR technology has also been shown, during pilot-scale and engineering scale testing discussed in Section 3.3 to be Hazardous Waste Combustor (HWC) Maximum Achievable Control Technology (MACT) compliant for Hg, Cl, CO, total hydrocarbons, and heavy metals [103,104]. A significant benefit of the FBSR process is that it produces zero-liquid releases. All water is released as water vapor.

3.1 Waste Form Process Description

The simulant waste feed for the TTT ESTD engineering-scale plant is made-up using reagent chemicals in a large tank according to a recipe that emulates the waste constituents and concentrations to be processed. It is transferred in batches to one of the two waste feed tanks where it is slurried with the desired quantity of aluminosilicate clay that will allow the FBSR process to create the types of minerals that would provide leach resistant (durable) waste forms for the immobilization of the hazardous and radioactive constituents of the waste stream. This has been approached by selecting a kaolin clay type with the appropriate Al:Si mole ratio that would suitably react with the cations (largely Na in the Hanford streams) and anions in the waste based on the MINCALC™ process control discussed in Section 6.0.

The slurried waste feed is metered into the DMR via a pump and the flow rate is monitored by a mass flow meter. The bed in the DMR is fluidized via a combination of hot steam, nitrogen, and minimal oxygen and is operated in a reducing mode. The simulant is atomized into the DMR bed with air via a

specially designed feed nozzle. The feed droplets coat the bed particles, consisting of granular mineral solids, and are instantly dried at 700 – 750°C. The large active surface of dried nitrates readily reacts with hot carbon reductant particles, carbon monoxide and hydrogen gases, and the reduced metal and metal oxide particles in the fluidized bed. This reducing environment results in the near complete destruction of nitrates and nitrites, with only trace levels remaining in the solid product. An IOC is used to enhance denitration and sequester any chromium from the waste.

It is important to maintain a stable particle size distribution in the DMR fluidized bed and the atomizing gas flow rate and nozzle atomizing ratio (NAR, the ratio of the volumetric flow rates of the atomizing gas and the atomized slurry) can affect the particle size through jet grinding and controlling the atomized feed droplet size. Increasing the velocity of the atomizing air, up to the point where sonic velocity is reached, increases the momentum of the feed spray. This increases the intensity of the particle-particle collisions in the vicinity of the feed nozzle. The collisions result in particle fracturing (attrition). The gas injected through the fluidizing rails fluidizes the bed and causes particle collisions, but the fraction of fines attributed to the fluidizing gas is considered minor compared to the feed nozzle atomizing gas and can be minimized, from a design standpoint, by the correct sizing of the upper disengagement section. Other operating parameters that can affect particle size in the fluidized bed include (a) amounts and properties of slurried clay particles and other undissolved solids in the waste feed stream, (b) DMR operating temperature, (c) properties such as resistance to attrition of the product particles, and (d) fluidizing gas velocity.

The granular solid products are removed from the DMR either at the bottom or as fine material elutriated with the process gas stream at the top of the unit. Particle elutriation is affected by the fluidizing gas velocity at the top of the bed, by bubbles exiting at the fluidized bed surface, and by the diameter and length of the upper disengagement section. The solids that accumulate in the PGF are drained from the bottom of the vessel and transferred to the PR as shown in Figure 3-1.

Product solids are periodically removed from the bottom of the DMR, to maintain fluidized bed height, by an auger and are pneumatically transferred to the PR via a nitrogen jet. The PR is fitted with four sintered metal candlestick filters similar to those used in the PGF. The off-gas from the PR is vented to the freeboard region of the DMR or alternatively to a location further downstream in the off-gas train. Product solids are drained from the bottom of the PR into collection containers. The product solids from the PR and PGF are combined to form the immobilized FBSR waste form.

3.2 Gaseous Reactions

The bed particles in the steam reformer are reacted by introduction of near ambient pressure superheated steam (~600°C). Granular carbon, typically calcined coal, is added directly to the DMR bed as a fuel source and a reductant. The DMR bed temperature is maintained by the injection of some oxygen mixed in with the fluidizing gas injected through the upper distributor of the two stacked fluidizing rails. A portion of the carbon oxidizes to produce the bulk of the necessary process energy (autocatalytic heating) according to the following reaction:

$$C + O_2 \rightarrow CO_2$$

The reducing environment in the DMR is maintained by controlling the hydrogen gas composition to about 1 vol% on a wet basis, via the quantity and rate of granular carbon added directly to the bed. Carbon reacts with the fluidizing steam and water in the feed to produce H_2 and CO via the water gas reaction:

$$C + H_2O \rightarrow CO + H_2$$

The CO reacts further via the water gas shift reaction to produce additional H_2:

$$CO + H_2O \rightarrow CO_2 + H_2$$

Several of the possible reaction mechanisms whereby nitrites and nitrates are converted to nitrogen gas are shown below:

$$NO_3 + 2C \rightarrow NO + 2CO$$
$$NO_3 + C \rightarrow NO_2 + CO$$
$$2NO_3 + 4C \rightarrow N_2 + 2CO + 2CO_2$$
$$2NO_2 + 3C \rightarrow N_2 + 2CO + CO_2$$
$$2NO + 2C \rightarrow N_2 + 2CO$$
$$2NO + 2CO \rightarrow N_2 + 2CO_2$$
$$2NO + 2H_2 \rightarrow N_2 + 2H_2O$$

Any organics in the slurry feed to the DMR are initially volatized and steam reformed into carbon dioxide, carbon monoxide, hydrogen, and a small quantity of light hydrocarbons, with methane being the main constituent:

$$C_xH_y + xH_2O \rightarrow xCO + (x+y/2)\ H_2$$
$$C_xH_y + (2x-y/2)H_2 \rightarrow xCH_4$$
$$CO + H_2O \rightarrow CO_2 + H_2$$

The process gases exiting the DMR consist mostly of steam, N_2 (from process reactions, instrument purges, and fluidizing gases), and CO_2 with small quantites of CO and H_2. There are also low levels of NO_X, acid gases, and short chained organics present. The process gas from the ESTD DMR flows to the PGF, which captures any small sized DMR mineral product and carbon solids elutriated from the DMR into the process gas stream. The PGF is equipped withcandlestick filters that are automatically back-pulsed with nitrogen during operation to remove built-up filter cake, based on the differential pressure across the filters

In the ESTD, the process gases flow from the PGF to the fluidizing gas inlet distributors of the CRR located near the bottom of the vessel. The volatile hydrocarbons and the carbon monoxide and hydrogen gases generated in the DMR are further steam reformed in the lower portion of the CRR, and then oxidized to carbon dioxide and water vapor by addition of oxygen to the fluidizing gases in the upper portion of the CRR:

$$CO + H_2O \rightarrow CO_2 + H_2$$
$$2CO + O_2 \rightarrow 2\ CO_2$$
$$2H_2 + O_2 \rightarrow 2\ H_2O$$

The CRR's semi-permanent bed media is composed of alumina, although other than minor elutriation the material is typically removed only at the end of an operating period, since solid product does not accumulate in the CRR bed. Oxygen diluted with nitrogen is injected into the CRR in the upper fluidized bed region along with glycol. The bed region between the inlet distributors and this oxygen injection level operates in a reducing mode to enhance overall process NO_X destruction, while the bed region above operates in an oxidizing mode to convert residual CO, H_2, and volatile hydrocarbons to CO_2 and water.

Higher in the CRR, additional oxygen is injected to control the process outlet gas oxygen concentration, which in turn keeps the process off-gas carbon monoxide concentration low. The injection of oxygen and glycol also provides the heat source necessary to allow the CRR to operate at approximately 950°C.

The gases exiting the CRR (mainly carbon dioxide, nitrogen, and water vapor) are cooled in the off-gas cooler (OGC), filtered in the off-gas filter (OGF), and then vented to the atmosphere through a HEPA filtration and a monitored stack. If mercury is present in the feed stream, it is volatized in the DMR and is

captured in a mercury absorber at the back end of the off-gas system employing sulfur impregnated granular activated carbon (GAC).

3.3 Pilot-scale and Engineering-scale FBSR Testing (Non-Radioactive Hanford LAW and INTEC SBW)

When kaolin clay, the main mineralizing additive, is added to a basic alkali-rich waste (Hanford LAW) or an acidic waste (INTEC SBW) and then processed using the THOR® FBSR process, a "mineralized" waste form is produced that is composed of various NAS feldspathoid minerals as discussed in Section 2.2. All the waste clay reactions occur by nano-scale reaction of the clay and waste (see Section 6.1) and there is experimental evidence to show that reaction between the clay and waste initiates in the feed/mixing tank.[10]

All the FBSR pilot-scale and engineering-scale tests using kaolin clay have used the MINCALC™ process control (see Section 6.2) developed at SRNL to control the chemistry of the process so that the desired NAS mineral assemblages are formed with a variety of legacy US DOE waste simulants. A summary of the pilot scale and engineering scale tests is given in the upper portion of Table 3-1. In Table 3-2, the references are summarized that document the characterization of the FBSR products, the durability tests performed, and whether or not monolithic waste forms were fabricated and also tested.

An FBSR granular waste form was produced (Table 3-1) with simulated Hanford LAW waste (Envelope C high organic waste known as AN-107) in the TTT pilot-scale facility at Hazen Research Incorporated (HRI) in late 2001 [57,60]. The identification of the crystalline phases is discussed in more detail in Section 8.2.3 and compared to the data generated in the 2004 pilot-scale testing, the 2008 engineering-scale testing, and the 2010-2011 BSR testing. TCLP testing had been performed by a Denver Environmental Protection Agency (EPA) certified laboratory and demonstrated that the product met the Universal Treatment Standards (UTS) for listed wastes. The TCLP data is presented in Section 8.2.9 and compared to the data generated in the 2004 pilot-scale testing, the 2008 engineering-scale testing, and the 2010-2011 BSR testing. Additional durability testing of this Hanford waste granular product ensued and American Society for Testing and Materials (ASTM) C1285 (PCT) was performed at SRNL. The PCT data is presented in Section 8.2.4 and compared to the data generated in the 2004 pilot-scale testing, the 2008 engineering-scale testing, and the 2010-2011 BSR testing.

Single Pass Flow Through (SPFT) and Pressure Unsaturated Flow-through (PUF) testing were performed at PNNL on the AN-107 FBSR material [61,105,106]. A preliminary Performance Assessment (PA) [107] demonstrated[f] that the release rates for the FBSR mineral product were the same as glass LAWA44 and 100 times slower than glass LD6-5412 formulated with the same AN-107 waste simulant.

Additional pilot-scale tests of the FBSR technology were performed from 2003-2004 at the SAIC-STAR facility in Idaho Falls, Idaho. The pilot-scale tests [108] were performed on a Hanford LAW (Rassat blend high sodium waste) [109] and an INL SBW [104,110] by the INL and TTT team. The wastes were 2-5 M Na^+, with a $NaReO_4$ spike (5.2-5.4 x 10^{-4}M) to simulate $NaTcO_4$, Cs, Cl, F, and I. The LAW waste had total organic carbon of ~3.5 g/L [109]. Additional focus on the Hanford LAW durability tests included ASTM C1285 and SPFT at SRNL, and TCLP testing by a South Carolina EPA certified laboratory. [111,112,113]. The identification of the crystalline phases is discussed in more detail in

[f] The PA evaluation required the pH dependence of the nepheline dissolution rate (η) since the NAS phases in the waste form (nepheline, nosean, and sodalite) all share the basic nepheline crystallographic framework structure. Values of η were available in the literature for natural single crystal nepheline and for nepheline glass but the published η values differed widely allowing only bounding PA calculations to be performed

Section 8.2.3 and compared to the data generated in the 2001 pilot-scale testing, the 2008 engineering-scale testing, and the 2010-2011 BSR testing.

The granular products (bed and fines from the 2003-4 testing and fines from the 2001 AN-107 testing, see Table 3-2) were determined to be ~2 orders of magnitude more durable than the LAW glass specification of NL_{Na}=2 g/m^2 when the Brunauer, Emmett, and Teller [114] (BET) surface area is used in the calculation instead of the geometric surface area as suggested by McGrail, et. al. [61]. When the geometric surface area was used, e.g. the leach rate is still expressed in g/m^2 (NL_i) but is not dependent on the surface roughness of the waste form being tested, the leach rate of the FBSR product is comparable to LAW glass.[‡] The PCT data is presented in Section 8.2.4 and compared to the data generated in the 2001 pilot-scale testing, the 2008 engineering-scale testing, and the 2010-2011 BSR testing.

[‡] Durability results can be expressed as a normalized concentration (NC_i) which have units of $g_{waste\ form}/L_{leachant}$, as a normalized release (NL_i) in $g_{waste\ form}/m^2$, or as a normalized rate (NR_i) in $g_{waste\ form}/\ m^2 \cdot$day where "i" is the chemical element of interest. Units of NL_i or NR_i necessitate the use of the surface area (SA) of the sample releasing species "i" and the volume (V) of the leachant being used which is expressed as the SA/V ratio.

Table 3-1. Comparison of Pilot-scale, Engineering-scale, and Bench-scale FBSR Size and Operation

Facility	Scale	Radioactive or Non-Radioactive?	FBSR Column Diameter	Externally or Autothermaly Heated?	Dual or Single Reformer Flowsheet?	Reductant of Choice	Catalyst?	Waste
TTT 2001-2002	Pilot	Non-Radioactive	6”	external and autothermal with coal	Single	BB charcoal	Yes	AN-107
SAIC-STAR 2003-2004	Pilot		6”	external and autothermal with coal	Single	BB charcoal	No	INTEC SBW Rassat LAW
TTT ESTD 2006	Engineering		15”	autothermal with coal	Dual	Bestac coal	Yes	INTEC SBW
TTT ESTD 2008	Engineering	Non-Radioactive	15”	autothermal with coal	Dual	Bestac coal	Yes	WTP-SW (*Module A*)
SRNL BSR 2009	Bench-scale	Radioactive and Non-Radioactive	2.75”	external and autothermal with coal	Dual	Bestac coal	No	WTP-SW (*Module A*)
START OF THE DOE-EM WFQ PROGRAM								
TTT ESTD 2008	Engineering	Non-Radioactive	15”	autothermal with coal	Dual	Bestac coal	Yes	Rassat LAW (*Module B*)
SRNL BSR 2010-2011	Bench-scale	Radioactive and Non-Radioactive	2.75”	external and autothermal with coal	Dual	Bestac coal	Some tests	Rassat LAW (*Module B*) SX-105 (*Module C*) AN-103 (*Module D*)
SRNL BSR 2011	Bench-scale	Non-Radioactive					Yes	AZ-101/ AZ-102 (*Module E*)

WTP-SW = WTP Secondary Waste

Table 3-2. References for FBSR Granular/Monolith Product Durability Testing

Pilot Scale Facility	Date	FBSR Diameter	Acidic And Basic Wastes	Granular PCT Testing	TCLP of Granular Form	Granular SPFT Testing	Preliminary Risk Assessment	Product Tested	Coal	Particle Size Distribution (PSD)	MonoLith	Monolith PCT Testing	Monolith SPFT Testing	MonolithANSI/ANS 16.1/ ASTM C1308 Testing	TCLP of Monolith
Non-Radioactive Testing															
HRI/ TTT	12/01 Ref 60	6”	LAW Env. C AN-107	Ref. 115	Ref 60,115	Ref 61,105 and PUF testing (106)	Ref. 107	Bed	Removed By Hand	Gaussian	No	N/A			
		6”		Ref 111,112,113		None	“Tie-back” Strategy 3	Fines	Removed by 525°C Roasting						
SAIC/ STAR	7/03 Ref 103, 104	6”	SBW			None	None	Bed			Yes (Samples were combined; 20% LAW, 32 % SBW and 45% Startup Bed	Ref 116,117	N/A		
SAIC/ STAR	8/04 Ref. 108	6”	LAW Rassat			Ref 6,113 , 118,119 and PUF 6,120	Data from Ref 113,118,119 “Tie-back” Strategy 3	Bed and Fines Separate							
SAIC/ STAR	7/04 and 11/04 Ref. 110	6”	SBW			Ref 113,118	None								
HRI/ TTT	12/06	15”	SBW	Ref 121		None	None				No	N/A			
HRI/ TTT	2008 Ref. 122		LAW Rassat	Ref 3,98 , 123,124, 125	Ref 123, 124, 125	126	“Tie-back” Strategy 3	Bed and Fines Together	Not removed	Bi-Modal	Yes	Ref 123	PNNL	Ref 3	
			WTP-SW			None	None						None	Ref 127, 128	Ref 123,124 125
Radioactive Testing															
SRNL/ BSR	2010-2013	2.75”	LAW Rassat	Ref. 3, 129		126,130 and PUF 131 ,132	“Tie-back” Strategy 3	Bed and Fines Together	Not removed	Gaussian	Yes	Ref 3	Ref 130	Ref 3	
			WTP-SW	Ref 127,129		None	None					Ref 127	None	Ref 127	Ref 127

PCT – product consistency test method (ASTM C1285-08); SPFT – single pass flow-through test method (ASTM C1662); ANSI/ANS16.1/ASTM C1308/EPA 1315 – monolith emersion tests all similar with different leachate replenishment intervals; Pressure Unsaturated Flow Test (PUF); -LAW Env. – low activity waste envelope A, B, and C; PSD - particle size distribution; FY11 – Joint program between SRNL, PNNL, ORNL; SRNL Test Results are complete and documented [3,4] PNNL Test Results are complete and documented; N/A – not applicable.

EPA TCLP tests were also conducted on the 2003-2004 LAW waste forms. The granular product passed TCLP at the UTS when spinel minerals were encouraged to form by using the IOC denitration catalyst [111,112]. The TCLP data is presented in Section 8.2.9 and compared to the data generated in the 2001 pilot-scale testing, the 2008 engineering-scale testing, and the 2010-2011 BSR testing.

The 2003-2004 LAW FBSR waste forms were also tested with the SPFT test by Lorier [113,118,119] in order to provide comparisons to the 2002 SPFT durability testing of McGrail [61,105]. The SPFT testing performed by Lorier, et. al. [118] included 5 different pH values and 4 different temperatures for 3-14 day test durations [118]. This allowed the pH dependence of the dissolution rate (η), and the activation energies of dissolution to be derived.[119] The durability data is in agreement with the 2002 SPFT testing performed by McGrail [61,105] and the preliminary PA modeling performed by McGrail [61,105] for the FBSR waste forms. Additional PUF testing on the 2004 pilot-scale SAIC-STAR FBSR products was performed by Pierce and these experiments are documented in Reference [6].

FBSR testing of a Hanford LAW simulant and a WTP-SW simulant at the engineering-scale was performed by TTT at HRI in April/May 2008.[122] The Hanford LAW simulant was the Rassat 68 tank blend [109] and the target concentrations for the LAW was increased by a factor of 10 for Sb, As, Ag, Cd, and Tl; 100 for Ba and Re (Tc surrogate); 1,000 for I; and 254,902 for Cs based on discussions with the DOE field office and the environmental regulators and an evaluation of the Hanford Tank Waste Envelopes A, B, and C.[133] It was determined through the evaluation of the actual tank waste metals concentrations that some metal levels were not sufficient to achieve reliable detection in the off-gas sampling.[122] Therefore, the identified metals concentrations were increased in the Rassat simulant processed by TTT at HRI to ensure detection and enable calculation of system removal efficiencies, product retention efficiencies, and mass balance closure without regard to potential results of those determinations or impacts on product durability response such as TCLP.[122]

A WTP-SW simulant based on melter off-gas analyses from Vitreous State Laboratory (VSL) was also tested at HRI in the 15" diameter ESTD dual reformer at HRI in 2008.[122] The target concentrations for the RCRA metals were increased by 16X for Se, 29X for Tl, 42X for Ba, 48X for Sb, 100X for Pb and Ni, 1000X for Ag, and 1297X for Cd to ensure detection by the analytic laboratory used for the demonstration.

Characterization of the granular 2008 products and the associated durability testing (ASTM C1285) and TCLP testing are summarized in Sections 8.2.4 and 8.2.9 and the details given in references 98 and 123. The FBSR PR samples had been taken from the Product Receiver Tank, while the PGF samples were the fines that also undergo mineralization and are collected as carryover from the DMR. The product was ~60% PGF fines due to the processing parameters used during the mineralization test.

Characterization of these crystalline powder samples indicates they are primarily Al, Na and Si, with < 1wt% Fe, K and S also present. The PR samples contained less than 2.1 wt% carbon with a bulk density of ~ 1 g/cc, and the PGF samples ranged from 8.6 to 13 wt% carbon.[123]

Crystalline phases observed in the aggregate and blends from the Hazen ESTD testing show two forms of $NaAlSiO_4$ (Low-Carnegieite and Nepheline), Nosean (the sulfate containing sodalite), and a halide containing sodalite similar to previous FBSR testing results. The identification of the crystalline phases is discussed in more detail in Section 8.2.3 and compared to the data generated in the 2001 pilot-scale testing, the 2004 pilot-scale testing, and the 2010-2011 BSR testing.

The as-received PR and PGF samples were roasted in air to determine coal content by loss-on-ignition at 525°C and to prepare the samples for durability testing. Durability testing of the PR and PGF samples using the ASTM C1285 PCT 7-day leach test at 90ºC was performed along with several reference glass

samples. Normalized release rates from the PR and PGF samples were all less than 0.08 and 0.14 g/m^2, respectively, with NL_S giving the highest of the measured releases. Measured leachate values were normalized using BET surface areas that measured in the range of 3.8 to 5.5 m^2/g for the 100-200 mesh fractions obtained from the FBSR aggregates. Note that BET measurements were performed on a PCT prepared sub-specimen so that the surface area of the mineral product and not the coal is used during release calculations.

Additional characterization of the 2008 ESTD simulant testing is reported in reference 122 and summarized in Table 3-2. Prior to the reference 122 studies the FBSR bed products and fines had been studied independently to determine the leaching mechanisms and appropriate leach tests to perform. In reference 122, the FBSR bed products were studied separately and together: it was shown that the mineral phases observed in the PGF fines are the same as the mineral phases in the FBSR bed products and have comparable durability.

3.4 Characterization and Testing of FBSR Waste Forms: Pilot- and Engineering-Scale Tests

Prior to the DOE-EM WFQ program that funded the work summarized in this document, a considerable amount of durability testing had already been performed by SRNL, PNNL, and ORNL on the FBSR granular waste form and the FBSR monolithed waste form: see Table 3-2, References 6 and 62, Appendix B, and Section 3.3 of this document for summaries of the work performed. The durability testing includes the (ASTM C1285 (PCT-A and PCT-B) durability testing, SPFT or ASTM C1662, PUF testing, and the EPA TCLP. Coupled together these test results can be used to demonstrate the waste form will meet preliminary waste acceptance criteria for the Hanford IDF. All of the non-radioactive durability testing was found to be consistent between the FBSR pilot studies (2001 and 2004) as discussed in Reference 6. This report demonstrates that data derived before the DOE-EM WFQ program and after the DOE-EM WFQ program, as depicted in Table 3-2, are consistent and demonstrate that the FBSR mineral waste form has comparable performance to glass.

The durability performance requirements are met by the FBSR granular mineral product because mineral dissolution involves the breaking of atomic bonds between cations and anions in the mineral structure in the same fashion that atomic bonds are broken in vitreous waste forms. Hence, the reason mineral (ceramic) waste forms and glass waste forms were competitors for HLW stabilization in the 1980's as discussed in Section 2.1. The long-term performance of both glass and mineral waste forms are controlled by a rate drop that is affinity controlled.

The discussion regarding monolith formulation versus durability is, therefore, considered supplementary to FBSR product performance but is given in Section 9.0. The choice of the binder and its particular formulation, and thus its performance with the granular product, is considered secondary to the basic FBSR process and therefore represents relatively low technical risk relative to the down select process.

Monolithing was investigated in geopolymers made from both fly ash and clay, various cements (Ordinary Portland Cement (OPC) and three high alumina cements), Ceramicrete, and hydroceramics. The durability of the monolithed FBSR waste forms were then compared to the granular product durability responses (Table 3-2). Monolith studies from 2008 to the present were performed on bed and fines products co-mingled at the relative ratios that they were produced during engineering scale testing. Monolithing in an inorganic geopolymer binder, which is amorphous, macro-encapsulates all the granules and retards the onset of leaching. More details will be given in Section 9.0.

3.5 FBSR Process Maturity

A commercial facility to continuously process radioactive wastes at moderate temperatures in a hydrothermal steam environment was built by Studsvik in Erwin, Tennessee in 1999.[56] The Erwin facility uses the THOR® process to pyrolyze ^{137}Cs and ^{60}Co organic resins from commercial nuclear facilities. The Erwin facility has the capability to process a wide variety of solid and liquid streams including: ion exchange resins, charcoal, graphite, sludge, oils, solvents, and cleaning solutions at radiation levels of up to 400R/hr. Erwin has been processing low and intermediate level radioactive wastes (e.g., Class A, B and C) from U.S. commercial nuclear power plants for the last 14 years.[134] The granular product is containerized and buried at the EnergySolutions/Chem Nuclear Low Level Radwaste (LLRW) Atlantic Compact site in Barnwell, South Carolina, at the Waste Control Specialists site in Andrews County, Texas, and at the EnergySolutions facility in Clive, Utah.

The commercialization of the FBSR technology at the Erwin, Tennessee facility created interest in this technology for the immobilization of a wide variety of radioactive wastes across the US DOE complex. Of special relevance is the capability of the FBSR technology to destroy organics while converting alkali/alkaline earth/rare earth salts to aluminosilicate minerals that are suitable for direct geological disposal and/or to carbonate or silicate species for subsequent vitrification or disposal. A significant benefit of the FBSR process is that liquid secondary wastes from process gas treatment are not produced. All water is released as water vapor.

The first application of the THOR® FBSR technology for stabilization of a liquid LAW radioactive waste in the DOE Complex was built at INTEC to treat 900,000 gallons of SBW. The SBW acidic waste, designated as Transuranic (TRU) waste, will be made into a granular FBSR product (carbonate based not NAS mineral based) for disposal in the Waste Isolation Pilot Plant (WIPP) [103,104]. The INTEC FBSR facility is known as the IWTU as discussed in Section 1.0.

The IWTU design work commenced in 2005 and the facility construction was completed in early 2012 when start-up activities and an ORR commenced. During the initial system heat-up testing, the IWTU experienced a pressure control shutdown event on June 16, 2012. Only carbon-based solids, inert bed materials, oxygen, and nitrogen had been added to the process equipment. No radioactive or hazardous materials had been introduced. Numerous modifications were made to the IWTU to address the causal factors related to the 2012 event as well as modifications related to overall process improvements that were identified post event. Some modifications directly addressing the causes of the event included:

- changing the location of introducing oxygen into the process to allow for more thorough carbon reaction and more efficient heating during start-up;
- securing the process filter bundles in the solids separation filter vessels;
- testing and upgrade of the fluidizing gas distributors in the primary FBSR vessel;
- testing of pressure control systems;
- installing additional pressure-relief valves; and
- adding additional monitoring to detect pressure variations in the process.

The causes of the event were related to scale-up design issues and not the technology.[134] The changes to the IWTU delayed re-start until late December 2013.

The DOE-EM WFQ R&D summarized in this document has substantially increased the TRL level of the FBSR process to a TRL of 6, which is the TRL required for a technology to enter design. With the recent process maturity, full scale FBSR operation at INTEC, the FBSR technology has reached a TRL of 7. The IWTU underwent an Operational Readiness Review (ORR) in March 2014. From late 2014 through January 2015, the initial non-radioactive IWTU start-up campaign, referred to as the TI-102 campaign, processed over 60,000 gallons of non-radioactive simulated SBW. The facility is currently in restart after

a planned outage for inspection of the equipment. The IWTU will resume processing simulated waste feed and perform another shutdown/inspection before beginning to process additional simulants and/or 900,000 gallons of radioactive SBW. When the IWTU begins radioactive operations, the FBSR technology will have reached a TRL of 8 for a waste stream similar to Hanford LAW.

Another FBSR facility had been under design at the SRS to convert a salt supernate LAW type waste (Tank 48) containing nitrates, nitrites, and cesium tetraphenyl borate (NaTPB), an organic, to an FBSR carbonate product that could be returned to the tank farm once free of organics and subsequently vitrified [135,136]. During design of the FBSR facility, the need to recover the Tank 48 space in the tank farm became less of a necessity at SRS so near-term treatment was abandoned. In-tank chemical destruction of the NaTPB organics is being further investigated as a long-term processing alternative.

Pilot-scale and engineering-scale testing has been performed on a variety of DOE wastes producing aluminosilicate waste forms for INTEC's SBW, Hanford's LAW, and LAW melter recycle (WTP-SW) as discussed in the previous Section 3.3.

4.0 Waste Form Criteria for Disposal in IDF

A key driver for maturing and qualifying the FBSR waste form and immobilization process is to ensure that the waste forms will be acceptable for disposal on site at the 200-East area IDF. Wastes intended for disposal in the IDF must meet requirements of DOE Order 435.1 and RCRA permit requirements established by the Washington State Department of Ecology. Figure 4-1 shows regulatory authorities and relationships that apply to ILAW disposal in the IDF.

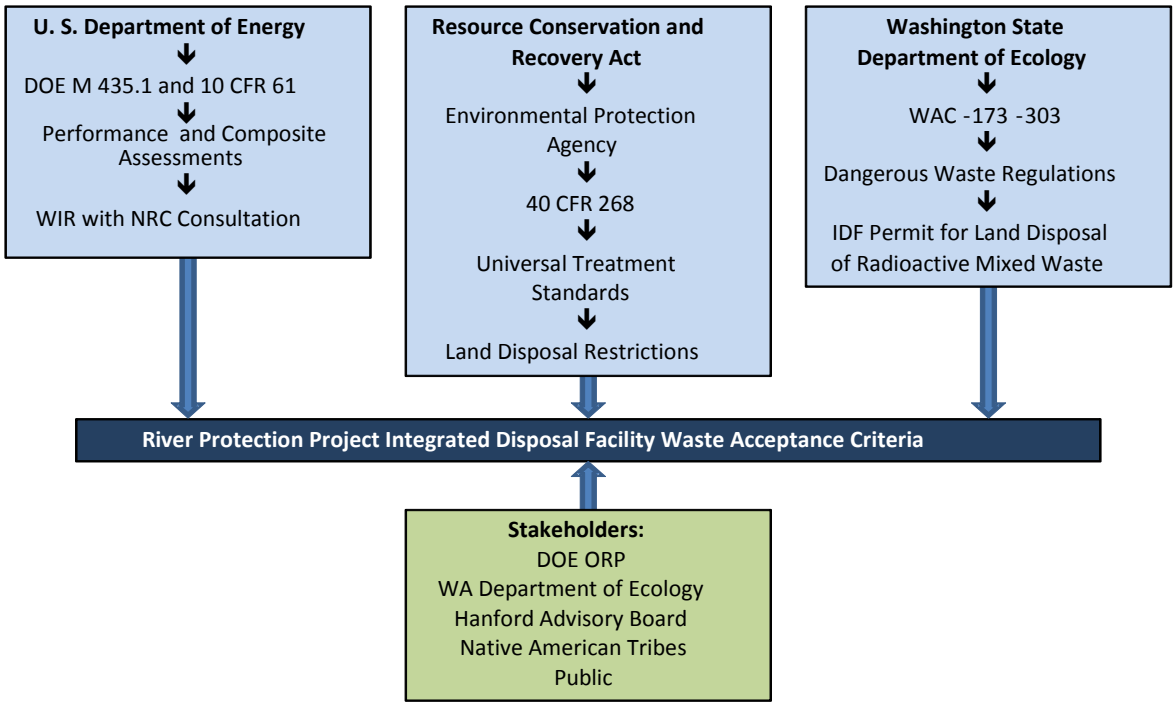

Figure 4-1. Regulators, Regulations and Stakeholders Relevant to IDF Waste Disposal

DOE Manual 435.1 Chapter IV describes the requirements for management of DOE LLW and Mixed Low Level Waste including requirements for treatment, storage, and disposal. The manual describes

waste determination procedures for identifying waste incidental to reprocessing (WIR) that can be managed as LLW. The manual delineates disposal facility design requirements and performance objectives to ensure radiation doses to the public are limited to 25 mrem/yr from all exposure pathways. DOE 435.1 requires a site-specific radiological PA be prepared and maintained, including calculations for a 1,000 year period after closure of potential doses to members of the public, to provide a reasonable expectation that the performance objectives will not be exceeded as a result of operation and closure of the facility. Performance assessments shall include a demonstration that projected releases of radionuclides to the environment shall be maintained as low as reasonably achievable (ALARA). For purposes of establishing limits on radionuclides that may be disposed of near-surface, the performance assessment shall include an assessment of impacts to water resources.

A PA for the ILAW Disposal Facility (later renamed the IDF) was approved in 2001.[137] After the PA was approved DOE issued a Disposal Authorization Statement that called for establishing waste acceptance criteria to provide specific radionuclide disposal limits, waste form restrictions, and descriptions of acceptable waste packages. The waste acceptance criteria were to be based on facility performance assessments, special analyses, and composite analyses as well as safety documentation and criticality considerations. The initial Waste Acceptance Criteria were developed and issued in 2002.[138] However, those criteria only addressed ILAW glass waste forms and included numerous requirements derived from WTP contract specifications that were not necessarily driven by performance objectives or the PA. An ILAW waste form would be considered "as good as glass" if it could meet all of the criteria established for the glass waste form. Alternatively, a non-glass waste form would be acceptable if it could be shown by the PA analyses to meet the performance objectives described in DOE Order 435.1

Waste acceptance criteria for the hazardous constituents in the ILAW waste form can be derived from the Washington State Dangerous Waste Regulations, WAC-173-303, including Washington State Department of Ecology's implementation of the Federal Land Disposal Restrictions found at 40 CFR 268 and WAC-173-303-140. Ultimately those requirements are incorporated in the waste acceptance criteria for the RCRA operable unit (IDF) and permit conditions for the facility.

The IDF portion of the Hanford Site RCRA permit does not identify waste acceptance criteria for Immobilized LAW waste forms other than ILAW glass and Demonstration Bulk Vitrification System (DBVS) waste. It does require the Permittee to submit a Permit modification request prior to first accepting ILAW to establish: 1) waste analysis requirements and waste acceptance criteria for each waste stream, 2) criteria and processes for demonstrating compliance with Land Disposal Restriction (LDR) treatment standards, and 3) any other sampling and analysis requirements necessary to ensure compliance with the Dangerous Waste Regulations.

For compliance with LDR, non-wastewaters are subject to the EPA High Level Vitrification (HLVIT) technology-based treatment standard. An alternative technology would require a Determination of Equivalent Treatment (DET) to be accepted in lieu of vitrification. For LAW streams that meet the criteria for wastewaters at a new point of generation, the applicable treatment standards would be re-evaluated and would include compliance with the UTS for toxic metals and underlying hazardous constituents and concentration-based limits for hazardous organics.

Finally, the waste form must meet minimum compressive strength criterion of 500 psi, as recommended in the Nuclear Regulatory Commission (NRC) Branch Technical Position on LLW forms.[139] This requirement is derived from an NRC Branch Technical Position on LLW forms discussed above which somewhat arbitrarily specifies 500 psi to preclude subsidence in the waste disposal. It is also noted that a monolithic waste form would reduce the impact to human health for the intruder scenario in the waste site

PA. While a monolith is desirable there are other means by which this requirement can be met, e.g. waste stabilization in HICs.

4.1 Performance Assessment Testing

4.1.1 *Durability Requirements*

For HLW, Waste Acceptance Product Specifications (WAPS) [140] and a Waste Compliance Plan (WCP) [141] were developed for the waste form to ensure the acceptance of the product to the federal geologic repository. Similar durability requirements were developed for LAW glass at Hanford, which are delineated in Specification 2 of the WTP contract.[142] The WAPS and extensive characterization of the borosilicate glass both before and after production began was required. In order to satisfy the WAPS and WCP product consistency requirement, a leach test was needed that could reliably and easily provide rapid confirmation of the consistency of the waste form being produced. So the PCT, now ASTM C1285, was developed.[†]

Lithium, sodium, and boron releases were monitored as nonradioactive indicator(s) in the waste form and in a standard glass of the maximum radionuclide release. A great deal of research had been performed [143,144,145,146,147,148,149,150,151] to demonstrate that in high level borosilicate waste glass, ^{99}Tc, present at ~4.1 x 10^{-4} wt. % in the waste form, was released at the same maximum normalized concentration as boron, lithium, and sodium. Technectium is the radionuclide released from HLW at a rate higher than all the other radionuclides. Therefore, for borosilicate glass waste forms, the leachates are routinely analyzed for boron, lithium, and sodium if these elements are present at > 1 mass % in the glass as an indicator of the maximum radionuclide release, i.e., the ^{99}Tc release, because these elements have been shown to leach congruently with B, Li, and Na.

While relating ^{99}Tc release to Na, Li, B release for a material that leaches congruently[‡] is an acceptable practice once the congruent relationship among these elements has been established, this has to be done for each phase present in a glass-ceramic or mineral waste form because each phase leaches at a different rate, i.e., the multiphase waste form leaches incongruently.[†] For multiphase materials like glass-ceramics and mineral waste forms, the most important elements to be analyzed in the leachate are those that represent the maximum dissolution of the radionuclides from the waste form. Elements that are not sequestered in precipitates that participate in surface alteration reactions and elements that are not solubility limited are good indicators of waste form durability. In the case of a multi-phase glass or mineral waste form, it may be important to analyze for elements from each significant phase present as these waste forms leach incongruently. Extensive testing [143-151] of any glass or glass ceramic waste form must be performed in order to determine what these elements are unless the radionuclide release (or surrogate radionuclide release) is measured which is what has been done in this study, i.e. either a Re analog of ^{99}Tc or ^{99}Tc release has been measured directly.

[†] C.M. Jantzen, N.E. Bibler, D.C. Beam, W.G. Ramsey, and B.J. Waters. "Nuclear Waste Product Consistency Test Method Version 5.0," U.S. DOE Report WSRC-TR-90-539, Rev. 2 (January 1992) now ASTM C1295, latest version.

[‡] Congruent dissolution of a waste form, like glass, is the dissolving of species in their stoichiometric amounts. For congruent dissolution, the rate of release of a radionuclide from the waste form is proportional to both the dissolution rate of the waste form and the relative abundance of the radionuclide in the waste form. Thus, for borosilicate glass, ^{99}Tc has been shown to be released at the same rate, congruently as Na, Li and B.

[†] Incongruent dissolution of a waste form means that some of the dissolving species are released preferentially compared to others. Incongruent dissolution is often diffusion-controlled and can be either surface reaction-limited under conditions of near saturation or mass transport-controlled. Preferential phase dissolution, ion-exchange reactions, grain-boundary dissolution, and dissolution-reaction product formation (surface crystallization and recrystallization) are among the more likely mechanism of incongruent dissolution, which will prevail in a complex polyphase ceramic waste form.

The use of the PCT test protocol for HLW vitrified waste [152] was applied at Hanford for testing the consistency of both the Hanford HLW vitrified waste and the immobilized LAW waste form.[142] The PCT is used to determine the waste form leaching and durability (granular and crushed monoliths) in conjunction with ANSI/ANS-16.1 for intact monoliths [153], and the PCT is used for determining waste form stability.[142] The Hanford contract [154] and the ILAW Product Compliance Plan specify the following:

> "The normalized mass loss of sodium, silicon, and boron shall be measured using a seven day product consistency test run at 90°C as defined in ASTM C1285. The test shall be conducted with a glass to water ratio of 1 gram of glass (-100 +200 mesh) per 10 milliliters of water. The normalized mass loss shall be less than 2.0 grams/m^2. Qualification testing shall include glass samples subjected to representative waste form cooling curves. The product consistency test shall be conducted on waste form samples that are statistically representative of the production glass."

In addition, the Hanford contract [154] requires durability testing for LAW glass by the Vapor Hydration Test (VHT) [155] as follows:

> "The glass corrosion rate shall be measured using at least a seven day vapor hydration test run at 200°C as defined in the DOE concurred upon ILAW Product Compliance Plan. The measured glass alteration rate shall be less than 50 grams/(m^2 day). Qualification testing shall include glass samples subjected to representative waste form cooling curves. The vapor hydration test shall be conducted on waste form samples that are representative of the production glass."

Because the VHT test interpretation for waste forms other than glass has not been investigated and the results of this test are used solely for engineering calculations of contaminant release [142]. the PCT durability test was used in this study as the screening test for the FBSR granular and monolith products.

4.1.2 *Durability Testing and Preliminary Risk Assessment*

All of the PCT testing on various FBSR LAW products is summarized in Table 3-2. The granular waste form must meet the Hanford performance standard of <2g/m^2 release during ASTM C1285 (PCT) testing. Since Re release, as a surrogate for ^{99}Tc, does not track Na release in the mineral product, it is the Re release that must meet the 2g/m^2 limit during PCT testing. The references cited in Table 3-2 confirm that the LAW FBSR releases are <2g/m^2 Re, and the radioactive test results given in References 3 and 4 and summarized in this report supports this conclusion for ^{99}Tc as well (see Sections 8.2.4 and 8.2.5).

In addition, SPFT testing was conducted on the 2001 FBSR AN-107 LAW products, and the results were used to perform a preliminary Risk Assessment (RA). In the preliminininary RA, the release of radionuclides ^{99}Tc and ^{129}I from the granular NAS waste forms was hypothesized to be limited by nosean solubility as the rhenium releases during durability testing tracked the sulfate releases.[61,105,106,107] The predicted performance of the granular NAS waste form was found to be comparable to the glass waste form in the initial supplemental LAW treatment technology risk assessment (Figure 4-2) [107].

Wastes intended for disposal in Hanford's IDF must meet requirements of DOE Order 435.1 and permit requirements established by Washington State Ecology as discussed in the previous section. The IDF waste acceptance criteria have not been established for waste disposal in the facility although there have been several draft Waste Acceptance Criteria (WAC) proposed. Initial draft waste acceptance criteria for a secondary waste form are based on the draft IDF waste acceptance criteria [138] and criteria related to free liquids, compliance with land disposal restrictions, compressive strength, and leachability.

For a FBSR waste form the following requirements would likely apply [156]:

- LDR: The waste form will meet the land disposal requirements in 40 CFR Part 268 by meeting the UTS in 40 CFR 268.48 via the TCLP test.
- Free Liquids: The waste form shall contain no detectable free liquids as defined in EPA SW-846 Method 9095 [157].
- Leachability Index (LI): The waste form shall have a sodium LI greater than 6.0 when tested in deionized water using the ANSI/ANS-16.1 method. The waste form shall have a rhenium or technetium LI greater than 9.0. These requirements are based on the 1991 NRC Technical Position on Waste Forms [139] and on early waste disposal RA and PA analyses.
- Compressive Strength: The compressive strength of the waste form shall be at least 3.54 E6 Pa (500 psi) when tested in accordance with ASTM C39/C39M (ASTM 2010c). This is based on the NRC's Technical Position on Waste Forms [139], which is more restrictive for cement-based waste forms.

Interestingly, in a 2010 NRC document, the NRC declares that the variance in sampling intervals in the ANS 16.1 method and the use of the average value from different intervals are not consistent with the diffusion-controlled mechanism that is used to calculate the leach index. Because of this, the document asserts that the leachability index does does not provide a reliable measure of the effective diffusion coefficient that is needed for performance modeling or any other characteristic of the material that is used in the test.[158] Therefore, the NRC prefers ASTM C1308 [159], which is essentially an ANSI 16.1 prototcol that standardizes the leaching intervals. Recently, the excel program, which accompanies ASTM C1308, for calculation of monolith diffusivity has been revised by Argonne National Laboratory (ANL).[160] The excel program, called REALM (REgression Analyses of Leaching Models) fits diffusivity equations and/or affinity release equations to waste form data sets from ASTM C1308 giving a partial mechanistic understanding to the test results.

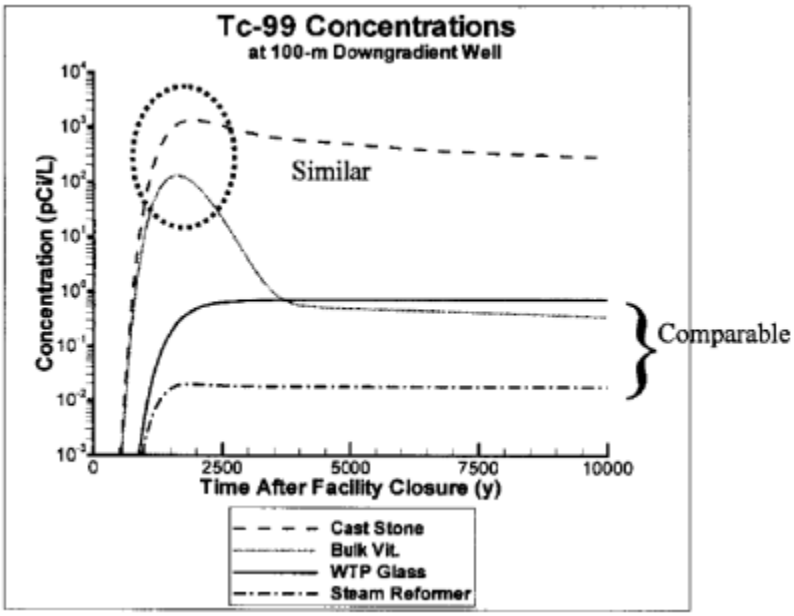

Figure 4-2. Comparison of Tc-99 concentration in a well 100 m downgradient of the IDF as a function of time from Mann et.al. (2003) RA.[107]

4.1.3 *Compressive Strength*

In the 1983 version (Revision 0) of 10 CFR 61.56(b)(1) regarding the stability of a waste form for shallow land burial, it is stated that "a structurally stable waste form will generally maintain its physical dimensions and form under expected disposal conditions (45 feet) such as weight of overburden and compaction equipment…". Assuming a cover material density of 120 lbs/ft^3, a minimum compressive strength criterion of 50 psi after curing for minimum of 28 days was established, although it was also stated that the waste forms should achieve the "maximum practical compressive strength" not just the "minimum acceptable compressive strength". Later, the burial depth was increased to 55 feet and the minimum compressive strength criterion was increased to 60 psi after curing for a minimum of 28 days.

In the early 1990's, the compressive strength criterion was re-evaluated. Because OPC mortars (cement, lime, silica sand and water) are capable of achieving compressive strengths of 5000-6000 psi, the minimum compressive strength for a waste form for shallow land burial was increased to 500 psi after curing for a minimum of 28 days. The rationale was that low-level radioactive waste material constituents are not capable of providing the physical and chemical functions of silica sand in a cement mortar and so a reasonable compressive strength was 1/10th that of a cement made with silica sand.[139]

Thus, to be accepted for near-surface disposal at Hanford, a waste form is required to meet this acceptance criterion for compressive strength of 500 psi. This requirement is derived from an NRC Branch Technical Position on LLW forms discussed above, which somewhat arbitrarily specifies 500 psi to preclude subsidence in the waste disposal. It is also noted that a monolithic waste form would reduce the impact to human health for the intruder scenario in the waste site PA. While a monolith is desirable there are other means by which this requirement can be met, e.g. waste stabilization in HICs.

The Hanford contract [154] for LAW specifies the following:

> *"The mean compressive strength of the waste form shall be determined by testing representative non-radioactive samples. The compressive strength shall be at least 3.45E6 Pa (500 psi) when tested in accordance with ASTM C39/C39M-99 [161] or an equivalent testing method"*

Monoliths were made and tested with the non-radioactive and radioactive BSR Rassat 168 tank LAW blend. No monoliths were made with the Hanford SX-105 or AN-103 non-radioactive or radioactive granular FBSR products produced in this study. The granular material was archived under the RCRA sample exclusion should funding become available for further monolith testing.

4.1.4 *Waste Loading*

For disposal of FBSR wastes at Hanford in Richland, WA, there is an additional specification that governs the waste loading for glass. Waste loading for Hanford LAW wastes are specified in terms of the amount of Na_2O from the waste that can be accommodated in the waste form. The most stringent of these criteria is for Envelope A waste. The specification (Section 2.2.2.2 of the Product Requirements) [154] states:

> "Waste Loading: The loading of waste sodium from Envelope A in the ILAW glass shall be greater than 14 weight percent based on Na_2O. The loading of waste sodium from Envelope B in the ILAW glass shall be greater than 3.0 weight percent based on Na_2O. The loading of waste sodium from Envelope C in the ILAW glass shall be greater than 10 weight percent based on Na_2O."

All of the Na_2O in the Hanford LAW granular FBSR products made during pilot scale testing in 2003-2004 [111,112] contained 20.87 wt% Na_2O. All of the Na_2O in the FBSR product is from the waste because the kaolin contains no sodium. If the FBSR granular product needs to be monolithed versus disposal in a HIC, it should not dilute the product Na_2O concentration to less than ~14 wt.% Na_2O so that the Na_2O content will be comparable to LAW Envelope A glass. Therefore, the FBSR loading in a monolith should be ~67 wt.% for Envelope A type wastes to be comparable to LAW glass. Table 4-1 summarizes the requirements that an FBSR granular or monolithic waste form would likely need to meet.

For a cementitious grout waste form, there is a PA requirement on nitrate/nitrite leaching that currently limits the grout waste loading.[156] There are also LDR limits for concentrations of hazardous organics from grout waste forms as well.[156 and 40 CFR 268] Nitrate/nitrite and solvents/organics get destroyed in the FBSR process so this requirement is always met for the FBSR waste form but the requirement is listed in Table 4-1 for completeness.

Table 4-1. Summary of Requirements for an FBSR LAW Waste Form

Test Criteria	Requirement for FBSR Granular Product in HIC	Requirement for FBSR Monolithic Product
Compressive Strength (psi)	≥500	
Crystalline Phases	Phase Identification	
PCT Re and/or ^{99}Tc (g/m^2)	< 2.0	
TCLP	< UTS	
Nitrate/nitrite leaching requirement for grout PA	N/A as nitrate/nitrite destroyed in processing	
Solvent/organic leaching requirement for LDR	N/A as solvents/organics destroyed in processing	
ANSI/ANS 16.1 or ASTM C1308 (LI after 90 days leaching)	N/A	^{99}Tc and/or Re ≥ 9 Na ≥ 6
FBSR (21 wt.% Na_2O from waste in granular product)*0.67 = 14 wt.% Na_2O in LAW Envelope A glass (wt.%)	N/A	67

N/A = not applicable

5.0 DOE-EM Waste Form Qualification (WFQ) Program Goals

The need for advanced waste forms and processes was discussed in the NRC report "Advice on the Department of Energy's Cleanup Technology Roadmap: Gaps and Bridges", Waste Processing gap number 5 (WP-5):

> *"The baseline tank waste vitrification process significantly increases the volume of high-level waste to be disposed".*

This report comments that waste forms that include little or no additives compared to glass should be investigated for Hanford and INL.

The current DOE site baseline technologies include: 1) vitrification of the HLW fractions of tank wastes at Hanford and Savannah River for disposal at a Federal repository; 2) vitrification of the LAW fraction at Hanford for disposal at the IDF; 3) cementation of the LAW fraction at Savannah River; 4) FBSR of the

tank waste at INL for disposal at the WIPP; 5) hot isostatic pressing of the calcined HLW at INL; and, 6) treatment and disposal of various secondary LLW at each site. These treatment options are reasonably proven technologies and those remaining technological gaps are being filled by site contracts. However, some of the disposal options are currently risky and may not be ideal. In addition there are likely more cost effective treatment/disposal options that should be considered to reduce risk and cost of tank cleanup in the U.S. This task explores one such option, FBSR, and develops the necessary technology to implement a promising waste form.

As discussed above, Fluidized Bed Steam Reforming is one of four immobilization technologies under consideration as part of the Supplemental Treatment Program for WTP Hanford LAW. It is anticipated that the FBSR product would reduce the treatment costs, processing time, and waste volumes at increased waste throughput for Hanford LAW compared to LAW vitrification or cementation. FBSR granular and monolithic waste forms have already been developed for several Hanford LAW waste streams (the Rassat 68 tank blend and AN-107) [60,61,105,106,107,111,115], and data has been generated on the granular waste form to demonstrate preliminary acceptance in the IDF [3,126,130,131,132]. See also Table 3-2 and the next section (Section 5.1) for the radioactive Hanford wastes chosen to be tested.

The EM-30 WP 5.2.1 test program objective is to reduce the risk associated with implementing the FBSR technology as a supplemental LAW treatment by addressing the remaining technical uncertainties, and, thereby, demonstrate acceptable performance for FBSR product after being disposed in a near-surface burial facility. Data and updated models are required to demonstrate the performance of the FBSR NAS waste form. The results from the updated models are required to support the schedule for the supplemental technology decision under the *Hanford Federal Facility Agreement and Consent Order (Tri-Party Agreement) Proposed Consent Decree and Tri-Party Agreement Modifications for Public Comment*. The tasks performed as part of this test program are designed to support the application of FBSR as a supplemental Hanford LAW treatment option. The current primary programmatic objective is to develop performance testing data on the geopolymer encapsulated FBSR waste forms. Data required for such an assessment includes, but is not limited to, determining an acceptable waste loading that provides the need performance while minimizing the volume of waste being produced and meeting the IDF product performance requirements of compressive strength and leach testing.

The test program includes the following activities designed to support the decision point to proceed with supplemental treatment of Hanford LAW:

1. Characterization of FBSR product from the HRI/TTT P1-B runs blended bed and fines products made from the Hanford Rassat 68 tank blend simulant.
2. Production of a similar Hanford Rassat simulant and radioactive LAW simulant from SRS LAW with added Tc, I, Cs, and Re. Process both materials in the SRNL BSR to produce NAS product.
3. Receipt, characterization, and performance of BSR processing on three Hanford LAW samples representing low anion, high anion, and high sulfur waste streams. As necessary, increase (spike) ^{99}Tc and ^{129}I levels in the NAS feed and thus in the product to support spectroscopic measurements, i.e. synchrotron x-ray absorption spectroscopy (XAS).
4. Determination of the speciation of ^{99}Tc and ^{129}I (or ^{127}I) and the distribution of ^{99}Tc and ^{129}I amongst the different mineral phases of the FBSR product.
5. Determination of a mass balance for ^{99}Tc and ^{129}I in the SRNL BSR system.
6. Assessment of whether the FBSR granular products and monolith products pass the TCLP.
7. Synthesis of phase pure minerals to determine the parameters for Item #15 in this list.
8. Determination of the fraction of minerals formed in the FBSR product through X-ray Diffraction (XRD) measurements.

9. Development of dissolution rate law parameters for each significant phase in the waste form. Use SPFT testing to isolate individual rate law parameters along with selected tests for multi-phase waste forms. Determine the thermodynamic parameters of key individual phases as well as the phases formed during reaction of FBSR materials with water.
10. Preparation of monolithic waste forms containing mineralized FBSR product.
11. XRD analysis of the monolithic waste forms.
12. Demonstration through SPFT experiments that the binder used for monolithic waste forms does not significantly impact the release rate or dissolution behavior.
13. Determination through ASTM C1308 type testing of the transport properties of the monolith waste forms.
14. Determination of the common ion effect of Al, Si, and nepheline saturated solutions on Re and Tc release from the FBSR product needed for source term model accounting.
15. Development and validation of a modified waste form release and radionuclide source term model for inclusion in the IDF performance assessment code. Additions to existing models needed include: a) the release rates for each phase, b) updated thermodynamic data for solid solution phases, c) common ion effect seen in preliminary experiments, d) transport properties measured in monolith samples, and e) ^{99}Tc and ^{129}I partitioning between phases in the waste form.

The required testing to meet these goals is given in Section 5.2 and summarized in Table 5-4. All of the items above are discussed in this document and in References 3, 4, 5 and 6 except items 9 and 15 which are reported elsewhere.[162]

5.1 Defining the Hanford Radioactive Wastes for FBSR Demonstrations

As part of the DOE-EM enhanced tank waste strategy at Hanford this multi-laboratory FBSR work scope was initiated under the DOE EM-31 TDD Program Task Plan WP-5.2.1-2010-001.[163 and Appendix A] The objective was to perform treatability studies in the SRNL BSR using three actual Hanford tank waste samples to demonstrate the range of Hanford LAW to be treated by FBSR (representing the middle 80% of the total LAW feeds based on anion content).

Prior to performing tests with actual Hanford LAW, a test with a radioactive SRS LAW that was compositionally adjusted to reflect the expected composition of a Hanford 68 tank blend, known as the Rassat simulant, was performed.[109] The Rassat 68 tank blend waste simulant was also tested in 2008 at TTT's ESTD Facility in Golden, CO and tested in 2004 at INL's SAIC-STAR's Facility in Idaho Falls (see Table 3-1 and Table 3-2). Testing in the SRNL BSR with the Rassat formulation (non-radioactive and radioactive) was designated as Module B testing and provided a "tie-back strategy" discussed in Section 5.3 and the earliest scientific data regarding the FBSR waste form leachability and the fate of ^{99}Tc in the FBSR mineral waste form.

Based on direction from DOE/ORP, three Hanford LAW samples were selected for steam reformer treatability testing in the SRNL BSR. A Data Quality Objectives (DQO) process was undertaken to ensure appropriate samples were selected.[164] The BSR campaigns with Hanford Tank SX-105 were designated Module C, campaigns with Hanford Tank AN-103 were designated Module D, and campaigns with a blend of AZ-101/AZ-102 were designated Module E (see Table 3-1).

The following considerations guided the development of Hanford LAW sample selection criteria:

- Because schedule considerations to obtain data from the treatability studies were critical, LAW samples were selected from the existing sample archives in Hanford's 222-S Laboratory.
- SRNL advised that two of the tests (Modules C & D) required approximately one liter of LAW solution at the target 5M sodium concentration. For the third sample, 1.5 to 2 liters would be required to facilitate inter-laboratory comparison of the diffusion (ASTM C1308 run at the same temperature and time intervals as ANSI/ANS 16.1 so the data are comparable) and PCT (ASTM C1285) test results.
- The samples were chosen to be representative of full-scale feed in respect to Na molarity (4-7 M Na, i.e., ≥100g Na).

WRPS identified thirty nine tank waste samples (supernatant or salt cake) as having sufficient sample material. Past experience suggested that sample handling in the hot cell environment and the amount of undissolvable solids in salt cake samples could result in losses on the order of 30%. This more conservative approach yielded a set of 25 samples (9 saltcakes and 15 supernates) as potential candidates for treatability testing.

Additional criteria were used in conjunction with the DQO process to select samples for treatability testing. The chosen criteria were as follows:

1. Scientists at SRNL and PNNL noted that certain anions (sulfate (SO_4^{2-}) chloride (Cl^-), fluoride (F^-), and phosphate (PO_4^{-3})) play an important role in determining which NAS mineral phases are formed. For example, sulfate and chloride are known to be bound in the sodalite cage structure and consequently do not readily leach out of the NAS matrix. Therefore, variations in the relative abundance of these anions and their impact on the quality of the NAS product formed needed to be examined.
2. Samples were chosen from tanks that had been evaluated for treatment by LAW vitrification, including radioactive, crucible-scale melts. This allowed direct performance comparisons for ^{99}Tc retention, durability, and leach resistance. Data from these samples would help to address regulatory/stakeholder concerns of glass-versus mineral waste forms.
3. Select samples that had been used in previous demonstrations of the FBSR process using simulants of that tank composition were chosen. This allowed a comparison of products made from the bench-scale reformer and the pilot-scale or engineering-scale FBSR and provided data to validate the use of simulants instead of real waste.
4. Both supernate and saltcake samples were represented to replicate the likely feed to any Supplemental Treatment technology.

To support the qualification of the FBSR process and waste form, the samples were representative of the majority of the LAW to be treated; the project determined the extreme ends of the compositional ranges do not need to be tested at this time. To evaluate samples relative to the 1st criterion above, anion concentrations in waste feed batches were taken from the Hanford Tank Waste Operations Simulator (HTWOS) output for the proposed ORP-11242, River Protection Project System Plan (System Plan 6) modeling case [165]. The LAW feed batches were sorted from low to high anion content for each of the four anions of interest with the lower 10th and upper 90th percentiles selected as the bounding limits. Conceptually, this target range represents the middle 80% of total LAW feed and eliminates the compositional outliers. Table 5-1 provides a summary of the target anion concentrations at the 10th and 90th percentiles.

Table 5-1. Molar Anion to Sodium Ratios in WTP Feed Batches

	SO_4^{-2}/Na Ratio [mol/mol]	Cl/Na Ratio [mol/mol]	F/Na ratio [mol/mol]	PO_4/Na Ratio [mol/mol]
High = 90th percentile	0.032	0.016	0.060	0.040
Low = 10th percentile	0.008	0.007	0.013	0.008

In reality, the waste samples available for FBSR mineralization and product testing were not likely to contain all of the anions of interest at high or low concentration ranges simultaneously. Further, SO_4^{-2} and Cl^- are considered more important since they are associated with specific mineral phases. Therefore, first it was identified which criteria were met for each sample, and then the sample selection was narrowed down for high or low anion content through a process of elimination with greater weight given to SO_4^{-2} and Cl^- ratios compared to F- and PO_4^{-3} ratios.

The results of the sample selection relative to this criterion are shown in Table 5-2.

Table 5-2. Molar Anion-to-Sodium Ratios for Hanford LAW Samples

	SO_4^{-2}/Na ratio [mol/mol]	Cl/Na Ratio [mol/mol]	F/Na Ratio [mol/mol]	PO_4/Na ratio [mol/mol]
SX-105	0.011	0.013	0.0007	0.016
AN-103	0.002	0.011	0.003	0.002
AZ-101/AZ-102 composite	0.033	0.006	0.015	0.005

Based on archive sample analysis data, the SX-105 sample (Module C) was initially selected as a high anion case. However, due to the heterogeneity of this salt cake sample, the final SO_4^{-2} concentration was much lower than anticipated and this sample only scored near the high end with respect to Cl^- concentration. The AN-103 sample (Module D) was selected to represent the low anion case particularly for SO_4^{-2} concentration. The third sample, a composite of AZ-101 and AZ-102 (Module E), was selected after the first two had been shipped to SRNL and to fulfill the criterion for high SO_4^{-2} concentration.

With respect to the 2nd criterion, prior vitrification tests with actual waste samples, only six tank waste samples have been tested with LAW vitrification: AW-101, AN-103, AN-102, AN-107, AZ-101, and AZ-102. Thus, results from the AN-103 and AZ-101/AZ-102 samples selected for FBSR treatability testing will be available for comparison to results for vitrified waste forms. The waste feed that is not represented is Envelope C, high organic complexant concentrate, but this Envelope represents less than 5% of the Hanford LAW to be treated on a metric tons of sodium (MT Na) basis.

The 3rd criterion was selection of samples that matched the composition of previous FBSR tests with simulants. Two Hanford LAW compositions have been used to produce a mineralized NAS waste form at the pilot-scale and engineering-scale (see Table 3-1 for the details regarding these campaigns and the references cited in Table 3-2):

- Simulated AN-107 (complexant tank)
  - in a 6-inch reformer (2001)
- Simulated Rassat 68-tank LAW composite

- in a 6-inch reformer (2004), and
- in a 15-inch reformer (2008-9).

By far the most material produced and tested is from the 2008-9 demonstration, which is represented by the SRS LAW chemically adjusted to match the Rassat 68 tank blend (Module B in Table 3-1). No compelling reason existed to attempt to replicate this composition with a sample of actual Hanford LAW and the SRS LAW sample from Tank 50 was used instead (see reference 3 for complete details).

Three Hanford Tank Samples were successfully identified and in conjunction with the two chemically adjusted SRS samples provided test samples for the FBSR program that largely spanned the target compositional ranges for the anions of interest.[166] The resulting data, summarized in this report, has expanded the body of knowledge on the FBSR product as a waste form for the immobilization of Hanford LAW.

5.2 Defining the Testing Program for Hanford FBSR Waste Forms

As part of the current DOE-EM enhanced tank waste strategy at Hanford this multi-laboratory FBSR work scope was initiated under the DOE EM-31 TDD Program Task Plan WP-5.2.1-2010-001.[163 and Appendix A] Treatability studies were performed in the SRNL BSR using the Tank 50 SRS LAW shimmed to represent the Hanford 68 Tank salt cake blend [109] and the three Hanford wastes. The Hanford LAW treated by BSR represented the middle 80% of the total LAW feeds based on anion content.

The data resulting from the demonstration test programs and data in previous publications and in this document are summarized in Table 5-4 and Appendix B. The shading in this table represents the required elements needed for a downselect of the FBSR technology and the rationale for this minimum suite of tests is given in Appendix C. All monolith activities are not required for the downselect and are indicated in Table 5-4 by italics. The data summarized in Table 5-4 will also be used to support the IDF performance assessment and decisions regarding deployment of a non-vitrification technology to immobilize LAW. A review was also produced [6] summarizing all previous and current leaching results and their impact on acceptance of the granular FBSR waste form in the IDF.

All of the data from the steam reformer treatability and waste form performance testing shown in Table 5-4 were not likely to be available in time to support the immobilization technology down select process. However, it was recognized that the greater the number of available data points, the broader the range of sample compositions tested, and the stronger the agreement with the results from prior testing with simulants would contribute to lower risk and greater confidence in the down select decision process. Therefore, a summary of the types of data to be collected from the five BSR tests is provided in Table 5-4. Data that are expected to be the minimum set of information needed for the down select were agreed to with the Supplemental Treatment Immobilization Technology Project and are indicated with shading (see also Appendix C). These are primarily data from Module B with SRS LAW and Modules C and D with Hanford LAW. The data from real waste samples will be evaluated in conjunction with data from prior tests with simulants.

A primary objective is to show that the results of these radioactive BSR tests correlate well with prior simulant work at the bench-scale, pilot-scale and engineering-scale, i.e., produce the same mineral phases and the same range of short-term PCT and other durability test results. If that is the case, that correlation will provide a basis for confidence that the prior FBSR tests with LAW simulants [108,122] are representative of FBSR process and product performance with actual wastes. This would enable the previous surrogate testing results to play a stronger role in informing the go / no-go down select

decisions. This would enable the critical decision process to proceed and support the Enhanced Waste Treatment Strategy for Hanford while reducing the need for additional hot testing.

The analytical methods and approaches are detailed in the Task Plans for each module and are given in References 3 and 4. The methods being used to generate the primary data to support the go / no-go decision in support of the down select process are summarized below from that plan.

With respect to Steam Reforming waste forms, granular product data rather than final monolith waste form data will be a primary input for the technology down select evaluation. This approach allows for direct comparisons of the performance with that of the granular product from prior simulant tests. The latter represents a larger data set. This approach also doesn't necessarily attribute any enhanced performance that is expected from the monolithic waste form. Monolithing the granular product will be necessary to satisfy the IDF requirements for compressive strength. A monolith form could improve the overall performance of the FBSR waste form since the binder matrix provides an additional diffusion barrier for water contacting the waste form. The monolith is also intentionally formulated to be similar in chemical composition to the mineral product so as to not degrade the performance of the FBSR granular product. The monolith binder could in fact impart buffering capacity to the infiltration water and thereby slow the dissolution rate of the primary waste form, i.e. known as the "common ion effect."

If it is determined that the FBSR process can reliably produce granular products from actual waste that exhibit a durability and leach resistance performance similar to those from previous tests with LAW simulants such as the performance described by McGrail [105] or Pierce [106], then there would be minimal risk in including FBSR in the down select process, and if selected, moving forward to develop a Conceptual Design for FBSR. Various studies have established that the NAS granular waste form performs as good as or better than LAW glass within limits of uncertainty. For example, Pierce [106] reported that LAW glass (LAW AN102) was dissolving approximately 11 times faster than an FBSR product (but cautioned that the uncertainty in the reactive surface area for the FBSR product complicated the interpretation of a direct comparison between the ^{99}Tc release rate from glass and the rate of Re release from the FBSR product). McGrail [105] concluded that fractional release rates from the FBSR granular waste form (based on rhenium as a surrogate for ^{99}Tc) calculated from PUF experiments with the FBSR granular product showed essentially identical performance with a reference LAW glass (LAWA44) tested under the same conditions. Should the granular product exhibit characteristics (similar mineralogy, similar short-term PCT response) that are consistent with the products studied by Pierce and McGrail, then this gives a high degree of confidence that the FBSR process can generate a granular product that can satisfy the performance requirements for the treatment of Hanford LAW.

The SRS LAW tests (Module B) provided the earliest scientific data regarding waste form leachability and the fate of ^{99}Tc in the mineral phase waste form followed by additional testing with actual Hanford LAW (Modules C,D,E). The test protocols shown in Table 5-3 were used to determine the key input data required to assess the long-term performance of the FBSR NAS waste form with the Subsurface Transport Over Reactive Multiphases (STORM) code. The SPFT test and the PUF test methods focus on different aspects of the mineral–water reaction. Linkages between the test methods, their principal function, and the data they provided for modeling are highlighted in Table 5-3. For additional details on the theory of each test method and the role these methods play in evaluating long-term durability of the FBSR NAS waste form in the disposal environment, the reader is encouraged to consult Appendix D in this document and Appendix D in Reference 6. Which of these characterization and durability tests were performed on which Hanford FBSR LAW samples (non-radioactive and radioactive) and which were considered critical inputs to FBSR WFQ are shown in Table 5-4 and discussed in Appendix C.

Table 5-3. Overview of Test Methods Discussed in this Report (see Appendix D for more detail)

Test Method	Temp. Range (°C)	Duration	Data Provided	Purpose
SPFT (ASTM C1662)	25-90°C	Weeks to months	Dissolution rate as a function of temperature, pH, and solution composition	Parameterization of kinetic rate law for glass dissolution
PUF	40-100°C	Months to years	Effluent chemical composition and dissolution rate as a function of temperature and flow rate, secondary phases, hydraulic property changes.	Highly accelerated test for waste form screening, secondary phases for STORM reaction network, validation of STORM code.
PCT-A or Short-Term PCT (ASTM C1285)	90°C	Week	Solution composition and dissolution rate at a fixed S/V ratio and temperature, secondary phases.	Screening test method to demonstrate the material or waste form has consistency.
PCT-B or Long-Term PCT (ASTM C1285)	90°C	Weeks to years.	Solution composition and dissolution rate at a fixed S/V ratio and temperature, and secondary phases equivalent to PUF testing.	Highly accelerated weathering test for waste form screening, secondary phases can be modeled in EQ3/EQ6 or Geochemist's Workbench.

The granular products from the treatability studies were subjected to the same regulatory and performance testing protocols as the non-radioactive tests. The test matrix is shown in Table 5-4 and the references for the testing and data are given in Table 5-5. The additional data from the study on the Hanford radioactive tank wastes (Modules C, D, and E in Table 3-2 in Reference 4) provided support to the previous testing with simulants and SRS Hanford LAW (Module B in Reference 3 and previous pilot scale test results summarized in Reference 6). All the data and resulting analyses from all the non-radioactive and radioactive testing will be used to minimize technical risk regarding waste form performance and to support critical decisions associated with enhanced tank waste strategy at Hanford for the deployment of the FBSR transformational technology.

In contrast to most waste form development programs where bench-scale research precedes pilot scale testing, the FBSR process has been run at the pilot and engineering scale (Table 3-1) with simulants but not at the bench-scale with either simulants or radioactive wastes. SRNL has successfully operated a BSR in the SRNL Shielded Cells Facility for the SRS Tank 48 wastes.[167,168] The BSR is a unique SRNL design and this radioactive capability does not exist elsewhere. SRNL also has unique expertise, analytical chemistry skills, and equipment for monolithing the granular FBSR product and measuring durability of waste forms (granular and monolithic). SRNL used two BSR's – one for non-radioactive testing and one for radioactive testing on the Hanford tank wastes and these will be described in Section 7.0.

Non-radioactive Re was added to the radioactive feed to determine the effectiveness of Re as a surrogate for ^{99}Tc during BSR processing. Data from the Rassat 68 tank farm blend (Module B) demonstrated that

Re and ^{99}Tc tracked each other in the off-gas and during subsequent durability measurement of the mineral product indicating that they substitute for each other atomically in the solid mineral product. Additional information regarding the mineral partitioning and how Re and ^{99}Tc responded to the REDOX in the BSR was determined from the Hanford tank waste radioactive testing (SX-105, AN-103, and AZ-101/AZ-102).

Table 5-4. Module B, C, D, and E ESTD and BSR Scale Tests (Shaded Elements Required for WFQ Downselect; see Appendices A, C and D)

Task	Module B	Module B (Rassat LAW)		Module C (SX-105)		Module D (AN-103)		Module E (AZ-101/102)	
	Hanford 68 Tank Salt Cake Blend [109]								
	ESTD Simulant	BSR Simulant	BSR Radioactive	BSR Simulant	BSR Radioactive	BSR Simulant	BSR Radioactive	BSR Simulant	BSR Radioactive
Mass Balance	&	●	●	●	●	●	●	○	○
Mineral Characterization (Granular)	●	●	●/▲	●	●/○	●	●/○	●	○/○
Tc & Re Speciation	■	■	■		■				○
Short-Term PCT (Granular) ASTM C1285	●	●	●	●	●	○	○	○	○
Long-Term PCT (Granular) ASTM C1285	●	●	●	●	●		○	○	○
TCLP (Granular)	●/▲	●/▲	●/▲	●	▲	●	▲	●	○
SPFT (ASTM 1662)	▲	▲	▲	▲	▲	○	○	○	○
PUF Testing	▲	▲	○	○	○	○	○	○	○
REDOX	●	●	●	●	●	●	●	●	○
Pure Phase Mineral Testing and Thermodynamic Constants	■ **Supplmentary Data for PA and Geochemical Modeling**								
Prepare Monoliths	●	●	●	○	○	○	○	○	○
Mineral Characterization (Monolith)	●	●	●/▲	○	○	○	○	○	○
Short-Term PCT (Monolith) ASTM C1285	●	●	●	○	○		○		○
Long-Term PCT (Monolith) ASTM C1285	●	●	●	○	○		○		○
Diffusion (Monolith) ASTM C1308/ANSI 16.1	●	●	○	○	○		○		○
SPFT/PUF Testing (Monolith)	▲/▲	▲/○	○/○	○/○	○/○		○/○		○/○
TCLP (Monolith)	●/▲	●/▲	●	○	○		○		○
Compressive Strength (Monolith)	●	●	●	○	○	○	○	○	○

Key [●] Completed at SRNL, [▲] Completed at PNNL, [■] Completed at ORNL and Univ. of Calif Davis, [&] Completed TTT, [○] Not Funded

Table 5-5. Bench-Scale Reformer (BSR) Tests Performed at SRNL for Hanford Wastes

BSR Module	Ref.	Test	Source of Radioactive Waste	Amount of Radioactive Product (g)	Amount of Non-Radioactive Product (g)
A	127	SRS WTP-SW	Shim of SRS DWPF melter recycle to resemble Hanford WTP- Secondary Waste	96	188
B	3	SRS-LAW	Shim of SRS LAW (Tank 50) to resemble Hanford LAW based upon Hanford 68 tank blend	640*	645
C	4	Hanford LAW Sample #1 (medium S, Cl, F, and P)	Hanford Tank 241 SX-105	317[f]	189
D		Hanford LAW Sample #2 (low S, Cl, F, and P)	Hanford Tank 241 AN-103	224	192
E		Hanford LAW Sample #3 (high Cr and high S)	Hanford Tank 241 Blend AZ-101/AZ-102	N/A	113

N/A – Testing not completed

* an additional 23.45g (~3.66%) was made at the desired REDOX with the enhanced ^{99}Tc spike and sent for XAS analyses and an additional 25.45g (3.98%) was made under more reducing conditions with the enhanced ^{99}Tc and sent for XAS analyses for comparison

f an additional 24.37 g (7.69%) was made at the desired REDOX with the enhanced ^{99}Tc spike and sent for XAS analyses.

During the radioactive Rassat 68 tank blend BSR campaigns (Module B), ~90% of the waste was processed with the ^{99}Tc and Re levels equivalent to the Rassat ESTD simulant processed by TTT, while the remaining ~10% of the waste (see Table 5-5 footnote for exact amounts) was doped with ^{99}Tc and Re at a minimum of 150 μg/g. This level was needed to detect these species during follow on X-ray Absorption Fine Structure (XAFS) analyses to determine the oxidation state and local bonding of the ^{99}Tc and Re in the mineral waste form. The 10% portion of the feed was processed at the end of the BSR campaigns, after the off-gas condensate was sampled and lines were flushed to ensure that the mass balance and leaching tests were not compromised by the elevated concentrations required by the XAFS.

During the Hanford radioactive BSR SX-105 (Module C) campaign, ~93% of the waste was processed with the Tc, Re, and I levels equivalent to the Rassat ESTD simulant processed by TTT, while the remaining ~7% (see Table 5-5 footnote for exact amounts) of the waste was doped with ^{99}Tc and Re at a minimum of 150 μg/g. As with the Rassat blend, the remaining ~7% of the feed was processed at the end of the BSR campaigns, after the off-gas condensate was sampled and lines were flushed.

5.3 Defining the "Tie-Back" Strategy

Data and updated models are required to demonstrate and confirm the performance of the FBSR NAS waste form. To help assess the suitability and effectiveness of the FBSR process for the treatment of Hanford LAW, a series of treatability studies were conducted at SRNL using a BSR test unit. Radioactive and non-radioactive BSR's were available at the SRNL from several Tank 48 radioactive and non-radioactive demonstrations. These BSR's were modified and used to treat actual radioactive LAW from SRS and Hanford to confirm the findings of the non-radioactive FBSR pilot-scale tests performed in 2001, 2004, and the FBSR engineering-scale tests performed in 2008. Radioactive testing of LAW with

the BSR commenced using SRS Tank 50 LAW chemically shimmed to look like Hanford's blended LAW known as the Rassat simulant (68 tank blend, 109) as this simulant composition had been tested in both the non-radioactive pilot scale FBSR at the SAIC-STAR facility in Idaho Falls, ID and in the TTT ESTD. This provided a "tie back" between radioactive BSR testing and non-radioactive BSR, the 2002 TTT/HRI pilot scale, the 2004 INL SAIC-STAR pilot scale, the TTT/HRI 2008 engineering scale testing,[118] and the Hanford RA performed on the 2001 pilot scale FBSR product.[107] See Figure 5-1 for a comparison of all the scale FBSR's that produced FBSR waste forms. Radioactive BSR testing also raised the TRL level of the FBSR technology from 4 to 6 which is the TRL required for a technology to enter design.

During Tank 48 LAW testing at SRNL, the BSR unit was determined to produce FBSR products with the same mineralogy and off-gases as the products produced by larger scale FBSR units [167]. This Hanford study used the first stage of the BSR unit but did not use the CRR, which was available, since organics were not in the feeds tested. The CRR converts off-gas hydrogen and CO to steam and CO_2. Since neither the SRS Tank 50 waste nor the Hanford's LAW wastes contained Hg, a Granular Activated Carbon (GAC) bed? was not used either.

The "tie-back" strategy, i.e. demonstrating the similarity of the radioactive mineral products and their durability to the non-radioactive tests, allows one to determine the suitability of the FBSR waste form for disposal at Hanford based on the 2003 RA of Supplemental Treatment Waste Forms. Detailed discussion of the preliminary RA results are included in Mann et.al.[107]

Principal contaminants of concern contained in the LAW stream that are expected to impact disposal are ^{99}Tc, ^{129}I, U, Cr, and nitrate/nitrite.[107] The mineral waste form volatilizes nitrates as N_2 and is primarily composed of nepheline (ideally $NaAlSiO_4$) and the sodalite family of minerals (ideally $Na_8[AlSiO_4]_6(Cl)_2$) and nosean (ideally $Na_8[AlSiO_4]_6SO_4$) as discussed in Section 2.2. During preliminary performance testing, the release of radionuclides ^{99}Tc and ^{129}I from granular Na-Al-Si (NAS) mineral waste forms was hypothesized to be limited by nosean solubility as the Re releases during durability testing tracked the sulfate releases [61,105,107]. The predicted performance of the NAS waste form (granular form) was found to be equivalent to glass waste form in the initial supplemental LAW treatment technology RA [107]. The granular product can be macro-encapsulated to meet transportation and disposal requirements discussed in Section 4.0 but this is not necessary to meet performance requirements, i.e. the granular product meets the performance requirements regarding durability and so disposal can be in a HIC.

The Hanford waste feed samples on which BSR tests were conducted are listed in Table 5-5. The first Hanford waste treated was a radioactive DWPF melter off-gas condensate shimmed to resemble a WTP-SW melter off-gas condensate. This treatability study, known as Module A, was not part of the DOE-EM FBSR waste qualification program. The data from Module A will likely be informative but is not expected to be directly applicable. Therefore, it will supplement the LAW immobilization down select process but is not expected to provide go/no-go information relative to applicability of FBSR to Hanford LAW. Details of the Module A tests and test results are given in Reference 127 and will not be discussed further in this document.

Module B with actual SRS LAW is intended to assess the performance of the FBSR process and waste form in the treatment of Hanford LAW. This test is important because the actual SRS LAW was chemically adjusted to represent a 68 tank blend of Hanford LAW.[109] Cumulatively the 68 single-shell tanks surveyed by Rassat, et. al [109] contain over 20 million gallons of saltcake, approximately 85 percent of the total saltcake inventory in all the single-shell and double-shell tanks.[169] This test also provides a tie back to the 2008 engineering-scale FBSR test, which used a simulant representing the same 68 tank blend [122] and to the 2004 pilot-scale testing at the SAIC-STAR facility [108]. The mineralized

product from the engineering test was further used in the monolith binder development and testing program that was initiated in the 2008-2009 time-frame and then the Module B FBSR products were made into the same type of monolith with the same starting materials and compared (see Table 5-4)

Thus, the early data from the SRS LAW (Module B) treatability study provides an important correlation using actual radionuclides to previous tests using surrogates at the bench and engineering-scales that produced a mineralized product as well as the monolith testing using the mineralized product (Table 5-4 and Table 5-5). Building correlations between work with radioactive samples and simulants is critical to being able to conduct future relevant simulant tests, which are more cost effective and environmentally sensitive than tests with radioactive wastes. These correlations also facilitate linking back to the performance comparisons between glass and FBSR mineral waste forms and the 2003 RA that has already been performed for the FBSR waste form [6,61,105,106,107]. These correlations will be discussed in the pertinent waste form performance testing sections of this document (Section 8.2). More complete details of the Module B tests and test results are given in reference 3.

Thus, the availability of data from the SRS LAW test provided in this study (Module B – the Rassat recipie), and comparisons to the 2004 SAIC/STAR facility pilot-scale and the 2008 HRI engineering-scale facility test results will provide an important correlation using actual radionuclides to the previous pilot- and engineering-scale tests that used surrogates. Specifically the following correlations can be derived since all the BSR, pilot-scale, and engineering-scale tests ran the Rassat simulant and the radioactive SRS LAW was shimmed to be like the Rassat simulant:

- Correlate radioactive bench-scale reformer to 15” HRI/TTT engineering-scale reformer tests (Figure 5-1, Tie back #1)
- Correlate radioactive bench-scale reformer to non-radioactive bench-scale reformer tests (Figure 5-1, Tie back #2)
- Correlate non-radioactive bench-scale reformer to 15” HRI/TTT engineering-scale reformer tests (Figure 5-1, Tie back #3)
- Correlate the non-radioactive 15” HRI/TTT engineering-scale reformer to the 6” SAIC-STAR facility engineering-scale reformer tests at INL (Figure 5-1, Tie back #4)
- Correlate radioactive bench scale reformer for Module C and D to Module B tests
- Correlate radioactive bench scale reformer to non-radioactive bench scale reformer tests for Modules C and D
- Correlate non-radioactive bench scale reformer with Module C and D to Module B tests

For this reason over 600 grams of non-radioactive and over 600 grams of radioactive Module B SRS Tank 50 LAW material was made in the SRNL non-radioactive and radioactive BSR’s in order to facilitate all the testing needed for the tie-back strategy (see Table 5-5).

Modules C, D, & E treatability studies were tests with the three actual Hanford LAW samples, of which only the first two were completed. These treatability tests were intended to assess the performance of the FBSR process and waste form when treating a range of actual Hanford LAW compositions. The waste samples to be used in the testing were selected to represent >80% of the compositional range of interest across the spectrum of Hanford tank wastes.[164,170] Collectively, these samples reflect most of the Hanford LAW that will require immobilization. Thus the early data from these BSR tests are important to establish confidence that the FBSR process, the resulting mineralized products, and subsequent monoliths produced using such wastes confirm results from prior surrogate testing. More complete details of the Module C, D, and E tests and results are given in Reference 4.

The importance of the BSR Hanford radioactive modules C, D, and E are how well they compare to the radioactive BSR Module B made with radioactive SRS LAW. The tie back of radioactive modules C, D and E tonon-radioactive and radioactive Module B provides a tie back to the 2008 ESTD simulant FBSR tests at HRI by TTT and the 2004 pilot-scale simulant FBSR tests at SAIC-STAR (see Figure 5-1).

Figure 5-1. Tie-back strategy between engineering scale non-radioactive pilot testing (top row) and BSR non-radioactive and radioactive testing (bottom row).

Notes: In order of importance, tie-back #1 is between the radioactive BSR run with the Tank 50 waste shimmed to be like the Rassat Blend (this study) and the non-radioactive engineering scale Rassat Blend tested in 2008. Tie-back #2 is between the non-radioactive BSR testing with Rassat Blend simulant and the radioactive BSR testing with the Tank 50 waste shimmed to be like the Rassat Blend. Tie-back #3 is between the non-radioactive BSR and the non-radioactive pilot testing with the Rassat Blend simulant. Tie-back #4 is between the pilot scale testing performed at SAIC-STAR in 2004 and the pilot scale testing performed at HRI in 2008 with the Rassat Blend simulant. Note that the radioactive BSR controllers and data acquisition are in a radioactive hood and not in the shielded cells (bottom right photo).

6.0 FBSR: Engineering, Pilot-Scale, and BSR Process Control

FBSR Process Control includes the following:

(1) the proper additives to produce the desired minerals,
(2) operating in a wide REDOX range to drive various species into insoluble mineral phases,
(3) reducing the amount of unreacted coal in the product,
(a) ensuring acceptable REDOX measurement results,
(b) maintaining a reducing enough atmosphere to ensure complete denitration of the feed,
(4) IOC control for denitration and chromium stabilization as insoluble Cr^{3+},
(5) controlling temperature to enable the correct mineralization reactions to occur, and
(6) controlling particle size control to maintain a sustainable bed in the DMR for engineering scale demonstrations/operations.

A process control strategy for the FBSR mineralizing process was developed by SRNL in 2004 and is based on composition control in the NAS oxide system (see discussion in Sections 6.2 and 8.2.8). The process control strategy is known as MINCALC™ and has been used to control the SAIC-STAR campaigns in 2004, the TTT/HRI ESTD campaigns in 2008 and the BSR campaigns (2004 and 2010-2011). Control of coal content based on nitrate and nitrite in the feed has also been a part of MINCALC™ since 2004 and control of the IOC was added in 2013 as a result of the testing described in Reference 4 and in Section 6.4. A description of these pilot and engineering-scale demonstrations is given in Section 3.3. A description of the DOE-EM WFQ bench-scale demonstrations is given in Section 8.0.

6.1 Mineralizing Reactions at the Nano-scale

In both the ESTD and the BSR, the non-volatile constituents in the waste feed are converted into highly leach resistant mineral forms by reaction with the aluminosilicate clay additive. The mineral species formed are principally alkali aluminosilicates, also referred to as feldspathoid mineral species. These minerals also incorporate other ions elsewhere in their molecular structures. Examples of the waste plus clay reactions that form these minerals (nepheline, nosean, and sodalite) are shown below written with NaOH in the waste reacting with clay:

Equation 1

$$\underbrace{2NaOH}_{waste} + \underbrace{Al_2O_3 \bullet 2SiO_2}_{kaolin\ clay\ additive} \rightarrow 2\ \underbrace{NaAlSiO_4}_{Nepheline\ product} + H_2O$$

Equation 2

$$\underbrace{8NaOH + SO_4}_{waste} + \underbrace{3(Al_2O_3 \bullet 2SiO_2)}_{kaolin\ clay\ additive} \rightarrow \underbrace{Na_6Al_6Si_6O_{24}(Na_2SO_4)}_{Nosean\ product} + 3H_2O + 2OH^-$$

Equation 3

$$\underbrace{8NaOH + 2Cl}_{waste} + \underbrace{3(Al_2O_3 \bullet 2SiO_2)}_{kaolin\ clay\ additive} \rightarrow \underbrace{Na_6Al_6Si_6O_{24}(2NaCl)}_{Sodalite\ product} + 3H_2O + 2OH^-$$

Equation 4

$$\underbrace{8NaOH + 2ReO_4^-}_{waste} + \underbrace{3(Al_2O_3 \bullet 2SiO_2)}_{kaolin\ clay\ additive} \rightarrow \underbrace{Na_6Al_6Si_6O_{24}(2NaReO_4)}_{Sodalite\ product} + 3H_2O + 2OH^-$$

Equation 5

$$\underbrace{6NaAlSiO_4}_{\text{nepheline product}} + \underbrace{2NaReO_4}_{\text{waste}} \rightarrow \underbrace{Na_6Al_6Si_6O_{24}(2NaReO_4)}_{\text{Sodalite}}$$

Equations 1 through 4 could also have been written with $NaNO_3$ in the LAW as the reactant and N_2 as one of the gaseous products. The cations in the salt waste; Na, Cs, Tc, etc, and other species such as Cl, F, I, and SO_4^{-2} are immediately available to react with the added clay as the clay dehydrates at the DMR temperatures and the aluminum atoms in the clay become charge imbalanced as the stabilizing OH^- atoms are lost (Figure 6-1). Once the hydroxides are lost, the clay becomes amorphous (loses its crystalline structure) and very reactive at the FBSR temperatures. This amorphous clay is called meta-kaolin. Stable crystalline clays (kaolin) are known [171] to become reactive amorphous clays (meta-kaolin) when they lose their hydroxyl groups above 550°C. The cations and other species in the waste react with the reactive amorphous meta-kaolin to form new stable crystalline mineral structures allowing formation and templating of the aluminosilicate structure at the nanoscale at moderate temperatures (see Figure 6-1). In addition, nepheline, once formed by reaction of the waste and clay can further react with the waste (Equation 5) to form sodalite(s) as shown in the last reaction above as sodalite is six nepheline unit cells that form the aluminosilicate cage structure that surrounds and is bound to $2NaReO_4$.

The stable nepheline and sodalite crystalline structures leave the process as a granular solid product. Kaolin clay has been found to template the feldspathoid group of minerals (nepheline, sodalites, nosean, etc.) for LAW and the illite clays have been found to template the dehydroxylated micas as radionuclide hosts for rare earth species.[58] The IOC stabilizes many of the RCRA hazardous species present in a waste in durable spinel phases, i.e. Cr^{3+}, Ni^{2+}, Pb^{2+} iron oxide minerals, see Section 2.2.5.

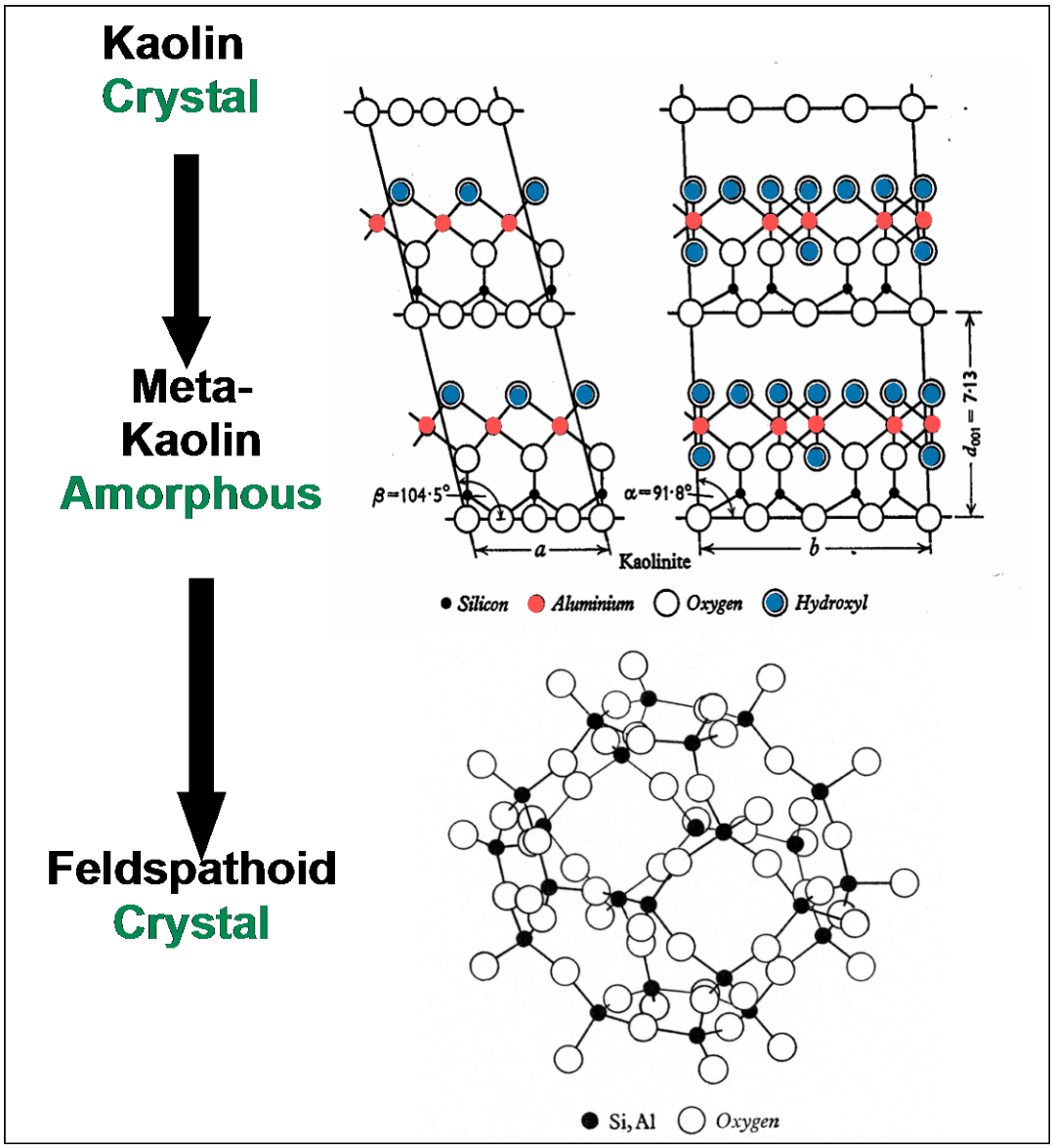

Figure 6-1. Kaolin transformation to meta-kaolin to Feldspathoid (Sodalite) Crystal by loss of hydroxyls and alkali activation as a function of increasing temperature (after reference 171).

6.2 Control of Mineralization

The MINCALC™ process control strategy for the FBSR mineralizing process was developed by SRNL in 2004 for the INL SAIC-STAR FBSR campaigns with SBW and LAW. MINCALC™ is based on composition control in the NAS oxide system (Figure 6-2). MINCALC™ controls the simulant or radioactive LAW FBSR product in the region of nepheline/sodalite formation. In Figure 6-2, the region where the blue rectangle for AN-107 lays is the composition of stoichiometric nepheline ($NaAlSiO_4$), i.e. the composition needed to form nepheline and the sodalites. The large shaded region in Figure 6-2 is where nepheline ($NaAlSiO_4$) melts incongruently to a liquid of a different composition, i.e. the melt has a different composition from stoichiometric nepheline. Because of the reactivity of the amorphous clay and the presence of

hydrothermal conditions, i.e. steam, the FBSR minerals form from solid state reaction and no melting occurs.

MINCALC™ converts the molar compostions of the waste to element weight percent on a wet basis and then to oxide weight percent on a dry calcine basis. The Al_2O_3 and SiO_2 from the clay additive and the $(Na,K,Cs)_2O$ and Al_2O_3 contributions from the waste are weighted by the desired waste loading to retain the maximum Na_2O and SO_4^{-2} content of the waste (100-waste loading), respectively, until the tie-line between the clay composition on the SiO_2-Al_2O_3 binary and the waste composition on $(Na,K,Cs)_2O$-Al_2O_3 binary pass through the AN-107 region of Figure 6-2.

The nepheline composition, based on the AN-107 FBSR pilot scale tests in 2001, was chosen as the most favorable base FBSR composition due to the extensive testing performed on the AN-107 products. The AN-107 FBSR product performed well in PCT testing [60,115], SPFT testing [6,61], and the preliminary RA[107]. All subsequent FBSR testing (engineering, pilot and bench-scale) has used MINCALC™ to control the FBSR product to the same AN-107 chemistry in the NAS ternary system shown in Figure 6-2 (~41 wt% SiO_2, 24 wt% $\Sigma(Na,K,Rb,Cs)_2O$, 35 wt% Al_2O_3) by adjusting the composition of the clay added (see Figure 6-2 and Table 6-1). The AN-107 composition used 1041grams of clay per liter of LAW (Table 6-1).

MINCALC™ was used during the 2004 INL pilot scale tests [108], the 2008 TTT/HRI ESTD campaigns [122], and the INL SBW BSR campaigns in 2004 [172] and the BSR treatabilities studies discussed in this report and discussed in References 3, 4, and 5. Most of the pilot scale campaigns were run with excess clay and hence excess Al_2O_3[ξ] and SiO_2 appear in the species predictions (Table 6-1) and during the characterization of the products. During the 2001 TTT pilot scale testing of AN-107 [60,115], MINCALC™ had not yet been developed and that campaign ran with only a little excess clay. The INL pilot scale tests with the Rassat simulant (Table 6-1) ran with 670 grams of clay per liter of LAW, which produced ~10% excess clay content. The ESTD initial MINCALC™ target was projected based on 716 grams of clay per liter of solution (Table 6-1) to be similar to the INL pilot scale campaigns. However, the amount of clay was reduced to 675 grams of clay per liter of LAW and finally 640 grams of clay per liter of LAW (see Table 8-7). The 640 grams of clay per liter of LAW proved to make successful product at the same composition of the AN-107 but without all the excess kaolin clay. This and process improvements to the ESTD facility help maximize reactivity between the clay and LAW so that unreacted clay cores were no longer observed in the product granules (compare Figure 2-3 to Figure 7-2) to maximize Na_2O loading. Therefore, the BSR testing in this study and References 3, 4, and 5 demonstrated that excess clay was not needed: the NAS mineral assemblages are flexible enough to accommodate small concentration changes in the Al_2O_3/SiO_2 ratio (Table 6-1). This helps maximize Na_2O waste loadings.

MINCALC™ also calculates the theoretical weight percent of each of the mineral phases that will be formed. The sum of all predicted phases has not been normalized to 100%, so sums shown at the bottom of Table 6-1 do not add completely to 100% but show how accurate MINCALC™ is in accounting for the major mineral species. For most LAW concentrations, the major mineral species are primarily nepheline (60-80 wt.%) and the sulfate sodalite known as nosean (6-12 wt.%). See the shaded values in Table 6-1.

[ξ] Al_2O_3 is also used as a startup bed during the engineering and pilot scale demonstrations. An Al_2O_3 startup bed was not used during the BSR treatability testing.

If more anions such as Cl, F, and I are present or oxyanions such as TcO_4^- or ReO_4^-, more sodalite forms. If more SO_4^{-2} is present the sodalite structured phase, nosean forms. If anions, SO_4^{-2}, Re and Tc are low, then less sodalite and nosean forms and more nepheline forms. Cs and K can be accommodated in either nepheline or sodalite where they substitute for Na. Theoretically[ξ], a pure sodium chloride waste stream would make a chloride sodalite and could accommodate 12.06 wt.% NaCl or 7.32 wt.% Cl. A pure iodide waste stream in sodalite could accommodate 22.03 wt.% I and a pure fluoride sodalite could accommodate 4.06 wt.% F. A pure sodium sulfate waste stream could accommodate up to 9.65 wt.% SO_4^{-2} or 14.28 wt.% as Na_2SO_4 in nosean. Likewise the Re and Tc sodalites can accommodate 13.31 wt.% Re or 8.00 wt.% Tc-99, respectively. In the simulant Module E studies discussed in Sections 5.1 and 5.2, 3.70 wt.% SO_4^{-2} was accommodated in the nosean or ~40 wt. % of the theoretical SO_4^{-2} that could have been accommodated in the absence of significant quantities of other anions or oxyanions.

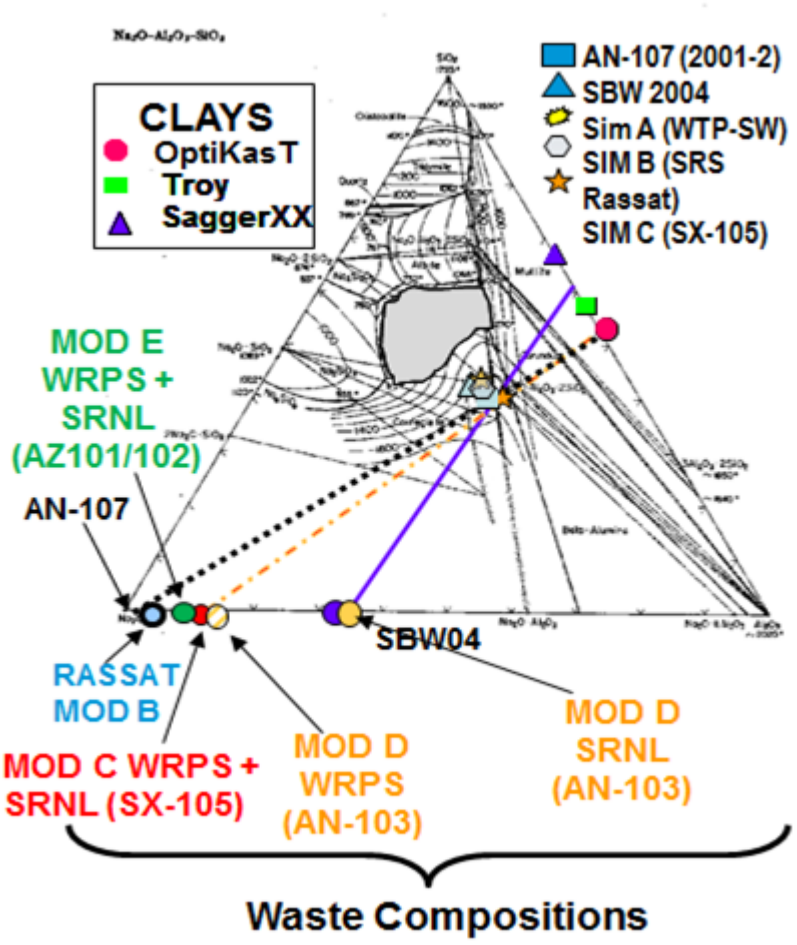

Figure 6-2. Na_2O-Al_2O_3-SiO_2 (NAS) Ternary

Note: Tie lines between waste compositions (triangle base) and clay compositions (triangle right side) give the relative amounts of waste vs. clay that should be used. Mincalc™ calculates these values on a wet clay basis and inputs include the clay compositions (sometimes a mixture of two clays is used), the clay moisture content, and the waste composition on a wet basis.

ξ Calculation is performed as follows: (2NaCl molecular wt./molecular wt. of chloride sodalite), i.e. (58.44*2/969.21)*100=12.06% NaCl, as there are 2NaCl's in sodalite (see atomic formula given in Table 6-1) or (35.45*2/969.21)*100= 7.3 wt.% Cl as there are 2Cl's in each sodalite.

Table 6-1. Mineral Speciation for Non-Radioactive Pilot and Engineering Scale LAW (AN-107 and Rassat Simulant) Predicted from MINCALC™-Version 3

Mineral Component	Chemical Component	Non-radioactive		
		AN-107 Simulant* (wt.%)	Rassat Simulant from INL Testing (wt.%)	Rassat Simulant from ESTD Testing (wt.%)
Na Nepheline	$Na_2Al_2Si_2O_8$	75.43	67.58	63.75
K Nepheline	$K_{0.5}Na_{1.5}Al_2Si_2O_8$ or $K_2Na_6Al_8Si_8O_{32}$	4.73	2.43	2.38
Cl Sodalite	$Na_8Al_6Si_6O_{24}(Cl_2)$	1.58	2.83	2.69
F Sodalite	$Na_8Al_6Si_6O_{24}(F_2)$	4.96	1.97	1.87
I Sodalite	$Na_8Al_6Si_6O_{24}(I_2)$	0.73	1.31	1.25
Nosean	$Na_8Al_6Si_6O_{24}(SO_4)$	6.48	11.93	11.33
Re Sodalite	$Na_8Al_6Si_6O_{24}(ReO_4)_2$	2.17	0.04	0.15
Tc Sodalite	$Na_8Al_6Si_6O_{24}(TcO_4)_2$	---	---	---
Free Silica	SiO_2	0.81	5.32	7.30
Free Alumina	Al_2O_3	0.21	3.49	5.15
	SUM	97.10	96.89	95.85
	$g_{(wet\ clay)}/L_{LAW}$	1041	679	716
	Type of Clay	Snobrite™	OptiKasT™	
	Na Molarity	8.30	5.02	5.02
AN-107 Target	**Normalized Wt% In Ternary Phase Diagram – Figure 6-2**			
41	SiO_2	41.25	42.96	43.35
24	$(Na,K,Li,Cs,Rb)O_2$	23.10	21.64	20.96
35	Al_2O_3	35.65	35.39	35.69

*see Table 3-2 and References 60,61,105,106,107,115

6.3 Control of Unreacted Coal in the Product

Carbon is added to the DMR in both the FBSR and the BSR in the form of coal. The carbon performs three important functions in the DMR. First, the carbon reacts with the steam to create the water gas shift reactions (see Section 3.2) and the highly reducing atmosphere that are essential to the pyrolysis reactions. Secondly, the carbon creates heat as it is oxidized and so the FBSR process is auto-catalytically heated. Thirdly, the carbon in balance with air bled in to create steam from excess H_2 sets up the proper atmosphere (-log fO_2 ~18 to 22 atm) in the DMR to attain the desired REDOX of various species, such as Re, ^{99}Tc, I, and Cr, so that these species can form the desired mineral phases.

Some unreacted coal remains in the FBSR and BSR products. It is unlikely that the coal ash formed from the portion of the coal that does react during auto-thermal heating remains as residual alumino-silicate ash. There is evidence from SEM that there is no separate aluminosilicate phase, so it is likely that the sodium from the waste is reacting with the coal ash to form additional feldspathoid (nepheline and sodalite) minerals. There is always some residual coal in the product and this can be minimized during processing.

Based on past SRNL studies, if greater than 10 wt.% of the product is unreacted coal, then the $Fe^{+2}/\Sigma Fe$ measurement becomes inaccurate leaving the species distribution in the product uncertain. The unreacted coal in the product is measured based on the weight loss change after the residual coal in the product is burned off in a furnace (i.e. Loss-on-Ignition or LOI measurement). The goal is to keep the residual coal as low as possible by reacting it in the DMR. For the ESTD, this is accomplished by the residence time in the bed. In the BSR, it is accomplished after feeding is completed and before furnace shutdown. The LOI was controlled by reacting away the excess coal in the reformer until the cumulative value of CO_2/ml fed to the DMR reached a predetermined endpoint. This ensured the product did not contain excessive unreacted coal. This is discussed in more detail in References 3 and 4.

6.4 Control of Denitration and Chromium Sequestration

The desired 100% denitration of the product is essentially achieved within the control boundaries required to make a good mineral product so no other controls are required but an IOC is often added as a denitration catalyst.

The IOC is also used to provide a reduced iron spinel that can sequester chromium as the insoluble Cr^{3+}. Using the data in References 3 and 4 for the TCLP response of Cr from the simulant and radioactive Modules B, C, and D, one can derive a dependency of Cr leaching on the product REDOX. For all of the BSR campaigns and data in Table 6-2, the IOC catalyst was not added to sequester chromium into the iron oxide mineral structure as $FeCr_2O_4$. Therefore, it is likely that the reducing REDOX of the BSR forced the chromium into a Cr_2O_3 structure instead. This Cr leaching versus REDOX dependency is shown in Figure 6-3 from Reference 4.

Table 6-2. Measured Cr_2O_3, REDOX and TCLP Response for Module B, C, and D FBSR Product without the IOC Catalyst Present

BSR Feed	Sample ID	Cr_2O_3 (wt.%) in FBSR Product$^{\xi}$	Measured REDOX $Fe^{2+}/\Sigma Fe$	Pass or Fail Cr UTS during TCLP Testing
Module B	Radioactive	0.0989	0.41	Pass
	Simulant	0.0998	0.36	Fail
Module C	Radioactive	0.2017	0.17	Fail
	Simulant On Spec	0.1754	0.34	Pass
	Simulant Oxidized	0.1754	0.15	Fail
	Simulant Reduced	0.1754	0.55	Pass
Module D	Radioactive	0.01973	0.18	Pass
	Simulant	0.01652	0.30	Pass

ξ calculation performed on Cr+3 as that was the desited Cr REDOX in the FBSR product

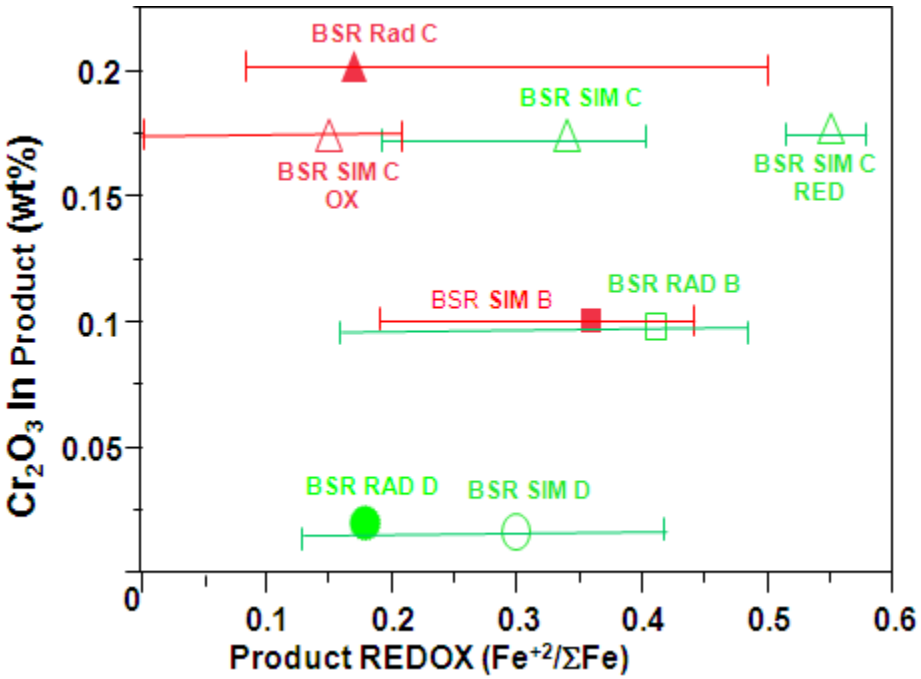

Figure 6-3. Dependency of Cr_2O_3 Leaching on FBSR Product REDOX

Note: The red symbols denote samples that failed TCLP for chromium leaching, while the green symbols denote samples that passed TCLP for chromium leaching. While the error bands on the REDOX measurements are large (as explained in the text), samples that failed chromium leaching in TCLP were definitely more oxidized than those that passed the TCLP testing.

Figure 6-3 shows the radioactive campaigns as solid symbols and the simulant campaigns as open symbols. Because "on specification" FBSR product was a composite of multiple runs with multiple measured REDOX values, the average value of the turbula mixed sample is plotted in Figure 6-3 and the ranges from Table 5-5 in Reference 3 and Table 5-9 in Reference 4 are given as error bars. The wide ranges of the REDOX error bars complicates the interpretation of Figure 6-3, but in general the samples below (more oxidized) than an $Fe^{2+}/\Sigma Fe$ of <0.25-0.3 fail TCLP

for chromium leaching at the UTS levels implying that chromium is present in the soluble +6 form. Samples that are more reduced ($Fe^{2+}/\Sigma Fe$ >0.30) pass TCLP for chromium leaching at the UTS levels implying that chromium is present in the non-soluble +3 form, i.e. likely Cr_2O_3. More data is needed to better define the Cr leaching limit on samples that have not been composited. Additional data is needed due to the poor reproducibility of the TCLP test response and the complications imposed by compositing the samples. The errors from compositing will be minimized when the BSR can be run with REDOX control using either REDOX probes or effluent gas mixtures as is done in the steel industry.[173]

Because more oxidizing values are favorable to the retention of Re and ^{99}Tc in the sodalite cage (see discussion in Section 8.2.8), an alternative way to sequester the chromium at oxidizing REDOX ranges is to provide the Fe_3O_4 host IOC, which forms the isostructural $FeCr_2O_4$ spinel where the chromium is in the +3 oxidation state. There is limited data available to look at the impacts of the IOC and the available data are presented in Reference 4 and Table 6-3.

Table 6-3. Measured Cr_2O_3, REDOX and TCLP Response for Module B, C, and D FBSR Product with the IOC Catalyst Present

Sample ID	IOC (g/100 grams wet feed)	Cr_2O_3 (wt.%) in FBSR product	Measured REDOX $Fe^{2+}/\Sigma Fe$	Pass or Fail Cr UTS during TCLP Testing
HRI Module B	14	0.1069	0.5	Pass
HRI Module B	14	0.1069	0.5	Pass
BSR Simulant Module E	17	0.16	0.13	Fail
AN-107 (TTT 2001)	14	0.0497	0.15	Pass
IOC	100	0	0.567	N/A

This limited data set was used to develop a "control strategy" for adding the necessary amount of IOC to sequester the chromium in the FBSR product in an iron chrome spinel while keeping the overall REDOX of the FBSR more oxidizing so that the Re and ^{99}Tc oxidation states are oxidizing enough to enter the sodalite structures.[4] Using the same dependent axis (Cr_2O_3 in the FBSR product) as in Figure 6-3 above, an x axis was derived which uses the IOC algorithm given in

Equation 6

$$desired\,REDOX * \left(\frac{IOC(\,g\,/\,100\,g\,wet\,feed\,)}{100} \right) * 0.567$$

where 0.567 is the $Fe^{2+}/\Sigma Fe$ of 100% pure IOC from Table 6-3. Plotting the IOC algorithm against the Cr_2O_3 in the FBSR product gives Figure 6-4 so that the amount of IOC can be calculated from the known Cr_2O_3 in the sample (via MINCALC™) and the REDOX desired to keep the Re and ^{99}Tc in the correct oxidation states for incorporation into sodalite. Since there are only 3 data points to fit the IOC algorithm, the intercept of the equation shown in Figure 6-4 is assumed to be zero. From this equation, the necessary IOC (in grams per 100 grams of wet feed/100) for chromium leaching control is back calculated to be

Equation 7

$$\left(\frac{IOC(\,g/100g\,wet\,feed\,)}{100}\right) \geq \frac{Cr_2O_3\,in\,FBSR\,product}{1.167 * desired\,REDOX}$$

From Figure 6-4, it can be seen that the Module E BSR simulant feed (AZ-101/AZ-102) did not have enough IOC added to ensure that all the chromium was tied up in an iron chrome spinel. Clearly, the data used from Table 6-3 indicates that FBSR products can be made at oxidizing REDOX with the IOC and that the presence of the IOC, when sufficient, ties up the chromium in the waste in an insoluble mineral phase related to the IOC structure.

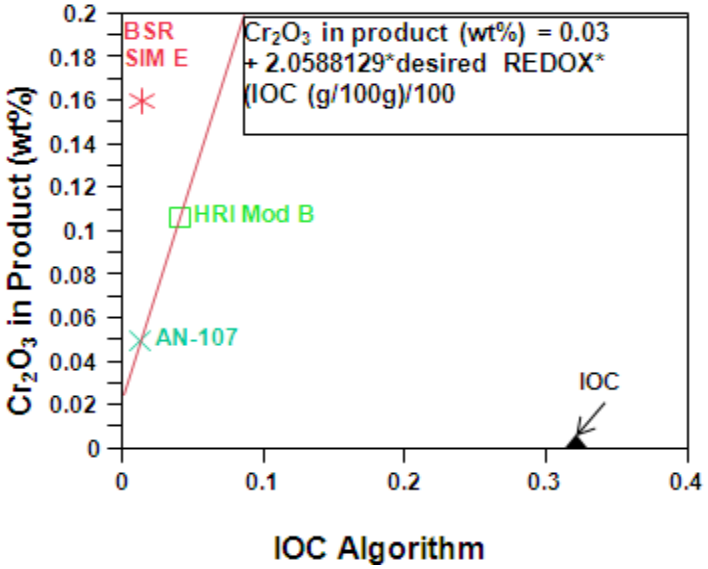

Figure 6-4. Dependency of the IOC on the Cr_2O_3 Content of the FBSR Product and the Desired REDOX

7.0 Overview of the SRNL Bench-Scale Steam Reformer Process

7.1 FBSR Process Chemistry

The THOR® mineralizing FBSR process and the SRNL BSR both destroy nitrates, nitrites, and organic materials present in the waste feed and produce a dry, leach-resistant alkali aluminosilicate mineral product containing the radionuclides, alkali metals, sulfates, halides, and non-volatile heavy metals present in the waste feed. The process converts nitrates and nitrites directly to nitrogen gas. Any organic material is converted to carbon dioxide and water vapor in the steam reformers by a combination of steam reforming and oxidizing reactions. A simplified THOR® mineralizing "dual reformer" FBSR process flow diagram for the treatment of Hanford LAW is given in Figure 3-1. A typical simplified BSR process flow diagram is given in Figure 7-1 for comparison.

To summarize Section 3.0, the THOR® process consists of several primary subsystems including: 1) feed systems for gases, liquids/slurry, and solid additives, 2) the fluidized bed DMR consisting of the bed bottom receiver and fluidizing gas distributor section, the fluidized bed section, the upper larger diameter freeboard (bed particulate disengaging) section, 3) the process

product/solids filtration, collection and management systems (PGF and PR), 4) the CRR which operates to enhance overall process NO_X destruction and to convert residual CO, H_2, and volatile hydrocarbons to CO_2 and water, 5) the off-gas treatment/emissions-control systems, and 6) the process monitoring and control system.

The simplified BSR flowsheet uses a quartz wool plug instead of an PGF to catch any particulate carryover. The BSR also does not have a PR product collection system as the product is harvested from the DMRonce it cools. The BSR has a CRR but it was not used for the experiments discussed in this report since the Hanford LAW streams being tested do not contain significant organic constituents. The BSR does have downstream condensers and the exiting gases are bubbled through these condensers. This assisted in mass balances performed in the BSR so that the amount of volatiles such as I, ^{99}Tc, Re, Cl, F, SO_4^{-2} could be accounted for.

The BSR designed at SRNL is a two-stage unit used to produce the same mineralized products and gases as the ESTD FBSR. A schematic of the single staged unit as used is shown in Figure 7-1. Unlike the FBSR, the BSR is not fluidized since it had to fit in the SRNL Shielded Cells and there is not enough height in the cells to allow for gravity disengagement of the product. The lack of fluidization does not impact the gaseous or mineralizing reactions but only impacts particle growth which has been determined not to impact product durability (see Sections 8.2.4 and 8.2.5 and Reference 111).

Steam, the fluidizing media, does flow though the BSR product freely, which is in the form of a porous biscuit, and SEM analysis shows well reacted particles in the BSR are similar to those in the HRI/TTT engineering-scale FBSR, i.e. both are fully reacted (Figure 7-2) and do not contain any unreacted clay cores as was observed in SEM of FBSR bed samples from the 2001 and 2004 pilot-scale tests. The biscuit stays porous so that steam can flow through it and all the gaseous and mineralization reactions can occur. Homogenization of the sample was done mechanically at the end of the campaign. Thus, the BSR is a batch process rather than a continuous process.

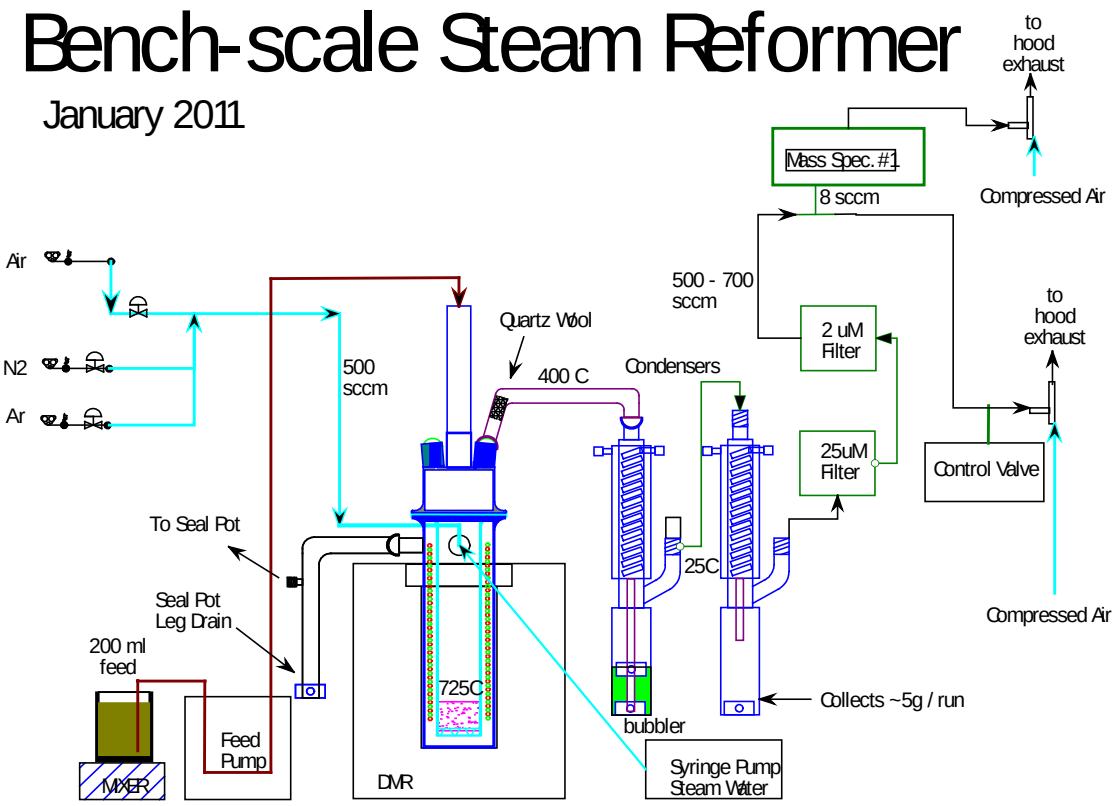

Figure 7-1. Schematic of the Bench-Scale Steam Reformer

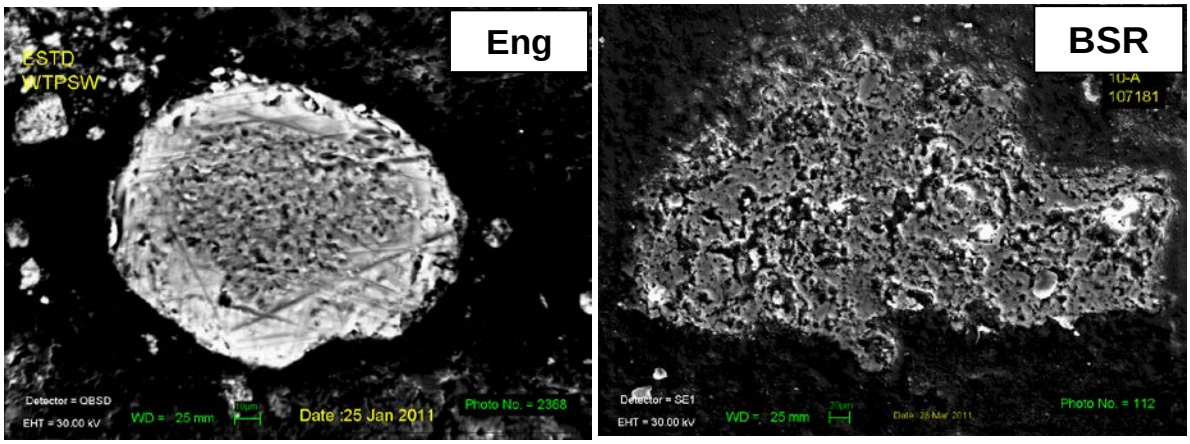

(a) (b)

Figure 7-2. Comparison of the product texture of an individual particle from the engineering-scale FBSR and the BSR. Note that unreacted clay cores as observed in the 2001 and 2004 samples are not present which indicates complete particle reactivity.

The nomenclature for the reformer came directly from the ESTD FBSR unit. During a typical run, approximately 200 ml of feed slurry was kept agitated with a stir bar mixer, while a peristaltic pump feeds the slurry through the center feed port in the lid of the DMR at about 0.9 ml/min. A mineralized product formed in the DMR in the presence of superheated steam, clay, and carbon and the off-gases flow toward the DMR condenser.

The DMR off-gas treatment system consists of the quartz wool in the crossover bar from the DMR to the condenser/bubbler, the condenser/bubbler, the second condenser, 25 μm paper filter, and 2 μm paper filter. The quartz wool filtered out most of the particulate carry over as the off-gases passed through it on the way to the condenser. This quartz wool was added at the beginning of Module C after solids carryover into the condenser had been observed in Modules A and B.

The condenser cooled the off-gas stream down to about 25°C and condenses the steam. A bubbler in the trap section of the condenser removed the particulate carry-over. The off-gas was further cooled by a second condenser which condenses out about 5 g of water per run. The off-gas then passed through a 25 μm filter and then a 2 μm filter prior to being measured by a Mass Spectrometer (MS) for H_2, O_2, CO_2, N_2, and Ar. An eductor drew the gases through the system and expelled them into the process exhaust system (chemical hood or shielded cell for SRNL) along with the motive air used to operate it. A control valve bled air into the suction side of the eductor to control the pressure of the DMR outer chamber to -4 inches of water column (inwc). See Figure 7-3 for a schematic of the DMR.

The DMR received the salt waste mixed with clay and coal as a single stream and converted it to a solid mineralized product in the presence of 725°C superheated steam and a controlled flow of air, N_2, and Ar.

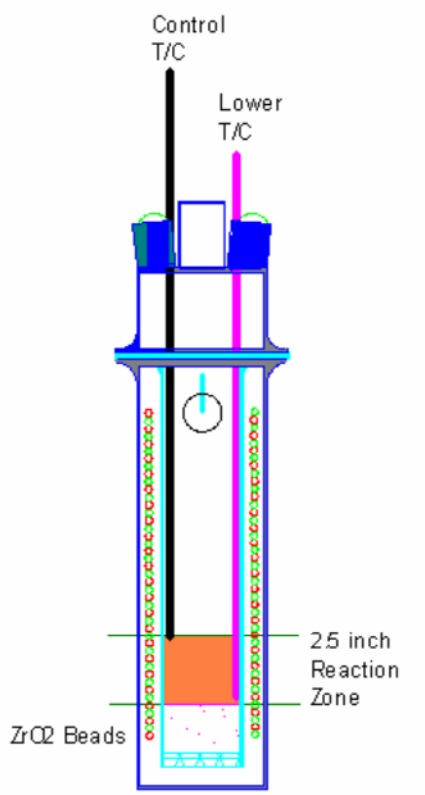

Figure 7-3. The Denitration Mineralization Reformer

The SRNL BSR DMR inner reaction chamber is 70mm ID x 385mm tall with a porous bottom. The bottom 50 mm (2 inches) is filled with zirconia beads. The zirconia beads were heavy enough not to be suspended by the gases and steam flowing up past them, acted as a base for the product to form on, allowed easy removal of the product from the reaction chamber, allowed easy separation of the product from the beads for analytic purposes, and provided a heat transfer medium for the gases that flow up through them. Zirconia beads are inert at the temperatures and oxygen fugacity at which the DMR operates and the beads do not affect the steam reforming chemistry.

The DMR outer chamber has a 120 mm ID and is 400 mm tall and provides connections for the outer chamber pressure relief and measurement line, and each of the two 20 foot coils which are housed between the DMR inner reaction chamber and the outer chamber. The outer chamber is sealed by the top flange of the inner chamber, and thus has a pressure relief line going to a seal pot which relieves at about 15 inwc. Water, N_2, Ar, and air enter the DMR via the coils, which are between the inner and outer walls of the DMR and are converted to superheated steam and hot gases with heat provided by the furnace that surrounded the DMR as an external heat source. The steam and gases leave the coils and flow through the bottom of the DMR inner well mixed reaction chamber, the zirconia beads, the product, and out through the top of the DMR to the DMR condenser. The N_2 plus Ar plus Air total flow rate was held at a constant 500 sccm to minimize particle carryover. The relative flow rates are varied in order to control the process REDOX potential.

7.1.1 *DMR Reaction Zone as Defined by Thermocouple Placement and Bead Height*

The DMR lid is 120 mm ID x 80 mm tall and was sealed to the top of the inner chamber. The lid holds two type K thermocouples, the centered feed line that is cooled with standing water, the inner chamber pressure relief and measurement line, and the off-gas line going to the DMR condenser. In the event of an off-gas line pluggage, the inner chamber and lid have a pressure relief line going to a seal pot which relieves at about 15 inwc. One thermocouple is positioned at the level of the zirconia bead bed and the control thermocouple is positioned 2.5 inches above the surface of the bead bed. This 2.5 inch height is the upper point of the reaction zone in the DMR. The control temperature ranged from 710°C to 740°C in the DMR for this set of runs.

The DMR off-gas treatment system consists of the quartz wool in the crossover bar (see Figure 7-4, with quartz wool not shown) from the DMR to the condenser/bubbler, the condenser/bubbler, the second condenser, 25 µm paper filter, and 2 µm paper filter. It was necessary for pretreatment of the off-gas to prevent pluggage or damage to the mass spectrometer. The system treated a combined controlled flow of 500 sccm of Ar, N_2, and air along with about 200 sccm of reaction gases from the reforming process. It condensed 0.4 ml/min water from the superheated steam plus about 0.7 ml/min water from the slurry feed. The condenser/bubbler was capable of reducing the off-gas stream temperature from 400°C down to 25°C.

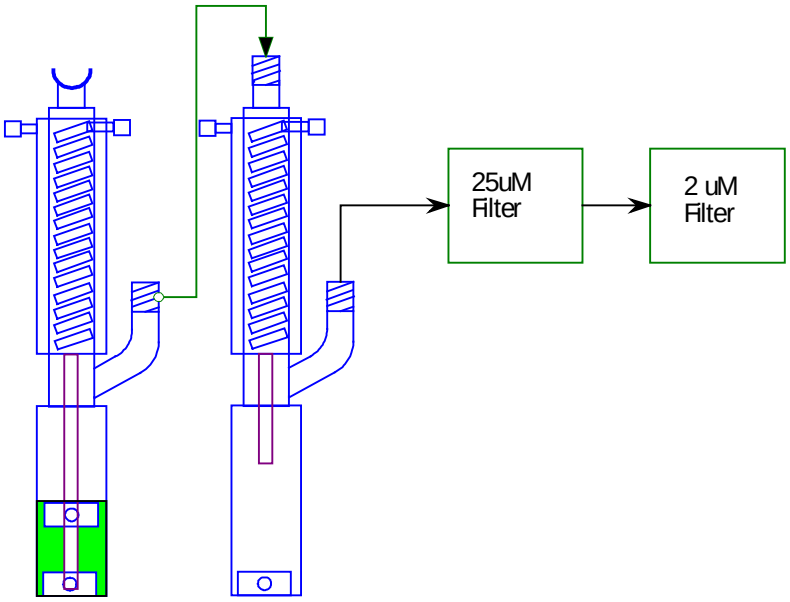

Figure 7-4. DMR Off-gas Treatment

A removable piece of quartz wool filtered out most of the particulate carry over as the off-gases passed through it on the way to the condenser/bubbler. The off-gases and steam entered at the top of the condenser/bubbler and flowed and condensed down through the center tube which ended at the bottom of a 75 mm deep water reservoir filled with zirconia beads. The condenser cooled the off-gas stream down to about 25°C and removed the steam and feed water. A bubbler in the trap section of the condenser removed the remainder of the particulate carry-over. Excess water from the bubbler would overflow into a sealed reservoir (not shown). The off-gas was further cooled by a second condenser which condensed out about 5 g of water per run. The off-gas then passed through a 25 µm filter and then a 2 µm filter prior to being measured by a Mass Spectrometer.

The 25 µm filter trapped most of the vaporized sealing grease (that sealed the DMR flanges) such that the 2 µm filter was seldom blinded. There were no pluggages of the mass spectrometer as a result of this system. The quartz wool and the bubbler water also provided some natural sampling points for off-gas analysis.

The BSR used a Monitor Instruments LAB 3000 Cycloidal mass spectrometer (MS) for the reformer real time off-gas analysis (see Figure 7-5). The spectrometer was set up to measure H_2, O_2, N_2, CO_2, and argon. The MS would measure the DMR off-gas on channel 2. Channel 1 was used for the calibration gas. Both channels had 7 micron sintered metal filters in the 1/8" lines going to the instruments to prevent plugging the lines inside the MS.

Since the line pressure near the MS could go down to -25 inwc, it was necessary to run a second eductor and vacuum regulator to draw the sample gases through the MS. The vacuum was controlled to -40 inwc while the flow rate of gases pulled by an MS sample line was kept at 8 sccm. The flow rate of the gases coming from the DMR condenser varied between 500 to 700 sccm.

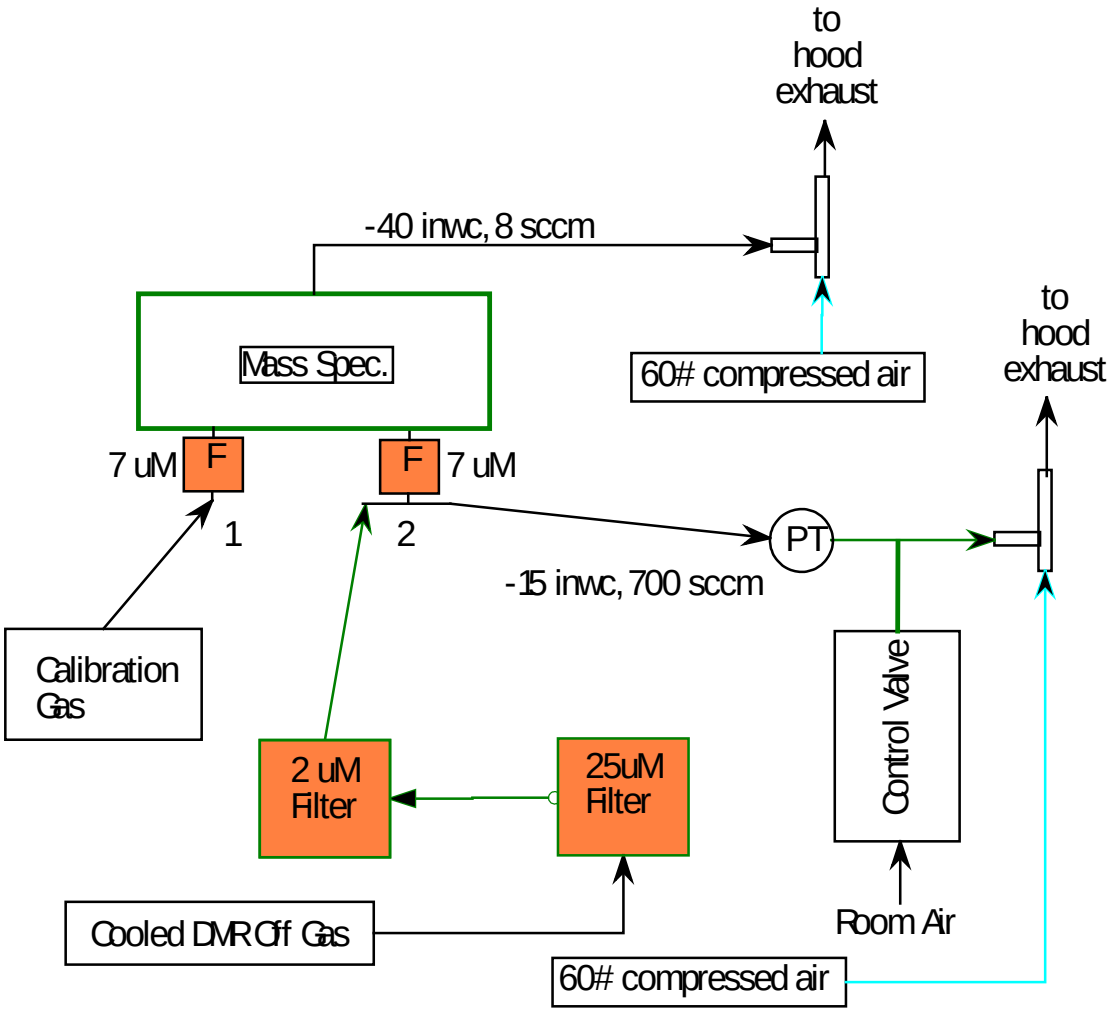

Figure 7-5. The BSR Mass Spectrometer

The MS was controlled by a Personal Computer with Monitor Instruments proprietary software loaded. Data from the MS computer was transferred to the control computer in real time via a serial connection.

The dry basis DMR H_2 values were continuously trended on the control computer and, originally, operating personnel would manually vary the air flow into the DMR to control the DMR H_2 value between 1.0% and 2.0%. However, from 10/19/10 forward, air flow was controlled to achieve the proper product REDOX based on a "gas REDOX" correlation.

The LOI was controlled by reacting away the excess coal in the reformer until the cumulative value of CO_2/ml fed to the DMR reached a predetermined endpoint. This ensured the product did not have excessive unreacted coal in it. This was based on an imperfect mass balance of carbon since the MS did not measure CO which also is present in the off-gas.

(Carbon fed into DMR) – (Carbon Leaving as CO_2) = Unreacted carbon in product

The MS would determine and transmit the gas concentration data about once every 14 seconds. However, the lag time between the measurement and the conditions in the DMR ranged between 3 to 4 minutes depending on flow rates. See Figure 7-6 for a diagram of the configuration of the control system in the SRNL Shielded Cells.

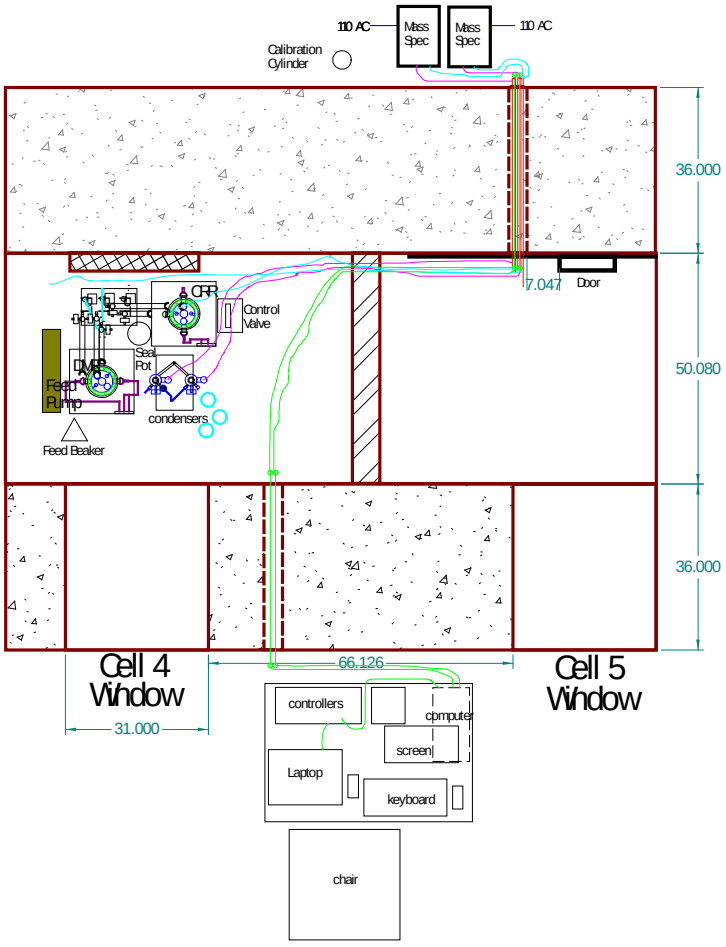

Figure 7-6. Total Rad System Layout at Cell 4 (Simplified)

The computers for the MS and process control system along with the steam water pumps, MKS gas flow controllers, furnace controllers, furnace safety relays, and input/output box were located external to the cell on the operational side. The MS is in a radio-hood behind the cell on the maintenance side. Connections between process and control systems required the use of 9 inner wall connection tubes (known at SRNL as KAPL plugs which were first developed at Knolls Atomic Power Laboratory).

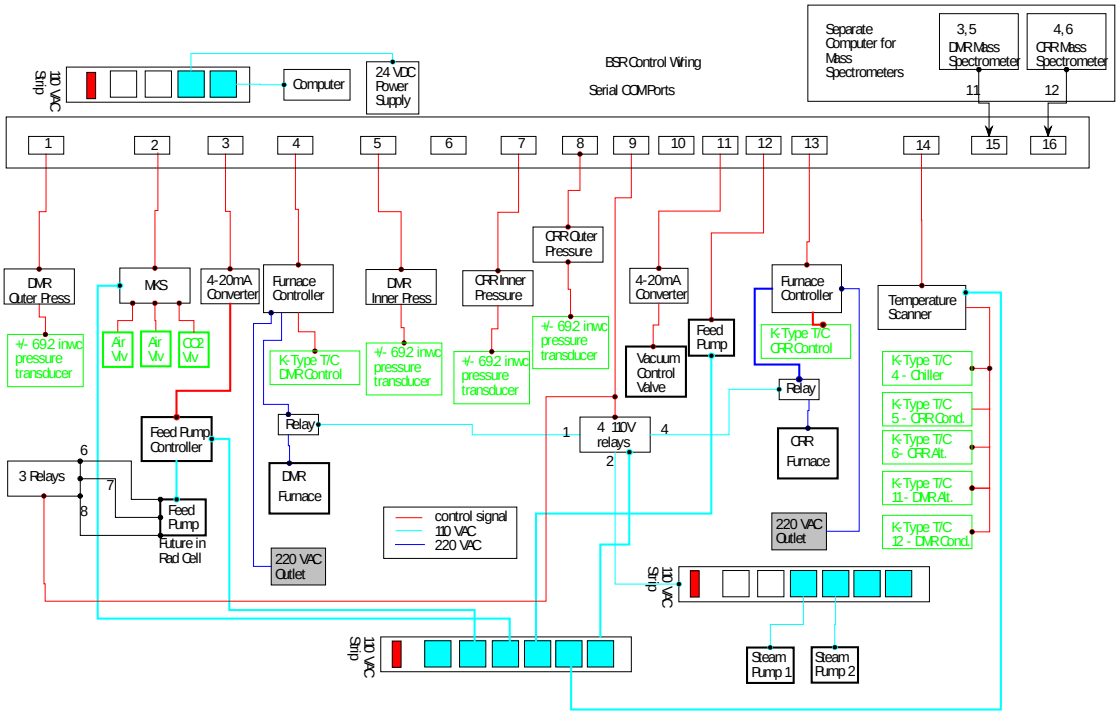

Figure 7-7. BSR Process Controller Diagram

The BSR was controlled by a single PC running Windows XP with 16 serial port connections (see Figure 7-7). Omniserver software was used as the server software to communicate through the serial ports. Intouch software was used as the client software and man machine interface. Data acquisition was continuous and trended in real time on screen as the process ran. Real time data was also saved to a file on a frequency of once per minute. Control logic was programmed into Intouch to provide operator aid (including a Pressure Indicating Device (PID) pressure controller).

Process parameters measured were:

Slurry Feed Rate, DMR outer pressure, DMR Inner Pressure, DMR Bed Temperature, DMR Control Temperature, DMR H_2, DMR O_2, DMR N_2, DMR CO_2, DMR argon, filter pressure inlet, Filter Pressure outlet, and chiller bath temperature.

Process parameters controlled were:

Slurry Feed Rate, DMR Control Temperature, DMR outer pressure, and the DMR Air flow-rate coupled to the N_2 and Ar flowrates.

See Table 7-2 below for specific control parameters for each module.

7.1.2 *BSR Operating Conditions*

The BSR did not use scaled values to the ESTD FBSR operation for this study. However, the BSR did feed slurry at about 1/800th the rate that the ESTD FBSR did for reference. BSR operation was modified to minimize non-condensable gases to reduce the carryover of particles from the reformer. BSR operation was also modified to control product REDOX instead of H_2 concentration. Since the non-radioactive and radioactive BSR systems were identical, the operating parameters determined for the non-radioactive runs were used in the radioactive runs.

The slurry feed rate of 0.9 ml/min worked well with this unit to form the needed biscuit shaped product, allow adequate pressure control, and minimize product carryover to the off-gas system.

The temperature range of 710 – 740°C was specified by TTT. The range was measured across the lower thermocouple at the bottom of the reaction zone and the upper controlled thermocouple at the top of the reaction zone. Typically, the control temperature would start at 725°C and would have to be lowered over the course of a run until it was set to 710°C. Many times slurry feeding was stopped signaling the end of the feeding stage of a run because the lower thermocouple reached 740°C after the control was already at 710°C. Thus, no new product was formed at temperatures above 740°C. However, it was normal for the lower temperature to spike to 750°C for a short time at the end of feeding because the temperature control system could not react quickly enough to offset the sudden loss of cold feed entering the DMR. Higher temperatures are typically avoided to avoid making amorphous glass out of the product. No glass was detected in any of the products formed from the campaigns discussed in this report.

The superheated steam rate was scaled to the ESTD FBSR rate based on the BSR slurry feed rate (~1/800th). Pressure control was set such to minimize process positive pressure.

The total controlled gas flow refers to the sum of the flow of N_2, Ar, and air flowing into the DMR. The control system automatically adjusted the air, N_2, and Ar flows when the operator changed the % air such that the total combined flow always remained at 500 sccm. This total flow is reduced from the ESTD scaled flows in order to reduce product carryover. The important parameter for product formation and REDOX control is O_2 (air) concentration, not flow as long as there is enough O_2 to complete all of the reactions. The ESTD FBSR needed much greater flows to support fluidization which is not a factor for the BSR.

7.1.3 *Product Composition and REDOX Control for the BSR*

BSR product criteria were set to mimic the successful 2004 pilot-scale and 2008 engineering-scale compositions with the Rassat simulant, REDOX, and coal carryover into the product. Product criteria were therefore established:

- Correct mineral assemblages (nepheline, nosean, sodalite)
- Acceptable REDOX based on the bed REDOX achieved in the 2008 testing[§]
- <2.5 wt.% residual coal also based on the bed composition of the 2008 LAW engineering testing

[§] It was undesirable to mimic the REDOX of the fines as it is believed that the REDOX measurement is compromised in the presence of the coal fines.

If the BSR product met the three criteria above, it was deemed "on spec" and if it failed any of the three criteria, it was deemed "off spec" and not used in subsequent WFQ testing.

The initial BSR REDOX target for the Rassat simulant (Module B) was between 0.4-0.6 $Fe^{+2}/\Sigma Fe$, which matched the values measured experimentally for the ESTD Module B testing (Table 7-1). The ESTD sample contained the IOC, which has its own REDOX, while the BSR simulant and radioactive products will be tested without the IOC as it complicates the interpretation of the REDOX measurement. The initial target range for Simulant Module C was lowered to allow more oxidizing feeds to be made, i.e. $Fe^{2+}/\Sigma Fe$ of 0.2-0.6 (Table 7-1). The Module C radioactive campaign lowered the upper limit to 0.5, i.e. $Fe^{2+}/\Sigma Fe$ of 0.2-0.5 (Table 7-1). During the course of these studies and in consortium with the ORNL who was measuring the amount of Re and ^{99}Tc in the sodalite cage, the upper limit $Fe^{+2}/\Sigma Fe$ was reduced to <0.5 as more reduced values volatilized too much SO_4^{-2} as $SO_3\uparrow$ or $S_2\uparrow$ gas and left 30-33% of the Re in the reduced oxidation state of Re^{+4} which would not go into the sodalite cage. Therefore, the upper REDOX limit for Module C was lowered to 0.5 to ensure a high percentage of the Re was present as Re^{+7} for the sodalite cage (Table 7-1). For Module D (AN-103), the REDOX target was lowered yet again to match the AN-107 FBSR product value of 0.18, which kept the chromium from leaching but maximized the Re^{+7} incorporation in the sodalite cage. The Module D targets (simulant and radioactive) were 0.15-0.5. The Module E target was lowered again, but the IOC was added to tie up the chromium as it was recognized that without a host phase to sequester the chromium, that the oxidizing REDOX might create soluble chromium +6 species instead of the desired insoluble chromium +3 species.

The REDOX range started out being $Fe^{+2}/\Sigma Fe$ of 0.4-0.6 to reproduce the range of REDOX values from the 2008 engineering-scale campaigns (Table 7-1). As a result of the XAS studies discussed in Section 8.2.2, it became apparent that a more oxidizing REDOX range was more favorable to $(Re,^{99}Tc)^{+7}$ and the REDOX range was shifted to more oxidizing values (see Table 8-8).

Table 7-1. REDOX Targets for Hanford Rassat Simulant, SX-105, AN-103 and AZ-101/AZ-102

Demonstration	Measured REDOX	Target REDOX			
	Module B (Rassat Simulant)	Module B (Rassat Simulant)	Module C (SX-105)	Module D (AN-103)	Module E (AZ-101/ AZ-102)
BSR Simulant	0.41	0.4-0.6	0.20-0.60	0.15-0.50	≤0.15
BSR Radioactive	0.36	0.4-0.6	0.20-0.50	0.15-0.50	
ESTD Product Receipt (PR)	0.41-0.58				
Iron Oxide Catalyst (IOC)	0.567				

The control began with the MINCALC™ calculation for the type and amount of clay and the stoichiometric amount of carbon required to complete the denitration process. This stoichiometric amount of carbon is then converted to an amount of the actual type of coal that is

being used. However, some of the carbon goes into making heat, some doesn't react, and some is lost as off-gas carryover. Therefore, more coal is needed than is calculated. At this point, the required amount of coal must be determined experimentally and is usually expressed as a factor times the stoichiometric amount.

Many parameters can affect the REDOX potential in the BSR and they all must be kept as constant as possible (once determined). The parameters that are kept constant are:

- Reactor temperature (710-740°C)
- Slurry feed rate (0.9 ml/min)
- Slurry feed concentration (if slurry has to be diluted to improve rheology, then the air flow to get the same REDOX must be lowered by a linear amount)
- Gas REDOX used for Module B.
- Air% used for Module C, D, E
- O_2 concentration (controlled by air% bled in or determined experimentally from REDOX as it is not measurable by the mass spectrometer, ~10^{-21} to 10^{-18} atm)
- Contact time of coal with the slurry feed (either by adding coal immediately before the run to minimize pre-reaction or allowing coal to react to completion in slurry prior to feeding to the BSR)
  - Since pilot-scale tests were performed with reductants added to the slurry in advance and engineering-scale tests co-added coal with feed, the coal was added immediately before each run for Module D and E.
- Superheated steam rate (0.4 g/min) and total gas flow (Air + N_2 + Argon = 500 sccm) kept constant and it is unknown at this point how much these affect REDOX.

See Table 7-2 for the specific parameters for each module. See References 3 and 4 for specific parameters for each run within each module and strategies for controlling REDOX should it be shown to be necessary.

Table 7-2. BSR Process Operation Conditions

Campaign	Module B (Rassat 168 Tank Blend LAW)		Module C (SX-105)		Module D (AN-103)		Module E (AZ-101/ AZ-102)
	SIM	RAD	SIM	RAD	SIM	RAD	SIM
Slurry Feed Rate (ml/min)	0.9	0.9	0.9	0.9	0.9	0.9	0.9
DMR Temp (^oC)	710 – 740	710 – 740	710 – 740	710 – 740	710 – 740	710 – 740	710 – 740
Superheated Steam (g/min)	0.40	0.40	0.40	0.40	0.40	0.40	0.40
DMR Control Pressure (inwc)	-4	-4	-4	-4	-4	-4	-4
Carbon times Stoichiometric	1.3x	1.3x	1.3x – 2.56x	1.3x – 1.54x	2.25x	2.25x	1.3x
Total Controlled Gas Flow (sccm)	500	500	500	500	500	500	500
Gas REDOX	na	Control 16 - 18	13.6 – 15.2	15.8 – 16.2	8.1 – 10.5	7.2 - 9	na
Controlled Air% during Feeding	na	na	Control 50%	Control 50%	24% air w/ new coal	25% w/new coal 15% w/aged coal	25%
Post Feed Air%	20	20	50	20	Kept [O_2] < 0.01%	12.75 - 15	15 to 6 over 40 minutes
CO_2/ml fed	27.8	27.8	34 - 53	25.2 – 36.9	24.5	19.7 – 24.5	16.6-18.8

8.0 Test Results

8.1 Bench-scale Reformer Treatability Testing: Prerequisites for Waste Form Performanc Testing

Prerequisits to the WFQ testing (Section 8.2) include knowing the following (1) how the LAW simulant and radioactive feeds were made and controlled, (2) how the LAW simulants and tank waste feeds were analyzed, and (3) how the LAW FBSR products were made and analyzed. These analyses were especially critical for the evaluation of the mass balance of the BSR and because the analyzed product compositions are used in the calculation of the waste form durability response as measured using ASTM C1285 (PCT), ASTM C1662 (SPFT), and the PUF testing. Details are given in References 3 and 4 but are summarized below.

8.1.1 *Feed compositions, feed formulation, and clay additives-*

8.1.1.1 *All BSR Campaigns*

MINCALC™ was used to determine the amounts and type of clays and the amount of coal to be mixed with each feed as discussed in Section 6.0. In all campaigns, the clay was mixed with the waste in a large batch to accommodate all of the expected runs. The number of batches varied with each module.

The same Bestac® coal was used in all the BSR campaigns and is the same coal used by the ESTD FBSR as a reducing agent. However, for the BSR, the coal was ground, then sifted through an 80 mesh sieve (177 microns) and mixed with the feed slurry prior to being pumped into the DMR versus the ESTD coal that was much larger and was added as a separate stream in the FBSR. The coal for the BSR had to be ground to flow through the peristaltic pump. In the Module B (Rassat 168 LAW Tank Blend) and Module C (SX-105) campaigns, the coal was mixed with the salt waste in a large batch to accommodate all the expected runs. Issues with the clay coating the coal particles were encountered. Therefore,in the Module D (AN-103) campaign, the coal was added the day of the run on the assumption that the coal loses ~40% of its reactivity after sitting in the salt/clay slurry for more than 2 days (it is believed to remain constant after the 3rd day). Adding the coal at the day the slurry is pumped mimics the ESTD method of coal feeding, which is to add it as a co-additive to the clay and waste.

In addition, a small amount of $Fe(NO_3)_3 \bullet 9H_20$ was added to the BSR runs to act as an analytical indicator for the REDOX potential in the product. The REDOX measurement was used to determine the expected distribution of multivalent species such as Cr, Re, and ^{99}Tc. Ferric nitrate nona-hydrate was added to have ≥1.5 wt% Fe in the final BSR product as there is little to no iron in the LAW waste. The IOC (Fe_3O_4) was not added in the early campaigns because it would complicate the measurement of the iron REDOX since it is a source of partially reduced iron.

Re was added as ReO_2 to all simulant and radioactive campaigns to track the fate of Re in the FBSR product and off-gas to determine how Re and ^{99}Tc tracked each other. The Re was added as $NaReO_4$ and ^{99}Tc was added as $NaTcO_4$ to the radioactive Module B (Rassat 168 Tank LAW Blend) so that significant quantities of Re and Tc would be available and could be detected. In Module C (SX-105) and Module D (AN-103), no additional ^{99}Tc was added as there was suffienct ^{99}Tc already in the LAW tank waste. The ^{125}I and ^{129}I were added as potassium iodide in solution. The ^{125}I has a shorter half-life but a stronger radiochemical signature and gives a more accurate measurement for mass balance purposes. The dopings of Tc and I are summarized in Table 8-1.

Table 8-1. Radioactive and Rhenium Spikes Added for Mass Balance Tracking and FBSR Product Durability

Spike	Species	Rad Mod B (Rassat 168 Tank Blend)	Rad Mod C (SX-105)	Rad Mod D (AN-103)	Rad Mod E (AZ-101/ AZ-102
^{125}I	Potassium iodide[a]	Yes	No	No	No
^{129}I	Potassium iodide[b]	Yes	No	No	No
Re	Sodium perrhenate[c]	Yes*	Yes	Yes	Yes
^{99}Tc	Sodium pertechnetate[d]	Yes*	Yes**	No	No

* Re and ^{99}Tc added to all Module B radioactive runs; enhances levels of ^{99}Tc added for final run for XAS analyses per Table 5-5 footnote

** ^{99}Tc only added to final run at enhanced levels for XAS analyses per Table 5-5 footnote

a. Added as radioactive standard in 0.1M NaOH from Eckert & Ziegler Analytics

b. Added as radioactive standard in caustic solution from SRNL stock

c. Added as sodium perrhenate ($NaReO_4$) reagent grade chemical

d. Added as $NaTcO_4$ standard in 0.01M NaOH from Eckert & Ziegler Analytics

The feed compositions for Modules B (Rassat Blend), C (SX-105), D (AN-103), and E (AZ-101/AZ-102) are shown in Table 8-2 through Table 8-5. The simulant recipes are those obtained following addition of Re, but prior to addition of clay, coal, Fe nitrate used to measure REDOX in the final BSR product, and/or the IOC. For Modules C, D, and E, the WRPS analysis as well as the SRNL analysis is given in the respective tables. Analyses include elemental composition as determined by Inductively Coupled Plasma - Atomic Emission Spectroscopy (ICP-AES) and ICP - Mass Spectroscopy (ICP-MS) measurements on either supernate or digested slurry samples; separation and counting techniques for ^{137}Cs, ^{99}Tc, ^{125}I (where applicable), and ^{129}I; Ion Chromatography (IC) anion measurements on filtered, weighted dilutions of slurry or supernate; total base, free OH^-, and other base excluding CO_3^{2-} titration of unfiltered, weighted dilutions of slurry or supernate; Total Inorganic Carbon (TIC) measurement for carbonate; and solids measurements where insoluble solids were present in a sample that was processed in the BSR. Details of the analyses methods can be found in Reference 3 for the Rassat Blend and in Reference 4 for SX-105, AN-103, and AZ-101/AZ-102.

8.1.1.2 *Rassat Simulant*

Table 8-2 provides the Rassat recipe [109] both as prepared at the INL pilot scale FBSR [108] without elevated RCRA metal ions and as prepared at the engineering scale FBSR known as the ESTD [122] with elevated RCRA metal ions. The simulant compositions in this table labeled as B1 and B2 were measured following removal of any precipitated solids from the simulant. The granular product produced in the Module B simulant runs was roughly an equal mixture of these two simulants.

The Rassat simulant for this testing was made using the formulation given in Table 8-2. The target concentration for the LAW was increased by a factor of 10 for Sb, As, Ag, Cd, and Tl; 100 for Ba and Re (Tc surrogate); 1,000 for I; and 1,000,000 for Cs as done in the TTT engineering scale demonstrations of the Rassat simulant[122] in order to observe their behavior during mass balance of the process. The HRI/TTT levels were chosen to achieve reliable detection in the off-gas sampling without regard to potential results of those determinations or impacts on product durability response such as TCLP.

The simulant for Module B had been specified to be exactly the same as that processed in the ESTD with the increased RCRA metals discussed above. When it was made in the laboratory,

some of the RCRA metals precipitated and were removed through filtration. They were filtered in case the precipitates were soluble precipitates that could give erroneous TCLP responses when the FBSR product was tested. Since the HRI/TTT simulants had not been filtered, comparison of the BSR FBSR product to the ESTD FBSR product would also give a comparison as to how well any precipitates in the simulant were incorporated into the FBSR mineral phases. Details of the analyses can be found in Reference 3.

8.1.1.3 *Radioactive Sample Shimmed to Match Rassat Composition*

A SRS LAW sample from Tank 50 was adjusted to the Rassat recipe composition, and then filtered to remove any precipitated solids to produce the Module B radioactive material. This sample was shimmed with ^{125}I, ^{129}I, ^{99}Tc, Re, and the excess RCRA metals. Precipitates formed when the solubility of the RCRA species were exceeded in the Tank 50 sample. The precipitates were sampled and identified by XRD as enriched in sodium antimony (+5) hydroxide, lead phosphate, lead carbonate, and barium nitrate. Since the precipitates were primarily RCRA species, which had exceeded their solubility, they were filtered out causing the analyzed compositions shown in Table 8-2 to be lower than the RCRA species added initially. Details and the XRD analyses can be found in Reference 3.

8.1.1.4 *Hanford Tank SX-105 (Module C)*

The Hanford Tank SX-105 samples, which had undergone cesium removal, were received in two separate bottles that were eventually composited for the SRNL BSR testing. Figure 8-1 provides a picture of the samples after they were unloaded in the Shielded Cells. Table 8-3 provides the SRNL analysis of the Hanford SX-105 Tank sample used in Module C, the WRPS analysis of SX-105 [174], and the SRNL simulant analysis that was prepared based upon the WRPS analysis of this sample prior to its shipment to SRNL. During simulant preparation, any components that were below detection limit (<) in the WRPS analyses were omitted from the simulant as their impact on durability, i.e. TCLP, would be detected in the radioactive sample if it were a significant impact.

Both the simulant, though to an immeasurable degree, and the LAW samples had visible solids of gibbsite (identified by XRD analysis in Reference 4) that were not removed prior to processing. The SX-105 sample solids did appear to increase between the visible receipt inspection and the start of BSR processing. The solids measurement data in the table below was made after the sample had been at SRNL for a number of months and prior to the addition of clay, coal, or REDOX tracer Fe nitrate. The significant difference in the Re level between the SRNL and WRPS analyses reflects the addition of Re to the sample prior to characterization in SRNL. The characterization in Table 8-3 does not reflect the additional ^{99}Tc spike of the Hanford LAW sample done for the last two BSR runs in order to provide material for XAS analyses by ORNL personnel aimed at determining the ^{99}Tc bonding and crystallographic location.

Table 8-2. Feed Compositions for Module B Recipes, Simulants, and SRS LAW Shimmed to the Rassat Simulant Recipe after Re Addition but Prior to Clay, Coal, or Fe Addition

Species	SRNL Analysis Radioactive B	SRNL Analysis Simulant B2	SRNL Analysis Simulant B1	Rassat Recipe HRI/ TTT	Rassat Recipe INL	Rassat Recipe [109]
	Molar	Molar	Molar	Molar	Molar	Molar
Ag	<1.74E-05	<1.97E-04	5.56E-04	1.61E-03		
Al	2.57E-01	6.28E-02	7.64E-02	6.37E-02		
As	6.94E-04	<1.11E-06	1.25E-03	1.37E-03		
B	5.80E-03					
Ba	1.08E-05	<2.23-04	1.15E-03	7.51E-03		
Cd	4.72E-06	<9.98E-04	<9.98E-04	4.20E-03		
Cr	8.90E-03	5.87E-03	1.01E-02	1.04E-02		
^{133}Cs	4.67E-06	1.41E-02	1.41E-02	1.30E-02	5.10E-07	5.10E-07
Fe	<1.02E-05					
Hg	6.26E-05					
K	1.40E-02	1.59E-02	4.08E-02	1.24E-02		
Li	<2.49E-04					
Mg	<1.03E-05					
Mn	<2.00E-05					
Na	5.36E+00	5.05E+00	5.05E+00	5.02E+00		
Ni	<3.27E-05	<6.60E-03	<6.60E-03	1.06E-02		
P	5.10E-02			4.92E-02		
Pb	5.60E-03	1.90E-03	5.00E-03	6.06E-03		
Re	1.60E-03	1.83E-03	1.83E-03	1.70E-03	3.95E-04	
Sb	2.00E-04	1.53E-04	3.58E-03	4.34E-03		
Se	1.04E-06	9.54E-04	7.91E-04	1.23E-03		
Si	5.00E-04					
Sr	<9.13E-07					
Ti	<1.55E-05	NA*	NA*			
Tl	NA	3.02E-04	6.37E-03	2.02E-03		
U	<3.15E-04					
Zn	1.00E-04					
^{137}Cs	3.44E-08					
^{99}Tc	6.69E-06					
$^{125}I^-$	2.99E-12					
$^{129}I^-$	2.04E-04					
$CH_3CO_2^-$	NA	NA	NA	1.32E-01		
CO_3^{2-}	3.40E-01	NA	NA	4.75E-01		
Cl^-	5.82E-02	4.40E-02	4.25E-02	4.38E-02		
F^-	1.95E-02	<5.26E-03	<5.26E-03	3.16E-02		
HCO_2^-	5.60E-03	NA*	NA*			
OH^-	8.53E-01	NA	NA	7.40E-01		
$^{127}I^-$	7.84E-03	7.13E-03	NA	1.30E-02	1.34E-04	
NO_3^-	3.80E+00	2.69E+00	3.00E+00	2.51E+00		
NO_2^-	3.12E-02	4.23E-01	5.34E-01	4.24E-01		
$C_2O_4^{2-}$	1.01E-02	1.06E-02	8.50E-03	1.18E-02		
SO_4^{2-}	1.13E-01	8.93E-02	9.08E-02	9.00E-02		
	Wt.%	Wt.%	Wt.%	Wt.%	Wt%	Wt.%
Insoluble Solids	removed	removed	removed	not removed	not removed	Not Applicable
	g/mL	g/mL	g/mL	g/mL	g/mL	g/mL
Density	1.32	1.25	1.26	N/A	N/A	1.24

NA not analyzed but was in simulant; NA* not part of simulant

Table 8-3. Feed Composition for Module C Simulant and Hanford Tank SX-105 after Re Addition but Prior to Clay, Coal, or Fe Addition

Species	SRNL Analysis SX-105	WRPS Analysis SX-105 [174]	SRNL Analysis Simulant C
	Molar	Molar	Molar
Al	3.74E-01	3.74E-01	3.78E-01
B	2.45E-03	2.95E-03	2.53E-03
Ba	1.40E-04	<2.18E-05	<5.08E-06
Be	<1.86E-05	<1.11E-04	NA
Ca	1.60E-03	<1.25E-03	<2.06E-04
Cd	<5.91E-06	<4.45E-05	<6.83E-06
Ce	<7.20E-05	<2.14E-04	<8.78E-05
Co	<3.08E-05	<1.70E-04	<4.27E-05
Cr	1.99E-02	1.79E-02	1.71E-02
Cs	NA	NA	4.01E-05
Fe	8.41E-04	<8.95E-05	1.75E-04
K	2.21E-02	1.42E-02	1.34E-02
La	<1.10E-05	<2.16E-05	<2.41E-05
Li	<1.66E-03	<4.32E-04	<4.08E-04
Mg	2.97E-04	<2.06E-03	<3.67E-05
Mn	9.54E-06	<5.46E-05	<1.72E-05
Mo	3.57E-04	<2.08E-04	<4.20E-05
Na	5.34E+00	5.13E+00	5.19E+00
Nb	NA	NA	<3.19E-05
Ni	8.56E-04	<3.41E-04	<3.65E-05
P	5.28E-02	8.81E-02	7.75E-02
Pb	2.30E-06	<2.41E-04	<2.76E-05
Re	1.67E-03	2.28E-05	2.20E-03
S	6.61E-02	5.74E-02	5.58E-02
Sb	<8.63E-05	<4.11E-04	NA
Si	4.96E-03	NA	<3.65E-04
Sn	<8.84E-04	NA	<4.94E-05
Sr	4.52E-06	<3.42E-05	<6.62E-06
Th	<3.29E-07	4.44E-09	NA
Ti	1.12E-04	<1.04E-04	<2.46E-05
U	1.18E-06	1.53E-06	NA
Zn	1.58E-04	1.07E-04	1.14E-04
Zr	1.90E-05	<5.48E-05	<1.17E-05
^{137}Cs	6.49E-11	3.26E-11	NA
^{99}Tc	4.11E-05	4.28E-05	NA
^{129}I	2.91E-06	3.57E-06	NA

NA is Not Analyzed.

Table 8-3. Feed Composition for Module C Simulant and Hanford Tank SX-105 after Re Addition but Prior to Clay, Coal, or Fe Addition (Continued)

Species	SRNL Analysis SX-105	WRPS Analysis SX-105 [174]	SRNL Analysis Simulant C
	Molar	**Molar**	**Molar**
$C_2H_3O_2^-$	NA	6.61E-03	NA
CO_3^{2-}	4.26E-01	8.20E-02	3.15E-01
Cl^-	7.21E-02	6.63E-02	5.11E-02
Br^-	<1.56E-03	<1.54E-03	<1.25E-02
F^-	<6.57E-03	3.70E-03	<5.26E-03
HCO_2^-	1.70E-02	1.12E-02	5.77E-03
$C_2H_3O_3^-$	NA	<2.65E-03	
OH^-	4.99E-01	5.41E-01	7.13E-01
I^-	NA	NA	2.98E-03
NO_3^-	2.30E+00	2.24E+00	2.47E+00
NO_2^-	8.15E-01	7.87E-01	8.07E-01
$C_2O_4^{2-}$	<1.42E-03	6.44E-03	4.36E-03
PO_4^{3-}	3.48E-02	8.37E-02	7.24E-02
SO_4^{2-}	5.31E-02	5.49E-02	5.51E-02
	Molar	**Molar**	**Molar**
Total Base	1.27E+00	NA	1.59E+00
Other Base Excluding CO_3^{2-}	2.74E-01	NA	4.61E-01
	Wt.%	**Wt.%**	**Wt.%**
Total Solids	30.38	NA	30.16
Dissolved Solids	29.92	NA	NA
Soluble Solids	29.72	NA	NA
Insoluble Solids	0.67	NA	~0
	g/mL	**g/mL**	**g/mL**
Density	NA	1.28	1.25

NA is Not Analyzed.

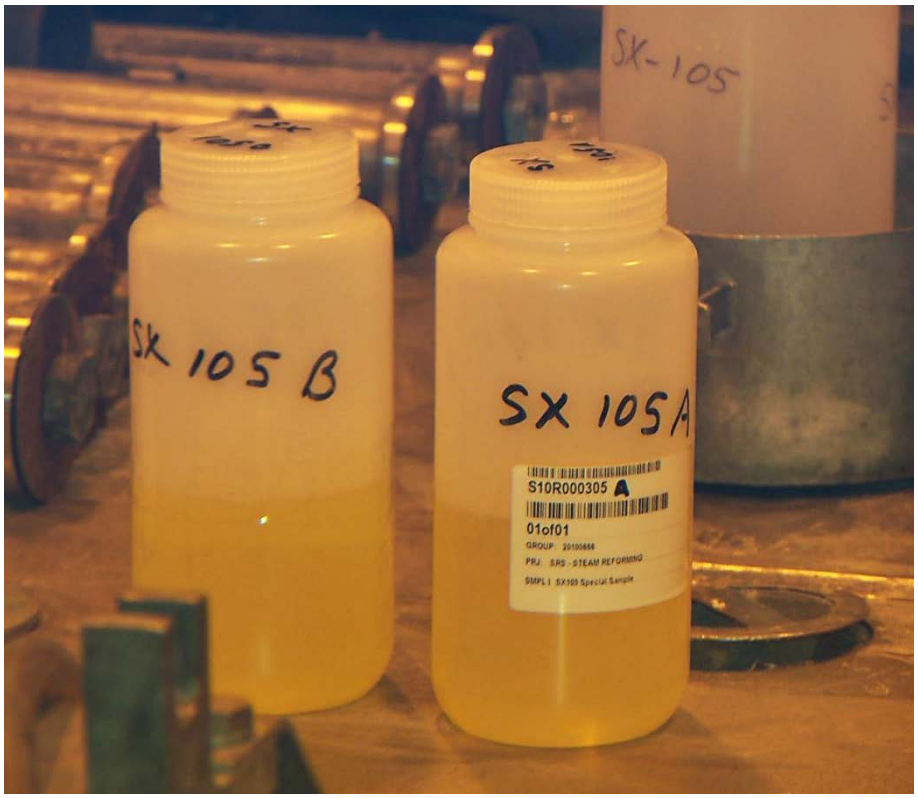

Figure 8-1. As-Received Hanford Tank SX-105 (Module C) Samples

8.1.1.5 *Hanford Tank AN-103 (Module D)*

The Hanford Tank AN-103 samples were also received in two separate bottles that were composited for the SRNL BSR testing. Figure 8-2 provides a picture of the samples after they were unloaded in the Shielded Cells. Table 8-4 provides the analysis of the Hanford AN-103 Tank sample used in Module D testing. The SRNL simulant was prepared based upon the SRNL analysis of this tank sample as the WRPS analysis had been performed on a filtered sample and SRNL was processing an unfiltered sample with the gibbsite precipitates. Both the actual waste sample, which contained approximately 3 wt.% insoluble solids when measured several months after receipt at SRNL, and the Module D simulant had gibbsite, $Al(OH)_3$, solids as determined by XRD analysis (identified by XRD analysis in Reference 4). A programmatic decision was made to process the material through the BSR unit without removing the solids prior to addition of clay, coal, or REDOX tracer Fe nitrate. Again, the significant difference in the Re level between the SRNL and WRPS analyses (Table 8-4) reflects the addition of Re to the sample prior to characterization in SRNL. The concentration of Al^{3+} as determined by SRNL was higher by a factor of 3.5X as SRNL analyzed the sample with the precipitates suspended, while WRPS measured the supernate without the gibbsite solids (Table 8-4 and Figure 6-2).

Since the BSR demonstration was intended to demonstrate that the FBSR technology can process precipitated solids, the analysis and the Module D campaigns were performed with the gibbsite solids present. The rationale was that the solids are expected to behave like the clay additive in the FBSR process, i.e. at the processing temperature the hydroxides from the $Al(OH)_3$ will be stripped and the activated Al^{3+} will react and become part of the mineral product in an identical fashion to how the hydroxides are stripped from the clay additives and become reactive (see

Figure 6-1). The additional Al was accounted for in the MINCALC™ process control spreadsheet as demonstrated in Figure 6-2.

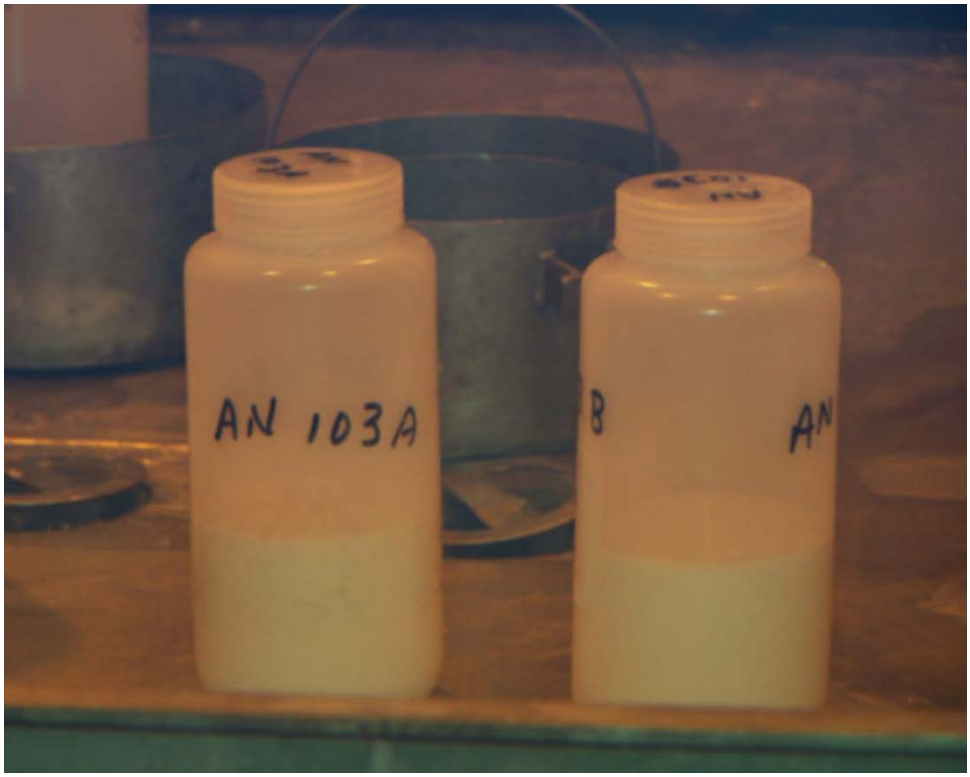

Figure 8-2. As-Received Hanford Tank AN-103 Samples

Table 8-4. Feed Composition for Module D Simulant and Hanford Tank AN-103 after Re Addition but Prior to Clay, Coal, or Fe Addition

Species	SRNL Analysis AN-103	WRPS Analysis AN-103 [174]	SRNL Analysis Simulant D
	Molar	Molar	Molar
Al	1.53E+00	4.41E-01	1.50E+00
B	8.27E-04	<2.77E-03	<7.43E-04
Ba	<4.73E-06	<2.18E-05	<4.77E-06
Be	1.73E-05	<1.11E-04	NA
Ca	3.64E-04	<1.25E-03	7.61E-04
Cd	3.97E-06	<4.45E-05	<6.46E-06
Ce	<5.18E-05	<2.14E-04	<9.90E-05
Co	<2.22E-05	<1.70E-04	<5.12E-05
Cr	3.96E-04	3.69E-04	3.25E-04
Cs	NA	NA	1.19E-04
Cu	3.04E-05	<7.87E-05	<3.62E-05
Fe	6.96E-04	<8.95E-05	1.74E-04
K	7.33E-02	8.90E-02	7.44E-02
La	<7.92E-06	<2.16E-05	<1.74E-05
Li	<2.74E-05	<4.32E-04	<3.85E-04
Mg	8.26E-05	<2.06E--03	2.35E-04
Mn	<2.20E-05	<5.46E-05	<1.02E-05
Mo	2.63E-04	2.79E-04	2.83E-04
Na	5.03E+00	5.18E+00	5.11E+00
Ni	<1.74E-04	<3.41E-04	<1.76E-05
P	1.12E-02	2.39E-02	9.46E-03
Pb	9.07E-06	<2.41E-04	7.24E-05
Re	1.67E-03	2.03E-05	2.14E-03
S	1.37E-02	1.51E-02	1.41E-02
Sb	<9.39E-05	<4.11E-04	NA
Si	7.61E-03	NA	<1.97E-04
Sn	9.73E-03	NA	<6.26E-05
Sr	6.81E-05	<3.42E-05	<4.47E-06
Th	<6.02E-05	9.91E-06	NA
Ti	2.33E-04	<1.04E-04	<2.25E-05
U	9.89E-06	9.62E-06	NA
Zn	1.68E-04	<7.64E-05	<2.97E-05
Zr	1.25E-04	<5.48E-05	<1.10E-05
	Molar	Molar	Molar
^{137}Cs	8.33E-11	9.57E-11	NA
^{99}Tc	2.00E-05	2.04E-05	NA
^{129}I	3.92E-06	5.36E-06	NA

NA is Not Analyzed.

Table 8-4. Feed Composition for Module D Simulant and Hanford Tank AN-103 after Re Addition but Prior to Clay, Coal, or Fe Addition (Continued)

Species	SRNL Analysis AN-103	WRPS Analysis AN-103 [174]	SRNL Analysis Simulant D
	Molar	**Molar**	**Molar**
$C_2H_3O_2^-$	NA	7.79E-03	NA
CO_3^{2-}	2.68E-01	5.55E-02	3.15E-01
Cl^-	6.07E-02	5.92E-02	5.70E-02
Br^-	<1.51E-02	<8.06E-04	<3.00E-03
F^-	<6.37E-03	1.84E-02	<1.26E-02
HCO_2^-	6.98E-03	4.80E-03	6.80E-03
$C_2H_3O_3^-$	NA	<1.39E-04	NA
OH^-	1.91E+00	2.12E+00	2.13E+00
I^-	NA	NA	4.19E-03
NO_3^-	1.03E+00	1.02E+00	9.88E-01
NO_2^-	8.01E-01	7.52E-01	8.03E-01
$C_2O_4^{2-}$	5.95E-03	6.27E-03	5.79E-03
PO_4^{3-}	6.44E-03	7.78E-03	6.61E-03
SO_4^{2-}	8.72E-03	1.16E-02	1.06E-02
	Molar	**Molar**	**Molar**
Total Base	2.82E+00	NA	3.09E+00
Other Base Excluding CO_3^{2-}	4.08E-01	NA	3.03E-01
	Wt.%	**Wt.%**	**Wt.%**
Total Solids	28.33	NA	28.90
Dissolved Solids	26.03	NA	27.03
Soluble Solids	25.22	NA	26.34
Insoluble Solids	3.11	NA	2.57
	g/mL	**g/mL**	**g/mL**
Density	NA	1.27	1.28

NA is Not Analyzed.

8.1.1.6 *Hanford Tank Blend AZ-101/102 (Module E)*

Table 8-5 provides the analysis of the third Hanford Tank sample, a blend of AZ-101 and AZ-102 tank waste, used in Module E and the SRNL simulant that was prepared based upon the SRNL analysis of this tank sample. The tank sample has no visible solids, but there is a minor insoluble solids fraction, 0.09 wt.%, in the Module E simulant that appears to be due to Fe precipitation. Trace complexant materials may also be present that are not fully characterized and are able to solubilize (hydrolyze) all of the measurable Fe (as an iron III hydroxide colloid which ages to other oxides) in the radioactive sample. These complexants are not present in the simulant. Once again, the significant Re level measured by SRNL reflects the addition of Re to both the waste tank sample and simulant prior to characterization.

Table 5-1 summarized the molar anion (SO_4^{-2}, Cl, F, I, P) content to molar sodium content of the Module C and D wastes. The SX-105 Module C waste was considered high anion to sodium LAW, and the AN-103 was considered low anion to sodium LAW. However, AZ-101/AZ-102 was higher in SO_4^{-2} than either SX-105 or AN-103 (compare analyses in Table 8-5 to Table 8-3).

Table 8-5. Feed Composition for Module E Simulant and Hanford Tank Blend AZ-101/AZ-102 after Re Addition but Prior to Clay, Coal, or Fe Addition

Species	SRNL Analysis AZ-101/-102	WRPS Analysis AZ-101/-102	SRNL Analysis Simulant Module E
	Molar	Molar	Molar
Al	2.41E-01	2.30E-01	2.21E-01
B	<6.51E-04	<2.77E-03	<5.56E-05
Ba	<1.72E-05	<2.18E-05	<3.60E-06
Be	<4.88E-05	<1.11E-04	NA
Ca	1.19E-04	<1.25E-03	1.23E-04
Cd	1.25E-05	<4.45E-05	<1.08E-06
Ce	<1.88E-04	<2.14E-04	<7.92E-06
Co	<5.77E-05	<1.70E-04	<4.91E-06
Cr	1.39E-02	1.48E-02	1.39E-02
Cs	NA	NA	3.28E-05
Cu	<8.94E-05	<7.87E-05	1.52E-05
Fe	2.15E-04	1.45E-04	1.55E-04
Hg	NA	5.08E-08	NA
K	9.50E-02	9.36E-02	7.60E-02
La	<1.84E-05	<2.16E-05	<2.18E-06
Li	<9.97E-04	<4.32E-04	5.42E-05
Mg	<4.11E-05	<2.06E-03	8.87E-05
Mn	<1.46E-05	<5.46E-05	<2.85E-06
Mo	6.60E-04	6.47E-04	6.57E-04
Na	5.32E+00	4.92E+00	4.75E+00
Nb	8.24E-04	5.51E-04	2.89E-04
Ni	<1.60E-04	<3.41E-04	<3.36E-06
P	2.47E-02	2.55E-02	2.21E-02
Pb	5.05E-06	<2.41E-04	<4.98E-06
Re	1.70E-03	NA	1.60E-03
S	1.64E-01	1.52E-01	1.56E-01
Si	2.09E-03	2.02E-03	4.49E-03
Sn	1.59E-04	2.73E-04	<2.23E-05
Sr	<3.20E-06	<3.42E-05	7.76E-07
Th	<8.62E-08	<2.15E-04	NA
Ti	1.53E-04	1.35E-04	8.21E-05
U	1.57E-05	<4.20E-04	NA
Zn	<1.35E-05	<7.64E-05	7.62E-06
Zr	6.24E-05	6.85E-05	6.50E-05
	Molar	Molar	Molar
^{137}Cs	4.04E-11	3.18E-11	NA
^{99}Tc	1.87E-04	1.44E-04	NA
^{129}I	1.71E-06	1.89E-06	NA

NA is Not Analyzed.

Table 8-5. Feed Composition for Module E Simulant and Hanford Tank Blend AZ-101/AZ-102 after Re Addition but Prior to Clay, Coal, or Fe Addition (Continued)

Species	SRNL Analysis AZ-101/-102	WRPS Analysis AZ-101/-102	SRNL Analysis Simulant Module E
	Molar	**Molar**	**Molar**
$C_2H_3O_2^-$	NA	2.93E-03	NA
CO_3^{2-}	6.91E-01	1.36E-01	5.69E-01
Cl^-	2.90E-02	3.10E-02	3.05E-02
Br^-	<7.66E-03	<7.26E-04	<5.92E-03
F^-	2.64E-02	7.26E-02	2.56E-02
HCO_2^-	8.21E-03	6.98E-03	<1.05E-02
$C_2H_3O_3^-$	NA	7.70E-04	NA
OH^-	4.70E-01	5.64E-01	3.00E-01
I^-	NA	NA	9.44E-03
NO_3^-	1.09E+00	1.25E+00	1.21E+00
NO_2^-	1.23E+00	1.33E+00	1.34E+00
$C_2O_4^{2-}$	1.38E-02	1.60E-02	1.32E-02
PO_4^{3-}	2.18E-02	2.50E-02	2.42E-02
SO_4^{2-}	1.33E-01	1.61E-01	1.52E-01
	Molar	**Molar**	**Molar**
Total Base	1.31E+00	NA	1.33E+00
Other Base Excluding CO_3^{2-}	2.92E-01	NA	2.99E-01
	Wt.%	**Wt.%**	**Wt.%**
Total Solids	NA	NA	27.53
Dissolved	NA	NA	27.47
Soluble Solids	NA	NA	27.44
Insoluble Solids	0	NA	0.09
	g/mL	**g/mL**	**g/mL**
Density	1.24	1.24	1.23

NA is Not Analyzed.

8.1.2 *Prepare and Analyze the BSR Feed for MINCALC™ Process Control*

The general goals for making BSR slurry feed included preparation of a simulant or actual waste composite, trimming with Rassat-specified reagents to boost levels of various (mainly RCRA) elements, addition of Re, spiking with radioactive isotopes for iodine and technetium tracking and synchrotron analysis (radioactive feeds only), filtration, and slurry makeup. Clay, coal, and ferric nitrate levels were provided by reviewed MINCALC™ spreadsheets and the amounts of each additive are given in Table 8-6. Slurry makeup included OptiKasT® clay (Sagger® XX clay was mixed in for Module D), Bestac® coal, and $Fe(NO_3)_3 \cdot 9H_2O$. The coal addition goal was to provide product within REDOX targets without leaving unused coal as measured by LOI. The ferric nitrate was added to provide 1 to 1.5 wt.% Fe in the granular product to allow determination of the $Fe^{2+}/\sum Fe$ REDOX ratio. Two Simulant B runs had 3 wt.% Fe to check the effect of extra ferric nitrate; both runs were found to make good product.

The simulant for Module B had been specified to be exactly the same as that processed in the ESTD with the increased RCRA metals discussed above. When it was made in the laboratory some of the RCRA metals precipitated and were filtered as discussed above. The filtrate was analyzed by ICP-AES and IC. Clay was added at the calculated MINCALC™ level of 640 g/liter of filtrate for each of two simulant batches. Coal was added at 1-1.3x times the calculated MINCALC™ stoichiometric level.

Radioactive Module B was made starting with a composite of SRS Tank 50 samples. The 2.4 L of Tank 50 material was trimmed with Rassat reagents to levels given in Table 8-2. The batch was heated to between 50°C and 70°C and agitated overnight so that reagents would have time to dissolve. As expected the batch contained significant solids as described above that did not dissolve overnight. All of the material was filtered and the 2.4 L of filtrate was spiked with ^{99}Tc, ^{125}I, and ^{129}I for further work. After further sampling the (now 2.1 L) batch had 1370 g of OptiKasT® clay (652g/L clay x 2.1L), 292 g of Bestac® coal, and 120 g $Fe(NO_3)_3 \cdot 9H_2O$ added to make the final slurry. After five runs, it was found that REDOX could not be increased from near zero and the coal content was raised from 1.0x to 1.3x the stoichiometric MINCALC™ value in order to adjust the "Gas REDOX". Radioactive Module B provided good product consistently at the 1.3x coal level as noted in Table 8-6 and the accompanying footnotes for exceptions. It is noted that the calculation for the coal addition considers reduction of the nitrate added as the ferric salt, since this significant oxidizing capacity must also be reduced. The slurry was diluted as needed in further runs when viscosity was found to be too high for feeding.

Module C showed the need to increase the coal level from 1.3x to 2.3x the stoichiometric MINCALC™ value for simulant work because of difficulties in balancing REDOX and LOI for this feed. The use of the 1.3x stoichiometric coal value for simulant work was abandoned in favor of higher coal loadings because only one run in the first nine BSR campaigns gave the desired product REDOX. Radioactive Module C often provided on-spec product (REDOX/LOI) at the 1.3x coal level, but higher coal levels were also run.

Module D simulant work started out with only Sagger® XX clay based on the low alumina value in Table 8-4 WRPS analyses but then moved to a mixture of Sagger® XX and OptiKasT® clays when a higher alumina value was determined at SRNL, i.e. MINCALC™ was recalculated. Only the Simulant D granular product produced from the dual clay mixture was used in the final composite material. Radioactive Module D was thus run with the same mixture of the two clays. Simulant D most often provided on-spec product (REDOX/LOI) at the 1.9x level of coal. All runs for Radioactive Module D were at 2.25x stoichiometric for coal.

The levels of clay per liter of LAW, the target coal concentrations, amount of ferric nitrate nona-hydrate and the waste loading, expressed on a dry calcine basis and as wt% Na_2O are summarized in Table 8-6. More details are given in References 3 and 4.

Table 8-6. Feed Slurry Composition from MINCALC™

Module	Target Clay g/L of Initial Solution	Target Coal g/L of Initial Solution	$Fe(NO_3)_3 \cdot 9H_2O$ g/L of Initial Solution	Waste Loading (Dry Calcine Oxide/Anion Basis) wt. %	Waste Loading (Na_2O Calcine Basis) wt.%
Sim B	640 OptiKasT®	139.0 for 1x	64.50	24.5	21.15
Rad B	652 OptiKasT®	139.0 for 1x 180.7 for 1.3x[e]	57.14	26.0	21.54
Sim C	660 OptiKasT®	255.7 for 2.3x[a]	64.50	25.5	20.52
Rad C	660 OptiKasT®	151.1 for 1.5x[a]	64.50	25.8	20.96
Sim D Batch 1-4	551.4 SaggerXX®	94.27 for 1.9x[b,c]	64.50	33.0	20.10
Sim D Batch 5-6	241.1 Sagger® XX, 294.7 OptiKasT®	94.27 for 1.9x[b,c]	64.50	34.0	21.96
Rad D	241.1 Sagger® XX, 294.7 OptiKasT®	94.27 for 1.9x[b,c]	64.50	33.9	21.67
Sim E	550.8 OptiKasT®	95.36 for 1.3x	64.50	28.0	21.52
Rad E (calculated)	611.8 OptiKasT®	86.55 for 1.3x	64.50	27.5[d]	21.91[d]

[a] At the time of the Module C simulant and radioactive campaigns, the anion analyses from SRNL were not available for the coal determinations. The coal requirement for denitration was based on the radioactive nitrate/nitrite analyses provided by WRPS: the coal target for Simulant C was 2.33x and the coal target for Rad C was 1.3x as discussed in the text but when the SRNL analyses became available the coal requirement was recalculated as given in this table.

[b] At the time of the Module D simulant and radioactive campaigns, the anion analyses from SRNL were not available for the coal determinations. The coal requirement for denitration was based on the radioactive nitrate/nitrite analyses provided by WRPS: the coal target for Simulant and Rad D was 1.3x as discussed in the text but when the SRNL analyses became available the coal requirement was recalculated as given in this table.

[c] The nitrate from the ferric nitrate nona-hydrate used as a REDOX indicator was included in the coal calculations for the Mod D campaigns but not for the Mod C and E campaigns: all values in this table were recalculated based on the SRNL analyzed nitrite and nitrate values only for consistency.

[d] The calculation was performed but no BSR campaigns were performed.

[e] After five runs of radioactive Module B at 1x coal, where the 1X is the amount calculated to force all the nitrates and nitrites to N_2, it was found that REDOX could not be increased from near zero. The coal content was raised from 1.0x to 1.3x the stoichiometric MINCALC™ value in order to adjust the "Gas REDOX" discussed in Section 7.1.1 and 7.1.3. Radioactive Module B provided good product consistently at the 1.3x coal level. It is noted that the calculation for the coal addition considers reduction of the nitrate added as the ferric salt, since this has significant oxidizing capacity that must also be reduced. The slurry was diluted as needed in further runs when rheoloy was found to be too high for feeding.

The feed targets given in Table 8-6 were projected to give the mineral phases in Table 8-7 based on MINCALC™. All modules make mostly nepheline $(Na,K)AlSiO_4$ in the 78-86 wt.% range except for Module E, which makes about 55-65 wt% nepheline as the SO_4^{-2} creates ~ 22 wt.% nosean ($Na_6Al_6Si_6O_{24} \bullet Na_2SO_4$). Module D made the highest amount of nepheline and the lowest amount of nosean, while module E made the highest amount of nosean and the lowest amount of nepheline. At the bottom of Table 8-7, the relative weight percentages of $(Na,K,Li,Cs,Rb)O_2$, SiO_2, and Al_2O_3 are given along with the relative weight percentages of these components in the target AN-107 region of Figure 6-2. It can be seen from the weight concentrations achieved for all the LAW BSR campaigns that MINCALC™ controlled each campaign within ±1.5 wt.% of

each component. It should be noted that in Table 8-7 it is shown that the BSR Rassat simulant composition was similar to the ESTD simulant composition and that the predicted mineralogy given in Table 8-7 was the same. This will also be discussed in Section 8.2.3 where the results of the mineralogy testing are given.

8.1.3 *BSR Granular Product Characterization: Composition, LOI, and REDOX*

The REDOX of certain species in the FBSR process and product were under study as discussed in Section 8.2.8 to see if REDOX impacted off-gas carryover of COCs or if REDOX impacted product durability. Based on the REDOX EMF series shown in Figure 8-29, one can calculate the relative amounts of Re^{+7} versus Re^{+4} and SO_4^{-2} available to form the various sodalite mineral phases (Table 8-8). Thus, the REDOX values were determined to confirm that the conditions achieved during BSR processing were consistent with the target conditions from the FBSR ESTD campaigns (Table 7-1).

The composite REDOX ratio, coal content (LOI-LOD difference), and mineralogy were measured on a Turbula® mixed composite of the "on-spec" granular product. Material with too high a coal content (LOI-LOD difference) and/or too high or low a REDOX ratio were segregated from the composite and are given in the table as "off-spec" material. The high coal content samples were rejected because high coal content can impact the REDOX measurement. The high and low REDOX samples were rejected as they were not in the REDOX range of the Engineering-scale (ESTD) tests that the BSR was emulating

Unreacted coal is not removed before the $Fe^{+2}/\Sigma Fe$ (REDOX ratio) is measured colorimetrically.[175] If the unreacted coal is present at >10 wt.%, interference can occur with the measurement of the REDOX ratio by the colorimetric procedure. For this reason, the unreacted coal concentration was kept as low as reasonably achievable in all the BSR Modules. For Module B, the coal as measured by the LOI was <2 wt.%, for Module C the coal was <4 wt.% and for module D the coal was <6 wt.% (Table 8-8 and Table 8-9).

The target range for the REDOX ratio and coal content (LOI-LOD difference) evolved as the program modules progressed. For instance during Module B, there was an effort to keep the coal content (LOI-LOD) below 2 wt.%, but this was not possible to achieve during Module D where a larger residual carbon content is observed in both the "on-spec" and "off-spec" granular products. The initial BSR REDOX target was between 0.4-0.6 $Fe^{+2}/\Sigma Fe$. The initial target range is the same as that for the 2008 pilot-scale test such that the mineral products produced in the BSR tests are representative of the 2008 testing (Table 7-1). The "on-spec" target REDOX ratio was maintained in the 0.1 – 0.5 range across Modules B and C. In Module D, the "on-spec" REDOX ratio was increased to a minimum of 0.2, while holding the 0.5 upper REDOX ratio for the reasons discussed above.

Table 8-7. Mineral Speciation for Non-Radioactive and Radioactive Module B, C, D, and E Predicted from MINCALC™-Version 3*

Mineral Component	Chemical Component	Module B (Rassat LAW Blend)			Module C (SX-105)		Module D (AN-103)		Module E (AZ-101/AZ-102)	
		TTT/HRI (wt.%)	BSR Simulant[a,b,c] (wt.%)	BSR Radio-active[a,b,c] (wt.%)	BSR Simulant (wt.%)	BSR Radio-active (wt.%)	BSR Simulant (wt.%)	BSR Radio-active (wt.%)	BSR Simulant (wt.%)	BSR Radio-active (wt.%)
Na Nepheline	$Na_2Al_2Si_2O_8$	68.47	72.30	71.78	81.86	82.35	86.87	85.13	55.31	64.91
K Nepheline	$K_{0.5}Na_{1.5}Al_2Si_2O_8$ or $K_2Na_6Al_8Si_8O_{32}$	2.47	2.45	2.52	2.48	3.12	9.17	9.10	8.03	8.93
Cl Sodalite	$Na_8Al_6Si_6O_{24}(Cl_2)$	2.89	2.97	3.67	3.22	4.50	3.43	4.11	2.21	1.90
F Sodalite	$Na_8Al_6Si_6O_{24}(F_2)$	2.02	2.07	1.19	BDL	BDL	BDL	0.42	1.79	1.67
I Sodalite	$Na_8Al_6Si_6O_{24}(I_2)$	1.20	0.001	1.15	0.26	2.54E-04	0.398	3.73E-04	0.96	0.0002
Nosean (SO_4-S_2 Sodalite)	$Na_8Al_6Si_6O_{24}(SO_4)$	12.18	12.51	11.68	7.11	6.81	1.47	1.21	22.56	17.90
Re Sodalite	$Na_8Al_6Si_6O_{24}(ReO_4)_2$	0.16	0.04	0.16	0.21	0.22	0.22	0.17	0.18	0.17
Tc Sodalite	$Na_8Al_6Si_6O_{24}(TcO_4)_2$	---	---	0.0006	---	3.54E-07	---	1.84E-03	---	1.47E-02
Free Silica	SiO_2	4.40	2.82	2.21	0.80	-0.17	-3.31	-2.63	2.03	0
Free Alumina	Al_2O_3	2.73	1.41	2.17	1.77	0.88	-0.87	-0.12	2.01	0.28
SUM		96.54	96.54	96.54	97.70	97.88[f]	101.57[f]	100.14[f]	95.09	95.77
$g_{(wet\ clay)}/L_{LAW}$		640	640	652		660	535	535	551	612
Type of Clay		OptiKasT™			OptiKasT™		45 wt% Sagger 55 wt% OptiKast™		OptiKasT™	
Na Molarity		5.02	5.05	5.36	5.13	5.34	5.11	5.03	4.75	5.32
AN-107 Target	**Normalized Wt.% In Ternary Phase Diagram (Wt.%) –** Figure 6-2									
41	SiO_2	42.70	42.36	41.66	41.66	41.44	40.29	40.35	41.00	40.87
24	$(Na,K,Li,Cs,Rb)O_2$	22.11	22.71	22.69	21.86	22.34	23.52	23.25	23.91	24.16
35	Al_2O_3	35.19	34.93	35.65	36.48	36.21	36.18	36.40	35.09	34.97

[a] RCRA metals (Sb, As, Ag, Cd, Ba, and Tl) and radionuclide surrogates (Re, I, Cs) were doped in at elevated concentrations

[b] LAW simulant used to produce the FBSR samples were based on Rassat et al. [109]

[c] Projections of mineralogy based on "as made" waste simulants as clay additions had to be performed before analysis of the simulants were complete

* Without any contributions from the ferric nitrate nona-hydrate REDOX indicator or the IOC since the mineral calculations do not include the potential substitution of Fe for Al in nepheline and the sodalites and the IOC forms iron rich spinels

f Sums without negative numbers

Table 8-8. LOI, REDOX and Speciation of Re and SO_4

Waste	Sample	LOI (%)	$Fe^{+2}/\Sigma Fe$	Re^{+7} (%)	SO_4 (%)
Module B HRI/TTT P-1B (Rassat Simulant)	PR	0-2.0	0.41-0.6	94	86
Module B (Rassat Simulant)	Simulant	1.14	0.36	98	99
	Radioactive	1.03	0.41	96	96
	Radioactive Tc-99 Spike "on-spec"	0.49	0.37	98	99
	Radioactive Tc-99 Spike "off-spec"	1.72	0.64	67	5
Module C (Tank SX-105)	Simulant	1.32	0.34	98	99
	Radioactive	3.50	0.17	100	100
	Radioactive Tc-99 Spike	3.35	0.39	97	98
Module D (Tank AN-103)	Simulant	1.62	0.30	99	100
	Radioactive	6.22	0.18	100	100
Module E (Tank AZ101/AZ102)	Simulant with IOC	0.70	0.13	100	100
	Simulant without IOC	1.15	0.06	100	100

Table 8-9. Summary of On-Spec and Off-Spec Granular Product Redox ($Fe^{2+}/\sum Fe$), LOI-LOD, and Mineralogy for BSR Module B, C and D

Module	Type	Composite $Fe^{2+}/\sum Fe$	Range of $Fe^{2+}/\sum Fe$	Composite LOI-LOD	Range of LOI-LOD	Composite Mineralogy	Range of Mineralogy
Simulant Module B (Rassat)	*On-Spec*	0.36	0.176 – 0.437	1.14%	0.23 – 1.77%	Nepheline (H) Nepheline (O) Nosean Anatase	Nosean, Nepheline (H) Nepheline (O) Sodalite Anatase, Quartz
	Off-Spec	*NA*	0.000 – 0.846	NA	0.05 – 3.59%	NA	Nepheline (H) Nepheline (O) Nosean Sodalite Anatase, Quartz
Radioactive Module B (SRS LAW)	*On-Spec*	0.41	0.164 – 0.537	1.03%	0.00 – 1.68%	Nepheline (H) Nepheline (O) Nosean Anatase	Nepheline (H) Nepheline (O) Sodalite Nosean, Anatase
	Off-Spec	*NA*	0.356 – 0.707	NA	0.70 – 2.38%	NA	Nepheline (H) Nepheline (O) Sodalite Nosean Anatase
Simulant Module C	*On-Spec*	0.343	0.194 – 0.414	1.32%	0.50 – 1.90%	Nepheline (H), Nepheline (O), Sodalite, Quartz, Anatase	Nepheline (H), Nepheline (O), Sodalite, Anatase, Quartz
	Off-Spec	*NA*	0.000 – 0.493	NA	0.12 – 8.09%	NA	Nepheline (H), Nepheline (O), Nosean, Sodalite, Anatase, Quartz
Radioactive Module C (SX-105)	*On-Spec*	0.165	0.090 – 0.522	3.50%	0.29 – 4.75%	Nepheline (H), Nepheline (O), Sodalite	Nepheline (H), Nepheline (O), Sodalite, Anatase, Quartz
	Off-Spec	*NA*	0.000 – 0.933	NA	2.48 – 6.89%	NA	Nepheline (H), Nepheline (O), Nosean, Sodalite, Anatase, Quartz
Simulant Module D	*On-Spec*	0.302	0.123 – 0.427	1.62%	0.88 – 2.03%	Nepheline (H), Nepheline (O), Quartz, Sodalite(Cl), Nosean	Nepheline (H), Nepheline (O), Sodalite(Cl), Nosean, Anatase, Quartz
	Off-Spec	*NA*	0.099 – 0.109	NA	0.51 – 0.76%	NA	Nepheline (H), Nepheline (O), Sodalite(Cl), Sodalite, Nosean, Quartz
Radioactive Module D (AN-103)	*On-Spec*	0.184	0.201 – 0.500	6.22%	2.33 – 6.27%	Nepheline (H), Nepheline (O), Quartz, Anatase, Sodalite	Nepheline (H), Nepheline (O), Sodalite(Cl), Sodalite, Nosean, Anatase, Quartz
	Off-Spec	*NA*	0.102 – 0.855	NA	2.88 – 5.22%	NA	Nepheline (H), Nepheline (O), Sodalite(Cl), Sodalite, Anatase, Quartz

Where Nepheline (H) is hexagonal $NaAlSiO_4$ (PDF 00-035-0424)
Nepheline (O) is orthorhombic $NaAlSiO_4$ which "may be synthetic low-carnegieite" [69] (PDF-00-052-1342)
Nosean is cubic $Na_8Al_6Si_6O_{24}SO_4$ (PDF 01-072-1614)
Sodalite is cubic $Na_8Al_6Si_6O_{24}Cl_2$ (PDF 00-037-0476)
Anatase is TiO_2 (PDF 00-021-1272)
Quartz is SiO_2 (PDF 00-046-1045)

The unreacted coal also does not contribute to the composition of the mineral product. Therefore, unreacted coal is removed before chemical analysis of the FBSR product. This can be done physically by (1) removing large coal manually, (2) roasting the coal out in an oxidized atmosphere, or (3) determining the amount of coal in the sample, performing the analysis with the coal present and then normalizing the composition mathematically for the coal content. Comparative studies have been performed at SRNL with methods 1-3 and the same compositions are achieved.[111]

Comparative studies have been performed at PNNL of roasted and unroasted samples and the same compositions were achieved.[105] Heating to remove the carbon was chosen as the preferential method of coal removal before analysis because it was a more thorough removal method and adaptable for the filter fines, i.e., hand removal of the carbon in the filter fines would be impossible due to the small size. Samples before and after this heating were examined by XRD to verify that the phase assemblages had not changed.[111]

In order to remove the coal by roasting first the Loss-on-Drying (LOD) is measured as the weight loss at 110°C from adsorbed water. The LOI is then performed at 525°C in air by heating the samples to 525°C overnight. This temperature was chosen because it is high enough to oxidize (remove) the carbon, but not high enough to change the composition or the phase assemblages. This is the temperature specified in a United States Geological Survey (USGS) procedure [176] for carbon removal in preparation for the analysis of coal combustion by-products. Samples before and after this heating were examined by XRD to verify that the phase assemblages had not changed.

Table 8-10 provides the analyses for Module B Rassat Tank Blend simulant from the ESTD campaigns. Table 8-11 provides the analyses for Module B simulant and radioactive granular product, while Table 8-12 provides the analyses for Module C and D simulant and radioactive granular product. The measured granular product densities are also provided, which are consistently in the 2.4 – 2.6 g/cc range. Many of the simulant constituents are listed as not present (NP) in the table and were not part of the simulant feed to the BSR. The Fe detected in the simulant product was not in the simulant feed but was added as the $Fe(NO_3)_3 \cdot 9H_2O$ component for REDOX measurements and is also present at trace levels in the added clay.[122] The Ti constituent in the simulant product was not analyzed for in the suite of metals from ICP-AES on dissolved simulant product but is derived from trace levels in the added clay.[122]

A comparison of the compositions measured by PNNL [132] and SRNL (Table 8-10, Table 8-11, and Table 8-12) for the ESTD P-1B Rassat Tank Blend, the BSR Rassat Tank Blend, and the radioactive SX-105 granular product are given in Table 8-13. In general, there is good agreement between the whole element analyses of the different laboratories but PNNL's values appear biased slightly lower than SRNL's analyses. The SiO_2 content of the BSR Rassat Tank Blend appears to be in error as it is low by about 10 wt.%. PNNL only provided a partial analysis for the radioactive SX-105 and they did not tabulate the LOI or LOD of each sample.

It should be noted that both "on-spec" and "off-spec" granular products had the same mineral phases, and hence this factor was not a discriminating characteristic. The composite mineralogy of the Turbula® mixed "on-spec" and "off-spec" FBSR products are given in Table 8-7 for the Module B, C, D simulant and radioactive campigns. The range of mineralogy observed over the individual campaigns that were combined in the "on-spec" and "off-spec" products is also given in Table 8-7. In most cases, the major phases are the same and only minor phase identifications differ. The major phases were primarily, nepheline, sodalite and nosean as expected from

MINCALC™. The mineralogy will be discussed in detail in Section 8.2.3 since it is a required Waste Form Performance criterion from Table 5-4.

Table 8-10. Analyses of ESTD FBSR Granular Products from Reference 123

Form	7-kg bag (08-1713)			Bucket (08-1714)		
Sample	P-1B (A)	P-1B (B)	Average	P-1B Bucket 1/5 (A)	P-1B Bucket 1/5 (B)	Average
	(wt.%)	(wt.%)	(wt.%)	(wt.%)	(wt.%)	(wt.%)
Ag_2O	0.04	0.04	0.04	0.04	0.04	0.04
Al_2O_3	34.39	34.58	34.48	34.77	34.96	34.86
As_2O_3	<0.26	<0.26	<0.26	<0.26	<0.26	<0.26
B_2O_3	<0.32	<0.32	<0.32	<0.32	<0.32	<0.32
BaO	0.13	0.13	0.13	0.13	0.13	0.13
CaO	0.06	0.06	0.06	0.06	0.06	0.06
CdO	0.05	0.05	0.05	0.05	0.05	0.05
Cl	0.23	0.2	0.22	0.21	0.22	0.21
Cr_2O_3	0.1	0.1	0.1	0.1	0.1	0.1
Cs_2O	0.24	0.22	0.23	0.18	0.18	0.18
F	<0.20	<0.20	<0.20	<0.20	<0.20	<0.20
Fe_2O_3	1.72	1.57	1.64	2.29	2.3	2.29
I	0.18	0.18	0.18	0.18	0.18	0.18
K_2O	0.23	0.22	0.23	0.22	0.23	0.22
MgO	0.02	0.02	0.02	0.02	0.03	0.03
MnO_2	<0.02	<0.02	<0.02	<0.02	<0.02	<0.02
Na_2O	19.95	20.49	20.22	20.89	20.62	20.76
NiO	0.1	0.09	0.09	0.1	0.1	0.1
PO_4	0.81	0.81	0.81	0.81	0.83	0.82
PbO	0.16	0.15	0.16	0.16	0.17	0.17
ReO_2	0.05	0.05	0.05	0.04	0.04	0.04
SO_4	1.55	1.5	1.53	1.47	1.46	1.47
Sb_2O_3	0.08	0.08	0.08	0.08	0.08	0.08
SeO_2	<0.01	<0.01	<0.01	<0.01	<0.01	<0.01
SiO_2	39.58	40	39.79	40	40.43	40.22
SrO	<0.01	<0.01	<0.01	<0.01	<0.01	<0.01
TiO_2	<1.14	<1.11	<1.12	<1.12	<1.15	<1.13
Tl	<0.01	<0.01	<0.01	<0.01	<0.01	<0.01
ZnO	<0.01	<0.01	<0.01	<0.01	<0.01	<0.01
Total	100.99	101.87	101.43	103.12	103.57	103.34
Coal	0.79 wt.%			1.72 wt.%		
Skeletal Density	2.39 g/cc			2.39 g/cc		
$Fe^{2+}/\Sigma Fe$	0.50			0.50		

Table 8-11. BSR Granular Product Analyses for Simulant and Radioactive Module B Samples

Species	Granular Product Simulant B (wt.%)	Granular Product Radioactive B (wt.%)
Al	1.77E+01	1.86E+01
As	1.37E-02	<9.92E-04
B	NP	1.18E-02
Ba	2.74E-03	6.94E-03
Ca	NP	1.63E-01
Cd	<2.00E-04	<9.24E-04
Ce	NP	<9.46E-03
Co	NP	9.16E-04
Cr	6.83E-02	6.77E-02
Cs	2.23E-01	1.01E-03
Cu	NP	2.26E-03
Fe	7.32E-01*	1.28E+00
K	1.34E-01	1.36E-01
La	NP	2.29E-03
Li	NP	<5.45E-03
Mg	NP	3.83E-02
Mn	<2.00E-04	1.09E-03
Mo	NP	<4.52E-03
Na	1.50E+01	1.56E+01
Ni	<2.00E-03	5.17E-03
P	2.44E-01	2.08E-01
Pb	5.04E-02	1.32E-01
Re	3.64E-02	3.62E-02
S	3.61E-01	4.35E-01
Sb	<2.00E-04	6.05E-03
Se	<2.00E-03	7.85E-03
Si	1.82E+01	1.87E+01
Sn	NP	<3.10E-03
Sr	NP	3.50E-03
Th	NP	1.73E-03
Ti	NP/NA	7.81E-01
U	NP	<9.02E-04
Zn	<2.00E-04	2.39E-03
Zr	2.26E-02	2.31E-03
^{137}Cs	NP	7.04E-07
^{99}Tc	NP	2.79E-05
^{129}I	NP	8.70E-04
Cl^-	2.10E-01	1.97E-01
Br^-	NP	NA
F^-	<5.00E-02	<9.84E-02
HCO_2^-	NP	NA
I^-	1.18E-01	6.32E-02
NO_3^-	<1.00E-01	<9.84E-02
NO_2^-	<1.00E-01	<9.48E-02
$C_2O_4^{2-}$	NA	<9.84E-02
PO_4^{3-}	4.34E-01	4.46E-01
SO_4^{2-}	1.31E+00	1.17E+00
	g/cc	**g/cc**
Density	2.39	2.59

NP – Constituents not added to simulant feed, NA – Not Analyzed
NP/NA – Ti was not added to simulant feed but is present in the simulant granular product from the added clay,
*Fe – Fe was not added to simulant feed but is present in the simulant granular product from both the added $Fe(NO_3)_3 \cdot 9H_2O$ and the added clay

Table 8-12. Granular Product Analyses for Simulant and Radioactive Module C and D Samples

Species	Module C – Tank SX-105		Module D - Tank AN-103	
	Radioactive	Simulant	Radioactive	Simulant
	Wt.%	Wt.%	Wt.%	Wt.%
Al	1.86E+01	1.77E+01	1.84E+01	1.67E+01
As	NA	NA	<1.08E-03	NA
B	1.42E-02	5.93E-03	1.15E-02	5.19E-03
Ba	4.93E-03	4.84E-03	1.18E-02	9.97E-03
Ca	4.05E-02	1.00E-01	6.14E-02	1.16E-01
Cd	<1.01E-03	<5.57E-04	6.89E-04	<1.06E-04
Ce	5.80E-03	<3.28E-03	6.27E-04	6.32E-03
Co	<9.35E-04	<6.72E-04	1.22E-03	<4.42E-04
Cr	1.38E-01	1.20E-01	1.35E-02	1.13E-02
Cs	high blank	6.84E-04	1.58E-04	*~1.35E-02*
Cu	6.60E-03	3.72E-03	7.30E-03	<4.92E-03
Fe*	1.38E+00	1.35E+00	1.76E+00	1.48E+00
K	1.88E-01	1.57E-01	5.71E-01	5.27E-01
La	3.29E-03	3.02E-03	4.05E-03	3.88E-03
Li	5.61E-03	4.37E-03	5.51E-03	2.95E-03
Mg	1.55E-02	1.95E-02	5.48E-02	5.45E-02
Mn	1.04E-03	8.33E-04	1.40E-03	1.14E-03
Mo	<4.92E-03	<1.35E-03	<4.86E-03	3.64E-03
Na	1.58E+01	1.52E+01	1.57E+01	1.57E+01
Ni	<7.31E-03	2.40E-03	<3.59E-03	2.09E-03
P	3.88E-01	3.16E-01	6.04E-02	4.55E-02
Pb	1.35E-03	<3.05E-03	2.64E-03	5.59E-03
Re	2.69E-02	4.70E-02	3.47E-02	4.69E-02
S	2.66E-01	2.92E-01	1.41E-01	1.22E-01
Sb	6.27E-03	NA	<8.25E-02	NA
Se	<2.16E-03	NA	<2.17E-03	NA
Si	1.89E+01	1.85E+01	1.75E+01	1.77E+01
Sn	<3.37E-03	<1.56E-03	<4.42E-03	<8.08E-04
Sr	2.93E-03	3.11E-03	7.68E-03	6.74E-03
Th	1.55E-03	NA	1.40E-03	NA
Ti	7.69E-01	7.33E-01	7.91E-01	8.15E-01
U	2.90E-04	NA	6.28E-04	NA
Zn	5.33E-03	2.65E-03	5.59E-03	2.21E-03
Zr	3.04E-03	<2.49E-03	5.70E-03	4.43E-03
^{137}Cs	1.66E-08	NA	3.04E-08	NA
^{99}Tc	3.99E-04	NA	2.23E-04	NA
^{129}I	3.01E-05	NA	4.68E-05	NA

NA – Not Analyzed, *Fe – Iron constituent was not added to simulant feed but is present in the simulant granular product from both the added $Fe(NO_3)_3 \cdot 9H_2O$ and the added clay; italicized numbers estimated from data in Table 8-7 and waste loading from Table 8-6

Table 8-12. Granular Product Analyses for Simulant and Radioactive Module C and D (Continued)

Species	Module C – Tank SX-105		Module D - Tank AN-103	
	Radioactive	Simulant	Radioactive	Simulant
	Wt.%	Wt.%	Wt.%	Wt.%
Cl^-	2.31E-01	2.06E-01	2.12E-01	2.27E-01
Br^-	NA	NA	NA	<9.46E-02
F^-	<5.02E-02	<2.13E-01	<4.69E-02	<9.46E-02
HCO_2^-	NA	NA	NA	<9.46E-02
I^-	NA	3.17E-02	NA	7.90E-02
	Wt.%	Wt.%	Wt.%	Wt.%
NO_3^-	<5.02E-02	<2.13E-01	<4.69E-02	<9.46E-02
NO_2^-	<5.02E-02	<2.13E-01	<4.69E-02	<9.46E-02
$C_2O_4^{2-}$	7.37E-02	<2.13E-01	<4.69E-02	<9.46E-02
PO_4^{3-}	9.64E-01	9.27E-01	1.81E-01	<4.73E-01
SO_4^{2-}	6.43E-01	6.71E-01	2.56E-01	<9.46E-02
	g/cc	g/cc	g/cc	g/cc
Density	2.60	2.49	NM	NM

NA – Not Analyzed, NM – Not Measured

Table 8-13. Comparison of Analyses of Granular Products Between SRNL and PNNL

Component (Wt.%)	P-1B Granular Rassat LAW Tank Blend From ESTD SIMULANT		BSR Granular Rassat LAW Tank Blend from BSR SIMULANT		LAW1 Granular LAW SX-105 RADIOACTIVE	
	PNNL [132]	SRNL*,**	PNNL [132]	SRNL*	PNNL [132]	SRNL*
Al_2O_3	31.74	34.48	32.50	33.44	32.50	35.14
Na_2O	19.01	20.22	19.55	20.22	19.14	21.30
SiO_2	38.51	39.79	38.94 [3]	38.94	40.43 [4]	40.43
$^{89}ReO_2$	0.02	0.05	0.04	0.04	0.02	0.03
TcO_2	NA	NA	NA	NA	5.2E-04	5.3E-04
I	0.06	0.18	0.07	0.12	NM	0.03
Cs_2O	0.14	0.23	0.30	0.13	NM	1.76E-08
SO_4	1.29	1.53	1.08	1.08	0.67	0.64
PbO	0.23	0.16	0.11	0.26	0.13	BDL
Fe_2O_3	2.43	1.64	1.43	1.05	1.72	1.97
Cr_2O_3	0.12	0.10	0.09	0.10	0.12	0.20
BaO	0.17	0.13	0.02	0.003	NM	5.50E-03
Coal	1.31	0.79	1.12 [3]	1.12	NM	2.26
moisture	0.35	0.27	0.31 [3]	0.31	1.32	1.30
SUM	95.38	99.57	95.54	96.81	96.05	103.27

*SRNL measured many other cations (see Table 8-10, Table 8-11, and Table 8-12) but PNNL did not; BDL means below detection limit; NM is not measured; NA is not applicable. ** Table 8-10 bag analysis

8.2 Waste Form Performance Testing (Granular Product)

The waste form performance will be discussed in the order in which the items appear in Table 5-4. The attributes of the FBSR granular product will be discussed in Section 8.2 and the attributes of the monolithic FBSR product, including the fabrication of the geopolymer monoliths, will be discussed in Section 9.0.

8.2.1 *Mass Balance*

Determining the disposition of key contaminants within a treatment process is a critical consideration for any technology selection process. Previous FBSR engineering-scale tests (ESTD) with LAW simulants indicated that >99.99% of the nonradioactive surrogates for ^{99}Tc and ^{137}Cs and >94% of the ^{129}I surrogate were captured in the mineral product and not released to the off-gas treatment system. The BSR is a simpler design than the ESTD facility in Golden, CO and so it is easier to perform a mass balance. For the radioactive BSR tests, mass balance data have been obtained for ^{99}Tc, ^{129}I, ^{125}I, ^{137}Cs and rhenium. This includes analyzing the granular product, liquid condensate, off-gas filters, and rinse solutions from the post-test cleanout of the BSR apparatus.

The key input and output streams for the mass balances for all the campaigns are given in Table 8-15 and Table 8-16. Due to the timing of the radioactive experiments and the limitations in the Shielded Cells Facility, no seal pot samples were collected for Module B (simulant or radioactive). As the program evolved, more portions of the BSR system were included in the mass balance and oxidizing rinsates were used instead of less aggressive deionized water to make the mass balance all inclusive.

The mass balance calculational approach for the Rassat 68 tank blend (Module B) simulant and radioactive campaigns consisted of identifying key input and output streams and then analyzing these streams for key species. Before each radioactive module, a simulant module was performed to identify the proper control parameters and sampling techniques. The mass balance streams that could be analyzed for the simulant campaigns were greater due to the limitations of the radioactive systems, i.e., accessibility to various streams given the physical constraints of the cells operations.

The output streams for the simulant Module C runs were the solid granular product, the cross bar rinse/solids, the DMR condenser/bubbler drains, and the seal pot drains/rinses. The output streams for the Radioactive Module C runs were the solid granular product, the cross bar rinse/solids, and the DMR condenser/bubbler drains.

For Module D simulant runs, more output streams were analyzed than the previous campaigns to try to close the mass balance more tightly. To try to capture more of the metal species for a better mass balance, a special solution of 5 wt.% HNO_3, 10 wt.% H_2O_2, 85 wt.% deionized water (hereafter referred to as the Oxidizing Solution) was prepared for Module D. This Oxidizing Solution was used for special rinses of the DMR condenser/bubbler and seal pot legs at the end of the Module D experiments. After the Oxidizing Solution rinse of the DMR condenser/bubbler, a 95 wt.% ethanol solution was used to rinse out the DMR condenser/bubbler to try to capture and characterize the black solids present for Module D. The various output streams for the Simulant Module D runs were the solid granular product, the cross bar solids, the DMR condenser/bubbler drains and Oxidizing Solution rinses, DMR Basket Oxidizing Solution rinses, the seal pot drains and Oxidizing Solution rinses, and the off-gas micron filters.

A special Simulant Module D run was performed to better quantify the masses of the input and output streams for the BSR system. For this special run, the Oxidizing Solution was used in the DMR condenser/bubbler instead of deionized water like for the normal Simulant D runs. For this special run, a 5 wt.% Spectrosol[τ] solution (hereafter referred to as the Spectrosol Solution) was used to rinse the crossbar and DMR condenser/bubbler after the Oxidizing Solution rinses. A scrubber with a 5 M KOH caustic solution on the off-gas vent was used to try to capture any volatile species like Iodide. The various output streams for the special Module D run were the solid granular product, the cross bar solids and Oxidizing/ Spectrosol Solution rinses, the DMR condenser/bubbler drains and Oxidizing/Spectrosol Solution rinses, DMR basket Oxidizing Solution rinses, the seal pot drains and Oxidizing Solution rinses, and the off-gas micron filters.

The key input and output streams for the modules B, C, and D are shown in Table 8-14 and Table 8-15, respectively. The most thorough mass balance was the Module D special simulant run. The schematic of the sampling points from this run are shown pictorially in Figure 8-3. Note that the mass balance input and output streams are in yellow boxes. More streams were analyzed for the special run shown in Figure 8-3 compared to the regular runs to try to close the mass balance. More details of this special run are given in Reference 4. Individual schematics, mass balance input values, and mass balance output values for the all campaigns can be found in References 3 and 4.

Table 8-14. Key Input Streams for Simulant and Radioactive Modules B, C, D

Input Stream	Comment
Feed-Supernate	Portion of Feed that is simulant or radioactive waste
Feed-$Fe(NO_3)_3*9H_2O$	Portion of Feed that is REDOX indicator
Feed-Coal	Portion of Feed that is unreacted Coal
Feed-Coal Ash	Portion of Feed that is assumed to be reacted coal or coal ash
Feed-Clay-OptiKast®	Portion of Feed that is OptiKast® Clay
Feed-Clay-Sagger®	Portion of Feed that is Sagger® Clay

[τ] A solution of ultra pure water and 37% fuming hydrochloric acid used to dissolve Al, Ba, Ca, Cd, Co, Cr, Cu, Fe, Hg, K, Mg, Mn, Na, Ni, Pb, Zn, Sr, Re and radionuclides into solution.

Table 8-15. Key Output Streams for Simulant and Radioactive Modules B, C, D

Campaign	Module B (Rassat LAW Blend)		Module C (Tank SX-105)		Module D (Tank AN-103)		
Output Stream	**Simulant Runs**	**Radioactive Runs**	**Simulant Runs**	**Radioactive Runs**	**Simulant Runs**	**Special Simulant Run**	**Radioactive Runs**
Granular Product	Product Solids	Product Solids	Product Solids	Product Solids	Product Solids	Product Solids	Product Solids
DMR Condenser/ Bubbler Drain	Deionized Water Filtrate & Filtered Solids	Deionized Water Filtrate & Filtered Solids	Deionized Water Filtrate & Filtered Solids	Deionized Water Filtrate & Filtered Solids	Deionized Water Filtrate & Filtered Solids	Oxidizing Solution Filtrate & Filtered Solids	Deionized Water Filtrate & Filtered Solids
DMR Condenser/ Bubbler Rinse	None	None	None	None	Oxidizing Rinse Filtrate & Filtered Solids	Unfiltered Oxidizing Rinse	None
DMR Basket Rinse	None	None	None	None	Oxidizing Rinse Filtrate & Filtered Solids	Unfiltered Oxidizing Rinse	None
Crossbar Rinse	Deionized Water Rinse Filtrate & Filtered Solids	Deionized Water Rinse Filtrate & Filtered Solids	Deionized Water Rinse Filtrate & Filtered Solids	Deionized Water Rinse Filtrate & Filtered Solids	None	Unfiltered Oxidizing Rinse	Unfiltered Oxidizing Rinse
Crossbar Solids	None	None	Quartz Wool Solids	Quartz Wool Solids	Quartz Wool Solids	Quartz Wool Solids	Quartz Wool Solids
Crossbar/ DMR Condenser Rinse	None	None	None	None	None	Unfiltered Spectrosol Rinse	None
Seal Pot Drain	None	None	Filtrate & Filtered Solids	None	Filtrate & Filtered Solids	Unfiltered Drain	None
Seal Pot Rinse	None	None	None	None	Oxidizing Rinse Filtrate & Filtered Solids	Unfiltered Oxidizing Rinse	None
25 Micron Off-gas Filter	None	None	None	None	Solids	Solids	None
2 Micron Off-gas Filter	None	None	None	None	Solids	Solids	None
Off-gas Caustic Scrubber	None	None	None	None	None	Unfiltered Drain	None

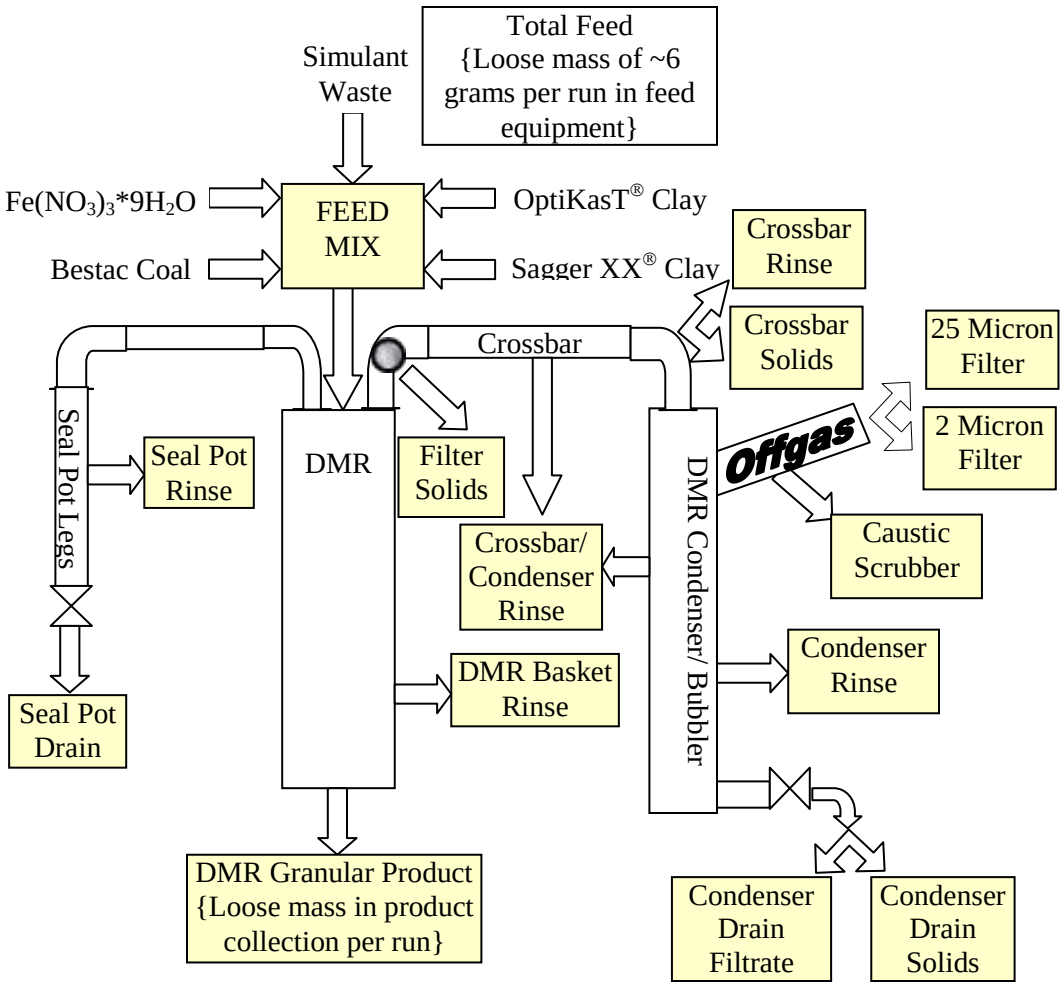

Figure 8-3. Mass Balance Input and Output Streams for Simulant Module D Special Run

The key species examined in the simulants and radioactive modules are shown in Table 8-16.

Table 8-16. Key Species for Mass Balance

Radioisotope Species	Non-Radioactive Species
^{137}Cs	^{133}Cs
^{125}I	Re
^{129}I	^{127}I
^{99}Tc	Al
	Cl
	Cr
	Na
	Si
	SO_4

Using the input and output streams described earlier, the mass balance calculational logic for the regular simulant and radioactive runs can be described as shown in Equation 8 noting that some streams are zero if not needed:

Equation 8

$$Waste*w_i + Fe*f_i + Coal_{ash}*ca_i + Coal_{un}*cu_i + O\_Clay*o_i + S\_Clay*s_i = Product*p_i + CD\_fil*cf_i + CD\_sol*cs_i + CDR\_sol*crs_i + CDR\_fil*crf_i + XR\_fil*xf_i + XR\_sol*xs_i + SP\_fil*sf_i + SP\_sol*ss_i + SPR\_fil*srf_i + SPR\_sol*srs_i + BR\_sol*brs_i + BR\_fil*brf_i + F25\_sol*f25_i + F2\_sol*f2_i$$

Where:

i = One of key species identified earlier

Waste = mass of simulant or radioactive waste stream

Fe = mass of $Fe(NO_3)_3 \bullet 9H_2O$ added to waste stream

$Coal_{ash}$ = mass of Bestac® Coal that remains in granular product as coal ash

$Coal_{un}$ = mass of Bestac® Coal that remains unreacted in granular product

O_Clay, S_Clay = mass of OptiKasT® and Sagger XX® Clay added to waste stream, respectively

w_i, f_i, ca_i, cu_i, o_i, s_i are concentrations of species i for waste, $Fe(NO_3)_3*9H_2O$, Coal Ash, Unreacted Coal, OptiKasT® Clay, and Sagger XX® Clay streams, respectively

Product = mass of solid granular product
p_i = concentration of species i in solid granular product

CD_fil = mass of DMR condensate filtrate
cf_i = concentration of species i in DMR condensate filtrate

CD_sol = mass of DMR condensate solids
cs_i = concentration of species i in DMR condensate solids

CDR_sol = mass of DMR Condenser dry solids (on- and off-specification material were both included in the mass balance as the designations on- and off-specification referred to product REDOX and coal content only) from filtering special rinse

crs_i = concentration of species i in DMR Condenser dry solids (on- and off-specification material were both included in the mass balance as the designations on- and off-specification referred to product REDOX and coal content only) from filtering special rinse

CDR_fil = mass of DMR Condenser special rinse filtrate (on- and off-specification material were both included in the mass balance as the designations on- and off-specification referred to product REDOX and coal content only)

crf_i = concentration of species i in DMR Condenser Solids special rinse filtrate (on- and off-specification material were both included in the mass balance as the designations on- and off-specification referred to product REDOX and coal content only)

XR_fil = mass of crossbar filtrate from rinse and filtering
xf_i = concentration of species i in crossbar filtrate from rinse and filtering

XR_sol = mass of crossbar solids from quartz wool (for modules C and D only) and/or rinse filtering
xs_i = concentration of species i in crossbar solids from quartz wool and/or rinse filtering

SP_fil = mass of seal pot leg filtrate from drains
sf_i = concentration of species i in seal pot leg filtrate from drains

SP_sol = mass of seal pot leg solids from drains
ss_i = concentration of species i in seal pot leg solids from drains

SPR_fil = mass of seal pot leg filtrate from rinses
srf_i = concentration of species i in seal pot leg filtrate from rinses

SPR_sol = mass of seal pot leg solids from rinses
srs_i = concentration of species i in seal pot leg solids from rinses

BR_sol = mass of DMR Basket dry solids (on- and off-specification material were both included in the mass balance as the designations on- and off-specification referred to product REDOX and coal content only) from special rinse

brs_i = concentration of species i in DMR Basket dry solids (on- and off-specification material were both included in the mass balance as the designations on- and off-specification referred to product REDOX and coal content only) from special rinse

BR_fil = mass of DMR Basket Solids special rinse filtrate (on- and off-specification material were both included in the mass balance as the designations on- and off-specification referred to product REDOX and coal content only)

brf_i = concentration of species i in DMR Basket Solids special rinse filtrate (on- and off-specification material were both included in the mass balance as the designations on- and off-specification referred to product REDOX and coal content only)

F25_sol = mass of 25 micron filter solids (on- and off-specification material were both included in the mass balance as the designations on- and off-specification referred to product REDOX and coal content only)

$f25_i$ = concentration of species i in 25 micron filter solids (on- and off-specification material were both included in the mass balance as the designations on- and off-specification referred to product REDOX and coal content only)

F2_sol = mass of 2 micron filter solids (on- and off-specification material were both included in the mass balance as the designations on- and off-specification referred to product REDOX and coal content only)

$f2_i$ = concentration of species i in 2 micron filter solids (on- and off-specification material were both included in the mass balance as the designations on- and off-specification referred to product REDOX and coal content only)

Due to feed remaining in the feed containers and the feed lines, a special BSR run was performed [4]. This special run was performed to better quantify the masses of the input and output streams for the BSR system. During the special BSR run for Module D, the masses of various equipment were taken before and after the run to determine the amount of feed actually fed and the amount of granular product actually produced. These special measurements showed that the feed mass per BSR run was overestimated by about 6 grams per run (feed hold up in the feed bottle and feed tube).

The special Module D run also showed that the granular product mass was being underestimated due to losses in the collection and processing of the granular product for each run. Since the granular product collection and processing techniques differed from the simulant versus radioactive modules as well as across different researchers and technicians, a calcine factor for the BSR was developed with respect to the mass of granular product produced per mass of feed coming into the system. This calcine factor was based on data from multiple campaigns as shown in Table 8-17. The average across all campaigns was 0.40 with a standard deviation of 0.03.

Table 8-17. Product to Feed Mass Ratios for BSR Runs

Run	Module B		Module C		Module D
	Simulant Runs	Radioactive Runs	Simulant Runs	Radioactive Runs	Radioactive Runs
1	0.42	0.42	0.36	0.36	0.43
2	0.38	0.41	0.43	0.38	0.38
3	0.39	0.40	0.42	0.38	0.41
4	0.39	0.42	0.37	0.44	0.36
5	0.39	0.41	0.42	0.43	0.34
6	0.39	0.42	0.35	0.43	0.40
7	0.39	0.36	----	0.42	0.39
8	0.39	0.43	----	0.38	0.49
9	0.37	0.44	----	0.41	0.37
10	0.40	0.46	----	0.38	----
11	0.40	0.40	----	0.45	----
12	0.39	0.41	----	----	----
13	0.40	0.38	----	----	----
14	0.40	0.46	----	----	----
15	0.39	0.46	----	----	----
16	0.40	0.40	----	----	----
17	0.41	0.38	----	----	----
18	----	0.39	----	----	----
19	----	0.37	----	----	----
Average	**0.39**	**0.41**	**0.39**	**0.41**	**0.40**
Standard Deviation	0.01	0.03	0.04	0.03	0.04

After studying the various granular product masses and corrected feed masses across the simulant and radioactive Module B, C and D activities, it was determined that:

Equation 9

$$C_f = \frac{\text{Product}}{\text{Waste} + \text{O\_Clay} + \text{S\_Clay} + \text{Fe} + \text{Coal}_{ash} + \text{Coal}_{un}} = 0.4$$

Where:

C_f = Calcined factor for BSR

Waste = mass of simulant or radioactive waste stream fed

Fe = mass of $Fe(NO_3)_3 \bullet 9H_2O$ fed

O_Clay, S_Clay = mass of OptiKasT® Clay and/or Sagger XX®Clay fed, respectively

$Coal_{ash}$ = mass of Bestac® Coal that remains in granular product as coal ash

$Coal_{un}$ = mass of Bestac® Coal that remains unreacted in granular product

To calculate the unreacted Bestac® coal remaining after the BSR processing, the LOI and LOD measurements were performed on each run's granular product. Using the LOI and LOD measurements, the wt% carbon remaining in the granular product at the end of each run (c_{wt}%) were calculated using Equation 10:

Equation 10

c_{wt}% = LOI (wt% of total mass) – LOD (wt% of total mass)

The Bestac® coal contains 82.49% wt% carbon based on analytical data received by SRNL from TTT. Using the c_{wt}% and the known wt% carbon in the Bestac® coal, the amount of unreacted coal per run was calculated using Equation 11:

Equation 11

$$Coal_{un} = \frac{\text{Product} * c_{wt}\%}{82.49\%}$$

Knowing the total mass of coal fed per run (Coal), the amount of coal that gets ashed per run ($Coal_{ashed}$) was calculated using Equation 12:

Equation 12

$Coal_{ashed} = Coal - Coal_{un}$

Using the measured wt% ash in the Bestac® Coal of 5.11%, the mass of coal ash that remains behind in the granular product per run ($Coal_{ash}$) was then calculated using Equation 13:

Equation 13

$$Coal_{ash} = Coal_{ashed} * 5.11\%$$

The mass of product produced per run was then calculated using the BSR calcined factor (C_f) and the various output masses as described above:

Equation 14

$$Product = \left(Waste + O\_Clay + S\_Clay + Fe + Coal_{ash} + Coal_{un}\right) * 0.4$$

Once the masses and concentrations have been determined, the percent recovery of species i for a particular output stream j was calculated using Equation 15:

Equation 15

$$Rec_{i,j} = Out_{i,j}/In_i$$

Where:

$Rec_{i,j}$ = Percent Recovery of species i for a particular output stream j

$Out_{i,j}$ = Output Stream j Mass of Species i, which would be Product*p_i, CD_fil*cf_i, CD_sol*cs_i, XR_fil*xf_i, XR_sol*xs_i for the various streams

In_i = Total Input Mass of Species i = Waste*w_i + Fe*f_i + Coal*c_i + O_Clay*o_i + S_Clay*s_i

The total recovery of species i for all streams j then becomes:

Equation 16

$$Rec_i = \sum_j Rec_{i,j}$$

Rec_i = Percent Total Recovery of species i across all output streams

The recovery of species i across j streams was then normalized to 100% by using Equation 17:

Equation 17

$$\overline{Rec}_{i,j} = \frac{Rec_{i,j}}{\sum_j Rec_{i,j}}$$

Where:

$\overline{\mathrm{Rec}}_{i,j}$ = normalized percent recovery of species i in stream j

The total recoveries of the key species for the key streams were calculated for the Module B campaigns using the logic presented above. The recoveries for Module B simulant from the BSR processing campaign are shown in Table 8-18. The recoveries for the Module B radioactive campaign are shown in Table 8-19.

Table 8-18. Recoveries for Key Streams and Species for Simulant Module B (Rassat Blend)

Method	Element	Total Recovery (%)	Normalized Recoveries				
			Product %	Condensate Filtrate %	Condensate Solids %	Crossbar Filtrates %	Crossbar Solids %
ICP-MS	^{133}Cs	92	99.3	0.3	0.2	0.004	0.1
	Re	83	98.1	1.6	0.2	0.02	0.03
	^{127}I	103	96.2	3.3	0.3	0.2	0.03
ICP-ES	Al	105	99.5	0.00	0.4	0.00	0.1
	Cr	152	99.5	0.1	0.4	BDL	0.1
	Na	99	99.3	0.3	0.3	0.03	0.1
	Si	103	100.0	0.02	0.0	0.00	0.00
IC	Cl	106	97.8	2.1	0.0	0.05	0.00
	SO_4^{2-}	114	98.5	1.4	0.1	0.01	0.02

Table 8-19. Recoveries for Key Streams and Species for the Module B Radioactive Campaign (Rassat Blend)

Method	Element	Total Recovery (%)	Normalized Recoveries				
			Product %	Condensate Filtrate %	Condensate Solids %	Crossbar Filtrates %	Crossbar Solids %
Radiochem	^{137}Cs	124	98.9	0.8	0.2	0.01	0.1
	^{125}I*	84	95.0	4.7	0.1	0.1	0.1
	^{129}I &	69	94.3	5.4	0.1	0.1	0.00
		75	94.8	5.0	0.1	0.1	0.00
	^{99}Tc	87	87.9	11.8	0.0	0.2	0.00
ICP-MS	^{99}Tc	Not performed					
	Re	98	97.8	2.1	0.1	BDL	0.00
	^{127}I	94	94.8	5.0	0.1	0.1	0.04
ICP-ES	Al	110	99.5	0.0	0.4	0.00	0.1
	Cr	120	99.4	0.1	0.3	BDL	0.2
	Na	104	99.2	0.5	0.3	0.03	0.00
	Si	110	99.4	0.03	0.4	0.01	0.1
IC	Cl	83	94.1	5.9	BDL	BDL	BDL
	SO_4^{2-}	113	95.6	4.3	0.1	BDL	0.1

*^{125}I values based on half-life decay from when sample pulled and actually analyzed. ^{125}I analytical more accurate than ^{129}I. &First row of ^{129}I recoveries use 3.41E+03 dpm/g for product concentration, while second row uses 3.73E+03 dpm/g.

The non-radioactive ^{133}Cs recovery was 92% for the simulant campaign. This recovery was good since the concentration of ^{133}Cs in the feed was about 1,874,000 ug/L with a total Cs mass fed of about 1.78 grams over 18 runs. The Re recovery was 83% and the ^{127}I recovery was 103% for the simulant campaign. The SO_4^{-2} recovery was about 114%. The SO_4^{-2} recovery was very dependent on the SO_4^{-2} coming in from the coal in the feed mix and how much of the coal in the

feed became ash. The approach on how to handle the feed coal SO_4^{-2} and other species was discussed in Section 4.6 and Appendix E of Reference 3 and in Equation 9 and Equation 10 above.

The Re recovery was 98% for the Module B radioactive campaign. The ^{127}I recovery was 94%. More details of the mass balance are given in Reference 3 (Appendix F). Most recoveries for the radionuclides in the Module B radioactive campaign were in the range of 84% to 124% except for ^{129}I. The ^{129}I value had higher variability in the granular product, which gave a range of 69-75% recovery using the average values. The 95% confidence interval for the 3.73E+03 dpm/g concentration is 627 dpm/g or the concentration could vary as high as 4,357 dpm/g giving a total recovery of ^{129}I of 87%. The ^{137}Cs and ^{99}Tc recoveries were 124% and 87%, respectively. The SO_4^{-2} recovery was about 113% in good agreement with the simulant recovery of 114%. Comparison of the total recoveries shown in Table 8-19 to the percent of each species in the product (Product % column) suggests that most analytes remain predominately with the FBSR granular product in processing the feed slurries in the BSR.

The recoveries for Module C simulant from the BSR processing campaign are shown in Table 8-18. More details of the mass balance are given in Appendix I of Reference 4. The non-radioactive ^{133}Cs recovery was 105% for the simulant campaign. This recovery was good since the concentration of ^{133}Cs in the feed was about 5,331 ug/L with a total Cs fed of about 1.37 milligrams over 7 runs. The Re recovery was 98% and the ^{127}I recovery was 76% for the simulant campaign. The SO_4^{-2} recovery was about 101%. As stated above, the SO_4^{-2} recovery is very dependent on the SO_4^{-2} coming in via the coal in the feed mix and how much of the coal in the feed is ashed.

Table 8-20. Recoveries for Key Streams and Species for Simulant Module C (SX-105)

Method	Element	Total Recovery (%)	Normalized Recoveries					
			Product %	Condensate Filtrate %	Crossbar Filtrates %	Crossbar Solids %	Seal Pot Filtrates %	Seal Pot Solids %
ICP-MS	^{133}Cs	104.96	97.77	0.87	0.03	0.12	0.32	0.29
	Re	97.69	97.98	1.55	0.00	0.05	0.31	0.04
	^{127}I	76.38	87.86	9.48	0.07	0.07	2.42	0.05
ICP-ES	Al	98.07	99.66	0.00	0.00	0.04	0.00	0.15
	Cr	107.46	99.65	BDL	BDL	0.04	BDL	0.15
	Na	96.31	99.62	0.13	0.00	0.03	0.03	0.08
	Si	104.13	99.74	0.01	0.00	0.00	0.00	0.11
IC	Cl	102.89	88.35	8.77	BDL	0.82	1.78	0.29
	SO_4^{2-}	100.86	95.54	3.02	BDL	0.59	0.47	0.30

BDL is Below Detection Limit

The recoveries for the Module C radioactive campaign are shown in Table 8-19. The radiochemistry and mass spectrometer recoveries were lower than expected and may be due to a mixing of the various feed batches for the runs. More details of the mass balance are given in Appendix J of Reference 4. The recoveries for the radionuclides in the Module C radioactive campaign were in the range of 71% to 83%. The ^{129}I granular product average concentration of 118 dpm/g had a high variability (19.39% RSD), which gives a 95% confidence interval of 92-143 dpm/g. Using the upper 95% confidence value of the ^{129}I granular product concentration, the total recovery of ^{129}I becomes 89%. The ^{137}Cs level is indeterminate because of the low concentrations in the feed and contamination from the shielded cells operations. Comparison of

the total recoveries shown in Table 8-19 to the percent of each species in the product (Product % column) suggests that most analytes remain predominately with the FBSR granular product in processing the feed slurries in the BSR.

Table 8-21. Recoveries for Key Streams and Species for the Module C Radioactive Campaign (SX-105)

Method	Element	Total Recovery (%)	Normalized Recoveries			
			Product %	Condensate Filtrate %	Crossbar Filtrates %	Crossbar Solids %
Radiochem	^{137}Cs	Indeterminate				
	^{129}I[&]	74.60 (88.70)[&]	86.15 (88.35)[&]	1.67 (1.41)[&]	BDL (BDL)[&]	12.18 (10.24)[&]
	^{99}Tc	80.24	98.00	0.25	0.01	1.74
ICP-MS	^{99}Tc	82.51	97.96	0.29	0.02	1.74
	Re	70.73	97.64	0.47	BDL	1.89
ICP-ES	Al	105.35	99.65	0.00	BDL	0.34
	Cr	107.75	99.73	BDL	BDL	0.27
	Na	103.82	99.52	0.04	0.00	0.43
	Si	108.52	99.98	0.02	0.00	0.00
IC	Cl	77.73	93.64	1.32	0.07	4.98
	SO_4^{2-}	100.33	96.23	0.97	BDL	2.79

[&] ^{129}I recoveries using upper 95% confidence interval value for granular product of 143 dpm/g; BDL is Below Detection Limit

The recoveries for Module D simulant from the BSR processing campaign are shown in Table 8-22. More details of the Module D simulant mass balance are given in Appendix K of Reference 4.

To try to better close the mass balance around the BSR system, the DMR condenser/bubbler, the DMR product basket, and DMR seal pots for the simulant campaign were rinsed with a 5 wt.% HNO_3, 10 wt.% H_2O_2 solution (balance is deionized water) to try to recover as many residue solids as possible. These special rinses were then filtered through 45-μm filters and the filtrates and solids submitted for analyses. The extra analyses showed that for key species there were about 0.3-0.4 wt.% in the DMR product basket, about 0.01-0.02 wt.% in the DMR condenser/bubbler, and about 0.04-0.10 wt.% in the Seal Pots. The 25 and 2 micron cellulose filters on the off-gas going to the mass spectrometer were also analyzed to see what species were making it to this point in the system. Note that these filters were in series, the 25 micron followed by the 2 micron filter. The analyses of the filters showed that very little of the key species make it to the filters. There was about 0.21% of the Re on the 25 micron filter but then below detection limit on the 2 micron filter. These additional analyses showed that the bulk of the BSR product remains in the granular product, crossbar solids, and DMR condenser/bubbler.

The non-radioactive ^{133}Cs recovery was indeterminate for the Module D simulant campaign due to the low amount in the feed (about 0.006 grams). The Re recovery was 90% and the ^{127}I recovery was 115% for the simulant campaign. The SO_4^{-2} recovery was about 134%. As with the other data, the SO_4^{-2} recovery is very dependent on the SO_4 coming in via the coal in the feed mix and how much of the coal in the feed is ashed.

There was a special run for the Module D simulant to try to quantify the feed and product mass losses in the other runs. The total recoveries of the key species for the key streams were calculated for this special Module D run using the logic discussed above. The recoveries for

Module D simulant special run are shown in Table 8-23. More details of the special Module D simulant mass balance are given in Appendix L of Reference 3.

The non-radioactive ^{133}Cs recovery for the Module D simulant special run was about 87%. There was high variability in ^{133}Cs measurements across campaigns so caution should be used in drawing any conclusions from the reported values. The Re recovery was about 95% and the ^{127}I recovery was about 104% for the special simulant run. The special off-gas caustic scrubber showed very little ^{127}I present (0.05%). This finding plus the operational problems of the caustic scrubber led to not using a caustic scrubber in future campaigns. The SO_4^{-2} recovery was indeterminate.

The recoveries for the Module D radioactive campaign are shown in Table 8-24. Note that fewer streams were analyzed for the radioactive campaign due to physical limitations imposed by the Shield Cells Operations or remote cell operations. More details of the mass balance are shown in Appendix M of Reference 3. The recoveries for the radionuclides in the Module D radioactive campaign were in the range of 86% to 100%. The ^{137}Cs level is indeterminate because of the low concentrations in the feed and contamination from the shielded cells operations. Comparison of the total recoveries shown in Table 8-24 to the percent of each species in the product (Product % column) suggests that most analytes remain predominately with the FBSR granular product in processing the feed slurries in the BSR.

A summary of the mass balance across the radioactive test modules is given in Table 8-25. A summary of the mass balance across the non-radioactive and radioactive test modules is given in Table 8-26.

Table 8-22. Recoveries for Key Streams and Species for Module D Simulant Runs (AN-103)

Method	Element	Total Recovery (%)	Normalized Recoveries													
			Granular Product	Conden-sate Filtrate	Conden-sate Solids	Condenser Rinse Filtrate	Condenser Rinse Solids	Basket Rinse Filtrate	Basket Rinse Solids	Crossbar Solids	Seal Pot Drain Filtrate	Seal Pot Drain Solids	Seal Pot Rinse Filtrate	Seal Pot Rinse Solids	25 Micron Filter Solids	2 Micron Filter Solids
ICP-MS	^{137}Cs	Indeterminate														
	Re	90.35	97.45	0.31	0.005	0.01	0.002	0.4	0.02	1.36	0.18	0.005	0.04	0.01	0.21	BDL
	^{127}I	115.43	97.01	0.70	0.0002	0.01	0.001	0.003	0.01	1.64	0.56	0.004	0.02	0.01	0.02	0.004
ICP-ES	Al	91.24	98.99	0.00	0.01	0.02	0.003	0.3	0.05	0.45	0.0004	0.013	0.10	0.01	0.003	0.02
	Cr	Indeterminate														
	Na	102.33	98.60	0.03	0.01	0.01	0.001	0.4	0.02	0.69	0.04	0.01	0.07	0.002	0.01	0.07
	Si	108.22	99.44	0.02	0.00	0.02	0.001	0.3	0.003	0.08	0.004	0.01	0.10	0.002	0.0004	0.00003
IC	Cl	85.64	99.11	BDL	BDL	BDL	BDL	BDL	BDL	0.55	0.34	BDL	BDL	BDL	0.0002	BDL
	SO_4^{2-}	134.27	44.35	BDL	BDL	10.73	BDL	22.7	0.05	7.47	0.81	BDL	13.87	0.08	0.0004	0.00002

BDL is Below Detection Limit

Table 8-23. Recoveries for Key Streams and Species for Module D Simulant Special Run (AN-103)

Method	Element	Total Recovery (%)	Normalized Recoveries												
			Granular Product	Condenser Drain Filtrate	Condenser Drain Solids	Condenser Rinse	Basket Rinse	Crossbar Rinse	Crossbar Solids	Spectrosol Crossbar/ Condenser Rinse	Seal Pot Drain	Seal Pot Rinse	25 Micron Filter Solids	2 Micron Filter Solids	Caustic Scrubber Solution
ICP-MS	^{137}Cs	87.08	79.32	BDL	0.50	0.04	4.36	0.04	5.84	0.09	0.25	0.13	0.79	0.09	8.55
	Re	95.39	94.75	0.15	0.00	0.01	2.58	0.01	2.12	0.01	0.13	0.06	0.19	0.0002	BDL
	^{127}I	103.58	98.48	0.36	0.00	0.03	0.15	0.02	0.00	0.02	0.72	0.18	NM	NM	0.05
ICP-ES	Al	101.09	99.28	NM	BDL	NM	NM	NM	0.71	NM	NM	NM	0.008	0.011	NM
	Cr	Indeterminate													
	Na	98.39	98.93	NM	0.0005	NM	NM	NM	1.07	NM	NM	NM	0.001	0.001	NM
	Si	Indeterminate													
IC	Cl	Indeterminate													
	SO_4^{2-}	Indeterminate													

NM=Not Measured

Table 8-24. Recoveries for Key Streams and Species for the Module D Radioactive Campaign (AN-103)

Method	Element	Total Recovery (%)	Normalized Recoveries			
			Product	Condensate Filtrate	Crossbar Filtrates	Crossbar Solids
Radiochem	^{137}Cs	Indeterminate				
	^{129}I	100.26	69.04	0.42	BDL	30.54
	^{99}Tc	86.15	97.62	0.29	0.02	2.08
ICP-MS	^{99}Tc	82.85	97.60	BDL	BDL	2.40
	Re	87.69	96.76	0.39	0.02	2.83
ICP-ES	Al	98.35	99.51	0.0045	0.0001	0.49
	Cr	Indeterminate				
	Na	101.70	99.51	0.03	0.003	0.46
	Si	105.00	99.97	0.023	0.0003	0.005
IC	Cl	Indeterminate				
	SO_4^{2-}	Indeterminate				

. BDL is Below Detection Limit

Table 8-25. Mass Balance of Radioisotopes and Re for BSR Radioactive Testing Acoss Modules

Method	Radio-isotope	RAD B (SRS LAW) [3]		RAD C (Hanford SX-105) [4]		RAD D (Hanford AN-103) [4]	
		Total %	Product %	Total %	Product %	Total %	Product %
Radiometric	^{137}Cs	124	99	Indeterminate			
	^{125}I*	84	95	Not shimmed			
	^{129}I	69-75	95	75-89	86-88	100	69
	^{99}Tc	87	88	80	98	86	98
ICP-MS	^{99}Tc	Analysis not Performed		83	98	83	98
	Re	98	98	71	98	88	97

*Signal for ^{125}I is stronger and more accurate than for ^{129}I

Table 8-26. Mass Balance for Non-Radioactive Species Across Modules

Method	Species	Total % Recovery (Output/Input)					
		Rassat Blend LAW		Hanford SX-105		Hanford AN-103	
		SIM	RAD	SIM	RAD	SIM	RAD
ICP-MS	^{133}Cs	92	Not Shimmed	105	Not Shimmed	Indeterminate	Not Shimmed
	^{127}I	103	94	76	Not Shimmed	115	Not Shimmed
ICP-ES or IC	Al	105	110	98	105	91	98
	Cl	106	83	103	78	86	Indeterminate
	Cr	152	120	107	108	Indeterminate	Indeterminate
	Na	99	104	96	104	102	102
	Si	103	110	104	109	108	105
	SO_4	114	113	101	100	134	Indeterminate

8.2.2 *Tc & Re Speciation*

One major assumption in the 2003 Risk Assessment [107] was that the release of ^{99}Tc— Re was used as a chemical analogue for technetium in non-radioactive production run sample used to collect the experimental data—from the NAS FBSR waste form was controlled by the weathering of a feldspathoid phase mineral (e.g., nosean which is a minor mineral present in the FBSR waste form). It is important to note that nosean was believed to be the sulfate analogue $[Na_6Al_6Si_6O_{24}](Na_2SO_4)$ for Re-sodalite $[Na_6Al_6Si_6O_{24}](NaReO_4)_2$ and/or or Tc-sodalite $[Na_6Al_6Si_6O_{24}](NaTcO_4)_2$. This conclusion was based upon the observation that the elemental release rate of sulfur and Re were within the experimental error of one another in PCT, SPFT experiments, and PUF experiments and the observed differences in XRD patterns of unleached and leached granular NAS FBSR samples.[60,61,105,107]

It is important to note the results documented in 2002 [62] and 2003 [61,105] represent the first set of chemical durability data collected on the granular NAS FBSR waste form. As a result of this early data, STORM simulations of ^{99}Tc release from the FBSR waste form was shown to be equivalent (within the experimental error) to low-activity waste glass at the compliance point (100-meter well down gradient of the disposal facility), and it was demonstrated that the release was controlled by the solubility of the feldspathoid phase, nosean/sodalite. The solubility controlled release of nosean/sodalite is probably dictated by the release of common elements—namely Al, Na, and Si—from nepheline—the dominant mineral phase contained in the FBSR product.

As a result of this assumption, the FBSR WFQ program initiated a series of experiments with the goal of determining the speciation, location, and distribution of rhenium in non-radioactive pilot-scale and bench-scale reformer tests and technetium in radioactive bench-scale reformer tests produced with actual Hanford low-activity tank waste. The samples used in these analyses include those shown in Table 8-27.

Table 8-27. List of Samples Used to Determine Re and Tc Speciation in the Granular NAS FBSR Product

Sample ID	Product	Scale	Year	Waste Type	Element
Non-Rad. FBSR 1125 [108]	fines	pilot	2004	Simulant	Re
Non-Rad. Hazen P-1B [122]	bed	engineering	2008	Simulant	Re
Non-Rad. Hazen P1B (Thin Section)	bed	engineering	2008	Simulant	Re
Non-Rad. Module B [3]	bed	bench	2010	Simulant	Re
Non-Rad. Module B (Thin Section)	bed	bench	2010	Simulant	Re
Rad. Module B [3] (spike)	bed	bench	2011	Radioactive	^{99}Tc & Re
Rad. Module C [4] (spike)	bed	bench	2011	Radioactive	^{99}Tc & Re

The series of non-radioactive granular FBSR products and radioactive granular FBSR products produced with actual Hanford LAW (Table 8-27) have been analyzed using XAS in order to address one key uncertainty in the overall performance of the NAS FBSR waste form: the location and release of ^{99}Tc from the mineral structures. To reduce this uncertainty, a series of XAS analyses were conducted on sub-samples of the non-radioactive engineering-scale FBSR and BSR product as shown in Table 8-27. The experimental details and the results collected as part of the XAS analyses are discussed in detail in the following sections.

8.2.2.1 *X-ray Absorption (XAS) Theory*

X-ray absorption (XAS) occurs when an x-ray photon travels through matter and ejects photoelectrons from a core shell of an atom in a target material. The transmission of the incident x-ray photon beam is reduced by the x-ray absorption event, and in the simplest approximation, the absorption coefficient is determined from the thickness of the material and the difference of intensities between incident and transmitted x-rays. The absorption threshold is the minimum energy required to eject an electron from the core shell of the specific atom of interest. This sharp increment in the absorption coefficient is referred to as the absorption edge. The absorption coefficient as a function of incident photon energy is used for XAS analysis. The photoelectron emitted by the x-ray absorption event can be partially backscattered by neighboring atoms.[177] Multiple scattering events occur in the x-ray absorption near edge structure (XANES) method, while single scattering mainly occurs in the extended x-ray absorption fine structure (EXAFS) technique. Both XANES and EXAFS spectroscopies probe only the local environment, because of the low energy of photoelectrons. XAS is element-specific and can provide local environmental information about the oxidation state, element identity, and bonding (coordination number and distance between the central and the nearest neighboring elements). The advantage of XAS is that most elements (except hydrogen) can be studied in any type of phase (crystalline, amorphous solid, liquid, gas, or mineral-water interface), even at low concentration levels (approximately 1-10 ppm). XAS is an in situ technique that does not need any special sample preparation like drying or vacuum conditions for analysis.[178,179] The disadvantage is that a high intensity x-ray source from a synchrotron radiation facility is required for complicated data collection. Even though EXAFS is a short-range order probe (approximate maximum range 4-6Å from the absorber) compared to XRD, it provides remarkably unique information about the local structural environment in most materials, so that it complements information from other spectroscopic methods to increase understanding of the binding and leaching mechanisms of contaminants in waste forms.

8.2.2.2 *X-ray Absorption Analyses and Approach for FBSR samples*

Based upon the RA simulations discussed in Section 4.1.2, one key uncertainty in the overall performance of the NAS FBSR waste form is the location and release of ^{99}Tc. To reduce the uncertainty, a series of X-ray absorption spectroscopy analyses were conducted on sub-samples of the non-radioactive engineering-scale FBSR and BSR product. The objective of the XAS measurement on the FBSR product was to determine the oxidation state of Re and ^{99}Tc, determine the nearest neighbor elements associated with Re and ^{99}Tc, identify the mineral(s) that are enriched in Re and ^{99}Tc, determine if Re is an adequate surrogate for ^{99}Tc.

Although these measurements appear fairly straight forward, the difficulty lies in the fact that the targeted elements represent less than 1% of the overall FBSR product. In other words, the technique is searching for a needle in a haystack, where the needle is represented by the sodalite phases and the haystack is the nepheline FBSR matrix (see relative amounts in Table 6-1 and Table 8-7) for the relative amounts of the Re and ^{99}Tc sodalites vs. nepheline. The XAS analyses are further complicated by the small contribution of Re and/or ^{99}Tc to the simulant matrix, which can result in mixed anion sodalite phases where a few unit cells contain Re and/or ^{99}Tc and the rest consists of other anions present in the low-activity waste stream at higher concentrations.

Because of the complicated FBSR mineral matrix, XAS represents a major advantage over other characterization approaches for this application because of its element selectivity—spectra are collected from specific X-ray absorption edges holding information on only those species and their surrounding environment—and insensitivity to long range order. Furthermore, a large amount of the standard XAS spectra required to determine the oxidation state and nearest neighbor for Re and ^{99}Tc has been documented in the literature [90,180,181,182]. This technique is highly complementary to traditional

techniques such as XRD. A number of excellent reviews that discuss XAS analysis are available in the literature (see Brown et al. 178 and the references therein). A brief discussion of the technique is provided below along with an example of the application of this technique to determine uranium speciation in a complex sediment matrix.

Over the last decade, a number of investigators have successfully applied XAS techniques to gain a detailed understanding of uranium speciation in sediment matrices. This sediment matrix is more complex than the FBSR matrix in terms of the number of mineral phases present. Furthermore, the uranium species contained in these sediments are extremely low and previous attempts using traditional characterization (bulk SEM, bulk TEM, and bulk XRD) approaches were equally unsuccessful. Three well know references include McKinley et al. [183], Catalano et al. [184], and Singer et al. [185] that examined uranium speciation in sediments.

Singer et al. [185] represents the most germane study to the work being performed to evaluate ^{99}Tc speciation in the FBSR product. In this study a combination bulk and micro-XAS techniques were used to determine uranium speciation as a function of depth in contaminated sediments removed from the 300 Area of the Hanford site. A similar approach is being used to determine the Re and ^{99}Tc speciation within the FBSR product using a sequence of steps:

1) determine Re oxidation of the HRI/TTT engineering-scale 2008 sample made using the Rassat simulant (P-1B) using bulk XAS,
2) identify Re enriched particles using beam line μ-XRF followed by μ-XAS to determine Re oxidation state using the HRI/TTT engineering-scale 2008 sample (P-1B),
3) conduct beam line μ-XRD of the enriched particle contained in the HRI/TTT engineering-scale 2008 sample (P-1B), and
4) use a focus ion beam (FIB) to remove the Re enriched particle and analyze the particle using a variety of traditional characterization approaches (SEM, Transmission Electron Microscopy , Raman, etc.) to corroborate the results collected on the beam line.

This approach will be repeated on several individual samples of the same material to demonstrate the repeatability of this technique. The same approach is being used for the non-radioactive and radioactive BSR samples that were made with the Rassat simulant and doped with Re (non-radioactive) and Re and ^{99}Tc (radioactive sample).

The Re and ^{99}Tc XAS studies discussed in this report were performed at the National Synchrotron Lightsource (NSLS) at Brookhaven National Laboratory (BNL), Stanford Linear Accelerator Collider (SLAC) at Stanford University, and the Advanced Photon Source (APS) at ANL.

For a detailed description of the experimental technique, specifically the materials and methods, and a more detailed explanation of the results see Appendix E. In the following section, a summary is provided of the XAS results collected to-date on non-radioactive and radioactive NAS samples listed in Table 8-27.

8.2.2.3 *Analysis of standard reference spectra.*

The standard spectra of the four rhenium compounds (Re metal [Re(0)], ReO_2 [Re(IV)], ReO_3 [Re(VI)], and $KReO_4$ [Re(VII)]), used to analyze the XAFS spectra discussed in this report were recorded by Lukens et al.[90] Two major features are observed in the standard reference spectra for rhenium species with different oxidation states (see Figure 8-4), Re(0) to Re(VII). First, the absorption edge shifts to higher energy because the binding energy of the electron increases as the formal oxidation state increases. The increase in the electron binding energy is because there are fewer electrons to screen the charge of the

nucleus from the 2p electrons. Second the area amplitude of the absorption edge is associated with the 2p to 4d transition—increases with increases in the rhenium oxidation state. This amplitude increase in the absorption edge is proportional to the number of core holes in the 4d shell, which increases with an increase in oxidation state (Table 8-28).

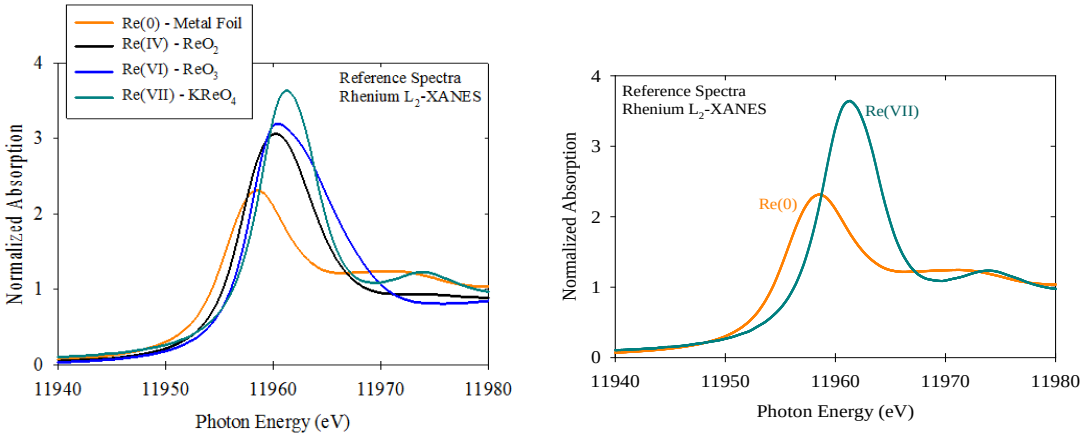

Figure 8-4. XANES spectra for rhenium reference samples from Lukens et al. [90]

Table 8-28. Relationship Between Number of Electron Vacancies in the Rhenium ([Xe]$4f^{14}4d^{5}6s^{2}$) 4d Shell and the Oxidation State

Chemical Formula	Oxidation State	Number of 4d electron vacancies
Re metal	Re(0)	5
ReO_2	Re(IV)	7
ReO_3	Re(VI)	9
ReO_4^-	Re(VII)	10

8.2.2.4 *Bulk XAFS analysis of FBSR Engineering-scale Samples.*

8.2.2.4.1 *Rassat Simulant from Engineering-scale Testing (P-1B)--particle sample measured at NSLS*

The results for fitting the XANES spectra are given in Table 8-29. The only components for which the amplitude is greater than the error are for Re(0) and Re(VII). However, the value of p(F) for Re(0) indicates that the data does not support the hypothesis that Re metal is present in the sample, whereas for ReO_4^-, the value of p(F) strongly supports the hypothesis that perrhenate is present in the sample. While it may appear surprising that p(F) is not smaller, the surprisingly large value of p(F) is due to the fact that the Re L_2 XANES spectra of ReO_2, ReO_3, and ReO_4^- are somewhat similar, so the spectrum of ReO_2 or ReO_3 can be used to fit the spectrum of ReO_4^- to some degree.

8.2.2.4.2 *Rassat Simulant from Engineering-scale Testing (P1B)-particle sample measured at APS*

In addition to the measurements performed on the P-1B material at NSLS, additional measurements were performed at APS. The results of these analyses are provided in Table 8-29. The XANES spectra were fit using the reference spectra for ReO_2, ReO_3, and $KReO_4$. In all cases, the fit using these reference spectra is not very good. The major issue is that the first post-edge feature in $KReO_4$ is at lower energy

than for ReO_4^- in Re-sodalite. It should be noted that even though the fit is not very good, with the exception of P-1B-packed, the data does not support the presence of any Re species other than ReO_4^-. In the case of P-1B-packed the data supports the presence of ~10 to 15 percent ReO_3 and 80 to 85 percent ReO_4^-.

Because $KReO_4$ was not an effective standard, the XANES spectrum of rhenium sodalite prepared by SRNL in 2004 (sodalite04) was used as the Re(VII) standard. The fits improved significantly in all cases, evident by the R-factor being an order of magnitude lower. For each of the samples, P-1B-packed and P-1B-particle, the data only supports the presence of Re(VII) in the samples. Although, the XANES spectrum of P-1B-particle is very noisy, the data still supports only the presence of Re(VII).

The P-1B-packed sample also had good fluorescence data out to a k = 12; therefore the EXAFS spectra were fit to confirm the findings of the XANES spectra. The results of this analysis are provided in Table 8-30. Although the spectrum is noisy, the number of neighbors and bond distance is consistent with a local structure identical to the theoretical structure for perrhenate. The number of neighbors and distance is provided in Table 8-30. For comparison the Re-O bond in $KReO_4$ is 1.723 ±0.004 Å.[186]

Table 8-29. Results of XANES Spectra Fitting for Pilot-scale FBSR Granular Product.

Sample	Beam line	Re(0)	[a]p(F)	ReO_2	p(F)	ReO_3	p(F)	ReO_4^-	p(F)	[b]*r*-factor
[c]P-1B-particle	NSLS	0.07 ±0.04	0.15	0.00 ±0.08	1	0.05 ±0.06	0.8	0.88 ±0.06	0.006	0.018
[c]P-1B-packed	APS	-	-	0.05 ±0.05	0.45	0.15 ±0.04	0.007	0.80 ±0.02	<0.001	-
[d]P-1B-packed	APS	-	-	0.03 ±0.02	0.25	0.04 ±0.02	0.11	0.93 ±0.01	<0.001	-
[d]P-1B-particle	APS	-	-	0.0 ±0.2	1	0.1 ±0.1	1	1.00 ±0.09	<0.001	-
[d]FBSR 1125	SSRL	-	-	0.07 ±0.05	-	0.00 ±0.04	-	0.93 ±0.03	-	-

[a]p(F) is the probability that the improvement to the fit due to including this component is due to random error. If p(F) < 0.05, the component can be considered to be present.
[b]*r*-factor is $[\Sigma(y_{obs}-y_{calc})^2/\Sigma y_{obs}^2]^{1/2}$, where the sum is over all data.
[c]data fit using $KReO_4$ as the Re(VII) reference spectra.
[d]data fit using Re-sodalite as the Re(VII) reference spectra measured at NSLS.

Table 8-30. Results of EXAFS spectra fitting for pilot-scale FBSR granular product.

Sample	Beam line	Neighbor	ΔE_0 (eV)	[a]R-factor	[b]N	[c]R (Å)	[d]σ^2 (Å^2)
P-1B-packed	APS	oxygen	5 ±3	0.020	4.2 ±0.8	1.72 ±0.01	0.002 ±0.001

[a]R factor =
[b]N – number of neighboring atoms. $S_0^2 = 1$ (fixed).
[c]R – distance to neighboring atoms
[d]σ^2 – mean-square disorder of neighbor distance
p(F) – meaningless for a fit with one shell

8.2.2.4.3 *FBSR 1125 (fines pilot-scale 2004) sample measured at SSRL*

Similar to the other pilot-scale FBSR samples, analysis of the rhenium oxidation state for the FBSR 1125 sample produced at the SAIC/STAR facility in Idaho, shows that only Re(VII) is present in this material (see Table 8-29).

8.2.2.4.4 *BSR Mod. B sample measured at SSRL*

The fit for rhenium in the BSR sample looks off because of the poor pre-edge correction (see Table 8-31). This sample contains antimony, which has an absorption edge just below the rhenium L_{II} edge. Consequently, the Re-edge is offset from zero in the pre-edge correction. This does not affect the fit. Similar to the FBSR pilot-scale samples, the only oxidation state present is Re(VII).

Table 8-31. Results of XANES Spectra Fitting for Granular Material Produced with the Bench-scale Reformer (BSR) at SRNL.

Sample	Beam line	ReO_2	ReO_3	ReO_4^-
[a]BSR	SSRL	0.00 ±0.04	0.00 ±0.03	1.00 ±0.02
[a]data fit using Re-sodalite as the Re(VII) reference spectra measured at NSLS.				

8.2.2.4.5 *Re-bearing sodalite samples, sodalite04 and ReZAA, measured at APS*

Two samples of Re-bearing sodalite were prepared by SRNL using a hydrothermal synthesis method. Briefly, the Re-sodalite [$Na_8Al_6(ReO_4)_2(SiO_4)_6$] was prepared by reacting Zeolite 4A with 8M NaOH in the presence of excess sodium perrhenate ($NaReO_4$) at 225°C at 400-psi in an autoclave for seven days. X-ray diffraction analysis of this sample was consistent with Re-sodalite and matched the powder diffraction file #04-013-6684. Two samples of this material were available and used in the XAS, one was prepared in 2004 and another prepared in 2010 by SRNL as part of the FBSR WFQ program. The results from XAS analyses of each sample are discussed in this section.

The XANES and EXAFS results for each sample are displayed in Table 8-32. The XANES spectra were initially fit using the reference spectra for ReO_2, ReO_3, and $KReO_4$. In all cases, the fit using these reference spectra is not very good. Similar to the fit for the P-1B sample, the first post-edge feature in $KReO_4$ is at lower energy than for ReO_4^- in the sodalite04 or ReZAA samples, which is the cause of the poor fit. This suggests that ReO_4^- in $KReO_4$ is slightly different than ReO_4^- in Re-sodalite. It is important to note that although the fit was less than optimal when using $KReO_4$ as the Re(VII) standard, the data only supported the presence of Re(VII) in the sample. This is consistent with the chemicals used to synthesize the samples and the XRD results. Additional XAS analyses are being performed on the Re-sodalite samples and the $KReO_4$ standard at both the L_{II} and L_{III} edge to elucidate the observed differences between the Re(VII) containing materials. The EXAFS results support the same conclusion obtained with XANES. The number of neighbors and distance is provided in Table 8-33 For comparison the Re-O bond in $KReO_4$ is 1.723 ±0.004 Å. [186]

Table 8-32. Results of XANES spectra fitting of the Re-sodalite samples.

Sample	Beam line	ReO_2	[a]p(F)	ReO_3	p(F)	ReO_4^-	p(F)	[b]*r*-factor
[c]Sodalite04	APS	0.03 ±0.05	0.71	0.11 ±0.04	0.061	0.79 ±0.03	<0.001	-
[c]ReZAA	APS	0.01 ±0.06	0.86	0.11 ±0.04	0.088	0.81 ±0.03	<0.001	-
[d]ReZAA	APS	0.00 ±0.01	0.77	0.00 ±0.01	1	1.00 ±0.01	<0.001	-

[a]p(F) is the probability that the improvement to the fit due to including this component is due to random error. If p(F) < 0.05, the component can be considered to be present.
[b]*r*-factor is $[\Sigma(y_{obs}-y_{calc})^2/\Sigma y_{obs}^2]^{1/2}$, where the sum is over all data.
[c]data fit using $KReO_4$ as the Re(VII) reference spectra.
[d]data fit using Re-sodalite as the Re(VII) reference spectra measured at NSLS.

Table 8-33. Results of EXAFS spectra fitting of the Re-sodalite samples.

Sample	Beam line	Neighbor	ΔE_0 (eV)	[a]R-factor	[b]N	[c]R (Å)	[d]σ^2 (Å^2)
Sodalite04	APS	oxygen	5 ±3	0.018	4.1 ±0.7	1.73 ±0.01	0.002 ±0.001
ReZAA	APS	oxygen	6 ±2	0.009	4.0 ±0.5	1.729 ±0.007	0.002 ±0.001

[a]R factor = $[\Sigma(y_{obs}-y_{calc})^2/\Sigma y_{obs}^2]^{1/2}$, where the sum is over all data.
[b]N – Number of neighboring atoms. Meaningless for a fit with one shell. $S_0^2 = 1$ (fixed).
[c]R – Distance to neighboring atoms
[d]σ^2 – Mean-square disorder of neighbor distance
p(F) – Meaningless for a fit with one shell.

8.2.2.4.6 *Radioactive BSR Module B sample measured at NSLS*

Two samples of technetium spiked BSR product was produced using actual Savannah River Site Defense Waste Processing Facility radioactive recycle and chemically adjusted to resemble the Hanford 68-tank blend low-activity waste (Module B Rassat simulant used in non-radioactive pilot-scale production runs). The redox for each sample was different and resulted in one sample being within the REDOX operating specifications for a pilot-scale system (low REDOX) and the other being outside this specification (high REDOX). These samples represented the first opportunity to determine the relationship between redox and Tc speciation in the BSR product. Re-bearing sodalite was prepared by SRNL using a hydrothermal synthesis method.

The results from the analysis of the XANES spectra for each sample are listed in Table 8-34. In both cases, the standard spectra fit the data well and support the presence of all three compounds in the sample. Although the percentages of Tc(VII) to T(IV) are clear, the relative ratios of $Tc_2S(S_3)_2$ versus $TcO_2 \cdot H_2O$ are not as accurate. For example, the sample could contain TcO_2 rather than $TcO_2 \cdot H_2O$, but the standard spectra for TcO_2 is not available. For example, the sample could contain TcS_2 rather than $Tc_2S(S_3)_2$, but the standard spectra for TcS_2 is not available. It is important to note that $Tc_2S(S_3)_2$ is a Tc(IV) sulfide that is formed in water at room temperature and it is also converted to TcS_2 by heating the material in an inert atmosphere.

From the EXAFS fit parameters for high REDOX sample (Table 8-35), it appears that this sample contains ~50% TcO_4^- as well as some other Tc species. The only scattering shell that is actually supported by the EXAFS data is the pertechnetate oxygen shell at 1.71 Å. Its value of F(p) is high because removing this shell in the fit allows the other oxygen shell to migrate and partially compensate for the missing pertechnetate oxygen. As is clear from both the large error on the number of neighbors as well as the value of p(F), the presence of the other oxygen shells cannot be considered to be supported by the data. It is not possible to determine what the other Tc species are from the EXAFS spectrum.

To summarize, both the EXAFS and XANES data give the same result, each sample contains both Tc(IV) and Tc(VII) species for both samples.

Table 8-34. Results of XANES Spectra Fitting for the Radioactive Module B BSR Samples.

Sample	Beam line	$Tc_2S(S_2)_3$	[a]p(F)	$TcO_2 \cdot 2H_2O$	p(F)	TcO_4^-	p(F)
Low Redox Mod B BSR	NSLS	0.22 ±0.02	<0.001	0.13 ±0.02	<0.001	0.65 ±0.01	<0.001
High Redox Mod B BSR	NSLS	0.28 ±0.02	<0.001	0.16 ±0.02	<0.001	0.56 ±0.01	<0.001
Mod C BSR	SSRL	0.08 ±0.01	<0.001	0.13 ±0.01	<0.001	0.79 ±0.01	<0.001

[a]p(F) is the probability that the improvement to the fit due to including this component is due to random error. If p(F) < 0.05, the component can be considered to be present.

Table 8-35. Results of EXAFS Spectra Fitting of the Radioactive "Out of Range" High REDOX Bodule B Samples from the BSR.

Sample	Beam line	Neighbor	ΔE_0 (eV)	[a]R-factor	[b]N	[c]R (Å)	[d]σ^2 (Å^2)	F(p)
Module B High REDOX	NSLS	oxygen	-	0.05	2.0 ±0.6	1.71 ±0.01	0.001 ±0.002	0.068
		oxygen	9 ±3	0.05	8 ±10	2.02 ±0.08	0.05 ±0.05	0.378

[a]R factor = $[\Sigma(y_{obs}-y_{calc})^2/\Sigma y_{obs}^2]^{1/2}$, where the sum is over all data.
[b]N – Number of neighboring atoms. Meaningless for a fit with one shell. $S_0^2 = 1$ (fixed).
[c]R – Distance to neighboring atoms
[d]σ^2 – Mean-square disorder of neighbor distance
F(p) – is the significance of the improvement to the fit created by adding an additional set of atoms. If the p-value is less than 0.05, the additional atoms have significantly improved the fit and can be consider "observed" in the EXAFS experiment.

8.2.2.4.7 *Radioactive BSR Module C sample measured at SSRL*

The results from the analysis of the XANES and EXAFS results for the sample are listed in Table 8-36 and Table 8-37. In both cases, the standard spectra fit the data well and support the presence of all three of the following compounds in the sample: TcO_4^-, $TcO_2 \cdot 2H_2O$, and $Tc_2S(S_3)_2$. Although the percentages of Tc(VII) to T(IV) are clear, the relative ratios of $Tc_2S(S_3)_2$ versus $TcO_2 \cdot H_2O$ are not as accurate. For example, the sample could contain TcS_2 rather than $Tc_2S(S_3)_2$, but the standard spectra for TcS_2 is not available. It is important to note that $Tc_2S(S_3)_2$ is a Tc(IV) sulfide that is formed in water at room temperature and it is also converted to TcS_2 by heating the material in an inert atmosphere.

The sample contains a mixture of Tc(IV) and Tc(VII). The XANES fit suggest that the sample actually contains Tc_2S_7 presumably due to reduction of the sulfate to sulfide during steam reforming. Only 80% of the Tc is present at pertechnetate. The presence of lower-valent Tc is not surprising as steam reforming creates reducing conditions conducive to the reduction of TcO_4^-.

The EXAFS spectrum is weak. The local environment has O atoms at 1.73 Å, which is indicative of TcO_4^-; however, the coordination number is low. If S^O_2=0.9 is used, then there should be 3.6 neighbors for TcO_4^-. The measured value of 2.6(5) implies that 0.7(1) of the Tc is present as TcO_4^-, which is in good agreement with the value of 0.79(1) found by XANES.

Table 8-36. Results of XANES Spectra Fitting for the Radioactive Module C BSR Samples

Sample	Beam line	$Tc_2S(S_2)_3$	[a]p(F)	$TcO_2 \cdot 2H_2O$	p(F)	TcO_4^-	p(F)
Mod C BSR	SSRL	0.08 ±0.01	<0.001	0.13 ±0.01	<0.001	0.79 ±0.01	<0.001
[a]p(F) is the probability that the improvement to the fit due to including this component is due to random error. If p(F) < 0.05, the component can be considered to be present. A value of p(F) <0.001 means that there is a >99% probability that adding the standard improved the fit.							

Table 8-37. Results of EXAFS spectra fitting of the module C BSR sample

Sample	Beam line	Neighbor	ΔE_0 (eV)	[a]R-factor	[b]N	[c]R (Å)	[d]σ^2 (Å^2)
Module C BSR	SSRL	oxygen	9 ±3	0.024	2.6 ±0.5	1.73 ±0.01	0.002 ±0.001
[a]R factor = $[\Sigma(y_{obs}-y_{calc})^2/\Sigma y_{obs}^2]^{1/2}$, where the sum is over all data. [b]N – Number of neighboring atoms. Meaningless for a fit with one shell. $S_0^2 = 0.9$ (fixed). [c]R – Distance to neighboring atoms [d]σ^2 – Mean-square disorder of neighbor distance							

8.2.3 *Mineralogy of Module B, C, D compared to Mineralogy of Pilot and Engineering-scale Tests and MINCALC™ Predictions*

The details of the XRD mineralogy for the various BSR campaigns are summcarized in Table 8-7. The species observed in the Turbula® mixed "on-spec" as well as the range of mineralogy observed were tabulated. The mineralogy observed for the BSR non-radioactive and radioactive samples for Module B (Rassat simulant) are the same as those of the ESTD bed products (see Table 8-7 and Figure 8-5 overlay). The phases were primarily, two types of nepheline (one of hexagonal symmetry and one of orthorhombic symmetry), and cubic nosean with minor cubic sodalite. The sodalite peaks are weaker than the nosean peaks and do not appear in every XRD. This is because there is a large region of solid solution between sodalite ($Na_8(AlSiO_4)_6Cl_2$ and nosean ($Na_8(AlSiO_4)_6SO_4$ [63,94] as shown in Figure 2-6 because the two species are isostructural. Therefore, when fitting XRD patterns to the "best matching" set of Bragg reflections, sometimes the nosean and sodalite are identified separately and sometimes as one or the other of the two species depending on the relative concentration of each present.

Other minor phases are anatase (TiO_2), which is a clay impurity, Al_2O_3, which is the ESTD/HRI startup bed material and quartz. The formulas for these species and the reference Powder Diffraction Files (PDFs) are given below and Figure 8-5. The hexagonal nepheline is the normal crystalline form of $NaAlSiO_4$ and the orthorhombic nepheline is $NaAlSiO_4$. The PDF file for the orthorhombic nepheline states that it may be low-carnegieite, a metastable form of nepheline. However, it is not a hydrated nepheline phase although it is made from a gel that dehydrates at ~800°C.[69] Throughout this document, this is referred to as nepheline (O) where the "O" is for orthorhombic but it should be recalled that it may be low-carnegieite (see discussion in Sections 2.2.2 and 2.2.3)

The phases found in the non-radioactive and radioactive BSR products agreed with the predicted mineralogy from MINCALC™ of more nosean (stronger Bragg reflections) than sodalite (weaker Bragg reflections) and quantities of 65-70 wt% of Na-K-Cs nepheline (Table 6-1).

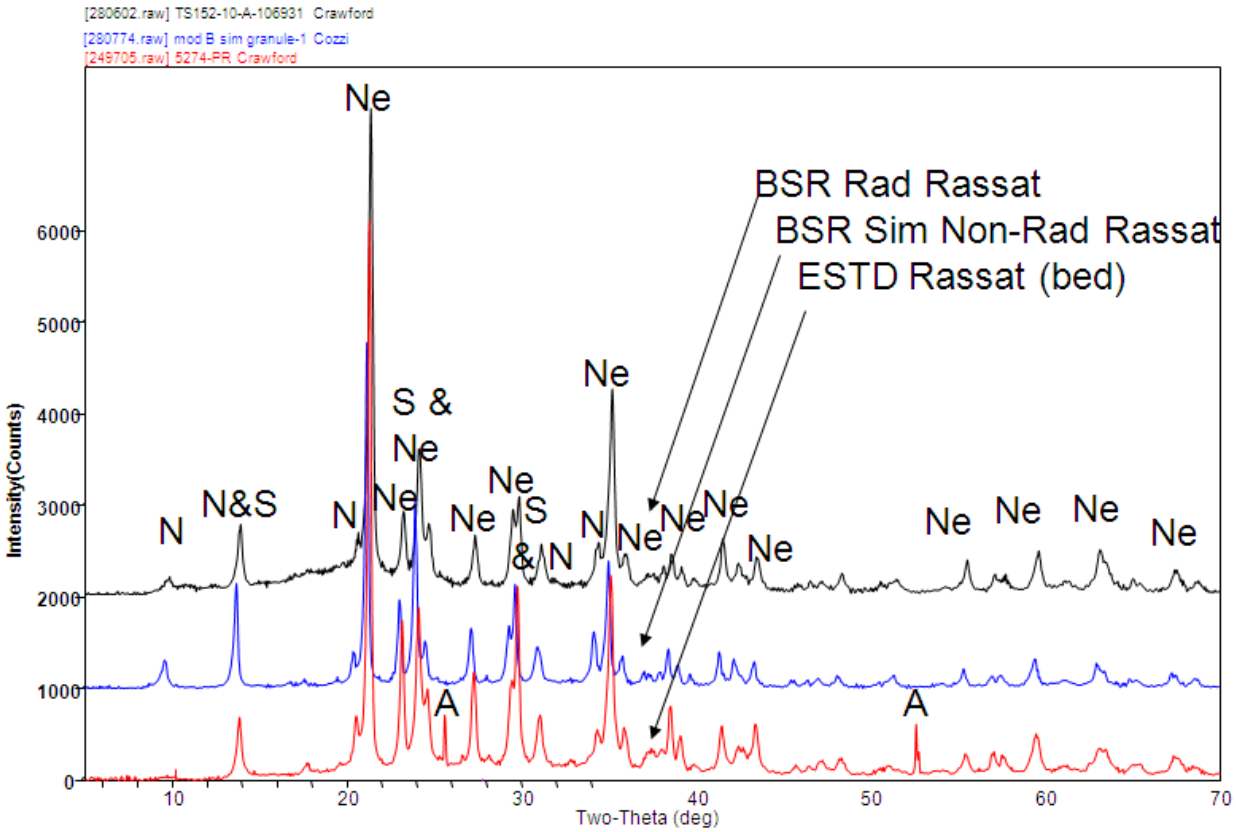

Figure 8-5. Overlay of X-ray Spectra for Module B (Rassat Formulation) for ESTD Engineering-scale DMR Products (P-1B), BSR Bench-scale Simulant and Radioactive Products.

Ne is Nepheline (H) and Nepheline (O) $NaAlSiO_4$ (PDF 00-035-0424 and PDF00-052-1342)
S is Sodalite (cubic) $Na_6Al_6Si_6O_{24}$ (PDF 00-042-0217)
N is Nosean, $Na_8Al_6Si_6O_{24}SO_4$ (PDF 01-072-1614)
A is Corundum, Al_2O_3 (PDF 01-089-3072)
Quartz is SiO_2 (PDF 00-046-1045)
Original XRD spectra fits are in Appendix I of Reference 3

For Module C, the mineralogy of the non-radioactive product from the BSR matched the mineralogy of the radioactive product from the BSR (see Table 8-7 and Figure 8-6). The phases observed agree with the predicted mineralogy from MINCALC™ (Table 6-1) of ~84-85 wt.% nepheline (stronger Bragg reflections) with ~11-12 wt.% sodalite and nosean (weaker Bragg reflections). In this case, the nosean is present in larger concentrations than sodalite as there is more SO_4^{-2} in the feed than halides.

For Module D, the mineralogy of the non-radioactive product from the BSR matched the mineralogy of the radioactive product from the BSR (see Table 8-7 and Figure 8-7). The phases observed agree with the predicted mineralogy from MINCALC™ (Table 6-1) of ~94-96 wt.% nepheline (stronger Bragg reflections) with ~5.5-6 wt.% sodalite and nosean (weaker Bragg reflections). In this case, the nosean is present in smaller concentrations than sodalite as there is more Cl in the feed than sulfate.

For Module E, the mineralogy from the non-radioactive BSR product matched the phases predicted from MINCALC™ (Table 6-1), as nosean was predicted to be ~20 wt.% in the FBSR product. The XRD pattern shown in Figure 8-8 for the Module E run with the IOC shows higher concentrations (stronger Bragg reflections) for nosean than those observed in Modules C or D (Figure 8-6 and Figure 8-8).

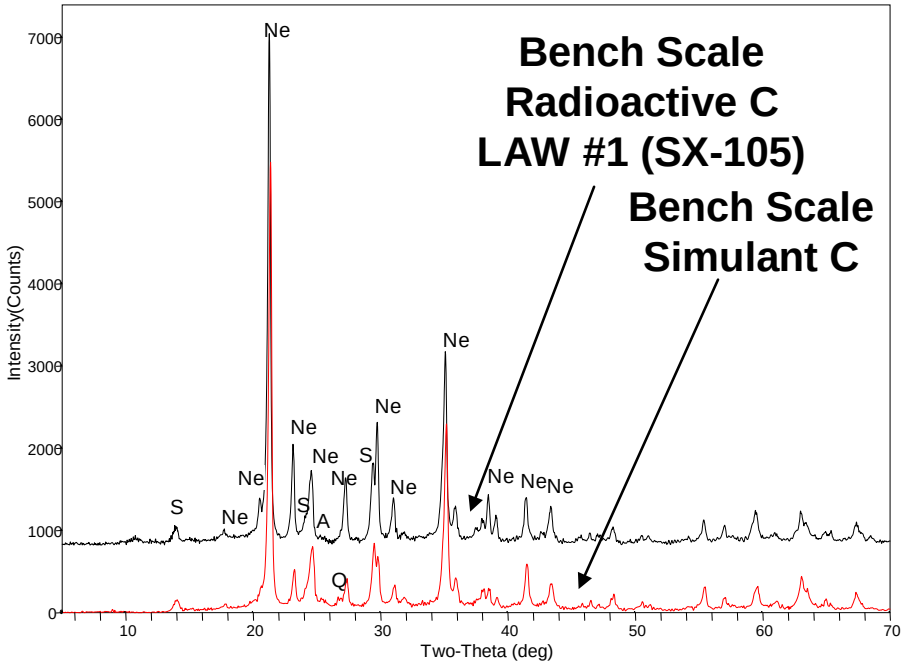

Figure 8-6. Overlay of X-ray Spectra for Module C (SX-105) for the BSR Bench-scale Simulant and Radioactive BSR Products.

Where Ne is Nepheline (H) and Nepheline (O) $NaAlSiO_4$ (PDF 00-035-0424 and PDF00-052-1342)
S is Sodalite (cubic) $Na_6Al_6Si_6O_{24}$ (PDF 00-042-0217)
N is Nosean, $Na_8Al_6Si_6O_{24}SO_4$ (PDF 01-072-1614)
A is Anatase, TiO_2 (PDF 00-021-1272) a clay impurity
Quartz is SiO_2 (PDF 00-046-1045) a clay impurity
Original XRD spectra fits are in Appendix N of Reference 4

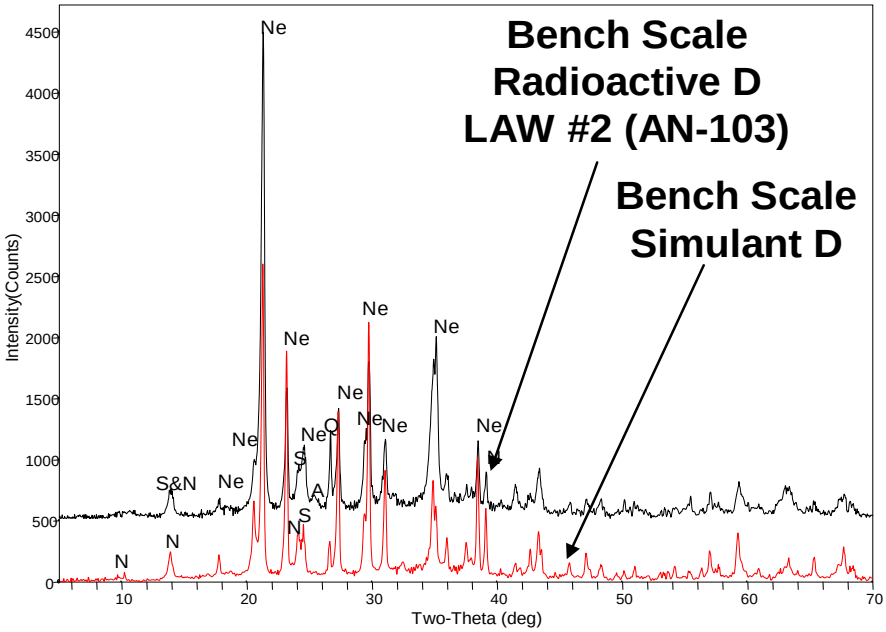

Figure 8-7. Overlay of X-ray Spectra for Module D (AN-103) for the BSR Bench-scale Simulant and Radioactive BSR Products.

Where Ne is Nepheline (H) and Nepheline (O) $NaAlSiO_4$ (PDF 00-035-0424 and PDF00-052-1342)
S is Sodalite (cubic) $Na_6Al_6Si_6O_{24}$ (PDF 00-042-0217)
N is Nosean, $Na_8Al_6Si_6O_{24}SO_4$ (PDF 01-072-1614)
A is Anatase, TiO_2 (PDF 00-021-1272)
Quartz is SiO_2 (PDF 00-046-1045)
Original XRD spectra fits are in Appendix N of Reference 4

.

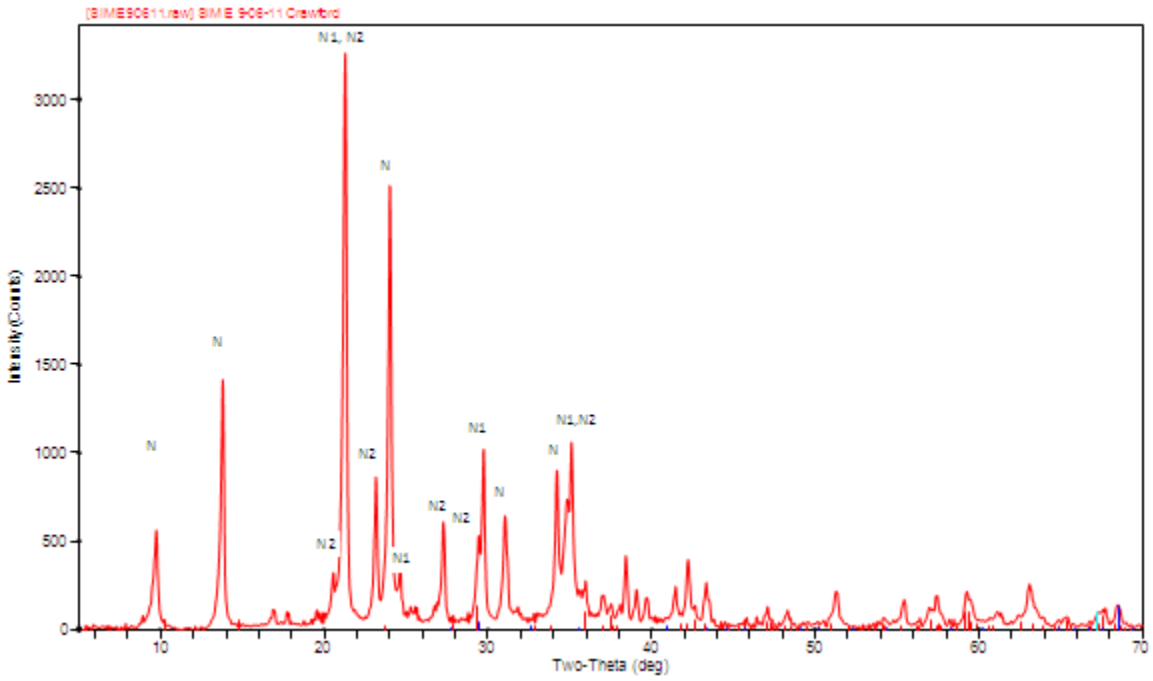

Figure 8-8. X-ray Spectra for Module E (AZ-101/AZ-102) for the BSR Bench-scale Simulant BSR Product run with the IOC.

Where N1 is Nepheline (O) $NaAlSiO_4$ (PDF00-052-1342)
N2 is Nepheline (H) $NaAlSiO_4$ (PDF 00-035-0424)
N is Nosean, $Na_8Al_6Si_6O_{24}SO_4$ (PDF 01-072-1614)
Original XRD spectra fits are in of Reference 4

The semi-quantative analysis based on stronger vs. weaker XRD Bragg reflections was used to compare the XRD percentages to the MINCALC™ predictions because single phase XRD calibration curves were not available. While each sodalite has a unique XRD signature (Figure 8-9), the literature suggests (1) that the sodalite lattice parameters vary slightly with the method by which the sodalite were prepared [94] and (2) there are high- and low-temperature forms of nosean, i.e. there are order-disorder distributions of the SO_4^{-2} in nosean,[94] and OH- often exchanges in the sodalite β-cages for other anions when the phase pure standards are made via a hydrothermal route.[12] While it is known [95] that the sodalite lattice itself is capable of hosting anions of unlike sizes, Cl and I or Cl and SO_4^{-2}, a solid solution with different sized anions creates a strain in the sodalite framework. The latter arises from the fact that sodalite cages are face-sharing. Thus the same set of Si-O-Al angles in a hexagonal ring shape in the sodalite structure is part of two different sodalite β-cages with two different central anions. The larger the difference in the sizes of the central anions, the more likely there will be the deviations from the random distribution of these anions in the sodalite lattice. Instead, the same species may be preferably incorporated during the lattice growth, eventually leading to the formation of "domains" of one of the species versus the other.[95] This is known as "domain segregation effects" and is known in the NaCl-NaI sodalite solid solution.[95]

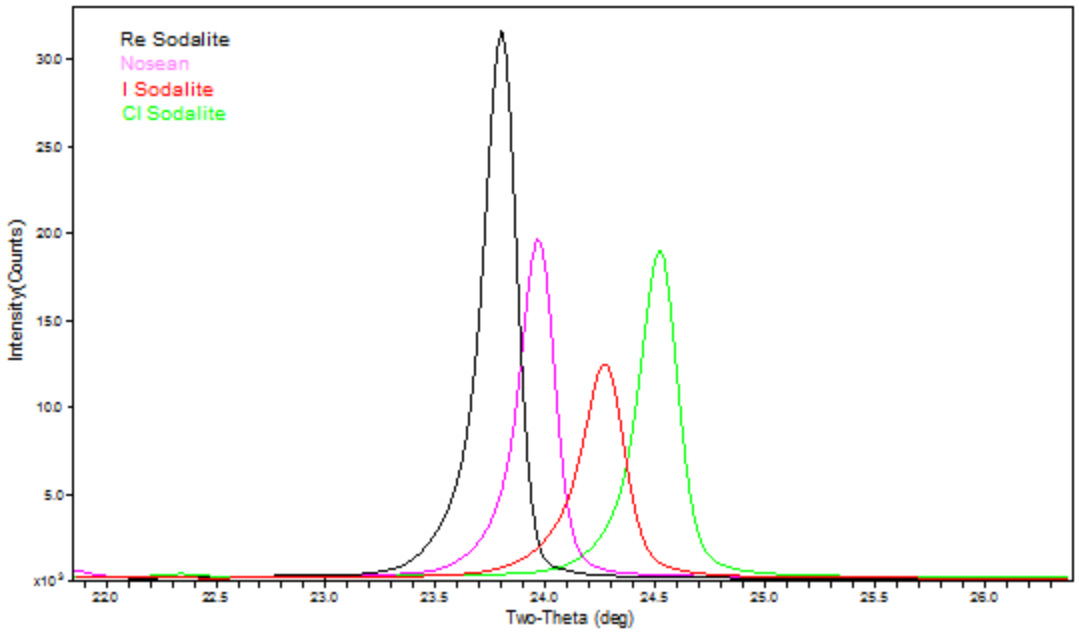

Figure 8-9. Individual XRD signatures of the various sodalite phases.

The mineralogy of the phases found in Module B, C, and D are similar to the phases found in the 2001 HRI/TTT testing with AN-107 (Table 8-38), to the phases found in the 2004 pilot-scale testing at SAIC-STAR (Table 8-38), and to the phases found in the 2008 HRI/TTT engineering-scale testing (Table 8-38). The AN-107 products had more Fe_2O_3 and Fe_3O_4 from the IOC process additive SphereOx. Less was added to the SAIC-STAR testing and to the HRI/TTT 2008 testing. None was added to the BSR testing until Module D when only limited testing was done on the IOC effect on TCLP response.

A comparison of the phases given in Table 8-7 and Table 8-38 shows that all the same phases formed providing the necessary tie back to the pilot and engineering-scale testing needed to demonstrate equivalency so that the 2003 RA for FBSR can be used in the FBSR technology down selection.

Table 8-38. Mineral Phases Analyzed in FBSR Products [98]**

	Low-Carnegieite[f] Nominally $NaAlSiO_4$	**Nepheline** Nominally $NaAlSiO_4$ or $K_{0.25}Na_{0.75}AlSiO_4$	**Nosean** $Na_6[Al_6Si_6O_{24}](Na_2SO_4)$ and/or **Sodalite** $Na_6[Al_6Si_6O_{24}](2NaX$ where X=Cl,F,I)	**Other Minor Components**
HANFORD ENVELOPE "C" LAW WASTES (2002) $Fe^{+2}/\Sigma Fe$ of Bed = 0.15				
SCT02-098-FM		X	Y	Al_2O_3, Fe_2O_3, Fe_3O_4
Fines PR-01	X	X	Y	Al_2O_3, Fe_2O_3, Fe_3O_4
HANFORD ENVELOPE "A" LAW WASTES (2004) $Fe^{+2}/\Sigma Fe$ of Bed = 0.28-0.81				
Bed 1103	X	X	Y	TiO_2
Bed 1104	X	X	Y	TiO_2
Fines 1125	X	Y		TiO_2
INL SBW WASTES (2003-4) $Fe^{+2}/\Sigma Fe$ of Bed = 0.51-0.61				
Bed 260	Y	X	TR	Al_2O_3 and TiO_2
Bed 272	Y	X	TR	TiO_2
Bed 277	Y	X	TR	TiO_2
Bed 1173		X	TR	Al_2O_3, SiO_2, $NaAl_{11}O_{17}$, $(Ca,Na)SiO_3$
HANFORD RASSAT LAW WASTES (2008) $Fe^{+2}/\Sigma Fe$ of Bed = 0.41-0.90				
PR Bed Product 5274 (P1A)	Y	X	X	Al_2O_3,
PR Bed Product 5316 (P1A)	Y	X	X	Pyrophyllite*
PGF Fines 5280 (P1A)	X	Y		$NaAl_{11}O_{17}$ (Diaoyudaoite),TiO_2
PGF Fines 5297 (P1A)	X	Y	X	SiO_2
PR Bed Product 5359 (P-1B)	Y	X	X	Pyrophyllite*
PR Bed Product 5372 (P-1B)	Y	X	X	Pyrophyllite*
PGF Fines 5351 (P-1B)	X	Y	Y	SiO_2
PGF Fines 5357 (P-1B)	X	Y	Y	TiO_2
Composite (P1A)	X	Y	Y	SiO_2 and TiO_2
Composite (P-1B)	X	Y	Y	SiO_2 and TiO_2
HANFORD MELTER OFF-GAS RECYCLE (WTP SW) WASTES (2008) $Fe^{+2}/\Sigma Fe$ =0.41-0.90				
PR 5475 (P2A)	Y	Y	X	Pyrophyllite*
PGF Fines 5471 (P2A)	X	X	X	SiO_2
PR 5522 (P2B)	Y	Y	X	Pyrophyllite*, TiO_2
PGF Fines 5520 (P2B)	X	X	X	SiO_2 and TiO_2
Composite (P2B)	Y	X	X	SiO_2

X = Major constituent ; Y = Minor constituent ; TR = trace constituent

f = the PDF for this phase states it is orthorhombic nepheline and possibly low-carnegeite (PDF 052-1342). Note low-carnegeite also has ring structures that are oval for sequestration of K, Cs, etc.

* $Al_{1.333}Si_{2\cdot.667}O_{6.667}(OH)_{1.333}$

** The XRD method gives information on the specific crystalline phases present by comparison to reference library spectra. Although this method is not used with any internal standards to allow for quantitative measurement of the various crystalline phases, it does provide information as to the 'major' and 'minor' and 'trace' phases present by intercomparison of the main peaks of each crystalline pattern within a given sample.

The mineralogy given in the XRD spectra shown in Figure 8-5, Figure 8-6, Figure 8-7, and Figure 8-8 qualitatively validate the MINCALC™ predictions based on the feed compositions shown in Table 8-6. Module B (BSR and Engineering-scale TTT/HRI) has more nosean than sodalite in a large amount of nepheline (68-71.6% nepheline). The amount of Re sodalite is in the 0.14-0.16 wt.% range even though the Re was shimmed in at 100X and the amount of Tc sodalite anticipated to form is in the 0.0005 wt.% range. For Module C (SX-105 the mid anion case), there is more nosean than nepheline but there was less nosean than in Module B (Rassat composition). The nepheline weight percentages for Module C were in the 76.5-78.5 range (higher than the Rassat Blend Module B). In Module D, the highest amount of nepheline occurred as this was the lowest anion feed campaign. The nepheline in Module D was ~83.7 wt.% (Table 8-6). In Module E, nosean dominated (>22 wt.%) as the AZ-101/AZ-102 feed was high in sulfate (Table 8-6).

Overall, the mineralogy of the BSR campaigns (Rassat simulant, SX-105, AN-103, and AZ-101/AZ-102) are the same phases obsereved in the 2001-2 pilot scale studies at HRI/TTT, in the 2004 INL pilot, and in the ESTD engineering scale FBSR runs. Semi-quantatitively, the amounts of each phase agree with the amounts predicted to form MINCALC™ used since 2004 for all testing at all scales. Coupling the results of this study with previous radioactive BSR studies demonstrates that when anions such as Cl, F, and I are present or oxyanions such as TcO_4^- or ReO_4^-, more sodalite forms. If more SO_4^{-2} is present, the sodalite structured phase nosean forms. If anions, SO_4^{-2}, Re and ^{99}Tc are low, then less sodalite/nosean forms and more nepheline forms. Cs and K can be accommodated in either nepheline or sodalite where they substitute for Na.

"Domain segregation" of sodalites of varying composition were not observed during SEM analysis of the BSR products but the domains may be on too fine a scale to be seen in SEM. Figure 8-10 through Figure 8-12 are SEM images of individual granules of BSR product, each about 200 microns in size. These granules are primarily nepheline ($NaAlSiO_4$), as can be observed by the fact that the back scattered images for Na, Al, and Si appear bright (illuminated) in the figures for Na, Al, and Si. The sodalite structures, which accommodate the sulfate, rhenium, and halides (primarily Cl), are structurally related to the nepheline. Six nepheline unit cells help define the sodalite cage in which the sulfates, rhenium and halides reside (see Equation 5). Therefore, local regions of the granule are atomically organized to accommodate these species, i.e. topotaxic[§] relationships. It should be noted that there is almost a complete solid solution between the NaCl sodalite and the Na_2SO_4 containing sodalite known as nosean (Figure 2-6) and "domain segregation" is known to occur between the NaCl and NaI sodalite.[95] Other mixed sodalite phases likely form but such studies have not yet been documented.

Figure 8-10 is for a BSR product made from radioactive WTP-SW, which had a large concentration of halides and had been shimmed with Re. Figure 8-10 shows the local Na, Al, Si regions that are enriched in these species. No "domain segregation" was observed but differing areas of this grain are locally rich in Na,Al, Si and Re and likely represent the Re sodalite. Other grains are rich in Na, Al, Si and Cl and likely represent the Cl sodalite.

Figure 8-11 is for the Rassat 168 LAW Tank Blend simulant (Module B), which had a large concentration of sulfate and had been shimmed with Re. Figure 8-11 shows the local Na, Al, Si regions that are enriched in these species. In Figure 8-11, it looks like the same grain is enrich in Re and Cl, which would imply that there may be a solid solution between these two sodalite.

[§] topotaxy = the conversion of a single crystal into one or more products which have a definite crystallographic orientation with respect to the original crystal from L.S. Dent Glasser, F.P. Glasser, F. P. , and H.F.W. Taylor, *Quart. Rev. Chem. Soc.*, 16, (4), 343 (1962).

Figure 8-12 is a Scanning Electron Microscope image of agglomerated granule of nepheline ($NaAlSiO_4$) from the ESTD Rassat LAW Tank Blend simulant (Module B) high in SO_4 and shimmed with excess I. Note that the Na, Al, Si, are enriched in the entire grain (illuminated). while the Cl, I, and SO_4 are enriched in swirls around the center. The SO_4^{-2} and I and Cl appear enriched in some of the same swirls indicating that solid solution may exist between these three sodalite.

The SEM images of BSR Module B (Figure 8-11) and ESTD Module B (Figure 8-12) confirm the findings of the Mass Balance (Section 8.2.1) that the halides, sulfate, and Re report to the FBSR minerals and do not volatilize in the off-gas. The SEM images of Re in sodalite in the ETD Module B and BSR Module B simulant samples also agrees with the findings of the XAS analysis dicussed in the next Section.

Figure 8-10. Scanning Electron Microscope image of agglomerated granule of nepheline ($NaAlSiO_4$) in which the Cl and Re sodalites have formed topotaxially due to the structural relationship of six $NaAlSiO_4$ unit cells that arrange such that they form the sodalite cage in which the Cl and Re reside.

Note: Sample is a radioactive WTP Secondary waste sample high in Cl and shimmed with Re.

Figure 8-11. Scanning Electron Microscope image of agglomerated granule of nepheline ($NaAlSiO_4$) in which the SO_4, Cl, and Re sodalites have formed topotaxially due to the structural relationship of six $NaAlSiO_4$ unit cells that arrange such that they form the sodalite cage in which the SO_4^{-2}, Cl, and Re reside.

Note: Sample is a BSR simulant Module B sample high in SO_4^{-2} and shimmed with Re. Note that the Na, Al, Si, Cl and Re scans all point to the same particle indicating it is enriched in all of these components and thus likely a Re, Cl sodalite. The S is in a different particle, which is also rich in Na, Si, and Al and likely nosean.

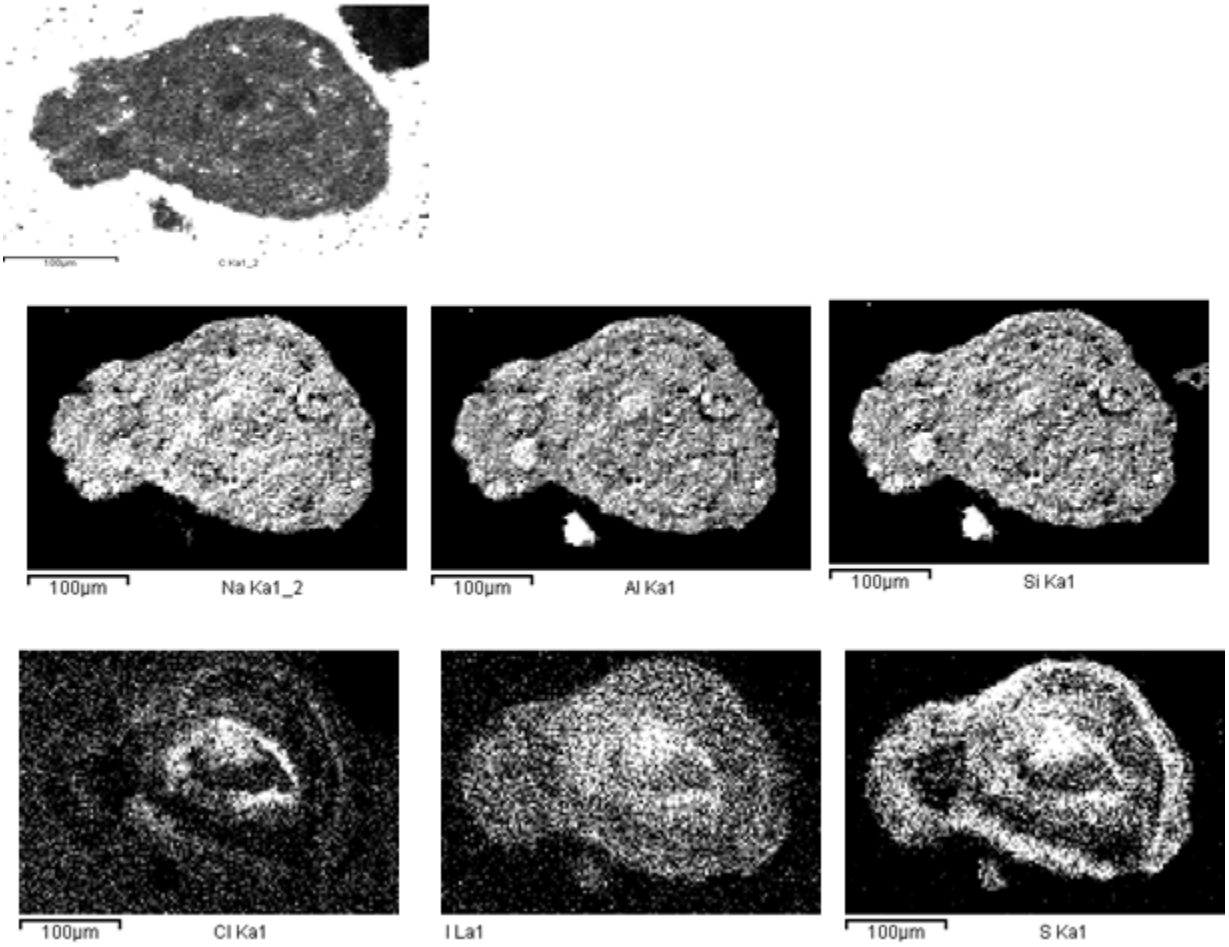

Figure 8-12. Scanning Electron Microscope image of agglomerated granule of nepheline ($NaAlSiO_4$) in which the SO_4^{-2}, Cl, and I sodalites have formed topotaxially due to the structural relationship of nepheline and sodalite.

Note: Sample is the ESTD simulant Module B sample high in SO_4 and shimmed with excess I. Note that the Na, Al, Si, are enriched in the entire grain (illuminated), while the Cl, I, and SO_4^{-2} are enriched in swirls around the center.

8.2.4 *Product Consistency Short-term Testing (Granular Product)*

The PCT was conducted on granular mineral and geopolymer monolith samples following the procedures described in ASTM C 1285-08.[152] More details about the Short-term, 7 day, PCT-A procedure can be found in Appendix D.

The samples were crushed and sieved using ethanol following the ASTM procedure sections 19.5 and 22.5. The samples were washed using only ethanol as described in section 19.6.1 of the PCT procedure. A portion of the washed and sieved material was analyzed using BET to determine the actual surface area of the BSR product rather than using the geometric hard sphere assumption given in the PCT procedure. Although use of the BET surface area may overestimate the true reactive surface area, the obvious microporosity indicates that use of the geometric surface area will underestimate the true dissolution rate. Therefore, the dissolution rates reported here have been normalized to the BET surface area. The true reactive surface area is probably less than the BET value, but also probably significantly higher than the geometric value.[106] When the durability of the FBSR product is calculated using the BET surface area, the durability is ~2 orders of magnitude lower than the leach rate of LAW glass. When the durability of the FBSR product is calculated assuming the hard sphere geometric surface area and not taking credit for the surface roughness of the FBSR product, the durability is equivalent to that of LAW glass. Data in this report used the BET surface area but the appendices contain the necessary data to calculate the durability from the hard sphere geometric surface area.

All tests were conducted in triplicate (at a minimum) and the results averaged. The PCTs were performed at 90°C for seven days (PCT-A) in either stainless steel or Teflon® vessels. The simulant leachates were then analyzed and the concentration of ions in the leachate measured by ICP-AES, IC, and ICP-MS.

Radioactive leachates were also analyzed using gamma spectroscopy and beta liquid scintillation. The elemental mass release of selected constituents was normalized by the initial concentration of each constituent after adjustment for moisture and unreacted carbon content, and reported in units of g/m^2.

Equation 18

$$NL_i = \frac{c_i(sample)}{f_i \cdot (SA/V)},$$

Where:

NL_i = normalized release, $g_{(waste\ form)}/m^2$

c_i (sample) = concentration of element "i" in the solution, g_i/L

f_i = fraction of element "i" in the unleached waste form (unitless)

SA/V = surface area of the final waste form divided by the leachate volume, m^2/L

The elemental mass release of selected constituents was normalized by the initial concentration of each constituent after adjustment for moisture and unreacted carbon content, and reported in units of g/m^2.The leached solids were analyzed for phase mineralogy using x-ray diffraction.

The 7-day PCT was conducted on the ESTD LAW P-1B Rassat FBSR granular product and BSR Module B Rassat simulant and radioactive Tank 50 Rassat BSR products. Data from the Rassat BSR products (Module B) non-radioactive and radioactive provides a comparison with PCT results from prior pilot-scale tests at INL and engineering-scale tests at TTT/HRI (ESTD) with simulants. All PCT data for the

Rassat LAW FBSR products in Table 8-39 and the raw data for the short-term PCT tests on the FBSR granular products are given in Appendix H of Reference 3.

All the PCT release rates for the ESTD and BSR Rassat LAW products were below 2 g/m^2 limit given in Table 4-1 as the durability limit for a vitreous waste form. Rhenium was added to the Module B radioactive Tank 50 salt solution to link durability release (performance) between the Re and ^{99}Tc species and between the simulant and radioactive products. As can be seen from the data in Table 8-39, the release of rhenium is consistent among the three granular products made from similar salt solutions (ESTD FBSR, the non-radioactive BSR, and the radioactive BSR), as well as with ^{99}Tc.

Table 8-39. 7-Day PCT Results for Granular Product Prepared from FBSR Product Made from the Rassat Simulant and Tank 50 Shimmed Radioactive Waste

Normalized Elemental Release	ESTD P-1B Granular		BSR Module B Simulant Granular		BSR Module B Radioactive Granular	
	(g/m^2)	Std. Dev.	(g/m^2)	Std. Dev.	(g/m^2)	Std. Dev.
Al	2.12E-03	2.01E-06	2.34E-03	7.09E-05	3.97E-03	1.33E-04
S	3.42E-01	2.17E-03	4.34E-02	1.59E-03	7.72E-02	1.47E-03
^{133}Cs	9.31E-03	8.78E-05	1.09E-02	2.36E-04		
^{137}Cs					2.29E-03	1.71E-04
Re	4.10E-03	4.07E-04	8.83E-03	3.45E-04	1.13E-02	1.22E-03
^{99}Tc					2.42E-02	5.86E-03
Na	2.15E-02	2.40E-04	1.14E-02	4.73E-04	1.24E-02	3.96E-04
Si	7.82E-04	2.50E-05	9.86E-04	4.71E-05	6.17E-04	4.83E-05
^{127}I	1.51E-02	4.13E-04	9.82E-04	1.06E-03	1.69E-03	8.04E-05
^{129}I					<3.61E-03	N/A
pH	11.63 (Blend)		11.4		11.25	

N/A = Not Applicable

Table 8-40 is data generated by PNNL[f] as replicate PCT samples on the ESTD Rassat LAW and the BSR Rassat LAW simulant. The data in Table 8-39 and Table 8-40 are comparable: PNNL and SRNL are achieving the same order of magnitude and similar PCT releases in g/m^2. The PNNL PCT leach data presented in this table have been normalized using composition (C_0 values-see Equation 18) and BET surface area data provided by SRNL on a coal free sample.

[f] The short-term PCT data (collected at a solid-to-solution ratio of 1:10 in Teflon vessels) generated by PNNL were acquired using a modified ASTM C-1285-08 method. Although the test conditions were performed according to ASTM C-1285-08, PNNL did not analyze standard waste glass reference materials as part of their tests. Additionally, PNNL ran one blank per PCT-B batch. The technical team has reviewed the data provided by PNNL and believe the data are unaffected by these procedure variations. The work performed by PNNL met the quality assurance requirements specified in the EM-31 Support Program Quality Assurance Program, Rev. 2. All analyses were performed in accordance with the Environmental Sciences Laboratory Quality Assurance Plan (QAP ESL, Rev. 3). The PNNL PCT leach data have been normalized using composition and surface area data provided by SRNL.

In addition, PNNL analyzed the samples with the coal and without the coal. The values obtained for the roasted coal sample are somewhat higher in Al and Si release, and this is to be expected as when the coal is roasted out of the sample, the ash remains which is higher in Al and Si.

Table 8-40. PNNL 7-Day PCT Results for Granular Product Prepared from LAW Simulants [132]

Normalized g/m^2	ESTD Rassat LAW P1-B Granular (not roasted)	BSR Rassat LAW Simulant Granular (not roasted)	ESTD Rassat LAWP1-B Granular (roasted)	BSR Rassat LAW Simulant Granular (roasted)
Al	1.71E-03	8.26E-04	2.07E-03	9.47E-03
S	NM	NM	NM	NM
Cs	NM	NM	NM	NM
Re	3.49E-02	1.43E-03	3.75E-02	3.74E-02
Na	1.40E-02	4.63E-03	1.64 E-02	2.01E-01
Si	4.27E-04	3.30E-04	5.16E-04	9.61E-04
I	NM	NM	3.55E-5-05	5.21E-03
pH	11.4±0.4	10.1±0.6	11.8±0.1	9.8±1.1
BET (m^2/g)	5.95	8.06	4.93	3.34

The 7-day PCT was conducted on the BSR Module C simulant and radioactive SX-105 BSR. All data is provided in Table 8-41 and Appendix O of Reference 4. The release rates were below 2 g/m^2 limit given in Table 4-1 as the durability limit for a vitreous waste form. Rhenium was also added to the Module C radioactive Hanford salt solutions to link durability release (performance) between Re and ^{99}Tc and, thus, between the simulant and radioactive products. As can be seen from the data in Table 8-41, the release of rhenium is consistent between the simulant and radioactive FBSR granular products made from the SX-105 solutions in the non-radioactive BSR and the radioactive BSR. Re and ^{99}Tc releases are shown to track each other well. The release rates from Module C FBSR granular products are also comparable to the Module B radioactive and simulant FBSR granular products reported in Table 8-39.

Due to funding and scope cutbacks, short-term leaching was not performed on Module D (AN-103) non-radioactive or radioactive BSR products. Short-term leaching was also not performed on Module E simulant BSR products (there were only 2 campaign runs), and no radioactive FBSR product was made with the Module E (AZ-101/AZ-102) radioactive LAW.

The short-term PCT leachate data from Table 8-39 and Table 8-41 along with the PNNL Re data[f] from Table 8-40 are shown graphically in Figure 8-13. These short-term PCT data are in agreement with the data generated in 2001 on AN-107 [115] and the 2004 SAIC-STAR facility samples with the Rassat simulant.[111,112] The correlations shown in Figure 8-13 were generated with the seven, then available,

[f] Additional PNNL data was not plotted due to the similarity of the SRNL and PNNL values to keep Figure 8-13 as simple as possible.

PCT responses from the 2001 and 2004 testing of both the DMR bed products and the PGF fines products. The HRI/TTT 2008 engineering-scale studies were then overlain for comparison for the Rassat LAW samples (P-1B bed samples, and Process Gas Filter, PGF, fines), which appear as "x" marks on the graphs. The HRI/TTT 2008 engineering-scale studies for the WTP-SW are overlain (bed and fines) as open diamonds. The BSR data for non-radioactive and radioactive Modules B and C are overlain with "doughnut" shaped circles around them for emphasis. Note that the data plotted in Figure 8-13 is plotted as the log of the release rates shown in Table 8-39, Table 8-40, and Table 8-41.

Table 8-41. 7-Day PCT Results for Granular FBSR Product Prepared from Module C Simulant and SX-105 Radioactive Waste

Normalized Elemental Release (g/m^2)	Module C Simulant (g/m^2)	Module C Simulant Std. Dev.	Normalized Elemental Release (g/m^2)	Radioactive Module C (g/m^2)	Radioactive Module C Std. Dev.
Al	3.43E-03	1.93E-04	**Al**	3.41-03	2.21E-04
S	1.51E-01	4.87E-03	**S**	1.64E-01	9.30E-03
^{133}Cs	7.60E-03	1.67E-03	**^{137}Cs**	1.03E-02	1.52E-03
Re	2.86E-02	1.45E-03	**Re**	1.49E-02	1.35E-03
Na	1.34E-02	6.88E-04	**Na**	1.65E-02	1.06E-03
Si	3.71E-04	2.35E-05	**Si**	2.50E-04	2.04E-05
^{127}I	2.35E-03	3.37E-05	**^{129}I**	<0.1644	N/A
			^{99}Tc	2.61E-02	7.17E-03
pH	10.79	0.04	**pH**	10.87	0.02

As with the 2001 and 2004 data, the pH increases (becomes more caustic) as the surface area of the material is decreased (see Figure 8-13a). For glass waste forms, pH usually increases with increasing surface area. This indicates that a buffering mechanism is occurring. Based on the trend of alkali (Na) release being co-linear with Al release (Figure 8-13b), it was hypothesized that this was an aluminosilicate buffering mechanism [112,113], which is known to occur in natural environments.

The Na release and Cs release are colinear with the Al release in the BSR and 2008 engineering scale data, as well as in the historical 2001 and 2004 data, as seen in Figure 8-13b and f. This is due to the aluminosilicate buffering mechanism. All the other cations appear to be released as a function of the solution pH (Figure 8-13c, d and e) for the Si, S, and Re and ^{99}Tc. This is also in agreement with the historical data and data from other leach testing and thermodynamic modeling.[6,126,131,156]

The Re release plot for the BSR (radioactive and simulant Module B), the 2008 engineering scale, and the historic data appear in Figure 8-13d. Due to the low concentrations of rhenium, it is a difficult element to measure. It is noteworthy that the Re release from the Module B simulant PCT tracks close to the Re release measured at SRNL for the radioactive Module B granular product. Note that the simulant Module B Re release tracks with the radioactive ^{99}Tc release. This demonstrates that Re and ^{99}Tc release are within experimental error of one another. The "tie back" strategy is, therefore, proven based on the fact that the radioactive and simulant BSR campaign products, i.e. releases of Re and ^{99}Tc, match each other and match the historic pilot and engineering scale data.

Thus, the FBSR minerals have been found to retain Re in the cage structure (~100%) of the granular mineral products as shown in Section 8.2.2 and Reference 120. Varying percentages of ^{99}Tc were

retained in the sodalite cage structure depending on the REDOX conditions (Table 8-34), and the lack of durability impact of REDOX of the FBSR product will be discussed in Section 8.2.8.

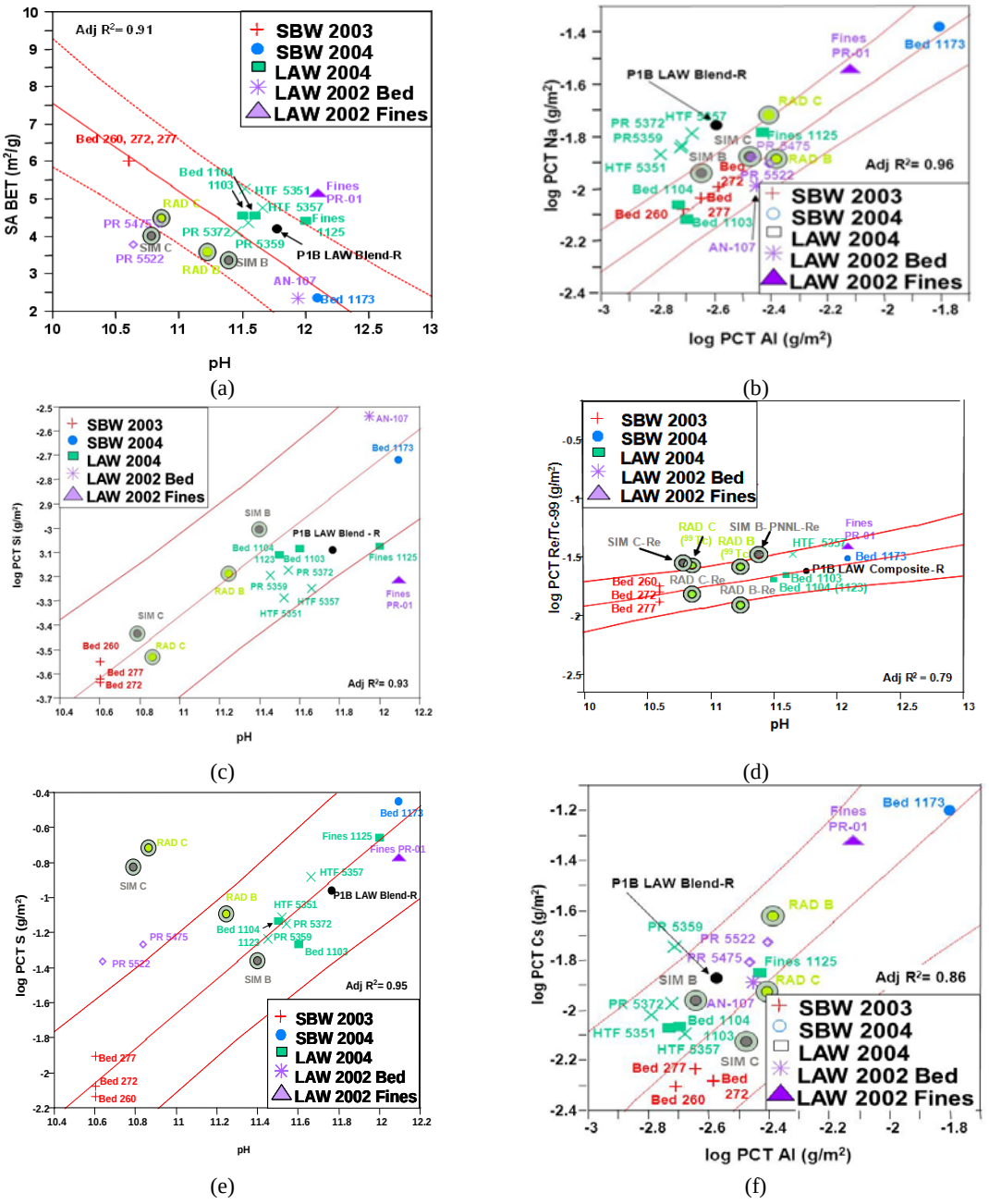

Figure 8-13. Short Term PCT Testing (ASTM C1285) Correlation Developed with INL Pilot-scale Test Results with Rassat Simulant from 2003-2004, and HRI/TTT Testing of LAW AN-107 Samples from 2001-2002 Testing with Current Module B PCT data from Engineering Scale ESTD samples and BSR samples Modules B and C (non-radioactive and radioactive).

8.2.5 *Product Consistency Long-term Testing (Granular Product)*

Long-term PCT tests are performed in the same manner as the short-term tests but PCT Method B [152] allows for longer time intervals, in this case, 1 month, 3 month, 6 month, and/or 12 month tests. More details about the long-term PCT-B testing and how the data generated can be used in conjunction with the results from PUF tests and geochemical modeling to evaluate waste form performance in a disposal environment in Appendix D.

The PCTs were performed at 90°C for extended times up to one year (PCT-B) in Teflon® vessels. The same analyses were performed on the long-term PCT leachates as the short-term PCT leachates. Due to the limited mass of product, all tests were conducted in duplicate and the results averaged. The elemental mass releases of selected constituents were normalized by the initial concentration of each constituent after adjustment for moisture and unreacted carbon content, and reported in units of g/m^2 as described the previous section. The leached solids were analyzed for phase mineralogy using x-ray diffraction looking for any mineral-water reaction products that could have formed. All of the raw data for the long-term PCT testing of the granular products are given in Appendix H of Reference 3.

PCT-B tests are useful for generating concentrated solutions to study chemical affinity effects on the dissolution rate. PCT Method B tests at high temperatures and high glass/solution mass ratios can be used to promote the formation of alteration phases to (1) identify the kinetically favored alteration phases, (2) determine their propensity to sequester radionuclides, and (3) evaluate the effect of their formation on the continued waste form dissolution rate. XRD was used as a tool to identify alteration phases but it should be noted that XRD sensitivity to minor phases is, in general, not very good.

Table 8-42 contains the PCT results for the engineering scale FBSR product of the LAW P-1B run at HRI and tracks the release rate of analytes as a function of time. PCT samples of the P-1B simulant granular product were leached for extended times. The 7-day results from Table 8-42 are shown with release results from samples leached for 1, 3, 6 and 12 months in Figure 8-14. For each of the elements analyzed, the release was consistent over the 1-year of testing. Silicon release was decreasing indicating solution saturation. Cesium release was decreasing as the silicon release was decreasing. Releases of other species held constant over the one year of testing indicating that the FBSR granular product was not undergoing a significant degradation. Re, I and Na were all released at about the same rate.

Table 8-42. Long-Term PCT Results for the Engineering Scale LAW P-1B Granular Product

Normalized Elemental Release (g/m^2)	Eng. Scale P-1B granular Test Interval				
	7 Days	1 Month	3 Month	6 Month	1 Year
Al	2.12E-03	2.86E-03	2.86E-03	2.93E-03	2.08E-03
S	1.41E-01	1.91E-01	1.42E-01	1.85E-01	1.61E-01
Cs	9.31E-03	1.66E-02	1.21E-02	1.58E-02	4.09E-03
Re	1.87E-02	3.56E-02	3.22E-02	3.92E-02	3.57E-02
Na	1.74E-02	2.53E-02	2.52E-02	2.94E-02	3.64E-02
Si	7.82E-04	6.84E-04	4.75E-04	3.39E-04	1.10E-04
I	1.51E-02	2.71E-02	2.59E-02	2.92E-02	2.79E-02
pH	11.63	11.65	11.50	11.43	10.29

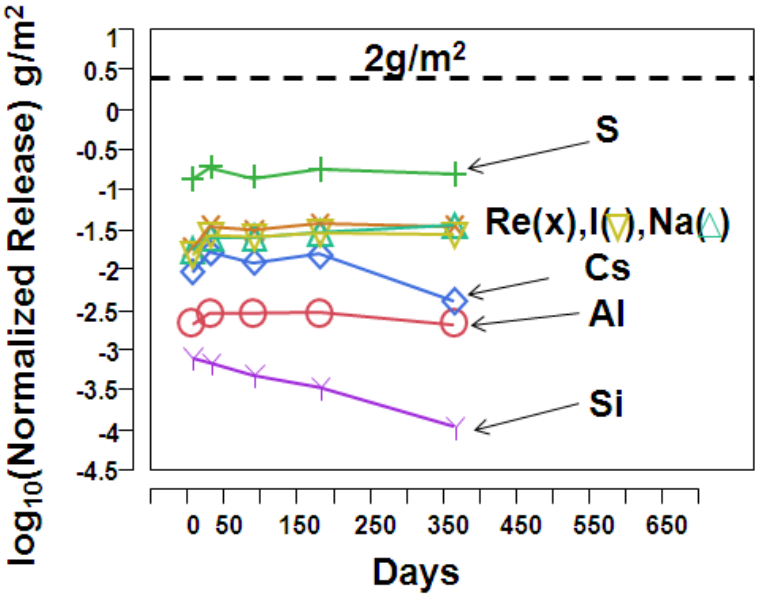

Figure 8-14. Release of Elements from P-1B ESTD Non-radioactive Rassat Simulant during 7 day, 1 month, 3 month, 6 month and 12 month Long-Term PCT Testing.

Figure 8-15 is an overlay of the XRD patterns of the ESTD FBSR LAW granules as received and after each leach interval. It is significant that all of the crystalline peaks of nepheline and sodalite have remained sharp and clear and of approximately the same height (intensity). This consistency implies that there has been little degradation to the mineral product throughout the 1-year leaching at 90°C. This is in agreement with the minimal change in leach rate over time shown in Figure 8-14.

Only one reaction product was noted in the XRD pattern, halloysite, indicated by the circle in Figure 8-15. Halloysite can form from many aluminosilicates and is the metastable reaction product that eventually forms kaolin clay. In other words, halloysite is the main metastable reaction product.[187,188] This indicates that excess and/or unreacted clay in the FBSR granular product may be degrading with time rather than the nepheline or sodalite phases formed during the FBSR processing. On geologic time scales halloysite will revert back to kaolin clay as a reaction product. However, since halloysite is only seen in the ESTD leaching experiments when ~10% excess kaolin was present and not in the BSR experiments where <5 wt% excess kaolin was present (Table 6-1 and Table 8-7), it is most likely that the halloysite formed from the excess clay. The diaoyudaoite seen in only one spectra is a mineral previously found in the ESTD FBSR products.[111,112]

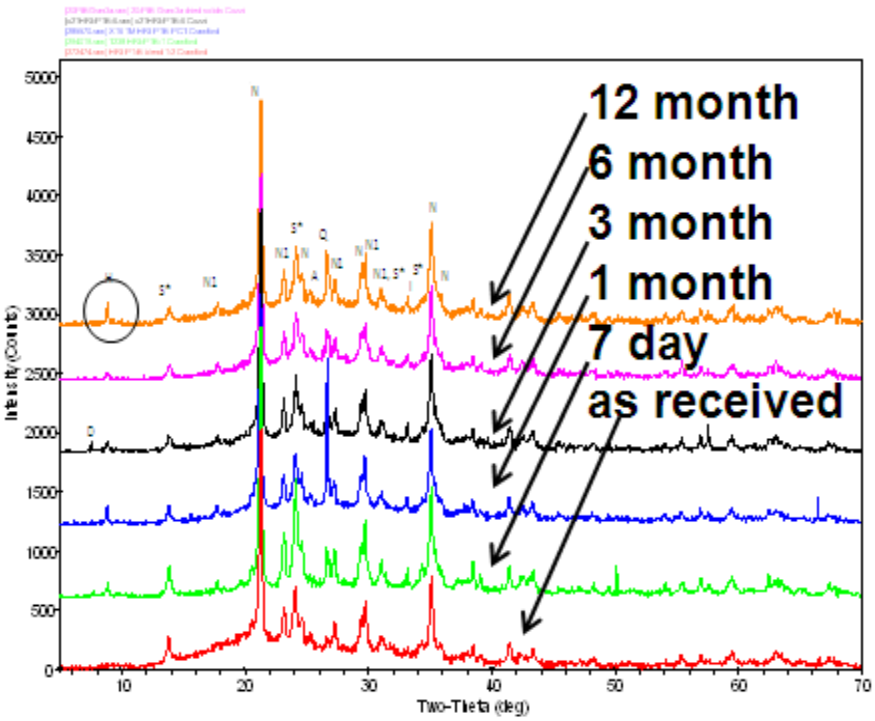

Figure 8-15. XRD Patterns of FBSR LAW P-1B Granules As-Received and After PCT Leaching.

N1 is Nepheline (O) $NaAlSiO_4$ (PDF 00-052-1342)
N is Nepheline (H) either $NaAlSiO_4$ (PDF 00-035-0424 top spectra)
S* is Sodalite (cubic) $Na_6Al_6Si_6O_{24}$ (PDF 00-042-0217)
A is Anatase, TiO_2 (PDF 00-021-1272)
Q is Quartz, SiO_2 (PDF 00-046-1045)
H is Halloysite, $Al_2Si_2O_5(OH)_4 \bullet 2H_2O$ (PDF 00-029-1489)
D is Diaoyudaoite, $NaAlO_{17}$, (PDF 00-021-1096)
Original XRD spectra fits are in Appendix I of Reference 3

For the BSR Module B granular product, the 7-day results are shown with release results from samples leached for 1, 3, 6 and 12 months in

Table 8-43 and Figure 8-16. For each of the elements analyzed, the release was consistent over the 1-year of testing. Silicon release was decreasing, while the other releases have held constant over the 1-year of testing indicating that the FBSR granular product was not undergoing significant degradation of the mineral species. Re, Cs and Na were all released at about the same rate with Na bounding the other releases. The sample REDOX was >0.36 Fe2+/ΣFe and indicates that iodine from more oxidized samples leaches less than in the more reduced P-1B sample.

Table 8-43. Long-Term PCT Results for the Bench Scale Module B Simulant Granular Product

Normalized Elemental Release (g/m^2)	Bench-Scale B Simulant Granular Test Interval				
	7 Days	1 Month	3 Month	6 Month	1 Year
Al	2.34E-03	2.32E-03	2.19E-03	2.30E-03	2.10E-03
S	4.34E-02	4.74E-02	5.04E-02	5.36E-02	6.00E-02
Cs	1.09E-02	NM	9.84E-03	8.05E-03	1.11E-02
Re	8.83E-03	8.65E-03	9.23E-03	9.86E-03	1.06E-02
Na	1.14E-02	1.22E-02	1.45E-02	1.66E-02	1.91E-02
Si	9.86E-04	8.24E-04	5.52E-04	3.32E-04	2.00E-04
I	9.82E-04	2.18E-03	2.19E-03	2.34E-03	2.10E-03
pH	11.40	11.10	10.48	10.01	10.30

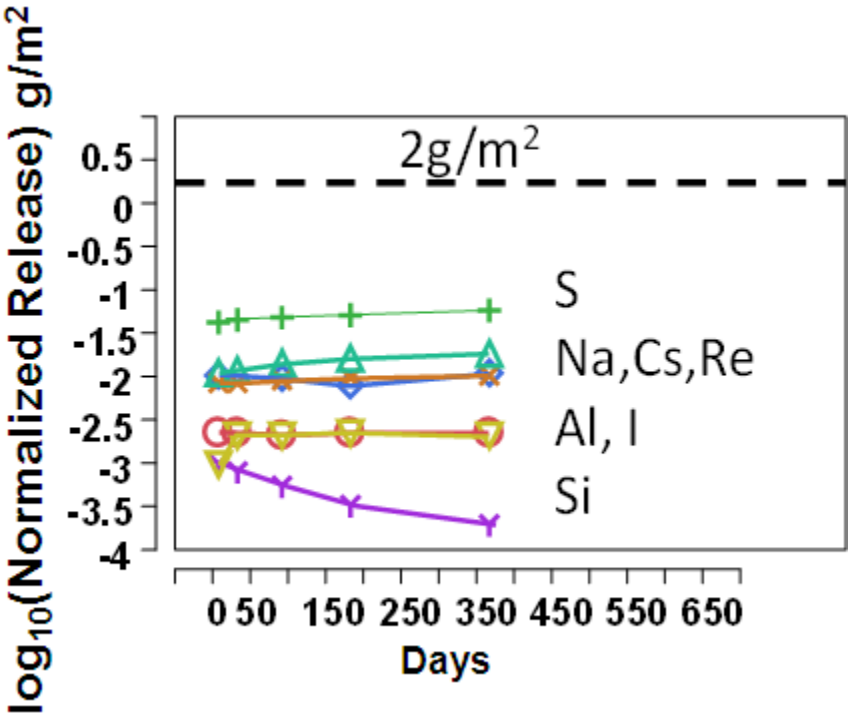

Figure 8-16. Release of Elements from BSR Simulant Module B during 7 day, 1 month, 3 month, 6 month and 12 month Long-Term PCT Testing.

Figure 8-17 is an overlay of the XRD patterns of the Module B simulant BSR product granules as prepared for PCT and after each leach interval. The XRD pattern for the as-received sample is on the bottom of the figure and the patterns are stacked with increasing leach duration. As with the FBSR LAW P-1B waste forms, the intensity and width of the major phases persist through all the leach intervals, indicating minimal degradation of the minerals. No reaction products were observed in any of the

powders after the long leaching intervals, as observed with the 1-year ESTD P-1B sample. This is likely because the BSR granules are completely reacted in the small chamber of the BSR.

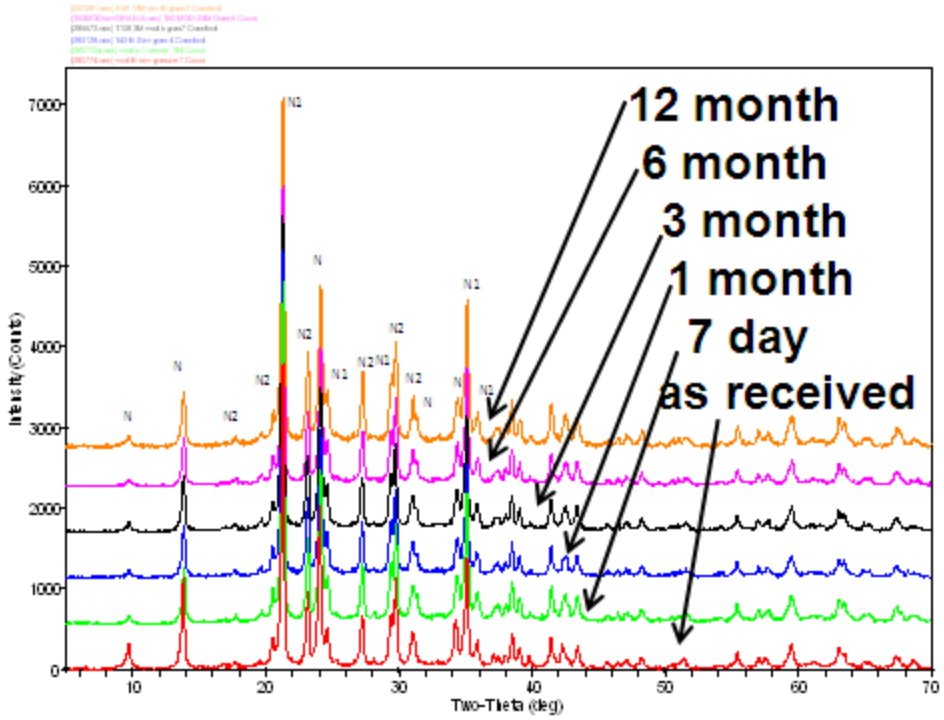

Figure 8-17. XRD Patterns of BSR Simulant Module B Granules As-Made and After PCT Leaching.

N1 is Nepheline (O) $NaAlSiO_4$ (PDF00-052-1342)
N2 is Nepheline (H) $NaAlSiO_4$ (PDF 00-035-0424)
N is Nosean (cubic) $Na_8Al_6Si_6O_{24}SO_4$ (PDF 01-072-1614)
Original XRD spectra fits are in Appendix I of Reference 3

For the Module B radioactive BSR granular product, the 7-day results are shown with release results from samples leached for 1, 3, and 12 months in

Table 8-44 and Figure 8-18. No 6 month interval was performed on the radioactive samples based on the results from the non-radioactive testing. For each of the elements analyzed, the release was consistent over the 1-year of testing. Silicon release was decreasing, while the other releases held constant over the 1-year of testing indicating that the FBSR granular product was not undergoing significant degradation of the mineral species. Tc-99 and Na were released at the same rate, which is similar to their congruent release with each other in glass. The sample REDOX was >0.41 Fe2+/ΣFe, which was similar to the 0.36 of the non-radioactive BSR samples. Iodine release rates were again lower than in the engineering scale P-1B sample, which was more reduced indicating that iodine release may be lower from more oxidized samples.

Table 8-44. Long-Term PCT Results for the Module B Radioactive Granular Product

Normalized Elemental Release (g/m^2)	BSR Rad B granular Test Interval			
	7 Days	1 Month	3 Month	1 Year
Al	3.97E-03	4.32E-03	4.39E-03	5.04E-03
S	7.72E-02	7.96E-02	9.14E-02	9.41E-02
^{137}Cs	2.29E-03	4.89E-03	4.18E-03	3.61E-03
Re	1.13E-02	9.26E-03	9.66E-03	1.12E-02
Na	1.24E-02	1.59E-02	1.76E-02	2.36E-02
Si	6.17E-04	6.39E-04	4.82E-04	3.30E-04
^{127}I	1.69E-03	1.61E-03	1.77E-03	2.16E-03
^{99}Tc	2.42E-02	<1.56E-02	1.96E-02	2.73E-02
^{125}I	<1.01E-01	<1.43E-02	<1.30E-02	<9.40E-01*
^{129}I	<3.61E-03	<2.92E-03	1.77E-03	<3.79E-03
pH	11.25	11.45	10.79	10.16

*Due to 60-day half life of I-125, the concentration at the 1-year interval had undergone numerous half lifes and is a very small concentration for the normalization [f_i – see section Equation 18]

Figure 8-19 is an overlay of the XRD patterns of the Module B radioactive granular product as received and after each leach interval. The XRD pattern for the as-received sample is on the bottom of the figure and the patterns are stacked with increasing leach duration. It can be noted from the figure that the intensity and width of the major phases persists through all the leach intervals, indicating minimal degradation of the mineral species. All of the original phases (nosean/sodalite, the two varieties of nepheline) from the BSR campaigns (radioactive Module B and non-radioactive Module B) appear in the XRD spectra and there are no reaction products present. The sodalite is reported as 42-0217 as in Figure 8-17 and is anhydrous. A hydrous sodalite pattern exists (42-0216) and the two structures are related and reported in the same reference by the same researchers. The sodalite in PDF 42-0217 states that the anhydrous sodalite was prepared from a hydrated sodalite with 8 waters of hydration, but that the sodalite prepared in PDF 42-0216 cannot be made that way and had to be prepared by slow rehydration of the anhydrous sodalite over a $NaNO_2$ solution at 65% relative humidity. Given that the sodalite formed over the $NaNO_2$ solution is not relative to the leaching scenario of the BSR product in deionized water, it is unlikely that the hydrated sodalite (PDF 42-0216) forms, otherwise it would contain 8 waters of hydration, which the XRD pattern fit does not support.

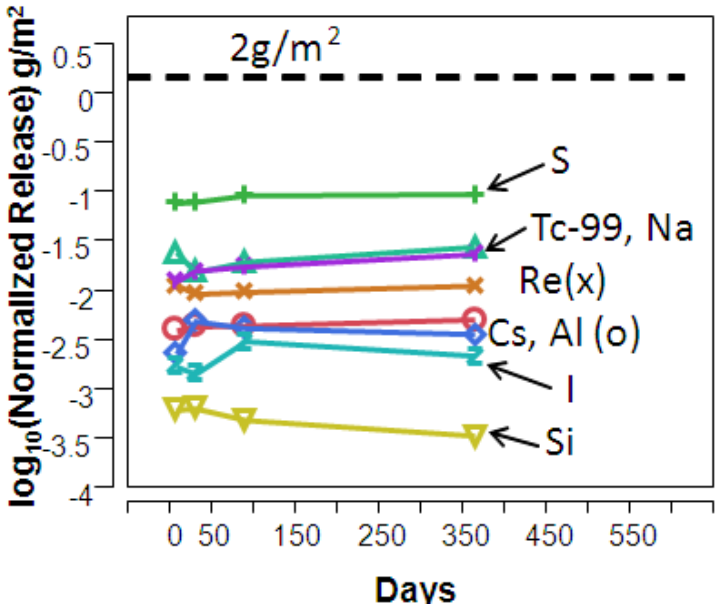

Figure 8-18. Release of Elements from BSR Radioactive Module B Granular Product during 7 day, 1 month, 3 month and 12 month Long-Term PCT Testing.

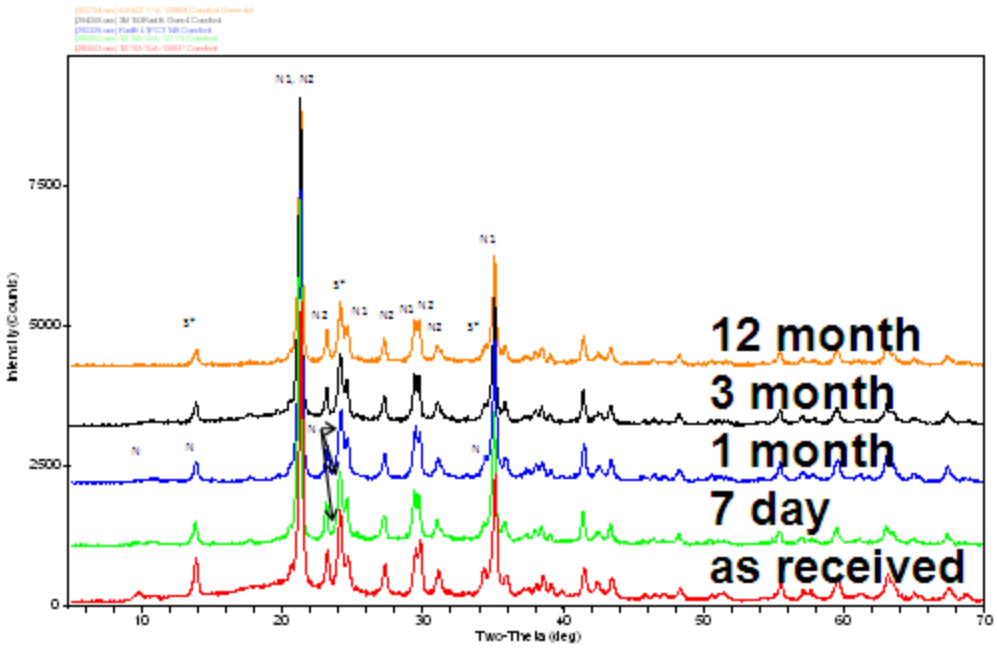

Figure 8-19. XRD patterns of Module B Radioactive Granules As-Made and After Long –Term PCT Leaching.

Where: N1 is Nepheline (O) $NaAlSiO_4$ (PDF00-052-1342)
N2 is Nepheline (H) $NaAlSiO_4$ (PDF 00-035-0424)
N is Nosean (cubic) $Na_8Al_6Si_6O_{24}SO_4$ (PDF 01-072-1614)
S* is Sodalite $Na_6(AlSiO_4)_6$ (PDF 00-042-0217)
Original XRD spectra fits are in Appendix I of Reference 3

8.2.6 *Single Pass Flow Through (SPFT) Testing (Granular Product)*

The SPFT method is frequently employed to measure the forward release rates of matrix elements and COCs in glasses and minerals [189,190,191,192,193,194]. More details about the SPFT test and how the data are used to determine the performance of a waste form in a disposal environment is given in Appendix D.

The SPFT test method involves running various *q/S (flow rate/surface area)* experiments that are designed to maximize the forward reaction (e.g., dissolution) and minimize the potential for back reactions (e.g., precipitation) at various temperatures. By maximizing the dissolution reaction, the effect of key environmental variables on the processes that control elemental release can be isolated and quantified. The trend shown in Figure 8-20 is typical of minerals and glasses and results from changes in the chemical potential difference between the mineral surface and the contacting solution. In other words, the dissolution rate decreases with decreasing *q/S* because when the flow rates are low or the total surface area is high, the concentration of elements in the contacting solution is also high. As the concentration of mineral components increase in solution, the solution approaches saturation with respect to some rate-limiting alteration phase(s). In other words, the dissolution rate slows down as the chemical potential difference between the mineral or glass and contacting solution decreases. In the case of a mineral or other solid phase, this effect can be expressed mathematically as the chemical affinity of reaction,

Equation 19

$$A = RT\ln\left(\frac{K}{Q}\right) = -\Delta G_r$$

Where:

A is the chemical affinity (kJ mol^{-1})

ΔGr is the free energy of reaction (kJ mol^{-1})

R is R is the gas constant (J mol^{-1} K^{-1})

T is the temperature (K)

K is the equilibrium constant (unitless

Q is the ion activity product (unitless).[195]

The chemical affinity is a measure of the departure from equilibrium. For additional details on the effect of chemical affinity on the dissolution rate, see Appendix A in Reference 6.

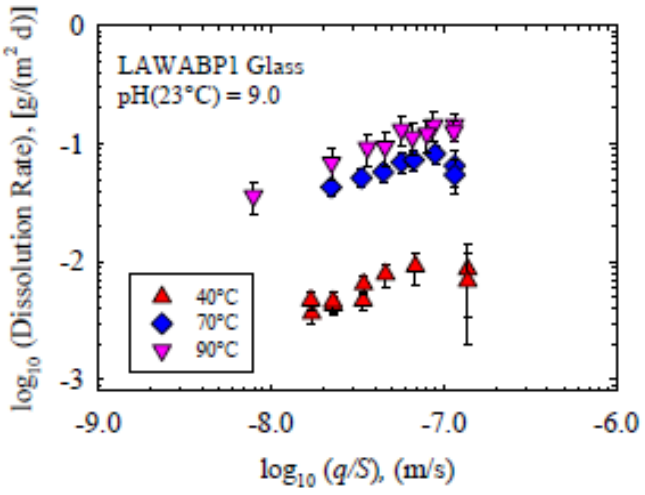

Figure 8-20. Dissolution rate, based on B release, as a function of flow-rate-to-sample surface area (*q*/*S*) for low-activity waste glass sample LAWABP1 at 40, 70, and 90°C and pH(23°C) = 9.0 (left).[196]

Equation 19 is derived from Transition State Theory (TST), which is based on the concept that a single elementary reaction is the rate-limiting mechanism.[197,198] As an intermediate step, a hydrated activated complex, which is transitional and short-lived, forms, and the breakdown of this activated complex limits the rate at which the overall reaction can proceed. The activated complex has a probability associated with it that can either decay into products or reform into reactants. Thus, activated complexes are in equilibrium with reactants, but the transformation into products is irreversible. The kinetic rate equation used to mathematically describe the hydrolysis reactions for minerals and glasses assumes that dissolution, via hydrolysis, is the driving reaction for the dissolution of the waste form matrix and subsequent release of radionuclides: a mineral or glass matrix must either dissolve or transform via replacement reactions before radionuclides can be released.

SPFT testing provides the parameters needed in the TST model for waste form diffusion, which is given by the general equation:

Equation 20

$$r = \vec{k} a_{H^+}^{-\eta} \; exp\left(\frac{-E_a}{RT}\right)\left[1-\left(\frac{Q}{K}\right)^{\sigma}\right]\prod_j a_j$$

Where:

r is the dissolution rate (g/m^2d)

k is the intrinsic rate constant (g/m^2d)

a is the hydrogen ion activity

E_a is the activation energy (kJ/mol)

R is the gas constant (kJ/mol·K)

T is the temperature (K)

Q is the ion activity product

K_g is the pseudoequilibrium constant

η is the pH power law coefficient

σ is the Temkin coefficient.

Quantification of parameters can be achieved by changing SPFT experimental conditions such as temperature, flow rate, pH, and the concentration of certain aqueous species. This method is only valid for homogeneous, single-phase materials. For the FBSR mineral product, which is a multi-phase material, the elemental composition of the effluent will be the signal from multiple materials dissolving simultaneously. If we assume a constant temperature and pH and a σ value of 1, Equation 1 simplifies to Equation 21.

Equation 21

$$r = k\left[1 - \frac{Q}{K}\right]$$

Therefore, by running the experiments in dilute conditions, Q goes to zero and the rate of mineral dissolution is equal to the temperature- and pH-dependent intrinsic rate constant.

Reaction kinetics were followed with the use of concentration measurements of the effluent concentrations of Al, Na, Si, Cs, I, and Re. When the concentration of a particular element is constant as a function of time then the system is assumed to be in steady-state conditions. The calculation of the dissolution rate in this steady state uses the following equation:

Equation 22

$$r_i = \frac{(c_i^{out} - c_i^{in}) \cdot q}{f_i \cdot S}$$

Where:

r_i is the normalized release rate of element i per unit area of glass (g/m^2d)

c_i^{out} is the concentration of element i in the effluent (g/m^3)

c_i^{in} is the elemental concentration of the influent (g/m^3)

q is the flow rate (m^3/s)

f_i is the mass fraction of the element in the original material (dimensionless)

S is the surface area of the sample (m^2).

In all cases, the background analyte was under the detection limit for the blank using the given analytical method and the mean limit of detection was used as the concentration of the element in the influent for calculations. The steady-state at each flow rate was determined when effluent concentrations of the analyte of interest differed by less than 10%. These conditions were obtained usually after three weeks of reaction time.

PNNL performed SPFT tests on the FBSR granular products from the ESTD (P-1B Rassat Tank Blend), BSR Rassat Tank Blend, and BSR radioactive SX-105 for periods of up to two months. The steady-state mineral release concentration was often achieved near 3 weeks of experimentation. At the smallest flow rates, steady-state concentrations were achieved on the order of 4 weeks of experimentation.

SPFT tests were conducted at 40°C for durations up to 2 months with a flow-through solution buffered at pH 9. The forward reaction rate of the simulant mineral product dissolution based on Si release for the granular product was measured to be $(6.2 \pm 2.1) \times 10^{-4}$ g/m^{2}d for the ESTD P-1B Rassat Blend product and $(13 \pm 4.9) \times 10^{-4}$ g/m^{2}d for the Rassat Blend BSR product. The SX-105 FBSR granular product created in the BSR using actual Hanford LAW gave similar release values and also demonstrated that Re and ^{99}Tc show similar release behavior with a dilute-condition release rate of $(1.1 \pm 0.5) \times 10^{-4}$ g/m^{2}d for ^{99}Tc and $(1.6 \pm 0.6) \times 10^{-4}$ g/m^{2}d for Re. These results indicate that the FBSR mineral product may be a suitable supplementary immobilization technique at the Hanford site and that both ^{99}Tc and Re occupy similar sites in the sodalite cage structure.[132]

When examining the release of the various species as a function of time, it is seen that the release of Cs, I, Re, and Tc have a different shape than Al, Na, and Si indicating that the release of these elements is controlled through a phase that has a different solubility compared with the bulk NAS phase. The release rates of all of the six elements listed here are near 1 x 10^{-3} g/m^{2}d. This in comparison to tests on similar materials conducted in unsaturated, non-dilute conditions (Pressure Unsaturated Flow Testing, PUF) where the releases of all these elements were dissimilar and I and Re were shown to be released at a rate roughly 100× times faster than the relatively insoluble Si when the experiment had reached a steady state.[131] This will be discussed in Section 8.2.7.

Figure 8-21 (top row) shows the normalized concentration of Al, Si, and Na (top row) and I, Re, and Cs (bottom row) at the SPFT outlet for the ESTD P-1B granular material (P-1BG) at 300, 150, and 10 mL/d. For the P-1BG granular material, at all flow rates and at short time periods, the release of Na is about an order of magnitude larger than the release of Si and Al, which appear to release concomitantly. The steady-state normalized concentration of Na is near 1×10^2 µmol/L at 300 mL/d and rises with decreasing flow rate to a value near 4×10^3 µmol/L at 10 mL/d. At higher flow rates, the Na concentration decreases sharply after the first sampling, whereas when the flow rate decreases the Na concentration stays constant for a few samplings and decreases more slowly suggesting that Na is supersaturated with respect to an unidentified mineral phase. Al and Si seem to be released concomitantly and the normalized concentration for the first sampling stays roughly the same across all flow rates (~1×10^3 µmol/L). Thereafter, Al and Si demonstrate similar release curves with lower flow rates giving higher steady-state normalized concentrations than higher flow rates. The concentration of these three elements converges for flow rates greater than 90 mL/d (not shown), but Na remains above the others for rates less than 90 mL/d. For the P-1B materials, the rates of the three elements seem to decrease after about 30 days at the higher flow rates suggesting that the mineral has dissolved to a point where the original measured surface area is no longer representative of the surface area available for dissolution.

Figure 8-21 (bottom row) shows the releases of Cs, I, and Re as a function of time for each flow rate. For the granular material, P-1BG, it is seen that Re and I follow similar trends, whereas Cs follows trends more similar to Na, Al, and Si. This is because the cationic species such as Cs can be substituted for Na

in the nepheline based or sodalite based mineral. Release of Re and I in the granular material seems delayed with respect to the bulk mineral product indicating that the aluminosilicate cage in the sodalite structure has to degrade before these species can be released. Initial high releases decrease and then go through a second maximum with time. The concentration of these elements at the second maximum is defined as the steady-state concentration of these two elements for the set of experiments because it is similar to the time when a transient steady-state release of Na, Al, and Si is observed.

The concentration of Na, Al, and Si released as a function of time from the granular Rassat Tank Blend made in the BSR, known as BSRG, follow similar trends and have similar graphs to the P-1BG material, see Figure 8-22 (top row). The only noticeable difference is that release concentrations stay constant for the entire testing period, whereas the P-1BG material seemed to show decreases in elemental concentrations at high flow rates and long time periods due to a diminishing surface area. Though, it is unclear if the BSRG materials would behave similarly because tests were not run for an equivalently long period of time. Releases of Cs, Re, and I from the BSRG as a function of time are shown in Figure 8-22 (bottom row). Cs shows nearly identical behavior in the granular to the P-1BG product. Along with these observations, one also sees a slight rise in Cs concentration with time as the experiments length increases similar to the phenomenon observed for the P-1BG mineral product.

Finally, the normalized concentrations as a function of time for Na, Al, and Si from the SX-105 radioactive granular product are given in Figure 8-23 (top row), while the releases of Re, Cr, and Tc are given in Figure 8-23 (bottom row). In general, similar conclusions can be drawn from this material as the granular products P-1BG and BSRG. The solution concentration for these elements is steady after 50 days of experiment.

The Re releases track the ^{99}Tc releases. For the SX-105 radioactive material, Cs and I data is not available. However, the release of ^{99}Tc and Re, are seen to release concomitantly from the material suggesting that they are present in the same phase and track each other in SPFT testing. The SX-105 material differs from the P-1BG and BSRG material in that there is not a sharp decrease in the concentration at short time periods. This observation supports the fact that only small amounts of perrhenate or pertechnetate salts are produced during fabrication and that Re and ^{99}Tc release is most likely controlled by sodalite dissolution rates.

Comparing the SPFT dissolution rate data of Neeway et al [126,132] from above on the ESTD FBSR Rassat simulant, the BSR Rassat simulant, and SX-105 to previous studies such as that by McGrail et al., [61] it is noted that McGrail et al. obtained the rate-law parameters required to model long-term performance by performing a series of SPFT experiments that were conducted as a function of flow rate (q) to sample surface area (S) and $pH_{(23°C)}$ from 7.0 to 11.0 at 90°C. They began by discussing the flow rate (q) to sample surface area (S) experiments, followed by pH sweep experiments. They observed a similar delay in the release of S and Re but McGrail et al. [61] did not identify this delay as resulting from sodalite dissolution at 90°C as Neeway et al. [132] do. There was also no data from the McGrail et al. study for I release, and the studies were conducted for 24 days but only at 90°C, which did not allow the observation of sodalite dissolution growth and slowing at the higher flow rates and lower temperatures. Of note is that Neeway et al. [132] were the first to show that Re and I have similar release behavior and that similar behavior of Re and Tc also occurs during SPFT testing. The release of these elements is assumed to be from the sodalite cage, which has been proposed as a getter in many nuclear waste immobilization processes.

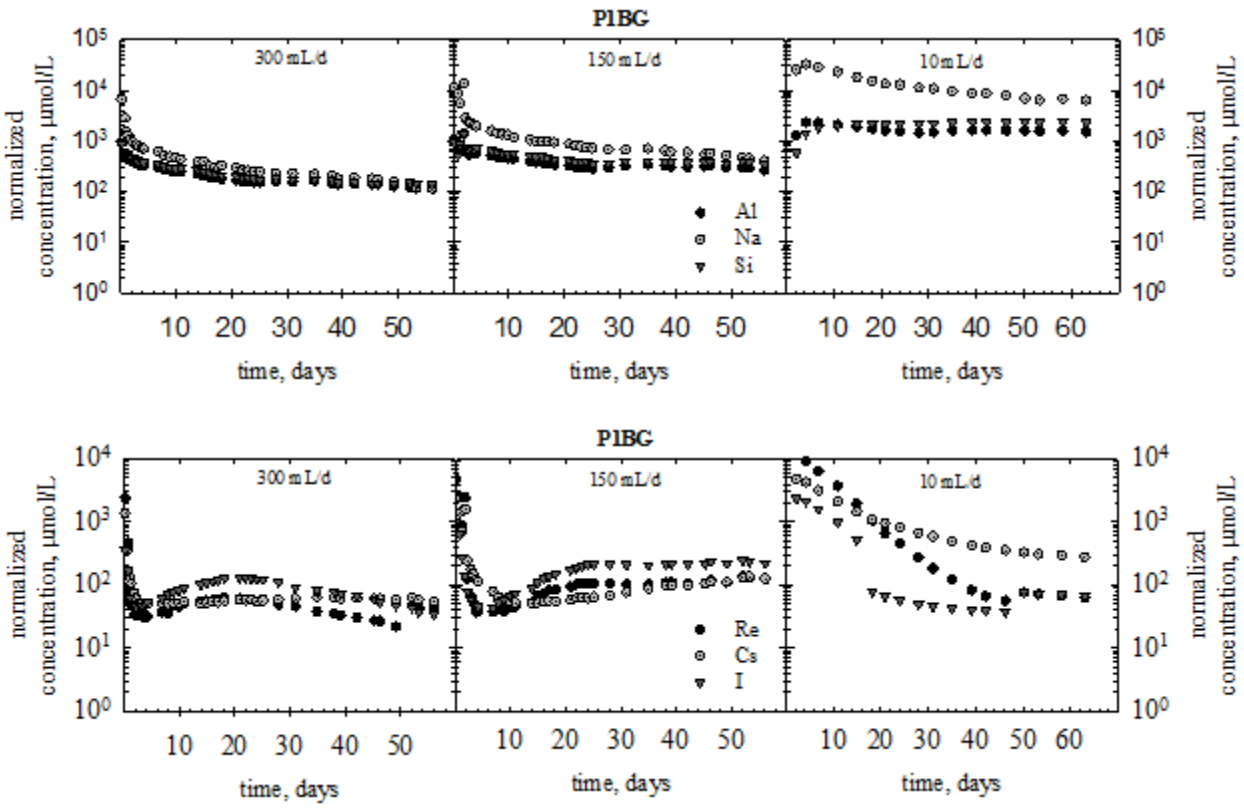

Figure 8-21. Normalized concentrations of Al, Na, and Si versus time for the P-1BG (top) and Re, Cs, and I (bottom) materials. The values are not corrected for background. Error from ICP-AES analysis is 10%.[132]

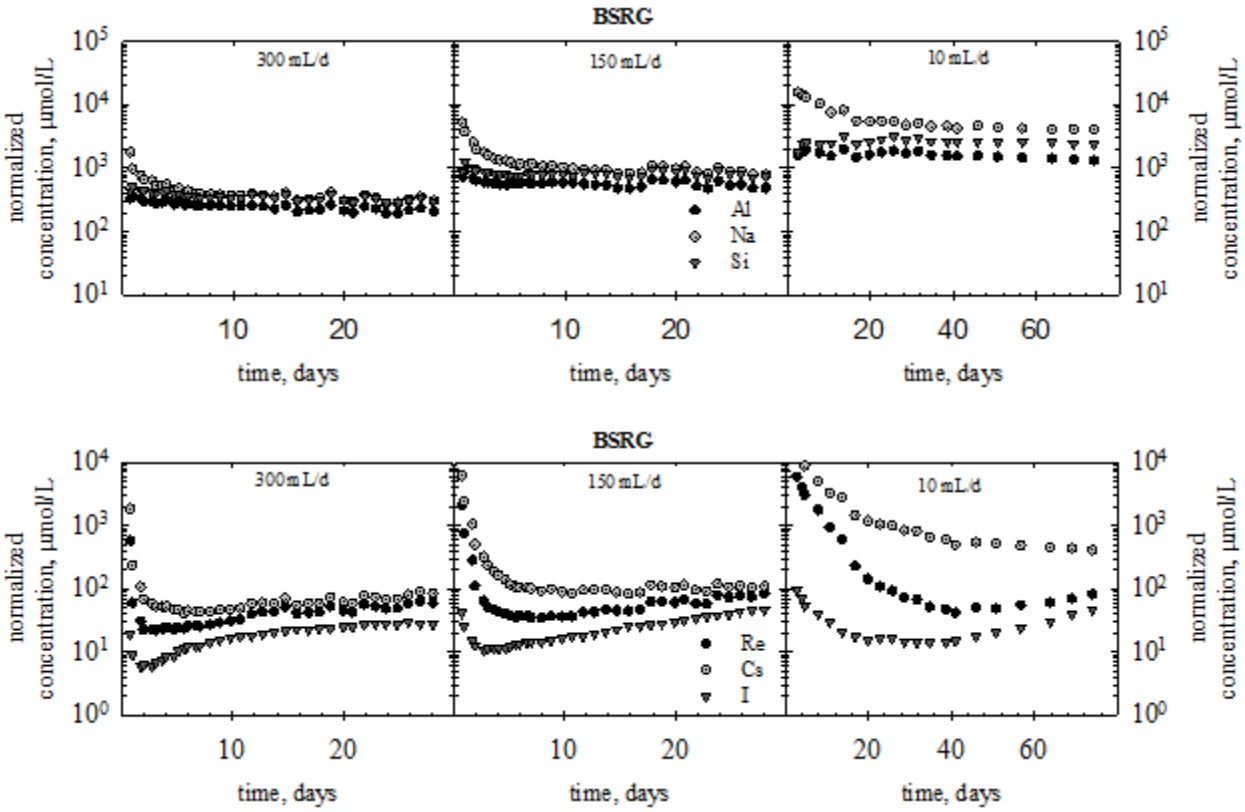

Figure 8-22. Normalized concentrations of Al, Na, and Si versus time for the BSRG (top) and Re, Cs, and I (bottom) materials. The values are not corrected for background. Error from ICP-AES analysis is 10%.[132]

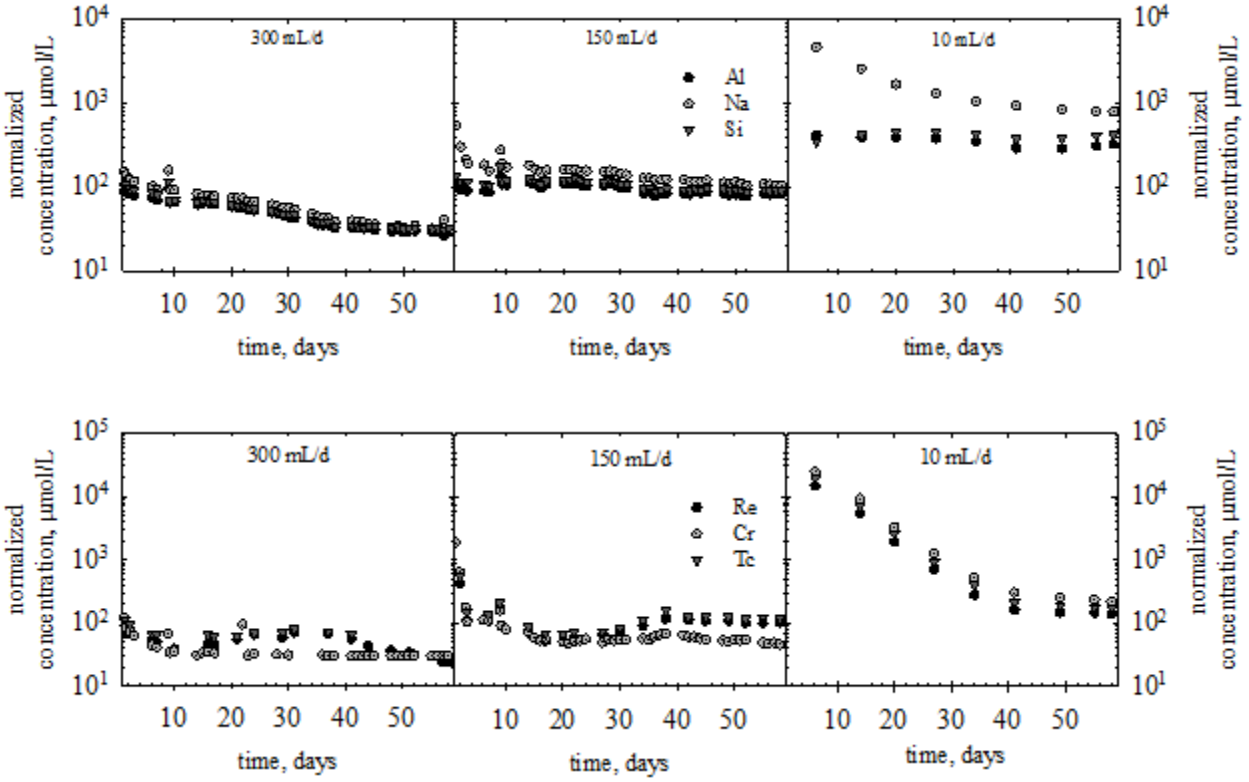

Figure 8-23. Normalized concentrations of Al, Na, and Si versus time (top) and Re, Cr, and Tc (bottom) for the BSR Radioactive SX-105 material. The values are not corrected for background. Error from ICP-MS analysis is 10%.[132]

A series of SPFT tests were performed by Lorier et al. [118] on the INL Rassat FBSR simulant samples. Analysis of the Lorier et al. data at 90°C suggested that these results were not conducted at the forward rate of reaction.[6] It appears that the data collected at 23 and 40°C may have been obtained at or near the forward rate of dissolution, but the short test duration (~14 days) prevented these experiments from achieving steady-state. Although these results cannot be used to compute the rate-law parameters needed for computer simulations of the FBSR waste form, these results provide an indication that Na and Si illustrate similar release behavior in experiments conducted under identical test conditions for the SCT02-98 AN-107 FBSR products [61] and the Rassat INL FBSR 1104/1123 samples. However, Al release appears to be significantly lower than previous measurements.[6] The comparison of the 40°C SPFT dissolution rates of Neeway et al. [132] on the Rassat simulant (ESTD and BSR scale) to the 40°C SPFT dissolution rates of INL SAIC-STAR 1123 Rassat simulant made at the pilot scale is given in Table 8-45. The magnitude of the releases is seen to be similar within the ranges of the errors tabulated recalling that the Lorier et al. [118] data may not have achieved steady-state.

Table 8-45. Release Rates derived from SPFT Testing for FBSR Engineering Scale and Bench Scale Rassat Simulant at 40°C and pH 9 Compared to Previous Testing on AN-107 at 90°C and pH 9.

	ESTD Engineering Scale P-1BG Rassat Blend Simulant at 40°C [132]	**BSR Bench-Scale BSRG Rassat Blend Simulant at 40°C** [132]	**INL SAIC-STAR Pilot Scale Rassat Blend Simulant LAW 1123 at 40°C** [118]
Al	$8.4\pm2.3 \times 10^{-4}$	$16\pm4.3 \times 10^{-4}$	$6.1\pm0.5 \times 10^{-4}$
Na	$10\pm2.9 \times 10^{-4}$	$18\pm5.0 \times 10^{-4}$	$5.9\pm0.8 \times 10^{-4}$
Si	$6.1\pm2.1 \times 10^{-4}$	$13\pm5.0 \times 10^{-4}$	$4.9\pm0.6 \times 10^{-4}$
Re	$19\pm5.3 \times 10^{-4}$	$24\pm6.5 \times 10^{-4}$	$4.5\pm1.8 \times 10^{-4}$
I	$28\pm7.6 \times 10^{-4}$	$32\pm8.8 \times 10^{-4}$	NA
Cs	$28\pm7.5 \times 10^{-4}$	$7.5\pm2.0 \times 10^{-4}$	NA
S	NA	NA	$11\pm14 \times 10^{-4}$

8.2.7 *Pressure Unsaturated Flow-Through (PUF) Testing (Granular)*

The PUF and PCT-B experiments conducted at elevated temperatures allow for the mineral–water and glass–water reactions to be accelerated; thereby allowing the researcher to gain insights into the mineral phases expected to form as a result of the weathering process. The process of mineral replacement is extremely important because the interplay between the primary minerals—nepheline, nosean, and sodalite in the case of FBSR—and secondary minerals will affect the chemistry of the solution in contact with the waste form. As previously stated, changes in solution chemistry will affect the rate of element release and subsequently radionuclide release. Accounting for these processes requires that a set of secondary phases that form from the long-term corrosion/weathering process and the precipitation-dissolution rate and/or solubility product for each of these phases be included in any PA calculation.

To demonstrate the durability of the FBSR product, which can be disposed of at the unsaturated IDF at Hanford, a series of tests has been performed using the PUF test system, which allows for the accelerated weathering of the solid materials. The system maintains hydraulically unsaturated conditions, thus mimicking the open-flow and transport properties that will be present at the IDF. A schematic representation of the instrument and more details about the PUF test and how the data are used to determine the performance of a waste form in a disposal environment is given in Appendix D.

Two materials were tested using the PUF system: 1) the P-1B granular product and 2) the P-1B granular material encapsulated in the GEO-7 flyash based geopolymer. The results of the graunular product are given here and the results of the geopolymer testing are given in Section 9.1.2.5.

Results of the year long PUF experiment on the P-1B material, shown as dissolution rates, is given in Figure 8-24. The dissolution rates demonstrate a trend of relatively constant effluent rates for Na, Si, Al, and Cs as a function of time. The elements I and Re show a steady release rate throughout the yearlong test from the granular FBSR product. This result suggests that these two elements may be present in the sodalite cage structure rather than in the predominant nepheline phase because their release is hindered due a possible shielding from the bulk nepheline ring structure.

Calculated one-year release rates for Si are on the order of 10^{-6} g/(m^2·d) for the granular FBSR P-1B product, while Re release is seen to be two orders of magnitude higher than Si release rates. The difference in these rates may be a result of the potential differences (or uncertainties) in the surface area measurements as the mineral waste form weathers.

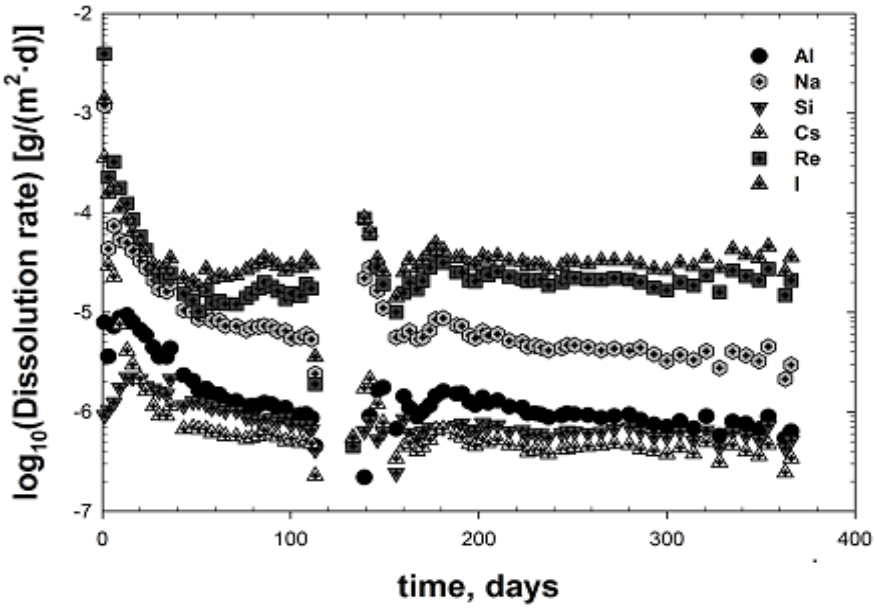

Figure 8-24. The normalized release rates for various elements from the ESTD P-1B Rassat LAW granular FBSR product as a function of time during the 1-year PUF test. Errors are typically on the order of 40% and are not shown to make the graph clearer.[131]

XRD analysis were performed on various subsamples of the reacted product as a function of depth in the column. The changes in mineralogy in the column area result of depth-dependent solution concentrations giving rise to chemical environments that may be supersaturated with respect to a number of mineral phases.

The XRD data, given in Figure 8-25, for the granular material shows a minor change in the phases that are present as a function of depth. All of the original mineral phases are still present in the sample at the end of the one year of testing whether at the top or the bottom of the column. The amorphous material is likely the excess clay in the P-1B, which becomes amorphous at the FBSR operating temperature since ~10 wt.% excess clay existed in the P-1B sample (see Table 6-1 and Table 8-7). This excess clay was shown to convert to halloysite during long-term PCT testing as identified by XRD (see Section 8.2.5 and discussion in Section 11.1). Halloysite can form from kaolin, it can be found associated with kaolin, and it can convert to kaolin.

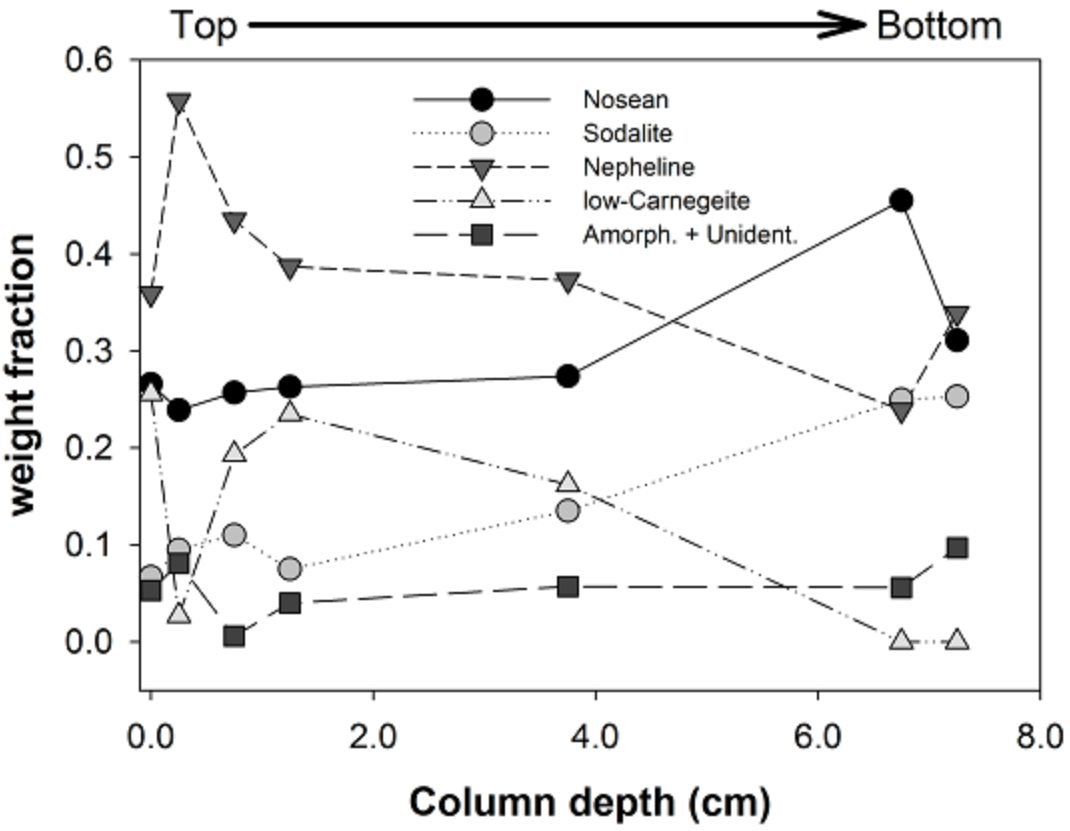

Figure 8-25. The weight fraction of mineral phases identified from subsamples of the PUF test for the ESTD P-1B Rassat LAW granular material using XRD as a function of depth in the PUF column. Each subsample uses roughly 0.5 cm in depth for analysis. The sample at zero gives the composition of an unaltered starting material.[131]

The data from the PUF testing of the P-1B material, which was made with the Rassat simulant on the engineering scale, can be compared to PUF testing performed by Pierce [6,106] and Pierce et al. [120] on the Rassat simulant made on the pilot scale at INL SAIC-STAR (bed products 1104/1123 and fines 1125) and the PUF testing performed by McGrail, et al. [61] on AN-107 made in a pilot scale FBSR. For example, Figure 8-26 shows the release of the elements from the AN-107 FBSR product to be lower than the release of B from LAWA44 glass. Note the similarity of the PUF plots for the P-1B Rassat similant FBSR product (Figure 8-24) and the AN-107 FBSR product (Figure 8-26). Of special interest is that the data in Figure 8-25 are two orders of magnitude lower than the data in Figure 8-26, which means that the Rassat FBSR product is ~2 orders of magnitude more durable than the LAWA44 glass shown in Figure 8-26 when BET data are used to calculate release rates.

The elemental release rate data for the AN-107 data is given in Figure 8-26 and shows a general decreasing trend with increasing reaction time. This behavior is typical of PUF experiments and is the result of the pore solutions achieving a steady-state concentration of elements released from the corroding FBSR matrix. The Re and S release are within the experimental error of one another in the PUF test. The steady state release of Al and Si is between one to two orders of magnitude lower than that for Na, Re, and S. This difference in release behavior suggests that Al and Si are being retained in the column, probably as a leach layer or alteration phase as noted in the P-1B sample. XRD analysis of reacted solids removed from different depths of the AN-107 PUF column after 100 days at 99°C suggests that all of the original minerals were still present at the top and bottom of the column as they are in the P-1B testing

(Figure 8-25). Although all of the original mineral assemblages were present along the vertical profile of each PUF column, McGrail et al. [61] suggests that nosean has diminished in the upper regions of the PUF test. This conclusion is based on a qualitative analysis of the XRD spectra and appears to be similar to what is seen in the P-1B Rassat FBSR product (Figure 8-26).

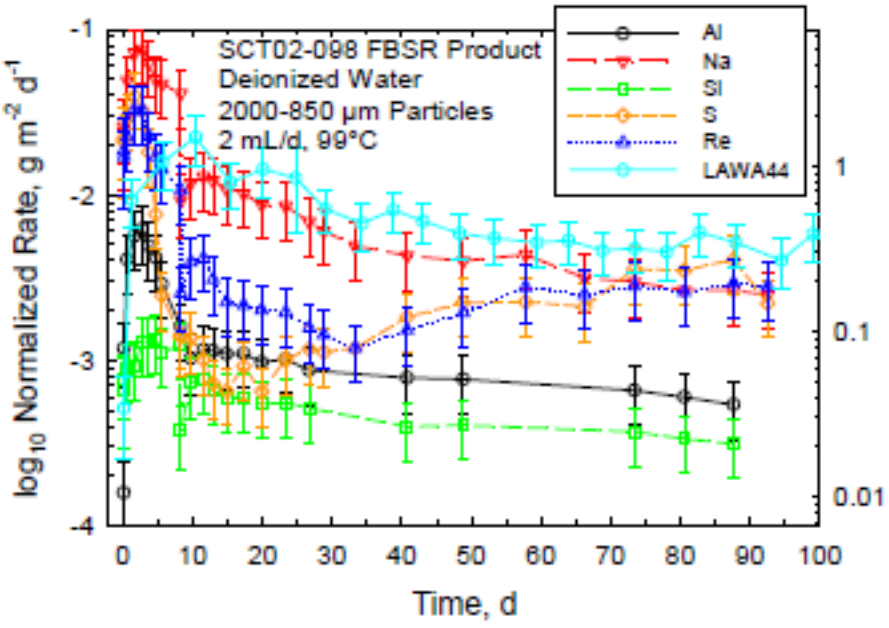

Figure 8-26. Dissolution rate, based upon Al, Na, Si, S, and Re release, for FBSR sample SCT02-98 as a function of time for PUF experiments conducted at 99°C.[6]

A comparison of the element release rates for the major components in the FBSR Rassat granular product made at SAIC-STAR is shown in Figure 8-27 from Pierce et al.[120] The rate of element release decreases as the reaction time increases in a similar fashion to the data for the P-1B Rassat simulant made at the engineering scale (Figure 8-25) and the AN-107 FBSR product made at the pilot scale (Figure 8-26). The results in Figure 8-27 also illustrate that the steady-state release rates (estimated to occur after 200 days of reaction) for Al [$(4.8 \pm 0.6) \times 10^{-5}$ g/(m^2d)] and Si [$(2.7 \pm 0.5) \times 10^{-5}$ g/(m^2d)] are equivalent and Na [$(1.1 \pm 0.2) \times 10^{-4}$ g/(m^2d)] release is ~2 to 4 times faster than Al and Si, respectively. In comparison to Al and Si, the steady-state release rate for Re [$(5.7 \pm 0.9) \times 10^{-4}$ g/(m^2d)] release is 10–20 times greater and S [$(2.0 \pm 0.4) \times 10^{-4}$ g/(m d)] release is 4–7 times greater.[120] Although the average steady-state Re release rate is ~2.8 times greater than the S release rate, the similarity in the observed time-dependent release behavior suggests that perrhenate sodalite and nosean may be associated with one another as was found in the AN-107 and P-1B samples. The slightly faster reaction rate for the perrhenate sodalite may be related to the possibility that Re may be present in the FBSR NAS product as a mixed salt anion-sodalite (see Section 2.2.1); in other words an anion-sodalite that contains multiple guest anions in the cage. There is a high probability for the formation of a mixed anion sodalite because other anions (i.e., Cl, F^-, SO_4^{2-} , etc.) are present in the FBSR feed material, specifically the LAW simulant, at concentrations that are several orders of magnitude greater than ReO^-_4.

Pierce et al. [120] also analyzed the reacted FBSR grains at various depths with powder XRD and confirmed that samples removed from the top of the column had the most extensive alteration. The XRD data suggests that the most reacted samples (from the 3.5-mm and 7.5-mm depth) have been significantly depleted in the $NaAlSiO_4$ phase that is similar to low carnegieite. Note that in Section 8.2.2 nepheline

(O), where "O" is for orthorhombic nepheline, is the phase identified as possibley being low-carnegieite) relative to the other phases present.

The fractional change of the phases as a function of depth in the PUF column is given in Figure 8-27 and indicates the reaction front has progressed ~30-mm (i.e., halfway) into the column. The fraction of anion-sodalite and nosean has been depeleted in the upper most samples (e.g., 3.5-mm and 7.5-mm) with the distribution of minerals contained in the remaining samples staying relatively constant (Figure 8-27). A similar trend is shown for nepheline in Figure 8-27 with the increase being largely associated with the depletion of the phase that resembles low carnegiete and the conversion of sodalite and nosean to nepheline.

The observed depth dependent XRD semi-quantative analyses are shown in Figure 8-28**.** The trends observed in Figure 8-28 occur because of the constant leaching of elements at the column inlet, which is caused by the addition of fresh deionized water that dilutes the equilibrated pore-water and provides the chemical potential needed for additional leaching of the FBSR NAS matrix. Additionally, the order of reactivity for each mineral phase also plays a role in the observed XRD profile because the thermodynamic stability of each mineral is different. Thermodynamic measurements indicate the order of reactivity is nepheline > nosean > Cl-sodalite > Re-sodalite. Although the XRD results are semi-quantitative, they suggest that the mineral phase that resembles low carnegieite dissolves first and is the least durable of all the mineral phases contained in the multiphase FBSR NAS waste form. The XRD results also indicate that the mineral distribution evolves with time but the dominant mineral phases contained in the FBSR NAS matrix are still present even after 2.5-years of leaching at 90°C and a high surface area-to-volume ratio.

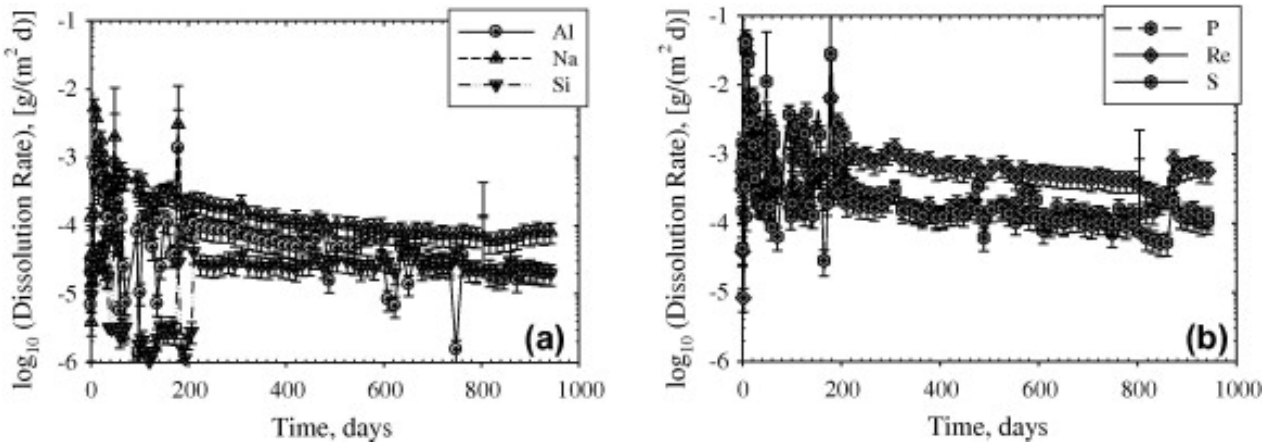

Figure 8-27. Normalized dissolution rate, in g/(m^2 d), as a function of time, in days, for Al, Na, and Si on the left (a) and P, Re, and S on the right (b).[120]

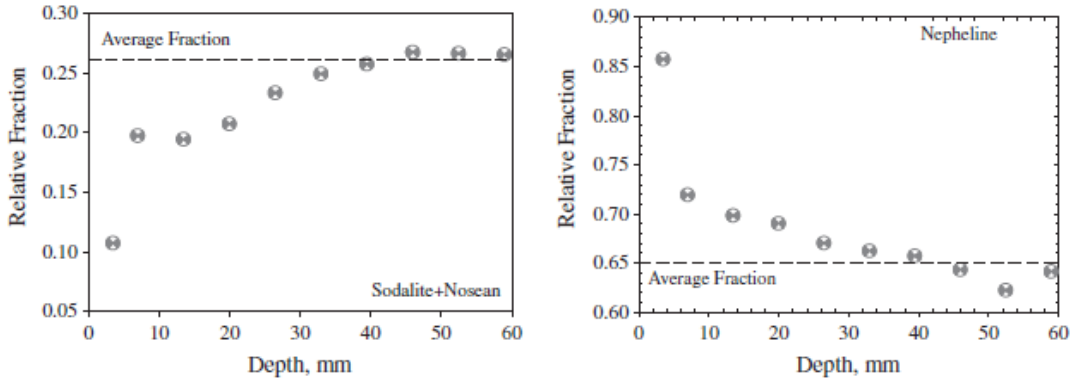

Figure 8-28. Relative fraction of the dominant minerals as a function of depth for the reacted NAS FBSR NAS waste form. The dashed line is the average fraction of the dominant minerals in the unreacted FBSR NAS waste form.[120]

In summary, all of the PUF testing on the AN-107 FBSR products made at the pilot scale [61], the P-1B Rassat LAW Blend FBSR products made at the engineering scale [131], and the Rassat LAW Blend FBSR products made at the INL SAIC-STAR pilot scale [6,106 ,120] are consistent with each other.

8.2.8 *FBSR REDOX: Is REDOX Control Needed as it is in Vitrification?*

8.2.8.1 *Vitrification REDOX Control*

In vitreous waste forms, the control of REDOX is important to the fate of ^{99}Tc, ^{104}Ru, and Cr.[199] The REDOX control in melters is also important for the fixation of leachable species from the glass such as Cr^{6+} and Tc^{7+} as a reducing melt retains these species in their less leachable oxidation states of Cr^{3+} and Tc^{4+}. Specifically, the DWPF melter at SRS maintains a reducing flowsheet (1) to minimize volatilization of radionuclides and hazardous species, (2) control melter foaming, (3) control undesirable metal nodule precipitation, and (4) atomically bond the radionuclides in their most durable oxidation state.

Chromium in the waste is volatile in a melter if it remains in the +6 oxidation state as $Na_2Cr_2O_7$ [200] and if the chromium remains in the +6 oxidation state in the glass it will be highly soluble in water/groundwater. At a REDOX, $Fe^{2+}/\Sigma Fe$, of 0.2 the Electromotive Force (EMF) series developed for melter REDOX control by Schreiber [201] predicts that 100% of the Cr^{6+} will be converted to the insoluble Cr^{3+} in a reducing melt. Thus the Cr is retained in the melt as Cr^{3+} and TCLP testing confirms that the Cr^{3+} is insoluble during durability testing.[202]

An extensive study by Vida [203] regarding the volatilitiy of ^{99}Tc during vitrification demonstrated that substantial amounts of ^{99}Tc is volatilized during vitrification in nitric acid (oxidizing) flow sheets regardless of whether laboratory or large scale melters were used for testing because the technetium +7 state forms a more volatile oxide (Tc_2O_7) than the +4 state (TcO_2). Laboratory scale testing with oxidized flow sheets by Lammertz, et al [204] quantified the ^{99}Tc loss as being nominally ~60% whether melter feeds were dry (calcine) fed or slurry fed. Under totally oxidizing conditions, the maximum ^{99}Tc that can be retained in borosilicate glass is ~33%, which is in the range (28-38%) of what has been observed in crucible studies [205,206] and 35.2% in pilot scale melters bubbled with air for single pass (no-recycle) melts when testing glass formulations for the Hanford Waste Treatment Plant.[207]

8.2.8.2 *FBSR Electro-motive Force (EMF) Series for REDOX Control*

Knowing that REDOX impacts volatility from HLW/LAW melt pools and that the REDOX of multivalent species plays an important part in glass durability, the fate of ^{99}Tc and Cr were investigated for the FBSR mineralized product (see References 3,4,5) and the discussion below.

Technetium has two dominant valance states where only one of the valance states will be captured into the sodalite/nosean type mineral structure. Tc^{+7} is the preferred valance state for the FBSR product as it forms the sodalite, $[Na_6Al_6Si_6O_{24}](NaTcO_4)_2$. On the other hand, Cr^{+6} is less desirable than the +3 valance states of Cr as Cr^{+6} is more mobile and toxic. To attain the preferred mix of valence states in the FBSR product, the impact of REDOX control was investigated. The first step to the investigation of REDOX on FBSR control, product performance, and off-gas performance was to have the same investigator, H.D. Schreiber, from Virginaia Military Institute (VMI) who developed the DWPF EMF series at the melter operating temperature of 1150°C, develop an EMF series for the FBSR process operating at ~725°C.[208]

Figure 8-29 is the FBSR EMF series developed by Schreiber [208]. The EMF allows one to take a measurement of the $Fe^{+2}/\Sigma Fe$ for the FBSR product and this defines the oxygen fugacity in the DMR at the time the sample was being processed. Fe is added as a REDOX indicator to the FBSR process feed as $Fe^{+3}(NO_3)_3$ and/or as the IOC denitration catalyst. Once the -log O_2 fugacity in the DMR is known, the percent of other reduced species can be determined for all the multivalent species given in Figure 8-29.

After the FBSR product is formed in the steam reformer, the product $Fe^{+2}/\Sigma Fe$ is measured colorimetrically to determine the overall product REDOX. A $Fe^{+2}/\Sigma Fe$ measurement between 0.15 and 0.5 is the range examined in this study (see also References 3 and 4). Reading from Figure 8-29, 0.15 $Fe^{+2}/\Sigma Fe$ gives 15% Fe^{+2} in the reduced state (top horizontal axis), which equates to log O_2 of -18 atmospheres. This oxygen fugacity gives >99% Re^{+7} and ~1% Cr^{+3}. At the other end of the range, 0.5 $Fe^{+2}/\Sigma Fe$ gives 50% Fe^{+2} in the reduced state (solid green vertical line on Figure 8-29), which relates to log O_2 of -21.2 atmospheres (solid horizontal green line on Figure 8-29), which relates to 8-10% Re^{+4} and 92% Re^{+7} (vertical dashed green line on Figure 8-29) and 75% Cr^{+3}. At $Fe^{+2}/\Sigma Fe$ of 0.5, the series indicate that ~38% of U (if it were present) would be U^{+4}, while 62% would be U^{+5} or U^{+6}. At this highly negative oxygen fugacity all the Mn is Mn^{+2}, all Ce is Ce^{+3} and most of the S is sulfide not sulfate, SO_4^{-2}.

In addition, the position of the Tc^{+4}/Tc^{+7} EMF was determined from the data in Table 8-8 and Table 8-34. The data in Table 8-46 is given in terms of wt% Tc+7 in sodalite, Tc+4 in sulfide, and Tc+4 in TcO_2. Since the EMF y-axis is oxygen fugacity and not sulfur fugacity, it was decided to normalize out the weight fraction of the Tc sulfide and calculate R, the log of the reduced species/oxidized species based on only the oxide components. The sulfide/sulfate EMF couple is shown in Figure 8-29 and Figure 8-30. At the more oxidized oxygen fugacities below the couple, sulfur exists as SO_4^{-2}, while above the sulfur couple the sulfur exists as sulfide: the sulfur couple takes into account the impacts of oxygen on sulfur. Therefore, the data shown in italics in Table 8-46 defines the elemental Tc ratios and the REDOX values used to add a Tc couple to the Schreiber EMF (see Figure 8-30). Figure 8-30 indicates that the Tc couple, the dark hatched line defined by the black and gray ellipses, are virtually an extension of the Re couple at more negative oxygen fugacities than the Re couple for the Tc oxide components.

Table 8-46. REDOX Measurements and X-Ray Absorption Spectroscopy (XAS) Speciation for ^{99}Tc (data from Table 8-34 and Table 8-8)

Waste	Sample	$Fe^{+2}/\Sigma Fe$ Original	$Fe^{+2}/\Sigma Fe$ Rerun	Log R (Fe^{2+}/Fe^{3+}) Original	Log R (Fe^{2+}/Fe^{3+}) Rerun	Tc^{+7} Sodalite (wt.%)	Tc^{+4} in TcO_2 (wt.%)	Log R (Tc^{4+}/Tc^{7+})
Mod B Tc Spike	RAD *(On-spec)*	0.37	0.29	*-0.23*	-0.44	83.62	16.38	*-0.71*
	RAD *(Off-spec)*	0.64	0.51	*+0.25*	*+0.02*	78.27	21.73	*-0.56*
Mod C Tc Spike	RAD *(On-spec)*	0.39	0.25	*-0.19*	-0.477	86.12	13.88	*-0.79*

R= reduced species/oxidized species

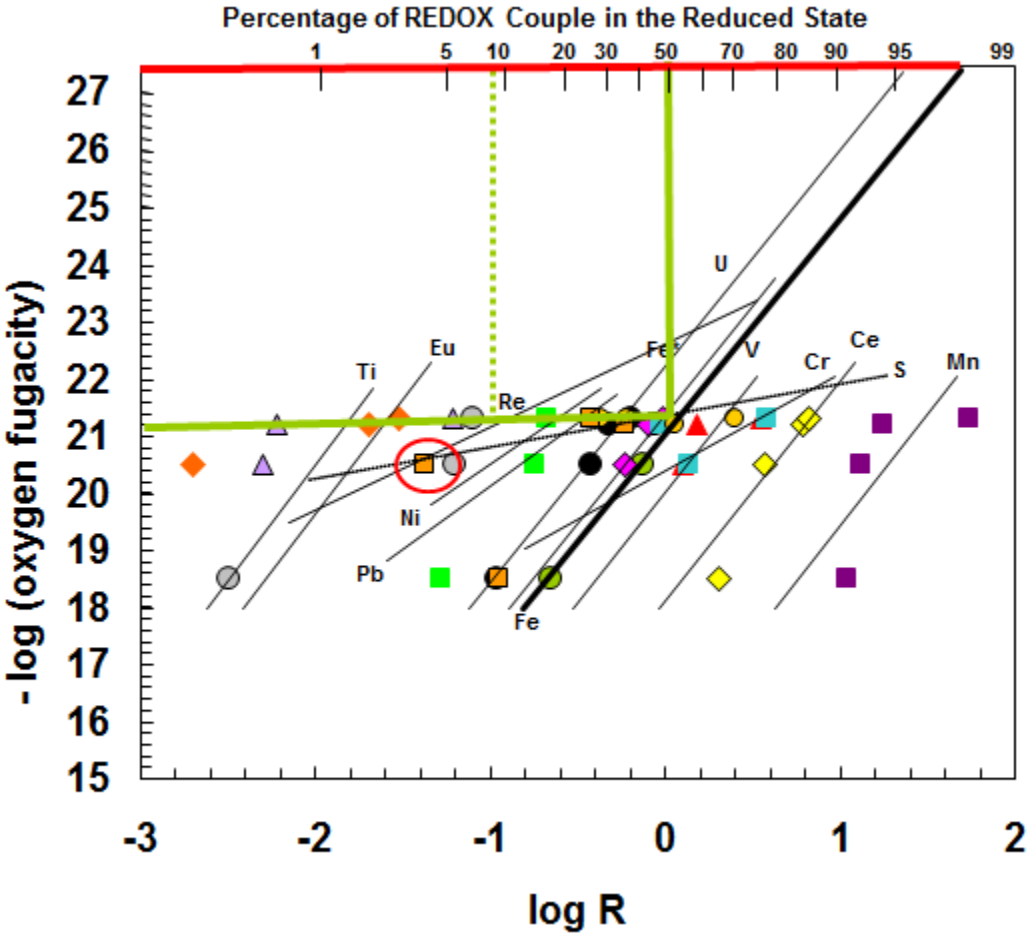

Figure 8-29. Species REDOX Target vs -log O_2 Fugacity [208]

Top axis is Reduced Species/Total amount of Species, i.e. $Fe^{2+}/\Sigma Fe$.
Bottom axis is Reduced Species/Oxidized Species, i.e. Fe^{2+}/Fe^{3+}.
REDOX keys off of the line labelled Fe (1 wt%) not Fe* (4.75 wt%).

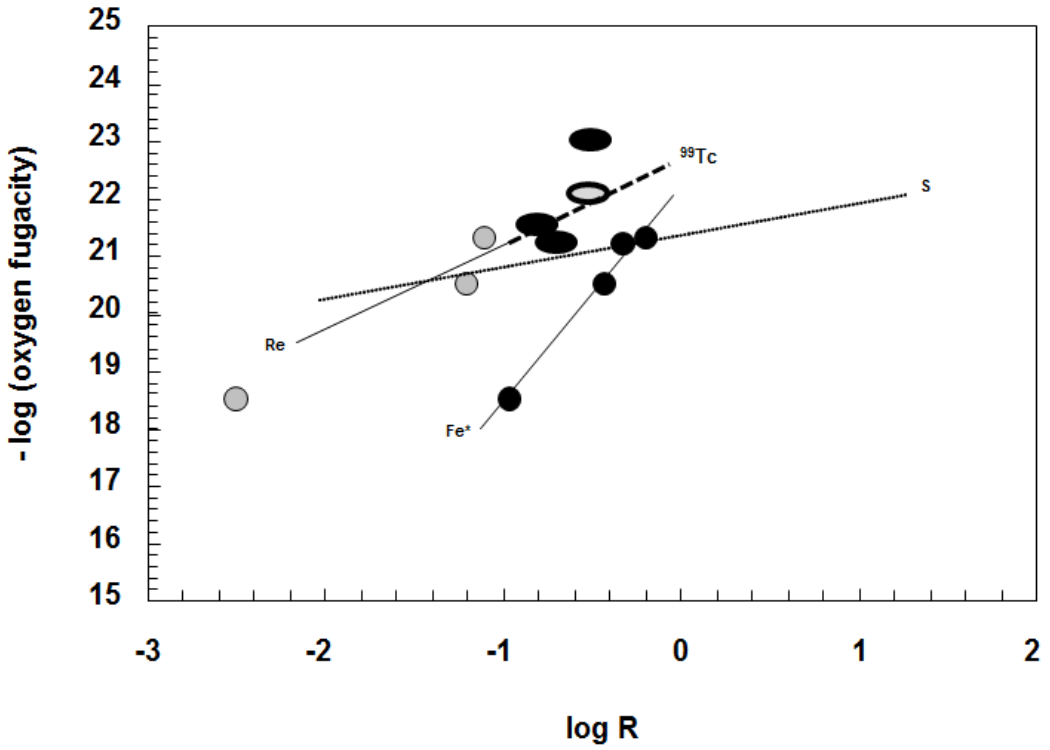

Figure 8-30. Species REDOX Target vs -log O^2 Fugacity for Tc^{4+}/Tc^{7+}. Data in italics in Table 8-46 was used to define the black and gray ellipses that define the Tc couple.

8.2.8.3 *Impact of REDOX on Volatilization: Mass Balance*

Since the various BSR radioactive and non-radioactive campaigns had slightly different REDOX conditions from each other (Table 8-8), the mass balance values from Section 8.2.1 were plotted against REDOX to see if the BSR processing REDOX had any impact on the releases of multi-valent and/or COC species to the off-gas. As can be seen in Figure 8-31, no trends of multi-valent species releases to the off-gas were noted as a function of REDOX.[5] The plots shown in Figure 8-31 for Cs, Re, ^{99}Tc, and I release have correlations with $R^2 < 0.50$, which means there is no discernable trend. The dashed line at 0 release of each component in Figure 8-31 to the off-gas indicates that the apparent trends are likely due to analytic error as the percentage releases are all <0.5%. The FBSR minerals were found to retain Re in the cage structure (~100%) of the granular mineral products and varying percentages of ^{99}Tc depending on the REDOX conditions (see Section 8.2.2).[6,120] It should also be noted that the percent sulfate/sulfide in the off-gas was zero, as all S species partitioned to the FBSR product. One can then conclude that there is no impact of REDOX on FBSR off-gas as there is for vitrification (see Section 8.2.8.1).

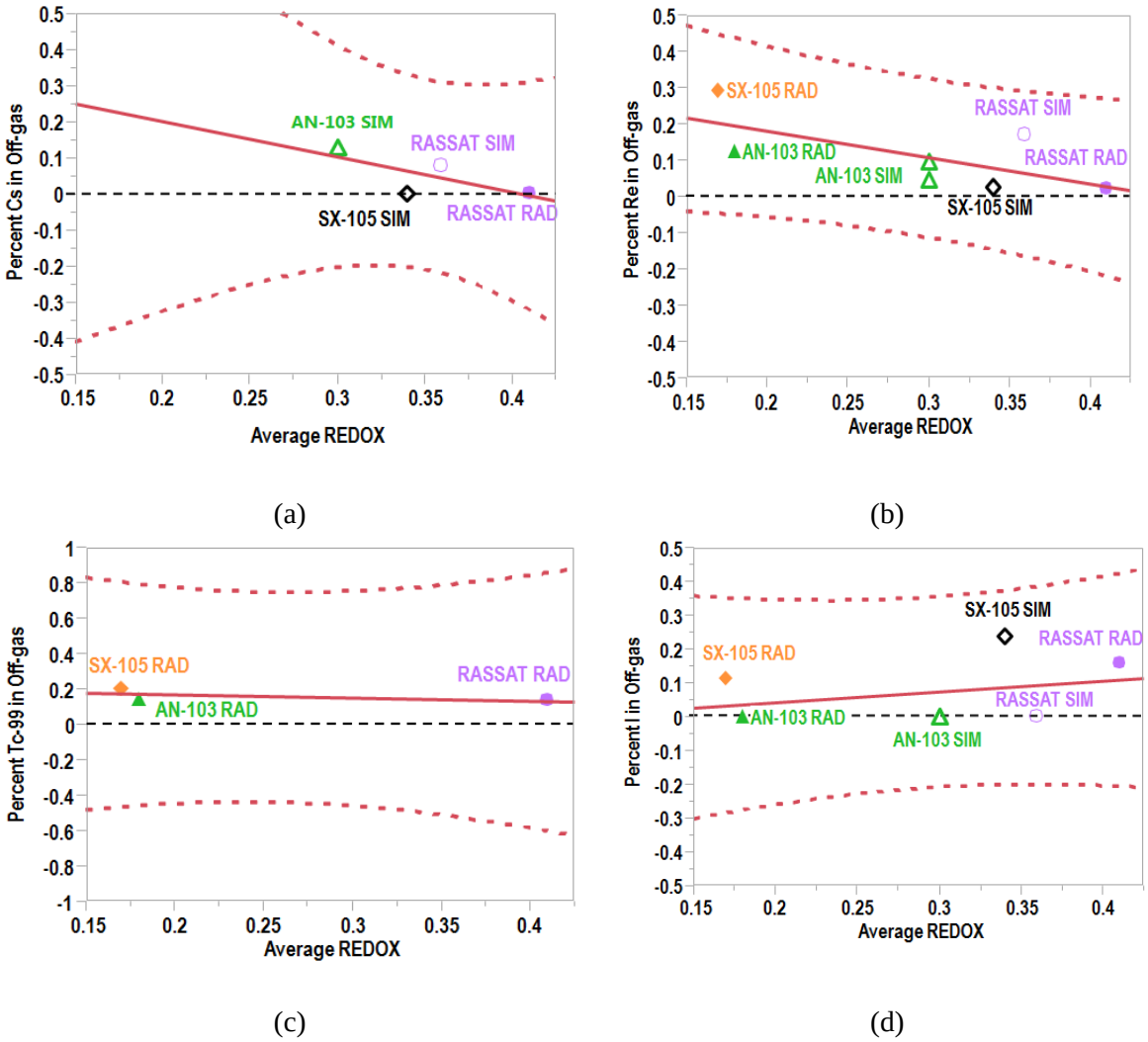

Figure 8-31. Lack of Correlation of REDOX and Multi-valent Species Release to BSR Off-gas.

8.2.8.4 *Impact of REDOX on FBSR Product Durability*

Since the various BSR radioactive and non-radioactive campaigns had slightly different REDOX conditions from each other (Table 8-8). the short-term PCT-A test values from Section 8.2.4 were plotted against REDOX to see if the BSR processing REDOX had any impact on the releases of multivalent and/or COC species to the leachate. As can be seen in Figure 8-32, no trends of multi-valent species (I, Re, ^{99}Tc) or Cs releases to the leachates were noted as a function of REDOX. The ^{99}Tc remains insoluble whether it is in the sodalite cage locally bonded in the +7 coordination with surrounding oxygen or whether it is in the +4 state as technetium (TcO_2) or technetium heptasulfide ($Tc_2S(S_2)_3$) (see Table 8-34). Since the relative position of the one year long-term PCT-B test responses follows the trends observed for the short-term PCT-A tests, one can conclude that there is no impact of REDOX on FBSR product durability as there is for vitreous waste forms (see Section 8.2.8.1).

Figure 8-32 does indicate that the release of I, Re, ^{99}Tc or Cs from the monolith is consistenly about one order of magnitude lower than the release from the granular product. However, all the FBSR leachate releases, granular and/or monolith are two orders of magnitude or more lower than LAW glass, i.e. the logarithm of 2 gm/m^2 is 3 x 10-1 g/m^2 on the axis given in Figure 8-32.

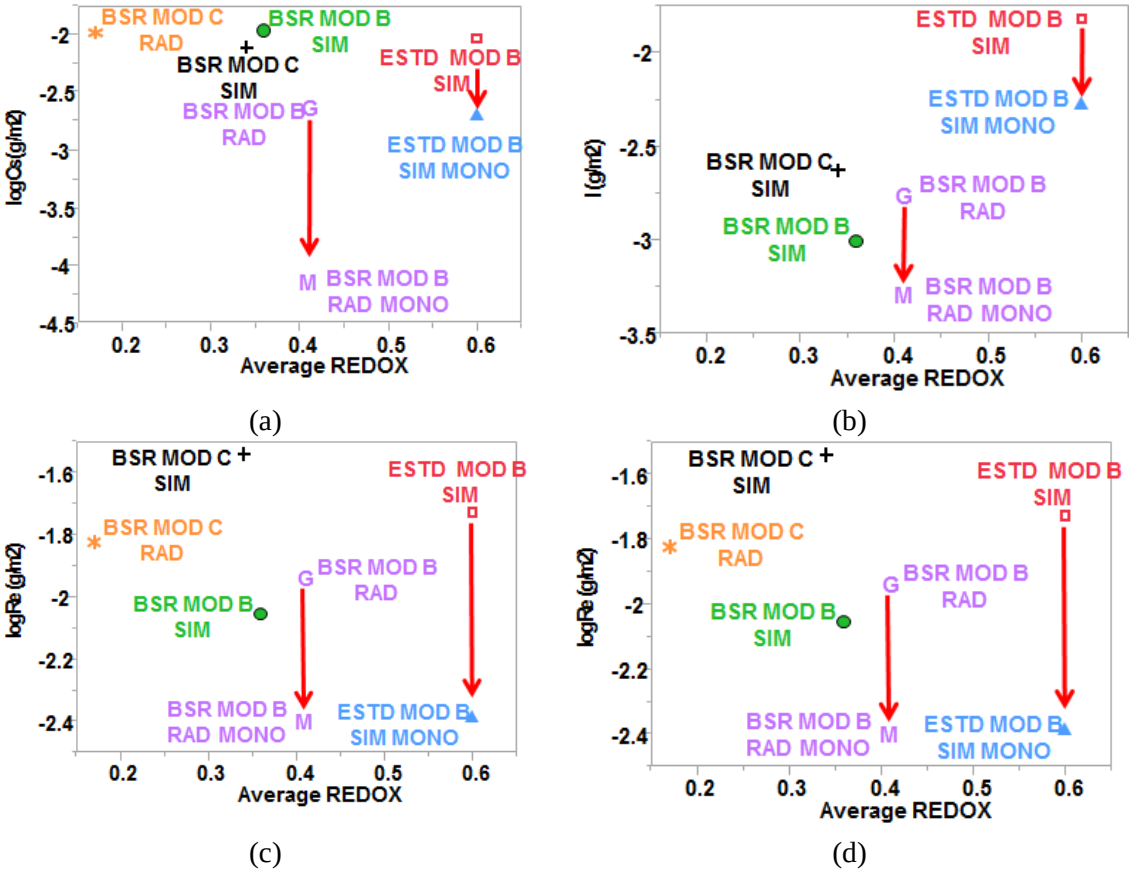

Figure 8-32. Lack of Correlation of REDOX and Multi-valent Species Release to Leachates in FBSR Samples from the ESTD and the BSR.

8.2.9 *Toxicity Characteristic Leaching Procedure (TCLP) (Granular Product)*

The TCLP Method 1311 was used to assess the release of RCRA metals from the granular BSR product. For the purposes of this evaluation, this section reports the TCLP results for the granular product, while Section 9.1.2.6 reports the TCLP results for various monolithic products.

The TCLP is an EPA approved procedure designed to determine the mobility of both organic and inorganic analytes present in liquid, solid, and multiphase wastes. The main purpose of this procedure is to determine whether the FBSR waste form will meet the requirements of the RCRA LDR since Hanford tank wastes contain hazardous constituents and are listed wastes. The initial focus of the TCLP analyses is on inorganic contaminants, because steam reforming effectively destroys organic materials[i]. TCLP data for the granular products are considered

[i] If FBSR is selected during the down select process, more rigorous RCRA testing will be conducted at a larger scale at a later time to support a Determination of Equivalent Treatment and (if required) a Treatability Variance in accordance with the Waste Form Qualification Program Plan (2).

inputs to the go / no-go evaluation process, primarily from Modules B and C (Table 5-4). The TCLP [209] was used to assess the release of RCRA metals from the granular BSR products for Modules D and E, as well. Samples submitted by SRNL were analyzed by General Engineering Laboratories (GEL), LLC, Charleston, SC or Davis & Floyd, Inc., Greenwood, SC. Figure 8-33 is a flowchart of the analytical process of the TCLP samples. A detailed description of the TCLP analysis is in References 3 and 4.

Since the BSR REDOX control strategy had not been worked out completely, some of the Module C BSR products had a REDOX more oxidizing than 0.20 (<0.20 $Fe^{2+}/\Sigma Fe$), some were in the desired range (0.20-0.60 $Fe^{2+}/\Sigma Fe$ for the simulant and 0.20-0.50 $Fe^{2+}/\Sigma Fe$ for the radioactive; Table 7-1), and others were more reduced than desired (>0.60 $Fe^{2+}/\Sigma Fe$ for the simulant and >0.5 $Fe^{2+}/\Sigma Fe$ for the radioactive). This allowed SRNL to have the TCLP measured on different REDOX samples to study the impact of REDOX on the Cr leaching. The Module B and C simulant samples were sent to GEL. The radioactive Module C BSR products were in the desired REDOX range, and TCLP was performed on the Module C radioactive material by PNNL.[ii]

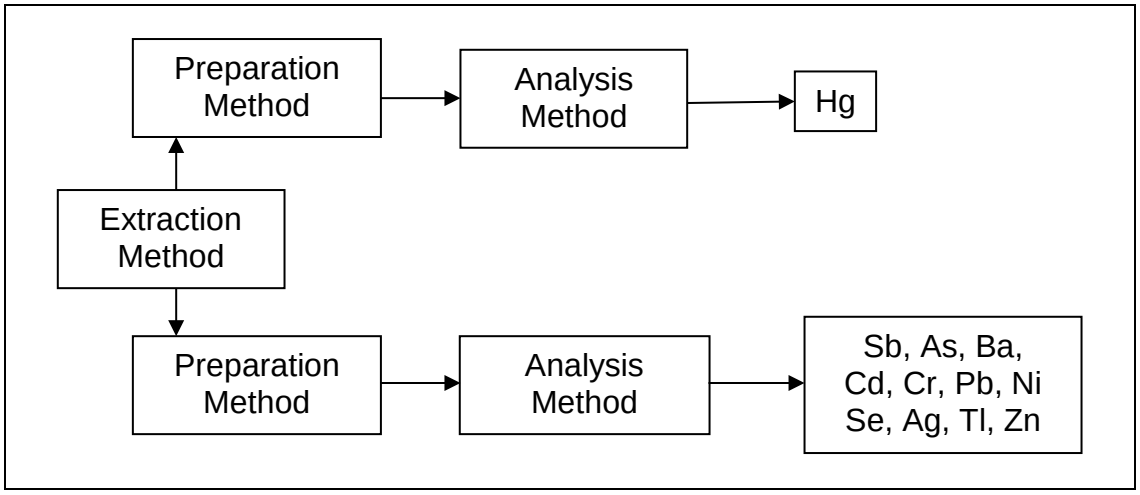

Figure 8-33. TCLP Analysis Sample Flow

The Module D simulant was in the correct REDOX range and SRNL submitted these samples to Davis and Floyd, an EPA certified laboratory for TCLP analyses. PNNL performed the radioactive Module D TCLP.

Two Module E simulant samples were made at a target REDOX of 0.15 $Fe^{2+}/\Sigma Fe$. One contained no IOC and the ferric nitrate nona-hydrate was the only additional source of iron, and the other contained the IOC and no ferric nitrate nona-hydrate. This was done to help evaluate the impacts of oxidizing REDOX on chromium leaching in the presence and absence of the IOC. Since the IOC has its own REDOX of 0.57 (Table 7-1), its presence can complicate the

[ii] Note that PNNL performed the TCLP in Washington at the Coastal Biogeochemistry Group at the Marine Science Laboratory (MSL). The MSL maintains national accreditation for its analytical services work with NTI (formerly called NELAC) (http://www.nelac-institute.org/index.php). MSL's accreditation is through the State of New Jersey, Department of Environmental Protection (Laboratory Certification ID# WA004). Among the analyses that MSL has accreditation for is the TCLP of wastes and soils for the analysis of metals.

measurement of the REDOX ratio, but attempts can be made to quantify how much IOC is needed at an oxidizing REDOX to retain the chromium as +3 chrome in the spinel mineral phase, which is isostructural with the IOC mineral phases.

Table 8-47 contains the TCLP results for the Module B granular products for all sets of testing with the Rassat material, i.e. ESTD engineering-scale, INL SAIC-STAR pilot-scale, and non-radioactive and radioactive BSR testing in SC and WA states. For comparison, results from the ESTD granular product, as reported in Reference 123, are given for material produced from the HRI/TTT engineering-scale tests, the results from the SAIC-STAR pilot scale facility products are given in References 111 and 112, and the results for the pilot scale AN-107 products are given in Reference 64. The results from the SAIC-STAR facility are provided since they had no IOC versus the HRI/TTT ESTD runs with IOC. The table also includes TCLP analysis performed on the Module B samples by PNNL, including the radioactive Module B granules. Green shaded elements were shimmed in at 10X and yellow shaded elements were shimmed in at 100X the concentrations given in the Rassat simulant recipe (see Section 8.1.1.2 and Table 8-2). All elements failing TCLP at the UTS limits are shown in bold italic print in Table 8-47.

Analytes detected but at concentrations too low to determine quantitatively have been flagged with the "J" qualifier. The engineering-scale ESTD samples were found to be above the UTS limits for Sb and Cd by GEL, but below the UTS by the PNNL laboratory. In the salt solution used to make these samples, these elements had been shimmed into the HRI/TTT simulant at 10X the concentration anticipated. During the engineering-scale experiments, the excess precipitates that were formed when the solubility for these RCRA elements were exceeded, were not filtered out as was done in the BSR simulants when the precipitates were observed.[3] The Sb precipitated as insoluble sodium antimony (+5) hydroxide in the BSR simulants and was removed through filtration.[3] The BSR granular products all passed TCLP below the UTS for Sb and Cd as these species are below their solubility limit in the granular FBSR products. Since antimony will not be present in the excessive amounts in LAW that they were in the engineering-scale ESTD TCLP results, these observations are considered not applicable.

The only remaining element that failed the TCLP at or below the UTS was Cr. SRNL and PNNL analyses identified a chromium concentration greater than the UTS limit. However, the granular product made using radioactive waste (Module B) passed TCLP for all contaminants of concern including chromium. It should be noted that in the engineering-scale tests IOC was used and this provided an insoluble spinel host phase for the Cr but the IOC was not used in the BSR Module B testing (non-radioactive or radioactive). It is apparent in Table 8-47 that when the IOC is present that elements such as Cr and Pb are sequestered in the spinel structure of the IOC. Conversely, for the columns of data tabulated for the granular product when IOC was not added to the process and Cr was at excess levels, almost all do not meet the UTS for Cr. Since the IOC is a process additive to enhance denitration, it can easily be added as a co-reactant to sequester Cr and an IOC algorithm to ensure that enough IOC is added to convert Cr+6 to $FeCr_2O_4$ is given in Section 6.4.

Table 8-47. TCLP Results for Granular Product Prepared from Rassat Simulants and Shimmed Tank 50 Radioactive LAW Solutions

Constituent	ESTD Simulant Granular with IOC		BSR Simulant Module B Granular		BSR Radioactive Module B Granular		SAIC-STAR Rassat Simulant Granular		HRI/TTT AN-107 Simulant Granular HRI/TTT [60] with IOC	Reporting Limit (RL)	UTS 40CFR 268.48 (Non-waste water std)
	SRNL[c] [123]	PNNL[b]	SRNL[c]	PNNL[b]	SRNL[c]	PNNL[b]	SRNL[c] [111,112] Bed	SRNL[c] [111, 112] Fines			
	(mg/L)	(mg/L)	(mg/L)	(mg/L)	(mg/L)	(mg/L)	(mg/L)	(mg/L)	(mg/L)	(mg/L)	(mg/L)
Sb	***2.13***	0.309 0.334	<MDL	0.009	0.0336 <MDL	0.0394	NM	NM	NM	0.1	1.15
As	<MDL	0.02 0.07	<MDL	0.009	0.00908 <MDL	0.0077 0.0085	NM	NM	NM	0.15	5
Ba	0.283	0.20 0.23	0.0394[J]	0.246 0.263	0.059 <MDL	0.066 0.142	0.069[a]	0.17[a]	NM	0.05	21
Cd	***1.02***	3.040 3.240	<MDL	<MDL	<MDL	0.00107	NM	NM	NM	0.05	0.11
Cr	<MDL	0.048 0.078	***1.35***	***1.09*** ***1.30***	0.310	0.074 0.083	***9.2***	***8.4***	0.015 0.06	0.05	0.6
Pb	<MDL	0.064 0.108	0.0475[J]	0.0076 0.05	0.0888[J]	0.01315	0.046[a]	<0.0310	0.002 0.067	0.1	0.75
Se	0.373	0.341 0.427	1.12	1.14 1.29	0.508	0.192 0.195	NM	NM	NM	0.15	5.7
Ag	<MDL	<MDL	0.0115[J]	0.0003 0.001	0.00339 <MDL	0.000389	NM	NM	NM	0.05	0.14
Hg	<MDL	0.000012 0.000026[J]	<MDL	<MDL	<MDL	0.004 0.013	NM	NM	NM	0.002	0.025
Ni	0.567	1.57 1.61	0.0249[J]	0.0229 0.0278	0.0083 <MDL	<MDL	NM	NM	NM	0.05	11
Tl	<MDL	NM	<MDL	NM	<MDL	<MDL	NM	NM	NM	0.2	0.2
Zn	0.0379[J]	0.151 0.183	0.0957[J]	0.272 0.325	0.0662[J]	<MDL	NM	NM	NM	0.1	4.3

Notes: Green shaded boxes were shimmed 10X and yellow shaded were shimmed 100X. MDL is the Method Detection Limit; NM is not measured. J indicates a detected value that was below quantitative limit. Where duplicate measurements were different, both values are reported. [a]Result is above method detection limit, but below reporting limit (reporting limit is 0.02 mg/L for Hg, and 1.0 g/L for the other metals). [b]PNNL performed the TCLP at the Coastal Biogeochemistry Group at the MSL which maintains national accreditation for its analytical services work with NTI (formerly called NELAC) (http://www.nelac-institute.org/index.php). MSL's accreditation is through the State of new Jersey, Department of Environmental Protection (Laboratory Certification ID# WA004). [c]SRNL performed TCLP in South Carolina with GEL in Charleston, SC.

During the Module C simulant campaigns, different REDOX conditions were achieved; those that were considered "on-spec" (Table 8-9) and those that were either more reduced or more oxidized than the target values given in Table 7-1. For the Module C simulant, the designation "off spec" included a reduced sample with a $Fe^{2+}/\Sigma Fe>0.6$ and an oxidized sample with a $Fe^{2+}/\Sigma Fe<0.2$. Two replicates of each sample type (1) off-spec (oxidized), (2) on-spec, and (3) off spec (reduced) were submitted to GEL . Duplicate samples of FBSR products that were >0.6 $Fe^{+2}/\Sigma Fe$, <0.15 $Fe^{+2}/\Sigma Fe$, and 0.34 $Fe^{+2}/\Sigma Fe$ were selected to aid in defining how the product REDOX impacted the TCLP response in the absence of the IOC. PNNL performed TCLP analysis of the radioactive Module C granules prepared with a REDOX of 0.17 $Fe^{+2}/\Sigma Fe$, which was below the oxidized REDOX limit set in Table 7-1 since this FBSR product was prepared without the IOC, which would act as an alternate Cr host in an oxidized FBSR product.

TCLP results in Table 8-48 show that the simulant sample deemed too oxidized exceeded the UTS limits for chromium implying that soluble chromium +6 was present. Analysis performed by PNNL on the Module C radioactive product also exceeded the UTS limits for chromium. This indicates a sensitivity of the chromium release to REDOX in the absence of the IOC spinel host. The "on spec" REDOX sample passed TCLP testing at the UTS for chromium indicating that the REDOX forced the chromium to Cr_2O_3 (Cr^{3+}) in the absence of the IOC spinel host. The sample designated "more reduced" in Table 8-48 also passed the TCLP testing at the UTS indicating the presence of Cr_2O_3 or an insoluble iron chrome spinel where chromium is in the +3 oxidation state. Analytes detected but at concentrations too low to determine quantitatively have been flagged with the "J" qualifier.

The Module D TCLP results are given in Table 8-49 and show that the non-radioactive sample was below the UTS for all contaminants of concern. The measured REDOX of the non-radioactive sample was $Fe^{2+}/\Sigma Fe = 0.30$ and the measured REDOX of the radioactive sample was $Fe^{2+}/\Sigma Fe = 0.18$. The Cr response for both the non-radioactive and the radioactive sample passed the TCLP at the UTS limits. Analytes detected but at concentrations too low to determine quantitatively have been flagged with the "J" qualifier.

The non-radioactive Module E TCLP results are given in Table 8-50 and show that the oxidized FBSR product with the IOC failed TCLP at the UTS limits only for chromium. The non-radioactive Module E TCLP results for the oxidized FBSR product without the IOC also failed TCLP at the UTS limits for chromium. All other contaminants of concern passed the TCLP for the non-radioactive TCLP. The measured REDOX of the non-radioactive samples with and without the IOC were $Fe^{2+}/\Sigma Fe = 0.13$ and 0.06, respectively (Table 8-50).

Using the data in Table 8-47 through Table 8-50 for the TCLP response of Cr from the simulant and radioactive Modules B, C, D, E and the engineering and pilot scale TCLP results (see References 3 and 4) in the presence and absence of the IOC, a dependency of Cr leaching on the product REDOX was derived (see Table 6-2, Table 6-3 and discussion in Section 6.4). Overall, with the correct IOC control or REDOX control and not shimming in excess RCRA metals to determine their fate in the off-gas, all FBSR products passed TCLP testing at the UTS limits.

Table 8-48. TCLP Results for Non-Radioactive and Radioactive FBSR Products from Module C (SX-105)

	Simulant Module C Granular Product						Radioactive Module C Granular Product* (REDOX =0.17)	Reporting Limit (RL)	Method Detection Limit (MDL)	TCLP Characteristic of Toxicity 40CFR 261.24	UTS 40CFR 268.48 (Non-waste water standard)
	"Off-Spec" (REDOX < 0.15)		"On Spec" (REDOX = 0.34)		"Off-Spec" (REDOX = >0.6)						
	1	2	1	2	1	2	4	--	--	--	--
	(mg/L)	(mg/L)	(mg/L)	(mg/L)	(mg/L)	(mg/L)	(mg/L)	(mg/L)	(mg/L)	(mg/L)	(mg/L)
Sb	<MDL	<MDL	<MDL	<MDL	<MDL	<MDL	0.0004	0.1	0.03	- - -	1.15
As	<MDL	<MDL	<MDL	<MDL	<MDL	<MDL	<MDL	0.15	0.05	5	5
Ba	***0.0449***^{J}	0.0566	***0.0891***	0.057	0.0208^{J}	0.0211^{J}	0.269-0.310	0.05	0.01	100	21
Cd	<MDL	<MDL	<MDL	<MDL	<MDL	<MDL	0.0026-0.00265	0.05	0.01	1	0.11
Cr	***0.790***	***0.826***	0.393	0.243	0.207	0.244	***0.69-0.72***	0.05	0.02	5	0.6
Pb	0.0947^{J}	0.110	0.0786^{J}	0.129	0.0336^{J}	0.0440^{J}	<MDL	0.1	0.025	5	0.75
Se	<MDL	<MDL	<MDL	<MDL	<MDL	<MDL	0.028-0.033	0.15	0.05	1	5.7
Ag	<MDL	<MDL	<MDL	<MDL	<MDL	<MDL	<MDL	0.05	0.01	5	0.14
Hg	<MDL	<MDL	<MDL	<MDL	<MDL	<MDL	0.012	0.002	0.0003	0.2	0.025
Ni	<MDL	<MDL	<MDL	<MDL	0.0204^{J}	MDL	<MDL	0.05	0.01	- - -	11
Tl	<MDL	<MDL	<MDL	<MDL	<MDL	<MDL	<MDL	0.2	0.05	- - -	0.2
Zn	0.115	0.115	0.0681^{J}	0.0599^{J}	0.0335^{J}	0.0408^{J}	<MDL	0.1	0.02	- - -	4.3

*Measured by PNNL; J are analytes detected but at concentrations too low to determine quantitatively; MDL is Method Detection Limit

Table 8-49. TCLP Results for Non-Radioactive and Radioactive FBSR Products from Module D (AN-103)

	Simulant Module D Granular Product			Radioactive Module D Granular Product*		Reporting Limit (RL)	Method Detection Limit (MDL)	TCLP Characteristic of Toxicity 40CFR 261.24	UTS 40CFR 268.48 (Non-waste water standard)
	REDOX <0.15	REDOX = 0.30	REDOX >0.5	REDOX = 0.18					
	(mg/L)	(mg/L)	(mg/L)	(mg/L)	(mg/L)	(mg/L)	(mg/L)	(mg/L)	(mg/L)
Sb	<MDL	<MDL	<MDL	0.00093	0.00086	0.1	0.1	- - -	1.15
As	<MDL	<MDL	<MDL	<MDL	<MDL	0.1	0.1	5	5
Ba	1.66	1.57	1.38	0.0565	0.0527	0.2	0.2	100	21
Cd	<MDL	<MDL	<MDL	<MDL	<MDL	0.05	0.05	1	0.11
Cr	0.184	0.120	0.165	0.07	0.0688	0.1	0.1	5	0.6
Pb	<MDL	<MDL	<MDL	0.0017[J]	ND	0.1	0.1	5	0.75
Se	<MDL	<MDL	<MDL	0.0209	0.0244	0.1	0.1	1	5.7
Ag	<MDL	<MDL	<MDL	<MDL	<MDL	0.1	0.1	5	0.14
Hg	<MDL	<MDL	<MDL	0.00167[J]	<MDL	0.002	0.002	0.2	0.025
Ni	<MDL	<MDL	<MDL	<MDL	<MDL	0.2	0.2	- - -	11
Tl	<MDL	<MDL	<MDL	<MDL	<MDL	0.04	0.04	- - -	0.2
Zn	<MDL	<MDL	<MDL	0.406	<MDL	0.2	0.2	- - -	4.3

*Measured by PNNL – duplicate results; U=unreportable due to interference; J are analytes detected but at concentrations too low to determine quantitatively; MDL is Method Detection Limit

Table 8-50. TCLP Results for Non-Radioactive FBSR Products from Module E (AZ-101/AZ-102) With and Without the IOC

	Simulant Module E Granular Product with IOC REDOX = 0.13	Simulant Module E Granular Product without IOC REDOX= 0.06	Reporting Limit (RL)	Method Detection Limit (MDL)	TCLP Characteristic of Toxicity 40CFR 261.24	UTS 40CFR 268.48 (Non-waste water standard)
	(mg/L)	(mg/L)	(mg/L)	(mg/L)	(mg/L)	(mg/L)
Sb	<MDL	<MDL	0.1	0.1	- - -	1.15
As	<MDL	<MDL	0.1	0.1	5	5
Ba	0.474	0.567	0.2	0.2	100	21
Cd	<MDL	<MDL	0.05	0.05	1	0.11
Cr	***12.2***	***10.3***	0.1	0.1	5	0.6
Pb	<MDL	<MDL	0.1	0.1	5	0.75
Se	<MDL	<MDL	0.1	0.1	1	5.7
Ag	<MDL	<MDL	0.1	0.1	5	0.14
Hg	<MDL	<MDL	0.002	0.002	0.2	0.025
Ni	0.221	<MDL	0.2	0.2	- - -	11
Tl	<MDL	<MDL	0.04	0.04	- - -	0.2
Zn	1.39	0.625	0.2	0.2	- - -	4.3

MDL is Method Detection Limit

8.2.10 *Phase Pure Standard Mineral Species*

The NAS waste form is primarily composed of nepheline (ideally $NaAlSiO_4$) and the sodalite family of minerals (ideally $Na_8[AlSiO_4]_6(Cl)_2$, which includes nosean (ideally $Na_8[AlSiO_4]_6SO_4$). Cesium and potassium can substitute for Na in the nephelines and sodalite. Oxyanions such as ReO_4^- and TcO_4^-, have been found to replace sulfate in the larger cage structured nosean.[75,210] Halides such as I^- and F^- are known to replace chlorine in the nosean-sodalite mineral structures (see Table 2-2) – immobilizing them.

In the FBSR waste form, each of various nephelines and sodalites can exist in a variety of solid solutions (see Figure 2-6 for example) that differ from the idealized forms observed in single crystals in nature. The lack of understanding of the durability of these stoichiometric or idealized mineral phases complicates the ability to deconvolute the durability of the mixed phase FBSR products since it is a combination of different NAS phases, some of which are likely solid solutions. However, the solid solutions share the same crystallographic topology so by better understanding the behavior of the stoichiometric phases in the FBSR product, the durability of the mixed phases can be approximated.

The SRNL prepared a series of phase-pure standards, consisting of nepheline, nosean, and Cl, Re, and I sodalite.[210] These standards have been subjected to subsequent characterization studies consisting of the following: SPFT testing and development of thermodynamic data which will be reported elsewhere.[162] In addition to the above mentioned phase-pure standards, SRNL fabricated a mixed Tc-Re sodalite.

SRNL completed the synthesis of 200 grams of five pure-phase standards - nepheline, nosean, Re-sodalite, Cl-sodalite, and I-sodalite - for the Hanford LAW FBSR program. X-ray diffraction analysis confirmed that single phases were fabricated, and particle size and surface area measurements for each of the pure-phase standards were determined.

SRNL was also able to synthesize a smaller quantity of a mixed sodalite containing rhenium and technetium. X-ray diffraction analysis confirmed that a single phase was fabricated, and the Scanning Electron Microscopy with Energy Dispersive X-ray Fluorescence confirmed the sodalite contained technetium. The mixed Re-^{99}Tc sodalite fabrication and testing are also documented in Reference 210.

9.0 Supplentary Monolith Testing

Monolithing of the granular FBSR product was investigated to prevent dispersion during transport or burial/storage (the 500 psi strength criteria). The granular product has a comparable durability to glass and could be disposed of in a HIC. Monolithing in an inorganic geopolymer binder, which is an amorphous aluminosilicate material, macro-encapsulates the granules (Figure 9-1). Geopolymers have an amorphous cross-linked three dimensional aluminosilicate structure: geopolymers remain amorphous because they contain insufficient water to crystallize zeolite phases like hydroceramics

The aluminosilicate geopolymers were chosen as a binder after a monolith down select (see Appendix G) of various types of binders [123] and because they are inorganic. They can be made of fly ash or kaolin clay as a source of the aluminosilicate, sodium hydroxide, and sodium silicate and so are rich in Al_2O_3, SiO_2 and Na_2O, the same chemistry as the NAS FBSR product. The synergy in chemistry means that if the geopolymer binder leaches into a solution or the groundwater that it will saturate the immediate solution with Na, Al, and Si and slow down the leaching of the macro-encapsulated particles. This is known as the “common-ion effect.”

(a) (b)

Figure 9-1. (a) Granules of FBSR product from the TTT/HRI 2001 campaign on a mm ruler and (b) how these granules which sequester COCs indicated by the small symbols inside the grains are micro-encapsulated in the gray amorphous geopolymer binder which contain no COCs.

9.1 Description of the WP 5.2.1 Test Program Regarding Monoliths and Monolith Testing

The EM-30 WP 5.2.1 test program objective is to reduce the risk associated with implementing the FBSR technology as a supplemental LAW treatment by addressing the remaining technical uncertainties and thereby demonstrate acceptable performance for FBSR product after being disposed in a near-surface burial facility (see Reference 163 and Appendix A). The tasks performed as part of this test program are designed to support the application of FBSR as a supplemental Hanford LAW treatment option. While the primary focus is on the FBSR granular product, there are also associated objectives to develop supplementary performance testing data on the geopolymer encapsulated FBSR waste forms.

The test program includes the following activities (in the order given in Table 5-4) designed to support the decision point to proceed with supplemental treatment of Hanford LAW:

1. Preparation of monolithic waste forms containing mineralized FBSR product.
2. Mineral characterization by XRD analysis of the monolithic waste forms.
3. Short-term and Long-term PCT testing
4. Demonstration through SPFT/PUF experiments that the binder used for monolithic waste forms does not significantly impact the release rate or dissolution behavior.
5. Determination through ASTM C1308 type testing of the transport properties of the monolith waste forms.
6. Assessment of whether the FBSR granular products and monolith products pass the TCLP.
7. Compressive Strength

A discussion of the monolith program prior to the WFQ program laid out in this document is given in Appendix G. A binder down select had been performed and various types of geopolymer binders were tested (see Appendix G and Reference 123), those that were fly ash based and several clay based geopolymers. The best geopolymers during the down select, for the Module B Rassat ESTD material appeared to be a fly ash based geopolymer (GEO-7). The formulations had assumed that the FBSR products had unreacted clay cores as as had been seen in the early FBSR products from pilot scale testing (TTT/HRI and INL SAIC-STAR pilot scales). It further assumed that this ureacted clay was >10 wt.% based on MINCALC™ of the TTT/HRI and INL feeds. When SEM of the ESTD and BSR products were performed (compare Figure 2-2 and Figure 2-3) there were no clay cores. Further investigation determined that process improvments in the ESTD and BSR had allowed more reactivity between the waste and the LAW and unreacted clay cores no longer formed. When the geopolymer formualtions were

recalculated assuming no unreacted clay cores in the ESTD and BSR FBSR granules, several of the formulations fell outside the desired G1 range for optimium geopolymer formulation (see Appendix G and References 3 and 123). This also meant that the early geopolymers contained excess NaOH which had been added to complex with the unreacted FBSR particle clay cores.

Therefore, in the Module B monolithing for the WQF program, a two-fold approach was taken to compare fly ash based geopolymers to geopolymers made with reactive clay. Formulations made with fly ash were made with minimal NaOH and in the G1 region. Other formulations were made with the reactive clays determined from an SRNL Laboratory Directed R&D (LDRD) program also in the G1 region. The fly ash based geopolymers were made first since the FBSR product contains some fly ash residue from coal degradation.

However, there are three primary reasons for preferring kaolin over fly ash:

(1) the unreactive nature of some of the components found in fly ash, e.g. the minerals mullite and quartz,
(2) the variable nature of fly ash compositions from various coal production facilities, and
(3) fluoride, if present as it was in the WTP-SW FBSR products [127], should not attack clay based binders as readily as those made from fly ash.[156]

Formulations with clays are preferred since clays are less variable in composition than fly ash and the clays can be chosen, as done in the LDRD study to have minimal unreactive components such as quartz and muscovite micas. Clays such as Troy®, Barden® and OptiKasT® were found to have good reactivity during the LDRD study. In addition, clays will continue to react with any excess alkali in the formulation as a function of time, while this is less likely in fly ash based geopolymers due to unreactive components such as mullite.

A discussion of the geopolymer formulation after the WFQ program is given in the next few sections. Comparisons are made between these clay based, lower NaOH containing geopolymers, and the earlier GEO-1 and GEO-7. Due to geopolymer reformulation at SRNL, the optimized geopolymers were only tested by short-term and long-term PCT and ASTM C1308/ANSI 16.1.

9.1.1 *Preparation of Monoliths*

All of the 1” x 2” cylinders formulated in the WFQ esting used a Kitchen Aid mixer fitted with a flat beater multipurpose agitator. All cylinder monoliths made in this project used standard plastic molds with fitted plastic caps. No heat treatment was applied to any of the monoliths fabricated in this project.

Initially monoliths were made by premixing the dry powders (BSR granular product and fly ash) followed by addition of the liquids sodium silicate, sodium hydroxide and water. Latter formulations involving clay used a different strategy of premixing the liquids, then blending in the dry clay powders to get asmooth consistent ‘slurry’. To this slurry, the final dry BSR granular powders were then added with final mixing. The latter methodology appeared to improve the compressive strength and form a more homogeneous monolith.

9.1.1.1 *Preparation of ESTD LAW P-1B Geopolymers Made with Fly Ash*

A geopolymer was made using the ESTD LAW simulant Rassat blend from the ESTD P-1B run. The blend was similar to the development of the geopolymer for the FBSR waste form given in Reference 123 with a 65% dry basis waste loading. The FBSR product and Class F fly ash were combined in the mixing bowl of a planetary mixer. The sodium silicate solution was added and mixed. After the sodium silicate was incorporated into the dry powders, the sodium hydroxide solution was added while mixing and mixed to resemble coarse granules. Water was then added during mixing. With continued mixing, the granules

coalesced into a "dough-like" ball. The ball transformed into a paste after approximately thirty seconds of additional mixing. Mixing continued for an additional thirty seconds. The paste then was transferred into two plastic cylinders and capped. Typical curing times were 28 days at ambient conditions on the benchtop. The monoliths were typically removed from the curing molds within about 1 week of planned compression testing and allowed a final cure open to the atmosphere.

Table 9-1. Composition of GEO-7 Geopolymer for Monoliths Prepared with ESTD LAW P-1B and Fly Ash

Component	Wet Basis Mass (g)	Wet Basis Mass %	Dry Basis Mass %
ESTD LAW P-1B	54.76	48.42	67.00
Class F fly ash	14.80	12.47	
Silica D (44.1 wt% $Na_2O \bullet SiO_2$)	20.60	17.36	
Caustic (50 wt% NaOH)	13.71	11.55	
Water (H_2O)	12.11	10.20	
Geopolymer Components			Mol%[f]
Geopolymer Na_2O			30
Geopolymer Al_2O_3			13
Geopolymer SiO_2			57
Total Mass	118.68	100.00	100.00
Geopolymer Water Content			Mol% Ratio
Geopolymer H_2O/Na_2O			15

[f] When the geopolymer program was initiated, all FBSR products had contained some unreacted kaolin clay and coal fly ash. It was assumed that between 10-20% of this excess clay would be available as a geopolymer formulation component. This gave a geopolymer $Na_2O/Al_2O_3/SiO_2$ ratio of 23/17/60 in the G1 region shown in Appendix G. SEM (Figure 9-8) showed no unreacted kaolin cores in the FBSR granules and so the composition was adjusted to that shown in this table which assumes no excess kaolin or fly ash in the FBSR product.

9.1.1.2 *Preparation of BSR Module B Simulant Geopolymers Made with Fly Ash*

The Module B simulant geopolymer was made using a similar methodology to the ESTD LAW simulant blend described above in Section 9.1.1. The composition of the geopolymer mixture, which made two cylinders is shown in Table 9-2. This formulation results in a 69% dry basis FBSR loading. Initial testing was performed using BSR product that did not meet REDOX and LOI requirements to confirm the mixing process and formulation. Results indicated that product from the BSR was coarser than that of the ESTD LAW blend (80% PGF and 20% PRB) used to develop the Rassat P-1B ESTD geopolymer. To obtain a similar particle size distribution, the Module B simulant BSR powders were milled in a high density polyethylene bottle with 6 mm partially stabilized zirconia grinding media for approximately one hour. Twelve one-inch by two-inch cylinders were prepared in six batches using the GEO-7 composition described in Reference 123.

The BSR product and Class F fly ash were combined in the mixing bowl of a planetary mixer. The sodium silicate solution was added and mixed. After the sodium silicate was incorporated into the dry powders, the sodium hydroxide solution was added while mixing and resembled coarse granules. Water was then added during mixing. In these tests, the water was partitioned in half, with the second half added drop wise until the mix had the same consistency as the mixes made with the ESTD LAW. With continued mixing, the granules coalesced into a "dough-like" ball. The ball transformed into a paste after

approximately thirty seconds of additional mixing. Mixing continued for an additional thirty seconds. The paste then was transferred into two cylinders, capped, and set aside to cure for 28 days prior to testing. The monoliths were typically removed from the curing molds within about 1 week of planned compression testing and allowed a final cure open to the atmosphere.

Table 9-2. Composition of GEO-7 Geopolymer for Monoliths Prepared with BSR Module B Simulant and Fly Ash

Component	Wet Basis Mass (g)	Wet Basis Mass %	Dry Basis Mass %
BSR Module B Simulant	51.13	47.35	68.00
Class F fly ash	13.82	12.80	
Silica D (44.1 wt% $Na_2O \bullet SiO_2$)	20.26	18.76	
Caustic (50 wt% NaOH)	13.48	12.48	
Water (H_2O)	9.30	8.61	
Geopolymer Components			Mol%[f]
Geopolymer Na_2O			31
Geopolymer Al_2O_3			13
Geopolymer SiO_2			56
Total Mass	107.99	100.00	100.00
Geopolymer Water Content			Mol% Ratio
Geopolymer H_2O/Na_2O			14

[f] When the geopolymer program was initiated all FBSR products had contained some unreacted kaolin clay and some coal fly ash. It was assumed that between 10-20% of this excess clay and fly ash would be available as a geopolymer formulation component. This gave a geopolymer $Na_2O/Al_2O_3/SiO_2$ ratio of 24/16/60 in the G1 region in Appendix G. SEM (Figure 9-8) showed no unreacted kaolin cores in the FBSR granules and so the composition was adjusted to that shown in this table which assumes no excess kaolin or fly ash in the FBSR product.

9.1.1.3 *Preparation of ESTD LAW P-1B and Module B Simulant Geopolymers Made with Metakaolin Clay*

For the WFQ geopolymer formulations made with clay, a different mixing strategy was used than was used with the fly ash geopolymers. The liquids were premixed then blended with the dry clay powders to get a smooth consistent 'slurry' representing all the 'binder' components. To this slurry, the final dry BSR granular powders were then added with final mixing.

Another approach for successful monolithing of the BSR granular product involved using a clay-based geopolymer monolith with lower dry-basis waste loading. Ultimately, it was decided through review of past monolith testing (Appendix G) to pursue the lower waste loading 'centroid' in the G1 region with clay.

Although this approach would use a lower waste loading than the GEO-7 recipe, scoping testing indicated that it would not require milling of the BSR granular product prior to monolithing. Apparently the coarser BSR mineral could be successfully monolithed using the lower waste loading and clay vs. the milling requirement discussed in Section 9.1.1.2 for the BSR mineral in the GEO-7 Fly Ash recipe.

Table 9-3 shows the centroid formulation recipe giving a maximum dry basis waste loading of 42% to make two 1"x 2" cylinders. This same recipe was used to make three different sets of clay centroid

geopolymer monoliths containing either ESTD LAW P-1B, ESTD LAW P-1A or the BSR Simulant B. This recipe is labeled as 'T-22-16-62-13' using the nomenclature previously used by SRNL geopolymer researchers.[211] 'T-22-16-62-13' represents the molar composition of 22% Na_2O, 16% Al_2O_3 and 62% SiO_2 (see Appendix G). The last number in the label indicates a literature-based suggested molar ratio of H_2O:Na_2O of 13.

Latter formulations involving clay used a different mixing strategy from the fly ash geopolymers discussed above. The liquids were premixed then blended with the dry clay powders to get a smooth consistent 'slurry' representing all the 'binder' components. To this slurry, the final dry BSR granular powders were then added with final mixing.

Table 9-3. Centroid 42% Waste Load Geopolymer ESTD LAW P-1B Simulant Monolith Recipe Made with Clay

T-22-16-62-13 Component Makeup	Wet Basis Mass (g)	Wet Basis Mass %	Dry Basis Mass %
FBSR ESTD LAW P-1B	28.2	28.98	42
Troy (Helmer) Kaolin (HT@650 °C)	24.4	25.08	
Silica D (44.1 wt% Na_2O•SiO_2)	23.8	24.46	
Caustic (50 wt% NaOH)	10.8	11.10	
Water (H_2O)	10.1	10.38	
Geopolymer Components			Mol%
Geopolymer Na_2O			22
Geopolymer Al_2O_3			16
Geopolymer SiO_2			62
Total Mass	97.3	100.00	100.00
Geopolymer Water Content			Mol% Ratio
Geopolymer H_2O/Na_2O			13

Further development of the G1 centroid recipe with 42% dry basis FBSR loading and H_2O:Na_2O ratio of 13 was pursued in order to fabricate geopolymer clay centroid monoliths with waste loadings approaching the previous nominal 65% dry basis FBSR loading of the fly ash GEO-7 monoliths. It was determined through scoping trials using the ESTD LAW P-1B that a 65% loading could be achieved by increasing the content up to the range of H_2O:Na_2O of 20. This higher waste loading clay centroid recipe is shown in Table 9-4 and was used to make two 1" x 2" cylinders.

Table 9-4. Centroid 65% Waste Load Geopolymer ESTD LAW P-1B Simulant Monolith Recipe Made with Clay

T-22-16-62-20 Component	Wet Basis Mass (g)	Wet Basis Mass %	DryBasis Mass %
FBSR ESTD LAW P-1B	44.8	46.52	65
Troy (Helmer) Kaolin (HT@650 °C)	14.9	15.47	
Silica D (44.1 wt% $Na_2O \bullet SiO_2$)	14.6	15.16	
Caustic (50 wt% NaOH)	6.7	6.96	
Water (H_2O)	15.3	15.89	
Geopolymer Components			Mol%
Geopolymer Na_2O			22
Geopolymer Al_2O_3			16
Geopolymer SiO_2			62
Total Mass	96.3	100.00	100.00
Geopolymer Water Content			Mol% Ratio
Geopolymer H_2O/Na_2O			20

9.1.1.4 *Preparation of BSR Module B Radioactive Monoliths*

The Module B radioactive geopolymers were made using similar recipes and methodology to the BSR Module B simulant metakaolin clay geopolymers in Section 9.1.1.3. The composition of the geopolymer to make two cylinders is shown in Table 9-5 for the 42% waste loading, which indicates that slightly higher water content was required to get the Module B radioactive granular product to set. The calculated molar ratio of H_2O:Na_2O in the binder is 16.2%. The same recipe, as was shown in Table 9-4 for simulant monolith formation at 65% waste loading, was successful in making the Module B radioactive geopolymers at 65% waste loading.

Table 9-5. Centroid 42% Waste Load Geopolymer Module B Radioactive Monolith Recipe Made with Clay Composition

T-22-16-62-16 Component	Wet Basis Mass (g)	Wet Basis Mass %	Dry Basis Mass %
BSR Module B Radioactive	26.5	27.24	42
Troy (Helmer) Kaolin (HT@650°C)	22.9	23.54	
Silica D (44.1 wt% $Na_2O \bullet SiO_2$)	22.4	23.02	
Caustic (50 wt% NaOH)	10.2	10.48	
Water (H_2O)	15.3	15.72	
Geopolymer Components			Mol%
Geopolymer Na_2O			22
Geopolymer Al_2O_3			16
Geopolymer SiO_2			62
Total Mass	97.3	100.00	100.00
Geopolymer Water Content			Mol% Ratio
Geopolymer H_2O/Na_2O			16

9.1.2 *Monolith Characterization Program*

Monoliths prepared above were all tested for compressive strength and for phase mineralogy by XRD. Some of the monoliths were also tested for durability via the PCT, and leachability using the ASTM C 1308-10. The monolith samples used in all tests following compressive strength testing were generally obtained by using the post-compressive strength fragments derived from running the compressive strength test to past failure resulting in cracked and/or fractured monoliths. A portion of some of the post-compression tested samples prepared for PCT were analyzed for surface area and this is described in Reference 3 and for loss on ignition.

Table 9-6 summarizes the various monolith testing and characterization methods used to test the geopolymers in this study to support waste form performance and PCT calculations.

After the monoliths were cured for 28 days, the compressive strength was measured using the ASTM procedure for compressive strength of cylinders see Table 9-6.

Compression testing of the ESTD LAW P-1B monoliths was performed at the URS 717-5N Civil Test Laboratory at SRS. Compression testing of the radioactive and simulant Module B monoliths were performed at SRNL with the same modifications to the ASTM compression test procedure as the ESTD LAW P-1B monoliths. Testing at SRNL used unbounded caps.

The broken pieces of monolith from compression testing were used for composition analysis, PCT testing, SPFT testing, and PUF testing (Table 9-6). The analytic techniques used are documented in Reference 3 and the leach test protocols are given in Reference 3 and Appendix D.

Figure 9-3 shows the position of the monoliths listed in Table 9-6 that underwent the majority of the WFQ testing. However, it should be noted that the fly-ash based geopolymers were not formulated in the optimized G1 region of the geopolymer ternary phase diagram in Figure 9-3. These included the fly-ash based geopolymer made from the ESTD granular product, the fly-ash based geopolymer made from the BSR granular product, and the clay based radioactive BSR granular product. The FBSR loadings were 68, 68 and 65 wt% respectively.

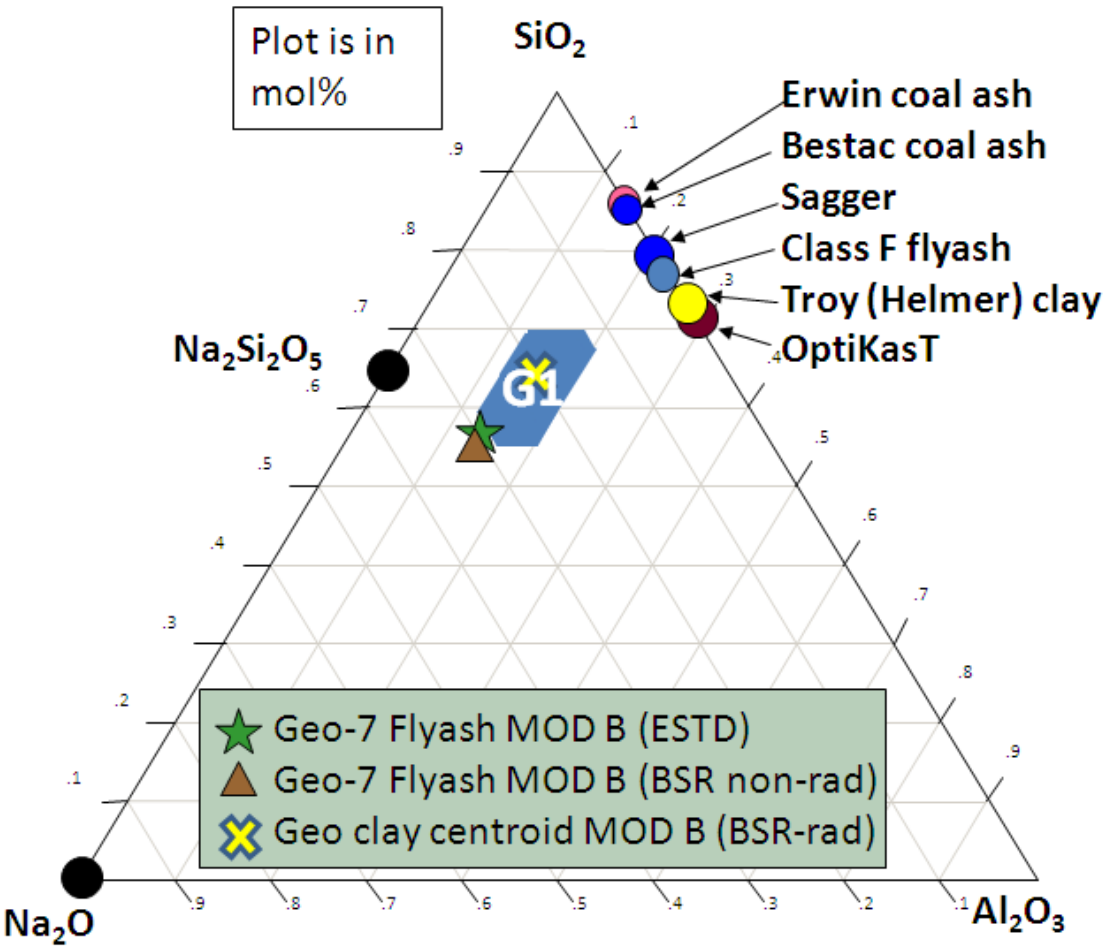

Figure 9-2. Position of the Two Fly Ash and One Clay Based Geopolymers that Underwent Long-Term PCT Testing, the Two Fly Ash Based Geopolymers that Underwent SPFT testing (ESTD and BSR), and the One Fly Ash Based Geopolymer (ESTD) that Underwent PUF Testing.

Table 9-6. Monolith Testing and Characterization Performed

Monolith	As Made Composition	Dry Basis Fbsr Loading (%)	Compress-Ion Tested	XRD Phases	PCT	Analyzed Chemical Composition	TCLP Testing	Bulk Density (G/Cc)	ANSI/ANS 16.1/ ASTM C1308 Leaching	SPFT/PUF Testing
Fly Ash GEO-7 ESTD LAW P-1B	Table 9-1	68	Yes	Yes	Short-Term and Long-Term	Yes	Yes	Yes	Yes	SPFT PUF
Fly Ash GEO-7 Mod B Sim	Table 9-2	68	Yes	Yes	Short-Term and Long-Term	Yes	Yes	Yes	Yes	SPFT
Clay ESTD LAW P-1B	Table 9-3	42	Yes	Yes	No	No[b]	No	Yes	Yes	No
	Table 9-4	65				No[b]	No	No	No	No
Clay Mod B Sim	Table 9-3	42	Yes	Yes	No	No[b]	No	Yes	Yes	No
Clay Mod B Rad	Table 9-5	42	Yes	Yes	Short-Term[a]	No[b]	Yes	No	No	No
	Table 9-4	65			Long-Term[a]	No[b]	Yes	No	No	No

a) Both the 42% WL and the 65% WL Mod B radioactive monoliths made with clay were tested with PCT. The lower 42% WL PCT leachates were archived and the 65% WL PCT leachates were analyzed and reported in this work.

b) Chemical compositions calculated from analyzed granular products and known Na, Al and Si oxide compositions of the binder additives.

9.1.2.1 *Chemical and Mineral Characterization (Monolith Product)*

The chemical compositions of the GEO-7 monoliths prepared from BSR simulant granular product are reported in Table 9-7. The elemental concentrations were converted to oxides and the measured LOI was taken into account to demonstrate full recovery of the sample. The LOI was then subtracted out and the oxides renormalized to 100% for PCT calculations. The difference in the sodium and silica values between the ESTD and BSR monoliths are attributed to the small change in the geopolymer composition that resulted from formulation and preparation work performed. This testing resulted in a slightly higher sodium hydroxide addition in the batch sheet.

Table 9-7. Chemical Composition of Simulant Monoliths Fabricated with Fly Ash

Component	ESTD Rassat Simulant Monolith GEO-7 SRNL	BSR Rassat Simulant Monolith GEO-7
	Wt.%	**Wt.%**
Al_2O_3	27.23	26.54
CaO	0.37	0.72
Cr_2O_3	0.07	0.08
Fe_2O_3	2.50	3.31
K_2O	0.99	0.59
Na_2O	21.07	24.51
P_2O_5	0.33	0.38
PbO	0.10	0.05
SO_4	0.99	1.26
SiO_2	44.95	40.78
TiO_2	0.99	0.99
ZrO_2	0.00	0.05
Cl	0.10	0.33
F	<0.06	<0.12
I	0.07	0.07
Cs_2O	0.14	0.18
Re_2O_7	0.03	0.03
Total	99.99	99.99
LOI	19.82%	18.67%

The chemical compositions of the centroid clay monoliths prepared from BSR simulant granular product were calculated from the simulant granular product analyses from Table 8-12 and the known Na, Al and Si oxide chemical compositions of the binder additives from Table 9-3 for the 42% waste loading. The centroid clay monolith oxide composition is shown in Table 9-8.

Table 9-8. Chemical Composition of BSR Simulant Monolith's Fabricated with Clay

Component	BSR Rassat Simulant - Centroid with Clay (wt%)
Al_2O_3	30.69
Cr_2O_3	0.04
Fe_2O_3	0.44
K_2O	0.07
Na_2O	19.86
P_2O_5	0.23
PbO	0.02
SO_4	0.45
SiO_2	46.35
ZrO_2	0.01
Cl	0.09
F	<0.02
I	0.05
Cs_2O	0.10
Re_2O_7	0.02
Total	98.45

The chemical compositions of the centroid clay monoliths prepared from ESTD P-1A and P-1B simulant granular product were calculated from the simulant granular product analyses from Reference 123 and the known Na, Al, and Si oxide chemical compositions of the binder additives from Table 9-3 for the 42% waste loading. These monolith oxide compositions are shown in Table 9-9.

Table 9-9. Chemical Composition of ESTD Simulant Monolith's Fabricated with Clay

Component	ESTD P-1A (wt%)	ESTD P-1B (wt%)
Ag_2O	0.02	0.02
Al_2O_3	31.18	31.54
As_2O_3	<0.11	<0.11
B_2O_3	<0.15	<0.14
BaO	0.05	0.05
CaO	0.03	0.03
CdO	0.02	0.02
Cl	0.08	0.09
Cr_2O_3	0.05	0.04
Cs_2O	0.12	0.08
F	<0.09	<0.08
Fe_2O_3	0.64	0.98
I	0.08	0.08
K_2O	0.09	0.10
MgO	0.01	0.01
MnO_2	<0.01	<0.01
Na_2O	20.18	20.24
NiO	0.03	0.04
PO_4	0.33	0.35
PbO	0.05	0.07
Re_2O_7	0.03	0.02
SO_4	0.42	0.62
Sb_2O_3	0.03	0.03
SeO_2	<0.004	<0.004
SiO_2	47.11	47.18
SrO	<0.004	<0.004
TiO_2	0.55	0.55
ZnO	<0.004	<0.004
Total	101.10	102.13

The chemical compositions of the centroid clay monoliths prepared from BSR radioactive granular product were calculated from the radioactive granular product analyses and the known Na, Al, and Si oxide chemical compositions of the binder additives from Table 9-5 for the 42% waste loading and Table 9-4 for the 65% waste loading. These monolith oxide compositions are shown in Table 9-10.

Table 9-10. Chemical Composition of Radioactive Monolith's Fabricated with Clay

Component	BSR Radioactive Module B (Rassat)	
	Centroid with Clay at 42% WL (wt%)	Centroid with Clay at 65% WL (wt%)
Al_2O_3	31.38	32.88
CaO	0.10	0.15
Cr_2O_3	0.04	0.06
Fe_2O_3	0.77	1.19
K_2O	0.07	0.11
Na_2O	20.24	20.55
P_2O_5	0.20	0.31
PbO	0.06	0.09
Re_2O_7	0.02	0.03
SO_4	0.55	0.85
SiO_2	46.79	44.07
TiO_2	0.55	0.85
ZrO_2	0.001	0.002
Cl	0.08	0.13
F	<0.04	<0.06
I	0.03	0.04
^{137}Cs	2.9E-07	4.6E-07
^{99}Tc	1.2E-05	1.8E-05
I-129	3.6E-04	5.7E-04
Total	100.89	101.38

Figure 9-3 and Figure 9-4 demonstrate that the phase assemblages of the granular products are not compromised when monolithed: the Bragg reflections remain sharp for the minerals in the FBSR granular product. Figure 9-3 shows the ESTD FBSR product monolithed at 42 wt.% FBSR loading in Troy (Helmer) clay (see Table 9-6 as both 42 wt.% and 65 wt.% FBSR loaded monoliths were made from the ESTD material but only the 42 wt.% loaded samples was submitted for XRD analyses). Figure 9-4 demonstrates that the phase assemblages are not compromised when the BSR radioactive Module B material was bound in a geopolymer made with Troy (Helmer) clay at a FBSR loading of either 42 wt.% (top) or 65 wt.% (bottom). See Table 9-6 for reference.

Figure 9-5 demonstrates that the phase assemblages are not compromised when the BSR simulant B material is bound in a geopolymer made with fly ash at an FBSR loading of 65 wt.%. Figure 9-6 demonstrates that the phase assemblages are not compromised when the BSR FBSR material is made into a clay based geopolymer at an FBSR loading of 42 wt.% either. Figure 9-6 shows the original spectra of the BSR minerals, a spectra of the monolithed BSR minerals, and an overlay of a geopolymer made with the Troy (Helmer) clay that does not contain any FBSR product. In Figure 9-6, Na_5FeO_4 and quartz are identified as impurities in the geopolymer clay and anatase (TiO_2) is an impurity in the OptiKasT™ clay used for FBSR processing. Faujasite is identified in Figure 9-5 as a minor phase. It is a known reaction product in geopolymers made of fly ash.[212]. Faujasite is a zeolite and similar to zeolite P or zeolite Y (non-stoichiometric

faujasite). However, faujasite (Zeolite Y), Zeolite X, and Zeolite P all have the identical cage structures as sodalite.[80]

It is note worthy that the individual Bragg reflections in Figure 9-5 and Figure 9-6 are less intense in the monolith patterns due to the dilution with the amorphous geopolymer matrix. The monolith peak intensities could also be lower if the granular FBSR product was being degraded by the geopolymer additives, specifically the NaOH additive, but the SEM shown in Figure 9-8 demonstrates that the individual FBSR granules have sharp grain boundaries in contact with the geopolymer matrix.

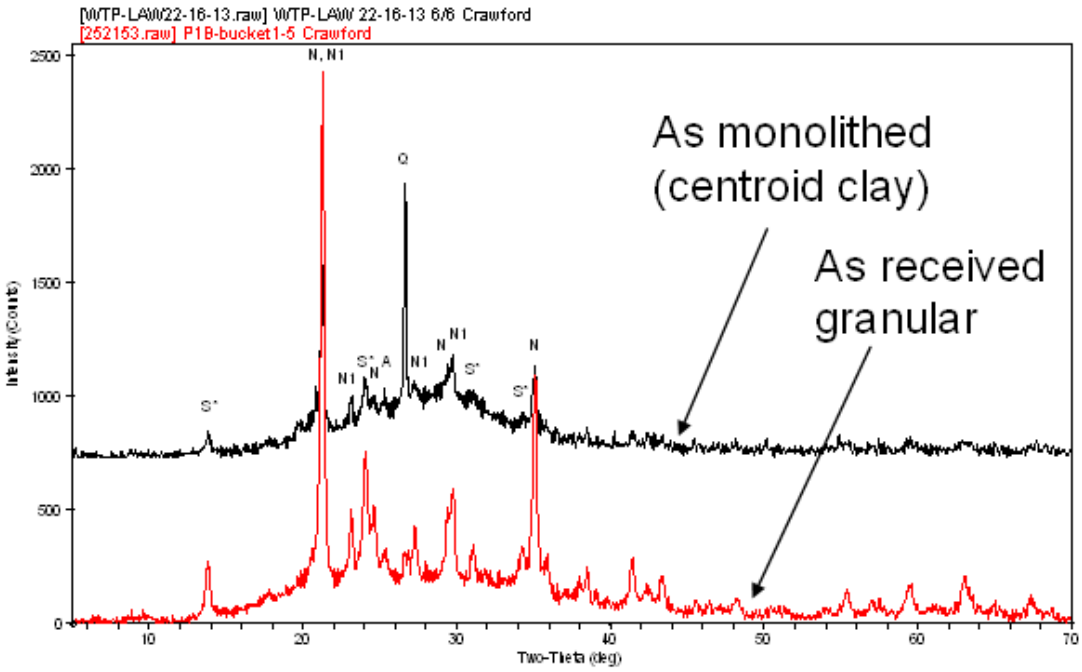

Figure 9-3. Overlay of As-received Engineering Scale Granular Product (P-1B) and Monolithed Geopolymer Made with Clay

Note that all the original phases survive in the XRD but are present at less intensity in the monolith pattern due to the dilution with the amorphous geopolymer matrix.
N1 is Nepheline (O) $NaAlSiO_4$ (PDF00-052-1342)
N is Nepheline (H) either $NaAlSiO_4$ (PDF 00-035-0424 top spectra) or $K_{0.17}Na_{0.75}AlSiO_4$ (PDF 01-072-7408 bottom spectra from TTT/HRI ESTD campaigns – high K containing wastes from INL had been processed recently and may have provided some K to the nepheline)
S* is Sodalite (cubic) $Na_6Al_6Si_6O_{24}$ (PDF 00-042-0217)
A is Anatase, TiO_2 (PDF 00-021-1272)
Q is Quartz, SiO_2 (PDF 00-046-1045)
Original XRD spectra fits are in Appendix I of Reference 3

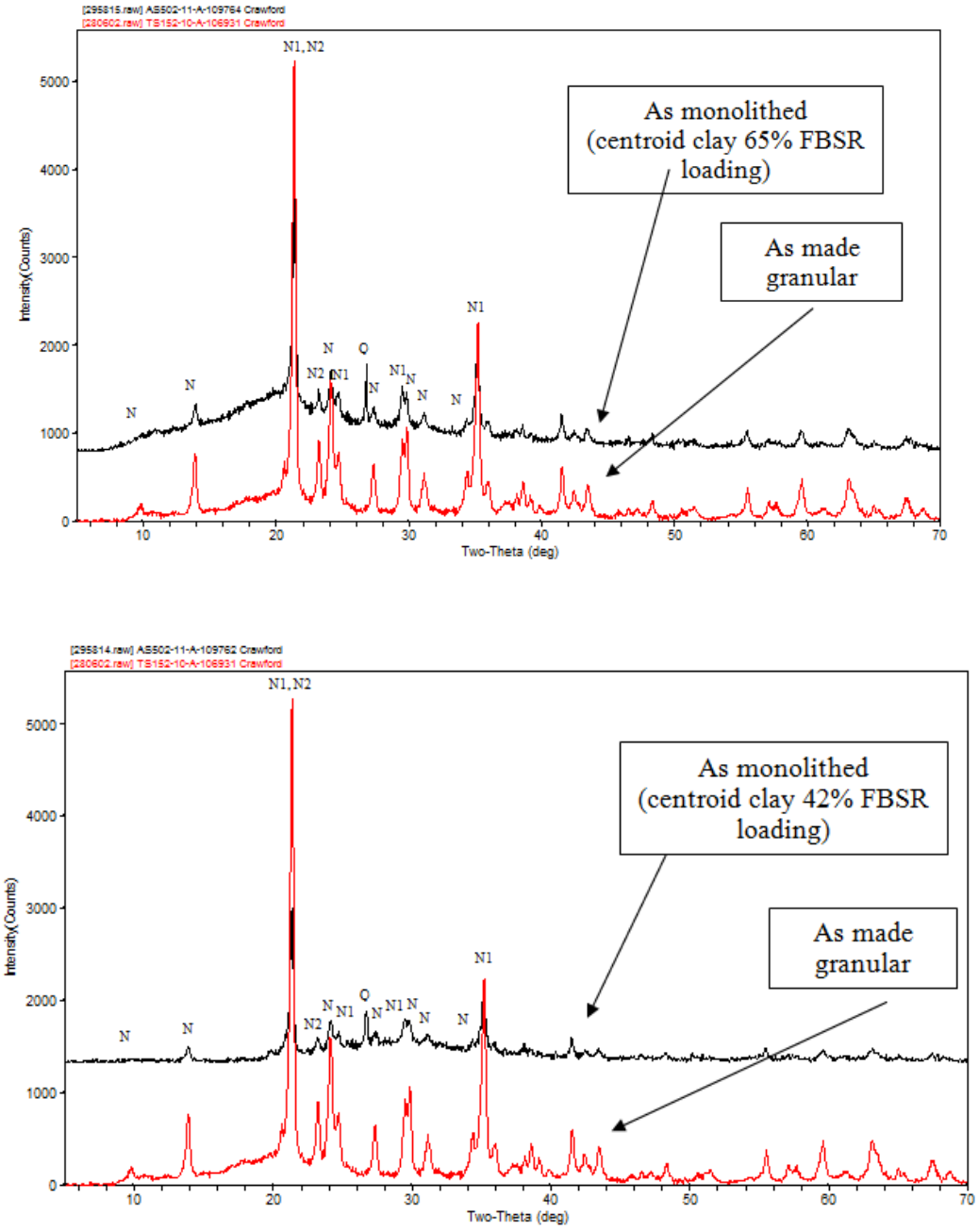

Figure 9-4. Overlay of As-made BSR Radioactive B Granular Product and Radioactive Monolithed Geopolymers Made with Clay at 42% and 65% FBSR Loading

Note that all the original phases survive in the XRD but are present at less intensity in the monolith pattern due to the dilution with the amorphous geopolymer matrix.
N1 is Nepheline (O) $NaAlSiO_4$ (PDF00-052-1342)
N2 is Nepheline (H) $NaAlSiO_4$ (PDF 00-035-0424)
N is Nosean (cubic) $Na_8Al_6Si_6O_{24}SO_4$ (PDF 01-072-1614)
Q is Quartz, SiO_2 (PDF 00-046-1045)
Original XRD spectra fits are in Appendix I of Reference 3

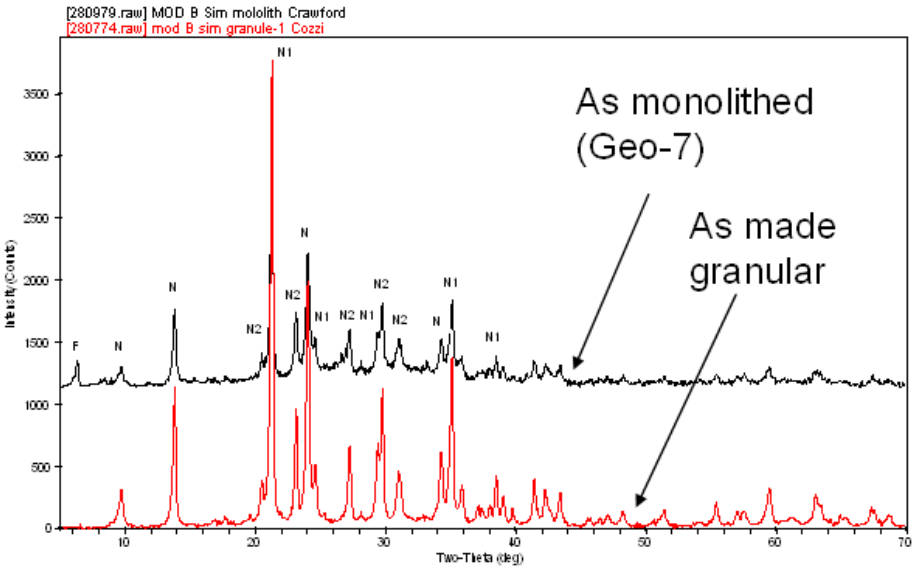

Figure 9-5. Overlay of As-made BSR Non-radioactive Granular Product and Monolithed Geopolymer Made with Fly Ash (GEO-7).

Note that all the original phases appear in the XRD of the monolith.

N1 is Nepheline (O) $NaAlSiO_4$ (PDF00-052-1342)
N2 is Nepheline (H) $NaAlSiO_4$ (PDF 00-035-0424)
N is Nosean (cubic) $Na_8Al_6Si_6O_{24}SO_4$ (PDF 01-072-1614)
Q is Quartz, SiO_2 (PDF 00-046-1045)
F is faujasite, $Na_2Al_2Si_40_{12}\bullet 8H_2O$ (PDF 00-039-1380) a geopolymer reaction product [Appendix G, 212]
Original XRD spectra fits are in Appendix I of Reference 3

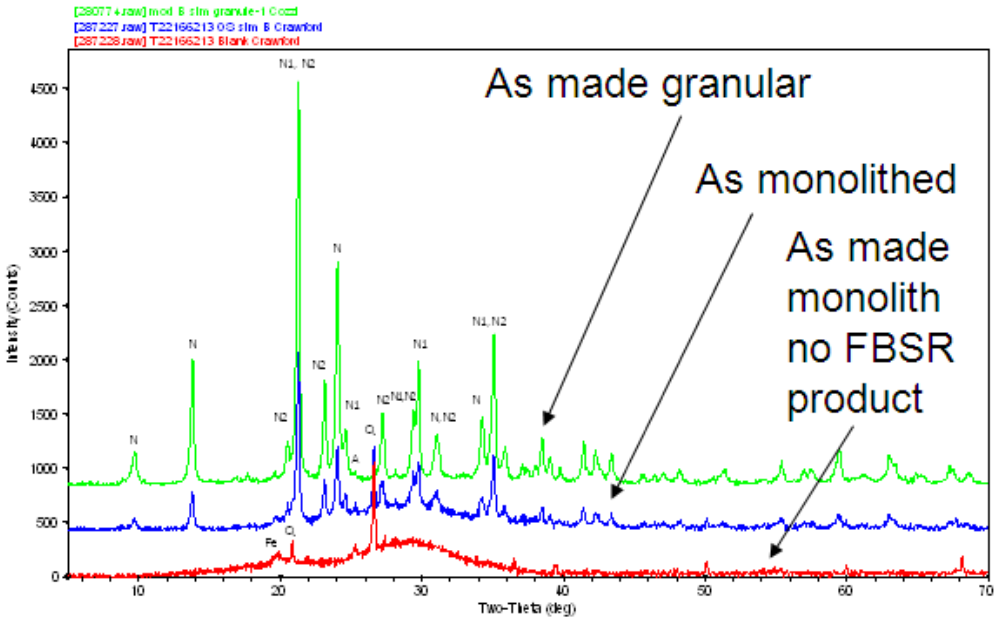

Figure 9-6. Overlay of As-made BSR Non-radioactive Granular Product, a Monolithed Geopolymer with the BSR product, and a Geopolymer with no FBSR product. The monolith with the BSR product contained 42 wt% FBSR product.

Note - all the original phases appear in the XRD of the monolith. The anatase is TiO_2 from impurities in the clay used in the FBSR process, but anatase is also an impurity in the geopolymer clay. In the geopolymer spectra, Na_5FeO_4, quartz, and anatase are present from the clay binder where the sodium iron phase is likely formed from the muscovite impurities in the clay (see Figure 9-7).
N1 is Nepheline (O) $NaAlSiO_4$ (PDF00-052-1342)
N2 is Nepheline (H) $NaAlSiO_4$ (PDF 00-035-0424)
N is Nosean (cubic) $Na_8Al_6Si_6O_{24}SO_4$ (PDF 01-072-1614)
Q is Quartz, SiO_2 (PDF 00-046-1045)
A is Anatase, TiO_2, (PDF 00-021-1272)
Fe is Na_5FeO_4 (PDF 00-036-0874)
Original XRD spectra fits are in Appendix I of Reference 3

During the production of the fly ash monolith formulations, all the ingredients were mixed together, i.e. the FBSR product, the metakaolin, the sodium hydroxide and the sodium silicate. This gave a less homogeneous monolith than desired. When the monolith formulations were made with clay, the geopolymer was made first from the metakaolin, the sodium hydroxide, and the sodium silicate to the desired composition in the G1 region shown in Appendix G. After the mixture reached the desired consistency, the FBSR granular product was added to ensure that the granules were macro-encapsulated.

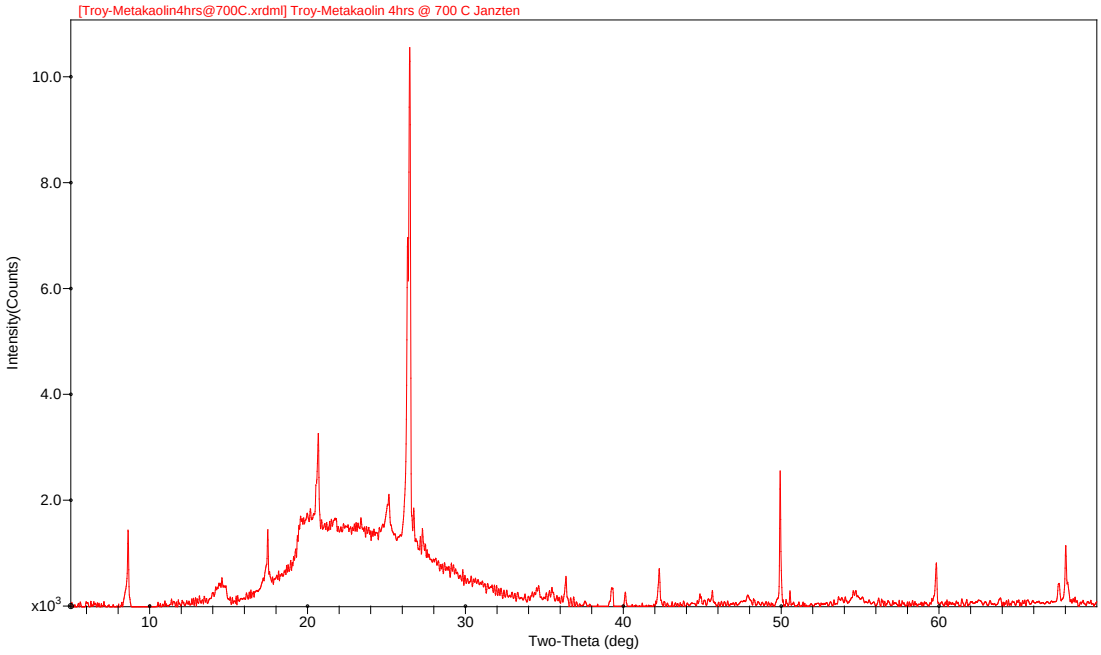

Figure 9-7. X-ray Diffraction Pattern of the Troy (Helmer) metakaolin after roasting at 700°C for 4 hours.

M is muscovite $(K,Na)(Al,Mg,Fe)_2(Si_{3.1}Al_{0.9})O_{10}(OH)_2$ (PDF 00-007-0042)
Q is Quartz, SiO_2 (PDF 00-046-1045)
T is Tridymite, SiO_2 (PDF 01-088-1535)
A is Anatase, TiO_2, (PDF 00-021-1272)
R is Rutile, TiO_2, (PDF 00-021-1276)
Original XRD spectra fits are in Appendix I of Reference 3

Figure 9-8 shows the ESTD engineering scale P-1B FBSR product embedded in a geopolymer made from fly-ash. The coal and Fe in the image come from the fly ash and the observed cracking in the geopolymer is due to SEM preparation. Note the three circular granules at the tips of the dashed triangles. They are rich in Cl, S, Al and Na and are sodalite/nosean solid solution FBSR minerals. The edges of the FBSR sodalite/nosean minerals are sharp and show no degradation or attack, which would cause irregular grain boundaries, from being embedded in the geopolymer (GEO-7).

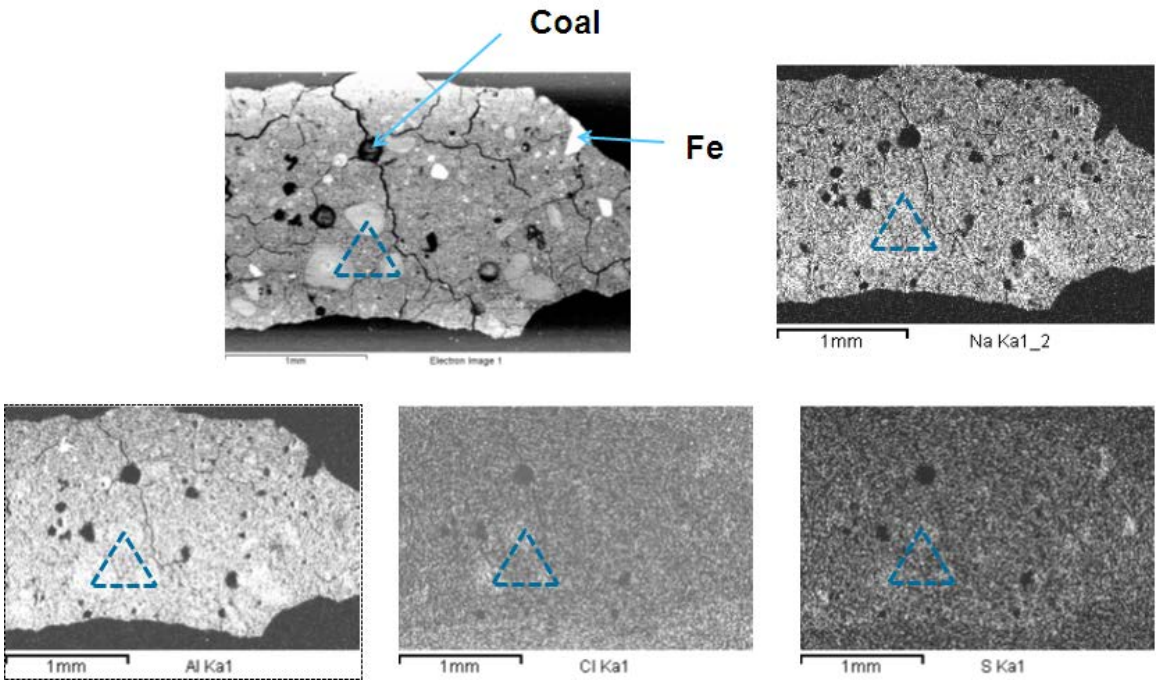

Figure 9-8. Scanning Electron Microscopy of ESTD FBSR Granular Product P-1B Embedded in a Fly Ash Geopolymer

Photographs of representative 1" diameter x 2" high right circular cylinder monoliths made during this study are shown in Figure 9-9. The Figure 9-9a shows ESTD GEO-7 made with fly ash at 65% FBSR loading and Figure 9-9b shows a Troy clay monolith made with BSR Module B at 42% BSR loading with the recipe of T-22-16-62-13. Figure 9-9c and Figure 9-9d photographs show Troy clay monoliths made with ESTD P-1B at two similar recipes of T-16-16-66-20 and T-20-20-60-20, respectively, each containing 60% FBSR loading. All of these monoliths show various small-sized indentions or craters that derive from trapped air pockets that form during initial loading of the monolith material into the plastic curing molds. The embedded coal may be from the FBSR product or the fly ash. The metallic Fe is an impurity in the fly ash.

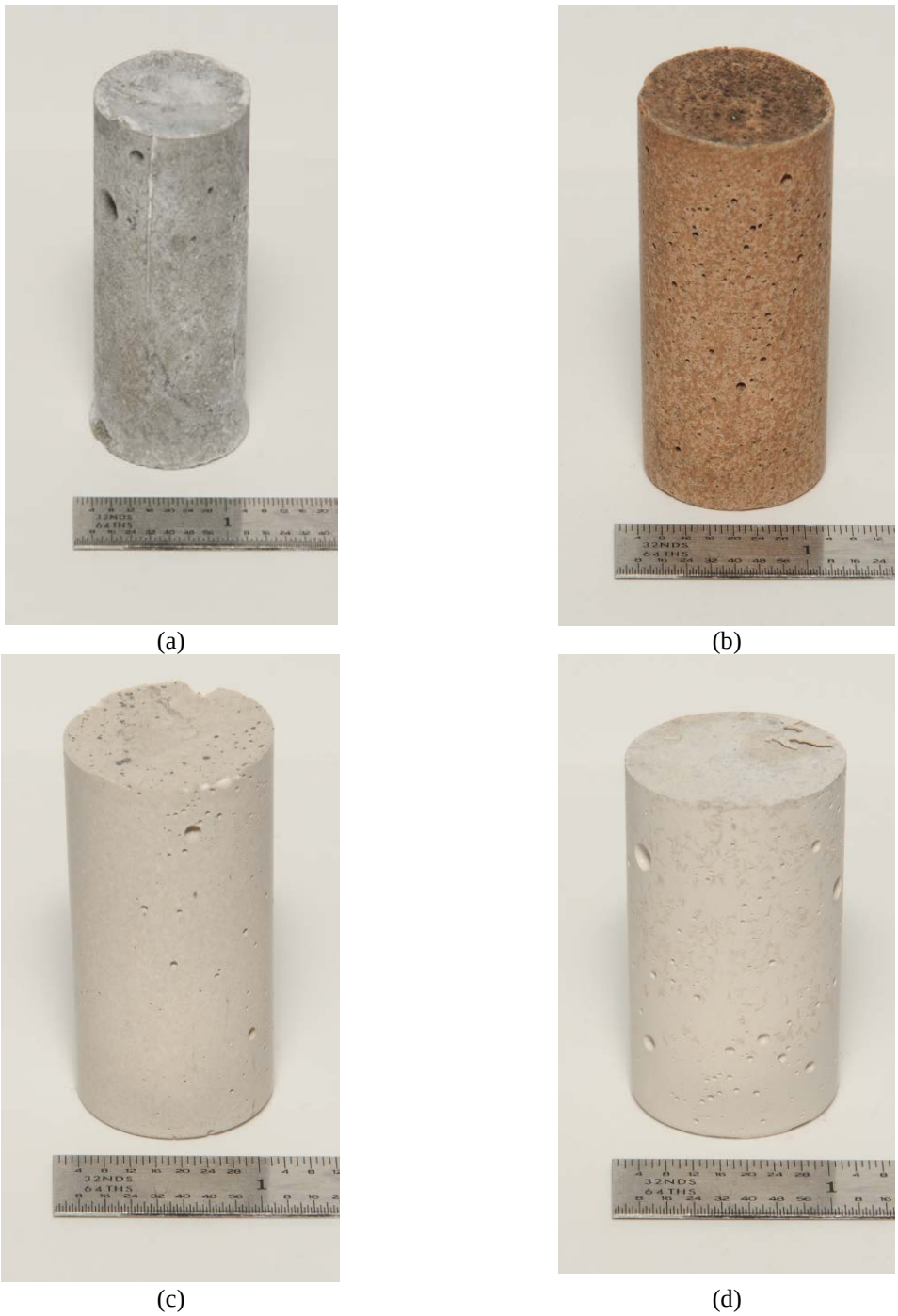

(a) (b)

(c) (d)

Figure 9-9. (a) ESTD GEO-7 made with fly ash at 65% FBSR loading; (b) Troy Clay Monolith made with BSR Module B at 42% BSR loading and T-22-16-62-13 recipe; (c) and (d) Troy Clay Monoliths made with ESTD P-1B at 60% FBSR loading and two similar recipes of T-16-16-66-20 and T-20-20-60-20, respectively

Note the difference in color between the fly ash and clay based geopolymer monoliths. Bubbles are due to setting without vibration to remove air pockets and dark coloration of GEO-7 made with fly ash is from the ESTD PR/PGF mixture and the fly ash binder.

9.1.2.2 *Product Consistency Short-term Testing (Monolith Product)*

The 7-day PCT was conducted on the Engineering scale LAW P-1B GEO-7 and the Module B simulant GEO-7 monoliths made with Fly Ash at 68 wt.% FBSR loading and on the radioactive monoliths made at 42 wt.% waste loading and 65% FBSR loading. The leachates were only analyzed for the 65 wt.% FBSR loaded monolith and the leachates from the 42 wt.% FBSR loaded monolith were archived (see footnote to Table 9-6). The results for the PCT of the engineering scale P-1B and Module B simulant monolith are shown in Table 9-11, and the raw data for the short-term PCT monolith tests are given in Appendix H of Reference 3. The granular PCT results from Table 8-39 are repeated in Table 9-11 for comparison. As can be seen from the data in Table 9-11, the release of rhenium is consistent among the monolith and granular products made from similar salt solutions.

Table 9-11. 7-Day PCT Results for Monoliths and Granules Prepared from Engineering Scale FBSR and Module B Simulants

Normalized Elemental Release (g/m^2)	Non-Radioactive				Radioactive	
	Fly Ash ESTD P-1B* GEO-7 Monolith (68% FBSR loading)	Fly Ash BSR Mod B GEO-7 Monolith (68% FBSR loading)	ESTD P-1B Granular	BSR Mod B Granular	BSR Mod B Clay Monolith (65% FBSR loading)	BSR Mod B Granular
Al	4.30E-05	4.47E-04	2.12E-03	2.34E-03	2.60E-04	3.97E-03
S	4.78E-02	1.02E-01	33.42E-01	4.34E-02	3.20E-02	7.72E-02
^{133}Cs	2.01E-03	4.60E-03	9.31E-03	1.09E-02		
^{137}Cs					7.00E-05	2.29E-03
Re	1.05E-02	1.99E-02	4.10E-03	8.83E-03	3.96E-03	1.13E-02
^{99}Tc					<8.35E-03	2.42E-02
Na	2.15E-02	7.30E-02	2.15E-02	1.14E-02	1.81E-02	1.24E-02
Si	2.70E-03	7.02E-03	7.82E-04	9.86E-04	2.40E-04	6.17E-04
^{127}I	5.27E-03	3.61E-03	1.51E-02	9.82E-04	5.00-E-04	1.69E-03
^{129}I					<2.66E-03	<3.61E-03
pH	12.39	12.56	11.63	11.40	10.33	11.25

* The elemental composition of the ESTD LAW P-1B monolith made with fly ash was reported in Table 37 of Reference 123.

9.1.2.3 *Product Consistency Long-term Testing (Monolith Product)*

Long-term PCT-B testing was also performed on GEO-7 monoliths made from the ESTD granular non-radioactive product and the BSR granular non-radioactive product (see Table 9-6 and Figure 9-2). Samples were collected at one month, three month, six month, and one year intervals. All of the raw data for the long-term PCT tests on the monoliths are given in Appendix H of Reference 3.

As with the long-term PCT-B tests on the granular products, the long-term PCT tests on the monolithic products are useful for generating concentrated solutions to study chemical affinity effects on the dissolution rate. PCT Method B tests at high temperatures and high glass/solution mass ratios can be used to promote the formation of alteration phases to (1) identify the kinetically favored alteration phases, (2) determine their propensity to sequester radionuclides,

and (3) evaluate the effect of their formation on the continued waste form dissolution rate. XRD was used as a tool to identify alteration phases but it should be noted that XRD sensitivity to minor phases is, in general, not very good.

Table 9-12 provides the PCT results over the PCT duration for the GEO-7 monolith prepared with the engineering scale FBSR product of the LAW P-1B run at HRI using the fly ash formulation. For each of the elements analyzed, the release was consistent over the duration of testing. Comparisons of the one year releases from the monolith samples (Table 9-12) to the granular product releases (Table 8-42) shows that the monolith releases are about an order of magnitude lower for S, R, I, Cs, Na, Al, and Si than the granular product releases due to the encapsulation of the granules by the monolith binder. The order of elemental release, i.e. which are slower vs. which are more rapid, is the same as the order in the granular P-1B (see Figure 8-14).

Table 9-12. Long-Term PCT Results for the GEO-7 Fly Ash Monolith Prepared with the Engineering Scale P-1B LAW Granules

Normalized Elemental Release (g/m^2)	Eng. Scale P-1B GEO-7 Monolith Test Interval				
	7 Days	1 Month	3 Month	6 Month	1-Year
Al	4.30E-05	2.98E-04	4.71E-04	1.30E-04	7.80E-04
S	3.42E-02	4.93E-02	6.30E-02	7.85E-02	6.26E-02
Cs	2.01E-03	2.70E-03	2.59E-03	3.58E-03	3.00E-03
Re	4.10E-03	9.24E-03	3.67E-02	4.70E-02	8.72E-02
Na	2.15E-02	3.12E-02	2.61E-02	2.31E-02	7.23E-03
Si	2.70E-03	1.89E-03	1.90E-04	2.80E-04	4.00E-05
I	5.27E-03	1.28E-02	6.31E-02	7.85E-02	1.20E-01
pH	12.39	12.45	12.49	12.79	11.94

The PCT results are shown in Table 9-12 and Figure 9-10. Silicon release decreases with time indicating solution saturation. The other releases held constant over the one year of testing indicating that the FBSR granular product was not undergoing significant degradation of the mineral species. Sodium release also decreased compared to the other elements. Aluminum release appeared erratic, while S, Re, and I release increased slightly with time. No reaction products were identified that were from reaction of the granular product with the leachant.

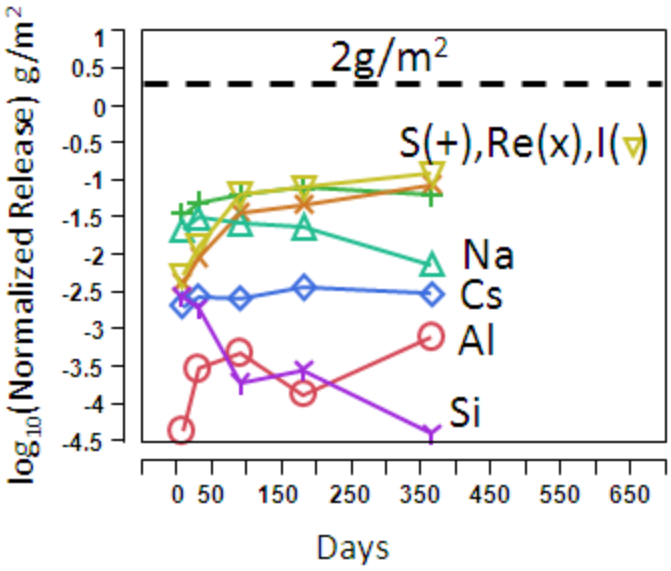

Figure 9-10. Release of Elements from ESTD P-1B Rassat GEO-7 Fly Ash Monoliths during 7 day, 1 month, 3 month, 6 month and 12 month Long-Term PCT Testing.

Figure 9-11 is an overlay of the XRD patterns of the ESTD B non-radioactive monolith product as received and after each leach interval. The XRD pattern for the as-received sample is on the bottom of the figure and the patterns are stacked with increasing leach duration. It can be noted from the figure that the intensity and width of the major granular phases persists through all the leach intervals, indicating minimal degradation of the mineral species.

The mineral faujasite was observed in XRD analysis (Figure 9-11), but that phase was present in the "as made" geopolymer. It is a zeolite that can form during geopolymerization in the presence of fly ash. Synchrotron radiation-based infrared microscopy (SR-FTIR) data processed via hierarchical clustering analysis was performed by researchers in Australia on geopolymers made from various fly ash compositions.[212] In general, fly ash was found to be composed of reactive components such as 36.6% amorphous SiO_2 and 15.3% amorphous Al_2O_3 with the remainder being unreactive crystalline mullite, quartz, and iron oxide phases. This was verified for the SEFA fly ash used by SRNL, which was found to contain crystalline mullite and quartz.[123]

In the Australian study [212], the formation of higher Si/Al ratio crystals such as faujesite occurred in samples with a slower alumina release rate. In other words, these samples had a lower availability of aluminum since the generally accepted reaction sequence of geopolymerization is that the first stage of reaction is the release of aluminate and silicate monomers by alkali attack on the solid aluminosilicate source (clay or fly ash), which is required for the conversion of solid particles to geopolymer gel. Hydrolysis reactions occur on the surface of the solid clay or fly ash particles, followed by the formation of dissolved species that cross-link to form oligomers, and then set and harden by polycondensation and the formation of a three-dimensional aluminosilicate network.

While the formation of faujasite has been well studied in fly ash based geopolymers [212], it is not a desired phase due to the 7 or 8 waters of hydration bound to its structure. However,

faujesite, Zeolite X, and Zeolite P, all have the identical cage structure as sodalite.[81] So while the sodalite in the FBSR mineral phases may be attracting structural waters of hydration to its structure the sodalite cage structure appears to remain in tact. Another zeolite, known as N3 or Zeolite Na-P1, was also observed but also forms from the alteration of fly ash according to the Australian study [212]. The fly ash is a geopolymer additive and not an FBSR mineral phase. Therefore, no reaction products were identified that were associated with the degradation of the granular FBSR phases.

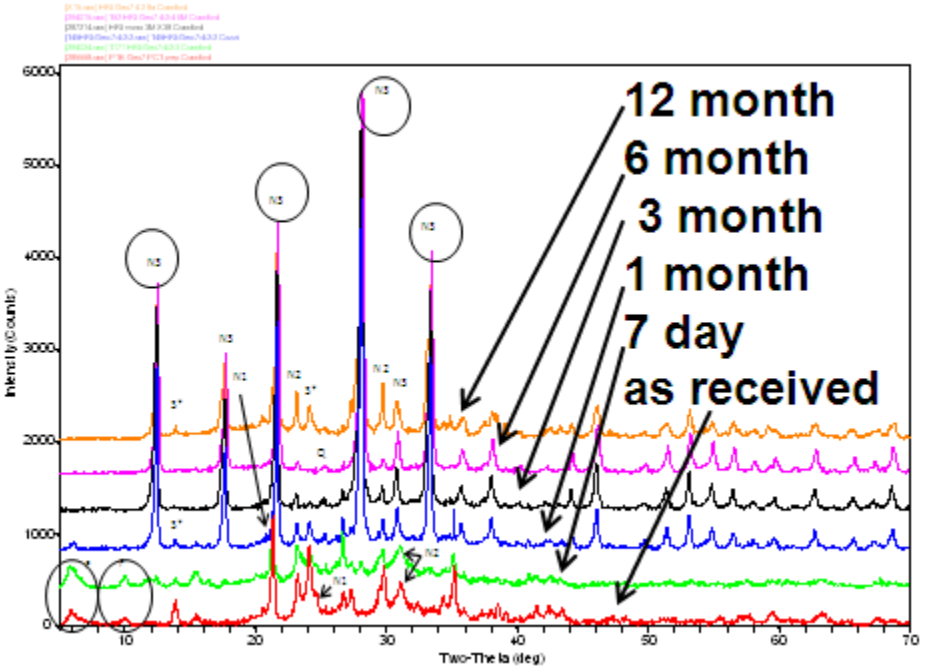

Figure 9-11. XRD patterns of Module B ESTD GEO-7 Fly Ash Monolith As-Made and after Long –Term PCT Leaching

N1 is Nepheline (O) $NaAlSiO_4$ (PDF00-052-1342)
N2 is Nepheline (H) $NaAlSiO_4$ (PDF 00-035-0424)
S* is Sodalite $Na_6(AlSiO_4)_6$ (PDF 00-042-0217)
N3 is Zeolite Na-P1, $NaAl_6Si_{10}O_{32}\bullet 12H_2O$ (PDF 00-039-0219)
F is Faujasite-K, $K_{48.2}Al_{48.2}Si_{143.8}O_{384}\bullet 243H_2O$ (PDF 00-026-0896)
Q is Quartz, SiO_2 (PDF 00-046-1045)
Original XRD spectra fits are in Appendix I in Reference 3

Table 9-13 contains the PCT results for the GEO-7 monolith prepared with the Module B simulant BSR product. As with the engineering scale long-term PCT, the release of the elements analyzed was consistent throughout the duration of the test.

The 7-day results from Table 9-13 are shown with release results from samples leached for 1, 3, 6, and 12 months in Figure 9-12. Silicon release is decreasing indicating solution saturation and so is aluminum in solution. The other releases are about constant over the one year of testing, which indicates that the FBSR granular product is not undergoing significant degradation of the mineral species.

Table 9-13. Long-Term PCT Results for the GEO-7 Fly Ash Monolith Prepared with the Module B BSR Simulant Granules

Normalized Elemental Release (g/m^2)	BSR Module B Simulant GEO-7 Test Interval				
	7 Days	1 Month	3 Month	6 Month	1 Year
Al	4.47E-04	1.21E-03	1.74E-03	1.99E-03	1.00E-04
S	1.02E-01	1.89E-01	1.86E-01	2.40E-01	3.11E-01
Cs	4.60E-03	NM	7.64E-03	5.93E-03	1.13E-02
Re	1.99E-02	8.51E-02	1.60E-01	2.16E-01	2.84E-01
Na	7.30E-02	7.48E-02	7.69E-02	7.94E-02	8.86E-02
Si	7.02E-03	2.28E-03	9.60E-04	5.80E-04	3.00E-04
I	3.61E-03	6.35E-02	1.48E-01	2.12E-01	2.22E-01
pH	12.56	12.64	12.56	12.48	13.07

NM – not measured

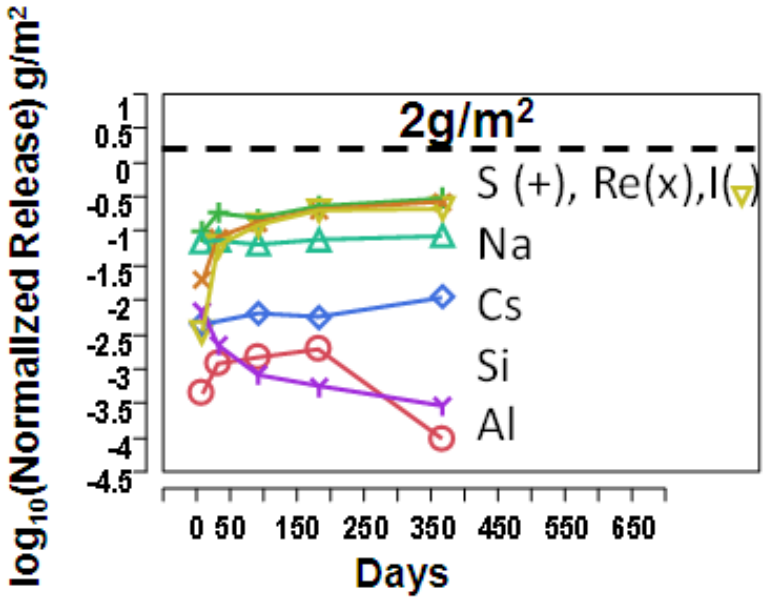

Figure 9-12. Release of Elements from BSR Module B GEO-7 Fly Ash Monolith Made from Rassat Simulant during 7 day, 1 month, 3 month, 6 month and 12 month Long-Term PCT Testing

Figure 9-13 is an overlay of the XRD patterns of the Module B simulant BSR monolith product as prepared for PCT and after each leach interval. The same secondary phases were found in the fly ash based BSR monolith as in the fly ash based ESTD monolith. Both contained faujasite in the as made monoliths, which is a reaction product of fly ash and NaOH. Both contained Zeolite N3, which is also a degradation product of fly ash. Halloysite was also found, which is the main reaction product of unreacted kaolin clay. No reaction products were identified that could have formed from the FBSR minerals, nepheline, sodalite, or nosean.

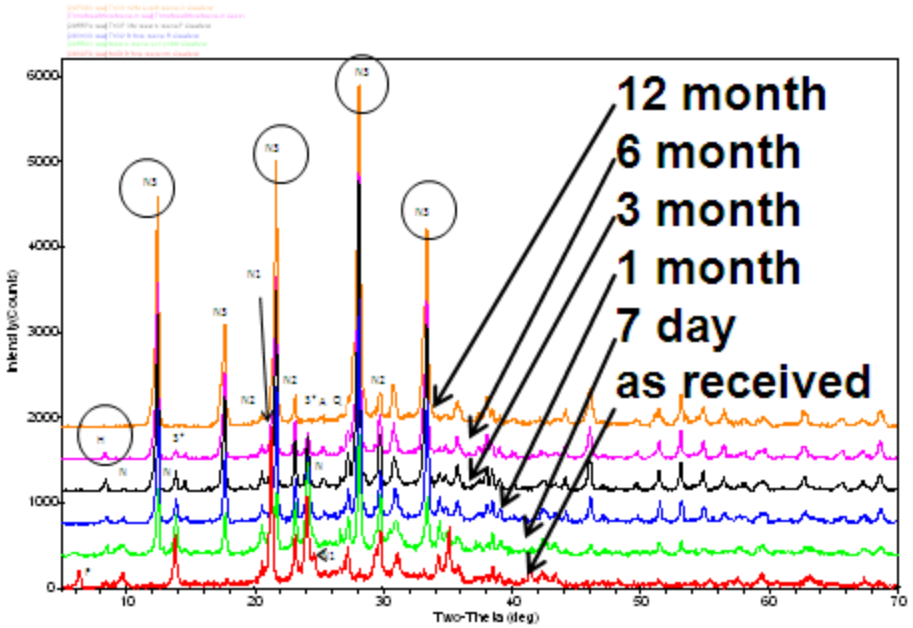

Figure 9-13. XRD Overlay for the GEO-7 Fly Ash Monolith Made from BSR Simulant Module B Rassat Granular Product

N1 is Nepheline (O) $NaAlSiO_4$ (PDF00-052-1342)
N2 is Nepheline (H) $NaAlSiO_4$ (PDF 00-035-0424)
S* is Sodalite $Na_6(AlSiO_4)_6$ (PDF 00-042-0217)
N is Nosean (cubic) $Na_8Al_6Si_6O_{24}SO_4$ (PDF 01-072-1614)
N3 is Zeolite Na-P1, $NaAl_6Si_{10}O_{32}\bullet 12H_2O$ (PDF 00-039-0219)
F is Faujasite-K, $K_{48.2}Al_{48.2}Si_{143.8}O_{384}\bullet 243H_2O$ (PDF 00-026-0896)
Q is Quartz, SiO_2 (PDF 00-046-1045)
H is Halloysite, $AlSi_2O_5(OH)_4\bullet 2H_2O$
Original XRD spectra fits are in Appendix I in Reference 3

As explained previously, during the monolith formulation and after the long-term durability testing had been initiated, SEM was performed (Figure 9-8) and unreacted cores were not found in either the FBSR products from the ESTD or BSR testing. Therefore, new formulations were made without including any interactions with the kaolin or fly ash in the FBSR product. A clay geopolymer formulation was used instead of fly ash and the old fly ash formulations were recalculated (see Table 9-1 and Table 9-2) based on zero extra aluminosilicate in the FBSR product. The positions of the three final monoliths that were durability tested are shown in Figure 9-2 relative to the desired G1 geopolymerization region.

The GEO-7 fly ash Module B monoliths made with fly ash and the ESTD and BSR non-radioactive FBSR products are barely outside the preferred G1 region of geopolymer formation (Figure 9-2). Since the long-term durability testing had already begun and the geopolymer formulations were close to the G1 region, the long-term testing was completed.

Geopolymers made with clay at 42 and 65 wt.% FBSR loading were also formulated (see Table 9-3, Table 9-4, and Table 9-5) and both radioactive geopolymer formulations (Table 9-5) were leach tested. Only short-term PCT testing was performed on this sample due to lack of funding and only the 65 wt.% FBSR loaded monolith leachates were analyzed, but the results of this short-term PCT testing will be discussed relative to the PCT long-term testing of the fly ash monoliths at 68 wt.% FBSR loading.

In Figure 9-14, the long-term releases from the granular and monolith PCT tests are compared for the mis-formulated GEO-7 fly ash monoliths made from the ESTD simulant. Of note is that the pH of the leachate is always higher for the monolith, likely due to the NaOH and/or Na silicate in the pore water due to the compounds used to form the geopolymers (Figure 9-14a). Even with the mis-formulation in the geopolymer binder and the high H_2O/Na_2O ratio used in this formulation, the monolith actually leached less than the granular product for all elements except Re and I.

In Figure 9-15, the long-term releases from the granular and monolith PCT tests are compared for the mis-formulated GEO-7 fly ash monoliths made with too much Na_2O and made from the BSR simulant. Note that the GEO-7 monolith for the simulated BSR sample is more outside the G1 geopolymer region than the GEO-7 ESTD monolith. For the BSR GEO-7 monolith, the leachate pH values are higher than that of the FBSR granular products (Figure 9-15). For most elements, the leaching was higher from the GEO-7 fly ash monolith than from the granular product except for Cs and Al.

In Figure 9-16, the long-term releases from the radioactive BSR granular and monolith PCT tests are compared for the correctly formulated clay based 65 wt.% FBSR loaded centroid geopolymer composition. A 42 wt.% FBSR loaded centroid geopolymer composition was also made with clay but was not durability tested due to lack of funding. Note that only short-term PCT testing was available for the radioactive clay based geopolymer.

For the clay monolith, the pH values are lower for the monolith than for the granular product (Figure 9-16a), which is due to better formulations in the G1 polyhedra of Figure 9-2. The Na releases of the leachate from the monolith are the only element that leaches more from the monolith than from the granular product (Figure 9-16b). However, all the other elements, including Tc-99, Re and I are released over an order of magnitude more slowly from a correctly formulated geopolymer than the granular product as the granular product is macro-encapsulated (see Figure 9-8). It should be noted that Figure 9-16g and h show comparable releases of Re and Tc-99 from the granular products and the monolith. It should also be noted that the releases of all elements, except Na from the monolith, follow the pH as noted in Section 8.2.4 on the short-term testing of the FBSR granular product. This trend with pH was also observed in the historical short-term PCT data (Figure 8-13) and data from other leach testing and thermodynamic modeling.[106,120,126,132,162]

In general, for a correctly formulated monolith, COC releases are an order of magnitude lower than the releases from the granular product due to the way in which the geopolymer encapsulates the granular product. It also demonstrates that the geopolymer matrix does not attack the FBSR granular product and cause any adverse reactions or releases from the FBSR granular product. Finally, the data demonstrate that the reaction products formed from the fly ash or kaolin clay (binder or FBSR additives) do not diminish the capacity of the FBSR granular product from retaining the COC.

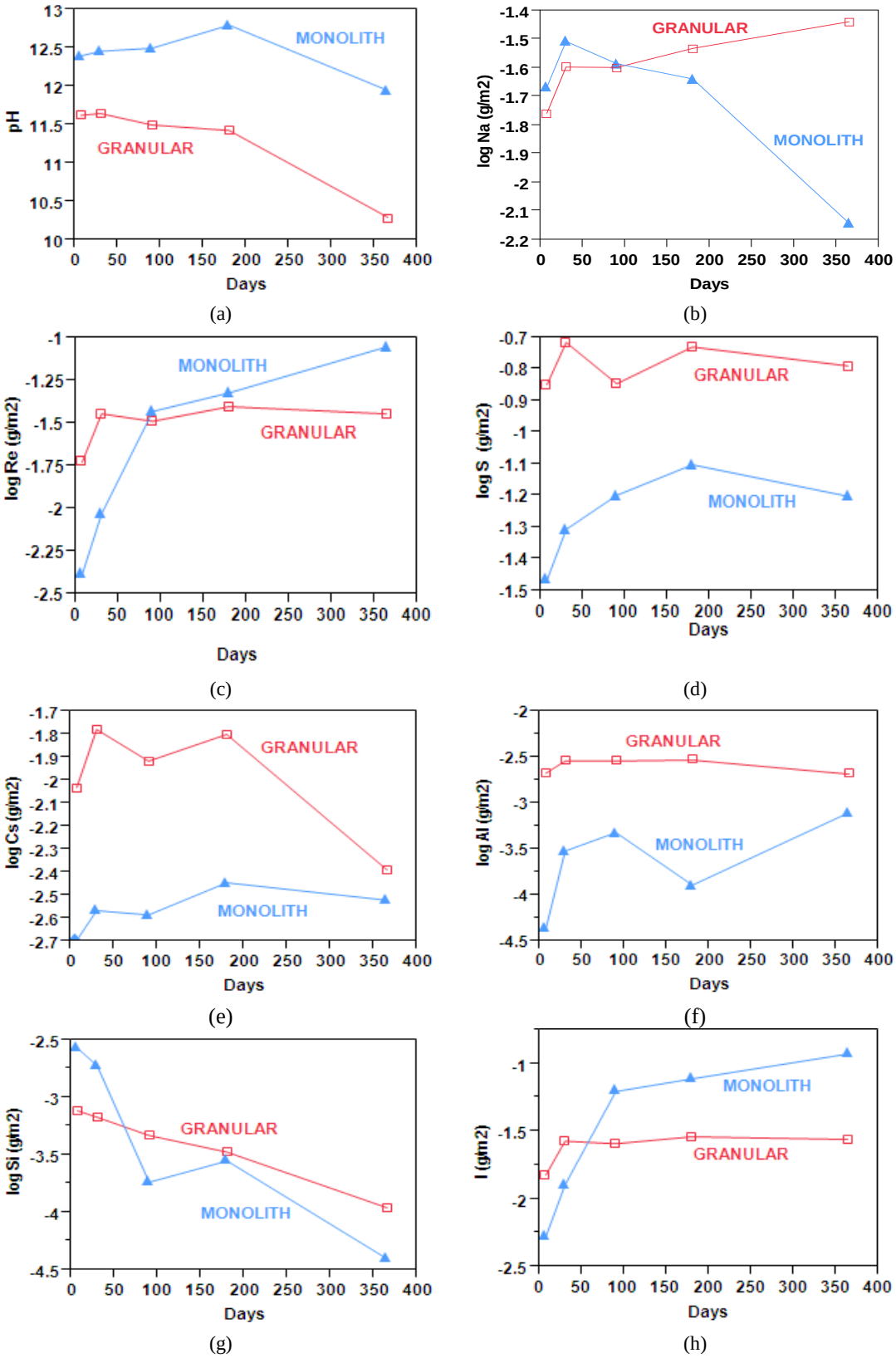

Figure 9-14. Overlay of the Simulated ESTD FBSR Granular Product Releases Compared to the Monolithed Product Releases for the GEO-7 Fly Ash Based Geopolymer at 67% FBSR Loading for PCT tests up to one year in duration.

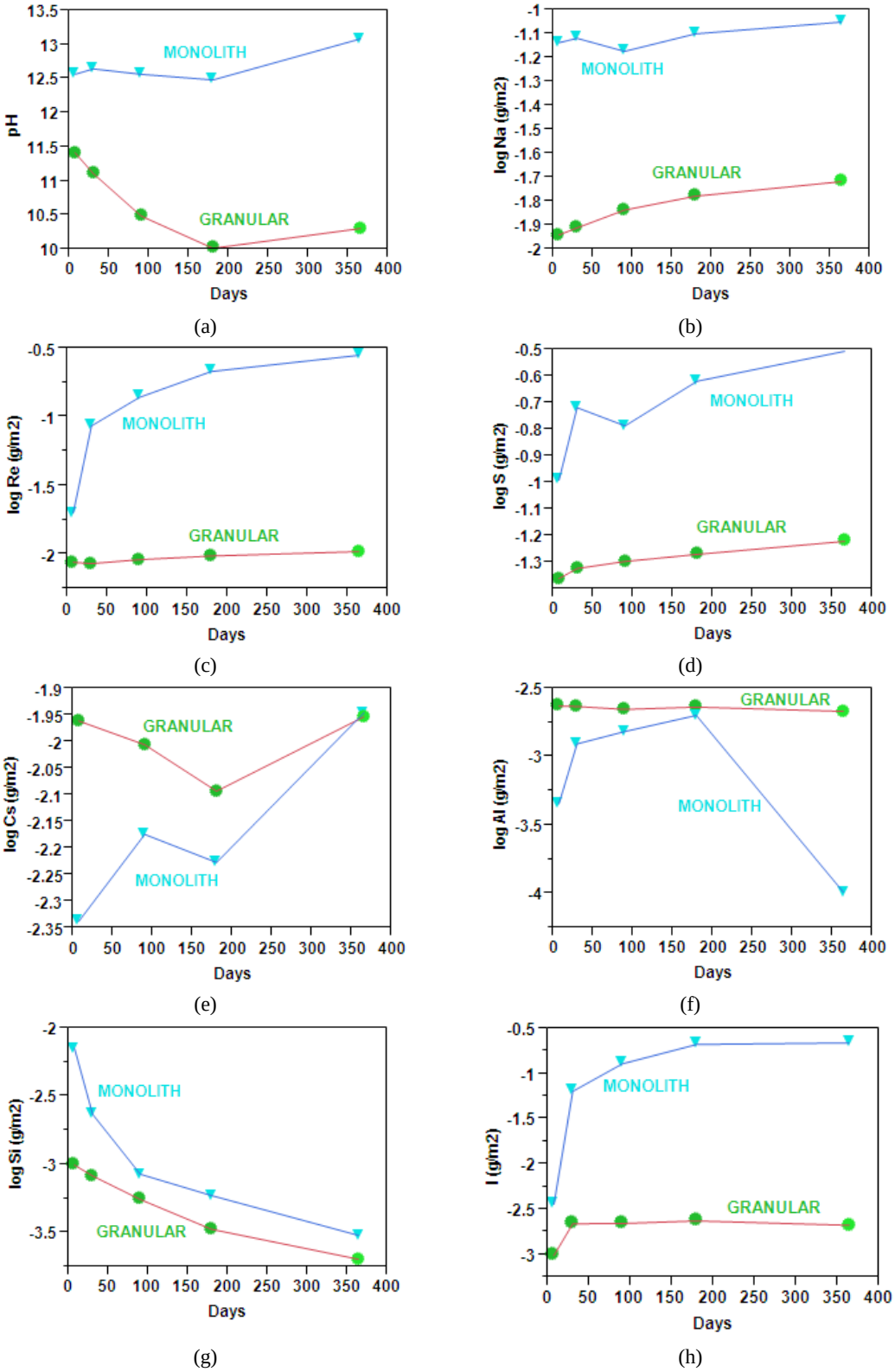

Figure 9-15. Overlay of the Simulated BSR Granular Product Releases Compared to the Monolithed Product Releases for the GEO-7 Fly Ash Based Geopolymer at 68% FBSR Loading for PCT testing up to one year in duration.

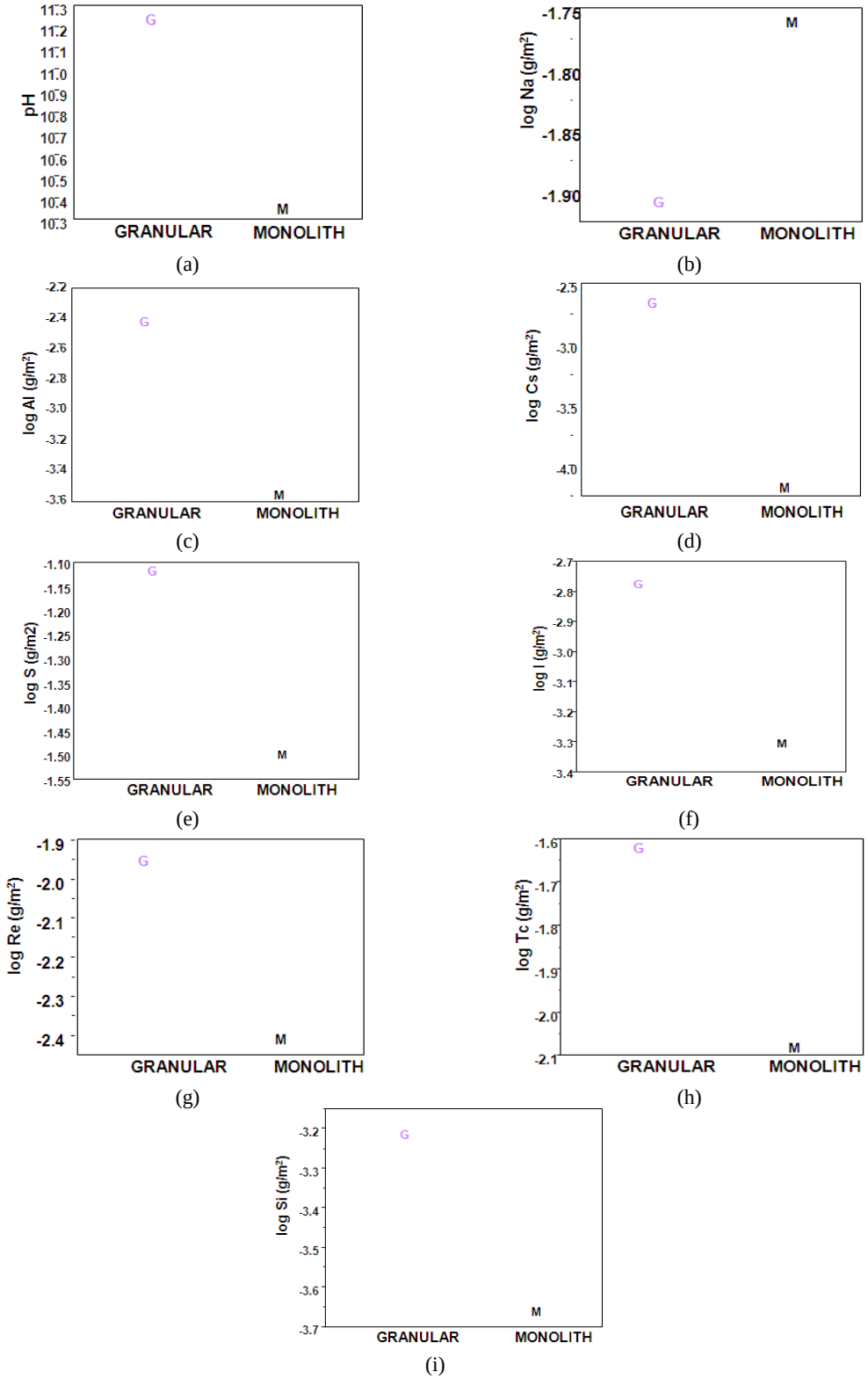

Figure 9-16. Overlay of the Radioactive BSR Granular Versus Monolithed Product Releases for a Clay Based Geopolymer at 65% FBSR Loading (that was correctly formulated) for 7-day PCT testing.

The ^{99}Tc release for the monolith is a less than number so the actual concentration of ^{99}Tc released is lower than shown from the monolith.

9.1.2.4 *Diffusion (ASTM C1308/ANSI 16.1) Testing*

Monolith leach testing was performed as given in Table 9-6 and included GEO-7 fly ash formulations with both ESTD and BSR simulants and centroid clay monoliths with both ESTD and BSR simulants. The monoliths were leached at ambient room temperature for the specified intervals and leachate data and cumulative mass fraction leached of the various analytes are shown in Appendix G of Reference 3. Pictures of the monoliths after leaching are provided in Figure 9-17 and they are seen to retain their shape and integrity. Mis-formulation of the fly-ash geopolymers is discussed in Appendix G and the preceding sections. The clay monoliths appear less corroded compared to the fly ash formulation.

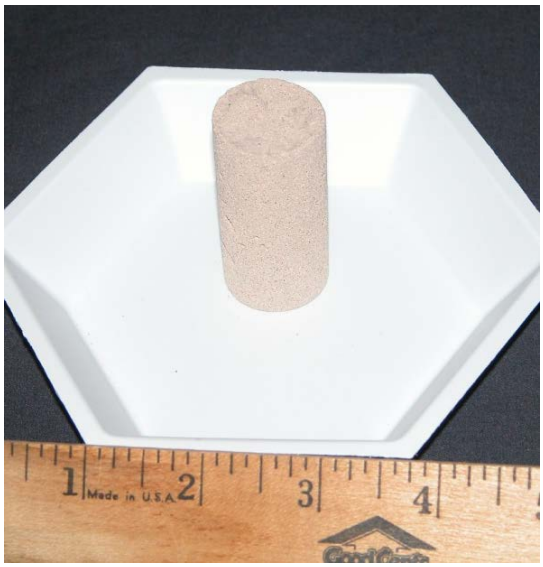

(a) BSR Module B Clay Monolith at 42% Loading

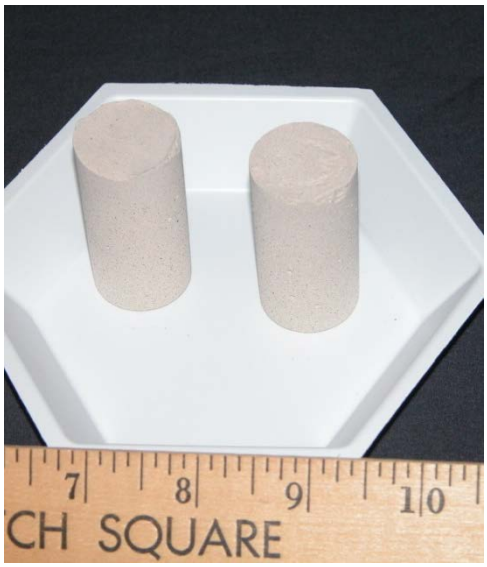

(b) ESTD P-1b Clay Monolith at 42% Loading

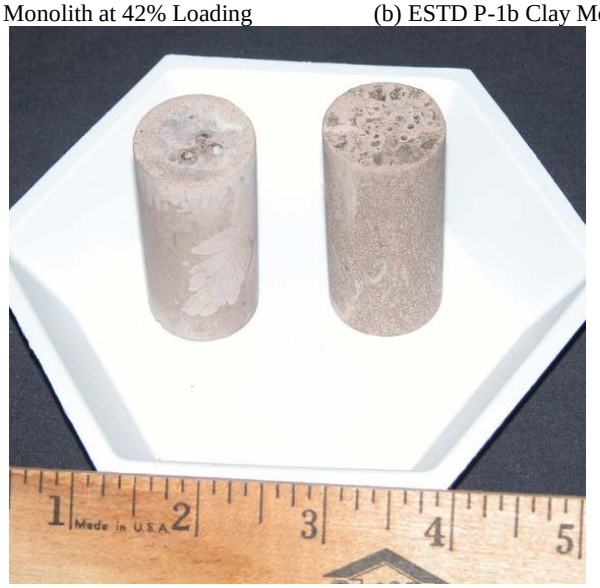

(c) BSR Module B Fly Ash Monolith at 65% Loading

Figure 9-17. Monoliths after ASTM C1308/ANSI/ANS 16.1 Testing

The pH values measured after each leaching interval are shown in Figure 9-18 for the HRI ESTD fly ash (top) and BSR Simulant Module B fly ash (bottom) monoliths. Data for the fly ash pH

shown in the top plot of Figure 9-18 indicate that the ESTD fly ash monoliths gave slightly higher leachate pH values and attained a maximum pH of 12 at 19 days versus the fly ash monoliths made with BSR Simulant Module B that are only slightly above a pH of 11 at 19 days. The centroid clay monolith leachate pH data show that the pH initially decreased from starting values of 11.5 down to 10.7 during the first 11 days, then slightly increased during the longer leach interval ending at 19 days, followed by a slight decrease to 11 and finally 10.7 for the 47 day and 91 day cumulative leach intervals. The pH values are also shown for blank solutions of the ASTM Type-I ultrapure water used in these tests which indicate that all blank solutions maintained a pH in the range of 6 to 7.

Representative cumulative leach fraction plots are shown in Figure 9-19 for the fly ash monoliths and Figure 9-20 for the centroid clay monoliths where each plot is plotted on the same scale for ease of interpretation. It is apparent from the Figure 9-19 and Figure 9-20 that P and S are released faster than Na for the ESTD geopolymers made from P-1B and P-1A where the unreacted coal concentrations were higher than in the BSR FBSR products. This indicates that the S released may be coming from the sulfur in the coal. For the BSR simulant monoliths made with fly ash, the S comes out slower than the Na (Figure 9-19) and for the BSR simulant monoliths made with clay (Figure 9-20), the S and Na are released at the same concentrations.

Re, Cs, and I are released at about the same concentrations as Si and Al in all monoliths irregardless of FBSR loading or whether the monoliths were made with clay or fly ash (Figure 9-19 and Figure 9-20). This indicates that the Cs is likely tied up in $CsAlSiO_4$ the Cs analog of nepheline and/or in a $(Na,Cs)_6Al_6Si_6O_{24}(NaI)_2$-$(Na,Cs)_6Al_6Si_6O_{24}(NaReO_4)_2$ sodalite solid solution so that the Cs, Re, and I are not released until the aluminosilicate framework structure of the minerals begins to degrade. All of the cumulative fraction leached plots in Figure 9-19 and Figure 9-20 show that steady state releases are reached after about 20 days during ASTM C1308 testing except for the HRI P-1B GEO-7 monolith made with fly ash (Figure 9-19 top).

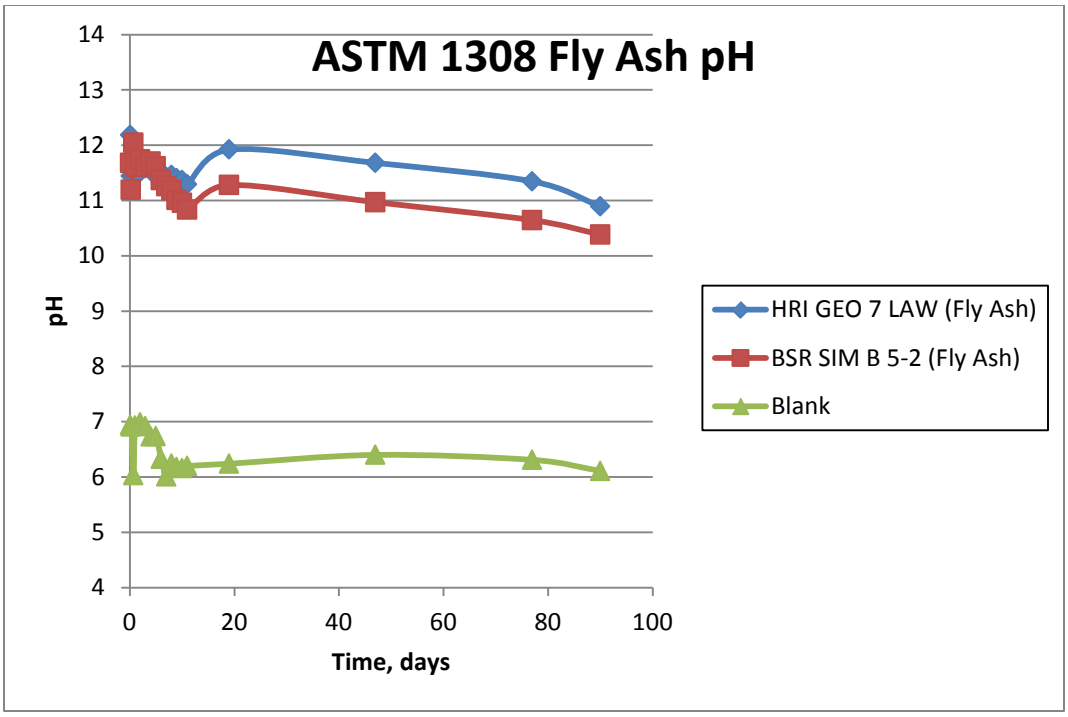

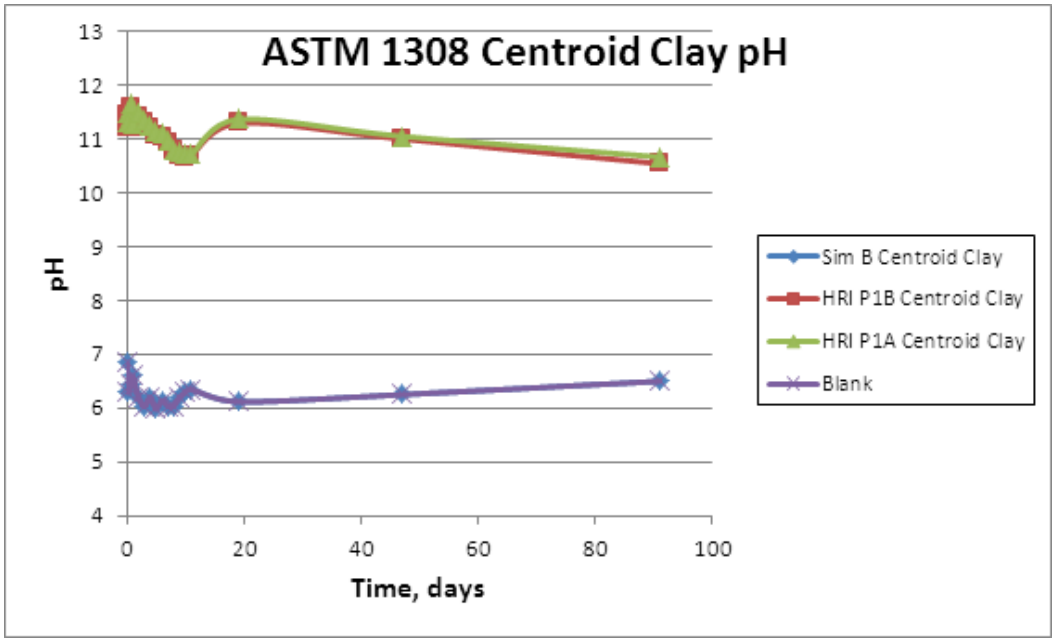

Figure 9-18. Measured pH for ASTM 1308 Leachates

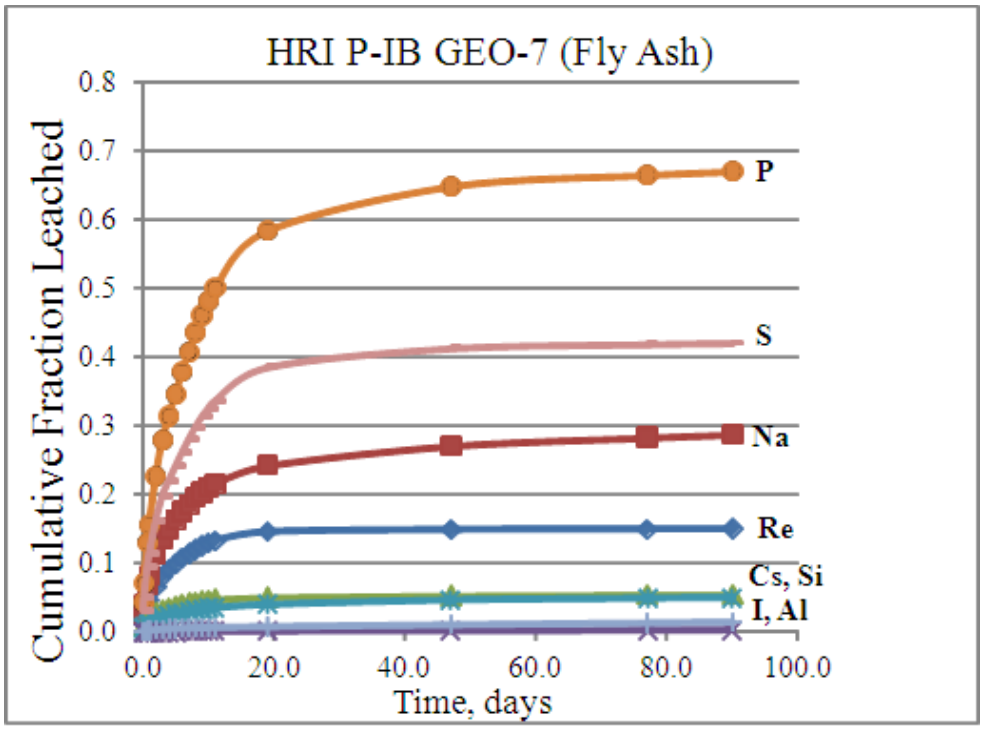

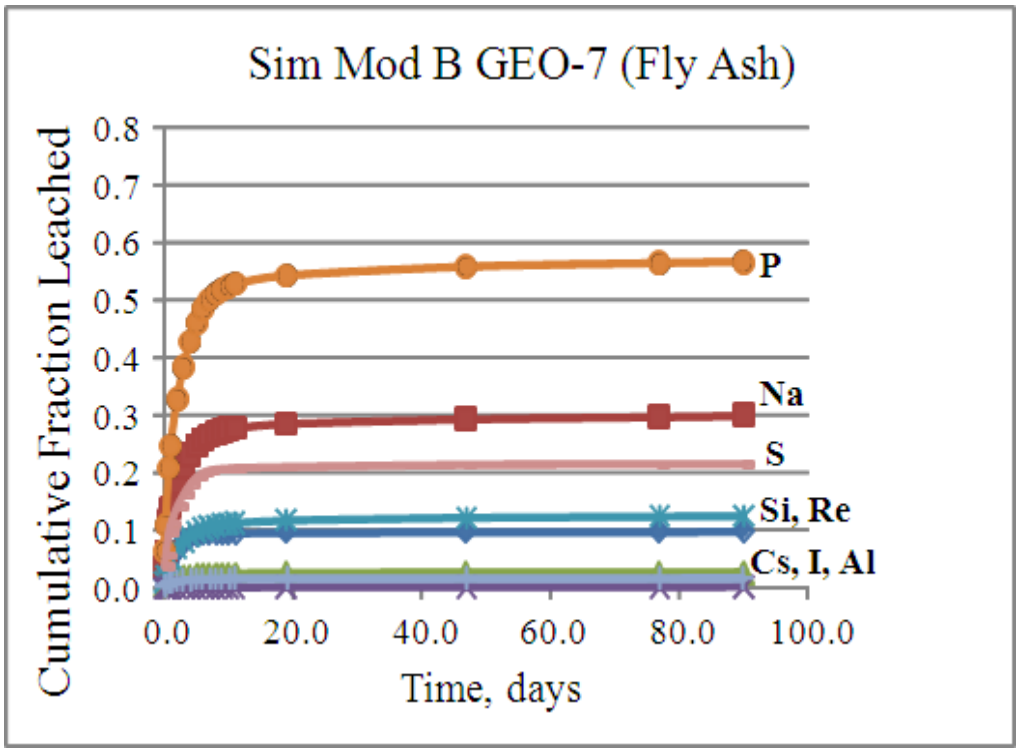

Figure 9-19. Cumulative Fraction Leached for Fly Ash Monoliths

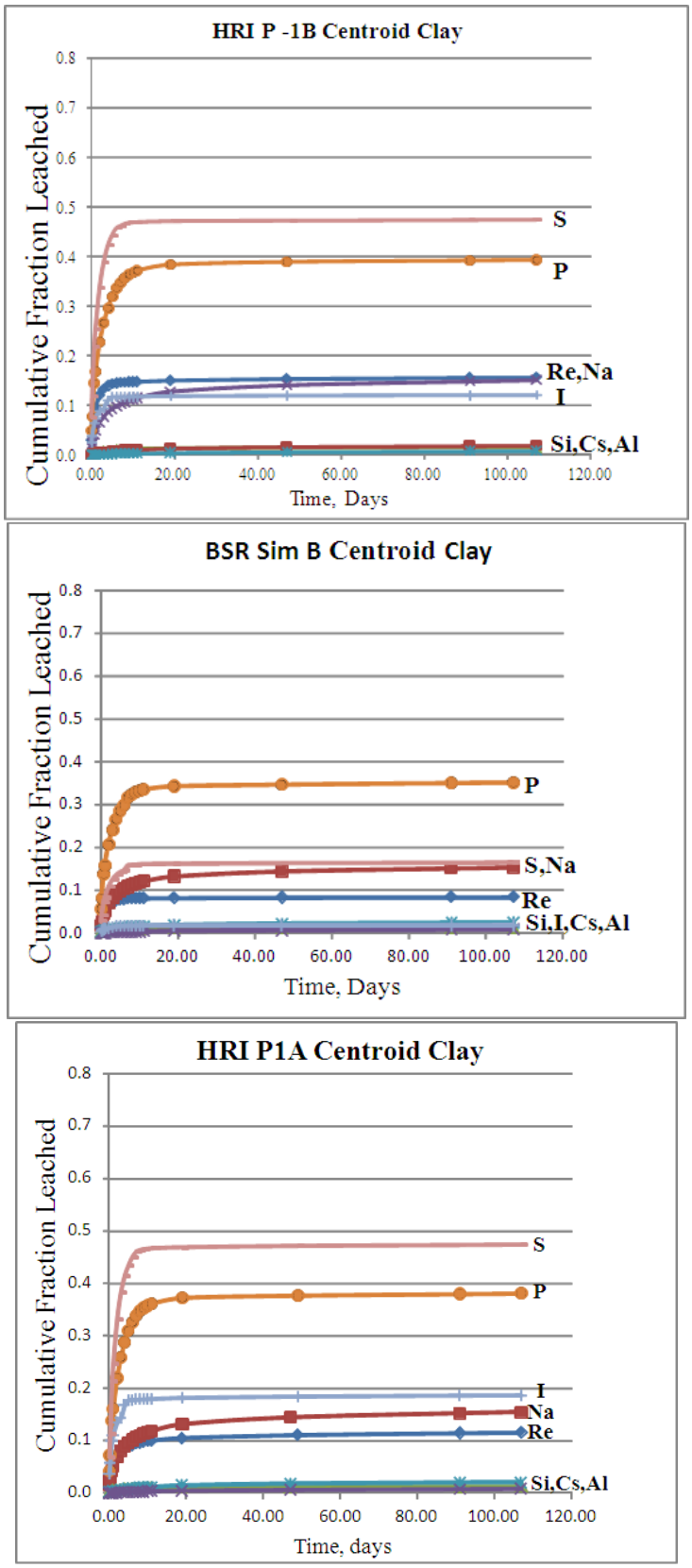

Figure 9-20. Cumulative Fraction Leached for Centroid Clay Monoliths

All of the ASTM 1308 leachate data from the initial testing on the fly ash monoliths (67-68 wt.% FBSR loading) and the latter testing on the centroid clay monoliths (42 wt.% FBSR loading) were used along with the various C_0 values and monolith densities to calculate the diffusivities. Details are given in Reference 3 and all the raw data is given in Appendix G of Reference 3. A summary of the calculated Leach Indices (LIs) for Re, Cs, I, and Na are given in Table 9-14.

Table 9-14. Summary Table of Leach Indices for Re, Cs, I, and Na from ASTM C1308 Testing

Monolith	Geopolymer Binder and FBSR Loading	Cumulative Time Days	Duplicate Diffusivities Converted to Leach Index			
			Re	Cs	I	Na
ESTD GEO- 7	Fly Ash 67% FBSR Loading	0.0833	8.37	8.87	10.9	7.77
		0.208	8.25	8.82	10.8	7.71
		0.708	8.27	9.08	10.9	7.81
		1	8.25	9.01	11.1	7.79
		2	8.23	9.17	10.8	7.86
		3	8.24	9.23	10.9	7.90
		4	8.49	9.47	11.2	8.08
		5	8.48	9.53	11.2	8.13
		6	8.45	9.56	11.2	8.10
		7	8.52	9.65	11.2	8.16
		8	8.54	9.68	11.1	8.17
		9	8.63	9.81	11.2	8.26
		10	8.76	9.95	11.3	8.35
		11	8.86	10.1	11.2	8.41
		19	9.44	10.7	11.6	8.80
		47	11.4	11.6	11.5	9.48
		77	12.4	12.1	11.4	10.0
		90	12.4	12.1	11.1	10.0
BSR SIM Module B	Fly Ash 68% BSR Loading	0.0833	8.22	9.50	9.62	7.40
		0.208	8.10	9.34	9.56	7.26
		0.708	8.19	9.57	9.79	7.33
		1	8.29	9.49	9.95	7.35
		2	8.47	9.73	10.0	7.60
		3	8.44	9.75	10.1	7.72
		4	8.78	9.97	10.4	7.81
		5	9.06	10.2	11.0	7.99
		6	9.49	10.4	11.5	8.25
		7	10.1	10.6	11.5	8.52
		8	10.7	10.8	11.8	8.77
		9	11.2	11.0	11.7	8.97
		10	11.3	11.2	12.0	9.13
		11	11.6	11.3	12.0	9.27
		19	12.0	12.0	13.3	9.89
		47	12.5	12.8	13.8	10.6
		77	13.0	13.1	13.9	11.0
		90	13.1	12.9	13.6	10.7

Table 9-14. Summary Table of Leach Indices for Re, Cs, I, and Na from ASTM C1308 Testing (Continued)

Monolith	Geopolymer Binder and FBSR Loading	Cumulative Time Days	Duplicate Diffusivities Converted to Leach Index			
			Re	Cs	I	Na
BSR SIM Module B Centroid Clay	Troy Clay 42% BSR Loading	0.0833	8.04	10.1	9.49	8.10
		0.208	8.12	10.2	9.62	8.16
		0.708	8.24	10.4	9.73	8.25
		1	8.42	10.4	10.0	8.27
		2	8.58	10.7	10.1	8.38
		3	8.89	10.7	10.8	8.44
		4	9.32	10.8	9.76	8.56
		5	9.82	10.9	10.5	8.67
		6	10.3	10.9	11.5	8.76
		7	10.8	11.0	11.4	8.87
		8	11.3	11.1	11.3	8.97
		9	11.4	11.1	11.3	9.04
		10	11.3	11.2	12.0	9.15
		11	11.3	11.3	11.9	9.16
		19	12.0	11.8	13.4	9.51
		47	12.5	12.6	14.2	10.3
		91	12.9	13.2	14.2	10.8
		107	12.8	12.6	13.5	10.7
HRI P-1B Centroid	Troy Clay 42% FBSR Loading	0.0833	7.60	10.2	7.80	8.22
		0.208	7.62	10.2	7.80	8.22
		0.708	7.69	10.3	7.96	8.29
		1	7.87	10.4	8.21	8.30
		2	8.06	10.5	8.48	8.41
		3	8.44	10.7	9.12	8.51
		4	8.87	10.7	8.06	8.60
		5	9.36	10.8	8.84	8.71
		6	9.77	10.7	11.1	8.83
		7	10.2	10.7	11.4	8.93
		8	10.5	10.9	11.6	9.01
		9	10.7	10.9	11.6	9.10
		10	10.8	10.8	11.6	9.20
		11	10.8	11.1	11.7	9.21
		19	10.9	11.6	11.8	9.45
		47	11.4	12.4	12.3	10.2
		91	11.8	13.0	12.7	10.7
		107	12.1	12.5	13.0	10.7

Table 9-14. Summary Table of Leach Indices for Re, Cs, I, and Na from ASTM C1308 Testing (Continued)

Monolith	Geopolymer Binder and FBSR Loading	Cumulative Time Days	Duplicate Diffusivities Converted to Leach Index			
			Re	Cs	I	Na
HRI P-1A Centroid Clay	Troy Clay 42% FBSR Loading	0.0833	8.32	10.3	7.42	8.21
		0.208	8.14	10.2	7.42	8.13
		0.708	8.17	10.4	7.53	8.25
		1	8.33	10.0	8.03	8.25
		2	8.41	10.7	8.10	8.36
		3	8.57	10.8	8.74	8.47
		4	8.79	10.8	7.69	8.57
		5	8.98	10.9	8.44	8.68
		6	9.21	10.9	10.5	8.79
		7	9.40	11.0	10.5	8.90
		8	9.56	11.1	10.9	9.00
		9	9.77	11.2	10.9	9.07
		10	9.87	11.3	10.9	9.17
		11	10.0	11.3	10.9	9.18
		19	10.2	11.8	11.0	9.44
		47	11.0	12.6	11.6	10.2
		91	11.3	13.1	12.0	10.7
		107	11.6	12.9	12.2	10.7

The leach indices for Re and Na are plotted in Figure 9-21. The data in Figure 9-21a show that all the Re leach indices are ≥9 after ~5 days for both the fly ash based and the clay based geopolymer monoliths. The ESTD GEO-7 fly ash monolith, which contained excess Na_2O likely as NaOH eventually goes to ≥9 Re release within ~19 days. The data in Figure 9-21b show that the Na leach indices are >7.75 even after 2 hours of leaching for all the geopolymers whether they are fly ash or clay based geopolymers. The formulations that meet Re >9 and Na >6 are the preferred formulations to meet the performance criteria for the Hanford IDF [156]. More testing with clay based geopolymers at higher FBSR loadings are needed to make a final comparison between using clay based versus fly ash based geopolymers.

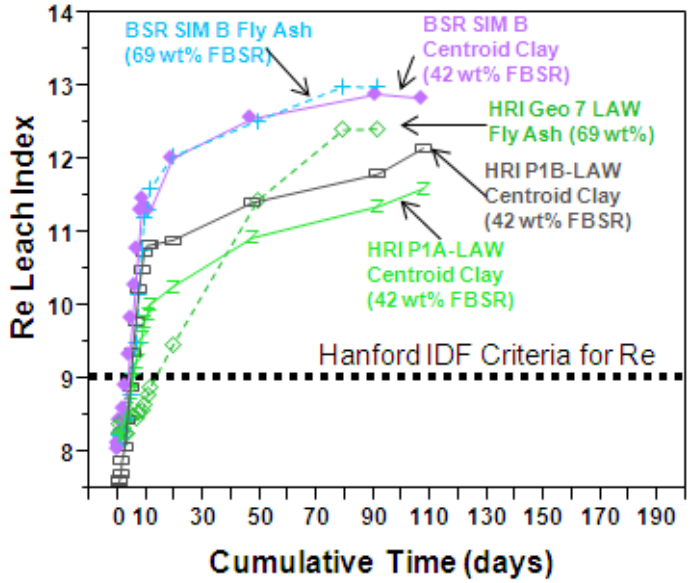

(a)

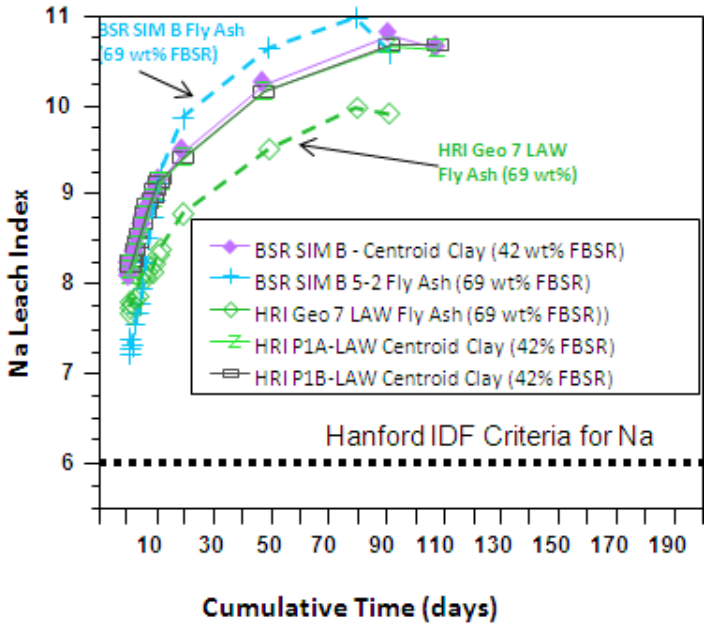

(b)

Figure 9-21. Log Diffusivity Plots for Re in ASTM C1308 Testing

Note: Fly ash based geopolymers are fitted with the dashed line and clay based geopolymers are fit with the solid lines.

9.1.2.5 *Single Pass Flow Through (SPFT) and Pressure Unsaturated Flor (PUF) Testing (Monolith Product)*

Only the non-radioactive monoliths made from the Rassat LAW Blend Simulant were tested by SPFT. These were the ESTD P-1B FBSR product monoliths and the BSR FBSR product monoliths made with the NaOH rich Geo-7 misformulation. Never-the-less the monoliths performed fairly well with release rates 2-3 times lower from the crushed monolith than from the

granular product. This result, indicates that the macroencapuslation may still be effective even though the monolithic product has been crushed in order to perform the SPFT testing.

The pH of the SPFT effluents was followed through the entirety of the experiment. Figure 9-22 shows the pH for the P-1B engineering scale ESTD Rassat LAW blend and the BSR Rassat LAW blend granular and monolithic samples. There is a marked increase in the pH at short time periods for the monolithic materials where the BSR monolith (BSRM) maximum pH was 10.2 at 10 mL/d flow rates. On the other hand, the maximum pH observed at the 10 mL/d flow rate for the BSR granular (BSRG) was 9.2, which is below the pH measured from the blank. The P-1B engineering-scale and BSR Rassat Simulant granular product pH values track each other and the monolith pH values track each other. For the other flow rates, the increase in the pH from the monolith is higher than the increase observed from the corresponding granular material. This increase in the pH of the solution is attributed to the release of OH^- from unreacted sodium hydroxide that is used as an activator in the production of the geopolymer.[213] Regardless, at longer reaction periods, the effluent was successfully buffered by the inlet solution. A similar trend is observed for the P-1B samples. Measured pH values are given in Reference 132.

The SPFT data for the monoliths are shown as a function of flow rate in Figure 9-23 and Figure 9-24 for the elements Si, Na, Al, Cs, I, and Re. For comparison, the granular SPFT data for the same FBSR products (ESTD and BSR scale) are given in Figure 8-21 and Figure 8-22. One way to compare the granular SPFT data to the monolith SPFT data from Figure 8-21 and Figure 8-22 with the data in Figure 9-23 and Figure 9-24 is to plot the dissolution rate for each element against the imposed flow rate divided by the surface area. The SPFT data is fit with regression lines with equations of the type $y=a(1-e^{-xb})$ in each graph for the granular and monolithic FBSR products. For Si, Al, and Na, this is shown in Figure 9-25 and for Cs, I, and Re in Figure 9-26. In each plot, one of the lines corresponds to the grouping of the granular materials and the other corresponds to the grouping of the monolithic materials. It is seen from Figure 9-25 that release values from the monoliths are 3-5 times smaller than the corresponding granular material. Normalized release rates of Cs, I, Re, and Tc as a function of *q/S* are seen in Figure 9-26. The release of Re and I show normalized release rates at the higher flow rates that are up to three orders of magnitude higher than release rates observed at the lower flow rates. Though one would expect rates to be lower at the lower flow rates because of the buildup of constituents in the contacting solution, this difference in releases, compared to similar ratios seen for the NAS backbone, seems quite high. An explanation for this is most likely that the steady-state concentration used to calculate the rates is an underestimation resulting from experiments that were too short in duration to observe the delayed growth in Re and I releases observed at the higher flow rates. The data also indicate that for I and Re there is no difference between the behavior of the granular and monolithic materials across the *q/S* range studied. Since these monoliths were misformulated, no further conclusions can be made about these results.

From the SPFT data collected, release rate calculations in dilute conditions were performed from flow rates at 200 and 300 mL/d. A summary of the rates comparing the non-radioactive ESTD and BSR monoliths to their respective granular products can be seen in Table 9-15. In all cases, the monolith release rates are lower than that from the granular products.

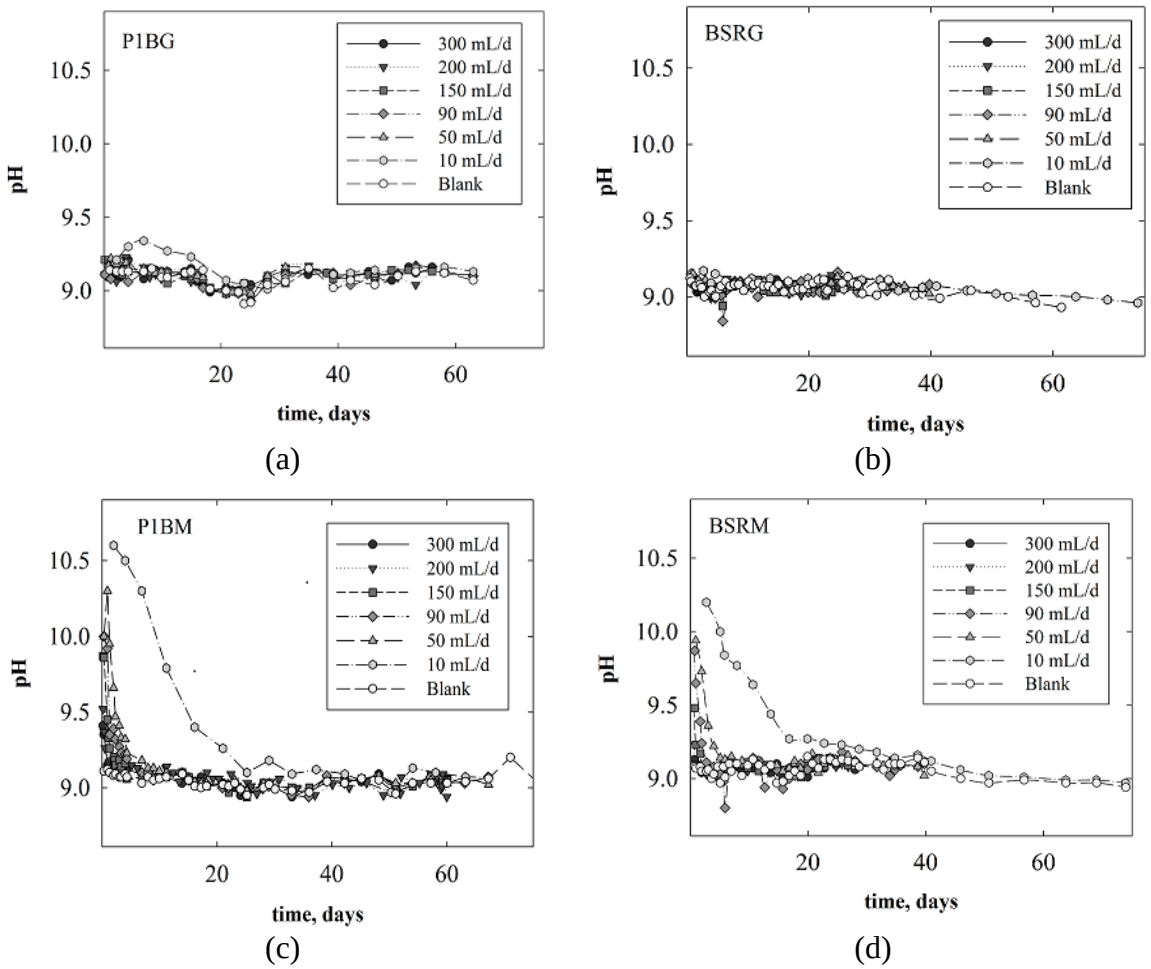

Figure 9-22. The pH of the effluent solution from the four non-radioactive test materials: (a) is the engineering scale ESTD P-1B Rassat LAW blend granular product, (b) is the bench-scale BSR Rassat LAW blend granular product, (c) is the GEO-7 monolith made with the P-1B granular Rassat LAW blend, and (d) is the GEO-7 monolith made with the BSR Rassat LAW blend.[132]

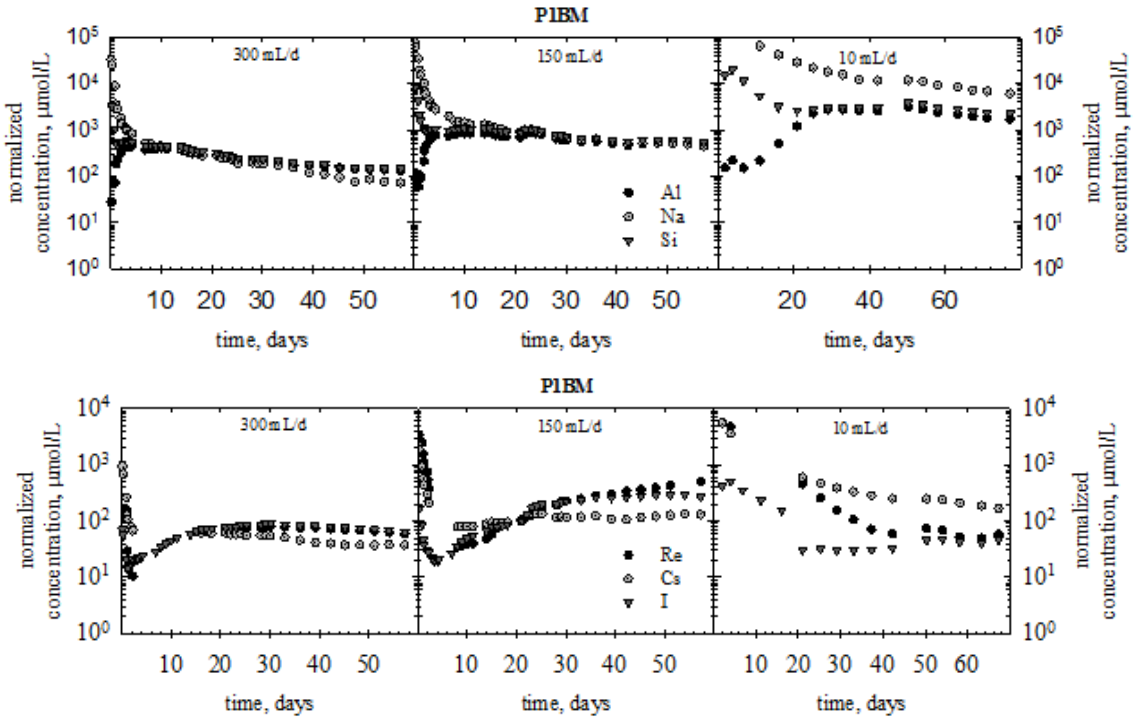

Figure 9-23. Normalized concentrations of Al, Na, and Si versus time for the P-1BM (top) materials. Normalized concentrations of Re, Cs, and I versus time for the P-1BM (bottom) materials. The values are not corrected for background. Error from ICP-AES analysis is 10%. Compare to data for granular products in Figure 8-21.[132]

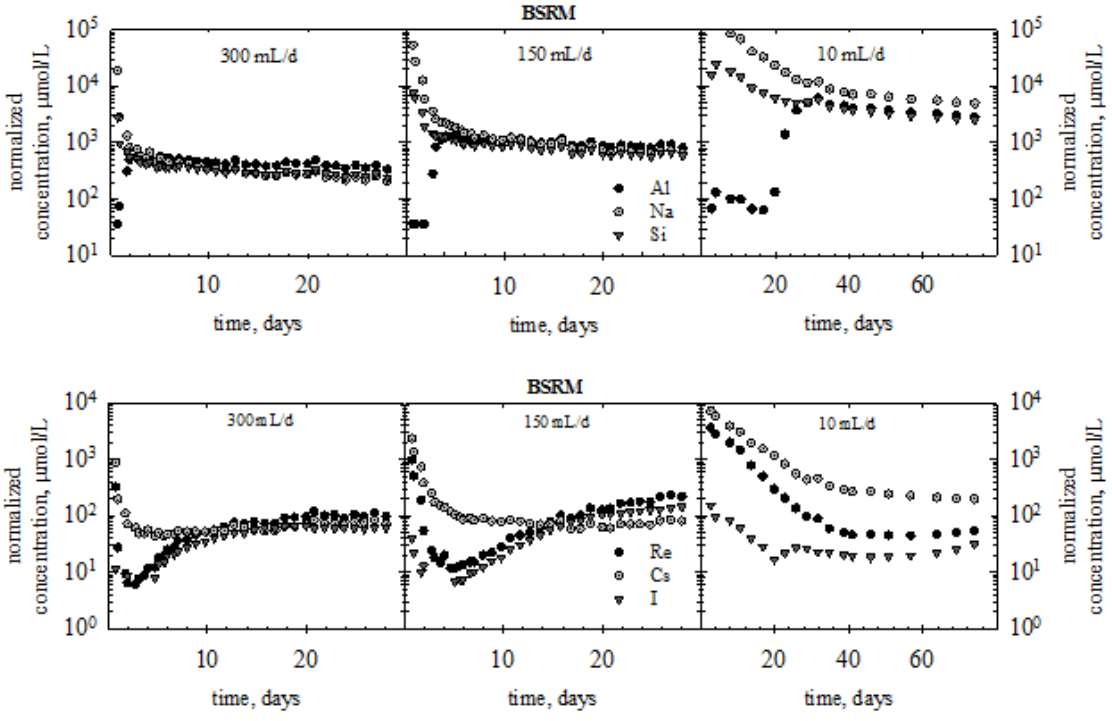

Figure 9-24. Normalized concentrations of Al, Na, and Si versus time for the BSRM (top) materials. Normalized concentrations of Re, Cs, and I versus time for the BSRM (bottom) materials. The values are not corrected for background. Error from ICP-AES analysis is 10%. Compare to data for granular products in Figure 8-22.[132]

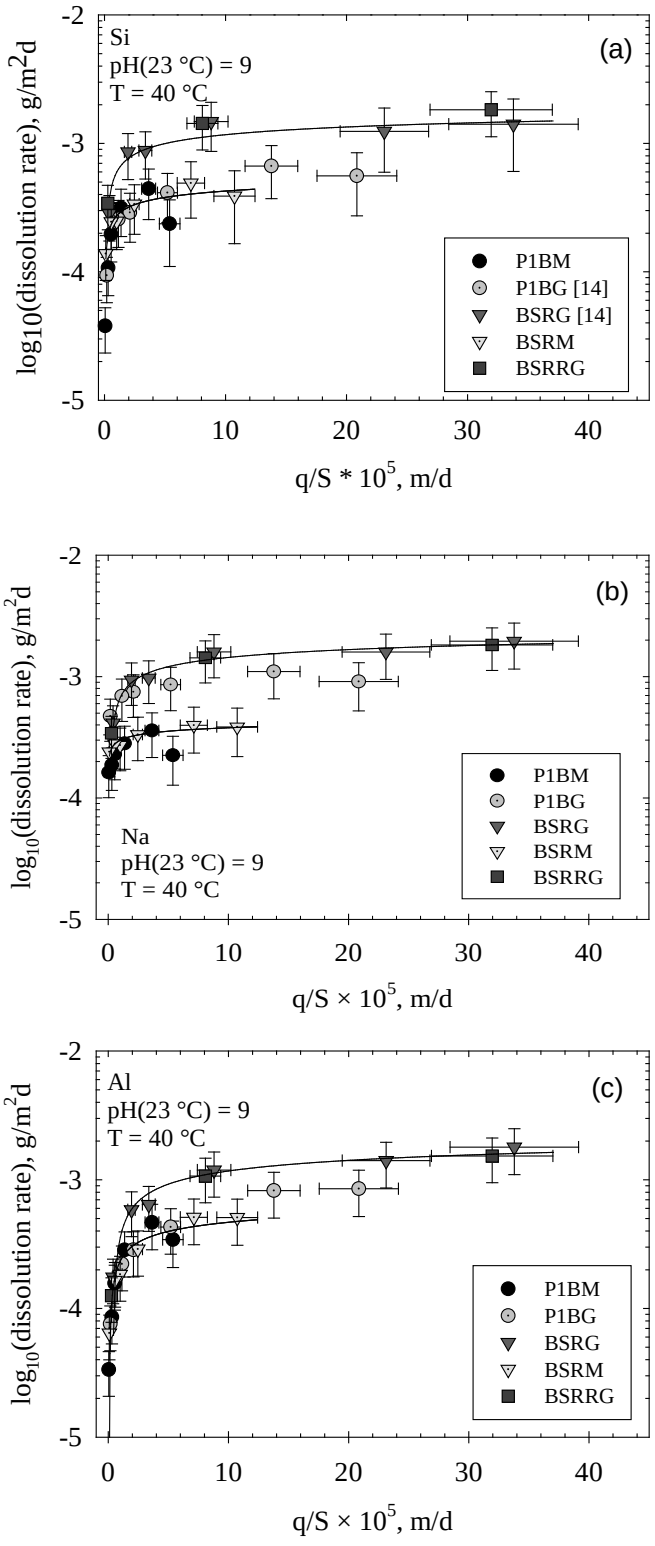

Figure 9-25. Release rates (g/m^2d) as a function of the ratio of the flow rate (q) to the sample surface (S) for (a) Si, (b) Na, and (c) Al.[132]

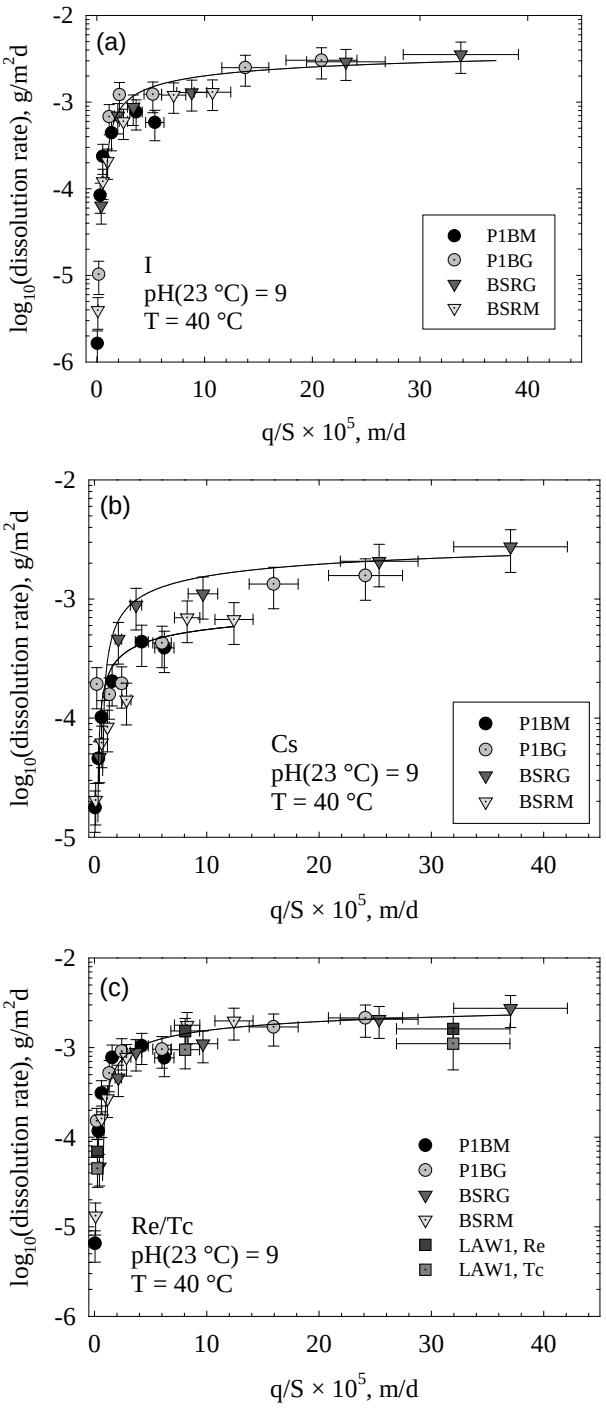

Figure 9-26. Release rates (g/m^{2}d) as a function of the ratio of the flow rate (q) to the sample surface (S) for (a) I, (b) Cs, and (c) Re/Tc.[132]

Table 9-15. Release Rates derived from SPFT Testing for FBSR Engineering Scale and Bench Scale Rassat Simiulant Monoliths at 40°C and pH 9 Compared to Previous Testing on AN-107 at 90°C and pH 9.

	ESTD Engineering Scale P-1B Rassat Blend Simulant at 40°C [132]		**BSR Bench-ScaleBSR Rassat Blend Simulant at 40°C** [132]	
	Granular	**Monolith**	**Granular**	**Monolith**
Al	$8.4\pm2.3 \times 10^{-4}$	$4.0\pm1.1 \times 10^{-4}$	$16\pm4.3 \times 10^{-4}$	$5.1\pm1.4 \times 10^{-4}$
Na	$10\pm2.9 \times 10^{-4}$	$2.9\pm0.8 \times 10^{-4}$	$18\pm5.0 \times 10^{-4}$	$3.9\pm1.2 \times 10^{-4}$
Si	$6.1\pm2.1 \times 10^{-4}$	$3.4\pm. 1.1 \times 10^{-4}$	$13\pm5.0 \times 10^{-4}$	$4.4\pm1.6 \times 10^{-4}$
Re	$19\pm5.3 \times 10^{-4}$	$9.1\pm2.4 \times 10^{-4}$	$24\pm6.5 \times 10^{-4}$	$19\pm5.1 \times 10^{-4}$
I	$28\pm7.6 \times 10^{-4}$	$6.8\pm1.8 \times 10^{-4}$	$32\pm8.8 \times 10^{-4}$	$13\pm3.4 \times 10^{-4}$
Cs	$28\pm7.5 \times 10^{-4}$	$4.1\pm1.1 \times 10^{-4}$	$7.5\pm2.0 \times 10^{-4}$	$6.9\pm1.9 \times 10^{-4}$
S	NA	NA	NA	NA

The PUF test was also performed on the P-1B ESTD Rassat LAW Blend. The data for the monolith and granular material are shown side by side in Figure 9-27. Data for the granular alone is given in Figure 8-24. Release rates for the granular product were calculated to be on the order of 10^{-6} g/(m^2 d) for Al, Si and Cs, 5×10^{-5} g/(m^2 d) for Na, and 10^{-5} g/(m^2 d) for Re and I, while for the monolith material values for Al and Si are on the order of 10^{-5} g/(m^2 d), Na is 10^{-4} g/(m^2 d), Re is 10^{-3} g/(m^2 d), and I is 5×10^{-3} g/(m^2 d). However, further studies are necessary on clay based monoliths that are correctly formulated.

As with the granular FBSR product, the monolith material, was analyzed by XRD data with depth in the PUF column. The monolith trends are shown in Figure 9-28 for comparison with the data given in Figure 8-26 for the granular FBSR P-1B product. The first 3 subsamples showed only minor deviations from the original material given as sample number "0" (Figure 9-28). There was a small increase in nepheline and a small decrease in the relative amount of an amorphous/unidentified material. This is not inconstistent with a geopolymer being primarily an amorphous NAS binder. SEM micrographs have also shown the existence of NAS platelets but it unclear what phase this may be.[131] Subsample number 1 contained a high proportion of sapphire (corundum from the XRD analysis) left over from column packing. When the sapphire contribution was removed from the subsample and the results were rescaled, the percentages of the minerals were consistent with subsample 2. However, the small fluctuations in nosean and quartz are most likely an artifact of the sapphire impurity and thus affect the quantitative results of this subsample. The major change in composition came between samples numbers 3 and 8. The amount of amorphous/unidentified material dropped by a factor of two (from 74% to 38%) with a corresponding rise in the content of zeolite P1 (gismondine structure), which had not been detected in subsamples 1 to 3. Nosean content dropped slightly but was offset in part by the appearance of a phase with the same structure but a smaller lattice parameter (in this case, assigned to sodalite). Nepheline increased slightly from around 16%. The last two samples along the column depth (14 and 15) had a similar composition to sample number 8. The amount of nosean plus sodalite increased slightly, but this appears to be barely significant. Sample number 15 was also compromised by the presence of 15% sapphire, which has been removed from Figure

9-28. The presence of zeolite P1 in fly ashed based geopolymers is also consistent with what it known about the reactivity of fly ash in geopolymers (see discussion in Appendix G regarding secondary phases forming in fly ash geopolymers and why SRNL switched to clay based geopolymers). Moreover, since the P-1B (ESTD Rassat LAW) monoliths were misformulated no further conclusions can be made about these results.

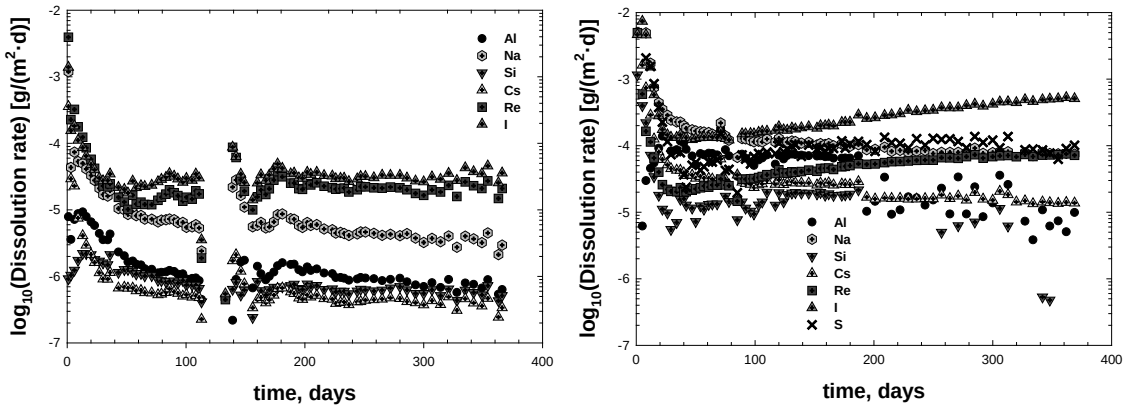

Figure 9-27. The normalized release rates for various elements of the a) P-1B granular material and b) P-1B monolith material as a function of time during the 1-year PUF test. Errors are typically on the order of 40% and are not shown to make the graph clearer.[131]

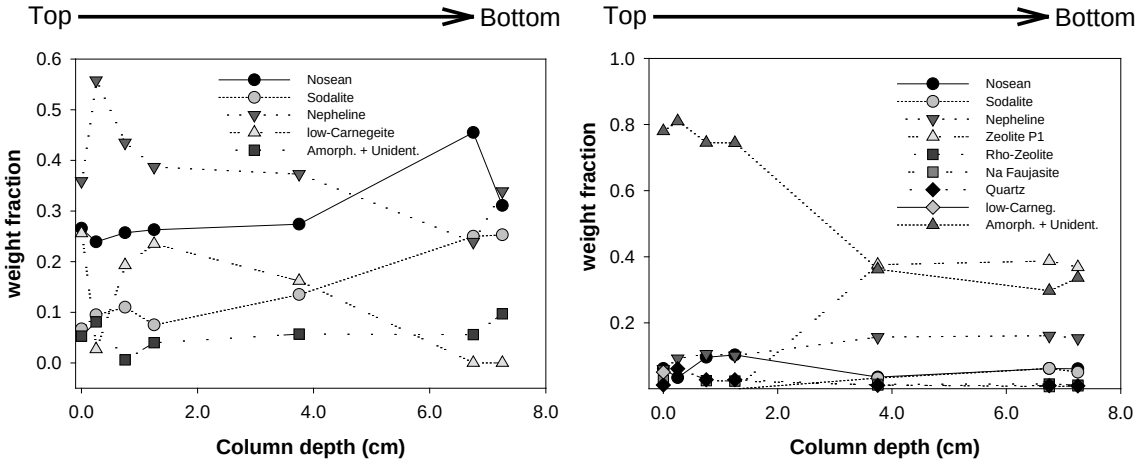

Figure 9-28. The weight fraction of mineral phases identified from subsamples of the PUF test for the P-1B granular material (left) and b) the P-1B monolith material using XRD as a function of depth in the PUF column. Each subsample uses roughly 0.5 cm in depth for analysis. The sample at zero gives the composition of an unaltered starting material.[131]

9.1.2.6 *Toxcity Characteristic Leaching Procedure (TCLP) (Monolith Testing)*

Table 8-47 contains the TCLP results for the Module B granular products for all sets of testing with the Rassat material. For comparison, results from granular product reported in Reference 123 for material produced from the HRI/TTT engineering-scale tests and for products from the SAIC-STAR facility are given. The results from the SAIC-STAR facility are provided since they had no IOC versus the HRI/TTT ESTD runs with IOC. The table also includes TCLP analysis performed on the Module B samples by PNNL, including the radioactive Module B granules. Green shaded elements were shimmed in at 10X and yellow shaded elements were shimmed in at 100X the concentrations given in the Rassat simulant recipe (see Table 8-2). All elements failing TCLP at the UTS limits are shown in bold italic print in Table 9-16 for leaching of the monoliths. These values can be compared to the TCLP response of the corresponding granular FBSR products which appears in Table 8-47.

Analytes detected but at concentrations too low to determine quantitatively have been flagged with the "J" qualifier. As discussed with the granular products, the engineering-scale ESTD samples were found to be above the UTS limits for Sb and Cd by the South Carolina GEL laboratory but below the UTS by the PNNL laboratory.[iii] In the salt solution used to make these samples, these elements had been shimmed into the HRI/TTT simulant at 10X the concentration anticipated. During the engineering-scale experiments, the excess precipitates that were formed when the solubility for these RCRA elements were exceeded, were not filtered out as was done in the BSR simulants when the precipitates were observed (see Section 8.1.1.2). Recall that the Sb precipitated as insoluble sodium antimony (+5) hydroxide (see Section 8.1.1.2) in the BSR simulants and was removed through filtration. The BSR granular products all passed TCLP below the UTS for Sb and Cd as these species are below their solubility limit in the granular FBSR products. Since antimony will not be present in the excessive amounts in LAW that they were in the engineering-scale ESTD TCLP results, these observations are considered not applicable.

Table 9-16 contains the TCLP results for the monolith prepared with the engineering scale P-1B LAW and the Module B simulant BSR granular product. In monolith testing of these geopolymers, the Sb and Cd are still released at greater than the UTS for the ESTD samples, i.e. only when they were shimmed into the FBSR product in excess of their solubility limit. When the granular sample was tested after monolithing, the chromium release was reduced by greater than 10x and is now 10x below the UTS limit (compare Table 8-47 to Table 9-16). Therefore, monolithing appears to help minimize Cr release in samples that were not processed with the IOC, where the IOC would have provided a host mineral phase for these species. This demonstrates that the monolith does encapsulate the FBSR granules and slow down release of COCs.

[iii] As with the granular FBSR products, PNNL performed the TCLP in Washington at the Coastal Biogeochemistry Group at the Marine Science Laboratory (MSL). The MSL maintains national accreditation for its analytical services work with NTI (formerly called NELAC) (http://www.nelac-institute.org/index.php). MSL's accreditation is through the State of New Jersey, Department of Environmental Protection (Laboratory Certification ID# WA004). Among the analyses that MSL has accreditation for is the TCLP of wastes and soils for the analysis of metals.

Table 9-16. TCLP Results for Monoliths Prepared with Simulant Rassat FBSR Product and Fly Ash

Constituent	ESTD Simulant Monolith GEO-7 (67% FBSR loading with Fly Ash)		BSR Simulant Module B Monolith GEO-7 (68% FBSR loading with Fly Ash)		BSR Radioactive Module B Monolith (42% FBSR loading with Kaolin)	BSR Radioactive Module B Monolith (65% FBSR loading with Kaolin)	Reporting Limit (RI)	UTS 40CFR 268.48 (Non-waste water standard)
	SRNL	PNNL	SRNL	PNNL	SRNL	SRNL		
	(mg/L)	(mg/L)	(mg/L)	(mg/L)	(mg/L)	(mg/L)	(mg/L)	(mg/L)
Sb	***2.32***	0.88 1.13	<MDL	0.0165 0.019	0.046[J]	0.0298 <MDL	0.1	1.15
As	3.07	1.89 2.05	2.48	2.16 2.32	0.00117 <MDL	0.059[J]	0.15	5
Ba	0.601	0.081 0.091	<MDL	0.132 0.179	0.278	0.257	0.05	21
Cd	***0.134***	0.009 0.027	<MDL	0.0005 0.0006	<MDL	0.00126 <MDL	0.05	0.11
Cr	0.112	0.035 0.056	<MDL	0.055 0.075	0.106	0.256	0.05	0.6
Pb	0.703	0.135 0.171	0.0473[J]	0.109 0.189	0.052[J]	0.0697[J]	0.1	0.75
Se	0.692	0.99 1.20	<MDL	0.443 0.473	0.207[J]	0.263[J]	0.15	5.7
Ag	<MDL	<MDL	0.0133[J]	0.0003 0.0004	0.00041 <MDL	0.00907 <MDL	0.05	0.14
Hg	NM	<MDL	<MDL	0.00005	<MDL	<MDL	0.002	0.025
Ni	0.0845	0.023 0.033	<MDL	0.0105 0.0139	0.00598 <MDL	0.0142 <MDL	0.05	11
Tl	<MDL	NM	<MDL	NM	<MDL	0.0067 <MDL	0.2	0.2
Zn	0.0694	0.024 0.113	<MDL	0.08 0.0989	0.0277 <MDL	0.111	0.1	4.3

Green shaded boxes were shimmed 10X and yellow shaded were shimmed 100X. MDL is the Method Detection Limit; NM is not measured. J indicates a detected value that was below quantitative limit. Where duplicate measurements were different, both values are reported.

9.1.2.7 *Compression Testing*

One replicate from each of the six batches of geopolymer monoliths prepared in Section 9.1.1 were tested for compressive strength at the URS 717-5N Civil Test Laboratory at SRS after 28 days of curing.[3] The remainder of the samples were either transferred to PNNL for further durability testing or reserved for leach testing.

Table 9-17 provides data from the compressive strength measurements of the samples representing each of the six batches produced. The geopolymers made with fly-ash had an average strength of 905.1 psi.

Table 9-17. Compressive Strength of the ESTD P-1B GEO-7 Monoliths Made with Fly Ash After 28 Days of Curing

ID	ESTD Rassat Simulant Monolith GEO-7 Compressive Strength (psi)
P-1B GEO-7 1-1	946.8
P-1B GEO-7 2-1	846.6
P-1B GEO-7 3-1	899.5
P-1B GEO-7 4-1	957.1
P-1B GEO-7 5-1	681.6
P-1B GEO-7 6-1	1099.4
Average	905.1
RSD	15.3%

Geopolymers prepared in Section 9.1.1 were tested for compressive strength at SRNL after 28 days of curing.[3] The first two samples were demolded, the ends were ground flat using 240 grit silicon carbide paper, and tested. Both of the samples failed before the instrument began recording data —1000 psi. It was noted that the samples were moist. The remainder of the samples identified for compression testing were demolded and stored in closed, zip-top bags for an additional seven days. Results of the compression tests are given in Table 9-18. Note that the average compressive strength was 1134 psi considering the two failed samples are counted as 0 psi—visual observation of the instantaneous compressive stress for both samples was >300 psi at the time of failure. Figure 9-29 is a representative compressive stress versus time plot for geopolymers made with steam reformed product. Jaggedness of the curve was due to the frequency of data sampling and the use of rubber end caps. It does not affect the test or the strength values.

Table 9-18. Compression Testing of Simulant BSR Module B GEO-7 Monolith After 28 Days Curing

Sample ID	Monolith GEO-7 Curing History	BSR Rassat Simulant Monolith GEO-7 Compressive Strength (psi)
Sim Mod B GEO-7 1-1	28 days in sealed mold; samples still moist when demolded	>300
Sim Mod B GEO-7 2-1		
Sim Mod B GEO-7 1-2	cured an additional 7 days out of mold but in a sealed zip top bag for more access to air/drying	750
Sim Mod B GEO-7 3-1		1098
Sim Mod B GEO-7 4-1		1404
Sim Mod B GEO-7 5-1		3550
Average	35 day cured samples	1700
RSD		74.2%

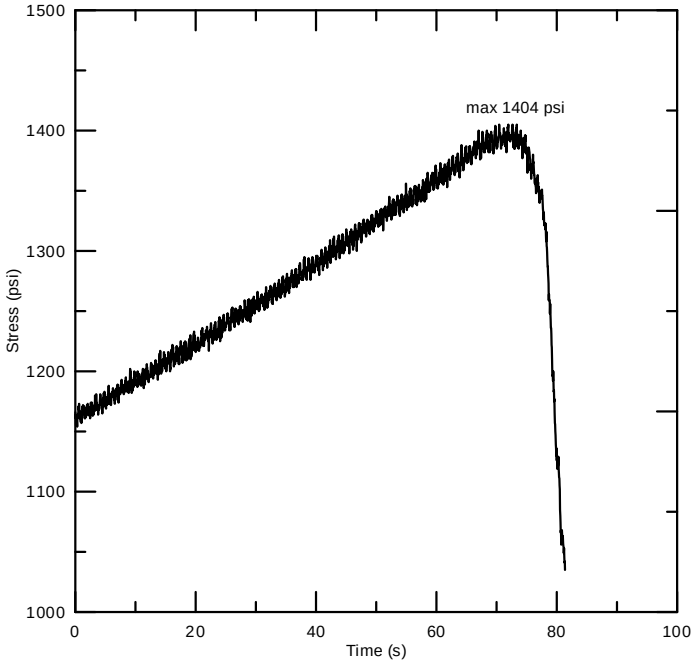

Figure 9-29. Typical Stress versus Time Plot for Geopolymers Made with Fly Ash and FBSR Product; Plot is for Simulant Module B GEO-7 4-1

Radioactive Module B (Rassat Blend) geopolymers prepared in Section 9.1.1.4 were also tested for compressive strength at SRNL after 28 days of curing.[3] Based on the observed behavior of freshly demolded samples in Section 9.1.2.1, the samples were demolded, and stored in closed, zip-top bags for an additional seven days. The ends were ground flat using 240 grit silicon carbide paper and tested. The first replicate of the 42%waste loading sample was too elastic and the steel end caps contacted, causing the test to be aborted. Since the equipment did not record a break, the data was not saved. It was noted that the stress on the display had exceeded 1500 psi prior to the excursion to much higher stresses associated with steel on steel. When the sample was removed from the equipment, it was apparent that the sample had failed, but the failure was not recorded by the equipment. The second sample of the 42%

waste loading was tested, Figure 9-30. Again the sample was elastic enough that the steel end caps met, however, the data was recoverable and the plot was annotated with the assumed break point and instant when the end caps met. The 65% waste loading samples was more brittle due to the reduced volume of geopolymer matrix and performed comparable to the monoliths prepared with either ESTD or BSR simulant granular FBSR product. The 65% waste loading sample, Figure 9-30, resulted in a compressive strength of 757 psi.

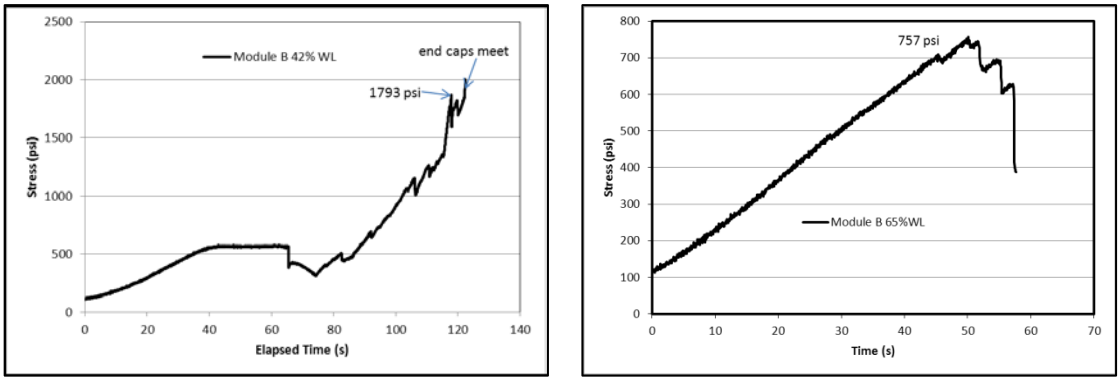

42% WL 65% WL

Figure 9-30. Compressive Stress/Time Plots for Radioactive Module B Geopolymers Prepared with Clay

An overall comparison can be made between compressive strengths of fly ash and clay monoliths using data presented above from this study, previous work on ESTD monoliths (Reference 123), and monoliths prepared with ESTD WTP-SW simulants (Reference 127). These data are shown in Table 9-19 with the first four rows of data from Reference 123 and the last row of data from Reference 127. Examination of the ESTD monoliths in the first five rows indicates that all of the 65% waste loading monoliths regardless of size and curing time have compressive strengths of about 1,000 psi or higher. Lowering the waste loading in the two Troy Clay monoliths in the sixth and seventh row of data shows a noticeable increase in compressive strength up to the range of 4600 to 5800 psi. This same trend of increased compressive strength with lower waste loading is noticed in comparing the Simulant Module B 65% waste loading GEO-7 fly ash monolith (avg. 1700 psi) with the Simulant Module B 42% waste loading centroid clay monolith (3300 psi). The final row of Table 9-19 shows that both the BSR Simulant Module B granular material and the BSR Simulant Module A granular material from the previous study when fabricated into the 42% waste loading centroid clay monolith give very high compressive strengths in the range of 3300 to 4356 psi. In general, the clay based geopolymers at equivalent FBSR loadings give a higher compressive strength than the geopolymers made with fly ash.

Table 9-19. Compressive Strengths of Geopolymer Monoliths Made with Fly Ash Vs. Clay

Size	Matrix	FBSR Loading (wt%)	Compressive Strength (psi)	Cure Time (days)	Bulk Density (g/cc)
Module B Engineering Scale					
3" x 6" (P-1B GEO-7)	Fly Ash	65	2500	14	1.90
3" x 6" (P-1B GEO-1)	Troy Clay	67	1690	14	1.85
6" x 12" (P-1B GEO-7)	Fly Ash	65	1920	18	NM
6" x 12" (P-1B GEO-1)	Troy Clay	67	1530	14	1.82
1" x 2" (P-1B GEO-7) **(See Table 9-17)**	Fly Ash	67	681-1099 905 (average of 6)	28	NM
1" x 2" (P-1B Centroid)	Troy Clay	42	4652	7	1.71
1" x 2" (P-1A Centroid)	Troy Clay	42	5844	7	1.72
Module B Bench-Scale Reformer (BSR) Simulant					
1" x 2" (SIM B GEO-7) (See Table 9-18)	Fly Ash	68	750-3550 1700 (average of 4)	29-35	1.88
1" x 2" (SIM B Centroid)	Troy Clay	42	3300	7	1.68
Module A Bench-Scale Reformer (BSR) Simulant (WTP-SW)					
1" x 2" (SIM A Centroid)	Troy Clay	42	4356	7	1.75

NM – Not measured

10.0 Disposal Volumes and WL

One of the attributes of any waste form for Hanford LAW should be to maximize the waste loading in the waste form as measured by the Na_2O content attributed to the waste (see discussion in Section 4.0). Maximizing the Na_2O content minimizes the disposal volumes for glass and ceramic waste forms, including FBSR mineral waste forms containerized in HIC's and/or as monoliths. The only glass formulation that does not maximize Na_2O loading is Envelope B glasses, i.e. made from AZ-101/AZ-102, because the waste loading is driven by the high sulfate in the Envelope B type wastes and not the Na_2O content. Cast stone waste forms maximize disposal volumes as not much Na_2O is accommodated in the cementitious formulations.

The disposal volumes for FBSR products in HIC's and/or as monoliths were compared to the disposal volumes for LAW glass and for the baseline Cast Stone for a 5M sodium LAW. The results are shown graphically in Figure 10-1 and tabulated in Table 10-1. The details of the calculations can be found in Appendix H. Figure 10-1 and Table 10-1 demonstrates that the FBSR waste forms (HIC's or monoliths) are comparable in lowering waste disposal volume to glass waste forms compared to Cast Stone. The HIC offers the largest Na_2O waste loading of any of the FBSR options with Na_2O waste loadings in the range of > 20 wt.%. High Na_2O waste loadings translate into more rapid processing of LAW. Other monolith options shown in Figure 10-1 have lower Na_2O waste loadings due to dilution by the monolithic binder but still provide for a disposal volume decrease. These binders include geopolymers (GEO), two high Al_2O_3 containing cements, and OPC. These calculations were performed assuming no compaction of the FBSR granular product. Even minimal compaction would give the granular FBSR product disposed of in a HIC the highest Na_2O loading and lowest disposal volume over glass and Cast Stone.

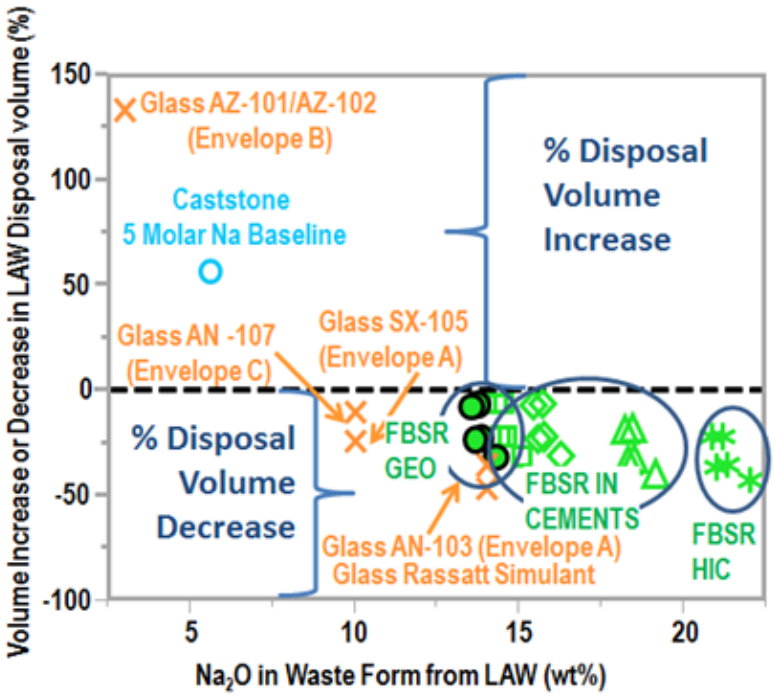

Figure 10-1. Volumes of waste form produced per volume of liquid LAW. All waste forms below the dashed line at 1.0 create a disposal volume reduction while those above the 1.0 create a disposal volume increase. FBSR waste forms are comparable to glass waste forms.

Table 10-1. Relative Volume Increases and Decreases for Glass, FBSR products (granular and monolith), and Cast Stone

Sample Type	Waste Type	Na_2O (wt%) in Final Waste Form	Volume (gallons WF/gallons LAW)	Volume Reduction (negative) vs. Volume Increase (positive)
FBSR HIC	AN-107 (Envelope C)	20.87	0.776	-22
	Rassatt Simulant (BSR)	21.03	0.642	-36
	SX-105 (Envelope A)	21.3	0.648	-35
	AN-103 (Envelope A)	21.16	0.781	-22
	AZ-101/AZ-102 (Envelope B)	21.98	0.575	-43
FBSR GEOPOLYMER	AN-107 (Envelope C)	13.57	0.921	-8
	Rassatt Simulant (rad centroid BSR)	13.67	0.762	-24
	SX-105 (Envelope A)	13.85	0.769	-23
	AN-103 (Envelope A)	13.75	0.927	-7
	AZ-101/AZ-102 (Envelope B)	14.29	0.682	-32
FBSR OPC	AN-107 (Envelope C)	18.16	0.812	-19
	Rassatt Simulant (HRI/TTT ESTD)	18.3	0.672	-33
	SX-105 (Envelope A)	18.53	0.678	-32
	AN-103 (Envelope A)	18.41	0.817	-18
	AZ-101/AZ-102 (Envelope B)	19.12	0.602	-40
FBSR Fondu (High Al Cement)	AN-107 (Envelope C)	14.32	0.937	-6
	Rassatt Simulant (HRI/TTT ESTD)	14.43	0.775	-22
	SX-105 (Envelope A)	14.61	0.783	-22
	AN-103 (Envelope A)	14.52	0.943	-6
	AZ-101/AZ-102 (Envelope B)	15.08	0.694	-31
FBSR Secar 71 (High Al Cement)	AN -107 (Envelope C)	15.44	0.932	-7
	Rassatt Simulant (HRI/TTT ESTD)	15.56	0.771	-23
	SX-105 (Envelope A)	15.76	0.778	-22
	AN-103 (Envelope A)	15.66	0.938	-6
	AZ-101/AZ-102 (Envelope B)	16.27	0.69	-31
LAW GLASS	AN-107 (Envelope C)	10	0.896	-10
	Rassatt Simulant	14	0.534	-47
	SX-105 (Envelope A)	10	0.764	-24
	AN-103 (Envelope A)	14	0.653	-35
	AZ-101/AZ-102 (Envelope B)	3	2.33	133
Cast Stone Baseline	5 Molar Na Caststone	5.63	1.56	56

11.0 Durability Mechanisms: Mineral (Ceramic) vs. Vitreous Waste Forms

In mineral waste forms, as in glass, the molecular structure and atomic bonding of COCs controls dissolution (contaminant release) by establishing the distribution of ion exchange sites, hydrolysis sites, and the access of water to those sites.[214] Mineral waste forms, like glass, are relatively insoluble which is why minerals and natural glasses formed by volcanic eruptions persist in nature for millions of years. Minerals and glasses dissolve by an affinity controlled reaction and should not be modeled using a matrix solubility limited-release model[4] for soluble materials as done recently in the Hanford Environmental Impact Statement (EIS).[215]

Minerals possess short range order (SRO), medium range order (MRO), and long range order (LRO). The SRO has a radius of influence ~1.6-3Å around a central atom of first nearest neighboring atoms, i.e. polyhedra such as tetrahedral and octahedral structural units.[216] Medium-range order has a radius of influence ~3-6 Å, which encompasses second- and third-nearest neighbor environments around a central atom, and the long range order extends beyond third-neighbor environments (>6 Å) and gives the crystalline mineral structures their crystallographic periodicity. Glasses do not possess LRO as mineral (ceramic) waste forms do, but they do possess SRO and MRO.[216] Sometimes glasses have more highly ordered regions, referred to as clusters or quasicrystals that have atomic arrangements that approach those of crystals, but no LRO.[216,217]

Because of the similarity of the SRO and MRO in mineral (ceramic) and vitreous waste forms the dissolution mechanisms that attack the Si-O and Al-O bonds are similar and the mechanisms that attack the network breaking cations in glass (i.e. Na+) and the interstitial cations in minerals (i.e. Na+) are similar. However, the mineral waste forms often afford better retention of the cationic species (including COCs) compared to glass waste forms due to the LRO of the mineral structure and the regularity of the coordination and bonding associated with a coordination polyhedra in which a cation, COC, or radionuclide is atomically bonded. The LRO provides shorter and more regular oxygen-cation (ionic) or oxygen-contaminant bonding and a periodic ordering, which makes the contaminant retention in mineral/ceramic waste forms as good as glass and often better than glass.

Many similarities between silicate glass and silicate mineral dissolution behavior exist. One such example is their dissolution leads to the formation of an alkali-depleted partially hydrated layer.[218]. However, the two materials do not behave completely the same. Bourcier et al. [219] have shown that crystalline albite ($NaAlSi_3O_8$) dissolves at a rate roughly 1-1.5 orders of magnitude slower than albite glass from pH 2-12 at 70°C (Figure 11-1) during SPFT testing. The author states, “the same mechanisms are operating with both glasses and minerals but at different rates,” where the glass of the same composition leaches faster than the mineral. This is why mineral waste forms are important within the DOE complex as discussed in Section 2.1.

Another comparison of mineral versus glass durability for materials of the same inorganic composition was performed by researchers at the Pennsylvania State University in 2001-2002 for albite ($NaAlSi_3O_8$ jadeite ($NaAl_2Si_2O_8$), and nepheline ($NaAlSiO_4$).[220,221] A durability comparison was made between these “mineral glasses” and the crystalline mineral of exactly the same composition. The durability response was found to be comparable over all pH ranges with respect to Si matrix dissolution.[220,221]

Moreover, when researchers at the PNNL performed Raman spectroscopy of nuclear waste glasses, they determined that the glasses contained discrete MRO clusters of nepheline [$NaAlSiO_4$] and that these

[4] Hazardous constituents are assumed to be uniformly distributed throughout a much larger mass of soluble material, such as salt cake. The matrix is porous and water flowing through the waste form dissolves the matrix and releases encapsulated constituents.

clusters or units had structures similar to crystalline nepheline.[222] Summaries of the similarities (breaking of bonds) and differences (congruent[f] dissolution for glass and incongruent[§] dissolution for mineral waste forms) in the durability of ceramics and glasses can be found in References 219-221, 223, and the references associated with the downselect between glass and ceramic (mineral) waste forms for HLW and Pu wastes.[17-26;34-40;50-54]

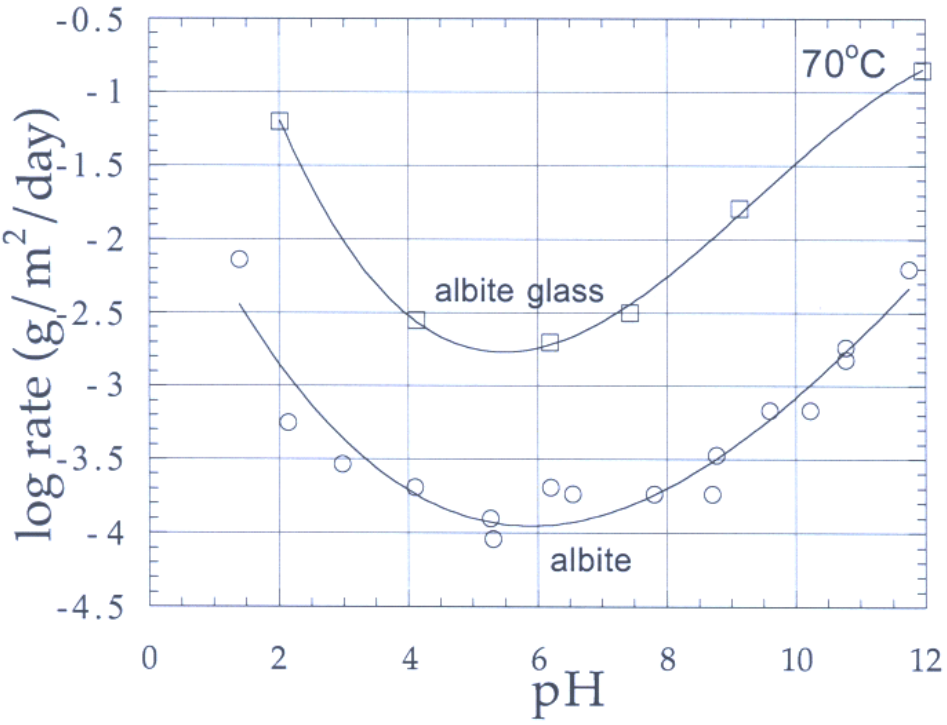

Figure 11-1. Comparison of dissolution rates of crystalline albite vs. albite glass from SPFT testing.[219]

A recent National Academy of Science report demonstrated how in mineral (ceramic) waste forms not every phase contains a sequestered radionuclide or constituent of concern.[26] The National Academy of Science schematic is reproduced in Figure 11-2 for reference. This demonstrates why glasses leach congruently when far from saturation and ceramics leach incongruently and why the total Na release from the ceramic cannot be compared to the total Na release from glass. In glass, Na and Re/^{99}Tc are released congruently, i.e. at the same rate. In ceramic waste forms, if the benign phases contain Na the Re/^{99}Tc, release is not directly related to the Na release. In this case, the Na release from glass must be compared to the Re/^{99}Tc release in the phase that hosts the COC, i.e. ^{99}Tc.

[f] Congruent dissolution of a waste form is the dissolving of species in their stoichiometric amounts from a single phase material like glass. For congruent dissolution, the rate of release of a radionuclide from the waste form is proportional to both the dissolution rate of the waste form and the relative abundance of the radionuclide in the waste form. Thus, for borosilicate glass, ^{99}Tc is released at the same rate, congruently, as Na, Li, and B.

[§] Incongruent dissolution of a waste form means that some of the dissolving species are released preferentially to others, i.e. the constituents of concern may only reside in one mineral phase and not in the others. Incongruent dissolution is often diffusion-controlled and can be either surface reaction-limited under conditions of near saturation or mass transport-controlled. Preferential phase dissolution, ion-exchange reactions, grain-boundary dissolution, and dissolution-reaction product formation (surface crystallization and recrystallization) are among the more likely mechanism of incongruent dissolution, which will prevail, in a polyphase mineral (ceramic) waste form.

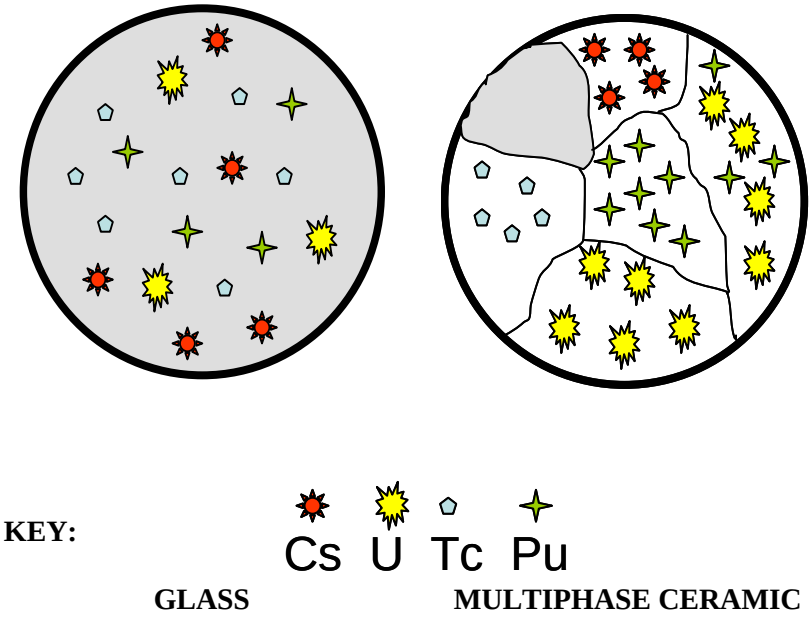

Figure 11-2. Schematic of the Manner in Which COCs are sequestered in glass and in ceramics. In both glass and ceramics the COCs are atomically bonded but in a ceramic the COCs report to different phases [26].

11.1 Relation of Durability Testing to Weathering of Nepheline and Sodalite

Nephelines are known to have survived anywhere from 879-1169 million years in nature as measured by K-Ar dating.[224] Weathering products from natural nepheline include but are not limited to analcite ($NaAlSi_2O_6$), boehmite (AlOOH), hydronepheline (nepheline with attached water molecules), kaolinite, muscovite, natrolite, and/or sodalite.[224] Sodalites are known to have survived thoroughout the Tertiary geologic period (696-732 million years ago) and age dating of sodalite deposits in South America range from 696-732 million years.[225] Thus, the stability of the non-radioactive and radioactive nepheline and sodalite FBSR granular mineral phases in 90-99°C deionized water for periods of up to 1 to 2.5 years underaccelerated weathering conditions of long-term PCT and PUF testing was anticipated and demonstrated (Sections 8.2.5 and 8.2.7).

Some data is available on the dissolution kinetics of pure crystalline nepheline and sparse data is available on the dissolution of pure crystalline sodalite. This data is discussed in Reference 6 by Pierce and summarized here. Tole et al. [226] studied the dissolution of pure crystalline nepheline (a natural specimen) and showed that elemental dissolution is congruent and that the initial dissolution rates drop due to the precipitation of new phases from solution. The new phases are initially aluminum hydroxides and, later, as the activity of silica in solution increases, amorphous aluminosilicates. All rates were estimated using the geometric surface area by Tole et al. because thin nepheline wafers were used.

A similar dissolution study on nepheline has shown that nepheline [220] shows a V-shape when the dissolution rate is graphed versus pH, similar to glass behavior, with a minimum dissolution rate near neutral pH (Figure 11-3). Studies on sodalite have also shown a similar V-shaped curve as a function of pH (Figure 11-4) and that the mineral is particularly vulnerable to acid attack with pronounced dissolution occurring below pH 5.5 [227,228].

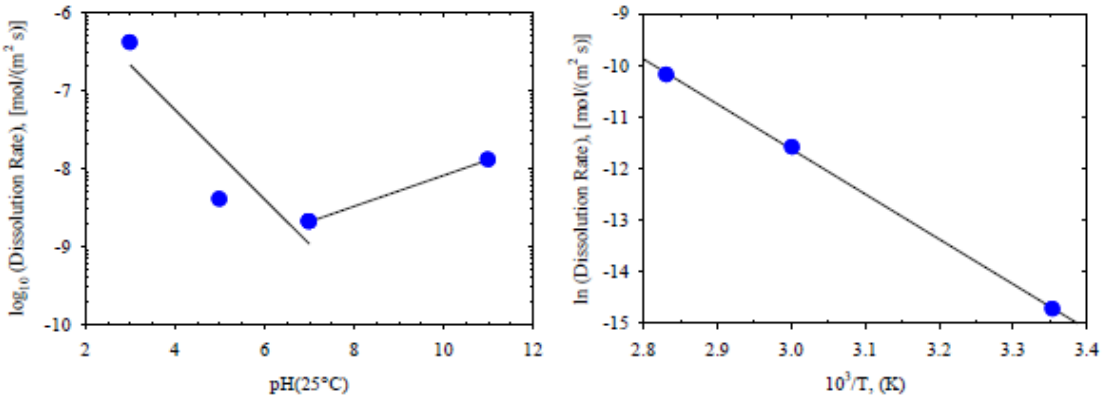

Figure 11-3. Nepheline dissolution rate as a function of pH and inverse temperature from Tole et al.[226]

As discussed in Section 2.2.1 on the sodalite minerals, the common attribute of the sodalite group of minerals is the flexible framework structure that can expand to enclathrate various guest anions by cooperative changes in the Al—O—Si bond angle.[7] This framework can collapse via tilting and deformation of the TO_4 tetrahedra to accommodate ions of various sizes. It is important to note that the sodalite cages are too small to allow for the exchange of ions (i.e., ion exchange of caged anions) from the structure without the destruction of the Al—O—Si framework.

A limited number of studies have examined the dissolution behavior of halide-sodalites under dilute and near-saturated conditions using a combination of MCC-1, PCT, and Soxhlet experimental approaches.[14, 228,229,230). All rates were estimated using the geometric surface area by Morss et al. [228] because a sodalite wafer was used. Although these experiments were conducted under static conditions, the results provide insight into the effect of two of key variables, pH and temperature, on sodalite dissolution. Understanding these two variables is critical to modeling the long-term performance of the FBSR waste form under near-surface disposal conditions.

In general, the sodalite dissolution experients [14,228,229,230] demonstrated that sodalite dissolves similarly to other framework aluminosilicate minerals under acidic and alkaline conditions, evident by the decrease in the dissolution rate as pH increases from 4.9 to 7.0, followed by an increase in the dissolution rate as pH increases from 7.0 to 10.0 (Figure 11-4). For example, at 90°C the average dissolution rate decreases by 6.7 times from 2.6 g/(m^2 d) at pH(23°C) = 5.1 to 0.39 g/(m^2 d) at pH(23°C) = 7.0. A similar increase (~6 times) occurs under alkaline conditions from pH (23°C) = 7.0 to pH (23°C) = 10.2. Reference 6 (Appendix B) provides a list of the rate law parameters obtained by Morss and colleagues [228] for sodalite dissolution. The apparent activation energy (E_a) for sodalite given in Reference 6 (Appendix B) suggests a surface reaction-controlled dissolution process, which is consistent with what has been observed with other framework aluminosilicate minerals (see next Section 11.1.1).

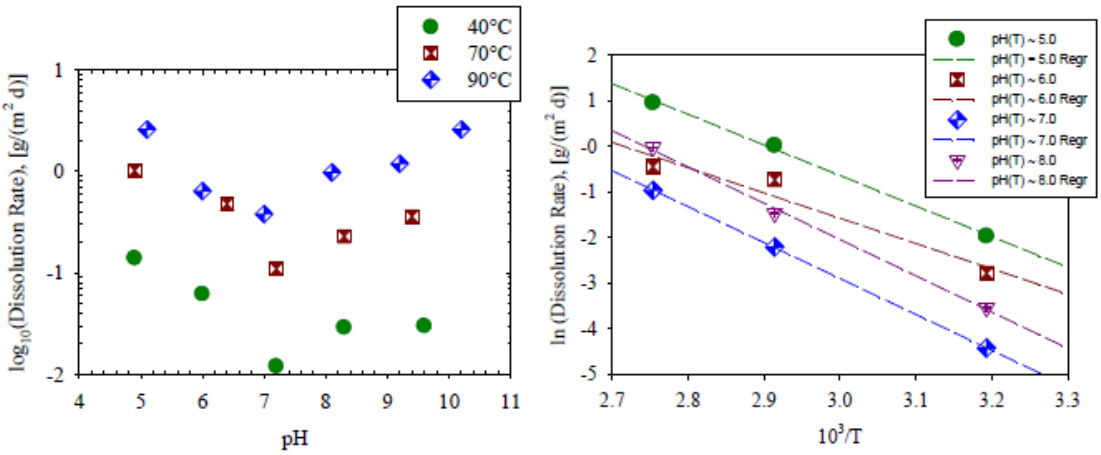

Figure 11-4. Normalized Dissolution Rate for Sodalite as a Function of pH and Temperature from Morss et al.[228]

11.1.1 *Mechanisms controlling Al, Na, and Si release in Minerals and Natural Glasses*

Although the reaction mechanism for silicate weathering (minerals and natural glasses) is still being actively investigated, the generally accepted concept that describes silicate weathering is the leaching mechanism.[120,231,232,233,234] The silicate leaching mechanism concept proceeds via a set of coupled processes that include (1) the selective removal of charge compensating cations (i.e., ion exchange of H^+ or H_3O^+ contained in bulk solution for cations in the mineral) and (2) protonation and rupture of Si–O–Si and Si–O–Al bonds (i.e., network hydrolysis) [see 235, 236, and the references contained therein]. Under near-saturated conditions, the aforementioned reaction mechanisms typically lead to the development of a hydrated surface layer that is depleted in aluminum, as well as alkali and alkaline-earth metals, and ranges in thickness from 20 to 1000 Å.

It has been postulated that reconstruction of the silica network, which creates a silica-rich surface layer, can occur via molecular-scale reorganization either by repolymerization of silanol groups [237,238], restructuring of the silica network [221], and/or readsorption of silica [239] at the mineral–solution interface. Hellmann et al. [240,241] have questioned the process of surface reconstruction in the formation of surface layers by studying the interface between experimentally altered and non-altered feldspar using high resolution transmission electron microscopy. Hellmann et al. [240,241] concluded that the interface was chemically and structurally sharp on an atomic scale and did not show the compositional profiles that would be expected from a solid state interdiffusion mechanism. They concluded that the data were better explained by an interfacial dissolution–reprecipitation mechanism, in which the dissolution reaction is initially stoichiometric, but is coupled with the precipitation of amorphous silica from a supersaturated boundary layer of fluid (i.e., a solution film in contact with the mineral surface that has a composition that is different than the bulk fluid).

11.1.2 *Geochemical Modeling of FBSR Mineral (Nepheline and Sodalite) Dissolution*

In an attempt to gain additional insight into mechanisms controlling Al, Na, and Si release from the FBSR NAS nepheline and sodalite matrix, geochemical modeling with PHREEQC [242] was used by Pierce et al. [120] to qualitatively evaluate the possibility of solubility limited release. For a brief description of the geochemical modeling simulations and the associated thermodynamic data used by Pierce et al., see the discussion contained in Reference 120 Supplemental Information.

Three simulations were conducted and compared to the measured Al, Na, and Si steady-state effluent concentrations (i.e., concentration after the first 200 days of PUF testing). The model simulations consisted of estimating the Al, Na, and Si concentration based on the nepheline solubility and Si concentration based on amorphous SiO_2 and chalcedony solubility. The results shown in Figure 11-5 suggest nepheline or the phase that resembles low carnegiete solubility is controlling the steady-state concentration of Al, whereas Na release is controlled by a combination of ion exchange and nepheline or the phase that resembles low carnegiete solubility, evident by the 2.3–3.7 higher release rate in comparison to Al. The deviation between the measured and predicted Si concentrations with respect to nepheline solubility (Figure 11-5) suggests that Si release is being controlled by the formation of another phase; probably a Si-rich phase similar to amorphous silica or chalcedony (Figure 11-6). The correlation between the measured Si concentrations to amorphous silica and chalcedony solubility suggests a hydrated surface layer may have formed on surface of altered FBSR grains. The inability to positively identify this phase in XRD and SEM analysis of reacted grains suggests the phase is amorphous and represents a minor component of the bulk sample, such as a surface coating on reacted grains.

Although the results presented cannot distinguish between the two mechanisms currently being debated (i.e., leaching versus dissolution–reprecipitation) within the geochemical community, the time-dependent evolution of the solution chemistry suggests the following steps are occurring: (1) the ion exchange as evident by the average Na (7.9×10^2 g/m^2) normalized release being 2.3 and 3.7 times greater than Al (3.4×10^2 g/m^2) and Si (2.2×10^2 g/m^2) normalized release, respectively; (2) the dissolution of the silicate matrix, specifically the phase that resembles low carneigeite, evident by the depth dependent alteration phase evolution (Figure 8-28); and (3) the formation of a silica-rich surface layer evident by the dissolved Si concentration being at or near the solubility of amorphous SiO_2 or chalcedony. The formation of a Si-rich surface layer indicates that the alteration mechanism controlling multiphase FBSR matrix weathering is similar to other silicate minerals.

While the SPFT data presented in Section 8.2.6 makes it appear that the Si, Al, and Na data may be leaching congruently, the PUF data presented in Section 8.2.7 (and the references contained therein) and the geochemical modeling summarized above indicates that the leaching of the elements from the FBSR is incongruent as with other multiphase ceramics.[40] The PUF data and geochemical modeling also demonstrates that the hypothesis of Jantzen et al. [119] that the "nepheline building blocks" common to the various FBSR NAS phases, i.e. nepheline, carnegietite, sodalite, and nosean, might be releasing Si, Al, and Na congruently based on Lorier's [118] short-term SPFT testing was incorrect.

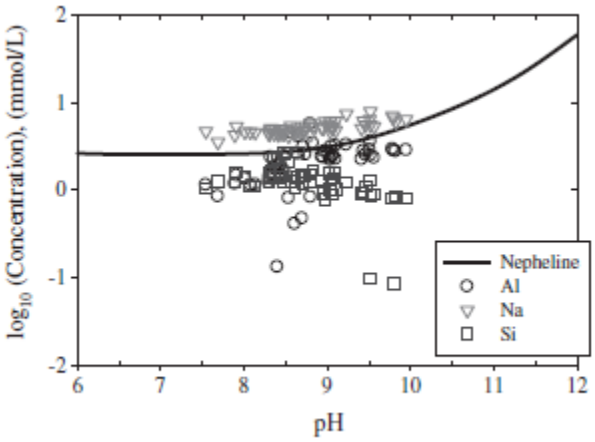

Figure 11-5. Steady-state effluent concentration (mmol/L) of Al, Na, and Si Measured in the PUF experiment starting at day 200 as a function of the average pH. Solid line represent the calculated solubility for nepheline.[120]

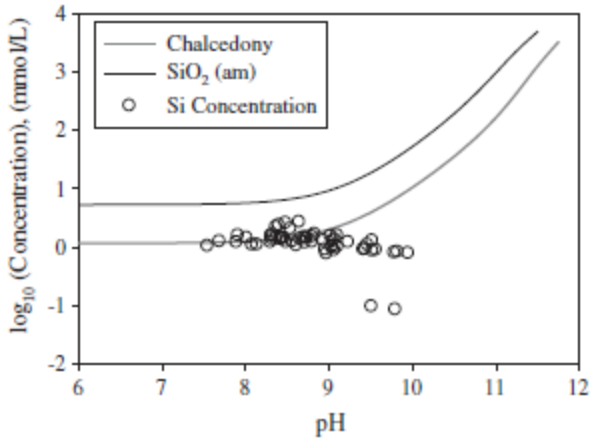

Figure 11-6. Steady-state concentration (mmol/L) of Si measured in the PUF experiment starting at day 200 as a function of the average pH. Solid black and dark gray lines represents the calculated solubility for SiO_2 (am) and chalcedony.[120]

In an attempt to gain additional insight into mechanisms controlling Re and S release from the FBSR NAS matrix, geochemical modeling was also performed using PHREEQC [242] by Pierce et al. [120] to qualitatively evaluate the possibility of solubility limited release. Two simulations were conducted and compared to the measured Re and S steady-state effluent concentrations (i.e., concentration after the first 200 days of PUF testing). The model simulations consisted of estimating the Re concentration based on the Re-sodalite solubility and S concentration based on the nosean solubility. The results shown in Figure 11-7 suggest the S and Re concentrations are within an order of magnitude of the nosean and Re-sodalite solubility, respectively. The order of magnitude difference between the observed and predicted concentration, along with the similarity in Re and S release profiles, provides additional indication for the existence of mixed anion-sodalites in the FBSR NAS products.

The multiphase FBSR NAS ceramic waste form (which is composed of nepheline, low carneigiete, nosean, and sodalite) was evaluated as a potential host material for Hanford LAW. These results illustrate that rhenium in the FBSR NAS matrix is in the Re(VII) oxidation state and incorporated into the sodalite structure [probably as mixed anion-sodalite type structure $Na_8(Al_6Si_6O_{24})(SO_4)$- $Na_8(Al_6Si_6O_{24})(ReO_4)_2$] solid solution. These results and the fabrication of a mixed Re-^{99}Tc sodalite discussed in Section 8.2.10 provide credibility to the proposed concept that Tc(VII), similar to Re(VII), can be incorporated into the sodalite structure while in the presence of the other anions contained in the LAW waste stream at significantly higher concentrations. Although it has been demonstrated that the REDOX chemistry for Re and ^{99}Tc in glass is significantly different [90], this large discrepancy is not observed in the FBSR EMF REDOX for these species discussed in Section 8.2.8. In addition the atomic radii for Re(VII) and Tc(VII) are similar [1.373 Å for Re(VII) and 1.358 Å for Tc(VII)], the ionic radii for Re(VII) and Tc(VII) at 0.56 Å, and the allows the perrhenate anion to serve as a close chemical analogue for the pertechnetate anion.[120]

A comparison of the results discussed in this study to data previously collected on LAW glass is given in Reference 120. The data presented indicates that Re release from the multiphase FBSR NAS granular product is an order of magnitude lower than ^{99}Tc release [$(2.1 \pm 0.3) \times 10^{-2}$ g/(m^2 d)] from LAWglass (LAW AN102) [243] when normalizing the rates using the BET surface area [$(6.1 \pm 0.9) \times 10^{-4}$ g/(m^2 d)] and comparable to glass when using the geometric surface area [$(1.32 \pm 0.02) \times 10^{-1}$ g/(m^2 d)]. In other words, the release rates normalized using the BET surface area reflect the inherent durability of the mineral phases present in the FBSR NAS ceramic waste form and suggest the material is durable or

possibly more durable than LAW glass under PUF test conditions. On the other hand, the release rates normalized by the geometric surface area reflect the high specific surface area of the FBSR NAS product. Although glass represents the primary treatment option for Hanford LAW, these results suggests the multiphase FBSR NAS ceramic waste form may be a viable alternative technology for providing the supplemental treatment capacity required to meet the schedule goals for Hanford cleanup.

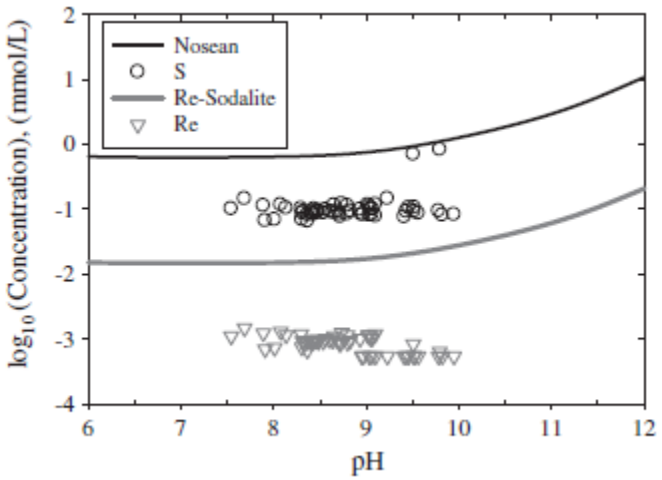

Figure 11-7. Steady-state concentration (mmol/L) of S and Re measured in the PUF experiment starting at day 200 as a function of the average pH. Solid black and dark gray lines represents the calculated solubility for nosean and Re-sodalite.[120]

12.0 Conclusions

FBSR treatability studies on Hanford LAW wastes (Rassat 68 tank LAW blend, SX-105, AN-103 and AZ-101/AZ-102) has demonstrated [3,4,5] the following:

- Atomic bonding of the radionuclides and constituents of concern (COC) comparable to glass
- Destruction of nitrates and organics comparable to vitrification
- No dependency of ^{99}Tc, $^{125/129}I$, Cl, S, Re, Cr, and Cs off-gas volatilization on REDOX (for glass this can be problematic)
  - Good mass balance closure and data indicates ^{99}Tc, Re, I, S, and Cl report to the sodalite mineral; Cs and Na to nepheline mineral product
- Short and long-term durability comparable to glass
  - No REDOX dependency of durability
  - No reaction phases form after 1 year of testing - suggests long-term stability
- Higher Na_2O and SO_4^{2-} waste loadings (WL) than glass
  - Higher WL contribute to low disposal volumes (as low as glass at higher WL) and provide for more rapid processing of LAW

The FBSR product is granular in nature. Monolithing of the granular product can prevent dispersion during transport and/or during burial/storage. While a monolith is desirable for control of dispersion, burial site subsidence, and intruder prevention, there are other means by which this requirement can be met for a granular waste form, e.g. waste stabilization in High Integrity Containers (HIC's). The primary waste form, the granular product, was the focus of the majority of the Waste Form Qualification (WFQ) testing summarized in this document. Testing of geopolymeric monoliths is also summarized in this document but is considered supplementary data to the testing of the primary waste form, i.e. the granular

mineral product. Monoliths and HIC's are compared in terms of IDF disposal volumes and the relative Na_2O oxide waste loading criteria for Hanford LAW. The disposal of the granular product is shown to give the highest Na_2O oxide waste loadings compared to glass at equivalent volume reductions. Higher volume reducions can be achieved by some compaction of the granular product.

The significant findings on the granular product to date of the testing primarily from the SRS Rassat LAW blend, the Hanford Tank SX-105, and the Hanford Tank AN-103 are given below:

- Good mass balance closure on ^{99}Tc, Re, Cs, and I in all BSR tests (radioactive and non-Radioactive)
  - SRS Rassat LAW blend - SRS Low Activity Waste shimmed to match Hanford LAW (Module B)
    - 98% recovery of Re in the product streams for the radioactive campaigns
    - 88% recovery of ^{99}Tc in the product streams for the radioactive campaign
    - 94-95% recovery of ^{129}I in the product streams for radioactive campaign and 95% recovery of ^{125}I in the radioactive campaign where the ^{125}I is a more accurate value
    - 103% recovery of ^{127}I in the non-radioactive campaign
  - Hanford LAW #1 - (Tank SX-105 or Module C)
    - 98% recovery of Re in the product streams for radioactive and simulant campaigns
    - 80-83% recovery of ^{99}Tc for once through processing with 98% of the ^{99}Tc in the product
    - ~75% recovery of ^{127}I (non-radioactive) and ^{129}I (radioactive); this is the difference of two very small concentrations (input and output) as no excess ^{127}I was shimmed in this waste
    - 78-100% recovery of chloride in non-radioactive and radioactive campaigns, respectively
    - ~100% recovery of Cs in the simulant campaigns; issues with cross contamination in the radioactive campaigns
  - Hanford LAW #2 – (Tank AN-103 - Module D)
    - 90-95% recovery of Re in simulant runs, 88% recovery in radioactive campaign
    - 83-86% recovery of ^{99}Tc for once through processing with 98% of the ^{99}Tc in the product
    - 100% recovery of ^{127}I (non-radioactive) in two simulant campaigns and 100% recovery of ^{129}I (radioactive) in the radioactive campaign
    - 86% recovery of Cl in the simulant campaigns
    - 87% recovery of Cs in the simulant campaigns, issues with cross contamination in the radioactive campaigns
- Data indicates ^{99}Tc, Re, Cs, and I (all isotopes) report to the mineral product and not to the off-gas
- ^{99}Tc and Re show similar behavior in partitioning between product and off-gas: for mass balance Re is an acceptable simulant for ^{99}Tc
- Mineralogy of radioactive and simulant products from the BSR and Engineering-scale Test Demonstration (ESTD) and the 2001 and 2004 pilot studies are the same
- XAS results for non-radioactive samples from ESTD 2004 and 2008 and BSR Module B shows that Re is in the VII oxidation state and contained in the sodalite structure at all REDOX values
  - XAS analyses have shown that ~65-79% of the ^{99}Tc is in the VII oxidation state when the BSR REDOX is in the REDOX range of the normal FBSR operation and ~56% of the ^{99}Tc is in the VII oxidation state at REDOX ranges more reduced than normal FBSR operation.
  - The remainder of the ^{99}Tc is present as +4 in TcO_2 oxide and/or $Tc_2S(S_3)_2$
  - No difference in the durability measurements attributed to sample REDOX were noted in any of the PCT, SPFT or PUF measurements which implies the following
    - the +7 fraction of the ^{99}Tc is insoluble in the sodalite cage, while the +4 fraction of the ^{99}Tc is insoluble as the oxide and/or sulfide

    - the REDOX range can be shifted to more oxidizing values to achieve higher VII oxidation states for ^{99}Tc but this appears to be unnecessary based on the durability testing
    - the XAS experiments have allowed a ^{99}Tc calibration line to be put on the existing EMF series
- TCLP data are acceptable when RCRA metals are not shimmed in excess and REDOX is controlled or an IOC is present as a spinel host for Cr
- ASTM C1285 (Product Consistency Test) releases are below 2 g/m^2 for the COC
    - Use of BET surface area to account for the surface roughness of the mineral granules demonstrates that the FBSR product is 2 orders of magnitude lower than the 2g/m^2
    - Use of the geometric surface area, which ignores the surface roughness of the mineral granules compared to glass gives an equivalent leach rate to vitreous waste forms
    - All the durability results for the non-radioactive constituents from the BSR testing and the ESTD testing are in agreement with the previous data from 2001and 2004
- Re is a good surrogate for ^{99}Tc during leaching experimentation proving that the current radioactive and simulant BSR campaign products using Re and ^{99}Tc match the historic and engineering scale data that used Re only proving the "tie back" strategy
- Long-term testing (1, 3, 6 and 12 month) at 90°C by ASTM C1285 has not shown any significant change in the mineral assemblages as analyzed by X-Ray Diffraction (XRD)
    - One exception was the Engineering-scale ESTD samples, which contain small amounts of halloysite, $Al_2Si_2O_5(OH)_4$, which is the main reaction product of kaolin clay
    - The halloysite does not increase in amount with time indicating that it is forming from a minor phase in the mineral waste form
    - The ESTD sample was the only sample made with ~10 wt% excess clay

For the non-radioactive Hanford LAW wastes

- Engineering and bench-scale product perform similarly in SPFT testing
    - Rates are one or two orders of magnitude lower than glass depeding on the element being compared, i.e. Si vs. Re [126,132]
    - Al, Na, Si have to break bridging oxygen bonds to release elements in sodalite cage [126,132]
    - Re and I are encapsulated in cages and have a delayed release [126,132]
    - I and Re release at similar rates [126,132]
    - ^{99}Tc and Re occupy similar sites in the sodalite cage structure [132]
    - Dissolution rates are all similar to ealier studies on pilot-scale FBSR products [126,132]
    - SPFT results suggest that forward or maximum dissolution rate for LAW glasses, based on B release from (LAWABP1, LAWE-1A, LAWE- 95A, and LAWE-290A), is approximately one order of magnitude greater than the FBSR NAS product dissolution rate, based on Na release, measured under the same conditions [6]
- Engineering and bench-scale product perform similarly in PUF testing
    - PUF tests of 1 year duration were performed on the non-radioactive Rassat LAW FBSR granular products made in the BSR and the ESTD [131]
    - The ESTD sample was 20% bed product and 80% fines [131]
    - The experiments showed a trend of decreasing release of Na, Si, Al, and Cs as a function of time [131]
    - The elements I and Re showed a steady release throughout the year long test [131]
    - The difference in the release rates of Na, Si, Al and Cs compared to I and Re suggests that the release I and Re species from the sodalite cage occurs at a different rate compared with the dissolution of the predominant nepheline phase [131]
    - Comparisons to PUF tests of a 2.5 year duration on the 2004 SAIC-STAR pilot scale FBSR products made with the Rassat LAW simulant were in agreement with the PUF testing of the BSR and ESTD products [120]

- The time-dependent elemental release rates were combined with geochemical modeling calculations and suggest that aluminum and sodium release is controlled by nepheline solubility, whereas silicon is being controlled by amorphous silica solubility after being released from the FBSR NAS matrix [120]
- For the duration of the experiment, Re and S releases were within the experimental error of one another, suggesting their release is either from the same phase or a phase with similar stability [120]
- The PUF data indicates that Re release from the multiphase FBSR NAS granular product is an order of magnitude lower than ^{99}Tc release [$(2.1 \pm 0.3) \times 10^{-2}$ g/(m^2 d)] from LAW glass (LAW AN102) [120]
- Geochemical calculations using PHREEQ-C on 200 day PUF data suggests the steady-state S and Re concentrations are within order of magnitude of solubility of phase pure nosean and Re-sodalite [120]
- PUF testing and modeling suggests that Re and S are being released from a “mixed-anion” sodalite phase (likey Re and SO_4^{-2} bearing), which has a different stoichiometry in comparison to the pure mineral end-members and a thermodynamic stability that lies between the pure phase end-members, e.g. such a solid solution is already known between the Cl and SO_4^{-2} sodalite/nosean endmembers and a mixed Re/^{99}Tc sodalitie was made at SRNL

13.0 References

1 Certa, P.J. and M.N. Wells, **"River Protection Project System Plan"**, ORP-11242, Rev. 5, DOE Office of River Protection, Richland, WA (November 2010).

2 U.S. Department of Energy Office of Environmental Management, **"Technology Readiness Assessment (TRA)/Technology Maturation Plan (TMP) Process Implementation Guide"**, Rev. 1 (November 2012).

3 Jantzen, C.M., C.L. Crawford, C.J. Bannochie, P.R. Burket, A.D. Cozzi, W.E. Daniel, D.M. Missimer, and C.A. Nash, **"Radioactive Demonstration of Mineralized Waste Forms Made from Hanford Low Activity Waste (Tank Farm Blend) by Fluidized Bed Steam Reformation (FBSR)"**, SRNL-STI-2011-00383, Savannah River National Laboratory, Aiken, South Carolina (August 2013).

4 Jantzen, C.M., C.L. Crawford, C.J. Bannochie, P.R. Burket, A.D. Cozzi, W.E. Daniel, D.M. Missimer, and C.A. Nash, **"Radioactive Demonstration of Mineralized Waste Forms Made from Hanford Low Activity Waste (Tank SX-105, AN-103, AZ-101/AZ-102) by Fluidized Bed Steam Reformation (FBSR)"**, SRNL-STI-2011-00384 , Savannah River National Laboratory, Aiken, South Carolina (September 2013).

5 Jantzen, C.M., C.L. Crawford, C.J. Bannochie, P.R. Burket, A.D. Cozzi, W.E. Daniel, C.C. Herman, D.H. Miller, D.M. Missimer, and C.A. Nash, **"Radioactive Demonstration of Mineralized Waste Forms Made from Hanford Low Activity Waste (Tank SX-105 and AN-103) by Fluidized Bed Steam Reformation (FBSR)"**, Paper #14317, Waste Management 2014, Phoenix, Arizona (2014).

6 Pierce, E.M., "**Review of Existing Fluidized-Bed Steam Reformer Sodium Aluminosilicate Waste Form Performance Data**". ORNL/TM-2012/19, Rev. 1, Oak Ridge National Laboratory, Oak Ridge, TN (2012; 2014 in revision).

7 Pauling, L., **"The Structure of Sodalite and Helvite"**, Zeitschrift fur Kristallographie, 74, 213-225 (1930).

8 Serne, R.J., J.M. Zachara, and D.S. Burke, **"Chemical Information on Tank Supernatants, Cs Adsorption from Tank Liquids onto Hanford Sediments, and Field Observations of Cs Migration from Past Tank Leaks"**, PNNL-11498/UC-510, Pacific Northwest National Laboratory, Richland, WA (1998).

9 Zhao, H., Y. Deng, J.B. Harsh, M. Flury, and J.S. Boyle, **"Alteration of Kaolinite to Cancrinite and Sodalite by Simulated Hanford Tank Waste and it's Impact on Cesium Retention"**, *Clays and Clay Minerals*, *52*[1], 1-13 (2004).

10 Lorier, T.H., C.M. Jantzen, J.C. Marra, and J.M. Pareizs, **"Feed Reactivity Study for Fluidized Bed Steam Reformer Processing"**, Ceramic Transactions V. 176, 111-119 (2006).

11 Babad, H. and D.M. Strachan, **"Method for Immobilizing Radioactive Iodine"**, U.S. Patent #4,229,317 (October 1980).

12 Brownell, L.E., C.H. Kindle, and T.L. Theis, **"Review of Literature Pertaining to the Aqueous Conversion of Radionuclides to Insoluble Silicates with Selected References and Bibliography"**, U.S. DOE Report ARH-2731, Atlantic Richfield Hanford Company, Richland, Washington (1973).

13 Barney, G., **"Fixation of Radioactive Wastes by Hydrothermal Reactions with Clays"**, Atlantic Richfield Hanford Company, Richland, Washington (1974).

14 Fanning, T., W.L. Ebert, S.M. Frank, M.C. Hash, E.E. Morris, L.R. Morss, T.P. O'Holleran, and R.A. Wigeland, **"Status of Ceramic Waste Form Degradation and Radionuclide Release Modeling,"** ANL-03/8, Argonne National Laboratory, Argonne, Illinois (2003).

15 Hatch, L.P., "**Ultimate Disposal of Radioactive Wastes"**, Am. Scientist, 41, 410-421 (1953).

16 Hench, L.L, R.J. Charles, A.R. Cooper, R.C. Ewing, J.R. Hutchins, D.W. Readey, F.L. VerSnyder, and S.M. Widerhorn, **"The Evaluation and Selection of Candidate High Level Waste Forms,"** Report No. 3, USDOE/TIC-11472, Alternative Waste Form Peer Review Panel (National Technical Information Service), Springfield, Virginia (1981).

17 Hench, L.L., D.E. Clark, and A.B. Harker, **"Nuclear Waste Solids"**, Journal of Materials Science, 21, 1457-1478 (1986).

18 Moschetti, T., W. Sinkler, T. DiSanto, M.H. Noy, A.R. Warren, D. Cummings, S.G. Johnson, K.M. Goff, K.J. Bateman, and S.M. Frank, **"Characterization of a Ceramic Waste Form Encapsulating Radioactive Electrorefiner Salt"**, in *Scientific Basis for Nuclear Waste Management XXIII*, R. Smith and D. Shoesmith, Eds.; Materials Research Society, Pittsburgh, Pennsylvania, 577-582 (2000).

19 Sinkler, W., T. O'Holleran, S. Frank, M. Richmann, and S**.** Johnson, **"Characterization of a Glass Bonded Ceramic Waste Form Loaded with U and Pu,"** in Scientific Basis for Nuclear Waste Management XXIII, R. Smith and D. Shoesmith, Eds.; Materials Research Society, Pittsburgh, Pennsylvania, 423-429 (2000).

20 Lutze, W. and R.C**.** Ewing, **"Radioactive Waste Forms for the Future"**, Elsevier Science Publishers, Amsterdam, The Netherlands (1988).

21 Lee, W., M. Ojovan, M. Stennett, and N. Hyatt, **"Immobilization of Radioactive Waste in Glasses, Glass Composite Materials, and Ceramics"**, Advances in Applied Ceramics, 105[1], 3-12 (2006).

22 Caurant, D., P. Loiseau, O. Majerus, V. Aubin-Chevaldonnet, I. Bardez, and A. Quintas, **"Glasses, Glass-Ceramics, and Ceramics for Immobilization of Highly Radioactive Nuclear Waste,"** Nova Science Publishers, Inc., New York (2009).

23 Donald, I.W., B.L Metcalfe, and R.N.J. Taylor, **"The Immobilization of High Level Radioactive Wastes Using Ceramics and Glasses"**, J. Materials Science, 32, 5851-5887 (1997).

24 Donald, I.W., **"Waste Immobilization in Glass and Ceramic Based Hosts"**, John Wiley Ltd., West Sussex, UK, (2010).

25 Stefanovsky, S., S. Yudintsev, R. Giere, and G. Lumpkin, **"Nuclear Waste Forms"**, in Energy, Waste, and the Environment: A Geochemical Perspective, R. Giere and P. Stille, Eds., Geological Society of London Special Publication, 36-63 (2004).

26 National Research Council, **"Waste Forms Technology and Performance Final Report"**, The National Academies Press, Washington, DC (2011).

27 Ebert, W.L., M.A. Lewis, and S.G. Johnson, **"Application of the PCT to the EBR II Ceramic Waste Form"**, Proceedings of the DOE Spent Nuclear Fuel and Fissile Materials Management Meeting, Charleston, South Carolina, September 17–20 (2002).

28 Ebert, W.L., M.A. Lewis, and S.G. Johnson, **"The Precision of Product ConsistencyTests Conducted with a Glass-Bonded Ceramic Waste Form"**, Journal of Nuclear Materials, 305, 37–51 (2002).

29 Goldman, M.I., J.A. Servizi, R.S. Daniels, T.H.Y. Tebbutt, R.T. Burns, and R.A. Lauderdale, **"Retention of Fission Products in Ceramic-Glaze-Type Fusions"**, Proceedings 2nd UN International Conference on Peaceful Uses of Atomic Energy, Geneva, 1958, 1827; United Nations, New York, 27 (1958).

30 Eliassen, R. and M.I. Goldman, **"Disposal of High-Level Wastes by Fixation in Fused Ceramics,"** in *Hearings on Industrial Radioactive Waste Disposal*, Vol. 3, R.L. Doan, Ed.: US Govt Printing Office, Washington, DC, 1966-1979 (1959).

31 Mawson, C.A., "**Management of Radioactive Wastes"**, D. VanNostrand Co., Inc., New Jersey, 1965.

32 Walton, R.D. ,Jr., W.B. Wilson, and D.E. Gordon, **"Department of Energy's Selection of High Level Waste Forms"**, in The Treatment and Handling of Radioactive Wastes, A.G. Blasewitz, J.M. Davis, and M.R. Smith, Eds.; Battelle Press, Columbus, Ohio, 307-311 (1983).

33 Office of Nuclear Waste Isolation, **"Interim Performance Specifications for Waste Forms for Geologic Isolation"**, NWTS-19 DRAFT, Columbus, Ohio (October 1981).

34 Kerr, R.A., **"Nuclear Waste Disposal: Alternatives to Solidification in Glass Proposed"** Science, 204, 289-291 (1979).

35 Kerr, R.A., **"Academy Squabbles Over Radwaste Report"**, Science, 205, 287-289 (1979).

36 Clarke, D.R., **"Preferential Dissolution of an Intergranular Amorphous Phase in a Nuclear Waste Ceramic"**, J. Am. Ceram. Soc., 64[6], C–89–C–90 (1981).

37 Zhang, Z. and M.L. Carter, "**An X-Ray Photoelectron Spectroscopy Investigation of Highly Soluble Grain-Boundary Impurity Films in Hollandite"**, J. Am. Ceram. Soc., 93[3], 894-899 (2010)**.**

38 Buykx, W.J., K. Hawkins, D.M. Levins, H. Mitamura, R.St.C. Smart, G.T. Stevens, K.G. Watson, D. Weedon, and T.J. White, **"Titanate Ceramics for the Immobilization of Sodium-Bearing High-Level Nuclear Waste"**, J. Am. Ceram. Soc., 71[8], 678–88 (1988).

39 Cooper, J.A., D.R. Cousens, J.A. Hanna, R.A. Lewis, S. Myhra, R.L. Segall, R.St.C. Smart, P.S. Turner, and T.J. White, **"Intergranular Films and Pore Surfaces in Synroc C: Structure, Composition, and Dissolution Characteristics"**, J. Am. Ceram. Soc., 69[4], 347–52 (1986).

40 Jantzen, C.M., D.R. Clarke, P.E.D. Morgan, and A.B. Harker, **"Leaching of Polyphase Nuclear Waste Ceramics: Microstructural and Phase Characterization"**, J. Am. Ceram. Soc., 65[6], 292-300 (1982).

41 Garmon, L. **"The Box Within a Box Within a Box"**, Science News, 120, 396-399 (1981).

42 Morgan, P.E.D., D.R. Clarke, C.M. Jantzen, and A.B. Harker, **"High Alumina Tailored Nuclear Waste Ceramics"**, J. Am. Ceram. Soc. 64[5], 249-258 (1981).

43 Lutze, W., J. Borchardt, and A.K. De, **"Characterization of Glass and Glass Ceramic Nuclear Waste Forms"**, Sci. Basis for Nuclear Waste Mgt. *I*, G.J. McCarthy, Ed.; Plenum Press, New York, 69-81 (1979).

44 McCarthy, G.J., **"Quartz-Matrix Isolation of Radioactive Wastes"**, J. Mat. Sci. 8, 1358-59 (1973).

45 McCarthy, G.J. and M.T. Davidson, **"Ceramic Nuclear Waste Forms: I. Crystal Chemistry and Phase Formation"**, Bull. Am. Ceram. Soc. 54, 782-786 (1975).

46 Schoebel, R.O., **"Stabilization of High Level Waste in Ceramic Form"**, Bull. Am. Ceram. Soc, 54[4], 459 (1975).

47 Ringwood, A.E., V.M. Oversby, and S.E. Kesson, **"SYNROC: Leaching Peformance and Process Technology"**, in *Proc. Seminar on Chemistry and Process Engineering for High-Level Liquid Waste Solidification*, R.Odoj and E. Merz, Eds.; Julich Conference 42, Vol 1, 495-506 (1981).

48 Dunson, J.B. Jr., A.M. Eisenberg, R.L. Schuyler, III, H.G. Haight Jr., V.E. Mello, T.H. Gould Jr., J.L. Butler, and J.B. Pickett, **"Assessment of Processes, Facilities, and Costs for Alternative Solid Forms for Immobilization of SRP Defense Wastes"**, U.S. DOE Report DP-1625, E.I. DuPont deNemours & Co, Savannah River Laboratory, Aiken, South Carolina (March 1982).

49 De, A.K., B. Luckscheiter, W. Lutze, G. Malow, and E. Schiewer, **"Development of Glass Ceramics for the Incorporation of Fission Products"**, Ceramic Bulletin, 55, 500-503 (1976).

50 Ewing, R.C., **"Nuclear Waste Forms For Actinides"**, Proc. Natl. Acad. Sci. 96, 3432-3439 (1999).

51 Oversby, V.M., C.C. McPheeters, C. Degueldre, and J.M. Paratte, **"Control of Civilian Plutonium Inventories Using Burning in a Non-fertile Fuel"**, Journal of Nuclear Materials, 245, 17-26 (1997).

52 Ewing, R.C., W. Lutze, and W.J. Weber, **"Zircon: A Host-phase for the Disposal of Weapons Plutonium,"** Journal of Materials Research 10[2], 243-246 (1995).

53 Ryerson, F.J. and B. Ebbinghaus,**"Pyrochlore-rich Titanate Ceramics for the Immobilization of Plutonium: Redox Effects on Phase Equilibria in Cerium- and Thorium-substituted Analogs"**, U.S. DOE Report UCRL-ID-139092, Lawrence Livermore National Laboratory, Livermore, California (May 2000).

54 Meyers, B., G.A. Armantrout, C.M. Jantzen, A. Jostsons, J.M. McKibben, H.F. Shaw, D.M. Strachan, and J.D. Vienna, **"Technical Evaluation Panel Summary Report: Ceramic and Glass Immobilization Options"**, U.S. DOE Report UCRL-ID-129315, Lawrence Livermore National Laboratory, Livermore, California (January, 1998).

55 Roy, R. **"Hydroxylated Ceramic Waste Forms and the Absurdity of Leach Tests"**, Proc. Int. Sem. On Chemistry and Process Engineering for High-Level Liquid Waste Solidification, Vol. 2, Julich, JUL-Conf-42, R. Odoj and E. Merz, Eds., 576-602 (1981).

56 Mason, J.B., T.W. Oliver, M.P. Carson, and G.M. Hill, **"Studsvik Processing Facility Pyrolysis/Steam Reforming Technology for Volume and Weight Reduction and Stabilization of LLRW and Mixed Wastes"**, Waste Management 99, Tucson, Arizona (1999).

57 Mason, J.B., J. McKibben, K. Ryan, and D. Schmoker, **"Steam Reforming Technology for Denitration and Immobilization of DOE Tank Wastes"**, Waste Management 03, Tucson, Arizona (2003).

58 Jantzen, C.M., M.R. Williams, N.E. Bibler, C.L. Crawford, and A.R. Jurgensen, **"Fluidized Bed Steam Reformed (FBSR) Mineral Waste Forms: Application to Cs-137/Sr-90 Wastes for the Global Nuclear Energy Partnership (GNEP)"**, WSRC-MS-2008-00013 (2008).

59 Jantzen, C.M. and M.R. Williams, "**Fluidized Bed Steam Reforming (FBSR) Mineralization for High Organic and Nitrate Waste Streams for the Global Nuclear Energy Partnership (GNEP)",** Paper #8314, Waste Management 08, Phoenix, Arizona, (2008).

60 Jantzen, C.M., **"Engineering Study of the Hanford Low Activity Waste (LAW) Steam Reforming Process,"** U.S. DOE Report WSRC-TR-2002-00317, Westinghouse Savannah River Co., Aiken, South Carolina (July 2002).

61 McGrail, B.P., H.T. Schaef, P.F. Martin, D.H. Bacon, E.A. Rodriquez, D.E. McReady, A.N. Primak, and R.D. Orr, **"Initial Evaluation of Steam-Reformed Low Activity Waste for Direct Land Disposal"**, U.S. DOE Report PNWD-3288, Pacific Northwest National Laboratory, Richland, Washington (2003).

62 Jantzen, C.M., **"Mineralization of Radioactive Wastes By Fluidized Bed Steam Reforming (FBSR): Comparisons to Vitreous Waste Forms and Pertinent Durability Testing,"** U.S. DOE Report WSRC-STI-2008-00268, Savannah River National Laboratory, Aiken, South Carolina (December 2008).

63 Deer, W.A., R.A. Howie, W.S. Wise, and J. Zussman, **"Rock-Forming Minerals, Vol. 4B, Framework Silicates: Silica Minerals, Feldspathoids and the Zeolites"**, The Geological Society, London, UK (2004).

64 Smith, J.V. and O.F. Tuttle, **"The Nepheline-Kalsilite System, Part I, X-ray Data for the Crystalline Phases"**, Am. J. Sci., 255, 282-305 (1957).

65 Brenchley, M.E. and M.T. Weller, **"Synthesis and Structruer of $M_8[AlSiO_4]_6$ $(XO_4)_2$, M = Na, Li, K; X = Cl, Mn Sodalites"**, Zeolites, 14, 682-686 (1994).

66 Fechtelkord, M., **"Influence of Sodium Ion Dynamics on the ^{235}Na Quadrupolar Interaction in Sodalite: A High-Temperature ^{236}Na MAS NMR Study"**, Solid State Nuclear Magnetic Resonance 18, 70-88 (2000).

67 Gesing, T.M., and J.C. Buhl, **"Crystal structure of a carbonate-nosean $Na_8[AlSiO_4]_6CO_3$,"** European Journal of Mineralogy 10[1], 71-77 (1998).

68 Deer, W.A., R.A. Howie, and J. Zussman, "**Rock-Forming Minerals, V. 4"**, John Wiley & Sons, Inc., New York, 435pp (1963).

69 Nayak, M. and T.R.N. Kutty, **"Luminescence of Fe^{3+} Doped $NaAlSiO_4$ Prepared by Conversion"**, Materials Chem. And Phys. 57[2], 138-146 (1998).

70 Brookins, D.G., **"Geochemical Aspects of Radioactive Waste Disposal"**, Springer-Verlag: NY, 347pp (1984).

71 Thompson, J.G., R.L. Withers, A. Melnitchenko, and S.R. Paletthorpe, "Cristobalite-Related Phases in the $NaAlO_2$-$NaAlSiO_4$ System. I. Two Tetragonal and Two Orthorhombic Structures", *Acta Cryst.*, **1998**, *B54*, 531-546.

72 Thompson, J.G., R.L. Withers, A. Melnitchenko, and S.R. Paletthorpe, **"Cristobalite-Related Phases in the $NaAlO_2$-$NaAlSiO_4$ System. II. A Commensurately Modulated Cubic Structure"**, Acta Cryst. B54, 547-557 (1998).

73 Dana, E.S., **"A Textbook of Mineralogy"**, John Wiley & Sons, Inc., New York, 851pp (1932).

74 Klingenberg, R. and J. Felsche, **"Interstitial Cristobalite-type Compounds $(Na_2O)_{0.33}Na[AlSiO_4]$"**, J. Solid State Chemistry, 61, 40-46 (1986).

75 Mattigod, S.V., B.P. McGrail, D.E. McCready, L. Wang, K.E. Parker, and J.S. Young, **"Synthesis and Structure of Perrhenate Sodalite"**, J. Microporous & Mesopourous Materials, 91(1-3), 139-144 (2006).

76 Barrer, R.M. **"Hydrothermal Chemistry of Zeolites"**, Academic Press, New York, 360pp (1982): see references by St. J. Thugutt, Z. Anorg. Chem, 2, 65 (1892) and E. Flint, W. Clarke, E.S. Newman, L. Shartsis, D. Bishop and L.S. Wells, J. Res. Natl. Bur. Stds, 36, 63 (1945).

77 Srdanov, V.I., W.T.A. Harrison, T.E. Gier, and G.D. Stucky, **"Structure and Spectroscopy of Sodalite Containing MnO_4"**, Ions. Journal of Physical Chemistry B, 98, 4673-4676 (1994).

78 Buhl, J.Ch., G. Englehardt, and J. Felsche, **"Synthesis, X-ray Diffraction, and MAS N.M.R. Characteristics of Tetrahydroxoborate Sodalite"**, Zeolites, 9, 40-44 (1989).

79 Tobbens, D.M. and J.C. Buhl, **"Superstructure of Sodiumborate Sodalite"**, Berline Neutron Scattering Center (BENSC) Experimental Report E9, Helmholtz Zentrum fur Materialiene und Energie (formally the Hahn-Meitner Institute), Berlin, Germany (2000).

80 Depmeier, W., **"Structure of Cubic Aluminate Sodalite, $Sr_8[Al_{12}O_{24}](CrO_4)_2$"**, Acta Cryst., C43, 2251-2255 (1987).

81 Buhl, J.-C., T.M. Gesing, and C. Gurris, **"Synthesis and crystal structure of rhodanide-enclathrated sodalite $Na_8[AlSiO_4]_6(SCN)_2$"**, Microporous and Mesoporous Materials, 50, 25-32 (2001).

82 Campbell, B.J., J. Miguel Delgado, A.K. Cheetham, B.B. Iversen, N.P. Blake, S.R. Shannon, S. Satturner, and G.D. Stucky, **"The Cation-vacancy Ordering Transition in Dehydrated Na_6 Sodalite"**, Journal of Chemical Physics, 113[22], 10226-10239 (2000).

83 Shannon, S.R, B.J. Campbell, H. Metiu, and N.P. Blake, **"Cation-vacancy Ordering in Dehydrated $Na_6[AlSiO_4]_6$"**, Journal of Chemical Physics, 113[22], 10215-10225 (2000).

84 Fleet, M.E., **"Structures of Sodium Alumino-Germanate Sodalites"**, Acta Cryst., C45, 843-847 (1989).

85 Johnson, G.M., P.J. Mead, and M.T. Weller, **"Synthesis of a Range of Anion-containing Gallium and Germanium Sodalities"**, Microporous and Mesoporous Materials, 38, 445-460 (2000).

86 Peterson, R.C. **"The Structure of Hackmanite, A Variety of Sodalite, from Mont St-Hilaire, Quebec"**, Canadian Mineralogist, 21, 549-552 (1983).

87 Hassan, I. and H.D. Grundy, **"The Crystal Structures of Sodalite-Group Minerals"**, Acta Cryst. B40, 6-13 (1984).

88 Riley, B.J., M.J. Schweiger, D.S. Kim, W.W. Lukens, B.D. Williams, C. Iovin, C.P. Rodriguez, N.R. Overman, M.E. Bowden, D.R. Dixon, J.V. Crum, J.S. McCloy, and A.A. Kruger, **"Iodine Solubility in a Low-Activity Waste Borosilicate Glass at 1000°C"**, *J. Nucl. Mat.*, 452 [1-3], 178-188 (2014).

89 McKeown, D.A., H. Gan, I.L. Pegg, W.C. Stolte, and I.N. Demchenko, **"X-ray Absorption Studies of Chlorine Valence and Local Environments in Borosilicate Waste Glasses"**, J. Nucl. Materials, 408 [3], 236-245 (2011).

90 Lukens, W., McKeown, D.A. Buechele, A.C., Muller, I.S., Shuh, D.K, and I.L. Pegg, **"Dissimilar Behavior of Technetium and Rhenium in Borosilicate Waste Glass as Determined by X-ray Absorption Spectroscopy,"** Chemistry of Materials 19 [3], 559-566. (2007)

91 Liebau, F. **"Zeolites and Clathrasils – Two Distinct Classes of Framework Silicates"**, Zeolites, 3[7] 191-92 (1983).

92 Dickson, J.O., J.B. Harsh, W.W. Lukens, and E.M. Pierce, **"Perrhenate Incorporation into Binary Mixed Sodalites: The Role of Anion Size and Implications for Technetium-99 Sequestration,"** Chem. Geol., 395, 138-143 (2015).

93 Dickson, J.O., J.B. Harsh, M. Flurry, W.W. Lukens, and E.M. Pierce, **"Competitive Incorporation of Perrhenate and Nitrate into Sodalite,"** Environmental Sci. and Tech., 48, 12851-12867 (2014).

94 Tomisaka, T. and H.P. Eugster, **"Synthesis of the Sodalite Group and Subsolidus Equilibria in the Sodalite-Noselite System"**, Mineralogical Journal, 5, 249-275 (1968).

95 Trill, H., H. Eckert, and V.I. Srdanov, **"Mixed Halide Sodalite Solid Solution Systems. Hydrothermal Synthesis and Characterization by Solid State NMR"**, J. Phys. Chem. B, 107, 8779-8788 (2003).

96 Taylor, D. and C.M.B. Henderson, **"A Computer Model for the Cubic Sodalite Structure"**, Phys. and Chem. of Minerals, 2[4], 325-336 (1978).

97. P. Vulic, V. Kahlenberg, and J. Konzett, **"On the Exitence of a Na-deficient Monoclinic trinepheline with Composition $Na_{7.85}Al_{7.85}Si_{8.15}O_{32}$,"** Am. Min., 03, 1072-1079 (2008).

98 Jantzen, C.M. and C.L. Crawford, "**Mineralization of Radioactive Wastes by Fluidized Bed Steam Reforming (FBSR): Radionuclide Incorporation, Monolith Formation, and Durability Testing"**, Paper #10467 Waste Management 10, Phoenix, Arizona (2010).

99 Deer, W.A., R.A. Howie, and J. Zussman,**"Rock-Forming Minerals, Vol V, Non-Silicates"**, John Wiley & Sons, Inc., New York, 371pp. (1962).

100 Friak, M., A. Schindlmayr and M. Scheffler, **"Ab initio Study of the Half-Metal to Metal Transition in Strained Magnetite,"** New J. Phys., 9[1], Paper #5 (2007).

101 Jantzen, C.M. **"Fluidized Bed Steam Reforming of Organic and Nitrate Containing Salt Supernate"**, Environmental Issues and Waste Management Technologies X, J.D. Vienna, C.C. Herman, and S.L. Marra, Eds.; Ceramic Transactions 168, 68-79 (2005).

102 Jantzen, C.M. **"Disposition of Tank 48H Organics by Fluidized Bed Steam Reforming (FBSR)"**, U.S. DOE Report WSRC-TR-2003-00352, Westinghouse Savannah River Company, Aiken, South Carolina (September 18, 2003).

103 Soelberg, N.R., D.W. Marshall, S.O. Bates, and D.D. Taylor, **"Phase 2 THOR Steam Reforming Tests for Sodium Bearing Waste Treatment"**, INEEL/EXT-04-01493, Rev. 1, Idaho National Engineering and Environmental Laboratory, Idaho Falls, Idaho (2004).

104 Marshall, D.W., N.R. Soelberg, and K.M. Shaber, **"THOR^{sm} Bench-Scale Steam Reforming Demonstration"**, INEEL/EXT.03-00437, Idaho National Laboratory, Idaho Falls, Idaho (2003).

105 McGrail, B.P., E.M. Pierce, H.T. Schaef, E.A. Rodriques, J.L. Steele, A.T. Owen, and D.M. Wellman, **"Laboratory Testing of Bulk Vitrified and Steam-Reformed Low-Activity Forms to Support a Preliminary Assessment for an Integrated Disposal Facility"**, PNNL-14414, Pacific Northwest National Laboratory, Richland, Washington (2003).

106 Pierce, E.M., **"Accelerated Weathering of Fluidized Bed Steam Reformation Material under Hydraulically Unsaturated Conditions"**, Proceedings from Materials Science & Technology, September 16-20, 2007, Detroit, Michigan.

107 Mann, F.M., R.J. Puigh, R. Khaleel, S. Finfrock, B.P. McGrail, D.H. Bacon, and R.J. Serne, **"Risk Assessment Supporting the Decision on the Initial Selection of Supplemental ILAW Technologies"**, RPP-17675, Pacific Northwest National Laboratory, Richland, Washington (2003).

108 Olson, A.L., N.R. Soelberg, D.W. Marshall, and G.L. Anderson, **"Fluidized Bed Steam Reforming of Hanford LAW Using THOR[sm] Mineralizing Technology"**, INEEL/EXT-04-02492, Idaho National Laboratory, Idaho Falls, Idaho (2004).

109 Rassat, S.D. L.A. Mahoney, and R.L. Russell, **"Cold Dissolved Saltcake Waste Simulant Development, Preparation, and Analysis"**, PNNL-14194, Pacific Northwest National Laboratory, Richland, Washington (2003).

110 Olson, A.L., N.R. Soelberg, D.W. Marshall, and G.L. Anderson, **"Fluidized Bed Steam Reforming of INEEL SBW Using THOR[sm] Mineralizing Technology"**, INEEL/EXT-04-02564 Idaho National Laboratory, Idaho Falls, Idaho (2004).

111 Pareizs, J.M., C.M. Jantzen, and T.H. Lorier, **"Durability Testing of Fluidized Bed Steam Reformer (FBSR) Waste Forms for High Sodium Wastes at Hanford and Idaho"**, U.S. DOE Report, WSRC-TR-2005-00102, Savannah River National Laboratory, Aiken, South Carolina (2005).

112 Jantzen, C.M., J.M. Pareizs, T.H. Lorier, and J.C. Marra, **"Durability Testing of Fluidized Bed Steam Reforming (FBSR) Products"**, Ceramic Transactions, V. 176, C. C. Herman, S.L. Marra, D.R. Spearing, L. Vance, and J.D. Vienna, Eds.; 121-37 (2006).

113 Jantzen, C.M., T.H. Lorier, J.C. Marra, and J.M. Pareizs, **"Durability Testing of Fluidized Bed Steam Reforming (FBSR) Waste Forms"**, Paper #6373, Waste Management 06, Tucson, Arizona (2006).

114 Brunauer, S., P.H. Emmett, and E. Teller, **"Adsorption of Gases in Multimolecular Layers"**, Journal of Physical Chemistry, 60, 309-319 (1938).

115 Jantzen, C.M., **"Characterization and Performance of Fluidized Bed Steam Reforming (FBSR) Product as a Final Waste Form"**, Ceramic Transactions, Vol. 155, J. D. Vienna, and D.R. Spearing, Eds.: 319-29 (2004).

116 Jantzen, C.M., "**Fluidized Bed Steam Reformer (FBSR) Product: Monolith Formation and Characterization**", WSRC-STI-2006-00033, Savannah River National Laboratory, Aiken, South Carolina (2006).

117 Jantzen, C.M., **"Fluidized Bed Steam Reformer (FBSR) Monolith Formation"**, Paper #7075, Waste Management 07, Tucson, Arizona (2007).

118 Lorier, T.H., J.M. Pareizs, and C.M. Jantzen, **"Single Pass Flow through (SPFT) Testing of Fluidized Bed Steam Reforming (FBSR) Waste Forms"**, U.S. DOE Report WSRC-TR-2005-00124, Savannah River National Laboratory, Aiken, South Carolina (2005).

119 Jantzen, C.M., T.H. Lorier, J.M. Pareizs, and J.C. Marra, **"Fluidized Bed Steam Reformed (FBSR) Mineral Waste Forms: Characterization and Durability Testing"**, Scientific Basis for Nuclear Waste Management XXX, D. S. Dunn, C. Poinssot, and B. Begg, Eds.; 379-386 (2007).

120 Pierce, E.M., W.W. Lukens, J. Fitts, C.M. Jantzen, and G. Tang, **"Experimental Determination of the Sepeciation, Partitioning, and Release of Perrhenate as a Chemical Surrogate for Pertechnetate form a Sodalite-bearing Multiphase Ceramic Waste Form"**, Applied Geochemistry, 42, 47-59 (2014).

121 Crawford, C.L. and C.M. Jantzen, **"Durability Testing of Fluidized Bed Steam Reformer (FBSR) Waste Forms for Sodium Bearing Waste (SBW) at INL"**, U.S. DOE Report WSRC-STI-2007-00319, Savannah River National Laboratory, Aiken, South Carolina (2007).

122 THOR® Treatment Technologies, Project Number 29387, **"Report for Treating Hanford LAW and WTP SW Simulants: Pilot Plant Mineralizing Flowsheet,"** Document Number RT-21-002, Rev. 1 (April 2009).

123 Crawford, C.L. and C.M. Jantzen, **"Evaluation of THOR™ Mineralized Waste Forms (Granular and Monolith) for the DOE Advanced Remediation Technologies (ART) Phase 2 Project"**, U.S. DOE Report SRNL-STI-2009-00505, Savannah River Technology Center, Aiken, South Carolina (December 2011).

124 Jantzen, C.M., C.L. Crawford, P.R. Burket, W.E. Daniel, A.D. Cozzi, and C.J. Bannochie, **"Radioactive Demonstrations of Fluidized Bed Steam Reforming (FBSR) as a Supplementary Treatment for Hanford's Low Activity Waste (LAW) and Secondary Wastes (SW)"**, Paper #11593 Waste Management 11, Phoenix, Arizona (2011).

125 Evans, B., A. Olson, J.B. Mason, K. Ryan, C.M. Jantzen, and C.L. Crawford, **"Radioactive Bench Scale Reformer Demonstration of a Monolithic Steam Reformed Mineralized Waste Form for Hanford Waste Treatment Plant Secondary Waste"**, Paper #12306, Waste Management 12, February 2012, Phoenix, Arizona.

126. Neeway, J.J., N.P. Qafoku, B.D. Williams, M.M. Valenta, E.A. Cordova, S.C. Strandquist, D.C. Dage, and C.F. Brown, **"Single Pass Flow-Through (SPFT) Test Results of Fluidized Bed Steam Reforming (FBSR) Waste Forms used for LAW Immobilization"**, Paper #12252, Waste Management 12, February 2012, Phoenix, Arizona.

127 Crawford, C.L., P.R. Burket, A.D. Cozzi, W.E. Daniel, C.M. Jantzen, and D.M. Missimer, **"Radioactive Demonstration of Mineralized Waste Forms Made from Hanford Waste Treatment Plant Secondary Waste (WTP-SW) by Fluidized Bed Steam Reformation (FBSR)"**, U.S. DOE Report, SRNL-STI-2011-00331, Rev. 1, Savannah River National Laboratory, Aiken, South Carolina (2014).

128 Pires, R.P., J.H. Westsick, R.J. Serene, E.C. Golovich, M.M. Valenta, and K.E. Parker, **"Secondary Waste Form Screening Test Results - THOR® Fluidized Bed Steam Reforming Product in a Geopolymer Matrix"**, PNNL- 20551, Pacific Northwest National Laboratory, Richland, Washington (July 2011).

129 Jantzen, C.M., C.L. Crawford, P.R. Burket, C.J. Bannochie, W.E. Daniel, C.A. Nash, A.D. Cozzi, and C.C. Herman, **"Radioactive Demonstrations of Fluidized Bed Steam Reforming (FBSR) with Actual Hanford Low Activity Wastes: Verifying FBSR as a Supplemental Treatment"**, Paper #12317, Waste Management 12, February 2012, Phoenix, Arizona.

130 Neeway, J.J., N.P. Qafoku, C.F. Brown, and R.A. Peterson, **"Characterization and Leaching Tests of the Fluidized Bed Steam Reforming (FBSR) Waste Form for LAW Immobilization"**, Paper #14300, Waste Management 13, March 2013, Phoenix, Arizona.

131 Neeway, J.J., N.P. Qafoku, B.D. Williams, R. Kenton, M.E. Bowden, C.F. Brown, and E.M. Pierce, **"Performance of the Fluidized Bed Steam Reforming Product Under Hydraulically Unsaturated Conditions"**, Journal of Environmental Radioactivity, 131, 119-138 (2014).

132 Williams, B.D., J.J. Neeway, M.M. Valenta, M.E. Bowden, J.E. Amonette, B.W. Arey, E.M. Pierce, C.F. Brown, and N.P. Qafoku, **"Release of Technetium and Iodine from a Sodalite-Bearing Ceramic Waste Form in Dilute-Solution Conditions"**, Submitted to Applied Geochemistry 2015.

133 "**Flowsheet Basis and Assumptions Requirements Document**", 24590-WTP-RPT-PT-02-005, Rev.3, River Protection Project, Richland, Washington (June 30, 2005).

134 Binni, S., G. Balsmeier, K. Ryan, S. Rogers, and B. Mason, **"Update on Integrated Waste Treatment Unit (IWTU) Testing and Readiness for Start-up"**, Paper #14660, Waste Management 14, March 2014, Phoenix, Arizona.

135 Soleberg, N.R., D.M. Marshall, S.O. Bates, and D.D. Siemer,**"SRS Tank 48H Steam Reforming Proof-of-Concept Test Report"**, INEEL/EXT-03-01118, Rev 1, Idaho National Engineering and Environmental Laboratory, Idaho Falls, Idaho (May 2004).

136 THOR® Treatment Technologies, LLC, "**Pilot Plant Report for Treating Tank 48H Simulants Carbonate Flowsheet"**, Document Number 28927-RT-001 (May 2007).

137 U.S. Department of Energy, **"Hanford Immobilized Low-Activity Waste Performance Assessment: 2001 Version"**, DOE/ORP-2000-24, Office of River Protection, Richland, Washington (2001).

138 River Protection Project, **"Waste Acceptance Criteria for the Immobilized Low Activity Waste Disposal Facility,"** RPP-8402 CH2M Hill Hanford Group, Inc, Richland, WA, (July 2002 issued) and River Protection Project, **"Integrated Disposal Facility Waste Acceptance Criteria,"** RPP-8402, Rev 1, U.S. Department of Energy, Richland Operations Office, Richland, Washington (2005 draft not issued).

139 U.S. Nuclear Regulatory Commission, **"Technical Position on Waste Form (Revision 1)"**, U.S. NRC Low-Level Waste Management Branch Division of Low-Level Waste Management and Decommissioning (January 1991).

140 U.S. DOE Office of Environmental Restoration and Waste Management, **"Waste Acceptance Product Specifications for Vitrified High-Level Waste Forms"**, U.S. DOE Document EM-WAPS, Rev.0, Washington, DC (February 2003).

141 Borders, M.N., **"DWPF Waste Form Compliance Plan",** U.S. DOE Report WSRC-IM-91-116-0, Rev. 9, Savannah River Remediation, Savannah River Site, Aiken, South Carolina (June 2012).

142 Burbank, D.A., **"Waste Acceptance Criteria for the Immobilized Low-Activity Waste Disposal Facility"**, US DOE Report RPP-8401, CH2M HILL Hanford Group, Richland, Washington (May 2002).

143 Bibler, N.E., and J.K. Bates, **"Product Consistency Leach Tests of Savannah River Site Radioactive Waste Glasses"**, Scientific Basis for Nuclear Waste Management, XIII, V.M. Oversby, and P.W. Brown, Eds.; Materials Research Society, Pittsburgh, Pennsylvania, 327–338 (1990).

144 Bates, J.K., D.J. Lam, and M.J. Steindler, **"Extended Leach Studies of Actinide-Doped SRL 131 Glass"**, Scientific Basis for Nuclear Waste Management, VI, D.G. Brookins, Ed.; North-Holland, NY, 183–190 (1983).

145 Bibler, N.E. and A.R. Jurgensen, **"Leaching Tc-99 from SRP Glass in Simulated Tuff and Salt Groundwaters"**, *Scientific Basis for Nuclear Waste Management*, XI, M.J. Apted and R.E. Westerman, Eds.; Materials Research Society, Pittsburgh, Pennsylvania, 585–593 (1988).

146 Bradley, D.J., Harvey, C.O., and R.P. Turcotte, **"Leaching of Actinides and Technetium from Simulated High-Level Waste Glass"**, U.S. DOE Report PNL-3152, Pacific Northwest Laboratory, Richland, Washington (1979).

147 Fillet, S., J. Nogues, E. Vernaz, and N. Jacquet-Francillon, **"Leaching of Actinides from the French LWR Reference Glass"**, *Scientific Basis for Nuclear Waste Management*, IX, L.O. Werme, Ed.; Materials Research Society, Pittsburgh, Pennsylvania, 211–218 (1985).

148 Bazan, F., J. Rego, and R.D. Aines, **"Leaching of Actinide-doped Nuclear Waste Glass in a Tuff-Dominated System"**, Scientific Basis for Nuclear Waste Management, X, J. K. Bates and W. B. Seefeldt (eds.), Mat. Res. Soc., Pittsburgh, Pennsylvania, 447–458 (1987).

149 Vernaz, E.Y. and N. Godon, **"Leaching of Actinides from Nuclear Waste Glass: French Experience"**, Scientific Basis for Nuclear Waste Management, XV, C.G. Sombret, Ed.; Mat. Res. Soc., Pittsburgh, Pennsylvania, 37–48 (1992).

150 Ebert, W.L., S.F. Wolf, and J.K. Bates, **"The Release of Technetium from Defense Waste Processing Facility Glasses"**, Scientific Basis for Nuclear Waste Management, XIX, W.M. Murphy and D.A. Knecht, Eds., Mat. Res. Soc., Pittsburgh, Pennsylvania, 221–227 (1996).

151 McGrail, B.P., **"Waste Package Component Interactions with Savannah River Defense Waste Glass in a Low-Magnesium Salt Brine"**, Nuclear Technology, 75 [2] 168–186 (1986).

152 ASTM C1285, **"Standard Test Methods for Determinning Chemical Durability of Nuclear, Hazardous, and Mixed Waste Glasses and Multiphase Glass Ceramics: The Product Consistency Test (PCT)",** ASTM C1285-14, Annual Book of ASTM Standards, Vol. 12.02, West Conshohocken, Pennsylvania (2014).

153 ANSI/ANS-16.1, **"Measurement of the Leachability of Solidified Low-Level Radioactive Wastes by a Short Term Test Procedure"**, American National Standards Institute/American Nuclear Society, La Grange Park, Illinois.

154 DOE/ORP Contract with Bechtel National, Inc., **"Design, Construction, and Commissioning of the Hanford Tank Waste Treatment and Immobilization Plant"**, Contract Number DE-AC27-01RV14136, U.S. Department of Energy, Office of River Protection, Richland, Washington (December 2000).

155 ASTM C1663, "**Standard Test Method for Measuring Waste Glass Durability by Vapor Hydration Test"**, ASTM C1663-09), Annual Book of ASTM Standards, Vol. 12.02, West Conshohocken, Pennsylvania (2010).

156 Qafoku, N.P., J.H. Westsik, D.M. Strachan, M.M. Valenta, and R.P. Pires, **"Secondary Waste Form Down-Selection Data Package- Fluidized Bed Steam Reforming Waste Form"**, U.S. DOE Report PNNL-20704, Pacific Northwest National Laboratory, Richland, Washington (September 2011).

157 Environmental Protection Agency, **"Paint Filters Liquids Test – Physical and Chemical Methods"**, *SW-846*, Method 9095B, Rev. 2., U.S. Environmental Protection Agency, Washington, D.C. (2004)

158 U.S. Nuclear Regulatory Commission, **"Radionuclide Release from Slag and Concrete Waste Materials, Part I. Conceptural Models of Leaching from Complex Materials and Laboratory Test Methods"**, U.S. NRC Document No. NUREG/CR-7025 (March 2010).

159 ASTM C1308-10. **"Accelerated Leach Test for Diffusive Releases from Solidified Waste and a Computer Program to Model Diffusive, Fractional Leaching from Cylindrical Waste Forms"**, ASTM International, West Conshohocken, Pennsylvania (2010).

160 Chamberlain, F.D. and W.L. Ebert, **"REALM: A Speadsheet Calculator for Regression Analysis of Leaching Models",** ANL-13-DRAFT (in draft for ASTM C1308).

161 ASTM C39/C39M-10, **"Compressive Strength of Cylindrical Concrete Specimens"**, ASTM International, West Conshohocken, Pennsylvania (2010).

162 Pierce, E.M., K. Lilova, W. Lukens, A. Navrotsky, J. Fitts,C. Rawn, C.M. Jantzen, D.M. Missimer, and A. Huq, **"Structure and Thermochemistry of Perrhenate Sodalite and Perrhenate/Pertechnetate Guest-guest Sodalite,"** *Proc. Natl. Acad. Sci.* (submitted for publication).

163 DOE EM-31 Technology Development & Deployment (TDD) Program Task Plan, **"Fluidized Bed Steam Reformer Low-Level Waste Form Qualification,"** U.S. DOE Document No.: WP-5.2.1-2010-001 (October 2010).

164 Banning, D.L., **"Data Quality Objectives for Selecting Waste Samples for the Bench Steam Reformer Test",** RPP-47073, Washington River Protection Solutions, Richland, Washington (2010).

165 Bergmann, M. L., **"River Protection Project System Plan (System Plan 6) Modeling Case, SVF-2052"**, ArtOFF BEL Gen Sol-6.2-8.4r0-2010-10-20-at-13-26-22.xlsm, Washington River Protection Solutions, Richland, Washington (2011).

166 Robbins R.A., L.J. Johnson, K.D. Lokkins, J.B. Duncan, H.J. Huber, D.J. Swanberg, and L.E. Thompson, **"Sample Selection Process for Bench-Scale Steam Reforming Treatability Studies using Hanford Waste Samples"**, U.S. DOE Document RPP-48824, Washington River Protection Solutions, Richland, Washington (2011).

167 Burket, P.R., W.E. Daniel, C.A. Nash, C.M. Jantzen, and M.R. Williams, **"Bench-Scale Steam Reforming of Actual Tank 48 Waste"**, US DOE Report SRNL-STI-2008-00105, Savannah River National Laboratory, Aiken, South Carolina (September 2008)

168 Burket, P.R., W.E. Daniel, C.M. Jantzen, C.A. Nash, C.L. Crawford, M.R. Williams, and A.B. Barnes, **"Steam Reforming Technology Demonstration for the Destruction of Organics on Actual DOE Savannah River Site Tank 48H Waste"**, Paper #9138, Waste Management 09, Phoenix, Arizona (February 2009).

169 Gasper, K.A., K.D. Boomer, M.E. Johnson, G.W. Reddick, Jr., A.F. Choho, and J.S. Garfield, **"Recommendation for Supplemental Technologies for Potential Mission Acceleration,"** RPP-11261, CH2MHill Hanford Group Inc., Richland, Washington (July 2002).

170 "**Sample Selection Recommendations for Fluid Bed Steam Reforming Treatability Studies Using Hanford Low Activity Waste Underground Storage Tank Samples"**, RPP-RPT-47143, Washington River Protection Solutions, Richland, Washington (2010).

171 Grimm, R.E., **"Clay Mineralogy"**, McGraw Hill Book Co., New York, 384pp (1953).

172 Burket, P.R., J.C. Marra, J.M. Pareizs, and C.M. Jantzen, **"Evaluation of Fluidized Bed Steam Reforming (FBSR) Technology for Sodium Bearing Wastes From Idaho and Hanford Using the Bench-Top Steam Reformer (BSR),**" U.S. DOE Report WSRC-TR-2004-00560, Savannah River Technology Center, Aiken, South Carolina (2005).

173 Muan, A. and E.F. Osborn, **"Phase Equilibria Among Oxides in Steelmaking"**, Addison-Wesley Publishing Company, Inc., Reading, MA, 236 pp. (1965).

174 Seidel, C.M., **"Solubilization of Saltcake from Tanks 241-AN-103 and 241-SX-105 in Preparation for Shipment to Savannah River National Laboratory"**, WRPS-1002463, Washington River Protection Solutions, Richland, Washington (2010).

175 Baumann, E.W., **"Colorimetric Determination of Iron(II) and Iron(III) in Glass"**, Analyst, 117, 913-916 (1992).

176 Bullock, Jr., J.H., J.D. Cathcart, and W.J. Betterton, W.J., **"Analytical Methods Utilized by the United States Geological Survey for the Analysis of Coal and Coal Combustion By-products"**, US Geological Survey: Denver, CO (2002).

177 Teo, B.K. **"EXAFS: Basic Principles and Data Analysis"**, Springer-Verlag, New York, NY (1986).

178 Brown, G., G. Calas, G. Waychunas, and J. Petiau, **"X-ray Absorption Spectroscopy and Its Applications in Mineralogy and Geochemistry"**, in *Spectroscopic Methods in Mineralogy and Geology*, F. Hawthrone, Ed.; Mineralogical Society of America, Washington, DC (1988).

179 Koningsberger, D., and R. Prins, **"X-ray Absorption: Principles, Applications, Techniques of EXAFS, SEXAFS, and XANES"**, Wiley, New York, New York (1988).

180 Lukens, W., D. Shuh, N. Schroeder, and K. Ashley, **"Identification of Non-Pertechnetate species in Hanford Waste Tanks, Tc(1)-carbonyl Complexes"**, Environmental Science & Technology 38, 229-233 (2004).

181 Lukens, W., **"Evolution of Technetium Speciation in Reducing Grout"**, Environmental Science & Technology 39, 8064-8070 (2005).

182 McKeown, D.A., A.C. Buechele, W.W. Lukens, D.K. Shuh, and I.L. Pegg, **"Tc and Re Behavior in Borosilicate Waste Glass Vapor Hydration Tests"**, Environmental Science & Technology 41[2], 431-436 (2007).

183 McKinley, J., J. Zachara, J. Wan, D. McCready, and S. Heald, **"Geochemical Controls on Contaminant Uranium in Vadose Hanford Formation Sediments at the 200 Area and 300 Area"**, Hanford Site, Washington, Vadose Zone 6, 1004-1017 (2007).

184 Catalano, J., J. McKinley, J. Zachara, S. Heald, S. Smith, and G. Brown, **"Changes in Uranium Speciation Through a Depth Sequence of Contaminated Hanford Sediments"**, Environmental Science & Technology 40, 2517-2524 (2006).

185 Singer, D.M., J.M. Zachara, and G.E. Brown, Jr., **"Uranium Speciation as a Function of Depth in Contaminated Hanford Sediments - A Micro-XRF, Micro-XRD, and Micro- and Bulk-XAFS Study"**, Environmental Science & Technology 43, 630-636 (2009).

186 Lock, C., and G. Turner, **"A Reinvestigation of the Crystal Structure of Potassium Perrhenate"**, Acta Crystallographica, B31, 1764-1765 (1975).

187 Steefel, C.I. and P. Van Cappellen, **"A New Kinetic Approach to Modeling Water-Rock Interaction: The Role of Nucleation, Precursors, and Ostwald Ripening"**, Geochimica et Cosmochimica Acta, 54, 2657-2677 (1990).

188 Huang, W.H., **"Stabilities of Kaolinite and Halloysite in Relation to Weathering of Feldspars and Nepheline in Aqueous Solution",** Am. Min., 59, 365-371 (1974).

189 Icenhower, J.P., B.P. McGrail, W.J. Shaw, E.M. Pierce, P. Nachimuthu, D.K. Shuh, E.A. Rodriguez, and J.L. Steele, **"Experimentally Determined Dissolution Kinetics of Na-rich Borosilicate Glass at Far from Equilibrium Conditions: Implications for Transition State Theory"**, Geochimica et Cosmochimica Acta, 72, 2767-2788 (2008).

190 McGrail, B.P., W.L. Ebert, A.J. Bakel, and D.K. Peeler, **"Measurement of Kinetic Rate Law Parameters on a Na-Ca-Al Borosilicate Glass for Low-Activity Waste"**, Journal of Nuclear Materials, 249, 175-189 (1997).

191 McGrail, B.P., J.P. Icenhower, D.K. Shuh, P. Liu, J.G. Darab, D.R. Baer, S. Thevuthasen, V. Shutthanandan, M.H. Engelhard, C.H. Booth, and P. Nachimuthu, **"The Structure of Na_2O-Al_2O_3-SiO_2 Glass: Impact on Sodium Ion Exchange in H_2O and D_2O"**, Journal of Non-Crystalline Solids, 296, 10-26 (2001).

192 Pierce, E.M., L.R. Reed, W.J. Shaw, and J.P. Icenhower, **"Effect of Al/B Ratio on the Dissolution of Nepheline Glass, $Na_3(Al, B)_{1-4}Si_4O_{16}$"**, Geochimica et Cosmochimica Acta, 69, A781 (2005).

193 Pierce, E.M., L.R. Reed, W.J. Shaw, B.P. McGrail, J.P. Icenhower, **"Experimental Determination of the Effect of the Ratio of B/Al on Glass Dissolution Along the Nepheline ($NaAlSiO_4$)-Malinkoite ($NaBSiO_4$) Join,"** Geochimica Cosmochimica Acta, 74[9], 2634-2654 (2010).

194 Pierce, E.M., E.L. Richards, A.M. Davis, L.R. Reed, and E.A. Rodriguez, **"Aluminoborosilicate Waste Glass Dissolution Under Alkaline Conditions at 40 Degrees C: Implications for a Chemical Affinity-based Rate Equation"**, Environmental Chemistry 5, 73-85 (2008).

195 Lasaga, A.C., **"Fundamental Approaches in Describing Mineral Dissolution and Precipitation Rates"**, in Chemical Weathering Rates of Silicate Minerals, A.F. White, and S. Brantley, Eds.; Mineralogical Society of America, Washington, DC, 353-406 (1995).

196 McGrail, B.P., J.P. Icenhower, D.H. Bacon, H.T. Schaef, P.F. Martin, E.A. Rodriguez, and J.L. Steele, **"Low-Activity Waste Glass Studies: FY2001 Summary Report",** PNNL-13761, Pacific Northwest National Laboratory, Richland, Washington (2001).

197 Aagaard, P. and H.C. Helgeson, **"Thermodynamic and Kinetic Constraints on Reaction Rates Among Minerals and Aqueous Solutions, I. Theroretical Considerations"**, Amer. J. Sci., 282, 237-285 (1982).

198 Helgeson, H.C., W.M. Murphy, and P. Aagaard, **"Thermodynamic and Kinetic Constraints on Reaction Rates Among Minerals and Aqueous Solutions, II. Rate Constants, Effective Surface Area, and the Hydrolysis of Feldspar"**, Geochimica et Cosmochimica Acta, 48, 2405-2432 (1984).

199 Jantzen, C.M., F.C. Johnson, M.E. Stone, D.C. Koopman, J.R. Zamecnik, K.G. Brown, J.B. Pickett, and C.C. Herman, **"Melter REDuction/OXidation (REDOX) Control to Optimize Melting and Retain Radionuclides: Part I. High Level Waste Melter REDOX Requirements and Measurement"**, (submitted *International Journal of Applied Glass Science*).

200 Jantzen, C.M., **"Characterization of Off-Gas System Pluggages, Significance for DWPF and Suggested Remediation"**, U.S. DOE Report WSRC-TR-90-00205, Westinghouse Savannah River Company, Aiken, South Carolina (1991).

201 Schreiber, H.D. and A.L. Hockman, **"Redox Chemistry in Candidate Glasses for Nuclear Waste Immobilization"**, J. Am. Ceram. Soc., Vol. 70, No. 8, pp. 591-594 (1987).

202 Jantzen, C.M., J.B. Pickett and I. Joseph, **"Toxic Characteristic Leaching Procedure (TCLP) Testing of Waste Glass and K-3 Refractory: Revisited"**, Environmental Issues and Waste Management Technologies in the Ceramic and Nuclear Industries-V, G.T. Chandler, Ed.; Ceramic Transactions, V. 107, 271-280 (2000).

203 J. Vida, **"The Chemical Behavior of Technetium During the Treatment of High-Level Radioactive Waste"**, KFK 4642, Translated by J.R. Jewett, PNL-TR-497, Westinghouse Hanford Co. (1994).

204 H. Lammertz, E. Merz, and S.T. Halaszovich, **"Technetium Volatilization During HLLW Vitrification"**, Scientific Basis for Nuclear Waste Management, VIII, C.M. Jantzen, M.A. Stone, and R.C. Ewing, Eds.; Materials Research Society, Pittsburgh, Pennsylvania, 823-829 (1985).

205 Zamecnik, J.R., C.L. Crawford, and D.C. Koopman, **"Large-Scale Vitrification of 241-AN-107 (Envelope C) Sample"**, U.S. DOE Report WSRC-TR-2002-00093, Westinghouse Savannah River Company, Aiken, South Carolina (2002).

206 Kim, D.S., C.Z. Soderquist, J.P. Icenhower, B.P. McGrail, R.D. Scheele, B.K. McNamara, L.M. Bagaasen, M.J. Schweiger, J.V. Crum, D.J. Yeager, J. Matyáš, L.P. Darnell, H.T. Schaef, A.T. Owen, A.E. Kozelisky, L.A. Snow, and M.J. Steele, **"Tc Reduction Chemistry and Crucible Melting Studies with Simulated Hanford Low-Activity Waste"**, U.S. DOE Report PNNL-15131, Pacific Northwest National Laboratory, Richland, Washington (2005).

207 Matlack, K.S., H. Abramowitz, M. Brandys, I.S. Muller, R.A. Callow, N. D'Angelo, R. Cecil, I. Joseph, and I.L. Pegg, **"Technetium Retention in WTP LAW Glass with Recycle Flow-Sheet: DM10 Melter Testing"**, Vitreous State Laboratory and Energy Solutions Final Report VSL-12R2640-1 (June 18, 2012).

208 Schreiber, H.D., **"Redox State of Model Fluidized Bed Steam Reforming Systems Final Report Subcontract AC59529T"**, VMI Research Laboratories, VMI, Lexington, Virginian (2007).

209 EPA Test Method 1311, **"Toxicity Characteristic Leaching Procedure, TCLP**", U.S. Environmental Protection Agency (EPA), Washington, DC (2008).

210 Missimer, D.M. and R.L. Rutherford, **"Preparation and Initial Characterization of Fluidized Bed Steam Reforming Pure-Phase Standards"**, U.S. DOE Report SRNL-STI-2013-00111, Savannah River National Laboratory, Aiken, South Carolina (Febuary 2013).

211. Jantzen, C.M., P.R. Burket, A.R. Jurgensen, D.M. Missimer, and C.L. Crawford, **"Geopolymers: Low Temperature Waste Forms for Hazardous Wastes and Thermal Treatment"**, U.S. DOE Report SRNS-STI-2008-00127, Journal Am. Ceram. Soc. (in preparation) also U.S. DOE Slide Presentation WSRC-STI-2007-00584S (2007).

212 Hajimohammadi, A., J.L. Provis, and J.S.J. van Devente, **"Effect of Alumina Release Rate on the Mechanism of Geopolymer Gel Formation"**, Chemistry of Materials, 22, 5199–5208 (2010).

213 Pierce, E.M., R.J. Serne, W. Um, S.V. Mattigod, J.P. Icenhower, N.P. Qafoku, J.H. Westsik Jr, and R.D. Scheele, **"Review of Potential Candidate Stabilization Technologies for Liquid and Solid Secondary Waste Streams"**, U.S. DOE Report PNNL-19122, Pacific Northwest National Laboratory, Richland, Washington (2010).

214 Bunker, B.C., G.W. Arnold, D.E. Day, and P.J. Bray, **"The Effect of Molecular Structure on Borosilicate Glass Leaching"**, J. Non-Cryst. Solids, 87, 226-253 (1986).

215 U.S. DOE, **"Draft Tank Closure and Waste Management Environmental Impact Statement for the Hanford Site, Richland, Washington (TC & WM EIS)"**, Appendix M (October 2009).

216 Brown, G.E. Jr., F. Farges, and G. Calas, **"X-Ray Scattering and X-Ray Spectroscopy Studies of Silicate Melts"**, in Structure, Dynamics and Properties of Silicate Melts, J.F. Stebbins, P.F. McMillan, and D.B. Dingwell, Eds.; Reviews in Mineralogy, V.32, 317-410 (1995).

217 Burnham, C.W., **"The Nature of Multicomponent Aluminosilicate Melts"**, Phys. Chem. of the Earth, v13 & 14, 191-227 (1981).

218 Hellmann, R., C.M. Eggleston, M.F. Hochella, Jr., and D.A. Crerar, **"The Formation of Leached Layers on Albite Surfaces During Dissolution Under Hydrothermal Conditions"**, Geochim. Cosmochim. Acta, 54, 1267-1281 (1990).

219 Bourcier, W.L., **"Affinity Functions for Modeling Glass Dissolution Rates"**, U.S. DOE Report UCRL-JC-131186 prepared for the Atomic Energy Commisssion, Vallee due Rhone Summer Workshop: Glass: Scientific Research for High Performance Containment in Jejannes-le-Clap, France (1998).

220 Hamilton, J.P., S.L. Brantley, C.G. Pantano, L.J. Criscenti, and J.D. Kubicki, **"Dissolution of Nepheline, Jadeite, and Albite Glasses: Toward Better Models for Aluminosilicate Dissolution"**, Geochemica et Cosmochimica Acta, 65[21], 3683-3702 (2001).

221 Tsomaia, N., S.L. Brantley, J.P. Hamilton, C.G. Pantano, and K.T. Mueller, **"Solid State NMR Studies of Aluminate and Silicate Environments in Surface Layers of Leached Aluminosilicate Glasses and Crystals: Implications for Dissolution"**, Am. Min., 88, 54-67 (2003).

222 Li, H., Y. Su, J.D. Vienna, and P. Hrma, **"Raman Spectroscopic Study - Effects of B_2O_3, Na_2O, and SiO_2 on Nepheline ($NaAlSiO_4$) Crystallization in Simulated High Level Waste Glasses"**, Environmental Issues and Waste Management Technologies, V, G.T. Chandler and X. Feng, Eds.; Ceramic Trans. 107, 469-477 (2000).

223 Jantzen, C.M., K.G. Brown, and J.B. Pickett, **"Durable Glass for Thousands of Years"**, International Journal of Applied Glass Science, 1[1], 38-62 (2010).

224. Haaker, R.F. and R.C. Ewing, **"Naturally Occurring Crystalline Phases: Analogues for Radioactive Waste Forms",** U.S. DOE Report PNL-3505, Pacific Northwest Laboratory, Richland, Washington (January 1981).

225 DeLourdes, M., R. DaSilva, H. Conceicao, M.J.B. Macambira, M.A. Galarza, M.P. Cunha, R.C.L. Menezes, M.M. Marinho, B.E. DaCruz Filho, and D.C. Rios, **"Neoproterozoic Anorogenic Magmatism in the Southern Bahia Alkaline Province of NE Brazil: U–Pb and Pb–Pb Ages of the Blue Sodalite Syenites"**, Lithos, 97[1-2], 88-97 (2007).

226 Tole, M.P., A.C. Lasaga, C. Pantano, and W.B. White, "**The Kinetics of Dissolution of Nepheline ($NaAlSiO_4$)"**, Geochim. Cosmochim. Acta, 50(3), 379-392 (1986).

227 Jeong, S.-Y., L.R. Morss, and W.L. Ebert, **"Corrosion of Glass-Bonded Sodalite and Its Components as a Function of pH and Temperature"**, Sci. Basis for Nuclear Waste Mgt., XXV, B.P. McGrail and G.A. Cragnolino, Eds.; Mat. Res. Soc. Symp. Proc. 713, Pittsburgh, Pennsylvania, 413-420 (2002).

228 Morss, L.R., M.L. Stanley, C.D. Tatko, and W.L. Ebert, **"Corrosion of Glass-Bonded Sodalite as a Function of pH and Temperature"**, Sci. Basis for Nuclear Waste Mgt., XXIII, R.W. Smith and D.W. Shoesmith, Eds.; Mat. Res. Soc. Symp. Proc. 608, Pittsburgh, Pennsylvania, 733-738 (2000).

229 Morss, L., M. Lewis, M. Richmann, and D**.** Lexa, **"Cerium, Uranium, and Plutonium Behavior in Glass-bonded Sodalite, a Ceramic Nuclear Waste Form"**, Journal of Alloys and Compounds, 303-304, 42-48 (2002).

230 Lewis, M., W.L. Ebert, and L. Simpson, **"Comparison of the Corrosion Behaviors of the Glass-Bonded Sodalite Ceramic Waste Form and Reference HLW Glasses"**, Ceramic Transactions 107, American Ceramic Society, Westerville, OH, 281-288 (2000).

231 Blum, A. and L. Stillings, Eds., **"Feldspar Dissolution Kinetics. Chemical Weathering Rates of Silicate Minerals"**, Mineralogical Society of America, 31, Washington, DC, 291–351(1995).

232 Nugent, M., S.L. Brantley, C.G. Pantano, and P. Maurice, **"The Influence of Natural Mineral Coatings on Feldspar Weathering"**, Nature, 395[6702], 588–591 (1998).

233 Oelkers, E.H., **"General Kinetic Description of Multioxide Silicate Mineral and Glass Dissolution"**, Geochim. Cosmochim. Acta, 65[21], 3703–3719 (2001).

234 Oelkers, E.H., J. Schott, and J.L. Devidal, **"The Effect of Aluminum, pH, and Chemical Affinity on the Rates of Aluminosilicate Dissolution Reactions"**, Geochim. Cosmochim. Acta, 58[9], 2011–2024 (1994).

235 Oelkers, E.H. and J. Schott, Eds., **"Thermodynamic and Kinetics of Water Rock Interactions. Reviews in Mineralogy and Geochemistry,"** Mineralogical Society of America, 70, Chantilly, Virginia (2009).

236 Schott, J., O. Pokrovsky, and E.H. Oelkers, "**The Link Between Mineral Dissolution/Precipitation Kinetics and Solution Chemistry"**, in Thermodynamics and Kinetics of Water–Rock Interaction, Reviews in Mineralogy & Geochemistry, 70, E.H. Oelkers and J.Schott, Eds.; Mineralogical Society of America, Chantilly, Virginia, pp. 207–253 (2009).

237 Casey, W.H. and B.C. Bunker, **"Leaching of Mineral and Glass Surfaces During Dissolution"**, in "Mineral–Water Interface Geochemistry," M.F. Hochella, Jr. and A.F. White, Eds.; Mineralogical Society of America, Washington, DC, pp. 397–426 (1990).

238 Casey, W.H., H. Westrich, and G. Arnold, **"Surface Chemistry of Labradorite Feldspar Reacted with Aqueous Solutions at pH = 2, 3, and 12"**, Geochim. Cosmochim. Acta, 52, 2795–2807 (1988).

239 Banfield, J., G. Ferruzi, W.H. Casey, and H. Westrich, **"HRTEM Study Comparing Naturally and Experimentally Weathered Pyroxenoids"**, Geochim. Cosmochim.Acta, 59, 19–31 (1995).

240 Hellmann, R., J. Penisson, R. Hervig, J. Thomassin, and M. Abrioux, **"A EFTEM/HRTEM High Resolution Study of the Near Surface of Labradorite Feldspar Altered at Acid pH: Evidence for Interfacial Dissolution–Reprecipitation"**, Phys. Chem. Miner., 30, 192–197 (2003).

241 Hellmann, R., R. Wirth, D. Daval, J-P. Barnes, J-M. Pennisson, D. Tisserand, T. Epicier, B. Florin, and R.L. Hervig, **"Unifying Natural and Laboratory Chemical Weathering with Interfacial Dissolution–Reprecipitation: A Study Based on the Nanometer-scale Chemistry of Fluid-Silicate Interfaces"**, Chem. Geol., 294–295, 203–216 (2012).

242 Parkhurst, D.L. and C.A.J. Appelo, **"User's Guide to PHREEQC (Version 2): A Computer Program for Speciation, Batch-Reaction, One-dimensional Transport, and Inverse Geochemical Calculations"**, U.S. Geological Survey, Denver, Colorado (1999).

243 Pierce, E.M., B.P. McGrail, M.M. Valenta, and D.M. Strachan, **"The Accelerated Weathering of a Radioactive Low-activity Waste Glass Under Hydraulically Unsaturated Conditions: Experimental Results from a Pressurized Unsaturated Flow (PUF) Test"**, Nucl. Technol., 155(2), 133–148 (2006).

Appendix A. DOE EM-31 Technology Development & Deployment (TDD) Program Task Plan for Fluidized Bed Steam Reformer Low-Level Waste Form Qualification

DOE EM-31 Technology Development & Deployment (TDD) Program Task Plan	Document No.: WP-5.2.1-2010-001 Rev. No.: 0.0
Title: Fluidized Bed Steam Reformer Low-Level Waste Form Qualification	
Effective Date: Upon Final Signature	Page 1 of 113
Signatures:	

REVISION HISTORY

Revision Number	Interim Change No.	Effective Date	Description of Change
0	0	Upon final signature	Initial issuance.

Definitions/Acronyms

ART	Advanced Remediation technologies	PSD	Particle Size Distribution
BET	Brunauer, Emmett, and Teller	PSQAP	Project Specific Quality Assurance Plan
BSR	Bench scale reformer	QA	Quality Assurance
CSEMD	Contained Scanning Electron Microscopy	RCRA	Resource Conservation and Recovery Act
DI	Deionized water	REDOX	Reduction-Oxidation
DOE	U.S. Department of Energy	SAIC	Science Applications International Corporation
DWPF	Defense Waste Processing Facility	SAD	Selected Area Diffraction
EIS	environmental impact statement	SBW	Sodium Bearing Waste
FBSR	Fluidized Bed Steam Reforming	SPFT	Single Pass Flow Through
GCM	Glass Composite Material	SRNL	Savannah River National Laboratory
HRI	Hazen Research Inc.	SRS	Savannah River Site
HTF	high temperature filter	STAR	Science and Technology Applications Research
ICP-AES	inductively coupled plasma-atomic emission spectroscopy	TCLP	Toxic Characteristic Leaching Procedure
ICP-MS	inductively coupled plasma-mass spectroscopy	TDD	Technology Development and Deployment
IDF	Integrated Disposal Facility	TC&WM	Tank Closure and Waste Management
ILAW	Immobilized Low-Activity Waste	THOR	THermal Organic Reduction
JHCM	Joule Heated Ceramic Melters	TOC	Total organic carbon
LAW	Low-Activity Waste	TTT	THOR Treatment Technologies
LI	Leachability Index	USGS	United States Geological Survey
LLW	Low-Level Waste	VHT	Vapor Hydration Test
LOI	loss on ignition	VOC	Volatile Organic Compounds
NAS	sodium alumino-silicate	WDOE	Washington State Department of Ecology
OPC	ordinary portland cement	WFO	Work for Others
ORP	Office of River Protection	WIPP	Waste Isolation Pilot Plant
PA	Performance Assessment	WP	Waste Processing
PCT	Product Consistency Test	WTP	Waste Treatment and Immobilization Plant
PFA	perfluoroalkoxy	WTP SW	Waste Treatment and Immobilization Plant Secondary Waste
PNNL	Pacific Northwest National Laboratory	XRD	X-ray Diffraction
PR	product receipt		

TABLE OF CONTENTS

LIST OF TABLES

LIST OF FIGURES

1.0 Background

Resolution of the nation's high level tank waste legacy requires the design, construction and operation of large and technically complex one-of-a-kind processing waste treatment and vitrification facilities. Vitrification technology was chosen to treat the high-level waste (HLW) fraction of tank waste at Hanford and the Savannah River Site (SRS) and the low activity waste (LAW) fraction of tank waste at Hanford. Joule-Heated Ceramic Melters (JHCM) are being used at the Defense Waste Processing Facility (DWPF) and will be used at the Hanford Tank Waste Treatment and Immobilization Plant (WTP) to vitrify tank waste fractions. While the ultimate limits for waste loading and melter efficiency have yet to be defined or realized, significant reductions in glass volumes for disposal and mission life may be possible with advancements in melter technologies and/or glass formulations.

The need for advanced waste forms and processes was discussed in the National Research Council report "Advice on the Department of Energy's Cleanup Technology Roadmap: Gaps and Bridges," Waste Processing gap number 5 (WP-5): "The baseline tank waste vitrification process significantly increases the volume of high-level waste to be disposed." This report comments:

> *"Waste forms that include little or no added binder. Idaho calcine is one such example. Perhaps sintered or minimally bonded sludges could be developed for Hanford and SRS. Such work would probably rely heavily on computer modeling of waste and repository characteristics to show that they could meet their disposal requirements."*

The current site baselines include: 1) vitrification of the HLW fractions of tank wastes at Hanford and Savannah River for disposal at a Federal repository; 2) vitrification of the LAW fraction at Hanford for disposal at the Integrated Disposal Facility (IDF); 3) cementation of the LAW fraction at Savannah River; 4) fluidized bed steam reforming (FBSR) of the tank waste at INL for disposal at the Waste Isolation Pilot Plant (WIPP); 5) hot isostatic pressing of the calcined HLW at Idaho National Laboratory (INL); and, 6) treatment and disposal of various secondary low-level waste (LLW) at each site. These treatment options are reasonably proven technologies and those remaining technological gaps are being filled by site contracts. However, the disposal options are currently risky and may not be ideal. In addition there are likely more cost effective treatment/disposal options that should be considered to reduce risk and cost of tank cleanup in the U.S. This task explores one such option and develops the necessary technology to implement a promising waste form.

A FBSR facility is being designed and constructed at the INL for treatment of Sodium Bearing Waste (SBW) for potential disposal at the WIPP.[1,2] Another facility is being designed for the Savannah River Site to convert a salt supernate waste (Tank 48H) containing nitrates, nitrites, and organic cesium tetraphenyl borate, to carbonate minerals which are compatible with subsequent vitrification.[3] Pilot-scale facilities have also been used to produce aluminosilicate waste forms from simulants for Idaho's SBW[4] and Hanford's LAW[5,6] and LAW melter off-gas scrubber recycle (referred to as Waste Treatment Plant Secondary Waste, WTP SW).

The WTP is being constructed to treat most of Hanford tank wastes. However, the LAW will be generated at over twice the rate that the currently designed LAW vitrification facility can treat. Either a second LAW vitrification facility or other supplemental LAW treatment technology is needed to meet schedule objectives and approved tank closure deadlines. Based on the pilot scale testing described above, using FBSR to produce a sodium-aluminosilicate (NAS) waste form has been identified as a promising supplemental technology. The NAS waste form is primarily composed of nepheline (ideally $NaAlSiO_4$), sodalite (ideally $Na_8[AlSiO_4]_6Cl_2$), and nosean (ideally

$Na_8[AlSiO_4]_6SO_4$). Semi-volatile anions such as ReO_4^-, TcO_4^-, and I^- are expected to replace sulfate and chloride in the nosean-sodalite mineral structures – immobilizing them. The granular aluminosilicate FBSR products are appropriate for macro-encapsulation and study as final waste forms. Table 1.1 gives the pilot scale campaigns already tested at the Hazen Research Inc. (HRI) Engineering Scale Technology Demonstration (ESTD) for THOR Treatment Technologies (TTT) and at the Science Applications International Corporation/Science and Technology Applications Research (SAIC/STAR) facility. It is important to note that HRI ESTD is the TTT dual reformer flowsheet using autocatalytic heating with coal as a reductant, whereas SAIC/STAR facility was a single externally heated reformer flowsheet that used sugar as a reductant.

The release of semi-volatile radionuclides ^{99}Tc and ^{129}I from granular NAS waste form was assumed, based upon the available results, to be by preliminary performance test to be limited by nosean solubility[7]. The predicted performance of the NAS waste form was found to be equivalent or better than the glass waste form in the initial supplemental LAW treatment technology risk assessment as shown in Figure 1.1. There is uncertainty in the curves shown in Figure 1.1, therefore the results shown must be used with caution.

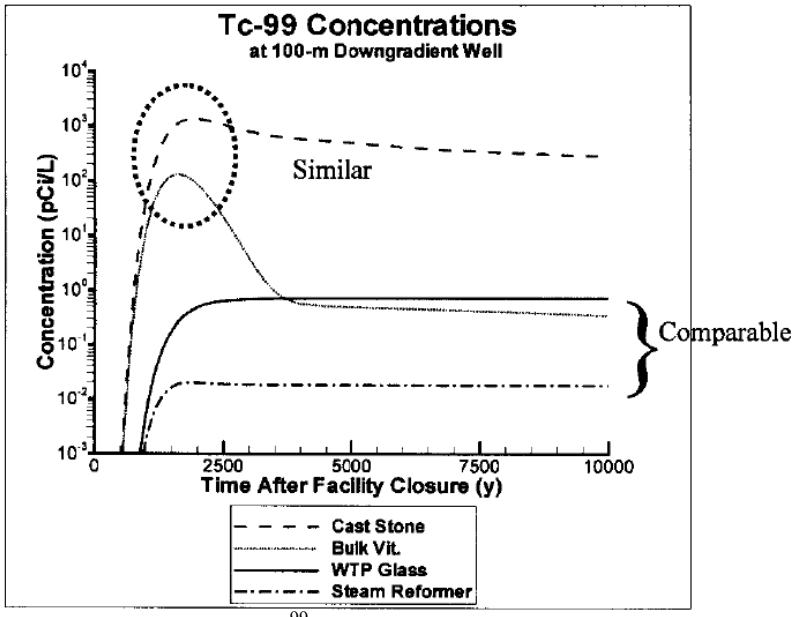

Figure 1.1. Comparison of ^{99}Tc Concentration in a Well 100 m Downgrade of the IDF as a Function of Time. See Mann et al. (2003) for additional details[7].

Table 1.1. Sources of Non-Radioactive FBSR Granular/Monolith Product Durability of Relevance to Performance Assessment

Pilot Scale Facility	Date of Pilot Scale Run	FBSR Diameter	Acidic and Basic Wastes	Granular PCT Testing	TCLP Granular Form	Granular SPFT Testing	Preliminary Performance Assessment	Product Tested	Coal	PSD	Monolith	Monolith PCT Testing	Monolith SPFT Testing	Monolith ASTM 1308 Testing	TCLP of Monolithic Form
HRI/ TTT	12/01	6”	LAW Env. C	Ref [8]	Ref [8]	Ref [9,10] also PUF testing	Ref [7]	Bed	Removed By Hand	Gaussian	No	N/A	N/A	N/A	N/A
HRI/ TTT	12/01	6”	LAW Env. C	Ref [9,10,11]	Ref [9,10,11]	None	None	Fines	Removed by 525°C Roasting	Gaussian	No	N/A	N/A	N/A	N/A
SAIC/ STAR	7/03	6”	SBW	Ref [9,10,11]	Ref [9,10,11]	None	None	Bed	Removed by 525°C Roasting	Gaussian	Yes (Samples were combined; 20% LAW, 32 % SBW and 45% Startup Bed	Ref [12,13]	No	No	No
SAIC/ STAR	8/04	6”	LAW Env. A	Ref [9,10,11]	Ref [9,10,11]	Ref [14,11,15] also PUF Testing	This study using data from Ref [14,11,15]	Bed and Fines Separate	Removed by 525°C Roasting	Gaussian			No	No	No
SAIC/ STAR	7/04 and 11/04	6”	SBW	Ref [9,10,11]	Ref [9,10,11]	Ref [14,11]	None	Bed and Fines Separate	Removed by 525°C Roasting	Gaussian			No	No	No
HRI/ TTT	12/06	15”	SBW	Ref [4]	Ref [4]	None	None	Bed and Fines Separate	Removed by 525°C Roasting	Gaussian	No	N/A	N/A	N/A	N/A
HRI/ TTT	2008	15”	LAW Env. A	Ref [3]	Ref [3]	This study	This study	Bed and Fines Together	Not removed	Bi-Modal	This Study, Partially Complete	This study	This study	This study	This study
HRI/ TTT	2008	15”	WTP-SW (melter recycle)	SRNL 2008 ART’s WFO	SRNL 2008 ART’s WFO	None	None	Bed and Fines Together	Not removed	Bi-Modal	Yes	SRNL 2008 ART’s WFO	None	PNNL Secondary Waste Form Testing Project	SRNL 2008 ART’s WFO

FBSR – Fluidized Bed Steam Reformer
PCT – product consistency test method
TCLP – toxic characterization leachate procedure
SPFT – single pass flow-through test method
PSD – particle size distribution
ASTM 1308 – monolith emersion test
HRI/TTT – Hazen Research Inc/THOR Treatment Technologies
SAIC/STAR – Science Applications International Corporation/Science and Technology Applications Research
LAW Env. – low activity waste envelope A, B, and C
SBW – sodium bearing waste
N/A – not applicable
SRNL – Savannah River National Laboratory
PNNL – Pacific Northwest National Laboratory
RL – Richland Operations
ART WFO – Advance Remediation Technologies Work for Others contract
Ref. – references
-3-, 4-, [8]Jantzen, C.M. (2004), [9]McGrail et al. (2003), [10]McGrail et al. (2003), [11]Pareizs et al (2005), [12]Jantzen et al. (2005), [13]Jantzen et al. (2006), [14]Jantzen (2006), [15]Jantzen (2007), [16]Lorier et al. (2005), [17]Jantzen et al. (2007), [18]Jantzen and Crawford (2010), [19]Jantzen (2008), and [16]Pierce et al. (2007).

In this Task Plan, FBSR is a proposed treatment method for Hanford LAW. If successful, it is anticipated that FBSR product would reduce the treatment costs and waste volumes at increased waste throughput. FBSR granular waste forms have been developed for several Hanford LAW waste streams (Envelope A and Envelope C)[5,6] and data has been generated on the granular waste form to demonstrate preliminary acceptance in the IDF[1,2 ,3,4,5,6,12,13,17,8]. This data has been partially summarized in Pareizs et al.[9]. As part of this work, a preliminary performance assessment will be generated based on all the pertinent data summarized in Pareizs et al.[9] and a white paper produced summarizing all previous and current leaching results and their impact on acceptance of the granular FBSR waste form in the IDF. Additionally a treatability study will be performed in the SRNL Benchscale Steam Reformer (BSR) using three actual Hanford tank waste samples to demonstrate the range of Hanford LAW to be treated by FBSR (representing the middle 80% of the total LAW feed relative to the anions and eliminates the outliers). The data resulting from the demonstration test program will be used to support the IDF performance assessment and decisions regarding deployment of a non-vitrification technology to immobilize LAW. Prior to performing tests with actual Hanford LAW, two tests with a radioactive SRS secondary waste sample from DWPF that is compositionally adjusted to reflect the expected composition of a Hanford WTP secondary waste and a SRS LAW shimmed to be compositionally the same as the 68 tank blend waste simulant[18,19] recently tested in 2008 at TTT's Engineering Scale Technology Demonstration (ESTD) Facility in Golden, CO will be performed. The SRS LAW test will provide the earliest scientific data regarding waste form leachability and the fate of ^{99}Tc in the mineral phase waste form. This data and resulting analysis will be used to ~~"m~~minimize" technical risk regarding waste form performance to support critical decisions associated with enhanced tank waste strategy at Hanford for the deployment of the FBSR transformational technology."

These granular products from the treatability studies will be subjected to the same regulatory and performance testing protocols as the nonradioactive tests given in Table 1.1, while some of the residual granular product will be monolithed for further testing.

Table 1.2. List of Bench-Scale Reformer Test to be Performed on Radioactive LAW and WTP Secondary Waste

Test Sequence	Test ID	Source of Radioactive Waste
#1	Secondary Waste Sample	Chemical shim SRS secondary waste sample from DWPF to resemble Hanford WTP SW
#2	SRS LAW Sample	Chemical shim SRS LAW to resemble Hanford LAW based upon 68 tank blend
#3	Hanford LAW Sample #1 (high S, Cl, F, and P)	Hanford Tank SX105
#4	Hanford LAW Sample #2 (low S, Cl, F, and P)	Hanford Tank AN103
#5	Hanford LAW Sample #3 (Complexants)	Hanford Tank AN107 – tentatively as of 08/26/2010

Ordinary portland cement (OPC), hydroceramics and Ceramicrete were tested in 2006 with a mixture of LAW Envelope A and SBW wastes[12,13]. In 2007-2009, seventeen different monolith matrices were made at the 2"×2" scale with FBSR granular product loadings between 63-85 wt % on a dry basis. These included 3 high alumina cement matrices at 2 different waste loadings, one OPC at 2 different waste loadings, 6 geopolymers made from kaolin clay and sodium silicate, 1 geopolymer (GEO-7) made from fly ash and NaOH, a NuCap material, and a Ceramicrete (CER) formulation at 2 different waste loadings[20]. In addition, preliminary scoping monolith preparation testing was performed using the L-TEM geopolymer with waste loadings of >80% on a dry basis. Three formulations were selected from these seventeen matrices based on a combination of optimized durability and

compressive strength. These three formulations were scaled up to 3"x6" and 6"x12" monoliths which were subjected to additional testing. GEO-7 was chosen as the most compatible benign binder tested, i.e., a binder that would not have deleterious impacts on the FBSR mineral phases encapsulated. Although Product Consistency Tests (PCTs) and Toxic Characteristic Leaching Procedure (TCLP) test were performed, few tests relevant to the long-term performance are available to determine the impacts of the process of making a monolith on the long-term performance of the NAS waste form produced by FBSR.

The key challenge with monolithic FBSR waste forms is the generation of sufficient data to demonstrate its acceptable performance in the IDF. An additional binder, a low temperature glass, is to be formulated for comparison. The waste form development and performance testing and collection of the pertinent data for performance assessment modeling will be performed under this task.

GEO-7 and potentially up to two additional binders matrices (e.g., GEO-1 and L-TEM) will be evaluated based upon the recent work conducted at SRNL. After evaluating this data, one binder matrix will be used for the preparation of monoliths of all the radioactive FBSR granular products. The monoliths will be tested with the durability tests and the necessary data generated for the Hanford IDF PA.

2.0 Objectives

The ability to demonstrate acceptable performance for FBSR product after being disposed in a near-surface burial facility is still faced with a number of key uncertainties. The goal of this Task Plan is to reduce the risk associated with implementing this technology as a supplemental LAW treatment by addressing the remaining the technical uncertainties. The information produced as part of this Task Plan will provide data and updated models which will be required to demonstrate the performance of the FBSR NAS waste form. The results from the updated models are needed to support the schedule for supplemental technology decision under the *Hanford Federal Facility Agreement and Consent Order (Tri-Party Agreement) Proposed Consent Decree and Tri-Party Agreement Modifications for Public Comment:*

> *M-062-40: …Not later than the System Plan Report due date of 10/31/2014, DOE will submit a one-time Hanford Tank Waste Supplemental Treatment Technologies Report, which will be required if a tank waste supplemental treatment technology is proposed, other than a 2nd LAW Vitrification Facility. …*
>
> *M-062-45: … 3. Supplemental treatment selection (a one time selection to be made not later than April 30, 2015) and milestones, which must be consistent with M-062-00 as established by M-062-45 item #5. A 2nd LAW Vitrification Facility must be considered as one of the options. *Milestones M-062-31-T01 through M-062-34-T01 are initially set as target dates and will be established (as may be modified) as interim milestones when they are converted to interim milestones in accordance with applicable HFFACO procedures at the conclusion of this negotiation. …*

A plan was developed to generate these data and models as part of the Tank Waste R&D Plan. The plan targets an early, technically defensible, evaluation of the FBSR process and the NAS monolithic waste form for Hanford LAW followed by a complete waste form source term model required for IDF performance assessment. The early evaluation will support a supplemental waste form down selection as early as possible with low risk upon receipt of the final risk assessment.

The task supports the application of FBSR as a supplemental Hanford LAW treatment option. This is a high-risk, high-benefit approach. The primary programmatic objective is to develop performance testing data on the geopolymer encapsulated FBSR waste forms and one additional FBSR waste form binder (glass) to generate the data necessary to demonstrate to the state of Washington that FBSR can produce a product that meets all regulatory constraints and is —..as good as glass…". It is believed that with this research the predicted release may be reduced (by a combination of improved waste form and improved knowledge of waste form performance). Demonstrating that the Hanford LAW FBSR waste form can meet the regulatory requirements is the necessary first step toward application of FBSR to Hanford LAW.

The primary programmatic objective is to develop performance testing data on the geopolymer encapsulated FBSR waste forms and one additional FBSR waste form binder (glass) to demonstrate acceptable performance in the IDF. Data required for such an assessment includes (but not limited to) determining an acceptable waste loading that provides the need performance while minimizing the volume of waste being produced and meeting the IDF product performance requirements (compressive strength and leach testing).

The logical steps to validate and confirm the corrosion behavior of materials whose life expectancies must greatly exceed the length of time over which experimental data can be obtained has been outlined in ASTM C1174 (2008). This procedure describes test methods and data analyses used to develop models for the prediction of the long-term behavior of materials, such as engineered barrier system (EBS) materials and waste forms, used in the disposal of waste forms in shallow subsurface disposal facility or a geologic repository. The alteration behavior of waste form and EBS materials is important because it affects the retention of radionuclides by the disposal system. The waste form and EBS materials provide a barrier to release either directly (as in the case of waste forms in which the radionuclides are initially immobilized), or indirectly (as in the case of containment materials that restrict the ingress of groundwater or the ingress of radionuclides that are released as the waste forms and EBS materials degrade). The logical steps include:

- Determining the likely range of environmental factors in the disposal system
- Identifying and characterizing materials that are likely to be present in the disposal system
- Performing tests under site-relevant conditions to determine important alteration processes for those materials
- Developing models for key alteration processes
- Performing tests that accelerate those processes.

The ASTM protocol also recommends tests to confirm the corrosion model and to use information provided by analog materials or systems. The technical strategy designed in this Task Plan is designed to answer the logical steps discussed above. The ASTM C1174 (2008) standard does not purport to address all of the safety concerns, if any, associated with its use.

3.0 Success Criteria

The success criterion for this task is to develop data and models necessary to provide data on the FBSR product necessary to support the Decision Point to Proceed with supplemental treatment. Activities described in Section 4 are planned to support this objective. The activities are designed to:

1. Characterize FBSR product from the HRI/TTT P1-B runs blended bed and fines products made from the Hanford Rassat (68 tank blend) simulant.

2. Make a similar Hanford Rassat (68 blend) radioactive LAW from SRS LAW with Tc, I, Cs, and Re. If the samples do not have sufficient ^{99}Tc and ^{129}I for spectroscopic measurements, namely XAS, additional ^{99}Tc and I (either as stable I or ^{129}I) will be added to a level equivalent to 150 μg/g in the final monolithic waste form.

3. Receive three Hanford LAW samples, a low anion, a high anion, and a complex waste sample. If the samples do not have sufficient ^{99}Tc and ^{129}I for spectroscopic measurements, namely XAS, additional ^{99}Tc and I (either as stable I or ^{129}I) will be added to a level equivalent to 150 μg/g in the final monolithic waste form.

4. Determine the speciation of ^{99}Tc and potentially ^{129}I in the FBSR product and the distribution of ^{99}Tc and ^{129}I amongst the different mineral phases. The speciation refers to oxidation state and nearest neighbor which requires the use of X-ray absorption spectroscopy (XAS). Selected area X-ray diffraction (XRD)/micro-XRD and electron microscopy of the Tc and I loaded material are also required. When combined with other data, these results will determine where Tc and I is located in the waste form. Contained Scanning Electron Microscopy (CSEM) will also be performed.

5. Determine the mass balance of ^{99}Tc and ^{129}I in the BSR system.

6. FBSR granular and monolith product passes the Toxic Characteristic Leaching Protocol (TCLP) on both the nonradioactive and radioactive.

7. Develop XRD calibration curves to determine relative range of mineral percentages. This activity will provide the basis for partitioning the product into the separate mineral assemblages.

8. Use XRD to determine the fractions of the minerals formed by FBSR. This will be performed on multiple different samples – primarily simulated waste samples but with confirmatory tests with actual LAW samples.

9. Develop dissolution rate law parameters for each significant phase in the waste form. Using SPFT testing to isolate individual rate law parameters along with selected tests for multi-phase waste forms (primarily Re containing, with selected Tc containing measurements to demonstrate Tc release is equivalent to Re-release). Additional tests will be needed to determine the phases formed during reaction with water. Thermodynamic parameters of key individual phases are needed.

10. Prepare monolithic waste forms containing mineralized FBSR product.

11. Perform x-ray diffraction (XRD) analysis on monolithic waste forms.

12. Demonstrate that the binder used for monolithic waste form does not significantly impact the release/dissolution behavior. This will require the use of SPFT experiments under dilute conditions of the binder with and without FBSR product.

13. Determine the transport properties of the monolithed waste form. This will be performed by diffusion tests such as ASTM C1308. These tests need to be performed for a number of samples

including Re-loaded simulants and actual waste samples containing Tc.

14. Determine the effect of Al, Si, and nepheline saturated solutions on Re and Tc release from the FBSR product. This will be used to quantify impact of the Al buffering effect seen in preliminary tests. This is mostly associated with the common ion effect and must be quantified so it can be accounted for in the source term model.

15. A modified waste form release/radionuclide source term model must be developed and validated for inclusion in the IDF performance assessment code. This source-term model will start with that developed by McGrail et al. 2003, but, include: a) the release rates for each phase, b) updated thermodynamic data for solid solution phases, c) common ion effect seen in preliminary experiments, d) transport properties measured in monolith samples, and e) Tc and I partitioning between phases in the waste form.

The primary milestones for this project are shown in Table 3.1.

Table 3.1. Primary Milestones for the Fluidized Bed Steam Reformer Low-Level Waste Form Qualification Project (WP- 5.2.1)

Milestone Number	Milestone	Organizations (lead)	Target Date*
5.2.1-01	Issue test plan for waste form qualification	(SRNL), PNNL	05/15/2010
	Regulatory Memorandum of Understanding Signed and Concurrence Received from WA and SC State Regulatory Agencies	WRPS/SRNL	09/2010
	Complete Secondary Waste Test Operations	SRNL/TTT	11/2010
	Complete SRS LAW Test	SRNL	12/2010
	Determine ^{99}Tc and ^{129}I mass balance in BSR for SRS LAW Test	SRNL	12/2010
5.2.1-02	Issue performance modeling strategy document	SRNL, PNNL	12/31/2010
Out Years			
--	Complete 1st actual Hanford LAW test (high S, Cl, F, P)	SRNL	02/2011[21]
--	Complete 2nd actual Hanford LAW test (low S, Cl, F, P)	SRNL	03/2011[21]
--	Complete 3rd actual Hanford LAW test (other)	SRNL	05/2011[21]
5.2.1-03	Complete advanced FBSR waste form characterization in support of CD-1 package	SRNL/PNNL	09/30/2011
	Submit Draft CD-1 to ORP	WRPS	09/30/2011
--	Preliminary data available to support M-62-40 System Plan Report	SRNL, PNNL	01/2012[21]
--	Preliminary data available to support M-62-45 Supplemental Treatment Selection	SRNL, PNNL	04/2012[21]
5.2.1-04	Complete performance testing/source term modeling for advanced waste form	SRNL, PNNL	10/17/2013
5.2.1-05	Complete independent technical review	DOE	12/30/2013
5.2.1-06	Decision point to proceed with FBSR	DOE	01/30/2014
*Target dates are based upon the availability of funding and meeting the regulatory requirements for shipping and receiving the Hanford LAW samples.			

4.0 Materials/Methods

4.1. Individual Phases of FBSR Products

X-ray diffraction analyses of the NAS waste form produced with simulated Hanford LAW has been shown to be composed of three framework silicate phases, nepheline (ideally $Na_3[Al_4Si_4O_{16}]$), nosean (ideally $Na_8[Al_6Si_6O_{24}]SO_4$), and sodalite (ideally $Na_8[Al_6Si_6O_{24}]Cl_2$, $Na_8[Al_6Si_6O_{24}]F_2$, $Na_8[Al_6Si_6O_{24}]I_2$, and $Na_8[Al_6Si_6O_{24}]ReO_4$). In the FBSR waste form, each of these phases can exist in a variety of solid solutions from the idealized forms observed in nature. Currently because of the lack of understanding of the weathering of these primary mineral phases, it complicates our ability to simulate the weathering of the FBSR product. Individual phases of the phase assemblage of the FBSR product will be prepared by ceramic processing methods, obtained from commercial vendors, or produced using hydrothermal methods. XRD analysis will be used to confirm the products to be phase pure. Develop quantitative XRD calibration curves, single-pass flow-through testing, and develop thermodynamic data for the pure phase materials.

4.2. NonRadioactive Simulant

Product from the Hazen Research Inc. (HRI) FBSR runs of Hanford Envelope A LAW simulant test P1B blended 1:4 (Product Receiver (PR):High Temperature Filter (HTF)) screened at one millimeter will be used for all testing conducted on simulated samples. The >1 mm fraction is >95% coal, this material will be removed from the product for a significant portion of the regulatory testing and performance testing discussed in this Task Plan. The purpose for removing the coal is because of the potential influence coal can have on understanding the key chemical and physical processes that control radionuclide release. Additional experiments will be conducted with both granular and monolith product in the presence of coal to quantify the effect of coal on contaminant release. Furthermore, a sample of the greater and less than 1-mm size fractions of coal will be analyzed using a variety of digestion techniques, specific to the contaminant or radionuclide of interest, to determine the chemical composition of the material before and after being run through the FBSR process. The goal of these analyses will be in support of the mass balance and determining the location of key contaminants in the FBSR product. The P1B material has been used to prepare geopolymeric waste forms[22]. The composition of the material from the HRI/TTT run ID P1B is compared to the composition of other FBSR products made from Simulated Hanford LAW in Table 4.1. The blended FBSR product will be characterized chemically and physically to provide a baseline to determine the effects of the formation of a monolith on the properties of the product.

Table 4.1. Composition of LAW Tested in This Study Compared to 2002 and 2004

	Component	[a,b]P1 A and B (LAW Envelope A @ HRI 2008) Rassat simulant (68 tank blend) mol/L	[c]AN-1073[18] (LAW Envelope C - @ HRI 2001) Rassat simulant (68 tank blend) mol/L	[b]LAW Envelope A @ SAIC/STAR (2004) mol/L
Oxalate	C_2O_4	0.0118	0.0704	0.0118
Acetate	CH_3COO	0.132	0.11938	0.132
Hydroxide	OH	0.74	2.69125	0.739
Carbonate	CO_3	0.475	0.9007	0.475
Sulfate	SO_4	0.09	0.0828	0.09
Chloride	Cl	0.0438	0.0394	0.0438
Fluoride	F	0.0316	0.13258	0.0316
Iodide	I	0.013	---	0.000134
Nitrite	NO_2	0.424	1.00289	0.424
Phosphate	PO_4	0.0492	0.0052	0.0492
Aluminum	Al	0.0637	0.32	0.0637
Potassium	K	0.0124	0.04	0.0124
Sodium	Na	5.0161	8.2955	5.0014
Nitrate	NO_3	2.58487	3.1941	2.31
Silver	Ag	0.00161	---	---
Arsenic	As	0.00137	---	---
Barium	Ba	0.00751	---	---
Cadmium	Cd	0.0042	---	---
Chromium	Cr	0.0104	0.0055	0.0104
Cesium	Cs	0.013	0.0001	0.00000051
Nickel	Ni	0.0106	0.0079	---
Lead	Pb	0.00606	0.0014	---
Rhenium	Re	0.0017	0.0000047	0.0003953
Antimony	Sb	0.00434	---	---
Selenium	Se	0.00123	---	---
Thallium	Tl	0.00202	---	---
Ammonium	NH_4	--	---	---
Calcium	Ca	--	0.0107	---
Iron	Fe	--	0.0464	---

[a]Resource Conservation and Recovery Act (RCRA) metals (Sb, As, Ag, Cd, Ba, and Tl) and radionuclide surrogates (Re, I, Cs) were doped in at 10-1000X

[b]LAW simulant used to produce the FBSR samples were based on Rasat et al. (2003)[18]

[c]Total Total organic carbon (TOC) 3.21 moles includes $Na_2EDTA.2H_2O$ where EDTA=$C_{10}H_{16}N_2O_8$, $Na_3HEDTA.2H_2O$, Sodium Acetate - $NaCH_3COO$, Sodium Formate NaCOOH, Sodium Oxalate - $Na_2C_2O_4$, Sodium Gluconate- $NaC_6H_{11}O_7$, Glycolic Acid - $C_6H_4O_3$, Nitrilotriacetic Acid - $C_6H_9NO_6$, Citric Acid - $C_6H_8O_7$ and Iminodiacetic Acid - $C_4H_4NO_4$

4.3. Radioactive Waste

Five radioactive test BSR runs will be conducted as part of this task plan. These include: one sample of DWPF recycle into WTP SW, one sample of chemically modified SRS LAW to resemble Hanford LAW, and three actual Hanford LAW samples. The first radioactive sample that will be produced will be in support of the Hanford secondary waste testing program. All of the remaining radioactive samples that will be produced using the BSR will resemble Hanford LAW. The first LAW sample to be produced will be a LAW from SRS that is chemically adjusted to reflect the composition of Hanford LAW blend per PNNL-14194[23], Rev 1, Table 3.1, and the composition of the nonradioactive simulant used in the 2008 Engineering-Scale Technology Demonstration (ESTD) test previously performed (see Table 4.1 in this document). Testing with a radioactive LAW that reflects this 2008 ESTD composition will allow for a direct comparison of the data of the radioactive BSR testing with the nonradioactive ESTD testing. Testing the nonradioactive BSR samples produced with the BSR with the nonradioactive samples produced at Hazen is expected to provide a direct comparison between the product produced by the BSR and FBSR process, therefore linking engineering scale results to the radioactive laboratory scale results being produced as part of this program. The other three Hanford LAW samples—from Tank AN103 (low anions), SX-105 (high anion), and tentatively AN107 (complexant)—to be treated represent the middle 80% of the total LAW feed relative to the anions and eliminates the outliers.

4.4. Prepare Feed for BSR

The first BSR run will be conducted using DWPF recycled chemically adjusted to be similar to WTP SW. After this test has been completed, a SRS low activity tank waste adjusted to meet Hanford LAW characteristics per Rassat et al.[23]. BSR run will be conducted. SRS LAW characterized as part of the SRS salt disposition program will be adjusted with reagents to more closely resemble this Hanford LAW composition. Prior to conducting BSR runs with actual radioactive waste at least one BSR run will be conducted with nonradioactive simulant to make certain the system performs as expected.

4.4.1. Process SRS Modified LAW

As previously stated, prior to operating the SRNL BSR to process the SRS modified LAW, a simulated waste will be prepared and processed through the SRNL BSR to confirm the efficacy of the BSR to process the salt solution and produce a mineralized waste form. After the demonstration that the SRNL BSR will produce an adequate mineralized product, the modified SRS LAW will be processed into a mineralized waste form and monolith.

4.4.2. Process Three Hanford LAW

Three samples of Hanford LAW will be used to prepare mineralized BSR product. These samples are expected to represent the majority of the waste expected to be treated by the FBSR process. Prior to processing each of these radioactive samples a BSR run will be performed with simulated waste to make certain the system performs as expected.

5.0 Monolith Process

5.1. Granular and Monolithic Waste Forms Preparation for Analyses

Waste forms will be prepared using the FBSR mineralized product made from the P1-B LAW Envelope A @HRI 2008 simulant given in Table 4.1 and from nonradioactive BSR product. The purpose of the monolithic waste form is to meet the compressive strength requirements of the IDF without negatively affecting the durability of the granular mineralized FBSR product. The chemical and physical characteristics of the monolithic waste forms will be measured and compared to the granular product baseline to determine if the materials or process used to produce the monolithic waste form effected the properties of the mineralized FBSR product. All of the granular material produced as part of the BSR process will be used to produce monolithic waste form samples for testing.

All subsequent radioactive waste forms will be prepared using the BSR mineralized product made from one SRS wastes shimmed to look like Hanford wastes (the Rassat 68 tank blend, WTP) and three actual Hanford LAW wastes. The radioactive BSR will be operated in the SRNL Shielded Cell Facility. The SRS wastes will be shimmed with ^{99}Tc and ^{129}I to a level sufficient for characterization and to provide a reasonable mass balance. It is important to note that in some cases, the element of interest can be below the detection limit of the analytical technique being used. All precaution will be taken to minimize this, but in some cases, measurements may result in less than values. For example, washing the BSR system to check for Tc and I condensed phases in the off-gas system, may result in values that are below the limit of detection. Depending on the amount measured in the product, estimates of the maximum amount that can be present in other parts of the BSR system can be made using detection limit values. Cast specimens will follow ASTM C 192 for making and curing concrete specimens modified to adapt to the specific waste form[23]. Curing time is 28-days at ambient temperatures.

Sufficient sample will be made from 1-2 L of radioactive waste to generate the following samples for durability testing. Many of the monolith samples used for compression testing can be subsequently sized reduce for performance testing. The amount of sample needed for testing is shown in Table 5.1.

Table 5.1. Sample Requirements for Testing. This is per Radioactive BSR Run.

Standard Test Method	Test	g/sample	# samples	Replicates	Total (gms)	Notes
ASTM C1662-07[24]	SPFT full suite-granular	0.5	144	2	144	6 soln's x 6pH x 4 temps = 144
	SPFT full suite-monolith or subset which would require ½ the number of samples.	0.5	144	2	144	6 soln's x 6pH x 4 temps = 144
-	PUF-granular	40	1	1	40	May require replicates
-	PUF-monolith product crushed	40	1	1	40	May require replicates
ASTM C1285-08[25]	PCT (short term) Granular product	4	6	2	48	2-4g/sample for rad PCT
ASTM C1285-08[25]	PCT (short term) Monolith product crushed (ASTM C1285-08)	4	6	2	48	2-4g/sample for rad PCT
ASTM C1285-08[25]	PCT (long term) granular (ASTM C1285-08)	2	3	2	12	2-4g/sample for rad PCT
ASTM C1285-08[25]	PCT (long term) Monolith product crushed (ASTM C1285-08)	2	3	2	12	2-4g/sample for rad PCT
	TCLP-granular	10	1	2	20	Use 10 gm modified TCLP for rad test
	TCLP-monolith crushed up	10	1	2	20	Use 10 gm modified TCLP for rad test
ASTM C1308-08[26]	*Diffusive release (monolith only)*	48.91	2	2	196	Assume 1" dia x 2" L cylinders
	Total - subset monolith w/10gm TCLP				264	
	Total subset granular				460	
	Total				724	

These amounts were calculated using a typical waste loading of Na_2O in FBSR granular product of ~28 wt %. Typical waste loading of FBSR granular product in monolith is approximately 65.2 wt %. Grinding losses when preparing samples for SPFT, PUF, PCT and TCLP testing are assumed to be ~50%

*Duplicate and replicate samples will not be performed using the LAW monoliths because the amount BSR product than can be produced using the available tank waste. Replicates will be performed on non-radioactive monolith samples and the radioactive SRS shim samples for inter-laboratory comparison.

5.1.1. Geopolymer

Geopolymer waste form GEO-7 was optimized based on the work performed in WFO-2008-001 (report in preparation) between TTT and SRNL. Samples will be cured for 28 days prior to characterization and testing.

6.0 Sample Characterization Methods

This section describes the characterization techniques that will be used to characterize the granular and monolithic form of the FBSR product. Solid analysis instruments can be used for identifying elements, minerals, solid-phase morphology, chemical composition of the bulk and solid surfaces, chemical bonding or interaction, and the oxidation state of selected elements within the solid. Each FBSR sample produced will be characterized using a suite of techniques that includes chemical digestion, X-ray diffraction (XRD), and scanning and/or transmission electron microscopy with energy dispersive spectroscopy (SEM-/TEM-EDS). Sample surface area will be determined by gas adsorption BET. Chemical digestion results will provide the elemental composition of each waste form and the information needed to normalize the measured elemental release rates. X-ray diffraction analyses will be performed on pre- and post-test samples to determine the sample mineralogy and evaluate the phase changes that occur during testing. Electron microscopy will be performed on pre- and post-test samples to gain insight into the distribution of elements and potential phase changes the waste form undergoes during testing. Although not discussed in detail here, XAS will be used to determine the oxidation state and, if possible, nearest neighbor environment for ^{99}Tc and possibly ^{129}I.

Instruments	Applications
XRD	Mineral identification, semi-quantitative bulk composition.
Chemical Digestion (Fusion)	Use a chemical fusion technique to dissolve the waste form. Specific fusions will be conducted in a manner that is consistent with the properties of the contaminant of interest.
Particle Size Distribution	Determine the particle size and distribution of the mineralize waste form.
Redox Measurement	Determine the reduction-oxidation state of the mineralized waste form.
SEM/EDS	Surface morphology along with elemental analysis of small regions of the solid.
TEM/EDS/SAD	Morphology, mineral identification, elemental analysis of very small regions of the solid (higher resolution than SEM).
FTIR/Raman	Chemical bonding, molecular structure, compounds identification.
XPS	Oxidation state of element in solid surface, depth profiles of element composition to correlate with dissolution data, and elemental composition of solid surfaces as a function of depth from the surface.
XAS (XANES/ EXAFS)	Oxidation state of element, element identity, and bonding information (coordination numbers and bonding distance between the central and the nearest neighboring elements).
Gas Adsorption	Surface area (BET), pore size distribution.

7.0 Regulatory Testing

This section discusses a series of regulatory test methods that must be performed to provide some of the data needed to screen potential secondary waste stabilization technologies. The methods discussed below include the compressive strength test, ASTM 1308 test, and Toxicity Characteristic Leaching Procedure (TCLP) test. Previous references also discuss the results of a series of TCLP test on both the granular and monolithic form of the FBSR product.

7.1. Compressive Strength — (ASTM C 39/C 39M–01)

The compressive strength of waste from samples will be measured using the ASTM C 39 method[27]. Dependent upon the waste form, samples will be either cast or machined to meet the dimensional requirements of the test method. Samples are loaded into a testing apparatus (i.e., servo-hydraulic test machine) so that the axis of the specimen is aligned with the center of the thrust of the spherically seated block of the apparatus. The load is applied at a rate of movement (platen to crosshead measurement) that corresponds to a stress rate on the sample of 0.25±0.05 MPa/s (35±7 psi/s) continuously and without shock until the load indicator shows that the load is decreasing steadily and the sample displays a well-defined fracture pattern. For each test, a constant displacement rate must be used for each waste form specimen for consistency. The compressive strength is calculated by dividing the maximum load carried by the sample during the test by the average cross-sectional area determined for the sample prior to testing. Compressive strength tests may also be conducted after thermal cycling, exposure to radiation, and immersion in water to assess the impact of each. Analysis of radioactive monolith samples will be performed using a similar testing protocol.

7.1.1. ASTM C1308

The ASTM C1308[28] will be used in this work to assess the durability of the monolithic LAW waste forms prepared in Section 4.2 and 4.3. A brief description of each test method and the associated calculations are provided below.

ASTM C1308 is a semi-dynamic leach test in which a cylindrical specimen is immersed in a leachant that is completely replaced after specified intervals. The concentration of an element of interest in the recovered test solution is measured after each exchange; this is referred to as the *incremental fraction leached (IFL)* (Equation 1). The accumulated amount of the species of interest in the intervals prior to and including the interval of interest is analyzed to determine if the release from the solid can be described using a mass diffusion model. The amount accumulated through a particular test duration is referred to as the *cumulative fraction leached (CFL)* (Equation 2). Leachate samples collected during these intervals will be used to measure pH, electrical conductivity, and Eh. It is important to note that Eh measurements made outside of a control atmospheric chamber can oxidize in the open atmosphere. Before submitting for chemical analyses, the samples will be filtered using a 0.45-µm syringe filter.

$$IFL_i = \frac{{}_i a_n}{{}_i A_o} \qquad [1]$$

$$CFL_i = \frac{\sum_{n=1}^{i} {}_i a_n}{{}_i A_o} = 2\frac{S}{V}\left[\frac{D_e t}{\pi}\right]^{1/2} \quad [2]$$

$$LI_n = -\log\left(\frac{D_n}{cm^2 s}\right) \quad [3]$$

where a_n is the total amount of species release in all leaching intervals through time t, A_0 = the initial amount of the species of interest in the specimen, S is the surface area of the specimen, V is the specimen volume, D_e is the effective diffusion coefficient, and LI is the leach index (Equation 3).

7.1.2. TCLP

The TCLP will be used in this work to assess the release of RCRA metals from the granular BSR product and the monoliths produced in Section 4.2 and 4.3. This procedure is designed to determine the mobility of both organic and inorganic analytes present in liquid, solid, and multiphasic wastes. The main purpose of this procedure is to determine if a waste will meet the definition of EPA Toxicity, that is, carrying a hazardous waste code under RCRA (40 CFR Part 261). Initially the focus of the TCLP analyses will be on inorganic contaminants, because organics are not expected to survive the processing conditions of the BSR and FBSR. To confirm this a screening analysis to determine total organic carbon content of each sample to access whether or not a more robust TCLP organic analysis is necessary. If the organic carbon content is sufficient a TCLP organic measurement will be performed. All TCLP measurements will be performed at a EPA certified laboratory.

8.0 Performance Testing

Quantifying the rate and extent of element or contaminant release from minerals, glasses, or other waste forms has been at the heart of predictive geochemistry studies for decades[28-42]. The majority of the geochemistry studies have focused upon understanding the weathering of primary minerals and basaltic glasses contained in the earth's crust for the purpose of predicting element cycles and the evolution of natural waters[28-42]. The concepts and theories, such as Transition State Theory of Chemical Kinetics, related to mineral and glass weathering developed within the geochemistry community have been carried forward and used to predict the release of contaminants from waste forms and other engineered materials[43-64]. The weathering of these materials is impacted by a series of sequential and/or simultaneous competing chemical and physical reaction/processes that may control the mass transfer of contaminants from the waste form into solution. These reaction/processes include, but are not limited to, the following:

- diffusion/advection
- dissolution/precipitation
- adsorption/absorption/desorption
- oxidation/reduction
- paragenetic sequence of mineral transformation

The overall impact of individual or coupled reactions/processes on the long-term performance of the FBSR waste form will depend on a number of different variables, such as composition, materials

resistance to physical and chemical degradation, dominant mechanism controlling contaminant release, and disposal system environment.

Therefore, performance testing must focus on the use of experiments that provide model parameters that explain the key processes and in some cases accelerate the weathering process in order to obtain the data needed to predict performance in a realistic time frame. The results produced from the laboratory-scale and experiments discussed in this section will be used to provide the parameters needed to predict performance and contaminant release over ~10,000 years, which is the expected period of performance for the engineered system.

Performance testing must address the following issues:

- Identify the key reactions and/or processes affecting waste form durability and contaminant release.
- Quantify the extent and rate of these reactions and/or processes.
- Obtain the model parameters needed to describe these reactions and/or processes and predict the behavior of the system.
- Verification of the derived model parameters.

In summary, performance testing is a strategic process that uses laboratory experimentation to quantify the needed parameters used in numerical or analytical predictive models to simulate the key reactions and/or processes affecting release over long-time frames.

8.1. Waste Form Performance Test Methods

8.1.1. Product Consistency Test (PCT)—(ASTM C 1285-08)

The PCT will be conducted on samples prepared in Section 4.2 and 4.3 following the procedures described in ASTM C 1285-08[65]. The monolithic waste forms will be crushed and sieved. The sieved (-100 to+200 mesh) powder will be wet sieved twice with pure ethyl alcohol to remove any small particles adhering to the surface of the larger particles. The samples will be dried at room temperature or 60°C and a particle size analysis performed on a representative subset. A second representative subset will roasted at 110° to determine moisture weight loss and then at 525°C to remove the coal fraction using the USGS procedure used in previous studies[66]. The loss-on-ignition (LOI) at both 110°C and 525°C will be measured to determine the weight percent moisture and coal volatilized (this is needed to normalize out the moisture and coal fractions of the sample from the leachate response). The roasted sample will be sent for both particle size analysis for comparison to the sample with the coal and for BET particle size analysis. PCTs will be performed at a mass to volume ratio (S/V) of 1/10 in Teflon® or stainless steel vessels held at 90±2 °C for seven days. After completion of the PCT, the leachate will be analyzed and the concentration of ions in the leachate will be measured by inductively coupled plasma-atomic emission spectroscopy (ICP-AES) and inductively coupled plasma-mass spectroscopy (ICP-MS). All tests will be conducted in triplicate (at a minimum) and the results will be averaged.

The normalized elemental mass release, NR_i, will be calculated as g/m^2 from Equation 4 after adjustment for moisture and coal content:

$$NR_i = \frac{c_{i,sample}}{(f_i)\left(\frac{SA}{V}\right)(t)} \quad [4]$$

where NR_i = normalized rate (g/(m^2•day))
c_i (sample) = concentration of element "i" in the solution (g$_i$/L)
f_i = fraction of element "i" in the unleached waste form (unitless)
SA/V = surface area of final waste form divided by the leachate volume (m^2/L)
t = time duration of test in days

If the units of time are omitted from the NR_i calculation, then the normalized release, NL_i, is calculated in Equation 5 as

$$NL_i = \frac{c_{i,sample}}{(f_i)\left(\frac{SA}{V}\right)} \quad [5]$$

where NL_i = normalized release (g/m^2)
c_i (sample) = concentration of element "i" in the solution (g$_i$/L)
f_i = fraction of element "i" in the unleached waste form (unitless)
SA/V = surface area of final waste form divided by the leachate volume (m^2/L)

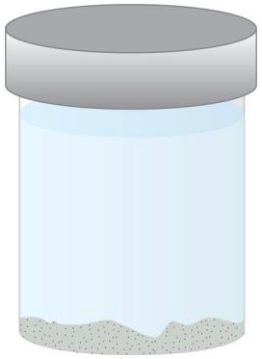

Figure 8.1. Example of Static Container for PCT

8.1.2. Single Pass Flow Through (SPFT) (ASTM C 1662)

Samples prepared in Section 4.2 and 4.3 as well as single phase pure standards will be evaluated for leach response using the SPFT method[30]. Flow rates and other testing conditions will be consistent with prior SRNL testing[14,11,15].

Dissolution experiments will be conducted with the SPFT apparatus. The SPFT apparatus consists of syringe pumps that transfer solution from input reservoirs to the reactors via Teflon tubing. The perfluoroalkoxy (PFA) Teflon reactor (Savillex, Minnetonka, MN) consists of two pieces that thread together to form a container with a 47.5 mm outer diameter and a 63.6 mm height, with a total inner volume of ~80 mL. The relatively large inner diameter of the reactor (40.8 mm) accommodates a thin layer of waste form particles that rest at the bottom. The experimental system pumps a continuous flow of fresh influent solution, which serves to (1) prevent the build-up of

reaction products, (2) maintain the bulk solution composition throughout the duration of an experiment, (3) allows an investigator to more directly quantify the dissolution rate rather than fitting a curve to a presumed reaction mechanism, and (4) allows for the study of the element release data from test materials over a wide range of experimental conditions. Therefore, by design, the SPFT experiment prevents the progressive accumulation of reaction products that would affect element release rates and the setup can be varied to retrieve rate parameters that will yield a mathematical description of the dissolution process. The SPFT system has been extensively described by others[51,60,61,67-69]; and the reader should consult these references, as well as the references contained therein for more detail.

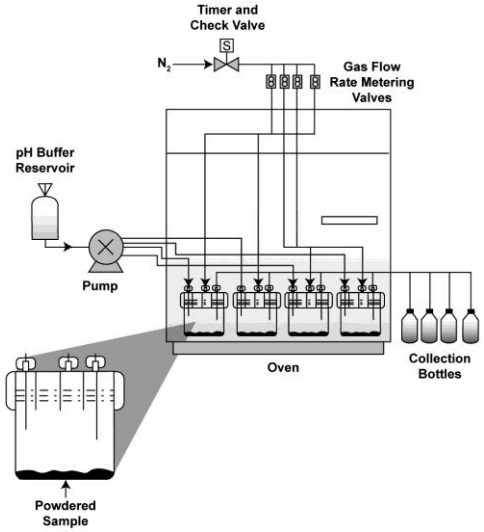

Figure 8.2. Schematic of the SPFT Test Method

Dissolution rates, based on steady-state concentrations of elements in the effluent, will be normalized to the amount of the element present in the sample by equation 6:

$$r_i = \frac{\left(C_i - \bar{C}_{i,b}\right) q}{f_i S} \qquad [6]$$

where r_i is the normalized glass dissolution rate based on the release of a particular element i [g/(m^2 d)], C_i is the concentration of the element i in the effluent (g/m^3), $\bar{C}_{i,b}$ is the average background concentration of the element of interest (g/m^3), q is the flow rate (m^3/day), f_i is the mass fraction of the element in waste form (dimensionless), and S is the surface area of the sample (m^2). Flow rates will be determined by gravimetric analysis of the fluid collected in each tared effluent collection vessel upon sampling. The background concentration of the element of interest is determined by analyses of the starting input solution and the three blank solutions. Typically, background concentrations of elements are below their respective detection thresholds. The detection threshold of any element is defined here as the lowest calibration standard that can be determined reproducibly during an analytical run within 10%. In cases where the analyte in the sample is below the detection threshold, the background concentration of the element will be set at the value of the detection threshold to represent a maximum release rate.

Determining the experimental uncertainty of the dissolution rate takes into account uncertainties of each parameter in Eqn. 6. For uncorrelated random errors, the standard deviation of a function $f(x_1, x_2,\ldots x_n)$ is given by:

$$\sigma_f = \sqrt{\sum_{i=1}^{n}\left(\frac{\partial f}{\partial x_i}\right)^2 \sigma_i^2} \qquad [7]$$

where μ_f is the standard deviation of the function f, x_i is the parameter i, and σ_i is the standard deviation of parameter i. Substituting Eqn. 6 into Eqn. 7 and converting to relative error, $\hat{\sigma} = \sigma / r_i$, yields:

$$\sigma_{r_i} = \sqrt{\frac{\left(\hat{\sigma}_{C_i} C_i\right)^2 + \left(\hat{\sigma}_{\bar{C}_{i,b}} \bar{C}_{i,b}\right)^2}{\left(C_i - \bar{C}_{i,b}\right)^2} + \hat{\sigma}_q^2 + \hat{\sigma}_{f_i}^2 + \hat{\sigma}_S^2} \qquad [8]$$

Relative errors of $\hat{\sigma}_{C_i}$, $\hat{\sigma}_{\bar{C}_{i,b}}$, $\hat{\sigma}_q$, $\hat{\sigma}_{f_i}$, and $\hat{\sigma}_{S_{geo}}$ are 10%, 10%, 5%, 3%, and 15%, respectively. The errors assigned to the parameters in Eqn. 8, in addition to the practice of substituting detection threshold values for situations where the sample results were below the background concentrations because of instrument limitations, results in typical 2μ uncertainties of approximately ±30% for SPFT-measured dissolution rates (or ±0.2 log units when reported as $\log_{10}$ rates).

8.1.3. Pressurized Unsaturated Flow Experiments

The PUF apparatus allows for accelerated weathering experiments to be conducted under hydraulically unsaturated conditions, thereby mimicking the open-flow and transport properties expected to occur in the IDF environment while allowing the corroding glass to achieve a final reaction state. The PUF apparatus provides the capability to vary the volumetric water content from saturation to 20% or less, minimize the flow rate to increase liquid residence time, and operate at a maximum temperature of 99°C. The PUF column operates under a hydraulically unsaturated condition by creating a steady-state vertical water flow, while maintaining uniform water content throughout the column; by using gravity to assist in drainage; and by maintaining a constant pressure throughout the column. Constant pressure is maintained with a porous Ti plate and gas pressure. For additional details on the PUF system see Pierce et al. [70-71] and the corresponding references contained therein.

The PUF system contains a 0.0762-m long and 0.0191-m diameter column fabricated from a chemically inert material, polyetheretherketone (PEEK), so that dissolution reactions are not influenced by interaction with the column material. A porous Ti plate with a nominal pore size of 0.2-μm is sealed in the bottom of the column to provide an adequate pressure differential for the conducting of fluid while operating under unsaturated conditions [72]. Titanium is chosen because it is highly resistant to dissolution and has excellent wetting properties. Once the porous Ti plate is water saturated, water but not air is allowed to flow through the 0.2-μm pores, as long as the applied pressure differential does not exceed the air entry relief pressure, referred to as the bubble pressure, of the Ti plate. If the pressure differential is exceeded, air will escape through the plate and compromise the ability to maintain unsaturated flow

conditions in the column. The PUF test computer control system runs LabVIEW™ (National Instruments Corporation) software for logging test data from several thermocouples, pressure sensors, inline sensors that measure effluent pH and conductivity, and from an electronic strain gauge that measures column weight to accurately track water mass balance and saturation level. The column also includes a PUF port, which is an electronically actuated valve that periodically vents the column gases. The purpose of column venting is to prevent reduction in the partial pressure of important gases, especially O_2 and CO_2, which may be consumed in a variety of chemical reactions.

9.0 Test Plan/Approach

This section discuss the testing approach that will be used to obtain the key information needed to model the performance of the FBSR product. In addition to the testing discussed below a number good housekeeping techniques will be used to maximize the scientific credibility of the results produced from the testing outlined in this Task Plan. Because the material produced by the FBSR and BSR process is a multi-phase material, some caution must be taken when crushing and sizing the material to perform experimental tests discussed below. These housekeeping checks should be performed to make certain that the size fractions being selected does not potentially bias the sample by segregating key mineral phases and/or contaminants of concern. Therefore it is suggested that all material required for testing either the granular or monolith product be sized at one time and then analyzed to demonstrate that no preferential segregation has occurred. This process may require the use of wet sieving techniques and washing the material in pure ethyl alcohol or equivalent.

9.1. Quantitative XRD

The FBSR product is a mixture phased material and it is currently assumed that the contaminants of concern are distributed amongst each of these phases. For example, it is assumed that ^{99}Tc has been sequestered in the nosean or sodalite structure. Therefore, to allow for long-term predictions to accurately describe the release of key contaminants of concern for the multi-phase FBSR product, quantitative XRD will be used to determine the percentage of these phases in the FBSR sample. It is not anticipated that this approach will distinguish between the various possible sodalite anion-bearing phases, but provide an estimate of the total amount of nepheline, sodalite, and nosean in the FBSR and BSR granular and monolith products. Mixtures of individual phases will be used to prepare calibration curves for quantitative XRD analysis of FBSR product. Confirmation of the predictability of the ability to provide quantifiable results will be demonstrated by testing a multi-phase sample prepared with known phase assemblage and comparing results with predictions. This analysis will be conducted on subsample of the previous nonradioactive granular and monolith FBSR product and a subsample from each batch of the four radioactive granular and monolith samples being prepared as part of the work discussed in this Task Plan.

9.2. Chemical Durability of Pure Phases

To accurately model the release of these contaminants that may have segregated into specific mineral phase within the FBSR product, an understanding of dissolution kinetics of the dominant pure phase mineral are needed. Therefore, dissolution rate law parameters (model parameters) will be measured using the SPFT test method using the individual phases, namely nepheline, sodalite, and nosean. Each of the possible anion-bearing sodalite phases (e.g., Re, I, SO_4, Cl, and F) will be produced and tested. These test will be conducted as a function pH, temperature, and solution composition. Confirmation of the predictability of the dissolution

process will be demonstrated by testing a multi-phase samples prepared with known phase assemblage and comparing results with predictions.

9.3. Chemical Durability of Non-radioactive FBSR Product

The granular and monolith form of the FBSR product will be evaluated using SPFT experiments to quantify the dominant dissolution mechanisms under IDF relevant conditions. These results will be compared to the results obtained for the individual pure phases to gain insight into the behavior of the FBSR matrix. Additionally, the influence of the process of preparing monoliths on the dissolution behavior will be obtain by comparing the results obtained for the granular and monolithic forms. These tests will be conducted as a function of pH, temperature, and solution composition. These results will be used to develop rate law parameters that will be used to predict the performance. Additionally, a series of PCT-B experiments will also be conducted to accelerate the weathering of the FBSR product. The goal of the PCT-B experiments is to provide information on the paragenetic sequence of alteration phases that form as a result of the FBSR waste form corrosion. Results from solution chemistry and solid phase analysis of the PCT-B samples will be used to conduct thermodynamic modeling with EQ3/6 code or Geochemist Workbench. The purpose of the thermodynamic modeling is to develop a chemical reaction network of solution and solid species that can be included in reactive chemical transport simulations of the near-field IDF environment.

9.4. Evaluate the Effect of Coal and Residual Coal on Contaminant Release

Coal has been used to sequester, via sorption, a variety of metals and radionuclides from natural waters. Because of the potential for coal particulates used in this process to concentrate specific contaminants of concern, specific test will be designed to evaluate the effect of residual coal contained in the FBSR and BSR products on the release of contaminants. A select number of PCT-A, PCT-B, and SPFT experiments will be conducted with a sample of non-radioactive FBSR sample and samples the non-radioactive and radioactive material produced with the BSR. Additionally, samples will be analyzed for to determined the total amount of specific contaminants of concern are associated with residual coal.

9.5. Chemical Durability of Radioactive BSR Product

A select number of SPFT experiments will be performed on radioactive samples of the granular and monolith form of the BSR product using SPFT experiments. These test will be used to compare the release of key contaminants of concern from radioactive samples to nonradioactive samples. These experiments will be performed using material obtained from each batch of material produced using actual radioactive simulant. Additionally, a series of PCT experiments will also be conducted.

9.6. Thermo-Chemical Measurements

A key component of performance assessment modeling is having an understanding of the thermodynamic stability of the starting minerals and mineral assemblages that form as a result of the weathering process. Therefore, thermo-chemical measurements will be performed on the pure phases as well as the nonradioactive FBSR product to determine the equilibrium constants that will be needed for modeling. In some cases, estimates of the thermodynamic constants will be calculate for a select number of solid-solutions that are difficult to synthesize[73].

9.7. Secondary Alteration Phase Formation

Determining the alteration phases that form as a result of the weathering process is a critical component of long-term PA calculations. Therefore, analysis of samples collected from a PUF experiment conducted for two-years at 90°C on nonradioactive granular FBSR product will be used to determine the amount and extent of alteration phases formed during weathering. In addition to PUF experiments, a series of long-term PCT experiments will be conducted on both granular and monolith samples of the FBSR product to determine the paragenetic sequence of alterations. The solution chemistry analyses and geochemical modeling of the PCT results should provided the aqueous chemistry input data needed for PA calculations of the long-term performance of the FBSR product.

9.8. Re, Tc, and I Speciation in BSR Product

A technical uncertainty in the performance of the BSR product is the location of key radionuclides, such as technetium. To reduce this uncertainty a series of X-ray absorption spectroscopy analyses will be conducted on sub-samples of radioactive granular and monolith BSR product to determine the Re, I, and ^{99}Tc oxidation state and nearest neighbors. Although XAS will be used as a primary technique to determine Re, I, ^{99}Tc speciation, a set of secondary analysis techniques will also be used. These include SEM-EDS, TEM EDS, and if necessary, micro-XRD, XPS, and electron microprobe. This analysis will aide in providing the technical justification for placing all or a percentage of ^{129}I and ^{99}Tc in the sodalite and/or nosean phase.

9.9. Diffusion Release from Monolith

The ASTM C1308 Test Methods discussed in Section 6.1.1.1 will be used to quantify diffusion release from the monolith for key contaminants of concern. These results will provide the technical basis needed to describe the diffusion related release from the FBSR monolith. This is another key model parameter that will be needed to model the long-term performance of the FBSR product.

9.10. Pressurized Unsaturated Flow Experiments

Pressurized unsaturated flow experiments will be conducted on one non-radioactive sample and one radioactive sample of granular and monolithic FBSR product (total of four). Because of the cost associated with these experiments and the length of time needed to obtain sufficient reaction product, these experiments will not begin until late 2012 after the technology has proceed beyond a number of the key evaluation points. The purpose of these tests will be determine the alteration phases expected to form as a result of the long-term weathering of the FBSR product under conditions that mimic the unsaturated, open flow and transport conditions expected in the IDF.

10.0 Evaluation Points

A key component of the overall strategy outlined in this Task Plan is to identify key points along the overall project time line that will be used to evaluate whether or not to continue. In addition to the evaluation points, a series of three progress briefings are planned to provide the principal investigators the opportunity to brief DOE and the project team with critical input when the data becomes available. In general, the key decision points will be based on the following:

- The first evaluation point is expected to occur after the SRS LAW shim sample is used in the BSR to produce FBSR product. This will be the first opportunity to estimate the amount of technetium and rhenium that has partitioned between the FBSR product and the other portions of the BSR system. The current conceptual model, based upon engineered scale tests and previous BSR process runs with rhenium, suggest that a significant portion of the rhenium spiked into simulated low-activity tank waste is contained in the FBSR product. Estimates from engineering scale tests suggest anywhere from 75%[6] to 99% (THOR 2009) of the total rhenium spike is contained within the FBSR product. It is important to note that two different systems were used at SAIC/STAR in 2004 and at TTT in 2008. A wash down of the BSR system, analysis of the off-gas, and an analysis of the FBSR product will provide some indication of the distribution of ^{99}Tc and Re in the BSR system. It is important to note that the BSR does not have a prototypic off-gas system. The information obtained in this step will be augmented with other supporting information, such as redox measurements and chemical digestion results of the FBSR product. This evaluation point applies for each of the four LAW radioactive waste samples as well as the radioactive secondary waste sample.

- The second point for evaluation of the FBSR waste form will be after the first two samples, SRS shimmed secondary waste and SRS shimmed LAW, have been analyzed to determine the ^{99}Tc oxidation state. This information will be augmented with the results of other supporting analyses, such as chemical digestion results, redox measurements and SEM-EDS analyses. Additionally, the results from SPFT experiments will be used to evaluate whether or not ^{99}Tc and ^{129}I release from the FBSR waste form is stochiometric or non-stochiometric with respect to sodalite and nosean. The purpose of this evaluation point is to confirm the premise that Tc is contained in the cage-like structure of sodalite and nosean.

- The third point of evaluation of the FBSR waste form will be after the analysis of the monolith immersion test results. A requirement for near surface disposal is the Leachability Index. Therefore, it is expected that release of ^{99}Tc and ^{129}I from the matrix will be consistent with the Nuclear Regulatory Commission guidance. This is an evaluation point because it could require changes in the binder/FBSR mix or selection of a different binder matrix.

11.0 Available Data

In accordance with DOE Order 413.3, the FBSR waste form qualification program is supporting a project acquisition process for a technology for the supplemental treatment of Hanford LAW. This project acquisition process includes a series of critical decisions. As data becomes available the results will be used in the critical decision (CD) process to reduce overall project risk. Provided below is a brief linkage between the available data and the project acquisition process.

- Critical Decision-0 – During the project planning phase, which includes pre-conceptual planning and conceptual design, the CD-0 package will be submitted to DOE in September 2010. The

purpose of the CD-0 package is to provide a justification of mission need and a acquisition strategy, along with pre-conceptual planning and mission need independent project review.

- Critical Decision-1 – In parallel with submitting the CD-0 package, a series of radioactive samples will be produced to evaluate the ability of the FBSR process to incorporate key radionuclides and to develop an understanding of the release of the radionuclides from the FBSR material. Only a portion of these results will be available to support the CD-1 package expected to be delivered in 09/30/2011. These include:

  - White-paper discussing all of the existing data on the FBSR product
  - Evaluation of Tc and I incorporation in the FBSR product when operating the BSR system
  - Diffusive release of key contaminants, namely Tc and I, from the FBSR monolith
  - Evaluation Tc and I release from the granular and monolith FBSR material for at least one radioactive LAW sample
  - Evaluation of speciation of ^{99}Tc and possibly ^{129}I in the granular and monolith FBSR material for at least one radioactive LAW sample.

- Critical Decision-2/3 – If selected, the full source term model that describes the performance of the FBSR material.

12.0 Key Assumptions

The following are a list of key assumptions that could impact the schedule or the ability to successfully complete the work scope outline in this Task Plan.

- The redox conditions for nonradioactive and radioactive BSR sample production runs are consistent with the redox conditions observed at the engineering scale. The contaminants of concern, namely ^{99}Tc and ^{129}I, are redox sensitive and the location of these contaminants in the waste form is also affected by the redox conditions. For example, $Tc(VII)O_4^-$ substitutes for other anions in the cage-like structure of nosean and sodalite; whereas a Tc(IV)-containing phase will form if the redox conditions become too reducing.

- The strategy outline in this Task Plan presumes that ^{99}Tc and ^{129}I are contained in the cage-like structure of sodalite and nosean. This assumption is based upon the best available scientific information on the FBSR process and product. Variations to this conceptual model will could result in changes in the overall strategy.

- There is no significant difference between the material (mineral assemblage and percentages) that is produced with the BSR versus the material that has been produced at engineering scale using similar starting compositions for the simulant and actual waste samples for specific Hanford waste envelopes (e.g., Envelope A, B, and C). Linking to the engineering scale is a critical aspect related to reducing the overall risk associated with a down selection process. Therefore, the radioactive samples produced in the BSR need to provide a link to existing engineering scale FBSR material that has been produced at Hazen and/or the STAR facility at INL.

- The majority of the testing to obtain valid model parameter estimates will be conducted with nonradioactive FBSR material. This will allow us to meet the anticipated schedule. It is assumed that these parameters will be consistent for both the nonradioactive and radioactive samples, evident by the dissolution rates being within the experimental error of one another. A similar

approach has been used for radioactive and nonradioactive LAW glasses as well as comparing crucible-scale and engineering scale glass from the bulk vitrification process.

13.0 Reporting

A performance modeling strategy document and a white paper summarizing all the pertinent durability testing outlined in Table 1.1 will be issued identifying the sequence of data and analysis fundamental to the support of the Performance Assessment (PA) of the FBSR waste form. A technical report documenting the testing and results will also be issued.

14.0 Quality Assurance

A graded Quality Assurance (QA) approach will be used to support the work performed under this DOE EM-31 Technology Development and Deployment (TDD) Task Plan. Initial tests will be performed using Standard Laboratory Procedures. As the project evolves, application and coordination of other Quality Assurance Requirements may be required. The determination shall be documented in Project Planning Contractual documents. The results produced as part of this effort will support a technology down select process for supplemental treatment and an evaluation of equivalent treatment. It is important to note, that additional information, in addition to what is being produced as part of this program, may be required to demonstrate equivalent treatment to other currently accepted immobilization options.

14.1. WRPS ESH&Q Requirements

The subcontractor shall comply with all Price-Anderson Amendment Act (PAAA) nuclear safety rules and reporting requirements as determined by their prime contracts negotiated with the Department of Energy

ESH Requirements Specific to this Task

The work activities for this statement of work have been designated as Full Quality.

The Subcontractor is required to conduct work in accordance with a Quality Assurance Program (QAP) that meets the Quality Assurance criteria specified in DOE O. 414.1, *Quality Assurance*, 10 CFR 830, *Nuclear Safety Management*, Subpart A, ~~–~~*Quality Assurance Requirements*", paragraph 830.122 and also meets the requirements of ASME NQA-1-2004, *Quality Assurance Requirements for Nuclear Facility Applications*. The Subcontractor shall implement an NQA-1-2004 program (as identified below) and be listed on an ESL for this scope of work:

Criterion #	Criterion Title	All Sections	Specific Sections as Listed:
1	Organization	☒	☐
2	Quality Assurance Program	☒	☐
3	Design Control	☐	☐N/A
4	Procurement Document Control	☒	☐
5	Instructions, Procedures, and Drawings	☒	☐
6	Document Control	☒	☐
7	Control of Purchased Items and Services	☐	☒ Sections 100, 400 & 800
8	Identification and Control of Items	☒	☐
9	Control of Processes	☒	☐
10	Inspection	☐	☐N/A
11	Test Control	☒	☐
12	Control of Measuring and Test Equipment	☒	☐
13	Handling, Storage, and Shipping	☒	☐
14	Inspection, Test, and Operating Status	☒	☐
15	Control of Nonconforming Items	☒	☐
16	Corrective Action	☒	☐
17	Quality Assurance Records	☒	☐
18	Audits	☐	☐N/A
Subpart 2.7	Computer Software for Nuclear Facility Applications*	☒	☐
*The development, procurement, maintenance, and use of the computer software shall comply with applicable requirements of ASME NQA-1-2004, Subpart 2.7, including problem reporting and corrective action.			

The implemented quality assurance program for Subcontractors located on the Hanford Site shall comply with DOE/RL 96-68 Hanford Analytical Services Quality Assurance Requirements Document (http://www.hanford.gov/orp/?page=141&parent=14). Subcontractors located off the Hanford Site shall have an implemented quality assurance program that complies with the (Department of Energy Consolidated Audit Program (DOECAP) Quality Systems for Analytical Services (QSAS) (https://doecap.oro.doe.gov/DOECAP_Public/documentsLab.aspx).

QAP Approval:
The Subcontractor's QAP shall be subject to review at all times by Buyer, including prior to award.

Changes to the Subcontractor's QAP:
The Subcontractor shall, during the performance of this Subcontract, submit proposed changes to the quality assurance program to the Buyer for review prior to implementation.

Treatability Study Materials Management

FBSR waste form, unused samples, laboratory samples, and treatability study residues generated by FBSR testing at SRNL will be managed in accordance with the provisions set forth below. For purposes of this Task Plan, "FBSR waste form" means Hanford tank waste samples that have been treated by the steam reforming process under the treatability study sample exclusion and "treatability study residues" or "residues" mean all other materials produced by the treatability studies, e.g., laboratory equipment, personal protective equipment, analytical residues, etc., that are contaminated by contact or commingling with Hanford-generated tank wastes that are not FBSR waste form or unused samples.

a. Unused Hanford waste samples not subjected to testing
Unused waste samples may be returned to the Hanford Site as an excluded treatability study material under the treatability study sample exclusion upon prior approval of USDOE-ORP. Unused samples must be returned within 90 days of completion of the study or within 1 year from the date of shipment of the sample – whichever occurs first.

b. **FBSR waste form**
FBSR waste form, including granular and monolith waste forms, or other treated waste forms determined not to be suitable for testing, may be returned to the Hanford site as an exempted treatability study material under the treatability study sample exclusion upon prior approval of USDOE-ORP. Unused archived exempted materials must be returned within 90 days of the completion of the study or within 1 year from the date of shipment of the sample – whichever occurs first.
FBSR waste form may also be archived at SRNL or Hanford for up to five years in order to perform future durability or other characterization testing as needed. The FBSR waste form archived at SRNL will be returned to Hanford within five years of receipt of the sample used to make the FBSR waste form as specified by regulation.

c. **Laboratory samples**
In the course of the activities addressed by this MOU, SRNL may generate samples from the FBSR process that are intended for or require analysis at off-site laboratories. SRNL shall not contract with any off-site laboratory to conduct these analyses but shall send any such samples to PNNL. PNNL shall manage these samples as well as any and all contracts to conduct said analyses with off-site laboratories.

d. **Treatability study residues**
Treatability study residues as defined above (in Sec. III) shall be managed as fully regulated hazardous wastes. Upon prior approval of USDOE-ORP, these treatability study residues wastes may be transported to Hanford using a Uniform Hazardous Waste Manifest for storage, treatment, or disposal. Alternatively, commercial waste vendors may be used for treatment and disposal of hazardous wastes upon prior approval of USDOE-ORP.

Residues resulting from testing of archived materials will be managed and disposed as specified above for treatability study residues.

14.2. PNNL – QA

In accordance with PNNL PQAP for EM-31 Support Project, dated 04.19.2010, the range of graded QA requirements for this Task Plan encompasses the following levels of QA requirements:

A. QL3; activities which lead to selecting programmatic paths, will be performed in accordance with best laboratory practices (NQA-1 Subpart 4.2 – based) as indicated in work flows and subject areas of the PNNL HDI standards-based system. Examples of programmatic paths include (but are not limited to) down selecting potential technologies and initial proof of concept testing.

B. QL2; activities which are eventually intended to support and could affect the quality of nuclear material applications, structures, systems, and components of nuclear facilities (i.e., waste management, nuclear material processing, other related facilities), will be

performed in accordance with applicable requirements of the PNNL-NQA-EQAM-1 (NQA-1 based). Examples of such activities include (but are not limited to) optimization testing and actual waste demonstrations.

C. QL1; activities that are Immobilized High Level Waste (IHLW) waste form affecting, will be performed in accordance with applicable requirements of the PNNL-NQA-EQAM-1 (NQA-1 based) supplemented with applicable requirements of DOE/RW-0333P.

In 2010, PNNL will perform activities under QL3, to issue a performance modeling strategy document and a white paper.

Summary of NQA-1 Applicable EED/EM-31SP Quality Assurance Documents

NQA-1-2004	Yes	No	QA Document Title	Justification for Exclusion
BR 1 100, 200, 300	X		PNNL-NQA-EQAM-1 Section 1.1, Organization PNNL-AP-205, Quality Assurance Plans	
BR 2 100 => 500	X		PNNL-NQA-EQAM-1 Section 1.1, Organization Section 2.1 QA Program and 2.2 Training, Section 10.1 Inspection, Section 15.1 Control of Nonconforming Items, Section 16.1 Corrective Action, Section 18.1 Audits, Section 8.1 Identification and Control of Items, Section 17.1 QA Records, PNNL-AP-1001, Preparation and Use of Inspection/Test Instructions PNNL-AP-1002 Project QA Surveillance, PNNL-AP-1003 Independent Inspection, PNNL-AP-1801 Internal Audits, PNNL-AP-201 Calibration Control System, PNNL-AP-1802 Supplier Qualification Procedure, PNNL-AP-1805 Qualification and Certification of Audit Personnel	BR 2_300: This work does not require qualified inspection and test personnel. NDE is not performed; therefore qualified NDE personnel are not required
BR 3 100 => 900		X	PNNL-NQA-EQAM-1 Section 3.1 Design Control Section 3.2 Computer Software PNNL-AP-300, Software Control PNNL-AP-301, Hand Calculations PNNL-AP-302, Assurance and Control of Engineering Design	Design activities will not be performed by PNNL; however, hand calculations may be performed per procedure PNNL-AP-301. For Basic R&D, BR 3 Design Control is not applicable. Commercially available software like Word, Excel, SigmaPlot, etc. will be used for data analysis in accordance with PNNL-AP-300. Unique computer codes will not be generated as part of these testing activities.
BR 4 100 =>400	X		PNNL-NQA-EQAM-1 Section 4.1 Procurement Document Control PNNL-AP-401 Procurement Document Control, PNNL-AP-402 Obtaining Products and Services,	
BR 5 100	X		PNNL-NQA-EQAM-1 Section 5.1 Instructions, Procedures, and Drawings Section 11.1 Test Control PNNL-AP-501 Preparation & Approval of Administrative Procedures PNNL-AP-1101 Test Planning, Performance, and	

Summary of NQA-1 Applicable EED/EM-31SP Quality Assurance Documents				
NQA-1-2004	**Yes**	**No**	**QA Document Title**	**Justification for Exclusion**
			Evaluation	
BR 6 110, 200, 300	X		PNNL-NQA-EQAM-1 Section 6.1 Document Control Section 5. 1 Instructions, Procedures, and Drawings PNNL-AP-501 Preparation & Approval of Administrative Procedures, PNNL-AP-601 Document Control, PNNL-AP-602 Procedure and Instruction Change Control PNNL-AP-604 Independent Technical Review PNNL-AP-606 Peer Review, PNNL-AP-1101 Test Planning, Performance, and Evaluation	
BR 7 100 => 800	X		PNNL-NQA-EQAM-1 Section 7.1 Control of Purchased Items and Services Section 7.2 Control of Work Package Items and Services Section 4.1 Procurement Document Control Section 4.2 Work Package Control Section 10.1 Inspection Section 18.1 Audits Section 15.1 Control of Nonconforming Items Section 17.1 QA Records PNNL-AP-701 Source Inspections, Tests, and Surveillances, PNNL-AP-401 Procurement Document Control, PNNL-AP-402 Work Package Control, PNNL-AP-1101 Test Planning, Performance, and Evaluation, PNNL-AP-1801 Internal Audits PNNL-AP-1701 QA Records,	
BR 8 100, 200, 300	X		PNNL-NQA-EQAM-1 Section 8.1 Identification and Control of Items PNNL-AP-801 Identification and Control of Test Materials, PNNL-AP-803 Item Identification and Control	
BR 9 100 => 400		X	PNNL-NQA-EQAM-1 Section 9.1 Control of Special Processes PNNL-AP-902, Control of Special Processes	Work will be controlled in accordance with BR 5 and BR 11.
BR 10 100 => 700		X	PNNL-NQA-EQAM-1 Section 10.1 Inspection PNNL-AP-604 Independent Technical Review, PNNL-AP-1101 Test Planning, Performance, and Evaluation, PNNL-AP-1002, QA Surveillance	Design inspection will not be performed; however, reports from the testing will be reviewed in accordance with procedure PNNL-AP-604, Independent Technical Review and testing activities will be performed in accordance with PNNL-AP-1101, Test Planning, Performance, and Evaluation. For Basic R&D, BR 10 Inspection is not applicable
BR 11 100 => 600	X		PNNL-NQA-EQAM-1 Section 11.1 Test Control Section 3.2 Computer Software PNNL-AP-1101 Test Planning, Performance, and Evaluation, PNNL-AP-300 Software Control	
BR 12 100 => 400	X		PNNL-NQA-EQAM-1 Section 12.1 Control of M&TE	

Summary of NQA-1 Applicable EED/EM-31SP Quality Assurance Documents				
NQA-1-2004	**Yes**	**No**	**QA Document Title**	**Justification for Exclusion**
			PNNL-AP-1201, Calibration Control System	
BR 13 100 => 600	X		PNNL-NQA-EQAM-1 Section 13.1 Handling, Storage, and Shipping QA-RPP-WTP-1301, Handling, Storing and Shipping	
BR 14 100	X		PNNL-NQA-EQAM-1 Section 14.1 Inspection, Test, and Operating Status PNNL-AP-1401, Inspection and Testing Status and Tagging	
BR 15 100 => 400	X		PNNL-NQA-EQAM-1 Section 15.1 Control of Nonconforming Items PNNL-AP-1501, Nonconformance Reports PNNL-AP-1502, Deficiency Reports	For Basic R&D, BR 15 Control of Nonconforming Items is not applicable.
BR 16 100	X		PNNL-NQA-EQAM-1 Section 16.1 Corrective Action Section 15.1 Control of Nonconforming Items PNNL-AP-1601, Corrective Action PNNL-AP-1605 Supplier Corrective Action, PNNL-AP-1501 Nonconformance Reports, PNNL-AP-1502 Deficiency Reporting	
BR 17 100 => 800	X		PNNL-NQA-EQAM-1 Section 17.1 QA Records QA-RPP-WTP-1701, Records System	
BR 18 100 =>800	X		PNNL-NQA-EQAM-1 Section 18.1 Audits PNNL-AP-1801, Internal Audits PNNL-AP-1802 Supplier Qualification Procedure PNNL-AP-1803 Evaluation of Qualified Suppliers PNNL-AP-1804 Projects Assessments	

14.3. SRNL – QA

SRNL work scope will be performed in accordance with 1Q, QAP 2-3 (Control of Research and Development Activities). Under this procedure, research and development work shall be classified as either a Task Activity or Scoping Activity based upon the work initiating documentation and customer requirements. The WP-5 Project Team for the Fluidized Bed Steam Reformer Low-level Waste Form Qualification task (WP-5.2.1) has determined that a graded approach will be utilized for this scope. Initial testing will be performed as "scoping" and will thus be controlled using SRNL L1 Manual, 7.10 (Identification of Technical Work Requirements) and other appropriate SRNL QA protocols. The scoping activities may be upgraded to a Task Activity during the course of the project. It should be noted that 1Q, QAP2-3 states that data collected in the scoping activities may be used if collected with sufficient and appropriate controls. In order to upgrade results, a Task Technical Plan and a Task QA plan shall be generated, and the Task Technical Plan shall specify the method of upgrading.

Implementing Procedures	Yes	No	AR
1.0. Organization			
1Q, QAP 1-1 Organization	X		
• L1, 1.02, SRNL Organization	X		
1Q, QAP 1-2 Stop Work			X
2.0. Quality Assurance Program			
1Q, QAP 2-1, Quality Assurance Program	X		
• L1, 8.02, SRNL QA Program Implementation and Clarification	X		
1Q, QAP 2-2, Personnel Training & Qualification	X		
• L1, 7.10 Identification of Technical Work Requirements	X		
1Q, QAP 2-3, Control of Research and Development Activities	X		
• L1, 7.10 Identification of Technical Work Requirements			
1Q, QAP 2-7, QA Program Requirements for Analytical Measurement Systems	X		
3.0. Design Control			
1Q, QAP 3-1, Design Control		X	
4.0. Procurement Document Control			
1Q, QAP 4-1, Procurement Document Control			X
• 7B, Procurement Management Manual			X
• 3E, Procurement Specification Procedure Manual			X
• E7, 3.10, Determination of Quality Requirements for Procured Items			X
5.0. Instructions, Procedures and Drawings			
1Q, QAP 5-1, Instructions, Procedures and Drawings	X		
• L1, 1.01, Administration of SRNL Procedures and Work Instructions	X		
• L1, 7.26 R&D Work Control Documents	X		
• E7, 2.30 Drawings		X	
6.0. Document Control			
1Q, QAP 6-1, Document Control	X		
• 1B, MRP 3.32, Document Control	X		
7.0. Control of Purchase Items and Service			
1Q, QAP 7-2, Control of Purchase Items and Services			X
• 7B, Procurement Management Manual			X
• 3E, Procurement Specification Procedure Manual			X
1Q, QAP 7-3, Commercial Grade Item Dedication		X	
• E7, 3.46 Replacement Item Evaluation/Commercial Grade Dedication		X	

Implementing Procedures	Yes	No	AR
8.0. Identification and Control of Items			
1Q, QAP 8-1, Identification and Control of Items			X
• L1, 8.02 SRNL QA Program Implementation and Clarification			X
9.0. Control of Processes			
1Q, QAP 9-1, Control of Processes		X	
1Q, QAP 9-2, Control of Nondestructive Examination		X	
1Q, QAP 9-3, Control of Welding and Other Joining Processes		X	
1Q, QAP 9-4, Work Planning and Control		X	
• 1Y, 8.20, Work Control Procedure			
10.0. Inspection			
1Q, QAP 10-1, Inspection		X	
• L1, 8.10, Inspection		X	
11.0. Test Control			
1Q, QAP 11-1, Test Control		X	
12.0. Control of Measuring and Test Equipment			
1Q, QAP 12-1, Control of Measuring and Test Equipment	X		
1Q, QAP 12-2, Control of Installed Process Instrumentation			X
1Q, QAP 12-3, Control and Calibration of Radiation Monitoring Equipment (not applicable to E&CPT)		X	
13.0. Packaging, Handling, Shipping, and Storage			
1Q, QAP 13-1, Packaging, Handling, Shipping, and Storage			X
• L1 8.02 SRNL QA Program Implementation and Clarification			X
14.0 Inspection, Test, and Operating Status			
1Q, QAP 14-1, Inspection Test, and Operating Status			X
• L1, 8.02 SRNL QA Program Implementation and Clarification			X
15.0. Control of Nonconforming Items			
1Q, QAP 14-1, Control of Nonconforming Items			X
L1, 8.02 SRNL QA Program Implementation and Clarification			X
16.0. Corrective Action System			
1Q, QAP 16-3			X
• 1B, MRP 4.23, Corrective Action Program			X
17.0. Quality Assurance Records			
1Q, QAP 17-1, Quality Assurance Records Management	X		
• L1, 8.02 SRNL QA Program Implementation and Clarification	X		
• L1, 7.16, Laboratory Notebooks and Logbooks	X		
18.0. Audits			
1Q, QAP 18-2, Surveillance			X
1Q, QAP 18-3, Quality Assurance External Audits			X
1Q, QAP 18-4, Management Assessment Program			X
• 12Q, SA-1, Self-Assessment			
1Q, QAP 18-6, Quality Assurance Internal Audits			X
1Q, QAP 18-7, Quality Assurance Supplier Surveillance			X
19.0. Quality Improvement			
1Q, QAP 19-2, Quality Improvement			X
• L1, 8.02 SRNL QA Program Implementation and Clarification			X
20.0. Software Quality Assurance			
1Q, QAP 20-1, Software Quality Assurance		X	
• E7, 5.0, Software Engineering and Control		X	
21.0 Environmental Quality Assurance			
1Q, QAP 21-1, Quality Assurance Requirements for the Collection and Evaluation of Environmental Data (E&CPT works to QAP 2-3 and is exempt from this QAP.)		X	
Special Requirements			
In addition to procedures noted above: special requirements (applicable if RW-033P QA program specified by customer) L1, 8.21, Supplemental Quality Assurance Requirements for DOW/RW-0333P		X	

The task being performed by SRNL can be categorized as the following:

Is the work Technical Baseline or Non-Baseline?	Baseline	Non-Baseline	
	X		
Is the work R&D, Routine Service, or Engineering Design?	R&D	Routine Service	Engineering Design
	X		
Is the work for an onsite or offsite customer?	Onsite	Offsite	

14.4. THOR Treatment Technology – QA

Quality Assurance (QA) implemented by THOR Treatment Technologies, LLC (TTT) is in accordance with the TTT Quality Assurance Plan. This document is based on ASME NQA-1-2000, DOE Order 414.1C, and 10 CFR 830.120. Personnel performing work are trained to this document and the implementing procedures and instructions to ensure that work is performed safely and in a consistent manner. Records for each involved individual are documented and maintained in a project training file.

TTT does not perform BSR operations or analytical procedures/analyses. These tasks are being performed by SRNL or PNNL, therefore TTT defers to the graded, but rigorous, QA Programs and QA Plan Procedure Matrices implemented by these two organizations.

THOR Treatment Technologies, LLC Quality Assurance Procedures Matrix

TTT Project Quality Assurance Program Element	TTT Applicability	Implementing Document Procedure	Exceptions/Deviations from QAP Requirements
1. Organization	X	TT/QA-100	A Quality Assurance Project Plan will be developed with the Project Specific Organization
2. QA Program	X	PQP 2.1, 2.2, and 2.3 and PQP 3.6	
3. Design Control	X	PQP 3.1, 3.5, and EP-0.0, 1.0, 2.0, 3.0, and 4.0	A new procedure may be developed to address the Project Specific Safety Categories and Quality Level Classifications
4. Procurement Document Control	X	PQP 4.1	
5. Instructions, Procedures, and Drawings	X	PQP 5.1	
6. Document Control	X	PQP 6.1 and 6.2	
7. Control of Purchased Items and Services	X	PQP 7.1 and 7.2	
8. Identification and Control of Items	X	PQP 8.1	
9. Control of Special Processes	X	PQP 9.1	
10. Inspection	X	PQP 10.1 and 10.2	
11. Test Control	X	PQP 11.1	
12. Control of Measuring and Test Equipment	X	PQP 12.1	
13. Handling, Storage, and Shipping	X	PQP 13.1	
14. Inspection, Test and Operating Status	X	PQP 14.1	

TTT Project Quality Assurance Program Element	TTT Applicability	Implementing Document Procedure	Exceptions/Deviations from QAP Requirements
15. Control of Nonconforming items	X	PQP 15.1	
16. Corrective Action	X	PQP 16.1	
17. QA Records	X	PQP 17.1 and 17.2	
18. Audits	X	PQP 18.1 and 18.2	
19. Software	X	PQP 3.1	
Note: X = applicability and N/A = Not Applicable			

15.0 Schedule Summary

Table 15.1 summarizes the key task activities, specific scope, and responsible organizations associated with the preparation and characterization of monoliths prepared from mineralized product from FBSR run P1-B. A time phased schedule to support the preparation and characterization of monoliths prepared from mineralized product from FBSR run P1-B activities is also shown in Table 15.1. Key Task Activities and Target Activity Dates Figure 15.1 and 15.2 is a high-level summary schedule of the activities to support FBSR waste form qualification. Table 15.2 summarizes the FY2010 key milestones for WP-5.2.1 for FY2010 and outyears.

Table 15.1. Key Task Activities and Target Activity Dates

Task Activity	Specific Scope	Performing Organization	*Target Activity Date	
Hanford LAW Sample Preparation and Shipping				
			Start	Finish
	Hanford LAW Sample #1	WRPS	08/2010	09/2010
	Hanford LAW Sample #2	-	08/2010	09/2010
	Hanford LAW Sample #3	-	09/2010	12/2010
Perform Bench Scale Reformer Tests and Granular/Monolith Samples for Testing				
			Start	Finish
Granular and Monolith Product	SRS Shimmed Secondary Waste Sample	SRNL/TTT	08/2010	11/2010
-	SRS LAW Sample	SRNL	08/2010	12/2010
-	Hanford LAW Sample #1	-	11/2010	02/2011
-	Hanford LAW Sample #2	-	01/2011	03/2011
-	Hanford LAW Sample #3	-	02/2011	05/2011
FBSR Product from 2008 HRI (Run P-1B) Prepare Monolith and Characterize Granular/Monolith Samples				
			Start	Finish
	Receive blended mineralized FBSR product	TTT/SRNL/PNNL	-	9/2010
	Characterize and Monolith FBSR Product	SRNL (support from PNNL)	09/2010	07/2011
Regulatory Testing				
			Start	Finish
TCLP	Perform TCLP Testing on Non-Radioactive and Radioactive BSR Product	SRNL/PNNL	08/2010	08/2011
	SRS LAW (non radioactive)	SRNL subcontractor	-	-
	SRS LaW (radioactive)	SRNL subcontractor	-	-
	Hanford LAW #1 (non radioactive)	SRNL subcontractor	-	-
	Hanford LAW #1 (radioactive)	PNNL	-	-
	Hanford LAW #2 (non radioactive)	SRNL subcontractor	-	-
	Hanford LAW #2 (radioactive)	PNNL	-	-
	Hanford LAW #3 (non radioactive)	SRNL subcontractor	-	-
	Hanford LAW #3 (radioactive)	PNNL	-	-
Compressive Strength ASTM C39/C39M	Perform Compression Testing on Non-Radioactive and Radioactive BSR Samples	SRNL	09/2010	10/2011
	SRS LAW	-	09/2010	05/2011
	Hanford LAW #1	-	01/2011	06/2011
	Hanford LAW #2	-	03/2011	08/2011
	Hanford LAW #3	-	04/2011	10/2011
Monolith Diffusion Test ASTM C1308	Perform Diffusion Testing on Non-Radioactive and Radioactive BSR Samples	SRNL	09/2010	10/2011
-	SRS LAW	-	09/2010	05/2011
-	Hanford LAW #1	-	01/2011	06/2011
-	Hanford LAW #2	-	03/2011	08/2011
-	Hanford LAW #3	-	04/2011	10/2011
	Documentation	-	10/2011	12/2011

Task Activity	Specific Scope	Performing Organization	*Target Activity Date	
Monolith Diffusion Test ASTM C1308	Perform Diffusion Testing on Non-Radioactive and Radioactive BSR Samples	PNNL	09/2010	12/2011
-	SRS LAW	-	09/2010	06/2011
-	Hanford LAW #1	-	02/2011	06/2011
-	Hanford LAW #2	-	04/2011	09/2011
-	Hanford LAW #3	-	05/2011	10/2011
-	Documentation of Results	-	10/2011	12/2011
Performance Testing				
			Start	Finish
Short-Term PCT-A ASTM C1285-08	SRS LAW	SRNL	09/2010	02/2011
	Hanford Sample #1	-	01/2011	03/2011
	Hanford Sample #2	-	03/2011	05/2011
	Hanford Sample #3	-	04/2011	06/2011
	Characterization/Results	-	05/2011	08/2011
Short-Term PCT-A ASTM C1285-08	SRS LAW	PNNL	09/2010	02/2011
	Hanford Sample #1	-	02/2011	04/2011
	Hanford Sample #2	-	04/2011	05/2011
	Hanford Sample #3	-	05/2011	07/2011
	Characterization/Results	-	06/2011	08/2011
Long-Term PCT-B ASTM C1285-08	SRS LAW	SRNL	09/2010	08/2011
	Hanford Sample #1	-	02/2011	09/2011
	Hanford Sample #2	-	02/2011	09/2011
	Hanford Sample #3	-	04/2011	11/2011
	Characterization/Results	-	07/2011	02/2012
Single Pass Flow-Through Testing ASTM C1662	Hazen 2008 – granular and monolith (full suite)	PNNL	09/2010	12/2011
	BSR Non-Rad SRS LAW – granular and monolith (subset)	-	01/2011	03/2012
	SRS LAW – granular and monolith (subset)	-	03/2011	11/2011
	Hanford Sample #1 – granular and monolith (subset)	-	03/2011	11/2011
	Hanford Sample #2 – granular and monolith (subset)	-	11/2011	07/2012
	Hanford Sample #3 – granular and monolith (subset)	-	11/2011	06/2012
Analysis of Previous PUF Test Samples	Characterize Samples from a PUF Test Conducted with FBSR product produced at SAIC/STAR in 2004 to determine alteration phases formed	PNNL	10/2010	09/2011
Pressurized Unsaturated Flow Testing	SRS LAW	PNNL	11/2010	01/2013
	Hanford Sample #1	-	01/2012	03/2013
	Hanford Sample #2	-	03/2012	05/2013
	Hanford Sample #3	-	05/2012	07/2013

Task Activity	Specific Scope	Performing Organization	*Target Activity Date	
Tc and I Location and Speciation	Determine the location and speciation of Tc and I using several analytical techniques on all radioactive spiked sample	PNNL/LBNL SRNL (CSEM/EDS)	08/2010	11/2011
Pure Phase Minerals – Preparation and Testing				
Preparation of Minerals	Prepare Nepheline	SRNL	09/2010	11/2010
	Prepare Cl-sodalite	-	10/2010	12/2010
	Prepare I-sodalite	-	11/2010	12/2010
	Prepare Re-sodalite	-	11/2010	02/2011
	Prepare F-sodalite	-	02/2011	04/2011
	Prepare Nosean	-	11/2010	03/2011
Measurement of Thermodynamic Constants of Pure Phase Minerals	Determine the thermodynamic constants for pure phases minerals and a select number of solid solutions via measurement and estimation techniques	PNNL/UC Davis	10/2010	03/2012
Single Pass Flow-Through Testing ASTM C1662	Nepheline dissolution and report - major mineral phases present in FBSR product (full suite)	ORNL	11/2010	08/2011
	Cl-sodalite dissolution and report - major mineral phases present in FBSR product (subset)	-	12/2010	03/2011
	I-sodalite dissolution and report - major mineral phases present in FBSR product (full suite)	-	01/2011	10/2011
	Re-sodalite dissolution and report - major mineral phases present in FBSR product (full suite)	-	03/2011	11/2011
	F-sodalite dissolution and report - major mineral phases present in FBSR product (subset)	-	04/2011	08/2011
	Nosean dissolution - major mineral phases present in FBSR product (full suite)	-	08/2011	02/2012
IDF Performance Assessment	Initial Model Calculations	WRPS/PNNL/SRNL	08/2010	12/2011
	Final Performance Assessment	WRPS/PNNL/SRNL	12/2011	10/2013
*Target dates are based upon the availability of funding and meeting the regulatory requirements for shipping and receiving the Hanford LAW samples.				

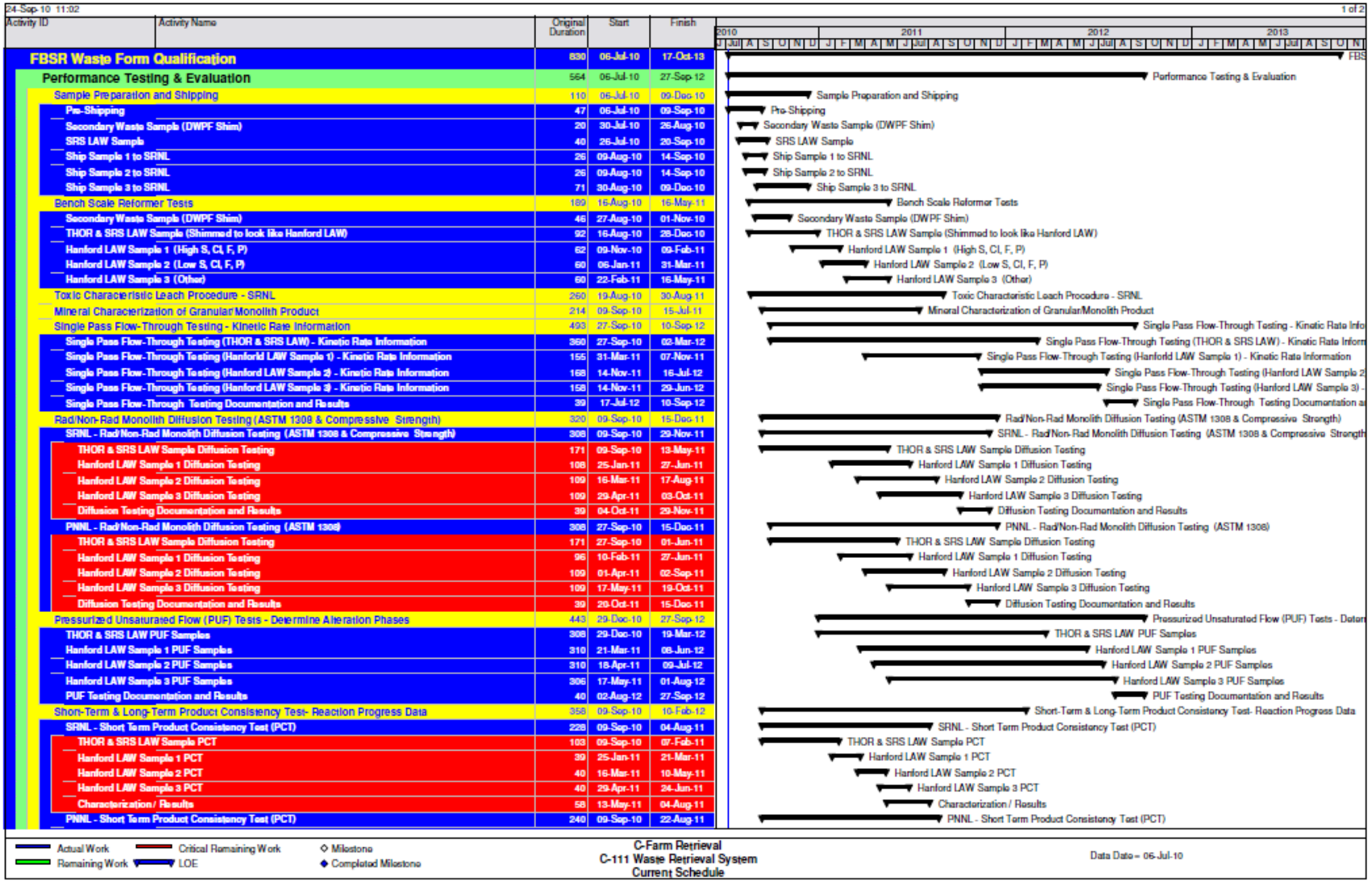

Figure 15.1. Final Project Schedule, page #1

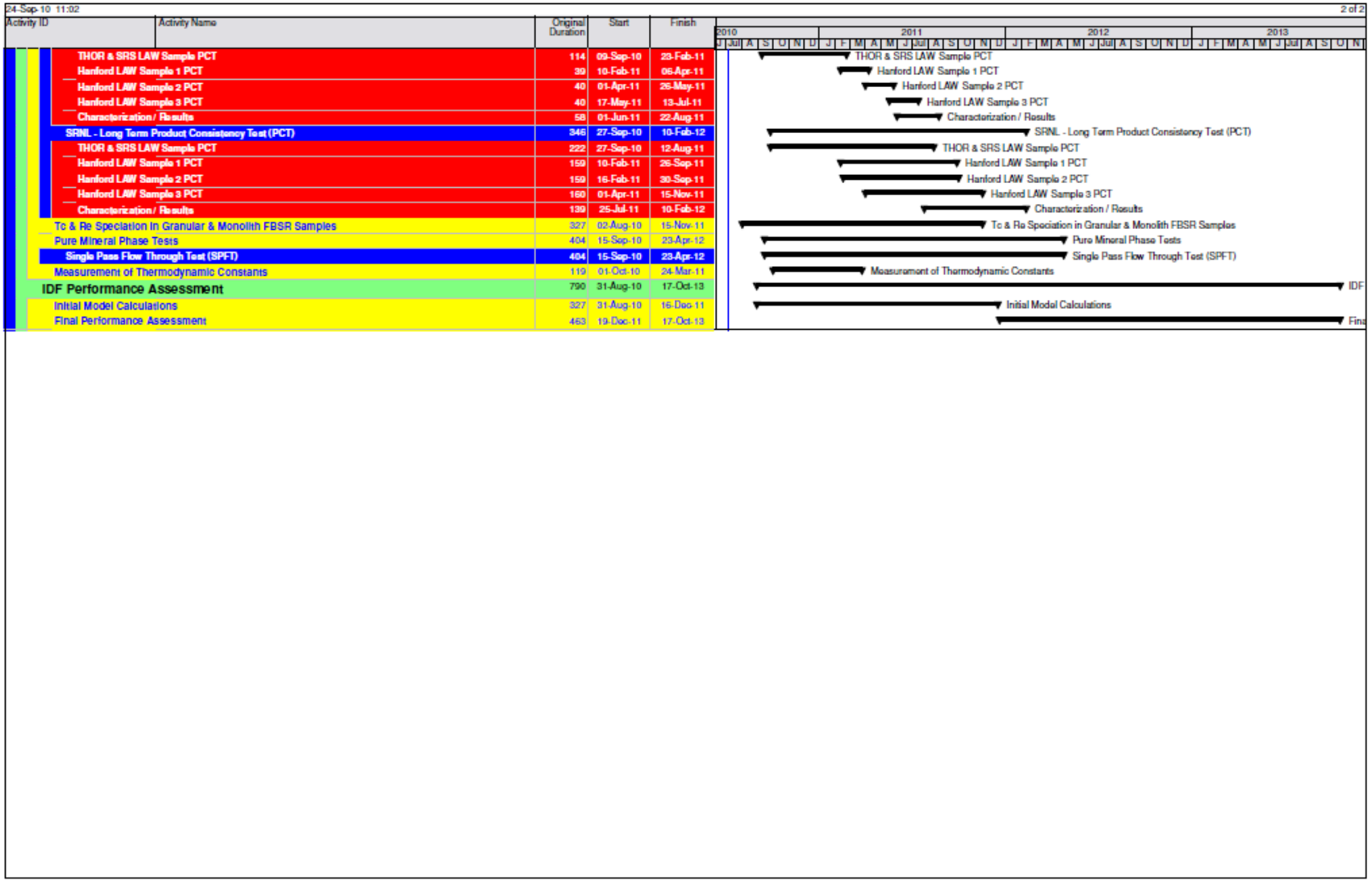

Figure 15.2. Final Project Schedule, page #2

Table 15.2. List of Milestones for WP-5.2.1 in FY2010 and Out Years

Milestone Number	Milestone Title	Completion date
	Description	
WP-5.2.1 Fluidized Bed Steam Reformer Low-level Waste Form Qualification		
WP-5.2.1-01	Issue test plan for waste form qualification	5/2010 complete
	Issue a joint task plan between SRNL, TTT, WRPS, and PNNL. Task plan documents key task activities, performers, and deliverables.	
WP-5.1.1-02	Issue performance modeling strategy document	12/2010
Complete 1st actual waste bench-scale test to demonstrate treatment of Hanford Secondary Waste Sample – DWPF shim		11/2010
Complete 1st actual waste bench-scale test to demonstrate range of Hanford LAWs – SRS shim (Rassat 68 tank simulant)		12/2010
Complete 2nd actual waste bench-scale test to demonstrate range of Hanford LAWs – high anion (S, Cl, F, P)		02/2011
Complete 3rd actual waste bench-scale test to demonstrate range of Hanford LAWs – low anion (S, Cl, F, P)		03/2011
Complete 4th actual waste bench-scale test to demonstrate range of Hanford LAWs – Other (complexant tank)		05/2011
WP-5.2.1-03	Complete advanced FBSR waste form development	9-30-2011
Out Year Milestones		
Preliminary data available to support M-62-40 System Plan Report		1/2012
Preliminary data available to support M-62-45 Supplemental Treatment Selection		4/2012
WP-5.2.1-04	Complete performance testing/source term modeling for advanced waste form	10/2013
WP-5.2.1-05	Complete independent technical review	12-30-2013
WP-5.2.1-06	Decision point to proceed with FBSR	1-30-2014

16.0 References

(1) Marshall, D. W., Soelberg, N.R., Shaber, K.M. *THOR^{sm} Bench-Scale Steam Reforming Demonstration*, Idaho National Laboratory, 2003.

(2) Olson, A. L., Soelberg, N.R., Marshall, D.W., Anderson, G.L. *Fluidized Bed Steam Reforming of INEEL SBW Using THOR^{sm} Mineralizing Technology*, Idaho National Laboratory, 2004.

(3) Soelberg, N. R., Marshall, D.M., Bates, S.O., Siemer, D.D. *SRS Tank 48H Steam Reforming Proof-of-Concept Test Report*, Idaho National Laboratory, 2004.

(4) Crawford, C. L., Jantzen, C.M. *Durability Testing of Fluidized Bed Steam Reformer (FBSR) Waste Forms for Sodium Bearing Waste (SBW) at Idaho National Laboratory*, Savannah River National Laboratory, 2007.

(5) Jantzen, C. M. *Engineering Study of the Hanford Low Activity Waste (LAW) Steam Reforming Process*, Savannah River Technology Center, 2002.

(6) Olson, A. L., Soelberg, N.R., Marshall, D.W., Anderson, G.L. *Fluidized Bed Steam Reforming of Hanford LAW Using THOR^{sm} Mineralizing Technology*, Idaho National Laboratory, 2004.

(7) Mann, F. M., Puigh, R.J., Khaleel, R., Finfrock, S., McGrail, B.P., Bacon, D.H., Serne, R.J. *Risk Assessment Supporting the Decision on the Initial Selection of Supplemental ILAW Technologies*, Pacific Northwest national Laboratory, 2003.

(8) Jantzen, C. M. In *Environmental Issues and Waste Management Technologies in the Ceramic and Nuclear Industries IX*; Vienna, J. D., and D.R. Spearing, Ed. 2004; Vol. 155, p 319.

(9) Pareizs, J. M., Jantzen, C.M., Lorier, T.H. *Durability Testing of Fluidized Bed Steam Reformer (FBSR) Waste Forms for High Sodium Wastes at Hanford and Idaho*, Savannah River National Laboratory, 2005

(10) Jantzen, C. M., Pareizs, J.M., Lorier, T.H., Marra, J.C. In *Environmental Issues and Waste Management Technologies XI* Herman, C. C., S.L. Marra, D.R. Spearing, L. Vance, and J.D. Vienna, Ed. 2005, p 121.

(11) Jantzen, C. M., Lorier, T.H., Marra, J.C., Pareizs, J.M. In *WM'06* Tucson, AZ, 2006.

(12) Jantzen, C. M. *Fluidized Bed Steam Reformer (FBSR) Product: Monolith Formation and Characterization*, Savannah River National Laboratory, 2006.

(13) Jantzen, C. M. In *WM'07* Tucson, AZ, 2007.

(14) Lorier, T. H., Pareizs, J.M., Jantzen, C.M. *Single Pass Flow Through (SPFT) Testing of Fluidized Bed Steam Reforming (FBSR) Waste Forms*, Savannah River National Laboratory, 2005.

(15) Jantzen, C. M., Lorier, T.H., Pareizs, J.M., Marra, J.C. In *Scientific Basis for Nuclear Waste Management XXX*; Dunn, D. S., C. Poinssot, B. Begg, Ed. 2007, p 379.

(16) Pierce, E. M. In *Material Science and Technology*; Apblett, A., Ed.; Material Science and Technology: Detroit, Michigan, 2007.

(17) Jantzen, C. M., Crawford, C.L. In *WM'10* Phoenix, AZ, 2010.

(18) Rassat, S. D., Mahoney, L.A., Russell, R.L., Bryan, S.A., Sell, R.L. *Cold Dissolved Saltcake Waste Simulant Development, Preparation, and Analysis*, Pacific Northwest National Laboratory, 2003.

(19) THOR *Report for Treating Hanford LAW and WTP SW Simulants: Pilot Plant Mineralizing Flowsheet*, THOR Treatment Technologies, LLC, 2009.

(20) Jantzen, C. M. *Mineralization of Radioactive Wastes By Fluidized Bed Steam Reforming (FBSR): Comparisons to Vitreous Waste Forms and Pertinent Durability Testing*, Savannah River National Laboratory, 2008.

(21) US DOE, Office of Environmental Management. *Tank Waste Research and Development Plan*. Washinton, DC, 2010.

(22) Jantzen, C. M., Crawford, C.L.; Savannah River National Laboratory: Aiken, SC, 2010.

(23) ASTM *Standard Practice for Making and Curing Concrete Test Specimens in the Laboratory*, ASTM International, 2007.

(24) ASTM *Standard Practice for Measurement of the Glass Dissolution Rate Using the Single-Pass Flow-Through Test Method*, ASTM International, 2007.

(25) ASTM *Standard Test Methods for Determining Chemical Durability of Nuclear, Hazardous, and Mixed Waste Glasses and Multiphase Glass Ceramics: The Product Consistency Test (PCT)*, ASTM International, 2008.

(26) ASTM *Standard Test Method for Accelerated Leach Test for Diffusive Releases from Solidified Waste and a Computer Program to Model Diffusive, Fractional Leaching from Cylindrical Waste Forms*, ASTM International, 2008.

(27) Crank, J. *The Mathematics of Diffusion*; Second ed.; Oxford University Press: New York, 1956.

(28) Chou, L.; Wollast, R. *Geochim. Cosmochim. Acta* **1984**, *48*, 2205.

(29) Oelkers, E. H.; Schott, J.; Devidal, J. L. *Geochim. Cosmochim. Acta* **1994**, *58*, 2011.

(30) Oelkers, E. H.; Schott, J.; Devidal, J. L. *Geochim. Cosmochim. Acta* **2001**, *65*, 4429.

(31) Wolff-Boenisch, D.; Gislason, S. R.; Oelkers, E. H.; Putnis, C. *Geochim. Cosmochim. Acta* **2004**, *68*, 4843.

(32) Holdren, G. R.; Speyer, P. M. *Geochim. Cosmochim. Acta* **1987**, *51*, 2311.

(33) Casey, W. H.; Westrich, H. R. *Nature* **1992**, *355*, 157.

(34) Icenhower, J. P.; Dove, P. M. *Geochim. Cosmochim. Acta* **2000**, *64*, 4193.

(35) Rimstidt, J. D.; Dove, P. M. *Geochim. Cosmochim. Acta* **1986**, *50*, 2509.

(36) Dove, P. M. *Am. J. Sci.* **1994**, *294*, 665.

(37) Devidal, J. L.; Schott, J.; Dandurand, J. L. *Geochim. Cosmochim. Acta* **1997**, *61*, 5165.

(38) White, A. F.; Brantley, S. L. *Chemical Weathering Rates in Silicates*; Reviews in Mineralogy ed.; Mineralogical Society of America: Washington, D.C., 1995; Vol. 31.

(39) Åagaard, P.; Helgeson, H. C. *Am. J. Sci.* **1982**, *282*, 237.

(40) Hamilton, J. P.; Brantley, S. L.; Pantano, C. G.; Criscenti, L. J.; Kubicki, J. D. *Geochimica Cosmochimica Acta* **2001**, *65*, 3683.

(41) Hamilton, J. P.; Pantano, C. G.; Brantley, S. L. *Geochimica Cosmochimica Acta* **2000**, *64*, 2603.

(42) Geisinger, K. L.; Oestrike, R.; Navrotsky, A.; Turner, G. L.; Kirkpatrick, R. J. *Geochim. Cosmochim. Acta* **1988**, *52*, 2405.

(43) Icenhower, J. P.; McGrail, B. P.; Shaw, W. J.; Pierce, E. M.; Nachimuthu, P.; Shuh, D. K.; Rodriguez, E. A.; Steele, J. L. *Geochimica Cosmochimica Acta* **2008**, *72*, 2767.

(44) Barkatt, A.; Gibson, B. C.; Macedo, P. B.; Montrose, C. J.; Sousanpour, W.; Barkatt, A.; Boroomand, M.-A.; Rogers, V.; Penafiel, M. *Nuc. Tech.* **1986**, *73*, 140.

(45) Bourcier, W. L. *Material Research Symposium Proceedings* **1991**, *212* 3.

(46) Bourcier, W. L. *Material Research Symposium Proceedings* **1994**, *333*, 69.

(47) Bunker, B. C.; Tallant, D. R.; Headley, T. J.; Turner, G. L.; Kirkpatrick, R. J. *Physics and Chemistry of Glasses* **1988**, *29*, 106.

(48) Casey, W. H.; Bunker, B. C. In *Mineral-Water Interface Geochemistry*; Hochella, M. F., Jr., White, A. F., Eds.; Mineralogical Society of America: Washington, D.C., 1990; Vol. 23, p 397.

(49) Hench, L. L.; Clark, D. E.; Harker, A. B. *Journal of Materials Science* **1986**, *21*, 1457.

(50) Icenhower, J. P.; Samson, S.; Luttge, A.; McGrail, B. P. In *Energy, Waste, and the Environment: A Geochemical Perspective*; Giere, R., Stille, P., Eds.; Geological Society of London: 2004; Vol. 236, p 579.

(51) McGrail, B. P.; Ebert, W. L.; Bakel, A. J.; Peeler, D. K. *J. Nuc. Mat.* **1997**, *249*, 175.

(52) Strachan, D. M.; Croak, T. L. *Journal of Non-Crystalline Solids* **2000**, *272*, 22.

(53) Werme, L. O.; Bjorner, I. K.; Bart, G.; Lutze, W.; Ewing, R. C.; Magrabi, C. *J. Mater. Res.* **1990**, *5*, 1130.

(54) Vernaz, E.; Dussossoy, J. L. *Applied Geochemistry* **1992**, *1*, 13.

(55) Vernaz, E.; Gin, S.; Jegou, C.; Ribet, I. *J. Nuc. Mat.* **2001**, *298*, 27.

(56) DOE *High-level Borosilicate Waste Glass: A Compendium of Corrosion Characteristics, vol. 1*, U.S. Department of Energy Office of Waste Management, 1994.

(57) DOE *High-Level Waste Borosilicate Glass: A Compendium of Corrosion Characteristics, vol. 2*, U.S. Department of Energy Office of Waste Management, 1994.

(58) Gin, S.; Jollivet, P.; Mestre, J. P.; Jullien, M.; Pozo, C. *Applied Geochemistry* **2001**, *16*, 861.

(59) Grambow, B. *Material Research Symposium Proceedings* **1985**, *44*, 15.

(60) Pierce, E. M.; Richards, E. L.; Davis, A. M.; Reed, L. R.; Rodriguez, E. A. *Environmental Chemistry* **2008**, *5*, 73

(61) Pierce, E. M.; Rodriguez, E. A.; Calligan, L. J.; Shaw, W. J.; McGrail, B. P. *App. Geochem.* **2008**.

(62) Abraitis, P. K.; McGrail, B. P.; Trivedi, D. P.; Livens, F. R.; Vaughan, D. J. *J. Nucl. Mater.* **2000**, *280*, 206.

(63) Abraitis, P. K.; McGrail, B. P.; Trivedi, D. P.; Livens, F. R.; Vaughan, D. J. *J. Nucl. Mater.* **2000**, *280*, 196.

(64) Abraitis, P. K.; Livens, F. R.; Monteith, J. E.; Small, J. S.; Trivedi, D. P.; Vaughan, D. J.; Wogelius, R. A. *Applied Geochemistry* **2000**, *15*, 1399.

(65) ASTM *Standard Test Method for Compressive Strength of Cylindrical Concrete Specimens*, ASTM International, 2001.

(66) Bullock Jr., J. H., Cathcart, J.D., Betterton, W.J.; U.S. Geological Survey: Denver, CO, 2002.

(67) Pierce, E. M.; Icenhower, J. P.; Serne, R. J.; Catalano, J. *J. Nuc. Mat.* **2005**, *345*, 206.

(68) Wellman, D. M.; Icenhower, J. P.; Gamerdinger, A. P.; Forrester, S. W. *Am. Min.* **2006**, *91*, 143.

(69) Icenhower, J. P.; Strachan, D. M.; McGrail, B. P.; Scheele, R. D.; Rodriguez, E. A.; Steele, J. L.; Legore, V. L. *Am. Min.* **2006**, *91*, 39.

(70) Pierce, E. M.; McGrail, B. P.; Valenta, M. M.; Strachan, D. M. *Nuclear Technology* **2006**, *155*, 133.

(71) Pierce, E. M.; McGrail, B. P.; Marra, J.; Martin, P. F.; Arey, B. W.; Geiszler, K. N. *Applied Geochemistry* **2007**, *22*, 1841.

(72) Wierenga, P. J.; Young, M. H.; Gee, G. W.; Hills, R. G.; Kincaid, C. T.; Nicholson, T. J.; Cady, R. E. *Soil Characterization Methods for Unsaturated Low-Level Waste Sites*, Pacific Northwest Laboratory, 1993.

(73) Mattigod, S.; McGrail, B. P. *Microporous, Mesoporous Materials* **1999**, *27*, 41.

Appendix A: Excerpt From EM "TANK WASTE RESEARCH AND DEVELOPMENT PLAN" June 2010, pp. 66 - 70

Appendix A: Excerpt From EM "TANK WASTE RESEARCH AND DEVELOPMENT PLAN" June 2010, pp. 66 - 70

Background - The Hanford Tank Waste Treatment and Immobilization Plant (WTP) is being constructed to treat most of Hanford tank wastes. However, the low-activity fraction of tank waste (LAW) will be generated at over twice the rate that the currently designed LAW vitrification facility can treat. Either a second LAW vitrification facility or other supplemental LAW treatment technology is needed to meet schedule objectives and approved tank closure deadlines. One promising supplemental technology is fluidized bed steam reforming (FBSR) to produce a sodium-alumino-silicate (NAS) waste form. The NAS waste form is primarily composed of Nepheline (ideally $NaAlSiO_4$), Sodalite (ideally $Na_8[AlSiO_4]_6Cl_2$), and Nosean (ideally $Na_8[AlSiO_4]_6SO_4$). Semi-volatile anions such as ReO_4^-, TcO_4^-, and I^- are expected to replace sulfate and chloride in the Nosean-Sodalite mineral structures – immobilizing them.

The release of semi-volatile radionuclides ^{99}Tc and ^{129}I from granular NAS waste form was found by preliminary performance test to be limited by Nosean solubility.[16] The predicted performance of the NAS waste form was found to be equivalent or better than the glass waste form in the initial supplemental LAW treatment technology risk assessment as shown in Figure 1.

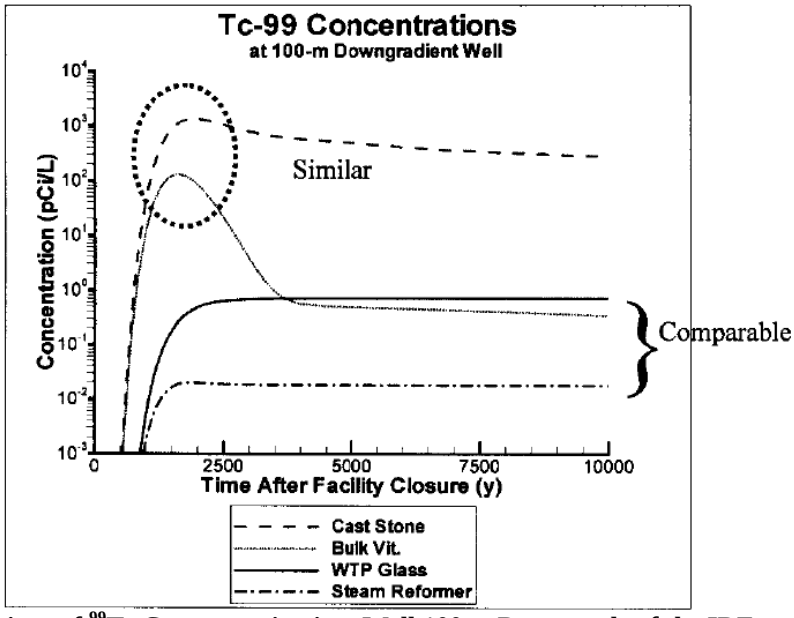

Figure A.1. Comparison of ^{99}Tc Concentration in a Well 100 m Downgrade of the IDF as a Function of Time (From Mann et al. 2003)

The granular FBSR waste form has high surface area, no resistance to mechanical deformation, and may contain respirable fines. Therefore, Savannah River National Laboratory (SRNL) and THOR® Treatment Technologies (TTT) developed a method to monolith the NAS waste form.[9, 10, 11] Five families of binders were developed:

- Ordinary Portland Cement, a binder of primarily calcium silicate with some calcium aluminate, and calcium aluminoferrite
- High alumina cements, composed mainly of calcium aluminates rather than calcium silicates (creates lower pH pore water than Ordinary Portland Cement)
- Geopolymers, which are amorphous to semi-crystalline, three-dimensional inorganic silico-

aluminate polymers formed by mixing clay with sodium silicate and/or NaOH
- Geopolymers, which are amorphous to semi-crystalline, three-dimensional inorganic silico-aluminate polymers formed by mixing fly ash with sodium silicate and/or NaOH
- Ceramicrete (ceramic cement), which is composed of $MgKPO_4 \bullet 6H_2O$ and made by mixing magnesium oxide, monopotassium phosphate, and Class F fly ash

The geopolymer made with fly ash and NaOH performed the best so far. Although Product Consistency Tests (PCTs) and Toxicity Characterization Leaching Procedure (TCLP) test were performed, little long-term testing is available to determine the impacts of the monolithing process and form on the long-term performance of the NAS waste form produced by FBSR.

The Hanford Tank Closure and Waste Management (TC&MW) Environmental Impact Statement (EIS) was recently issued as a draft for public comment.[12] For the FBSR NAS waste form the draft EIS risk assessment uses a waste matrix solubility limited release model without chemical feedback. The NAS is assumed to reach its solubility limit in water instantaneously. The results suggest that the granular NAS waste form is not only orders of magnitude less durable than LAW glass, but also well above the regulatory dose limits. These results suggest that NAS waste form is unacceptable for disposal in the Hanford Integrated Disposal Facility (IDF). Since the primary minerals in the NAS waste form are known to survive in natural environments as the minerals nepheline and sodalite this release model does not appear to be appropriate. Separate discussions are underway with the Office of River Protection (ORP) and their EIS contractor to determine if the assumptions used in the draft EIS are appropriate and if changes to the risk assessment should be performed (e.g., using a fractional release rate model) prior to issuing the final EIS.

Data and updated models are required to demonstrate the performance of the FBSR NAS waste form. The results from the updated models are needed to support the schedule for supplemental technology decision under the *Hanford Federal Facility Agreement and Consent Order (Tri-Party Agreement) Proposed Consent Decree and Tri-Party Agreement Modifications for Public Comment*:

> *M-062-40: …Not later than the System Plan Report due date of 10/31/2014, DOE will submit a one-time Hanford Tank Waste Supplemental Treatment Technologies Report, which will be required if a tank waste supplemental treatment technology is proposed, other than a 2nd LAW Vitrification Facility. …*
>
> *M-062-45: … 3. Supplemental treatment selection (a one time selection to be made not later than April 30, 2015) and milestones, which must be consistent with M-062-00 as established by M-062-45 item #5. A 2nd LAW Vitrification Facility must be considered as one of the options. *Milestones M-062-31-T01 through M-062-34-T01 are initially set as target dates and will be established (as may be modified) as interim milestones when they are converted to interim milestones in accordance with applicable HFFACO procedures at the conclusion of this negotiation. …*

A plan was developed to generate these data and models as part of the Tank Waste R&D Plan. The plan targets an early, technically defensible, evaluation of the FBSR process NAS monolithic waste form for Hanford LAW followed by a complete waste form source term model required for IDF performance assessment. The early evaluation will support a supplemental waste form down selection as early as possible with low risk upon receipt of the final risk assessment.

R&D Path Forward - Several key data gaps must be filled to conduct a performance assessment for the NAS waste form (either granular or monolith). These requirements are briefly described below:

1. The speciation of ^{99}Tc in the FBSR product and the distribution of ^{99}Tc amongst the different mineral phases. The speciation really refers to oxidation state and nearest neighbor which requires the use of X-ray absorption spectroscopy (XAS). Selected area X-ray diffraction (XRD)/micro-XRD and electron microscopy of the Tc loaded material are also required. When combined with other data, these results will determine where Tc is located in the waste form.
2. Determination of the fractions and compositions of the minerals formed by FBSR. This will be performed by XRD on multiple different samples – primarily simulated waste samples but with confirmatory tests with actual LAW samples.
3. Develop dissolution rate law parameters for each significant phase in the waste form. This will require a combination of single-pass flow-through (SPFT) testing to isolate individual rate law parameters. Some preliminary results of SPFT results were reported by McGrail et al. (2003) and Jantzen et al (2007) [13, 14], for two different multiphase waste forms (one with Envelope C LAW and one with Envelope A LAW). There is also SPFT data on single crystal natural nepheline (Tole et.al.1985).[15] To complete the rate law, parameters for each individual single phase are necessary along with selected tests for multi-phase waste forms (primarily Re containing, with selected Tc containing measurements to demonstrate Tc release is equivalent to Re-release). Additional tests will be needed to determine the phases formed during reaction with water. These measurements are generally performed by long-term product consistency test (PCT) and pressurized unsaturated flow through (PUF) tests. Finally, thermodynamic parameters of the key individual phases are needed. This data is available for some of the stoichiometric end members, but, not for the solid solutions formed during the process.
4. The impact of the monolithing process (e.g., binder and reactions with granules) on the release/dissolution behavior of the waste form, if any. This will require the use of SPFT and long-term PCT experiments under dilute conditions of the binder with and without FBSR product.
5. Determine the transport properties of the monolithed waste form. This will be performed by diffusion tests such as ANSI-16.1, ASTM 1308, or SW-846-1315. These tests need to be performed for a number of samples including Re-loaded simulants and actual waste samples containing Tc.
6. Determine the effect of Al, Si, and nepheline saturated solutions on Re and Tc release from the FBSR product. This will be used to quantify impact of the Al buffering effect seen in preliminary tests. This is mostly associated with the common ion effect and must be quantified so it can be accounted for in the source term model.
7. A modified waste form release/radionuclide source term model must be developed and validated for inclusion in the IDF performance assessment code. This source-term model will start with that developed by McGrail et al. 2003, but, include: a) the release rates for each phase, b) updated thermodynamic data for solid solution phases, c) common ion effect seen in preliminary experiments, d) transport properties measured in monolith samples, and e) Tc and I partitioning between phases in the waste form.

Three actual Hanford tank waste samples will be used to demonstrate the range of Hanford LAW to be treated by FBSR (representing the minimums and maximums of SO4/Na, Halide/Na, Tc/Na, and potentially other salts to sodium ratios of the waste). The data resulting from the demonstration test program will be used to support the IDF performance assessment and decisions regarding deployment of a non-vitrification technology to immobilize LAW. Prior to performing tests with actual Hanford LAW, a test using SRS waste adjusted to meet Hanford LAW characteristics will be performed. This test is to provide the earliest scientific data regarding waste form leachability and the fate of 99Tc in the mineral phase waste form. This data and resulting analysis will be used to ―buydown" technical risk regarding waste form performance to support critical decisions associated with enhanced tank waste strategy at Hanford for the deployment of the FBSR transformational technology.

A selected subset of this bench scale data will be accelerated for use in waste form selection and reduction

of risk in making this decision prior to a full performance assessment. These early data include Tc partitioning between phases, transport of Tc through a monolithic waste form, and rate law parameters (with only limited thermodynamic data for solid solutions). All of these data will be available for the first of three real waste tests along with engineering scaled Re-surrogate test already performed.

A FBSR waste form preliminary performance evaluation (i.e., risk assessment) will reduce the risk of early decisions by the DOE. In concert with this waste form development and qualification work there is a parallel schedule for process development and demonstration. Several process development activities also support waste form performance evaluation e.g., engineering scale FBSR tests with simulants of the actual wastes tested for waste form performance. These efforts support the target for FBSR waste performance to be completed by October 2013, and to support FBSR facility startup in 2018.

Milestones:

R&D Activity	Finish Date
Issue plan for FBSR waste form development	4/2010 complete
Complete 1st actual waste bench-scale test to demonstrate range of Hanford LAWs – Hanford complexant LAW	9/2010
Complete 2nd actual waste bench-scale test to demonstrate range of Hanford LAWs – high sulfur / Tc / Iodide Hanford LAW	2/2011
Complete 3rd actual waste bench-scale test to demonstrate range of Hanford LAWs – low sulfur / Tc / Iodide Hanford LAW	7/2011
Complete FBSR waste form preliminary performance evaluation	**9/2011**
Preliminary data available to support M-62-40 System Plan Report	1/2012
Preliminary data available to support M-62-45 Supplemental Treatment Selection	4/2012
Complete FBSR waste form performance testing	7/2012
FBSR waste form source term model results available for use in performance assessment	**2/2013**

Summary Chart

R&D Initiative	R&D Activity	FY10	FY11	FY12	FY13	FY14	FY15	FY16	FY17	FY18	FY19	Comments
Fluidized Bed Steam Reformer Low-Level Waste Form Qualification	Hanford LAW FBSR waste form development and qualificaiton											Transfer data in 2011 for waste form selection. Final data and model to support PA model in 2013

DOE Decision
Complete actual waste test
Complete pilot scale demo
Technology Insertion

Completed Work
Planned Work

Appendix B: Fluidized Bed Steam Reformer Briefing to Ines - July 22, 2010

Appendix B: Fluidized Bed Steam Reformer Briefing to Ines – July 22, 2010

Fluidized Bed Steam Reforming Hanford LAW Waste Form Development and Qualification

Description – Fluidized bed steam reformer (FBSR) process is being tested for Hanford low-activity waste (LAW) form development and qualification. If successful, FBSR would reduce the treatment costs and waste volumes at the Hanford site. One key challenge at Hanford is the formulation of a waste form and generation of sufficient data to demonstrate its acceptable performance in the Hanford Integrated Disposal Facility (IDF).

The FBSR will produce a sodium-alumino-silicate (NAS) waste form. The NAS waste form is primarily composed of Nepheline (ideally $NaAlSiO_4$), Sodalite (ideally $Na_8[AlSiO_4]_6Cl_2$), and Nosean (ideally $Na_8[AlSiO_4]_6SO_4$). Semi-volatile anions such as ReO_4^-, TcO_4^-, and I^- are expected to replace sulfate and chloride in the Nosean-Sodalite mineral structures – immobilizing them. The granular FBSR waste form has high surface area, no resistance to mechanical deformation, and may contain respirable fines. Therefore, Savannah River National Laboratory (SRNL) and THOR® Treatment Technologies (TTT) developed a method to monolith the NAS waste form.

Data and updated models are required to demonstrate the performance of the Hanford LAW FBSR NAS monolithic waste form. The results from the updated models are needed to support the schedule for supplemental technology decision. Hanford LAW FBSR waste form development and performance testing and modeling efforts performed under this task are being accelerated to facilitate an early decision on the efficacy of placing this process in the Hanford Site baseline. Testing will use both Hanford actual and simulated low-activity waste.

A plan is being developed to generate these data and models as part of the Tank Waste R&D Plan. The plan targets an early, technically defensible, evaluation of the FBSR process NAS monolithic waste form for Hanford LAW followed by a complete waste form source term model required for IDF performance assessment. The early evaluation will support a supplemental waste form down selection as early as possible with low risk upon receipt of the final risk assessment.

R&D Path Forward - Several key data gaps must be filled to conduct a performance assessment for the NAS waste form (either granular or monolith). These requirements are briefly described below:

8. The speciation of ^{99}Tc, ^{129}I, etc. in the FBSR product and the distribution of ^{99}Tc, etc. amongst the different mineral phases.
9. Determination of the fractions and compositions of the minerals formed by FBSR.
10. Develop dissolution rate law parameters for each significant phase in the waste form. This will require a combination of single-pass flow-through (SPFT) testing to isolate individual rate law parameters. To complete the rate law, parameters for each individual single phase are necessary along with selected tests for multi-phase waste forms (primarily Re containing, with selected Tc containing measurements to demonstrate Tc release is equivalent to Re-release). Additional tests will be needed to determine the phases formed during reaction with water. These measurements are generally performed by long-term product consistency test (PCT) and pressurized unsaturated flow through (PUF) tests. Finally, thermodynamic parameters of the key individual phases are needed.
11. The impact of the monolithing process (e.g., binder and reactions with granules) on the release/dissolution behavior of the waste form, if any.

12. Determine the transport properties of the monolithed waste form. This will be performed by diffusion tests such as ANSI-16.1, ASTM 1308, or SW-846-1315.
13. Determine the effect of Al, Si, and nepheline saturated solutions on Re and Tc release from the FBSR product. This will be used to quantify impact of the Al buffering effect seen in preliminary tests.
14. A modified waste form release/radionuclide source term model must be developed and validated for inclusion in the IDF performance assessment code.

Three actual Hanford tank waste samples will be used to demonstrate the range of Hanford LAW to be treated by FBSR (representing the minimums and maximums of SO4/Na, Halide/Na, Tc/Na, and potentially other salts to sodium ratios of the waste). The data resulting from the demonstration test program will be used to support the IDF performance assessment and decisions regarding deployment of a non-vitrification technology to immobilize LAW. Prior to performing tests with actual Hanford LAW, a test using SRS waste adjusted to meet Hanford LAW characteristics will be performed. This test is to provide the earliest scientific data regarding waste form leachability and the fate of ^{99}Tc in the mineral phase waste form. This data and resulting analysis will be used to "buy down" technical risk regarding waste form performance to support critical decisions associated with enhanced tank waste strategy at Hanford for the deployment of the FBSR transformational technology.

Milestones:

R&D Activity	**Finish Date**
Complete bench scale test of SRS actual LAW adjusted to Hanford LAW characteristic to provide early data on waste form viability.	10/2010
Begin shipping actual Hanford LAW decontaminated samples to SRNL	12/2010
Complete 1st actual Hanford LAW bench scale test to demonstrate range of Hanford LAWs – low sulfur / Tc / Iodide Hanford LAW	1/2011
Complete 2nd actual Hanford LAW bench scale test to demonstrate range of Hanford LAWs – Hanford complexant LAW	3/2011
Complete 3rd actual Hanford LAW bench scale test to demonstrate range of Hanford LAWs – high sulfur / Tc / Iodide Hanford LAW	4/2011
Complete FBSR waste form preliminary performance evaluation	**9/2011**
Preliminary data available to support M-62-40 System Plan Report	1/2012
Preliminary data available to support M-62-45 Supplemental Treatment Selection	4/2012
Complete FBSR waste form performance testing	7/2012
FBSR waste form source term model results available for use in performance assessment	**2/2013**

Figure B.1. FBSR Laboratory Scale Experimental System at SRNL

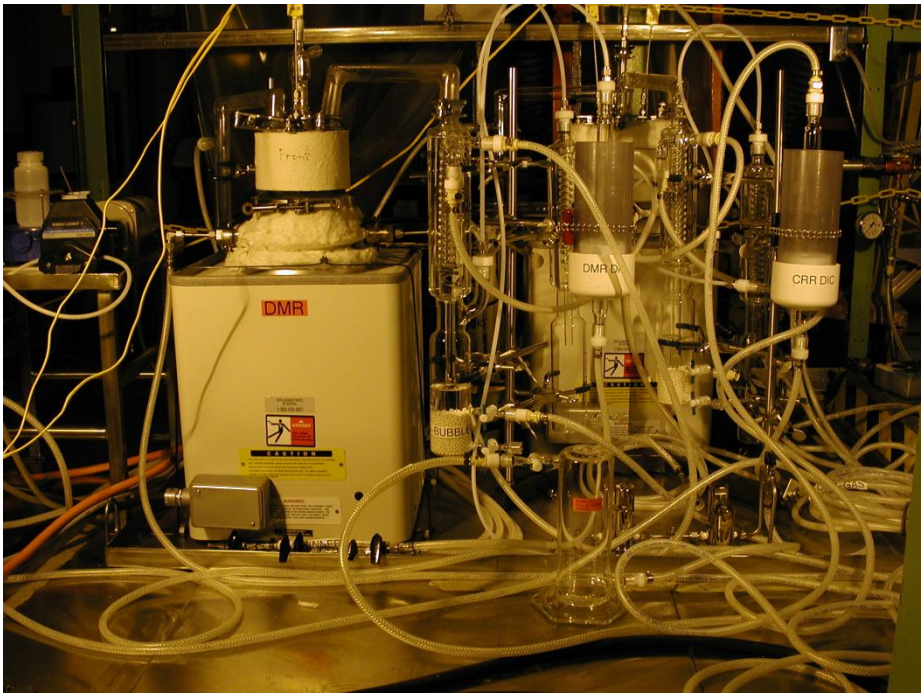

Figure B.2. FBSR Laboratory Scale Experimental System Installed in Hot-Cell Mock-Up at SRNL

Appendix C: Tc in Fluidized Bed Steam Reformer Memo Briefing to Ines – July 22, 2010

Appendix C: Tc in Fluidized Bed Steam Reformer Briefing to Ines – July 22, 2010

Date: 22 July 2010

cc: S.L. Marra, 773-A
C.C. Herman, 773-A
W.R. Wilmarth, 773-42A

To: Steve Schneider, DOE - EM

From: Carol M. Jantzen

Title: Fate of TECHNECIUM IN FLUIDIZED BED STEAM REFORMER (FBSR) PRODUCTS

Tc and Re exists in the +7, +6 and +4 oxidation states with +7 and +4 being the most stable oxidation states. The equilibrium between Re^{+7} to the Re^{+4} is shown in Figure C.1, an Electromotive Force (EMF) diagram developed by Dr. Henry Schreiber of Virginia Military Institute for SRNL's FBSR program in 2007.† This diagram shows the negative oxygen content (y axis) of the FBSR while the x axis shows the percentage of Re and S that will be in the oxidized vs. reduced state, i.e. +7 vs. +4. At the red circle ~ 5 % of the Re is in the +4 state and 95% in the +7 state. Likewise, at the red circle ~5% of the S is in the +2 state and 95% in the +4 state. Therefore Re will be present as $NaRe^{+7}O_4$ and the S will be present as Na_2SO_4.

Sodalite minerals are composed of a framework of $(SiO_4)^{-4}$ tetrahedra and $(AlO_4)^{-5}$ tetrahedra (Figure C.2). The negatively charged $(AlO_4)^{-5}$ and $(SiO_4)^{-4}$ tetrahedra that are arranged together to form the cage structure (Figure C.3Figure C.) and bond to various species inside the cage, such as 2NaI, 2NaF, 2NaCl, Na_2SO_4, and $2NaRe^{+7}O_4$. $Na_2S^{+4}O_4$ enters the cage structure of the sodalite mineral found in the FBSR products and this is confirmed by X-ray diffraction as the sodalite phase known as nosean $Na_6Al_6Si_6O_{24}(Na_2SO_4)$ is identified in the FBSR products (Figure C.3). Likewise it is anticipated that $2NaRe^{+7}O_4$ will enter the sodalite cage as Mattigod (PNNL, 2006)§ has made this structure in the phase pure state by hydrothermal reaction of aluminosilicate gels and sodium perrhenate solutions (Figure C.3). This hydrothermal mechanism is similar to the way alkali wastes react with kaolin clay (source of amorphous aluminosilicate) in the FBSR which operates with steam, i.e. hydrothermal conditions. It is anticipated that $2NaTc^{+7}O_4$ will also enter the sodalite structures as the sodium pertechnetate because the ionic radius of Re+7 in VI-fold coordination is 0.53Å while Tc+7 in VI-fold coordination is 0.56Å. Research is being initiated to substantiate that Tc enters the sodalite cage structure as does Re.

If Re or Tc are reduced to the +4 state, then sulfur would likely be reduced to the +2 state and either ReO_2 or ReS_2 would be the stable oxidation states with Tc forming TcO_2 or TcS_2 depending on the relative amounts of Tc, Re and S versus abundantly available oxygen. If ReO_2 or TcO_2 form these are the same stable coordinations found in HLW borosilicate glass when a reducing flowsheet is used as at the SRS DWPF.

---

† H.D. Schreiber, **"Redox State of Model Fluidized Bed Steam Reforming Systems Final Report Subcontract AC59529T,**" VMI Research Laboratories, VMI, Lexington, VA 24450 (December 2007).

§ S.V. Mattigod, B.P. McGrail, D.E. McCready, L.Wang, K.E. Parker and J.S. Young, **"Synthesis and Structure of Perrhenate Sodalite,"** J. Microporous & Mesopourous Materials, 91 (1-3), 139-144 (2006).

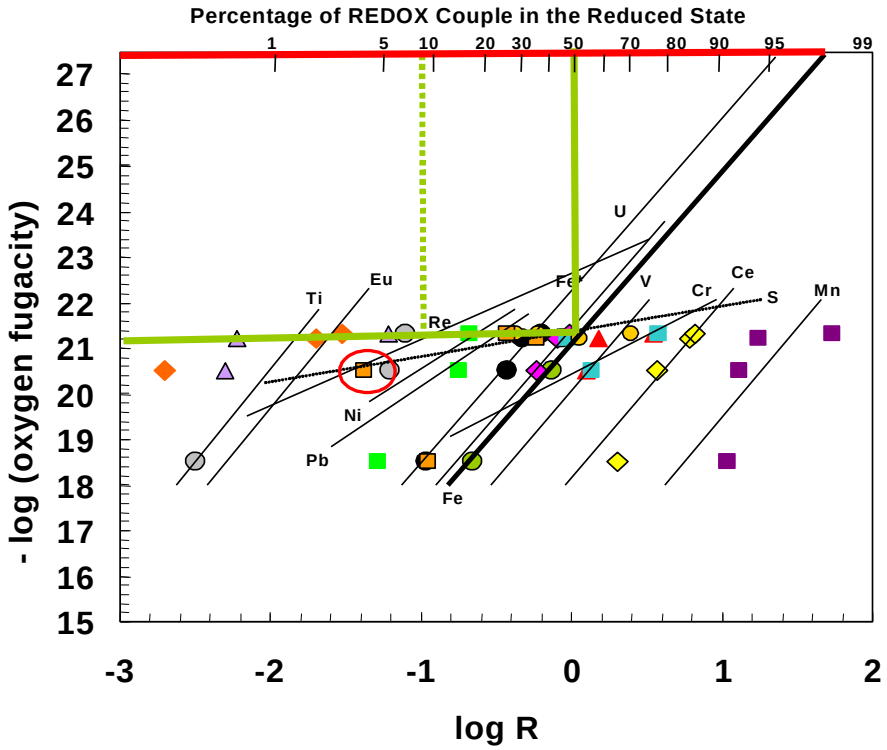

Figure C.1. Electromotive Force (EMF) series developed by Schreiber for FBSR reactions. Log R is log ($X^{red}/X^{oxidized}$) so measuring the ($Fe^{red}/Fe^{oxidized}$) in the FBSR product fixes the log (oxygen fugacity) as indicated by the solid green lines. Once the oxygen fugacity of the product at formation is known by measuring the Fe+2 to total iron content, the oxidation state of the other multivalent elements like Re and S (shown in BOLD) can be determined.

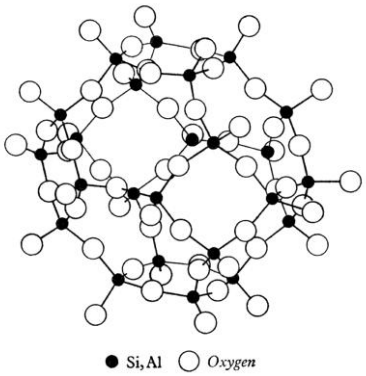

Figure C.3. Structure of Sodalite showing the tetrahedral oxygens (bridging and non-bridging) around each Al and Si but omitting the Al and Si atom ordering.

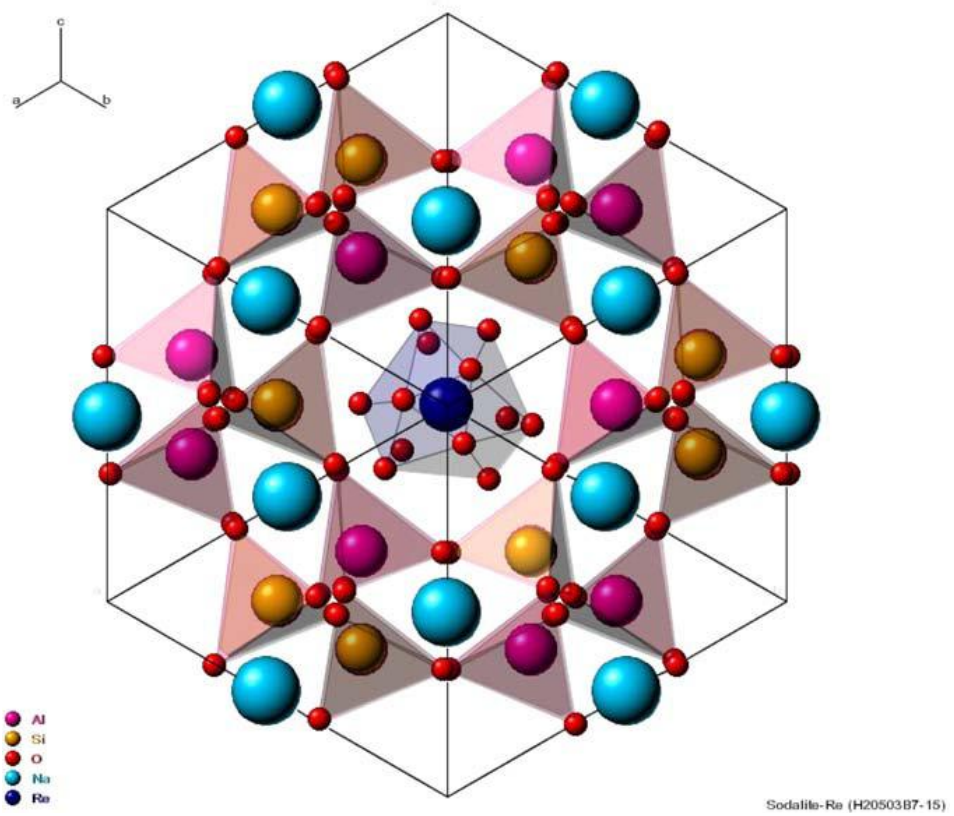

Figure C.4. Bonding of Re in the perrhenate sodalite. A single unit cell is shown.

Appendix D: Technetium Incorporation in Glass
Briefing to Ines – July 22, 2010

Appendix D: Technetium Incorporation in Glass
Briefing to Ines – July 22, 2010

Description – The Hanford Tank Waste Treatment and Immobilization Plant (WTP) design includes the separation of tanks waste to low-activity waste (LAW) and high-level waste (HLW) fractions followed by separate vitrification of both fractions. The current design assumes that the LAW vitrification facility will immobilize between 30 and 50% of the LAW fraction leaving the bulk of LAW to be treated by a supplemental treatment technology. One option for this supplemental treatment technology is a second, larger, LAW vitrification facility. This paper describes the current state of knowledge about Technetium (Tc) partitioning through the WTP process.

The WTP process models, based on testing and analyses, suggest that roughly 97% of the Tc partitions to the LAW fraction after pretreatment. This 97% of Tc would then split to roughly 58% to supplemental technology and 39% to LAW vitrification. Extensive testing with Rhenium (Re, the best known surrogate for Tc) in glass melting shows that roughly 35% of Re in the melter feed will partition to the glass while 65% will partition to the off-gas in a single pass through the melter. Recent tests at the Catholic University of America (CUA) have shown that for the current baseline melter feed compositions Re is a relatively good surrogate for Tc where partitioning between glass and off-gas are concerned (with an average of roughly 34% Tc retained in glass). [Note: if significant amounts of reductant are added, the differences in partitioning between Tc and Re become greater.]

The WTP design, therefore, includes a recycle of the primary off-gas scrub solution which sends nearly all of the 65% of the Tc from the LAW vitrification off-gas back to the melter feed. As the concentration of Tc in the melter feed increases, a *steady-state* is achieved where the amount of Tc coming from Tank waste, roughly matches the amount retained by glass as shown in Figure D.1. The partitioning of Tc from waste is shown roughly in Figure D.2.

- Off-gas system DF's and recycle must be considered in addition to retention in the melter
- Simple model:

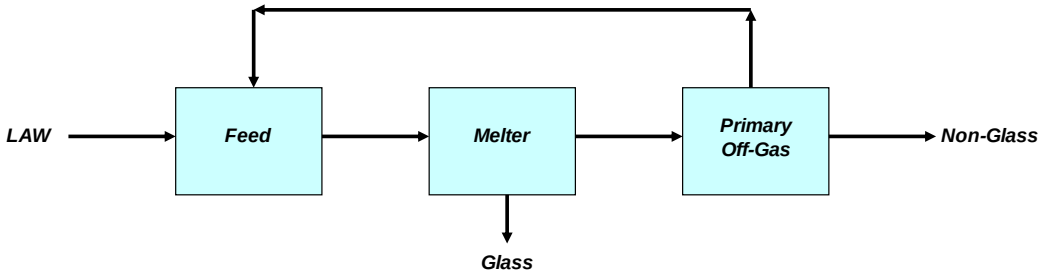

- If the fraction retained in glass in the melter is α
- And the fraction recycled from the primary off-gas system is β
- Then, at steady state, the non-glass fraction is given by:

$$\frac{(1-\beta)(1-\alpha)}{1-\beta(1-\alpha)}$$

Figure D.1. Impact of Recycle and Purge on Steady State Melter Feed Concentration.

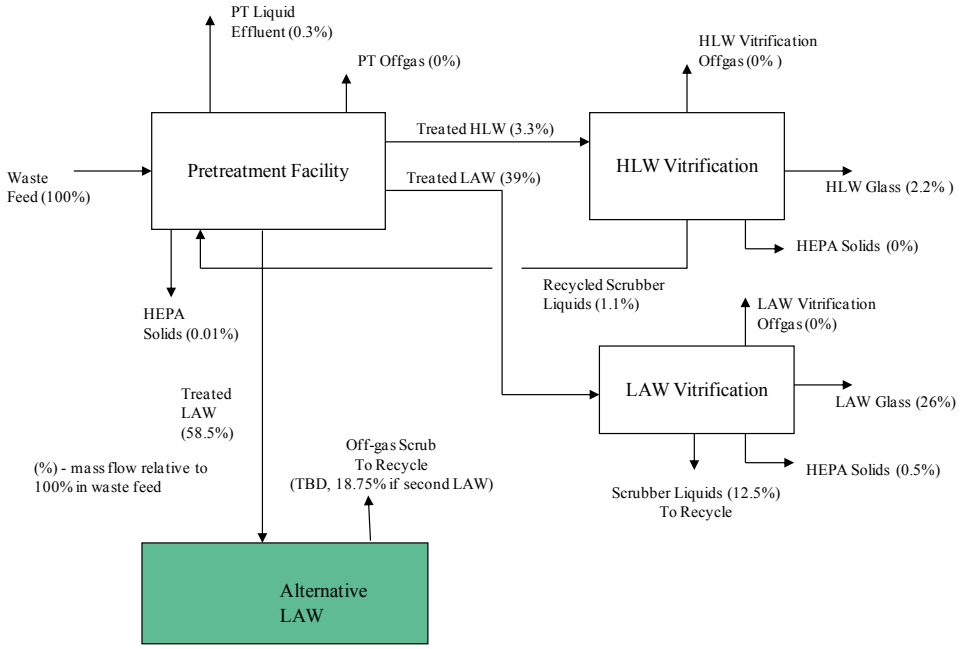

Figure D.2. Example Technetium Partitioning Scheme in Hanford Tank Waste Treatment and Immobilization Plant Design

No direct data is available to understand the partitioning of Tc between the off-gas treatment unit operations; however, that testing is ongoing. The model assumes, based on previous studies, that roughly all of the Tc volatilized from the melter is captured in the recycled scrub solution.

R&D Path Forward – Several key data gaps must be filled to demonstrate the range of Tc partitioning between LAW glass and off-gas unit operations. The ongoing research to fill these data gaps are described briefly below:

1. The retentions of Tc and Re in scaled melter tests are being compared in an ongoing Washington River Protection Solutions (WRPS) funded program at CUA. → Preliminary results suggest that for the reference feed compositions Tc and Re retentions are roughly equivalent at ~35% (with maximum values near 60%). They also suggest that the retentions tend to differ more with the addition of more reductants.
2. A scientific investigation into the behaviors of Tc and Re in melter environments has begun under an EM-31 funded program at University of Nevada at Las Vegas (UNLV) with collaboration from the Pacific Northwest National Laboratory (PNNL). → This study has just begun and no results are yet available.
3. Effects of melter feed composition variations on maximum potential Tc retention in glass on a single pass is being investigated under a WRPS funded program at CUA. → Preliminary results suggest that the replacement of ferric iron (Fe^{3+}) by ferrous iron (Fe^{2+}) reliably improves retention to roughly 50%. The impacts of organics from waste and other waste compositions are still being investigated.
4. A large scale melter test (~1:10) with Re and prototypic off-gas unit operations will be conducted under a WRPS funded project to verify the Re partitioning between off-gas streams.
5. A EM-31 funded program to evaluate the removal of Tc from LAW or melter off-gas scrub solution in the form of Goethite, [Fe,Tc]OOH, and feed that material into the HLW melter or encapsulate in low temperature waste forms is on-going. → Preliminary results indicate a 94 to 99% capture of Tc into Goethite. HLW melter tests with Goethite feed will be conducted this summer.

This joint WRPS -- EM-31 is ongoing and conclusions are premature. However, the results to-date indicates that: 1) Re is a reasonable surrogate for Tc with regard to retention in glass under relatively oxidizing conditions. 2) Retention of Tc in glass is likely to range from 30 to 60% in a single pass through the LAW melter. 3) The recycle loop or a robust waste form for melter off-gas scrub solutions will be required to successfully manage Tc from Hanford LAW vitrification. 4) Goethite precipitation appears to be a promising approach to Tc management that may allow breaking the recycle loop and managing Tc as a HLW.

Appendix E: Memorandum of Understanding Between Washington River Protection Solutions LLC and Savannah River Nuclear Solutions LLC for Conducting a Treatability Study

washington river protection solutions
PO Box 850
Richland, WA 99352

September 2, 2010 WRPS-1002400

Mr. John Temple, Director
Savannah River Nuclear Solutions, LLC
P. O. Box A
Building 730-1B9 / Room 316
Aiken, South Carolina 29802

Dear Mr. Temple:

CONTRACT NUMBER DE-AC27-08RV14800 - MEMORANDUM OF UNDERSTANDING BETWEEN WASHINGTON RIVER PROTECTION SOLUTIONS LLC AND SAVANNAH RIVER NUCLEAR SOLUTIONS LLC FOR CONDUCTING A TREATABILITY STUDY

Enclosed is the Memorandum of Understanding (MOU) that has been developed between our respective staffs to conduct a Treatability Study on Hanford tank waste samples using Fluidized Bed Steam Reforming technology. The samples to be treated in this treatability study currently are archived at the 222-S Laboratory at Hanford. Among other things, this MOU describes the respective roles and responsibilities of Washington River Protection Solutions LLC (WRPS) and Savannah River Nuclear Solutions (SRNS) and sets forth requirements for managing steam reforming product and residues.

I have signed the MOU on behalf of WRPS, and request that you sign for SRNS on page four of the enclosed document.

You may contact me at 372-9138, or your staff may contact Mr. J. W. Donnelly at 373-2119 with any questions regarding this matter.

Sincerely,

C. G. Spencer
President and Project Manager

AMH:LMM

Enclosure: Memorandum of Understanding Between Washington River Protection Solutions, LLC, and Savannah River Nuclear Solutions, LLC (38 pages)

cc: ORP Correspondence Control
S. E. Bechtol, ORP
S. L. Charboneau, ORP
T. W. Fletcher, ORP
L. A. Huffman, ORP
S. C. Johnson, ORP
B. M. Mauss, ORP
S. H. Pfaff, ORP
S. D. Stubblebine, ORP
W. J. Taylor, ORP

WRPS Correspondence Control
J. C. Allen-Floyd, WRPS
K. A. Colosi, WRPS
W. T. Dixon, WRPS
J. W. Donnelly, WRPS
A. B. Dunning, WRPS
L. D. Garcia, WRPS
A. M. Hopkins, WRPS
G. J. Johnson, WRPS
F. R. Miera, WRPS
P. L. Rutland, WRPS
T. L. Sams, WRPS
S. M. Sax, WRPS
R. J. Skwarek, WRPS
D. J. Swanberg, WRPS
L. E. Thompson, WRPS

MEMORANDUM OF UNDERSTANDING

BETWEEN

WASHINGTON RIVER PROTECTION SOLUTIONS, LLC

AND

SAVANNAH RIVER NUCLEAR SOLUTIONS, LLC

I. PURPOSE AND SCOPE

This Memorandum of Understanding (MOU) describes the responsibilities of Washington River Protection Solutions, LLC (WRPS)[1] and Savannah River Nuclear Solutions, LLC (SRNS)[2] for the coordination of activities to complete waste treatability studies on Hanford tank waste samples using Fluidized Bed Steam Reforming technology (FBSR). The samples to be treated in this treatability study currently are archived at the 222-S Laboratory at Hanford. An Inter-Entity Work Order (IEWO) was issued on August 30, 2010 for this scope of work. This MOU outlines the respective roles and responsibilities of WRPS and Savannah River National Lab (SRNL), sets forth requirements for managing steam reforming product and residues, as defined below, and unused samples, and identifies Points of Contact.

II. BACKGROUND

As stated in the IEWO, SRNL will be conducting treatability studies for WRPS. WRPS will ship samples of tank waste from the Hanford Site to SRNL in accordance with applicable requirements of the treatability study sample exclusion as set forth in 40 CFR 261.4(e) and WAC 173-303-071(3)(r). In general, three initial and separate waste treatability studies will be conducted at SRNL that will subject Hanford Site tank waste samples to the FBSR process in order to provide data on waste form characteristics after exposure to the FBSR treatment process, analysis of process conditions, and efficiency of the treatment process as it relates to specific aspects of the waste form characteristics.

Using bench-scale FBSR equipment, SRNL will process the waste samples into a solid granular treated waste form. A portion of the resulting granular material will be encapsulated using a geopolymer, forming a monolithic waste form. After treatment of the waste samples, some of the granular and monolith waste forms will be returned to the Hanford site for analysis. Some of the granular and monolith waste forms will temporarily remain with SRNL for analysis. A detailed Statement of Work (SOW) for this project is provided in the IEWO at Attachment 1. A summary test plan (Summary Plan For Bench-Scale Reformer and Product Testing Treatability Studies Using Hanford Tank Waste, RPP PLAN 47084, Rev.1) is provided for reference at Attachment 2.

[1] WRPS is the Tank Operating Contractor for the Office of River Protection (ORP) at the Hanford Site in Washington State.

[2] SRNS Manages and Operates the Savannah River National Lab (SRNL) on behalf of the U.S. Department of Energy (DOE).

III. REGULATORY ANALYSIS

The approach for the treatability studies will be consistent with Resource Conservation and Recovery Act (RCRA) 40 CFR 260-261 and applicable Washington State and South Carolina regulations for conducting treatability studies. An exclusion for waste samples used in small-scale treatability studies has been promulgated in these regulations in order to address the need to develop more effective hazardous waste treatment alternatives. In general, treatability study waste samples and treatment residues are exempted from a substantial portion of RCRA regulations provided that, among other things, applicable sample quantity, time limits, and recordkeeping requirements are followed. A regulatory analysis has shown that a compliant treatability study can be achieved with this project. Regulatory analysis and depiction of the treatability study process that will be implemented is provided by Figures 1 and 2.

IV. ROLES AND RESPONSIBILITIES

As provided in the regulations set forth above, USDOE and its Hanford facility co-operator WRPS, will be considered the "generator" of the treatability study waste samples. The SRNL, a facility located in the State of South Carolina, will be considered the "laboratory or testing facility" conducting the treatability study. Waste samples will be prepared for transport at the Hanford Site (EPA ID# WA7890008967) and shipped to SRNL (EPA ID# SC1890008989). Upon prior approval of USDOE-ORP, FBSR waste forms and unused samples shall be returned to Hanford under the treatability study sample exclusion; Hanford tank waste residues may be returned to Hanford upon prior approval of USDOE-ORP using a Uniform Hazardous Waste Manifest for subsequent storage, treatment, or disposal as set forth in Section VI of this MOU.

WRPS responsibilities include:

1. Developing the detailed test plan;
2. Obtaining regulator approval or making notifications as needed in Washington;
3. Selecting waste samples to be used in the treatability study by SRNL;
4. Preparing waste samples for transport;
5. Shipping waste samples to SRNL;
6. Receiving upon prior approval of USDOE-ORP, FBSR waste forms and unused samples from SRNL under the treatability study sample exclusion;
7. Receiving Hanford tank waste residues or debris, upon prior approval of USDOE-ORP, returned to Hanford using a Uniform Hazardous Waste Manifest, for subsequent storage, treatment, or disposal;
8. Analyzing FBSR waste forms for waste form performance and independent verification;
9. Providing oversight and validation for waste segregation to be performed by SRNL in Item 6 of SRNL responsibilities should residues be returned to the Hanford Site for disposal; and
10. Integrating with the Hanford Site Plateau Remediation Contractor for acceptance, should residues be returned to the Hanford Site for disposal.

SRNL/SRNS responsibilities include:

1. Obtaining regulator approval or making notifications as needed in South Carolina;
2. Receiving waste samples;
3. Conducting FBSR treatability studies;
4. Analyzing FBSR waste forms;
5. Managing and shipping FBSR waste forms and unused samples in accordance with section VI of this MOU and applicable regulations;

6. Segregating Hanford tank wastes, FBSR waste forms, unused samples, and residues from cross-contamination with any non-Hanford wastes; and
7. Shipping FBSR waste forms, unused samples, and study residues back to Hanford as specified in Section VI.

V. COMMUNICATION

Clear communication will be maintained by the parties throughout the treatability study process. In particular, the timing for shipments of treatability study samples, FBSR waste forms, unused samples, and residues will be communicated in order to facilitate recordkeeping and compliant waste management functions by all parties.

Single points of contact (POCs) will serve as a resource to integrate project, environmental and waste management needs for each party. POCs for each party are identified as follows:

Organization	POC	Title	Phone
USDOE-ORP	Stephen Pfaff	Supplementary Technology Federal Project Director	(509) 376-2188
USDOE-SRS	Patrick Jackson	SRS Office of Laboratory Oversight	(803) 725-1226
WRPS	Terry L. Sams	WTP Technology & Development	(509) 376-4653
SRNL	Sharon Marra	SRNL E&CPT Research Programs	(803) 725-5891

VI. TREATABILITY STUDY MATERIALS MANAGEMENT

FBSR waste forms, unused samples, laboratory samples, and treatability study residues generated by FBSR testing at SRNL will be managed in accordance with the provisions set forth below. For purposes of this MOU, "FBSR waste form" means Hanford tank waste samples that have been treated by the steam reforming process under the treatability study sample exclusion and "treatability study residues" or "residues" mean all other materials produced by the treatability studies, e.g., laboratory equipment, personal protective equipment, analytical residues, etc., that are contaminated by contact or commingling with Hanford-generated tank wastes that are not FBSR waste forms or unused samples. In the event that there is a conflict between the IEWO SOW Section 7.2 and MOU Section VI, the MOU shall control.

a. **Unused Hanford waste samples not subjected to testing**

Unused waste samples shall be returned to the Hanford Site as an excluded treatability study material under the treatability study sample exclusion upon prior approval of USDOE-ORP. Unused samples must be returned within 90 days of completion of the study or within 1 year from the date of shipment of the sample – whichever occurs first.

b. **FBSR waste forms**

FBSR waste forms, including granular and monolith waste forms, or other treated waste forms determined not to be suitable for testing, shall be returned to the Hanford site as an exempted treatability study material under the treatability study sample exclusion upon prior approval of USDOE-ORP. Unused archived exempted materials must be returned within 90 days of the completion of the study or within 1 year from the date of shipment of the sample – whichever occurs first.

FBSR waste forms may also be archived at SRNL or Hanford for up to five years in order to perform future durability or other characterization testing as needed. The FBSR waste forms archived at SRNL will be returned to Hanford within five years of receipt of the sample used to make the FBSR waste forms as specified by regulation.

c. **Laboratory samples**

In the course of the activities addressed by this MOU, SRNL may generate samples from the FBSR process that are intended for or require analysis at off-site laboratories. SRNL shall not contract with any off-site laboratory to conduct these analyses but shall send any such samples to Pacific Northwest National Laboratory (PNNL) under EPA ID# WA7890008967. PNNL shall manage these samples as well as any and all contracts to conduct said analyses with off-site laboratories.

d. **Treatability study residues**

Treatability study residues as defined above shall be managed as fully regulated hazardous wastes. Upon prior approval of USDOE-ORP, these treatability study residues wastes shall either be transported to Hanford using a Uniform Hazardous Waste Manifest for storage, treatment, or disposal or, in the alternative, be transported to a commercial waste vendor(s) for treatment and disposal of hazardous wastes.

Residues resulting from testing of archived materials will be managed and disposed as specified above for treatability study residues.

Date / /

Date / /

Figure 1

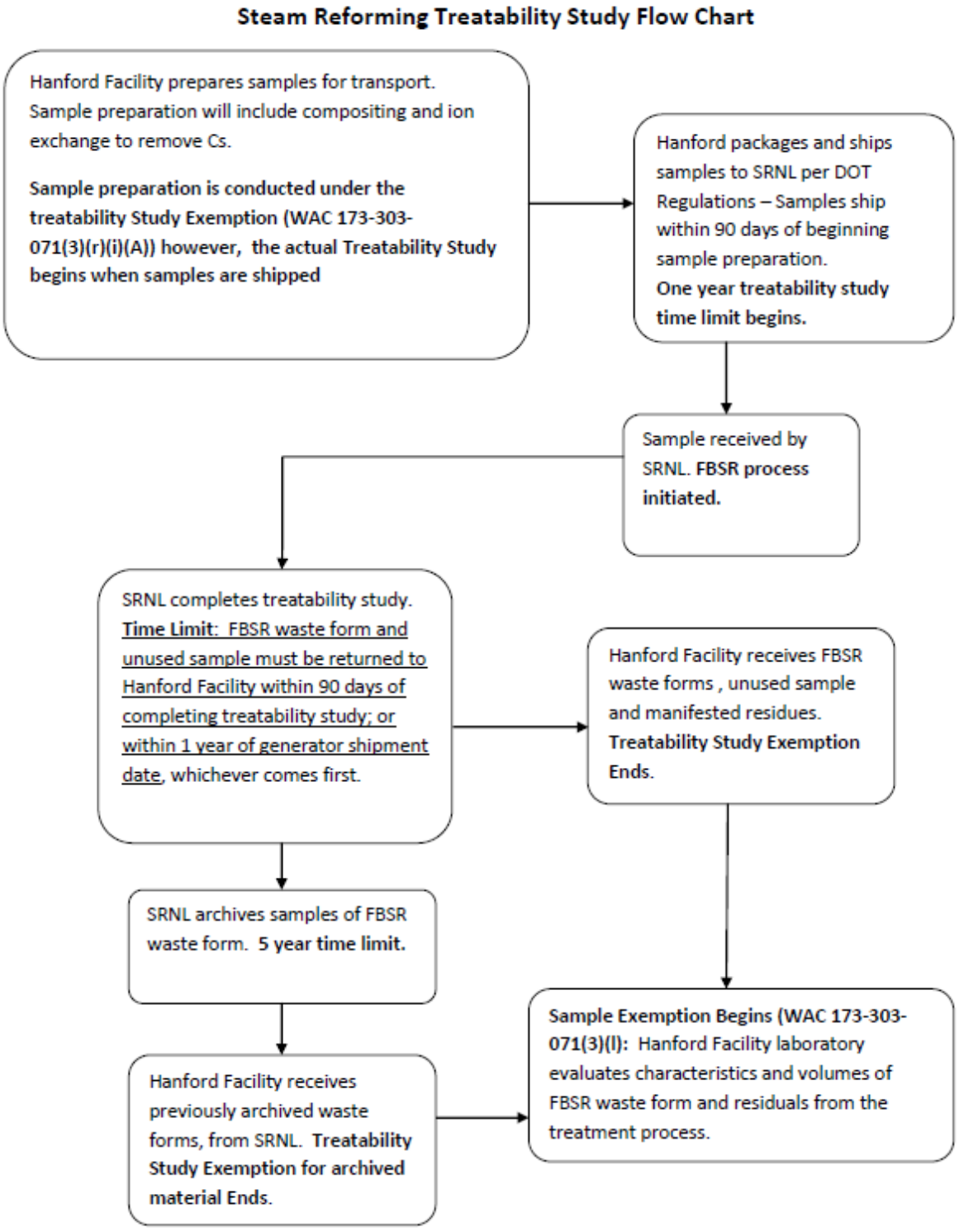
Steam Reforming Treatability Study Flow Chart
Hanford Facility prepares samples for transport. Sample preparation will include compositing and ion exchange to remove Cs.
Sample preparation is conducted under the treatability Study Exemption (WAC 173-303-071(3)(r)(i)(A)) however, the actual Treatability Study begins when samples are shipped
Hanford packages and ships samples to SRNL per DOT Regulations – Samples ship within 90 days of beginning sample preparation.
One year treatability study time limit begins.
Sample received by SRNL. FBSR process initiated.
SRNL completes treatability study.
Time Limit: FBSR waste form and unused sample must be returned to Hanford Facility within 90 days of completing treatability study; or within 1 year of generator shipment date, whichever comes first.
Hanford Facility receives FBSR waste forms , unused sample and manifested residues.
Treatability Study Exemption Ends.
SRNL archives samples of FBSR waste form. 5 year time limit.
Hanford Facility receives previously archived waste forms, from SRNL. Treatability Study Exemption for archived material Ends.
Sample Exemption Begins (WAC 173-303-071(3)(l): Hanford Facility laboratory evaluates characteristics and volumes of FBSR waste form and residuals from the treatment process.

Figure 2

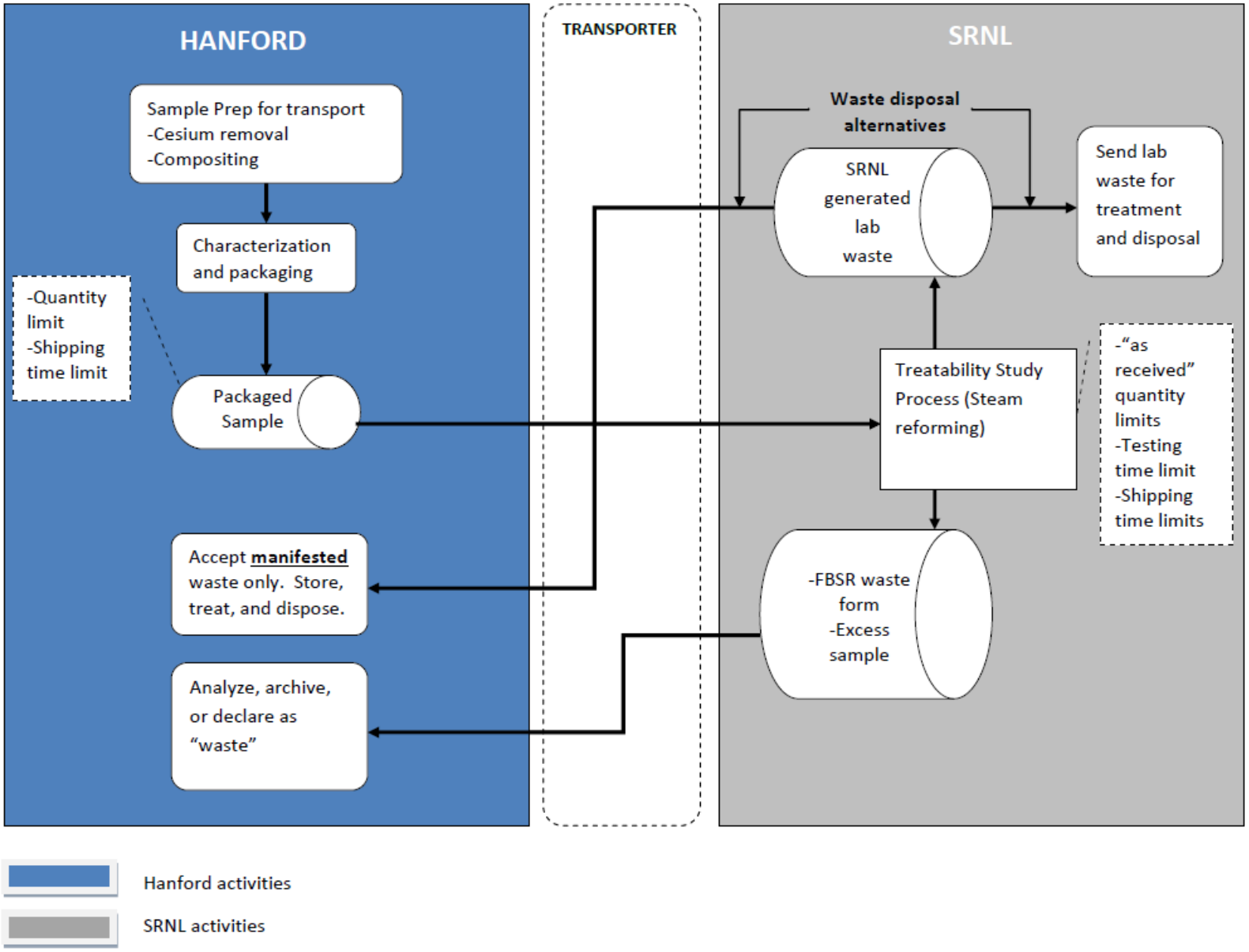
HANFORD
TRANSPORTER
SRNL
Sample Prep for transport
-Cesium removal
-Compositing
Characterization and packaging
-Quantity limit
-Shipping time limit
Packaged Sample
Accept manifested waste only. Store, treat, and dispose.
Analyze, archive, or declare as "waste"
Waste disposal alternatives
SRNL generated lab waste
Send lab waste for treatment and disposal
Treatability Study Process (Steam reforming)
-"as received" quantity limits
-Testing time limit
-Shipping time limits
-FBSR waste form
-Excess sample
Hanford activities
SRNL activities

ATTACHMENT 1

IEWO MOSRV00054, A1

SEPTEMBER 1, 2010

U.S. Department of Energy
INTER-ENTITY WORK ORDER

1. Work Order Number: M0SRV00054 **Amendment Number:** 1	**2. Month/Year to be recorded:** *(for use in DOE-DOE work only)* Aug-10

Authorizer

3. Authorizing Contractor or Field Office: DOE-Richland Operations Office (Office of River Protection)	
4. Authorizing Contractor or Field Office OPI Code: RL90	**5. Allotment Symbol:** RL9191

6. Budget Analyst: Dragana Etheridge
Telephone: 509.376.2394
E-Mail: Dragana_Etheridge@orp.doe.gov

7. ORP Technical Point of Contact Signature:
Stacy Charboneau — Date: 8/31/10

8. Funds Availability Authorization Official's Signature:
Tom Toon — Date: 8/31/10

9. Authorizing Contracting Officer Signature: (Required for IEWO >$1M life of project)
Susan Bechtol — Date: 8/31/10

10. Scope of Work (attach additional sheets if needed):
TDD funds deobligated from WRPS and obligated to SRNS for Fluidized Bed Steam Reforming Treatability Studies using SRS Low Activity Waste and Hanford Low Activity Waste Tank Samples .
The amendment 1 of this IEWO changes the Statement of Work and supersedes the Statement of Work attached to Work Order Number M0SRV00054 Amendment 0. Specifically, this amendment 1 changes the word "may" to "shall" in section 7.2.a, line 1, and section 7.2.b, line 2.

11. Period of Performance: ASAP-9/30/2010

12. Billing and Budgetary Information:
Address: "Accounts Payable - Work will be billed via VIPERS, with reference to Work Order Number"

Funding titles: Fund Type.Appo Year.Allottee.Rpt Entity.Obj Cls.Program.Project.WFO.Local Use.Future Use

Funding Source: 01250.2010.34.421301.25200.1111412.0004263.0000000.0000000.000000 (Current Funding)

Authority	Current Year	Cumulative
Previous Total	$ 1,000,000.00	$ 1,000,000.00
Current Action	$ -	$ 0.00
Revised Total	$ 1,000,000.00	$ 1,000,000.00

Performer

13. Performing Contractor: Savannah River Operations Office	
14. Performing Contractor OPI Code: SR90	**13. Allotment Symbol:**

16. Cognizant Contracting Officer: Robert Peters
Telephone: (803) 952-8648
E-Mail: Robert02.Peters@srs.gov

17. P

18. P

TEMPLATE "C-3"

STATEMENT OF WORK

Title: Fluidized Bed Steam Reforming Treatability Studies Using SRS Low Activity Waste and Hanford Low Activity Waste Tank Samples

Revision Number: n/a
Date: August 19, 2010

Prior SOW or Revision Date *n/a*

1.0 Objective:

The objective of this work scope is to generate waste form performance data to demonstrate that the THOR Fluidized Bed Steam Reformer (FBSR) technology will produce a waste form acceptable for disposal at the Hanford Integrated Disposal Facility (IDF).

This work scope will be conducted with a Bench-Scale Reformer (BSR) using Savannah River Site (SRS) actual radioactive waste that represents the chemical composition of Hanford LAW, and as an option, actual Hanford Low Active Waste (LAW). A portion of the granular product material produced for each sample will be encapsulated in a geo-polymer to form a monolith. The granular product and monolithic product will be then be packaged for shipment to Pacific Northwest National Laboratory, (PNNL).

2.0 Background/Introduction:

As part of its accelerated clean-up plan for the Hanford site, the US Department of Energy (DOE) is considering deploying supplemental technologies for the treatment and immobilization of a large proportion of the Hanford LAW. Three supplemental treatment options for LAW immobilization have been identified (bulk vitrification (BV), grout (saltstone), and, FBSR) and evaluated against criteria such as safety, environmental protection, schedule, cost, operations etc. A key criterion is the performance assessment of the waste form in the proposed low-level waste repository at Hanford (Integrated Disposal Facility). Sufficient data have already been gathered for BV and grout to allow an assessment of the performance of these waste forms in the IDF to be carried out. DOE have requested that the FBSR waste form be brought to the same level of understanding as BV and grout to allow a formal down select to be carried out.

Savannah River National Laboratory (SRNL) is the DOE's lead laboratory for EM 31 development work and has extensive experience with fluidized bed steam reforming (FBSR) technology. In order to generate waste form performance data both actual Hanford LAW and SRS LAW, chemically adjusted to resemble Hanford LAW, will be processed by SRNL's BSR to form a granular waste form, a proportion of which will be immobilized in a geo-polymer to form a monolith.

The purpose of the tests is to examine the ability of the FBSR product to include radioactive and Resource Conservation and Recovery Act, (RCRA) metals in the waste form matrix at an acceptable loading level and to examine the leach characteristics of the resultant product(s). The trials will also examine all radionuclides and RCRA metals of concern however, special attention will be paid to technetium (Tc) and iodine (I), both of which are conservative (i.e. their migration

is not retarded in the geosphere), and have been demonstrated to be difficult to be included in the glass matrix.

3.0 Scope:

The scope of the work will include tests on SRS LAW chemically adjusted to resemble Hanford LAW and three actual samples of Hanford radioactive waste. Simulants of each of the radioactive samples will be prepared and run through the BSR to ensure that the process conditions are such that a suitable NAS granular-like product can be prepared for each. All the radioactive waste samples will be processed through the BSR to form radioactive granular-like product. A proportion of the granular product from each sample will be immobilized in to form a number of monoliths. Both the granular and the monolith product will be characterized and subject to a number of product performance tests. Additionally, some of the granular and monolith product formed from each sample will be shipped to PNNL for additional testing.

Task 1. BSR Testing of Savannah River Site Low Active Waste Chemically Adjusted to Resemble Hanford Low Active Waste

The contractor shall conduct a FBSR BSR test using LAW from the Savannah River Site (SRS) that is chemically adjusted to reflect the composition of Hanford LAW per PNNL-14194, Rev 1, Table 3.1 to reflect the composition of the non-radioactive simulant used in the 2008 Engineering-Scale Technology Demonstration (ESTD) test previously carried out under the DOE Advanced Remediation Technologies (ART) program contract and reported by THOR Treatment Technologies (RT-21-002, Rev 1, April 2009). Testing with a radioactive LAW that reflects this 2008 ESTD composition will allow for a direct comparison of the data from the radioactive BSR testing with the non-radioactive ESTD testing.

The work includes a single LAW formulation processed using a mineralizing flow sheet to produce both an alkali aluminosilicate granular mineral product and a monolithic product including the primary analytical tests necessary to demonstrate the acceptability of the monolithic waste form for disposal on the Hanford Site. This will involve the following:

A. Perform a BSR run using a non-radioactive LAW simulant to functionally test the BSR equipment and make enough non-radioactive granular product to produce at least ten (10) 1" diameter × 2" tall product monoliths, plus ≈200 grams of granular product. The LAW simulant is to be compositionally consistent with the material used for the Hanford LAW ESTD testing as referenced above.

B. Produce a radioactive LAW material that is compositionally representative of the simulated Hanford LAW stream used in the 2008 ESTD run using SRS dissolved salt cake LAW (spiking with I-129 and Tc-99 as necessary).

C. Adjust this simulated radioactive Hanford LAW with aluminosilicate clay to make a feed for the radioactive BSR test that will produce leach-resistant alkali aluminosilicate granular solid product.

D. Perform sufficient operational runs of the radioactive BSR using the clay-adjusted radioactive SRS chemically adjusted LAW sample to produce sufficient granular product to make ten (10) 1" diameter × 2" tall product monoliths, plus ≈200 grams of additional granular product for analysis.

E. Collect process data during operations, including sufficient off-gas and product sampling to determine the partitioning of certain radionuclides between the solid product and the off-gas. This will include, but is not limited to, mercury, Cs-137, Tc-99, and I-129.

F. Perform a redox measurement on the mineral product

G. Determine the speciation of the mineral product using XRD, SEM with EDS, and other analytical methods, as appropriate. To the extent possible, determine the mineral form, percentages of mineral phases in the assemblages in the mineral product.

H. Form and cure ten (10) final radioactive product monoliths using the GEO-7 geopolymeric binder identified from the prior ESTD testing phase.

I. Perform compressibility strength tests on two (2) to three (3) radioactive monoliths using a method calibrated with ASTM-C-39/C39M-99.

J. Perform the following on three (3) of the radioactive monoliths, stating the number of replicates:

i. Product Consistency Test(PCT) (ASTM C-1285) --short-term and long-term
ii. Toxicity Characteristic Leach Procedure (TCLP) in accordance with SW-846
iii. Leachability of Solidified Low-Level Radioactive Wastes (using ASTM 1308, EPA 1315, or ANSI/ANS 16.1 as directed by WRPS).

K. Perform PCT (short-term and long-term) and TCLP on the radioactive granular product.

L. Ship two (2) intact monoliths, the remains of three (3) radioactive monoliths and 200 grams of radioactive granular product to PNNL for Single Pass Flow Tests (SPFT) and Pressurized Unsaturated Flow (PUF) tests on the monoliths and granular product. Additionally, minor amounts of characterization of the granular and monolith material, via micro-XRD and chemical digestion, will also be performed at PNNL. Finally these samples will also be prepared for XAS analyses of the granular and monolithic product. Testing by PNNL will be at no cost to the current contract (funding provided by others).

Task 2. BSR Testing of Actual Hanford LAW

The contractor shall conduct a BSR test using three different actual Hanford tank waste samples chosen by WRPS to reflect the range of Hanford LAW that may be processed in the future by FBSR (Hanford LAW Sample 1, Hanford LAW Sample 2, and Hanford LAW Sample 3). The actual Hanford tank waste samples shall represent a range of SO4/Na, Halide/Na, Tc/Na, and potentially other salts to sodium ratios of waste. The demonstration test program data will be used to support the IDF performance assessment and decisions regarding deployment of non-vitrification technology to immobilize Hanford LAW. For each of the three samples the following steps shall be followed:

A. Perform a chemical and radioactive analysis of the Hanford radioactive sample.

B. Prepare a non-radioactive simulant of the radioactive Hanford sample based on the analysis data from Task 2.A.

C. Perform a BSR run using the non-radioactive Hanford simulant to functionally test the BSR equipment.

D. Prepare the Hanford radioactive sample for treatment, by spiking it with I-129, and Tc-99 as necessary, and adjusting it with aluminosilicate clay to make a feed for the radioactive BSR test that will produce leach-resistant alkali aluminosilicate granular solid product.

E. Perform sufficient operational runs of the radioactive BSR using the clay-adjusted radioactive Hanford sample to produce sufficient granular product to make ten (10) 1" diameter × 2" tall product monoliths, plus ≈200 grams of additional granular product for analysis.

F. Collect process data during operations, including sufficient off-gas and product sampling

to determine the partitioning of certain radionuclides between the solid product and the off-gas. This will include mercury, Cs-137, Tc-99, and I-129.

G. Perform a redox measurement on the mineral product

H. Determine the speciation of the mineral product using XRD, SEM with EDS, and other analytical methods, as appropriate. To the extent possible, determine the mineral form, percentages of mineral phases in the assemblages in the mineral product.

I. Form and cure ten (10) final radioactive product monoliths using the GEO-7 geopolymeric binder identified from the prior ESTD testing phase.

J. Perform compressibility strength tests on two (2) to three (3) radioactive monoliths, using a method calibrated with ASTM-C-39/C39M-99.

K. Perform the following on three (3) of the radioactive monoliths, stating the number of replicates:

   i. Product Consistency Test(PCT) (ASTM C-1285) –short-term and long-term
   ii. Toxicity Characteristic Leach Procedure (TCLP) in accordance with SW-846
   iii. Leachability of Solidified Low-Level Radioactive Wastes (using ASTM 1308, EPA 1315, or ANSI/ANS 16.1 as directed by WRPS).

L. Perform PCT (short-term and long-term) and TCLP on the radioactive granular product.

M. Ship two (2) intact monoliths, the remains of three (3) radioactive monoliths and 200 g of radioactive granular product to PNNL for Single Pass Flow Tests (SPFT) and Pressurized Unsaturated Flow (PUF) tests on the monoliths and granular product. Additionally, minor amounts of characterization of the granular and monolith material, via micro-XRD and chemical digestion, will also be performed at PNNL. Finally these samples will also be prepared for XAS analyses of the granular and monolithic product. Testing by PNNL will be at no cost to the current contract (funding provided by others).

4.0 Deliverables:

The following deliverables are in addition to those listed in Section 3.0 above:

The contractor shall develop for WRPS a Fluidized Bed Steam Reformer Low-Level Waste Form Qualification Test Plan, incorporating input from WRPS, PNNL, Thor Treatment Technologies, and SRNL personnel. The Test Plan shall include:

A. Overall project scope summary
B. Detailed descriptions of work segmented into logical subtasks
C. Schedule to include:
    i. Milestones
    ii. Deliverables to include dates
    iii. Decision points/Hold Points with explicit determinations for continuation
    iv. Insertion points
D. Measurable criteria to demonstrate the accomplishment of project objectives. Identify the range of accuracy for the measured parameters. Indicate the methodologies that will be employed to verify or validate the test data. Describe any scoping tests that may be desirable prior to the development of the test matrix.
E. Description of test equipment configuration and test procedures used to include:
    i. A description of any specialized equipment required
    ii. A brief description of the test equipment maintenance and calibration procedures
    iii. Temperature control
    iv. Control of the solids concentration to the desired level
    v. Sampling methods to ensure a representative sample
F. Description of the procedures employed to implement the QA requirements
G. Relevant consensus standards
H. Identification of any external coordination required to execute the work scope and identification of relevant stakeholders
I. A mass balance indicating the distribution between the product and the BSR off-gas for each of the samples in Task 1 and Task 2
J. Final report to include at a minimum data generated, details of sample preparation and process conditions, investigative methods used, results and recommendations
K. Organization chart identifying key personnel
L. Detailed listing of all primary and secondary waste streams generated by this work scope identifying the disposition route of each
M. For each of the four samples (SRS LAW, Hanford LAW Sample 1, Hanford LAW Sample 2, and Hanford LAW Sample 3) provide a cost estimate for each of the activities outlined in Task 1., A. through K., and Task 2., A. through L., a cost estimate should be given for each subtask listed in Task 1. J. and Task 2. K.

5.0 Acceptance Criteria:

Work products and services provided must meet established applicable WRPS procedures for control and review of work products. Acceptance shall be based on validation by WRPS that Subcontractor has resolved and incorporated all WRPS comments. Subcontractor personnel provided under this subcontract shall possess the qualifications, certifications, and any other attributes required to complete the assigned work.

6.0 Configuration Management and Standards

6.1 Configuration Management Requirements:

Configuration management requirements for this Release are based upon the types of engineering services being procured and include the TOC standards listed in Section *6.2 Applicable Standards* and the statements below.

New or revised Technical Documents shall be prepared in accordance with TFC-BSM-AD-STD-02, *Editorial Standards for Technical Documents* and meet the document release criteria found in Table 3 of TFC-ENG-DESIGN-C-25, Technical *Document Control.*

6.2 Applicable Standards

The following Federal Regulation will be applied: Code of Federal Regulation (CFR) Rule 10 CFR 61.55.

The following engineering procedures apply:

APPLICABLE ENGINEERING CODES AND TOC ENGINEERING STANDARDS

	Number	Title
1.	TFC-BSM-AD-STD-02	Editorial Standards for Technical Documents
2.	TFC-ENG-DESIGN-C-25	Technical Document Control
3.	TFC-ENG-DESIGN-C-10	Engineering Calculations
4.	TFC-ENG-DESIGN-C-32	Spreadsheet Development and Verification
5.	TFC-BSM-IRM_HC C-01	Software Development, Implementation and Management

7.0 ESH&Q Requirements

The subcontractor shall comply with all Price-Anderson Amendment Act (PAAA) nuclear safety rules and reporting requirements as determined by their prime contracts negotiated with the Department of Energy

7.1 ESH Requirements Specific to this Task

The work activities for this statement of work have been designated as Full Quality.

The Subcontractor is required to conduct work in accordance with a Quality Assurance Program (QAP) that meets the Quality Assurance criteria specified in DOE O. 414.1, *Quality Assurance*, 10 CFR 830, *Nuclear Safety Management*, Subpart A, "*Quality Assurance Requirements*", paragraph 830.122 and also meets the requirements of ASME NQA-1-2004, *Quality Assurance Requirements for Nuclear Facility Applications*. The Subcontractor shall implement an NQA-1-2004 program (as identified below) and be listed on an ESL for this scope of work:

Criterion #	Criterion Title	All Sections	Specific Sections as Listed:
1	Organization	☒	☐
2	Quality Assurance Program	☒	☐
3	Design Control	☐	☐N/A
4	Procurement Document Control	☒	☐
5	Instructions, Procedures, and Drawings	☒	☐
6	Document Control	☒	☐
7	Control of Purchased Items and Services	☐	☒ Sections 100, 400 & 800
8	Identification and Control of Items	☒	☐
9	Control of Processes	☒	☐
10	Inspection	☐	☐N/A
11	Test Control	☒	☐
12	Control of Measuring and Test Equipment	☒	☐
13	Handling, Storage, and Shipping	☒	☐
14	Inspection, Test, and Operating Status	☒	☐
15	Control of Nonconforming Items	☒	☐
16	Corrective Action	☒	☐
17	Quality Assurance Records	☒	☐
18	Audits	☐	☐N/A
Subpart 2.7	Computer Software for Nuclear Facility Applications*	☒	☐

*The development, procurement, maintenance, and use of the computer software shall comply with applicable requirements of ASME NQA-1-2004, Subpart 2.7, including problem reporting and corrective action.

The implemented quality assurance program for Subcontractors located on the Hanford Site shall comply with DOE/RL 96-68 Hanford Analytical Services Quality Assurance Requirements Document (http://www.hanford.gov/orp/?page=141&parent=14). Subcontractors located off the Hanford Site shall have an implemented quality assurance program that complies with the (Department of Energy Consolidated Audit Program (DOECAP) Quality Systems for Analytical Services (QSAS)

(https://doecap.oro.doe.gov/DOECAP_Public/documentsLab.aspx).

QAP Approval:
The Subcontractor's QAP shall be subject to review at all times by Buyer, including prior to award.

Changes to the Subcontractor's QAP:
The Subcontractor shall, during the performance of this Subcontract, submit proposed changes to the quality assurance program to the Buyer for review prior to implementation.

7.2 Treatability Study Materials Management

FBSR waste form, unused samples, laboratory samples, and treatability study residues generated by FBSR testing at SRNL will be managed in accordance with the provisions set forth below. For purposes of this Statement of Work, "FBSR waste form" means Hanford tank waste samples that have been treated by the steam reforming process under the treatability study sample exclusion and "treatability study residues" or "residues" mean all other materials produced by the treatability studies, e.g., laboratory equipment, personal protective equipment, analytical residues, etc., that are contaminated by contact or commingling with Hanford-generated tank wastes that are not FBSR waste form or unused samples.

a. **Unused Hanford waste samples not subjected to testing**

Unused waste samples shall be returned to the Hanford Site as an excluded treatability study material under the treatability study sample exclusion upon prior approval of USDOE-ORP. Unused samples must be returned within 90 days of completion of the study or within 1 year from the date of shipment of the sample – whichever occurs first.

b. **FBSR waste form**

FBSR waste form, including granular and monolith waste forms, or other treated waste forms determined not to be suitable for testing, shall be returned to the Hanford site as an exempted treatability study material under the treatability study sample exclusion upon prior approval of USDOE-ORP. Unused archived exempted materials must be returned within 90 days of the completion of the study or within 1 year from the date of shipment of the sample – whichever occurs first.
FBSR waste form may also be archived at SRNL or Hanford for up to five years in order to perform future durability or other characterization testing as needed. The FBSR waste form archived at SRNL will be returned to Hanford within five years of receipt of the sample used to make the FBSR waste form as specified by regulation.

c. **Laboratory samples**

In the course of the activities addressed by this MOU, SRNL may generate samples from the FBSR process that are intended for or require analysis at off-site laboratories. SRNL shall not contract with any off-site laboratory to conduct these analyses but shall send any such samples to PNNL. PNNL shall manage these samples as well as any and all contracts to conduct said analyses with off-site laboratories.

d. **Treatability study residues**

Treatability study residues as defined above (in Sec. III) shall be managed as fully regulated hazardous wastes. Upon prior approval of USDOE-ORP, these treatability study residues wastes may be transported to Hanford using a Uniform Hazardous Waste Manifest for storage, treatment, or disposal. Alternatively, commercial waste vendors may be used for treatment and disposal of hazardous wastes upon prior approval of USDOE-ORP.

Residues resulting from testing of archived materials will be managed and disposed as specified above for treatability study residues.

8.0 Verification/Hold Points:

None

9.0 Reserved

10.0 Work Location/Potential Access Requirements:

The contractor will work off-site and may be requested to attend meetings in Richland, WA during execution of this contract.

11.0 Training:

No specific Hanford training will be required for this contract work.

12.0 Qualifications:

The contractor shall be knowledgeable of tank farm operations and waste. The contractor will have experience of operating a BSR in a high radioactive environment. This work requires a minimum of a bachelor degree in related engineering or science field.

13.0 Special Requirements:

Hanford Site Access

Performance of onsite work in other than administrative facilities (such as 2750 E) requires the individual to call the Base Operations shift office prior to accessing the facility.

Use of Government Vehicles

There is no anticipated need for any Subcontractor employees to use a Government-furnished vehicle in the performance of this statement of work. The Subcontractor's employees, therefore, are specifically prohibited from driving any Government-furnished vehicles under the performance of this statement of work unless this statement of work is formally so modified by the parties and a copy of any applicable driver's license provided to the BTR.

Government Property

No Government Property will be furnished to the contractor

14.0 Reporting/Administration:

A weekly status report will be provided to the technical POC identified by the Buyers Technical Representative (BTR).

Subcontractor information including reports and other documents shall be submitted in either hard copy or electronic format as designated by WRPS. If electronic formatted documents are

required, the documents must be viewable using Microsoft ® Windows®, Microsoft® Office, or Adobe® Acrobat® software.

The subcontractor is also required to meet the following requirements:

- Attend weekly status meetings/conference calls as requested.
- Provide weekly schedule status reports as directed by the Technical Point of Contact or designee.
- Provide monthly progress reports to the Technical Point of Contact or designee
- Attend Safety meetings as directed by the BTR.
- Provide weekly reporting of progress and expected delays and impacts to the BTR.

15.0 Workplace Substance Abuse Program Requirements:

A Workplace Substance Abuse Program is not required for this SOW.

16.0 Reserved

ATTACHMENT 2

RPP-PLAN-47084, REV 1

SEPTEMBER 1, 2010

SUMMARY PLAN FOR BENCH-SCALE REFORMER AND PRODUCT TESTING TREATABILITY STUDIES USING HANFORD TANK WASTE

J. B. Duncan
H. J. Huber
R. A. Robbins
D. J. Swanberg
Washington River Protection Solutions LLC

Date Published
July 2010
Prepared for the U.S. Department of Energy
Office of River Protection

Contract No. DE-AC27-08RV14800

Table of Contents

List of Tables

List of Figures

List of Terms

Abbreviations

AES	Atomic Emission Spectroscopy
ALARA	As Low As Reasonably Achievable
ANSI	American National Standards Institute
ASTM	American Society for Testing and Materials
ATL	Advanced Technologies and Laboratories International, Inc
BSR	Bench-scale Steam Reformer
CVAA	Cold Vapor Atomic Adsorption
DOE	Department of Energy
DOT	Department of Transportation
DQO	Data Quality Objectives
Ecology	Washington State Department of Ecology
EPA	Environmental Protection Agency
FBSR	Fluidized Bed Steam Reformer
GEA	Gamma Energy Analysis
HLW	High-Level Waste
ICP	Inductively Coupled Plasma
IDF	Integrated Disposal Facility
kg	Kilogram
LAW	Low-Activity Waste
LCS	Laboratory Control Sample
MS	Mass Spectroscopy
NAS	Sodium-alumino-silicate
NRC	Nuclear Regulatory Commission
PCB	Polychlorinated biphenyl
PCT	Product Consistency Test
TcO_4^-	pertechnetate
PNNL	Pacific Northwest National Laboratory
PPE	Personal Protective Equipment

PUF	Pressurized Unsaturated Flow Test
PVDF	polyvinylidene fluoride
QA	Quality Assurance
RPD	Relative Percent Difference
SEM	Scanning Electron Microscope
SCDHEC	South Carolina Department of Health and Environmental Control
SPFT	Single Pass Flow-Through Test
Sr	strontium
SRNL	Savannah River National Laboratory
TCLP	Toxicity Characteristic Leach Procedure
TRU	Transuranic
TSD	Treatment, Storage, Disposal
TTT	Thor Treatment Technologies
U.S. DOE	United States Department of Energy
WAC	Waste Acceptance Criteria
WTP	Hanford Waste Treatment and Immobilization Plant
XAS	X-Ray Absorption Spectroscopy
XRD	X-Ray Diffraction
XRF	X-Ray Fluorescence

Units

Kg	Kilogram
M	Molarity (moles/liter)
mL	Milli-liter (1×10^{-3} L)
µm	Micro-meter (1×10^{-6} m)
µCi	Micro-curie (1×10^{-6} Ci)

1.0 INTRODUCTION

The U.S. Department of Energy (DOE) Hanford tank farms contain approximately 57 million gallons of wastes, most of which originated during the reprocessing of spent nuclear fuel to produce plutonium for defense purposes. DOE intends to pre-treat the tank waste to separate the waste into a high level fraction, that will be vitrified and disposed of in a national repository as high-level waste (HLW), and a low-activity waste (LAW) fraction that will be immobilized for on-site disposal at Hanford. The Hanford Waste Treatment and Immobilization Plant (WTP) is the focal point for the treatment of Hanford tank waste. However, the WTP lacks the capacity to process all of the LAW within the regulatory required timeframe. Consequently, a supplemental LAW immobilization process will be required to immobilize the remainder of the LAW.

One promising supplemental technology is Fluidized Bed Steam Reforming (FBSR) to produce a sodium-alumino-silicate (NAS) waste form. The NAS waste form is primarily composed of nepheline ($NaAlSiO_4$), sodalite ($Na_8[AlSiO_4]_6Cl_2$), and nosean ($Na_8[AlSiO_4]_6SO_4$). Semi-volatile anions such as pertechnetate (TcO_4^-) and volatiles such as iodine as iodide (I^-) are expected to be entrapped within the mineral structures, thereby immobilizing them (Janzen 2008).

Results from preliminary performance tests using surrogates, suggests that the release of semi-volatile radionuclides ^{99}Tc and volatile ^{129}I from granular NAS waste form is limited by Nosean solubility. The predicted release of ^{99}Tc from the NAS waste form at 100 meters down gradient well from the Integrated Disposal Facility (IDF) was found to be comparable to immobilized low-activity waste glass waste form in the initial supplemental LAW treatment technology risk assessment (Mann 2003). To confirm this hypothesis, DOE is funding a treatability study where three actual Hanford tank waste samples (containing both ^{99}Tc and ^{125}I) will be processed in Savannah River National Laboratory's (SRNL) Bench-Scale Reformer (BSR) to form the mineral product, similar to the granular NAS waste form, that will then be subject to a number of waste form qualification tests. In previous tests, SRNL have demonstrated that the BSR product is chemically and physically equivalent to the FBSR product (Janzen 2005).

The objective of this summary plan is to describe the sample selection, sample preparation, and environmental and regulatory considerations for treatability studies of the FBSR process using Hanford tank waste samples at the SNRL. The SNRL will process samples in its BSR. These samples will be decontaminated in the 222-S Laboratory to remove undissolved solids and selected radioisotopes to comply with Department of Transportation (DOT) shipping regulations and to ensure worker safety by limiting radiation exposure to As Low As Reasonably Achievable (ALARA). These decontamination levels will also meet the Nuclear Regulatory Commission's (NRC's) definition of low activity waste (LAW). After the SNRL has processed the tank samples to a granular mineral form, SRNL and Pacific Northwest National Laboratory (PNNL) will conduct waste form testing on both the granular material and monoliths prepared from the granular material. The tests being performed are outlined in Appendix A.

2.0 ENVIRONMENTAL ISSUES

Testing of Hanford tank waste samples using the BSR at SRNL will be considered a treatability study as defined by 40 CFR 260.10, 261.4, Protection of Environment and WAC 173-303, Dangerous Waste Regulations. Samples used for the purpose of treatability studies are classified as an "excluded category of waste" under WAC 173-303-071(3)(r).

Treatability study samples are excluded from a substantial portion of the regulatory requirements in WAC 173-303 during collection, preparation for transport, transport to the laboratory or testing facility, and transport of the remaining unused waste sample or FBSR waste form back to the original generator from the laboratory or testing facility, as long as the following requirements are met:

1. **Mass of each sample shipment**: The mass of a sample shipment from a generator must not exceed 1000 kg. The facility conducting the treatability study may store no more than 1000 kg of "as received" treatability study samples (actual sample sizes will be limited to approximately 1 L) (WAC 173-303-071(3)(r)(ii)(B) and (s)(iv)).
2. **Packaging and Transport**: The samples must be packaged so they will not leak, spill, or vaporize from their packaging during shipment and such that the transportation of each sample shipment complies with United States Department of Transportation (DOT) requirements.
3. **Timeline for Shipping**: Sample must be shipped, within 90 days of being generated or of being taken from a stream of previously generated waste, to a laboratory or testing facility which is exempt under WAC 173-303-071(s) or has an appropriate final facility permit or interim status.
4. **Recordkeeping**: The generator or sample collector maintains the following records for a period ending three years after completion of the treatability study:
    A. Copies of the shipping documents;
    B. A copy of the contract with the facility conducting the treatability study;
    C. Documentation showing:
        - The amount of waste shipped under this exemption;
        - The name, address, and Environmental Protection Agency (EPA)/state identification number of the laboratory or testing facility that received the waste;
        - The date the shipment was made; and
        - Whether or not unused samples and FBSR waste form were returned to the generator.
    D. The generator reports the 4.C. documentation above in its Dangerous Waste Annual Report due March 1 for the preceding calendar year (WAC 173-303-220(1)).

Figure 1 provides a basic flow diagram for meeting these requirements. Figure 2 depicts roles and responsibilities for implementation of treatability study activities between the Hanford Site and SRNL, which are formalized in a Memorandum of Understanding.

Figure 1 Steam Reforming Treatability Flow Chart

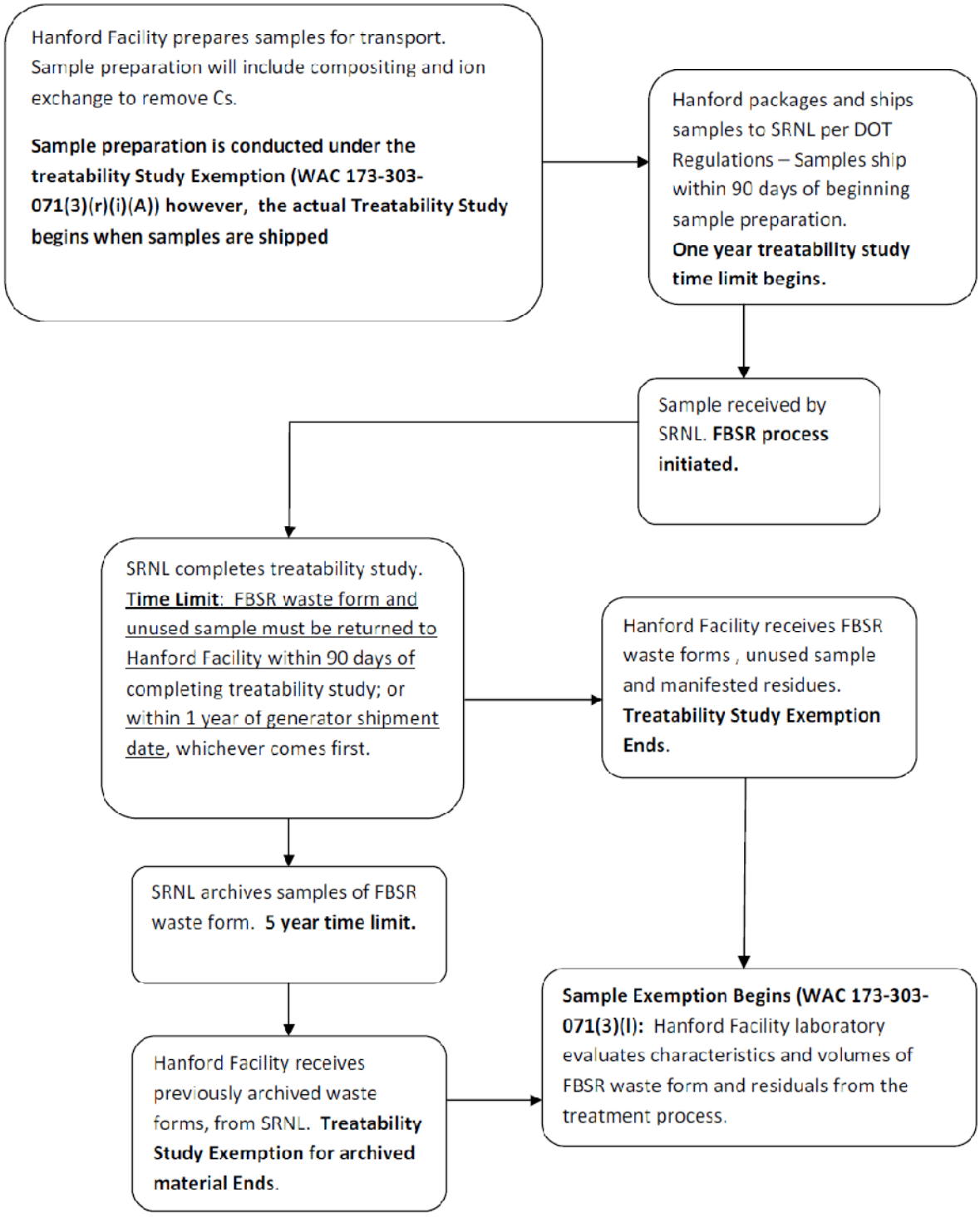

Figure 2. Material Compliance Obligations During Stages of Treatability Study

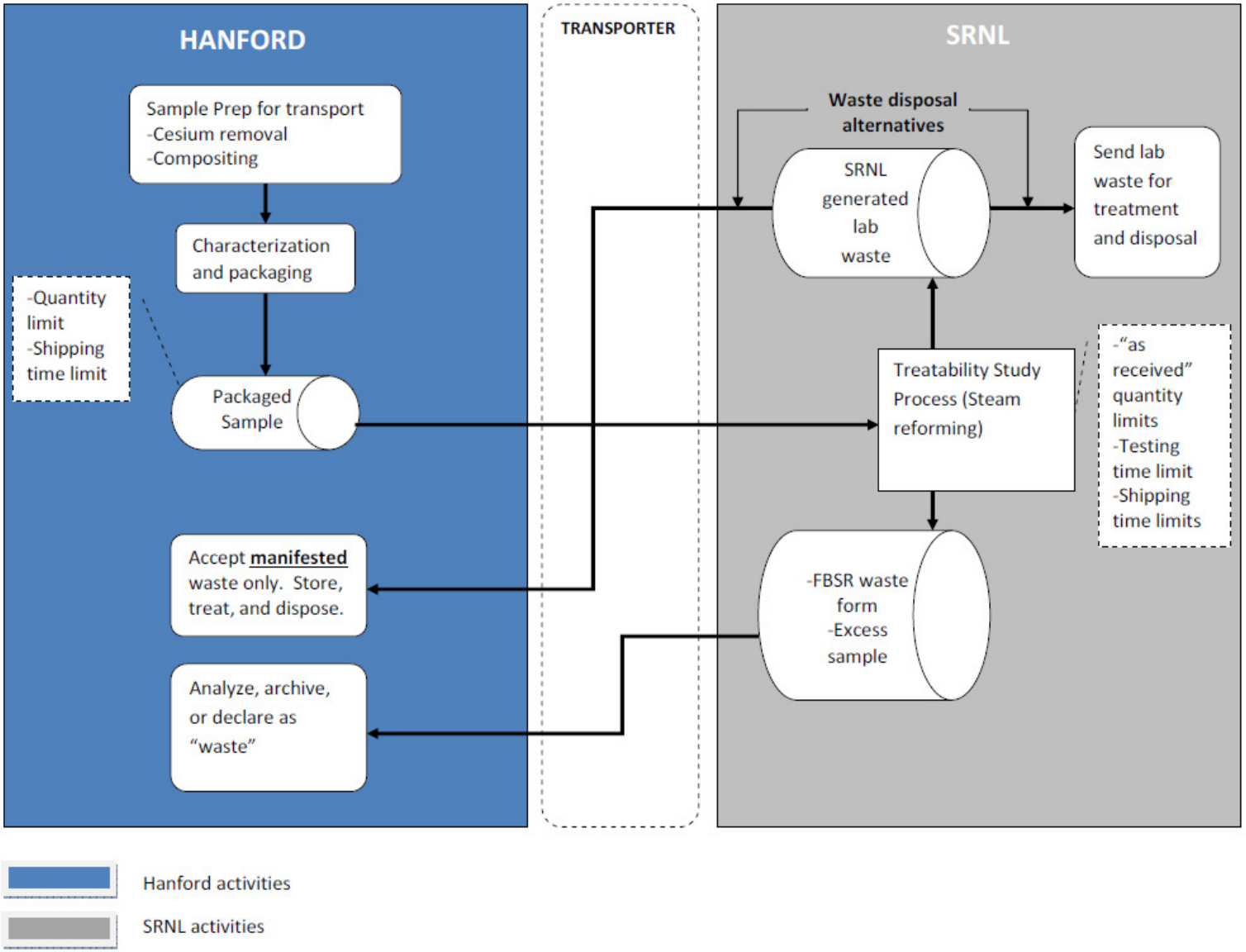

3.0 SELECTION OF TANK SAMPLES

The technical basis for the selection of candidate tank samples is described in RPP-RPT-47143, *Sample Selection Recommendations for Fluid Bed Steam Reforming Treatability Studies Using Hanford Low Activity Waste Underground Storage Tank Samples,* and in RPP-47073, *Data Quality Objectives for Selecting Waste Samples to Test the Fluid Bed Steam Reformer Process*.

The Data Quality Objectives (DQO) process is used to determine the type, quantity, and quality of data required to make a decision. It is the process employed in the selection of archived tank waste samples to be used for BSR process testing. Figure 3 is from RPP-47073 and shows the logic flow chart and decisions that will be made during the sample selection process.

As can be seen in Figure 3, the initial sample selection for BSR test samples is made using existing analytical data from archived tank samples in the 222-S Laboratory. The selected samples are analyzed and the results compared to test sample requirements and action limits outlined in RPP-47073. These data are used to determine if the selected samples are suitable for use as BSR test samples. The decisions to be made and the decision points in the selection process are shown in the logic flow chart in Figure 3.

Figure 3 Sample Selection Logic Flow Chart

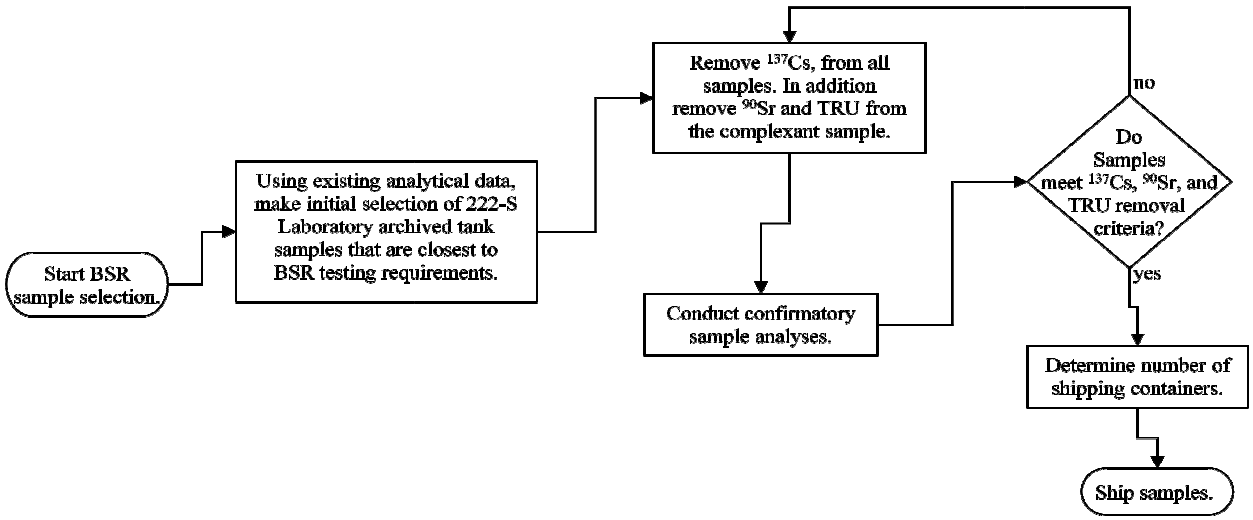

A number of criteria are used to select suitable radioactive waste samples:

- The samples should be representative of the bulk of the LAW to be treated and particular compositions of interest are:
    - High sodium (Na), low sulfate (SO_4^{-2}), chloride (Cl^-), fluoride (F^-), and phosphate (PO_4^{-3}) anions.
    - Low sodium (Na), high SO_4^{-2}, Cl^-, F^-, and PO_4^{-3} anions[1]
    - Complexant concentrate with other forms of Tc in solution besides pertechnetate (TcO_4^-)
- Where possible, samples should be from tanks that represent tank waste likely to be processed by FBSR within the first 5-7 years of operations
- Samples should be those that have previously been included in vitrification studies
- Samples should be those that have previously been demonstrated in simulant FBSR trials.

Using these criteria, the tanks selected for samples from the archive to be shipped to SNRL are:

- Tank 241-SX-105 (saltcake)
- Tank 241-AN-103 (saltcake)
- Tank 241-AN-107 (complexant concentrate)

Approximately 1-liter of each sample will be sent to SRNL.

[1] It is believed that anions such as $SO_4^{-2,}$ Cl^-, F^-, and PO_4^{-3} compete with pertechnetate $(TcO_4)^-$ for crystal locations within the NAS mineral structure

4.0 PREPARATION OF TANK SAMPLES FOR SHIPMENT

4.1 Sample Preparation

As stated above, three tank samples have been identified from within the archived samples of the 222-S laboratory and will be prepared to meet the LAW requirements.

Laboratories and/or subcontracted laboratories performing analyses in support of this DQO shall have approved and implemented Quality Assurance (QA) Plans. These QA plans shall meet DOE/RL-96-68, *Hanford Analytical Services Quality Assurance Requirements Documents* (HASQARD) minimum requirements as the baseline for laboratory quality systems. Advanced Technologies and Laboratories, ATL-MP-1011, *ATL Quality Assurance Project Plan for 222-S Laboratory* specifies the analyses conducted at the 222-S Laboratory. Analyses performed by WRPS shall be performed by ATS-MP-1032, *222-S Laboratory Quality Assurance Plan*.

The basic approach is to first adjust the identified samples to 5-7 M Na concentration by diluting with water. The resulting solution will be inspected to determine if any solids are present, thus requiring filtration (*As the strontium (Sr) and transuranic(TRU) components occur primarily in the solid phase, filtration will remove any Sr and TRU*). The Sr and TRU concentrations of the sample are required to be minimized for LAW requirements as well as for ALARA and shipping reasons. If solids are present, the filter media, for the initial and subsequent filtration, will be a 0.45 μm filter of polyvinylidene fluoride (PVDF) which is compatible with the tank samples from both radioisotope and highly alkaline aspects. After concentration adjustment and filtering (if required) each sample will be analyzed by sending an aliquot to the onsite analytical laboratory Advanced Technologies and Laboratories (ATL), International. Table 1 indicates the analytical methods and analytes.

Table 1 Analytical Method and Analytes

Analytes	Quality Control Acceptance Criteria				
	Proposed Analytical Methods	**LCS % Recovery[(a)]**	**Spike % Recovery[(b)]**	**Duplicate RPD[(c)] Liquids**	**Duplicate RPD[(c)] Solids**
Ag, As, Ba, Be, Cd, Cr, Hg, Pb, Na, Ni, Sb, Se, Tl, V, Zn	ICP/AES	80 - 120	75 - 125	≤20%	≤30%
Cl^-, F^-, PO_4^{3-}, SO_4^{2-}	IC	80 - 120	75 - 125	≤20%	≤30%
^{90}Sr	Beta Counting	80 - 120	N/A[(d)]	≤20%	≤30%
^{241}Am, ^{243}Am, ^{238}Pu, ^{239}Pu, ^{240}Pu, ^{242}Pu, ^{244}Pu ^{237}Np, ^{229}Th, ^{230}Th, ^{232}Th, ^{231}Pa, ^{233}U, ^{234}U, ^{235}U, ^{236}U, ^{238}U,	ICP/MS	80 - 120	75 - 125	≤20%	≤30%
^{99}Tc	Liquid Scintillation	80 - 120	75 - 125	≤20%	≤30%
^{137}Cs	GEA	80 - 120	N/A[(e)]	≤20%	≤30%
TOC	Silver catalyzed persulfate oxidation	80 - 120	75 - 125	≤20%	≤30%

Notes:

N/A = Not Applicable
TOC = total organic carbon

(a) LCS = Laboratory Control Sample. This sample is carried through the entire method. The accuracy of a method is usually expressed as the percent recovery of the LCS. The LCS is a matrix with known concentration of analytes processed with each preparation and analyses batch. It is expressed as percent recovery; i.e., the amount measured, divided by the known concentration, times 100.

(b) For some methods, the sample accuracy is expressed as the percent recovery of a matrix spike sample. It is expressed as percent recovery; i.e., the amount measured, less the amount in the sample, divided by the spike added, times 100. One matrix spike is performed per analytical batch. Samples are batched with similar matrices.

(c) RPD = Relative Percent Difference between the analytical samples. Analytical precision is estimated by analyzing duplicates taken separately through preparation and analysis. RPD for Polychlorinated biphenyl (PCBs) may be calculated using matrix spike and matrix spike duplicate results. Acceptable analytical precision is usually ≤20% RPD for liquids and ≤30% for solids, if the sample result is at least 10 times the instrument detection limit.

RPD = ((absolute difference between primary and duplicate)/mean) x 100

(d) Matrix spike analyses are not required for this method because a carrier or tracer is used to correct for constituent loss during sample preparation and analysis. The result generated using the carrier or tracer accounts for any inaccuracy of the method on the matrix. The reported results reflect this correction.

(e) The measurement is a direct reading of the energy and the analysis is not affected by the sample matrix; therefore, a matrix spike is not required.

Each sample will then be contacted with a cesium sorbent such as IONSIV[2] IE-911 or spherical Resorcinol Formaldehyde to remove radioactive cesium. An aliquot will be submitted to ATL for cesium analysis. When the radioactive cesium level is at the concentration agreed upon, then any additional Sr and TRU removal will proceed, if required.

Strontium and TRU will be removed from the tank 241-AN-107 complexant concentrate sample using the protocol reported by Nash, et al. in *Separation Science and Technology*, 2003. The protocol uses a non-radioactive 1 M strontium nitrate and a 1 M sodium permanganate solution, which is consistent with the strontium and TRU removal step in the current WTP flowsheet.

When the reaction is complete, an aliquot will be submitted to ATL to determine the success of the operation.

Conceptual flow sheets are presented in Appendix B.

4.2 Sample Shipment

The tank samples identified for the treatability studies will be prepared for packaging and shipment after filtration and cesium removal by sorbent/ion exchange processes. The complexant tank sample will be prepared for packaging and shipment after filtration and removal of Cs, Sr, and TRU radioisotopes. Shipment will occur via ground transportation and will commence no sooner than 45 days after SRNL has sent notification to the South Carolina Department of Health and Environmental Control (SCDHEC).

4.2.1 Hot Cell Activities

In order to prepare samples for shipping, a determination is made as to the dose rate of the sample. Once the dose rate is determined, a sample container size (125 mL, 250 mL or 1 L) will be identified for shipping. The material will be packaged in accordance with the Hedgehog operating manual: HNF-11651, *Operation and Maintenance Manual for the Hedgehog II Packaging System*. The laboratory will package using procedure LO-090-157, *Preparation/Loading of Type A Hedgehog II Packaging for Shipment*, and LO-090-156, *Tighten/Torque and Quality Control Verify Type A Packaging for Shipment*.

4.2.2 Department of Transportation Requirements

The samples will be packaged and shipped as Type A shipments per 49 CFR 173.

The laboratory data needed to support the shipment are:

- Activity per isotope, μCi/mL; μCi/g, etc.
- The sample weight
- The sample phase (solid or liquid)
- Sample dose at contact, at 1 meter
- Exact address at SNRL
- Contact person at SRNL, name, email, and phone number

[2] IONSIV® is a registered trademark of Universal Oil Products, Inc., Des Plaines, Illinois.

4.2.3 Shipping

Approval to ship will be provided by the Certified Hazardous Material Shipper (Eugene Juteau or delegate) once all appropriate approvals are in place at Hanford and SRNL.

A commercial shipping subcontractor will physically transport the samples to the SNRL as an "exclusive use" shipment. The configuration will most likely be a standard 40 foot enclosed van with tractor. The estimated time of delivery for team drivers is 2.5 days.

5.0 STEAM REFORMING PRODUCT AND PRODUCT TESTING

5.1 Savannah River National Laboratory Testing

SRNL will conduct a number of BSR tests on each of the Hanford LAW samples using the mineralizing flowsheet to produce an alkali aluminosilicate granular product in conjunction with Thor Treatment Technology (TTT) oversight as prescribed in DOE's contract DE-AC09-06SR22521, to ensure proper application of their proprietary technology. Data will be gathered during the operational radioactive BSR runs and equipment smears taken to ascertain the partitioning of key elements (for example, ^{137}Cs, ^{99}Tc, and ^{129}I) between the solid product and the off-gas. A portion of the granular product from each of the Hanford LAW samples will be immobilized in a geopolymer matrix to form a monolith. A number of performance tests will be carried out on the radioactive granular and monolithic product samples including the Product Consistency Test (PCT). Additional data will be gathered from redox measurements, X-ray Defraction (XRD), X-ray Fluorescence (XRF), Scanning Electron Microscope (SEM), and other analytical techniques as required. Compressibility strength tests will also be performed on the radioactive monoliths.

Radioactive samples of both the granular and monolith products will be sent to PNNL for further tests (see below)

5.2 Pacific Northwest National Laboratory Testing

PNNL will conduct a number of measurements on the LAW BSR product being produced at SRNL. The objective of the selected tests is to address the following issues:

- Identify the key reactions and/or processes affecting waste form durability and contaminant release
- Quantify the extent and rate of these reactions and/or processes
- Obtain the model parameters needed to describe these reactions and/or processes to better predict the behavior of the system
- Verification of the derived model parameters

These measurements will include the use of spectroscopic characterization techniques to evaluate technetium speciation and single-pass flow-through experiments to determine kinetic rate law parameters, effect of solution composition on the dissolution of granular and monolith BSR product, and effect of the binder on contaminant release from the BSR product. PNNL will also conduct the Toxicity Characteristic Leach Procedure (TCLP) and product consistency test (PCT) (duplication) for leachability, and the pressurized unsaturated flow (PUF) test. In addition, a combination of x-ray diffraction, scanning and/or transmission electron microscopy, and/or x-ray photoelectron spectroscopy, will be used characterize these radioactive samples.

6.0 MATERIAL TO BE RETURNED FOR TESTING

6.1 Disposition of Materials Generated by Savannah River National Laboratory

The SRNL is expected to generate materials from conducting FBSR activities that can be categorized as a FBSR waste form, unused samples, laboratory samples, or residues. For the purposes of this section: "FBSR waste form" means Hanford tank waste samples that have been treated by the steam reforming process under the treatability study sample exclusion and "residues" means all other materials produced by the treatability studies, e.g., laboratory equipment, personal protective equipment, that is contaminated by contact or co-mingling with Hanford generated tank wastes that are not FBSR waste form or unused samples.

A portion of the FBSR waste form either in granular or monolithic form will be transported to PNNL for testing. FBSR waste form and unused Hanford tank waste samples may be returned to the Hanford site under the treatability study exclusion upon prior approval from DOE-ORP.

Residues as described above including laboratory generated materials such as contaminated equipment and personal protective equipment (PPE) shall be dispositioned by SRNL and shall not be returned to Hanford under the treatability study sample exclusion. SRNL shall not return any residues as described above to Hanford except upon express prior approval from DOE-ORP.

7.0 REFERENCES

40 CFR 260.10, 261.4, "Protection of Environment", *Code of Federal Regulations* as amended.

49 CFR Part 173, "Shippers –General Requirements for Shipping and Packaging," *Code of Federal Regulations,* as amended.

AC 173-303, "Dangerous Waste Regulations," as amended, State of Washington.

ATL-MP-1011, 2009. Rev 9, *ATL Quality Assurance Project Plan for 222-S Laboratory,* 222-S Laboratory, Advanced Technologies and Laboratories International, Inc., Richland, Washington.

ATS-MP-1032, 2010, Rev 4, *222-S Laboratory Quality Assurance Plan*, 222-S Laboratory, Washington River Protection Solutions, Richland WA.

DE-AC09-06SR22521 Contract, Thor Treatment Technologies, LLC Aiken, South Carolina.

Jantzen, C.M., "Evaluation of Fluidized Bed Steam Reforming (FBSR) Technology for Sodium Bearing Wastes from Idaho and Hanford Using the Bench-Top Steam Reformer (BSR)", WSRC-TR-2004-00560, 2005.

Jantzen, C.M., "Mineralization of Radioactive Waste by Fluidized Bed Steam Reforming: Comparison to Vitreous Waste Forms, and Pertinent Durability Testing," WSRC-STI-2008-00268, 2008.

Nash, C. A., H.H. Soto and W.R. Wilmarth, "Strontium and Transuranic Precipitation and Crossflow filtration of a Large Hanford Tank 241-AN-102 Sample, Separation Science and Technology," 38(12&13):3189-3213, 2003.

HNF-11651, 2007, Rev 1, *Operation and Maintenance Manual for the Hedgehog II Packaging System,*CH2M Hill Hanford Group, Inc., Richland, Washington.

LO-090-156, 2009, "Tighten/Torque and Quality Control Verify Type A Packaging for Shipment," Rev E-0, Advanced Technologies and Laboratories International, Inc., Richland, Washington.

LO-090-157, 2009, "Preparation / Loading of Type A Hedgehog II Packaging for Shipment," Rev B-0, Advanced Technologies and Laboratories International, Inc., Richland, Washington.

ORP-11242, R 4, 2009, *River Protection Project System Plan*, US DOE Office of River Protection, Richland, Washington.

RPP-PLAN-47143, 2010 *Sample Selection Recommendations for Fluid Bed Steam Reforming Treatability Studies Using Hanford Low Activity Waste Underground Storage Tank Samples,* Washington River Protection Solutions, Richland, Washington

RPP-47073, 2010, *Data Quality Objectives for Selecting Waste Samples to Test the Fluid Bed Steam Reformer Process,* Washington River Protection Solutions, Richland, Washington.

RPP-17675, Rev. 0, 2003, *Risk Assessment Supporting the Decision on the Initial Selection of Supplemental ILAW Technologies,* CH2MHILL Hanford Group Inc., Richland, Washington

APPENDIX A

Steam Reforming Waste Form Tests

Savannah River National Laboratory (SRNL)

All the radioactive Hanford LAW samples will be subjected to:

- Processing through the bench-scale reformer run to produce a granular product
- Production of ten (10) 1"diameter by 2" cylindrical monoliths from granular product

The following tests will be performed on the granular and/or monolithic product from the radioactive BSR runs:

- Mineral characterization (Redox, XRD, XRF, SEM etc.)
- Short-term and long-term product consistency test (PCT) (ASTM C-1285)
- Compressive strength (ASTM-C-39/C39M-99)

Note: Any analyses that require a third party, off-site laboratory will be managed by PNNL. Samples requiring these analyses will be sent to PNNL and they will contract with the appropriate laboratory.

Pacific Northwest National Laboratory (PNNL)

Savannah River National Laboratory will ship samples of the granular product and the monolith formed from BSR processing of each of the radioactive Hanford LAW samples. PNNL will conduct the following tests on the granular and/or monolithic product:

- Single Pass Flow-Through (kinetic rate information)
- Pressurized Unsaturated Flow (PUF)
- Short-term and long-term product consistency test (PCT) (ASTM C-1285) - duplication
- Tc and Re speciation
- Measurement of thermodynamic constants (subcontracted to UC Davis)
- Mineral characterization (micro-XRD, XAS)
- Toxicity Characteristic Leach Procedure (TCLP) in accordance with SW-846
- Waste Package Release Testing (ANSI/ANS 16.1, EPA draft method 1315, or ASTM C1308) Monolith diffusion testing (ASTM 1308, EPA 1315 or ANSI 16.1)

Note: Duplicate tests (e.g., short and long-term PCT) may be carried out at either laboratory

APPENDIX B

Conceptual Flow Sheets for Sample Preparation

Figure B-1. Saltcake Dissolution Flowsheet.

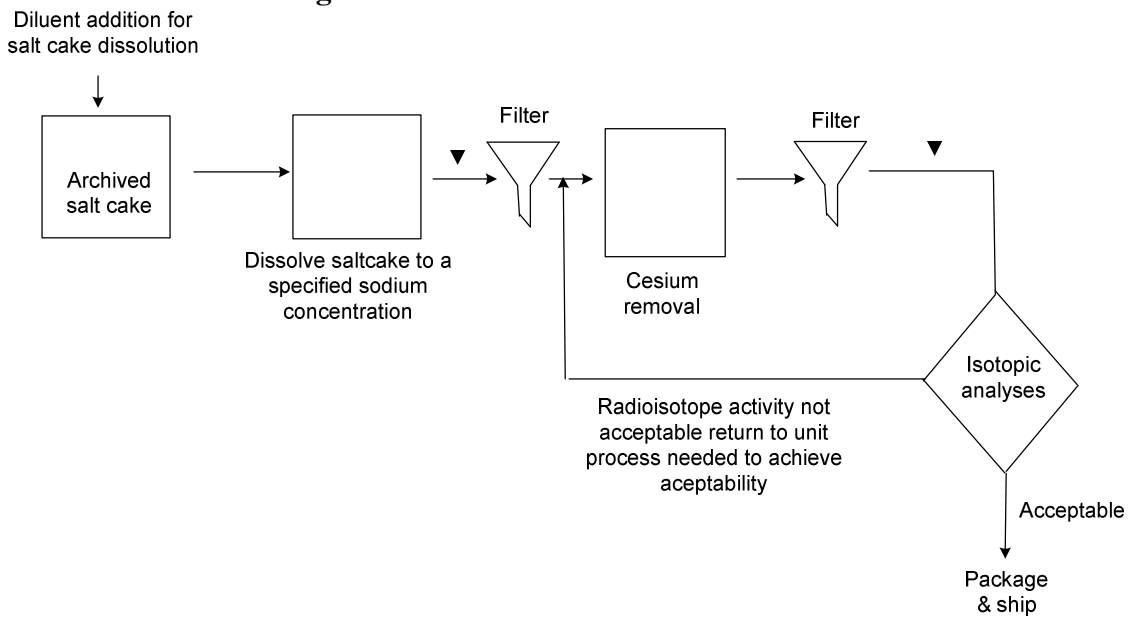

Note: The primary analysis of interest to pack and ship is the isotopic analyses. An aliquot for a full suite of analyses is taken where the symbol (▼) indicates. These analyses are not needed for packaging and shipping and will be sent to SRNL upon completion.

Figure B-2. Cesium, Strontium, TRU Removal Flowsheet.

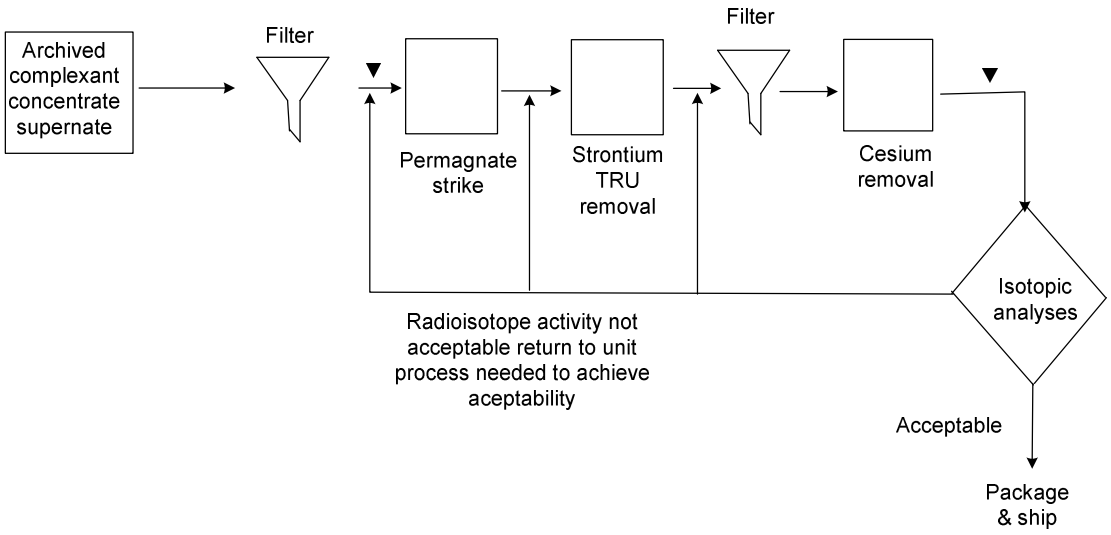

Note: The primary analysis of interest to pack and ship is the isotopic analyses. An aliquot for a full suite of analyses is taken where the symbol (▼) indicates. These analyses are not needed for packaging and shipping and will be sent to SRNL upon completion.

Appendix F: Chain of Custody Form

Chain of Custody Number:					Analyses Requested					
Laboratory name and address:			contact name and address:							
Date	Time	Sample ID#	Sample source	Sample description (volume, container, etc.)						

Appendix B. Summary of Scientific Research and Testing for Fluidized Bed Steam Reforming Process Applied to Immobilization of Key Radionuclides in Hanford Low Activity Waste

Leo E. Thompson

Appendix B represents an overview of FBSR mineral waste form testing (pilot and bench scale) and characterization that had been performed before the EM31 Technology Development and Deployment (TDD) Program (WP5.2.1-210-001) was begun. The document is entitled ""Summary of Scientific Research and Testing for Fluidized Bed Steam Reforming Process Applied to Immobilization of Key Radionuclides in Hanford Low Activity Waste," The document summarizes the testing and characterization of the granular mineral waste form, the initial studies performed at SRNL and PNNL, the Hanford Risk Assessment, and the initial studies to make the mineral waste form into monoliths. The overview is presented graphically and in writing in italics below since it was taken directly from a document written by Leo E. Thompson that was never issued. This overview helped define the remaining test program needed for a down selection for Hanford Supplementary LAW.

"Overview

A substantial body of information has been developed over the past decade regarding the use of a fluidized bed steam reforming (FBSR) process to treat U.S. Department of Energy (DOE) wastes. Although FBSR is already planned for use at other DOE sites, Hanford is a special case in that the waste form that would be produced would need to be mineralized in order to provide long-term protection against waste contaminant releases to groundwater and then converted to a monolith to meet compressibility requirements established for the Hanford Integrated Disposal Facility. Those two approaches are unique to Hanford if FBSR is selected to treat LAW at that site. The literature also contains numerous references to FBSR studies pertaining to sodium-bearing waste (SBW) at the Idaho National Laboratory and Tank 48 waste at the Savannah River Site. This summary does not specifically address those wastes given the differences in the waste forms to be produced (carbonate[1] waste form rather than a mineralized form) and the differences in the waste feed to the FBSR units.

The information in this report is primarily digested from scientific information published in the literature, vendor information, independent reports, and studies/plans funded by DOE as indicated in Table 1. This paper summarizes in tabular form the results from over 20 reports, articles, and technical papers that are relevant to the state of Tc-99 and I-129 in Hanford LAW feed when processed using FBSR to produce a mineralized waste form.

Of principal interest to DOE, its regulators, and stakeholders is the long-term fate of technetium-99 (Tc-99) and iodine-129 (I-129) in Hanford low-activity wastes if those wastes are processed using FBSR. Since 2001, a progressive series of bench, engineering, and pilot scale FBSR tests have been conducted with Hanford LAW surrogate wastes at the Savannah River National Laboratory (SRNL) in Aiken, SC; at the Science and Technology Applications Research (STAR) Center in Idaho Falls, ID; and at Hazen Research in Golden, CO. The mineralized waste forms produced have been analyzed by Pacific Northwest National Laboratory (PNNL) in Richland, WA and by SRNL and identified as a mixture of various Na-Al-Si (NAS) feldspathoid minerals including nepheline and sodalites such as nosean.

The mineralized waste form produced during the FBSR process generally consists of both granular materials and fines, both of which are reported by Jantzen to exhibit the same durability characteristics. The durability tests used for the FBSR waste form are, for the most part[2], the same tests that are used to test the durability of Hanford low-activity waste (LAW) glass formulations. The tests conducted include Product Consistency Tests (PCT) consistent with ASTM C1285 protocols, Single Pass Flow Through (SPFT) tests, and Pressurized Unsaturated Flow (PUF) tests. The waste forms were also tested in accordance with U.S. Environmental Protection Agency (EPA) Resource Conservation and Recovery Act (RCRA) Toxicity Characteristic Leaching Procedure (TCLP) test protocols for RCRA constituents.

---

[1] Mineralized FBSR runs were conducted for the SBW, however; the SBW feed is substantially different from Hanford LAW.
[2] Vapor Hydration Testing (VHT) is an exception at this point in time. VHT is used for glass but not for mineral waste forms.

The findings from the tests as reported in numerous scientific journal articles, technical symposia papers, and technical reports consistently indicate two key results as follows:

1. *Greater than 99.99 percent of the Tc-99 and Cs-137[3] are reported to be captured in the mineralized FBSR product, and*
2. *The durability of the mineralized product, within the uncertainties inherent in glass and FBSR testing/measurements, appears to be of the same order of magnitude as indicated by LAW glass tests.*

It is reported by Jantzen (Jantzen 2002) that the FBSR temperatures are "low enough not to vaporize radionuclides, but high enough to destroy volatile organic compounds. Whether that is the reason for the high radionuclide retention reported to be in the waste form or there is another cause needs further investigation.

Further testing and analysis is required (and is planned) for FBSR to better understand the mineralized and monolithic waste forms and provide higher confidence levels for information that will inform DOE decision-making pursuant to the process in DOE Order 413.3A. For example, several scientists have postulated that the mineralized waste form includes cage-like tetrahedra structures that form around Tc-99 and I-129. Those scientists (McGrail, Jantzen) postulate that the cage-like structures, in conjunction with ionic bonds, hold key radioisotopes more tightly within the mineral waste form than occurs with a vitrified waste form.

Questions remain with respect to leaching mechanisms that can release the radionuclides of interest. Studies of vitrified waste forms indicate that radioisotopes, such as Tc-99 and I-129, are released congruently (at the same time) as sodium is released from the waste form matrix. In the case of the FBSR mineralized waste form, it is reported that the dissolution is incongruent which means that sodium would leach from the waste form prior to constituents such as Tc-99 and I-129. The dissolution mechanism (congruent or incongruent) for the mineralized waste form is not fully understood, however; recent scientific reports focus on a leaching mechanism that correlates to aluminosilicate buffering and pH. Tests are currently underway and planned over the next year to analyze the mineralized waste forms at the atomic level to ascertain whether or not the mineral cage structures do contain key radionuclides such as Tc-99 and I-129.

Although the mixture of mineralized granules and fines produced during the FBSR process appear to have good durability characteristics based on analytical results identified in Table 1, those materials do not have sufficient compressive strength for direct disposal in the Hanford Integrated Disposal Facility (IDF). Consequently, DOE is also investigating the use of various binding agents that could be used to coalesce the FBSR product into a monolithic form. Preliminary results from those investigations are also provided in Table 1, however; additional testing and analysis will be conducted on binders to form monolithic waste forms and the net performance realized from monolithic waste forms.

Relative to the mineralized waste form durability, the manner in which test results are reported can cause confusion. For example, as identified in Table 1, several scientists report that the normalized release rates from the mineralized waste form which are generally expressed in grams/m^2, are a factor of 100 or so less than have been measured for LAW glass. The lower release rate is offset, however, by the much greater surface area resulting from the rough surface texture of the mineral waste. When the surface area differences are taken into account, the net leach rates appear to be of the same general order of magnitude for both.

[3] *Note that nonradioactive Re and Cs are used in place of the radionuclides Tc-99 and Cs-137 respectively.*

A variable that remains to be evaluated is the reduction in effective surface area of the mineralized waste once a binder is used to produce a monolith. Some preliminary results are provided in Table 1. The net impact of a binder on the leaching results is also the subject of currently planned tests.
Several of the tests planned for the upcoming year will be conducted using actual Hanford tank wastes. These tests will, among other things, provide a means of ascertaining whether the extensive testing conducted to date with LAW surrogates sufficiently correlates with results produced with actual wastes. This is important since the cost and time to conduct hot (radioactive) tests are substantially greater than to conduct tests with non-radioactive surrogates.

Although not the focus of this report, Table 1 also includes limited amounts of other pertinent regulatory information such as the ability of the FBSR process to meet RCRA and Clean Air Act requirements (e.g., destruction of organics), ability to essentially eliminate SOx and NOx emissions, and ability to meet RCRA Land Disposal Restrictions. Additional information relative to those requirements is contained in the references listed at the back of this report. The information and conclusions provided in Table 1 should be used with care. If information within this summary table is to be used elsewhere, it should be carefully reviewed within the context of the source document and in context with other studies cited.

Figure 1 on the following page depicts the relationship between FBSR testing that has been conducted for Hanford LAW and secondary wastes, reports that have been issued and summarized in Table 1 in this paper, and key findings and pertinent information that has been obtained"

Figure 1. Fluidized Bed Steam Reforming (FBSR) Investigations on Mineralized Products from Hanford LAW Waste, per Cited References

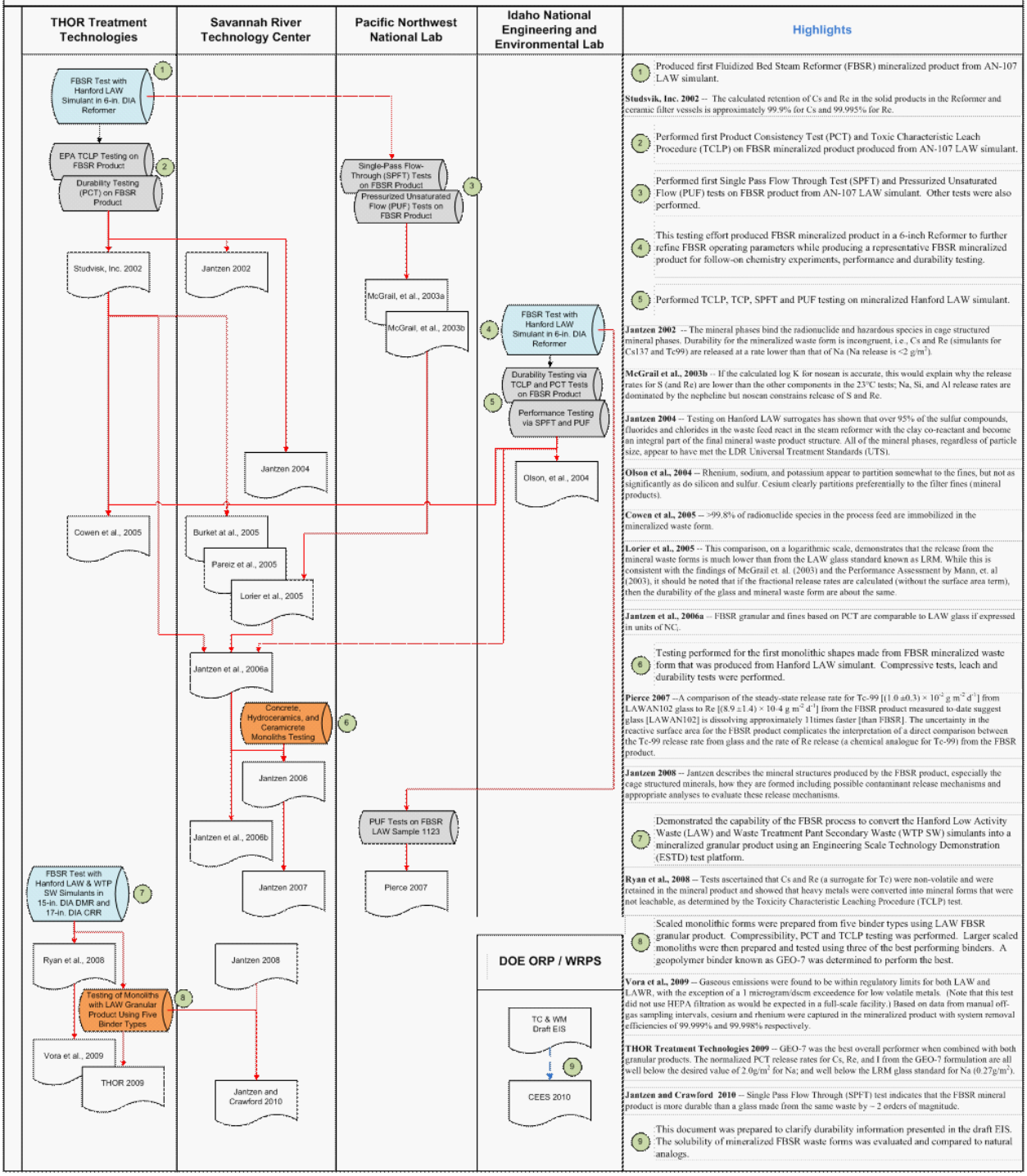

Appendix C. Immobilization Technology - Downselect Data Needs Pre-Decisional Draft (November 2, 2010)

Leo E. Thompson

The text below represents a Pre-Decisional November 2, 2010 Draft Document by Leo E. Thompson of Washington River Protection Solutions, LLC. The Pre-Decisional draft was never issued and so is given in the italicized text below as it was written in November 2010. This document lays out the logic for the testing that needed to be performed for a down selection of the FBSR mineral waste form for Hanford Supplementary LAW.

"FBSR Waste Form Qualification Testing Data Inputs Required to Support Technology Down Select Process for the Hanford Supplemental Immobilization Project

Introduction

The U.S. Department of Energy's Office of River Protection (ORP) has as its primary mission to retrieve, treat, immobilize, and dispose of Hanford's tank waste and subsequently close the emptied underground storage tanks. Currently there are approximately 56 million gallons of highly radioactive mixed wastes, resulting from the processing of irradiated fuels, that are being stored in a total of 142[a] single-shell tanks (SSTs) and 28 double shell tanks (DSTs) in the 200 Areas at Hanford (1). A key aspect of implementing the River Protection Project (RPP) cleanup mission is to construct and operate the Waste Treatment and Immobilization Plant (WTP). The WTP will separate the tank waste into high-level and low-activity waste (LAW) fractions, both of which will subsequently be vitrified.

However, the projected throughput capacity of the WTP LAW Vitrification Facility is insufficient to complete the RPP mission in the time frame required by the Hanford Federal Facility Agreement and Consent Order, also known as the Tri-Party Agreement (TPA). Without additional LAW treatment capacity, the mission would extend an additional 40 years beyond December 31, 2047, the Tri-Party Agreement milestone date for completing all tank waste treatment. The life-cycle cost of tank waste cleanup is strongly influenced by the WTP operating duration. Each year the WTP operates beyond 2047 costs taxpayers approximately $1 billion in today's dollars. Therefore, a significant life-cycle cost savings incentive exists to complete tank waste treatment processing at the earliest practical date.

Therefore, Supplemental Treatment is required both to meet the Tri-Party Agreement treatment requirements as well as to more cost effectively complete the tank waste treatment mission. The Supplemental Treatment Project will design, construct and operate the processes and facilities required to treat and immobilize into a solidified waste form that portion of the retrieved LAW that is not sent to the WTP's LAW Vitrification facility. The solidified waste will then be disposed on-site in the Integrated Disposal Facility (IDF).

Four immobilization technologies are under consideration as part of the Supplemental Treatment Program including:

- *second WTP LAW vitrification*
- *bulk vitrification*
- *cementitous solidification (cast stone)*
- *fluidized bed steam reforming (FBSR).*

DOE has made substantial past investments in evaluating each of the proposed vitrification processes (i.e., WTP LAW and bulk vitrification) and cementitious solidification processes at Hanford. Additionally, numerous other sites within the DOE complex have examined the performance of

[a] *There are 149 single shell tanks (SSTs). Seven SSTs have been fully retrieved and four SSTs have been retrieved to the limits of technology as noted in the River Protection Project System Plan.*

cementitious solidification of LAW for number of years. DOE has made some but not sufficient investments to date in the FBSR process to produce a monolithic, mineralized waste form for Hanford LAW immobilization. This paper is, therefore, focused on specifying the minimum essential data required to objectively evaluate the FBSR waste form as a LAW immobilization alternative to the other technologies.

The initial step in evaluating immobilization technologies will involve a go / no-go evaluation of waste form performance. If it is determined that the performance of a waste form for a given immobilization technology will likely satisfy the IDF disposal requirements, the technology will be included in the technology down select process. However, if the data indicates the waste form is unlikely to satisfy IDF disposal requirements, the immobilization technology will not be considered further. An FBSR waste form qualification (WFQ) program plan developed in 2010 provides a description of the logic, technical rationale, compliance strategy, and the testing needed for qualifying a monolithic FBSR waste form for disposal in IDF, should FBSR be selected as the Supplemental Treatment technology (2).

This paper describes the FBSR waste form data to be obtained from a series of bench-scale radioactive tests. The data from these tests will be used, in combination with other data on the FBSR mineral product, to assess whether or not the FBSR process is likely to satisfy IDF disposal requirements and therefore be included in the subsequent technology down select process.

Fluidized Bed Steam Reforming

An FBSR facility is being constructed at the Idaho National Laboratory (INL) for treatment of Sodium Bearing Waste (SBW) (3). The design of another FBSR facility is being developed for the Savannah River Site (SRS) to convert a salt supernate waste to carbonate minerals as a pre-treatment method to facilitate subsequent vitrification (4). A significant number of studies, assessments, reviews and tests have been carried out in support of these DOE applications, both of which involve a carbonate type of waste form. However, not as much work has been directed to the application of the FBSR technology for the production of a sodium aluminosilicate mineral waste form necessary for the immobilization of Hanford LAW and specifically there have been no tests with actual wastes. The most significant activity related to the application of the FBSR technology for Hanford LAW was an EM-31 funded program in 2008-2009 that involved an engineering-scale demonstration of the FBSR process using simulated Hanford LAW followed by a subsequent task at Savannah River National Laboratory (SRNL) to develop and test formulations to convert the granular FBSR product into a monolithic form (5). Conversion to a monolithic form is required to meet Hanford Integrated Disposal Facility (IDF) waste compressibility requirements.

As a result of the work to date, FBSR has been identified as a promising supplemental immobilization technology for Hanford LAW. For the immobilization of Hanford LAW, the FBSR would be operated to produce a sodium aluminosilicate (NAS) mineral form primarily composed of nepheline, sodalite, and nosean. Semi-volatile anions such as TcO_4^- and I^- are expected to be immobilized in the nosean-sodalite mineral structures (6). The granular aluminosilicate mineral products would be macro-encapsulated in a monolithic form to produce a structurally and environmentally stable final waste form.

The release of semi-volatile radionuclides ^{99}Tc and ^{129}I from granular sodium aluminosilicate mineral product was found by preliminary performance test to be limited by nosean solubility (7). The predicted performance of the NAS waste form was found to be equivalent or better than the glass waste form in an initial supplemental LAW treatment technology risk assessment (7). While the existing data are promising, additional testing with actual waste is required to mature the technology and to confirm the earlier findings from simulant tests.

Waste Form Qualification (WFQ) Testing

Data and updated models are required to demonstrate and confirm the performance of the FBSR NAS waste form. To help assess the suitability and effectiveness of the FBSR process for the treatment of Hanford LAW, a series of treatability studies are being conducted at SRNL using a Bench Scale Reformer (BSR) test unit. The BSR unit produces waste form products with the same mineralogy as well as similar off-gases as are produced by larger scale FBSR units (8). A program plan outlining the approach for the testing and monolithing as well as the sampling and analyses has been developed (9) to obtain the additional minimum essential information. The waste feed samples on which the tests will be conducted are listed in Table 1. The objectives of these tests, methods, and the data to be collected are described in the program plan (9) and summarized later in this paper.

Table 1. Radioactive Bench-Scale Reformer Tests Being Performed at SRNL

Test Sequence	*Test ID*	*Source of Radioactive Waste*
#1	*Secondary Waste Sample*	*Chemical shim of SRS secondary waste sample from DWPF to resemble Hanford WTP secondary waste*
#2	*SRS LAW Sample*	*Chemical shim of SRS LAW to resemble Hanford LAW based upon Hanford 68 tank blend*
#3	*Hanford LAW Sample #1 (low S, Cl, F, and P)*	*Hanford Tank 241-AN-103*
#4	*Hanford LAW Sample #2 (high S, Cl, F, and P)*	*Hanford Tank 241-SX-105*
#5	*Hanford LAW Sample #3 (Complexants)*	*Hanford Tank 241-AN-107 – tentative selection but currently being reviewed*

Test #1 will be with actual SRS Secondary Waste that is chemically shimmed to reflect the expected composition of Hanford WTP secondary waste. This test was planned as part of an existing EM-30 funded project to support the evaluation of the FBSR process to determine the suitability of the process to treat secondary wastes. This test will provide some useful information and contribute to the understanding of the FBSR process behavior and sodium aluminosilicate waste form and will also provide insights into the suitability of FBSR to treat WTP LAW vitrification secondary wastes if those wastes contain unacceptable quantities of Tc-99. However, the composition of the SRS secondary waste is markedly different than a Hanford LAW (e.g., very low sodium) (5). Consequently, the data from Test #1 is informative but not directly applicable. It will supplement the down select process but will not provide go/no-go information relative to the LAW immobilization selection process.

Test #2 with actual SRS LAW is intended to assess the performance of the FBSR process and waste form in the treatment of Hanford LAW. The test is important because the actual SRS LAW that will be used will be chemically adjusted to represents a 68 tank blend of Hanford LAW and also provides a tie back to the 2008 engineering-scale FBSR test which used a simulant representing the same 68 tank blend (5,10). The monolith work from 2008-2009 was generated using the product produced from that test program (5,11). Thus, the early data from the SRS LAW test will provide an important correlation using actual radionuclides to previous tests using surrogates at the bench and engineering scales that produced a mineralized product as well as the monolith testing using the mineralized product. Building correlations between work with radioactive samples and simulants is critical to being able to conduct future relevant simulant tests, which are more cost effective and environmentally sensitive than tests with radioactive wastes.

Test #s 3, 4, & 5 with the three actual Hanford LAW samples are intended to assess the performance of the FBSR process and waste form when treating a range of actual Hanford LAW compositions. The waste samples to be used in the testing were selected to represent more than 80% of the compositional range of interest across the spectrum of Hanford tank wastes (12,13). Collectively, these samples reflect most of the Hanford LAW that will require immobilization. Thus the early data from these BSR tests, particularly the first two Hanford LAW tests, will be important to establish confidence that the FBSR process, the resulting mineralized products, and subsequent monoliths produced using such wastes confirm results from prior surrogate testing.

Data resulting from the tests and subsequent analyses will be provided for evaluation at three progress briefings. The progress briefings will provide the principal investigators the opportunity to brief DOE and the Supplemental Treatment program team with critical inputs. The data will be used to minimize technical risk to support critical decisions associated with the potential deployment of the FBSR technology.

First Progress Briefing

The first progress briefing is scheduled for January 2011. Initial data from the Secondary Waste and SRS LAW tests will be available. The data available for the first briefing is expected to include mass balance estimates of ^{99}Tc, Re, and ^{129}I for the first two tests. This will be the first opportunity to estimate the technetium, rhenium, and iodine that has partitioned between the FBSR product and the other portions of the BSR system. It will also provide a correlation between technetium and rhenium behavior in the FBSR system.

Additional data will be available from these tests including BSR test operational data, Reduction / Oxidation (Redox) measurements of the granular product, short-term (7-day) Product Consistency Test (PCT) per ASTM C-1285, and chemical digestion results of the FBSR granular product.

Second Progress Briefing

The second progress briefing is scheduled for April 2011. This will occur after the first two samples, SRS shimmed secondary waste and SRS shimmed LAW, have been analyzed to determine the ^{99}Tc oxidation state. This information will be augmented with the results of other supporting analyses, such as chemical digestion results, redox measurements, crystalline phase mineralogy via XRD, and scanning and/or transmission electron microscopy (SEM or TEM) with energy dispersive spectroscopy (EDS) analyses. Early results from the first two Hanford LAW tests are expected to be available such as Toxicity Characteristic Leaching Procedure (TCLP), short term PCT analysis of the mineral phases, and mass balance results.

^{99}Tc speciation results for some of the initial tests should also be available by the time of the second progress briefing. Additionally, the results from shorter term Single Pass Flow Through (SPFT) tests will be used to evaluate whether ^{99}Tc and ^{129}I release from the FBSR waste form is stochiometric or non-stochiometric with respect to sodium in the sodalite and nosean. Collectively, these results should help to confirm the premise that ^{99}Tc is contained in the cage-like structure of sodalite and nosean.

Third Progress Briefing

The third progress briefing is scheduled for July 2011 and will provide an opportunity to present an overview of all of the results to date. The results from most of the monolith development and testing should be available by that time including diffusion test results. A requirement for near surface disposal is the Leachability Index. Therefore, it is expected that release of ^{99}Tc and ^{129}I from the matrix will need

to be consistent with the Nuclear Regulatory Commission requirements (i.e., 10 CFR 61 subpart C). The outcome could result in changes in the binder/FBSR mix or selection of a different binder matrix. However, this is considered a low risk assuming the granular product is exhibiting a durability and leach response that is consistent with previous tests with simulants since the previous tests showed the leach resistance of the NAS product to be several orders of magnitude better than required by the NRC requirement. An assumption that will be confirmed through testing is the binder matrix will not degrade the performance of the FBSR granular product.

Supplemental Treatment (Immobilization) Technology Selection Process

The Supplemental Treatment technology selection process will generate a decision document whose scope will be to:

- *clearly identify the immobilization technology options that are evaluated;*
- *identify those immobilization technology options not evaluated and provide a rationale as to why they were not further evaluated;*
- *rigorously evaluate each of the selected technology options using a set of defined, weighted, and measured evaluation criteria; and*
- *recommend to WRPS management and ORP the technology option that best meets RPP's programmatic needs.*

The down select process will result in a recommendation to ORP of which of the four immobilization technologies to pursue. Following approval of that decision by ORP, the Supplemental Treatment Program will commence a Conceptual Design project to develop a Critical Decision package for the selected immobilization technology in accordance with DOE Order 413.3. Thus, data from the FBSR WFQ test program will be needed by as soon as practical to support the go / no-go evaluation of waste form performance and the determination if the FBSR technology should be included in the subsequent technology down select process.

Data Needed for Go / No-Go Decision Prior to Down Select Process

A summary of the types of data to be collected from the five BSR tests is provided in Table 2. As illustrated in the table, the go / no-go evaluation to support the down select recommendation will be based primarily on data from Test #2 with SRS LAW and Tests #s 3 and 4 with Hanford LAW. These data will be evaluated in conjunction with data from prior simulant testing.

As noted previously, the SRS LAW test is important because it represents the 68 tank blend of Hanford LAW and also provides a tie back to the 2008 engineering-scale FBSR test and subsequent monolith development work (5,11). Together Test #s 2, 3 and 4 represent the bulk of Hanford LAW requiring immobilization (12).

Table 2. Primary BSR Test Data to be Used in Go / No-Go Evaluation Prior to Down Select Process

Test / Analyses		***Secondary Waste***	***SRS LAW***	***Hanford LAW 1***	***Hanford LAW 2***	***Hanford LAW 3***
	Test No.	*1*	*2*	*3*	*4*	*5*
Redox			*x*	*x*	*x*	
Minerology			*x*	*x*	*x*	
TCLP (granular)			*x*	*x*		
Mass Balance (Tc, Re, I)			*x*	*x*	*x*	
Short Term PCT (granular)			*x*	*x*		
Long Term PCT						
SPFT / Kinetic Rate Law						
PUF / Alteration Phases						
Tc Speciation (Re speciation if available)			*x*	*x*		
Pure Mineral Phase Tests						
Measurement of Thermodynamic Constants						
Compressive Strength						
Diffusion Testing						

Ideally, the results of these radioactive BSR tests will correlate well with prior simulant work, i.e., produce the same classes of minerals and the same range of short-term PCT/leach results. If that is the case, that correlation will provide a basis for confidence that the prior FBSR tests with LAW simulants (5,14) are representative of FBSR process and product performance with actual wastes. This would enable the previous surrogate testing results to play a stronger role in informing the go / no-go down select decisions. This would enable the critical decision process to proceed more rapidly and better support the Hanford treatment mission acceleration initiative while reducing the reliance on additional hot testing. The analytical methods and approaches are detailed in the Task Plan (9). The methods to be used to generate the primary data to support the go / no-go decision in support of the down select process are summarized below from the Task Plan.

<u>Redox / Mineralogy</u>

The Reduction / Oxidation (Redox) of certain species in the FBSR process are important because at a certain Fe+2/ΣFe ratio, the oxygen fugacity in the DMR is at an appropriate level to help ensure these species are in the right oxidation states to be sequestered in the target mineral phases (6). Thus, the Redox of the mineral products will be determined to confirm that the conditions achieved during BSR processing were consistent with the target conditions including those of the pilot scale test of 2008 such that the mineral products produced in these BSR tests are representative of the 2008 testing.

The FBSR product is a mixture of sodium aluminosilicate minerals comprised of feldspathoid mineral phases such as nepheline, nosean, and sodalite (6). It is currently assumed that the contaminants of concern are distributed amongst each of these phases. Therefore, to allow for long-term predictions to accurately describe the release of key contaminants of concern for the multi-phase FBSR product, quantitative XRD will be used to determine the percentage of these phases in the FBSR sample. The types of mineral phases found to be present should align with prior testing with simulant work in order to provide confidence that the radioactive product will exhibit a similar behavior relative to the durability response. Redox and mineralogy data are considered as required inputs for the go / no-go evaluation process from the three tests as indicated in Table 2, SRS LAW and the first two Hanford LAW tests.

Toxicity Characteristic Leaching Procedure (TCLP) Method 1311

The TCLP will assess the release of RCRA metals from the granular BSR product. For the purposes of this paper, the emphasis will be on the TCLP results of the granular product even though TCLP testing will be conducted on both the granular and monolithic products. This EPA approved procedure is designed to determine the mobility of both organic and inorganic analytes present in liquid, solid, and multiphase wastes. The main purpose for the use of this procedure is to determine whether the FBSR waste form will meet the requirements of the Resource Conservation and Recovery Act (RCRA) Land Disposal Restrictions (LDR) since Hanford tank wastes contain hazardous constituents. Initially[b] the focus of the TCLP analyses will be on inorganic contaminants, because steam reformation effectively destroys organic materials. TCLP data for the granular products are sought as inputs to the go / no-go evaluation process, primarily from Tests #s 2 and 3 (SRS LAW and the first Hanford LAW test).

Mass Balance

Determining the disposition of key contaminants within a treatment process is a critical consideration for any technology selection process. Previous FBSR engineering-scale tests with LAW stimulants have produced results indicating that >99.99% of the nonradioactive surrogates for ^{99}Tc and ^{137}Cs and >94% of the ^{129}I were captured in the mineral product (5) and not released to the off-gas treatment system. For the series of radioactive BSR tests that will be conducted, mass balance data will be obtained for ^{99}Tc, ^{129}I and rhenium. This will include analyzing the granular product, liquid condensate, off-gas filters, and rinse solutions from the post-test cleanout of the BSR apparatus.

Although mass balance does not directly relate to waste form performance, confirming the fate of Tc, Re and I from the actual waste tests is important to confirm prior data from tests with simulants. Reproducible mass balance results add confidence that the key contaminants of concern can be accurately accounted for within the limits of measurement accuracy and detection limits. Mass balance targets for previous demonstrations were to close within +/-10% for major constituents and +/- 30% for minor constituents (5). Tc, Re, I will all be present at levels considered minor constituents. Mass balance results from Tests 2, 3, and 4 will be used to inform the go / no-go evaluation process.

Product Consistency Test

The PCT will be conducted on granular mineral samples following the procedures described in ASTM C 1285-02. The PCTs will be performed at 90 degrees centigrade for seven days. After completion of the PCT, the leachate will be analyzed and the concentration of ions in the leachate will be measured by inductively coupled plasma-atomic emission spectroscopy (ICP-AES) and inductively coupled plasma-mass

[b] *If FBSR is selected during the down select process, more rigorous RCRA testing will be conducted at a larger scale at a later time to support a Determination of Equivalent Treatment and (if required) a Treatability Variance in accordance with the Waste Form Qualification Program Plan (2).*

spectroscopy (ICP-MS). All tests will be conducted in triplicate (at a minimum) and the results will be averaged. The normalized elemental mass release will be calculated as g/m^2 after adjustment for moisture and unreacted carbon content. Data from Tests 2 and 3 will be compared with PCT results from prior simulant tests (to ensure reasonable correlation of results) and to inform the go / no-go evaluation process.

Speciation

Although it has been scientifically inferred that certain key radionuclides, such as technetium, are contained in the cage structure of specific mineral phases that make up the NAS waste form, this needs to be demonstrated through testing and analysis if DOE intends to take credit for this property of the material in its risk analyses. To gain scientific credibility that this will in fact occur, a series of X-ray absorption spectroscopy (XAS) analyses will be conducted on sub-samples of radioactive granular and monolith BSR product to determine the ^{99}Tc oxidation state and nearest neighbors. Although XAS will be used as a primary technique to determine ^{99}Tc speciation, a set of secondary analysis techniques will also be used. These include SEM-EDS, TEM EDS, and if necessary, micro-XRD, XPS, and electron microprobe analyses. These analyses will aide in providing the technical justification for assuming all or a percentage of ^{99}Tc will be trapped within sodalite and/or nosean "cages" which will make it more resistant to release to groundwater. Even though other testing may demonstrate that the durability and leaching performance of the monolithic mineralized waste form will meet all relevant regulatory requirements based on performance assessment analyses that will be performed at a later time, ascertaining the location of key radionuclides within the waste matrix would add confidence that waste form performance will be satisfactory over the long-term. The FBSR process could still be included in the down select process if the results of this speciation analysis are ambiguous or reveal an unexpected result, for example, if ^{99}Tc is stabilized outside the cage but in a stable, low solubility state such that there is confidence in the long term performance such that the waste form will likely satisfy IDF requirements. Speciation results from two tests, SRS LAW and the first Hanford LAW, will be factored in to the go / no-go evaluation process.

Emphasis on Granular Product vs. Monolith Data

With respect to waste form, granular product data rather than final monolith waste form data will be a primary input for the go / no-go evaluation. This approach allows for a comparison of the performance with granular product data from prior simulant tests which represents a larger data set. This type of approach also doesn't necessarily attribute any enhanced performance that is expected from the monolithic waste form. Monolithing of the granular product will be necessary to satisfy the IDF requirements for compressibility. A monolithic form should improve the overall performance of the FBSR waste form since the binder matrix will reduce the total surface area of the product available to be in contact with water. The monolith is intended to address the intruder scenario but it may also add an additional layer of protection by reducing the total surface area of the product and potentially acting as a diffusion barrier. An assumption that will be confirmed through testing is the binder matrix will not degrade the performance of the FBSR granular product.

If it is determined that the FBSR process can reliably produce granular products from actual waste that exhibit a durability and leach resistance performance similar to those from previous tests with LAW simulants such as the performance described by McGrail (7) or Pierce (15) then there would be minimal risk in including FBSR in the down select process, and if selected, moving forward to develop a Conceptual Design for FBSR. Various studies have established that the NAS granular waste form performs as good as or better than LAW glass within limits of uncertainty. For example, Pierce (15) reported that LAW glass (LAWAN102) was dissolving approximately 11 times faster than an FBSR product (but cautioned that the uncertainty in the reactive surface area for the FBSR product complicated

the interpretation of a direct comparison between the ^{99}Tc release rate from glass and the rate of Re release from the FBSR product). McGrail (7) concluded that fractional release rates of the FBSR granular waste form (based on rhenium as a surrogate for Tc) calculated from Pressurized Unsaturated Flow (PUF) test experiments with the FBSR granular product showed essentially identical performance with a reference LAW glass (LAWA44) tested under the same conditions. Should the granular product exhibit characteristics (similar mineralogy, similar short term PCT response) that are consistent with the products studied by Pierce and or McGrail, then this will give a high degree of confidence that the FBSR process can generate a granular product that can satisfy the performance requirements for the treatment of Hanford LAW.

The choice of the binder and its particular formulation, and thus its performance with the granular product, is considered secondary to the basic FBSR process and therefore represents relatively little technical risk relative to the down select process.

References

1. *ORP-11242, River Protection Project System Plan, Rev. 4, US Department of Energy, Office of River Protection, Richland, Washington*

2. *Westsik, JH, Jr., RJ Serne, SV Mattigod, RP Pires. 2010. Fluidized Bed Steam Reforming Waste Form Qualification Program Plan. PNNL-16914 Limited Distribution. Pacific Northwest National Laboratory, Richland, WA.*

3. *Advice on the Department of Energy's Cleanup Technology Roadmap: Gaps and Bridges. National Research Council of the National Academies. Washington DC.*

4. *2009 Pilot Scale Fluidized Bed Steam Reforming Testing Using the THOR® (THermal Organic Reduction) Process: Analytical Results for Tank 48H Organic Destruction. M. R. Williams, et al. Savannah River National Laboratory. Aiken, South Carolina*

5. *Olsen, et al. 2009. Report for Treating Hanford LAW and WTP SW Simulants: Pilot Plant Mineralizing Flowsheet, RT-21-002, Rev. 1, THOR Treatment Technologies, Denver, CO*

6. *C.M. Jantzen, Mineralization of Radioactive Wastes by Fluidized Bed Stream Reforming (FBSR): Comparisons to Vitreous Waste Forms, and Pertinent Durability Testing, WSRC-STI-2008-00268, 2008*

7. *B.P. McGrail, J.L. Steele, E.M. Pierce, A.T. Owen, H.T. Schaef, D.M. Wellman, and E.A. Rodriguez. 2003. Laboratory Testing of Bulk Vitrified and Steam Reformed Low-Activity Waste Forms to Support a Preliminary Risk Assessment for an Integrated Disposal Facility, PNNL-14414, Pacific Northwest National Laboratory, Richland, WA*

8. *P. R. Burket et al. Bench-Scale Steam Reforming of Actual Tank 48H Waste. SRNS-STI-2008-00105, Revision 0. Savannah River National Laboratory, Aiken, South Carolina*

9. *DOE EM-31 Technology Development & Deployment (TDD) Program Task Plan: Fluidized Bed Steam Reformer Low Level Waste Form Qualification, Document WP-5.2.1-2010-001, Revision 0.0. September 2010. US Department of Energy, Office of Environmental Management, Technology Innovation & Development. Washington DC.*

10. *S.D. Rassat, L.A. Mahoney, R.L. Russell, et al., Cold Dissolved Saltcake Waste Simulant Development, Preparation, and Analysis, Pacific Northwest National Laboratory, PNNL-14194, 2003.*

11. *C.M. Jantzen. Fluidized Bed Steam Reformer (FBSR) Monolith Formation. 2010. Savannah River National Laboratory. Aiken, SC*

12. *Sample Selection Recommendations for Fluid Bed Steam Reforming Treatability Studies Using Hanford Low Activity Waste Underground Storage Tank Samples. RPP-RPT-47143. 2010. Washington River Protection Solutions. Richland, Washington*

13. *D.L. Banning. Data Quality Objectives for Selecting Waste Samples for the Bench Steam Reformer Test. RPP-47073. 2010. Washington River Protection Solutions. Richland, Washington*

14. *A.L. Olson et al. Fluidized Bed Steam Reforming of Hanford LAW Using THOR Mineralizing Technology. INEEL/EXT-04-02492. 2004. Idaho National Engineering and Environmental Laboratory. Idaho Falls, Idaho.*

15. *E. M. Pierce. Accelerated Weathering of Fluidized Bed Steam Reformation Material Under Hydraulically Unsaturated Conditions, Materials Science and Technology 2007, September 16 – 20, 2007, Detroit, Michigan"*

Appendix D. Laboratory Test Methods

Modified from Reference 1 (Appendix C in Reference 1) where more details and error analyses can be found.

Laboratory test methods must be focused on identifying key processes and quantifying the parameters that represent the processes to support calculations and simulations of waste form performance. In other words, useful test methods must identify the key mechanisms that affect performance and quantify these processes in a way that allows for an overall model to be developed that accurately estimates contaminant release. Three general classes of tests that serve as the foundation for this technical strategy are (1) characterization, (2) accelerated, and (3) service condition [2]

D1. CHARACTERIZATION TESTS

Characterization tests are used to isolate and provide specific information on processes or to parameterize theoretical models (commonly referred to as sub-continuum models). Test conditions are usually very different from expected service conditions of the disposal system environment to evaluate a particular process or mechanism while minimizing or holding constant other effects. In other words, the goal of characterization tests is to isolate the effect of a specific mechanism, such as Si–O–Al hydrolysis, with the intent to identify the dominant processes that control weathering. Examples of such characterization tests include measuring basic material properties, such as the hydrolysis reaction, as functions of pH or solution composition. The characterization test methods discussed in this section include monolith immersion test (MCC-1 ASTM C1220) (Figure C.1), (PCT-A ASTM C1285), Soxhlet, and SPFT (ASTM 1662) experiments, with the product consistency test (PCT) PCT-A and the SPFT method being proposed in this document as the primary approach for making these types of measurements.

D1.1 MONOLITH IMMERSION TEST (ASTM C1220)

The monolith immersion test method is based on the Materials Characterization Center (MCC) test method number one (MCC-1) [3,4]. This is a static leach test method (Figure D - 1) that uses a monolithic specimen to compare the durabilities of candidate waste forms developed to stabilize HLW. The method calls for placing a monolithic specimen of known geometric surface area into a volume of solution such that the surface area-to-volume ratio (S/V) is 10 m^{-1}. The MCC-1 test is typically performed with demineralized water, a reference silicate solution, or a reference brine. The reference temperature and time are 90°C and 28 days, although temperatures of 40 or 70°C and other durations can be used.[††] The MCC-1 test typically provides a solution-dominated system in that the leachate remains dilute as the glass dissolves. However, tests conducted for long time periods may be affected by changes in solution chemistry. Samples corroded in MCC-1 tests show details of the chemical and physical alteration of the mineral and glass surface and have provided insight into mechanisms controlling the initial stages of corrosion.[5,6]

While the MCC-1 method was originally designed to compare the relative chemical durabilities of candidate waste forms, the test can be used to characterize several aspects of the corrosion process in conjunction with a corrosion mechanism. Short-term MCC-1 tests provide a simple means of measuring the waste form corrosion rate under dilute conditions. Tests have been performed in buffer solutions or solutions spiked with various glass components to determine the effects of the leachate chemistry on the corrosion rate [7]. Longer-term MCC-1 tests can be run to monitor the alteration of the waste form surface during corrosion to investigate the corrosion mechanism [5,8]. However, because determining the effects of solution composition and identifying the dominant corrosion mechanism is more appropriately evaluated with the SPFT method, there is no compelling need to include MCC-1 tests in the testing strategy for FBSR NAS waste form.

[††] The MCC-2 test procedure is a variation of the MCC-1 procedure that permits reaction temperatures of 110, 150, and 190°C.

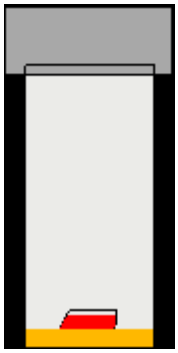

Figure D - 1. Monolith Immersion Test

D1.2 MCC-3 SOLUBILITY TEST

The MCC-3 test was designed to measure the maximum solubility of a waste form in the solution of interest. [3,9] This test method formed the basis for the PCT (Figure D - 2). The MCC-3 tests were to be conducted until the resulting solution composition did not vary with increased reaction time (i.e., until the glass ―saturated‖ the solution). However, when applying the test method Shade and Strachan [10] showed that (1) constant solution compositions were not achieved within a few weeks, and (2) the solution composition depended on the particle size of the waste form used. The first observation is a direct result of the waste form reactivity, while the second observation is from the different S/V that results from the different total surface areas of different sieve fractions. Tests conducted at higher S/V usually generate more concentrated solutions. The MCC-3 procedure was subsequently modified so that (1) a single size fraction is specified and (2) the test vessel is continuously agitated during the test, usually by placing it on a roller. The PCT (ASTM C1285) has effectively replaced the MCC-3 test in most laboratories, although all of the complications associated with the use of crushed material found during development of the MCC-3 tests are common to the PCT procedure, the MCC-3 test did not wash adherent fines off of the particles and did not control the particle size in the stringent manner that is done in the PCT. In addition, during MCC-3 testing the samples were constantly rotated which created impingement of particles upon each other and created varying size particles due to these collisions. The constant agitation in the MCC-3 protocol was therefore removed in the PCT procedure.

D1.3 PRODUCT CONSISTENCY TEST A (ASTM C1285, Reference 11)

The PCT method is a water-saturated and static (closed-system) test, based on the MCC test method number three (MCC-3). The PCT Method A was developed specifically for verifying process control of vitrified HLW forms and is conducted with specific test conditions: −100 +200 mesh size fraction material; demineralized water; and a solid/solution mass ratio of 1/10, 90°C, and 7 days. The approach can be represented in terms of linking several relationships [12]:

process control ↔ composition control ↔ dissolution rate control ↔ performance control ↔ acceptable performance

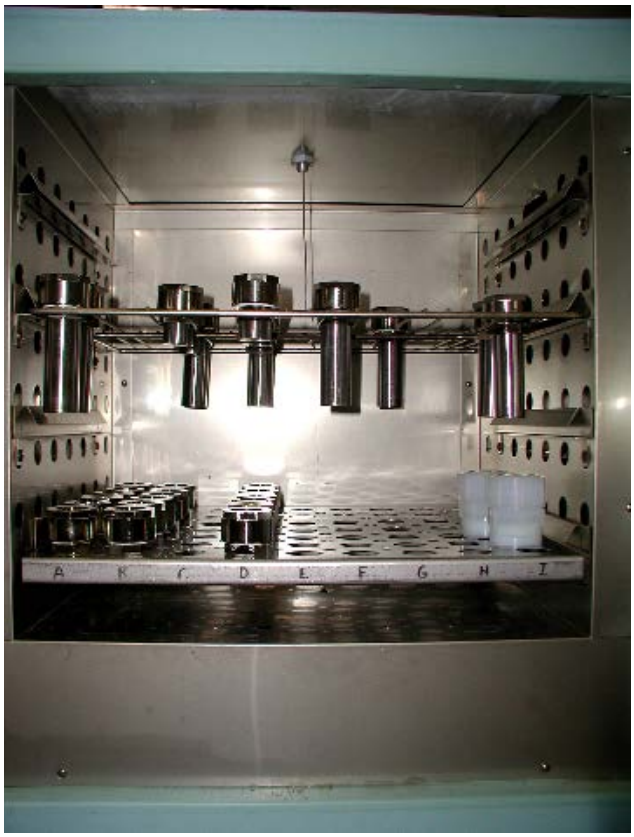

Forced-air circulation Blue M Oven with numerous 304L stainless steel and two Teflon vessels. Note that the Teflon vessels have white crushed glass in the bottom of the containers and that special racks are used to allow the forced air to circulate around the leach vessels to maintain the vessel and its contents at constant temperature.

Figure D - 2. Schematic of PCT

It is conducted by immersing a specimen of crushed waste form in a volume of leachant at a known S/V. The mass and size fraction of the crushed material in the test is known and used to estimate the surface area. The test vessel is sealed and placed in a constant-temperature oven for a prescribed duration. The solution concentrations of components of interest are measured at the end of the test. The tests are usually conducted in demineralized water but can be conducted with synthetic or actual groundwater.

For the PCT-A and PCT-B tests, the releases from the waste form can be calculated as the concentration in normalized units NC_i or $log[NC_i]$ for all waste forms including multiphase waste forms wherein the concentrations in g/L are normalized by the weight fraction of that element present in the entire waste form. This provides an estimate of the total mass of material that goes into solution. Normalization is based on the entire waste form rather than the particular phase containing it because the value of NC_i is used to represent the entire waste form. Normalization to the waste form composition allows for direct comparison of NC_i measured for different waste forms. The normalized concentration, NC_i, is a function

of (*1*) the mass fraction of the element of interest, *i* ,in the glass and (*2*) the concentration of element *i* in solution.[‡‡] The normalized concentration for each replicate is expressed as:

Equation 1

$$NC_i = \frac{C_i(sample)}{f_i}$$

where:

NC_i	=	normalized concentration, $g_{waste\ form}/L_{leachant}$,
$C_i(sample)$	=	concentration of element "*i*" in the solution from test with waste form, g_i/L, and
f_i	=	mass fraction of element "*i*" in the unleached waste form (g_i/g_{glass}).

The units of NC_i for PCT-A are normally expressed as grams of glass waste form dissolved per liter of leachant when all of the tests are performed at the reference volume of leachant (V_{soln}) to sample mass (m_{solid}) ratio, for example, $V_{soln}/m_{solid} = 10 \pm 0.5$ cm^3/g, and with the 100 to 200 mesh reference particle size (see Appendix X1 in ASTM C1285). Use of the reference conditions maintains the waste form surface area (*A*) to volume of leachant (*V*) at a constant for waste forms with the same density. As long as the glass waste form density and glass waste form particle size remain the same between leach tests, this parameter will remain a constant and need not be calculated every time.

Normalization of the concentration to the surface area of the waste form used in the test allows for comparison of tests conducted at different SA/V ratios with materials having different densities, and test samples of different size fractions. For comparing the results of these tests the geometric surface area is calculated by modeling the particles as spheres having a diameter equal to the arithmetic average of the sieve mesh sizes. The specific surface area of a sphere having a particular diameter is calculated as

Equation 2

$$SA_{sp} = \frac{6}{\rho d}$$

and the surface area is calculated as the product of the mass used in the test and the specific surface area of the material as

$$SA = \frac{6\,mass}{\rho d}$$

where:

ρ	=	density in g/cm^3
d	=	particle size diameter in cm
mass	=	mass in g
SA	=	surface area in cm^2
SA_{sp}	=	specific surface area in g/cm^2

The average diameter for particles in the -100 +200 mesh size fraction is 112.5 μm.

[‡‡]At the dilute solute concentrations utilized in this report, a 1 kg of solution is considered equivalent to 1 L of solution and so ppm and mg/L can be used interchangeably.

A normalized elemental mass loss, NL_i, can be calculated when the particle size, *or the* V_{soln}/m_{solid}, are varied between tests, or for test results on waste forms of different density. The following expression may be used to calculate NL_i:

Equation 3 $$NL_i = \frac{c_i(sample)}{(f_i) \bullet (SA/V)} \quad \textbf{or} \quad NL_i = \frac{NC_i}{SA/V}$$

where:

NL_i	=	normalized elemental mass loss, $g_{waste\ form}/\ m^2$,
$c_i(sample)$	=	concentration of element "*i*" in the solution, g_i/L,
f_i	=	mass fraction of element "*i*" in the unleached waste form (g_i/g_{glass}),
SA/V	=	surface area divided by the leachate volume, m^2/L

NL_i represents the total mass of glass dissolved over the test interval presuming all components dissolve congruently with element i and the surface area remains constant as the glass dissolves.

D1.4 PERIODIC REPLENISHMENT TESTS

Several test methods have been developed in which a leachate solution is periodically removed from an ongoing static test and replaced with an equal volume of fresh solution (Figure D - 3). Such replacement tests have been used to simulate very low flow rates that cannot be attained with mechanical pumps. [13,14] This test method was used by Tole et al. [15] to evaluate single-crystal nepheline dissolution. Either monolithic or crushed samples can be used, and different starting solution compositions can be used. Specific test methods have different replacement schedules and replace different fractions of the total solution volume. For example, the test designated by the International Standardization Organization (ISO) calls for replacing the entire solution volume daily for the first week, every week for 8 weeks, monthly for 6 months, and twice yearly thereafter [16] but the Nuclear Regulatory Commission (NRC) prefers more frequent exchanges so that forward diffusion is measured in the absence of back reactions.[17] Recent experiments at Argonne National Laboratory (ANL) have indicated that the frequent and constant exchanges are necessary throughout the duration of the experiment or the curvature of the diffusion equation changes with time.[18]

The American Nuclear Society test method ANSI 16.1 and variations of the ANSI 16.1, such as the Dynamic Leach Test (DLT), ASTM C1308 (previously known as the Accelerated Leach Test, ALT), and EPA 1315, are similar total volume exchange tests. They differ primarily in the replacement schedules (Figure D - 4). These tests were developed to characterize materials from which contaminants are assumed, a priori, to be released by a diffusion-controlled process, such as grouts and cements. Because monoliths may be the final form of the FBSR granular product, periodic replenishment tests were performed to obtain key information on elemental release via diffusion.

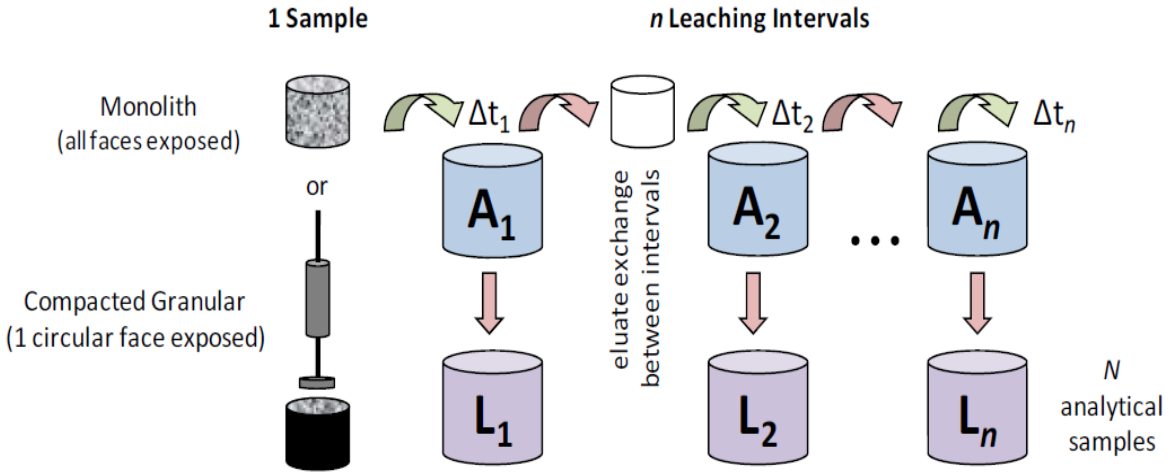

Figure D - 3. Schematic of the Semi-dynamic ASTM C1308/ANSI 16.1/EPA 1315 Monolith Leach Tests

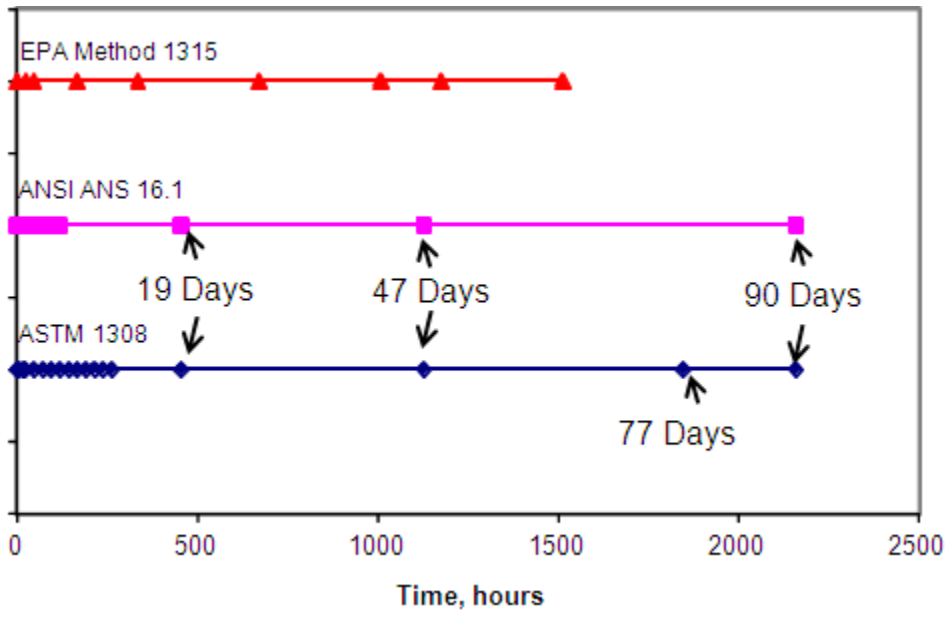

Figure D - 4. Leach exchange intervals for ANSI/ANS 16.1 versus ASTM C1308 versus EPA 1315

Table D - 1. Comparison of Leach Exchange Intervals for ANSI/ANS 16.1, ASTM C1308, and EPA 1315

Cumulative Time ANSI/ANS 16.1		Cumulative Time ASTM 1308 [19]		Cumulative Time EPA 1315		Cumulative Time This Study	
Hours	**Days**	**Hours**	**Days**	**Hours**	**Days**	**Hours**	**Days**
2	0.083	2	0.083	2	0.083	2	0.0833
		5	0.208333			5	0.208
7	0.291667						
		17	0.708333			17	0.708
24	1	24	1	25	1.04	24	1
48	2	48	2	48	2	48	2
72	3	72	3			72	3
96	4	96	4			96	4
120	5	120	5			120	5
		144	6			144	6
		168	7	168	7	168	7
		192	8			192	8
		216	9			216	9
		240	10			240	10
		264	11			264	11
				336	14		
456	19	456	19			456	19
				672	28		
				1008	42		
1128	47	1128	47				
				1176	49	1176	47/49
				1512	63		
		1848	77			1848/1896	77
2160	90	2160	90			2160/2184	90/91
2880	120					2568	107

The observed diffusivity for each constituent is calculated using the analytical solution shown below, for simple radial diffusion from a cylinder into an infinite bath as presented by Crank. [20]

Equation 4

$$D_i = \pi \left[\frac{M_{t_i}}{2\rho C_0 (\sqrt{t_i} - \sqrt{t_{i-1}})} \right]^2$$

where

D_i	=	observed diffusivity of a specific constituent for leaching interval, *i* [m^2/s]
i	=	Leaching interval
M_{ti}	=	mass released during leaching interval *i* [mg/m^2]
t_i	=	cumulative contact time after leaching interval, *i*[s]
t_{i-1}	=	cumulative contact time after leaching interval, *i-1*[s]
C_o	=	initial leachable content [mg/Kg-dry]
ρ	=	sample density [kg-dry/m^3].

The mean observed diffusivity for each constituent can be determined by taking the average of the interval-observed diffusivity with the standard deviation.

The leach index (LI), the parameter derived directly from immersion test results, evaluates diffusion-controlled contaminant release with respect to time. The LI is used as a criterion to assess whether solidified/stabilized waste will likely be acceptable for subsurface land disposal. In most cases, the solidified waste is considered effectively treated when the LI value is equal to or greater than 9. The LI is calculated from the D_i above with the following equation:

Equation 5 $$LI = -\log [D_n / cm^2/s]$$

where:

LI	=	leach index
D_n	=	effective diffusivity for the elements of interest (cm^2/s) during the leach interval n

D1.5 SINGLE-PASS FLOW-THROUGH TEST METHODS (ASTM 1662 Reference 21)

The SPFT test is an open system test in which a solution at a known flow rate and constant temperature flows through a reaction cell that contains the sample. The configuration precludes recirculation of a portion of the effluent and so makes a - single-pass through the reaction cell. Many different SPFT apparatuses have been developed, but these can all be classified as three basic types: (1) well-mixed batch reactor, (2) packed bed reactor, and (3) fluidized bed reactors. The advantages and disadvantages of each design are discussed in Reference 1. Only the well-mixed batch reactor (ASTM C1662) will be discussed below.

The experimental system pumps a continuous flow of fresh influent solution, which serves to (1) prevent the buildup of reaction products, (2) maintain the bulk solution composition nearly constant throughout the duration of an experiment, (3) allow an investigator to more directly quantify the dissolution rate rather than fit a curve to a presumed reaction mechanism, and (4) allow for the study of the element release data from test materials over a wide range of experimental conditions. Therefore, by design, the SPFT method minimizes the progressive accumulation of reaction products that would affect element release rates, and the setup can be varied to retrieve rate parameters that will yield a mathematical description of the dissolution process. Alternative SPFT system setups have been used to monitor the formation of alteration layers on mineral and glass surfaces and are discussed in Reference 1 as well.

D1.5.1 Well-Mixed Batch Reactor

Figure D - 5 shows a schematic of a typical batch flow-through cell. The batch flow-through cell has been extensively described by others [22,23,24,25,26,27] and the reader should consult these references as well as the references contained therein for more detail. Fluid and, optionally, a gas or gas mixture is pumped into the cell. Fluid exits the cell and is collected in a separate container for later chemical analysis. Mixing is accomplished by convection from the solution flow and (optionally) gas flow into the reactor. Some researchers have used a mechanical stirrer as well. The key advantages to this type of reactor include the ability to use powdered or monolithic samples, use and control a gas or gas mixture during the test, and eliminate the need to control bubble formation in the fluid inlet, as is necessary with a packed-bed reactor (see below). The only disadvantage to a batch flow-through cell is the need to verify that with powdered samples, sufficient mixing occurs to prevent agglomeration of the particles or formation of a stagnant solution around the sample.

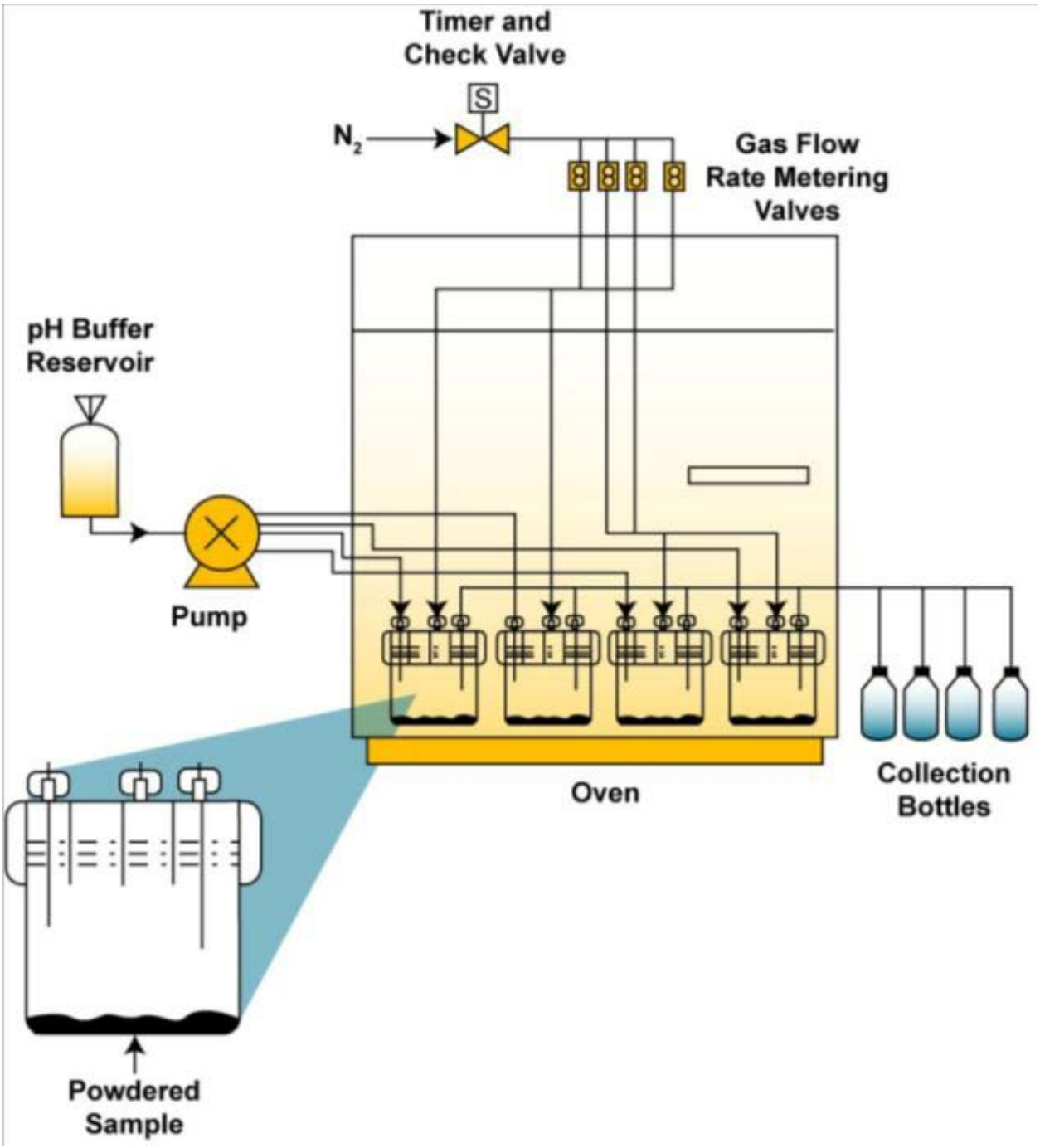

Figure D - 5. Schematic of the SPFT System Batch Flow-Through Reactor

D1.5.2 Quantification of dissolution rate and uncertainties

The SPFT test is used to measure the dissolution rate of a homogeneous silicate glass, including nuclear waste glasses, in various test solutions at temperatures less than 100°C. Tests may be conducted under conditions in which the effects from dissolved species on the dissolution rate are minimized to measure the forward dissolution rate at specific values of temperature and pH, or to measure the dependence of the dissolution rate on the concentrations of various solute species. Tests are conducted by pumping

solutions in either a continuous or pulsed flow mode through a reaction cell that contains the test specimen. Tests must be conducted at several solution flow rates to evaluate the effect of the flow rate on the glass dissolution rate. Tests may be conducted with demineralized water, pH buffer solutions, simulated groundwater solutions or actual groundwaters. Data from these tests can be used to determine the values of kinetic model parameters needed to calculate the glass corrosion behavior in a disposal system over long periods of time (see ASTM C1174). It should also be noted that the SPFT test originated for the geologic study of the degradation of single phase minerals in nature [28,29,30] and is now being applied to glass waste forms.

The intrinsic rate constant can be calculated using the forward glass dissolution rates measured at various temperatures and pH values in a mechanistic rate expression such as:

Equation 6

$$rate = k_0 \bullet 10^{\eta pH} \bullet \exp\left(\frac{-E_a}{RT}\right) \bullet \left(1 - \frac{Q}{K}\right)$$

where:

k_0	=	intrinsic rate constant
η	=	the pH dependence
E_a	=	the activation energy
R	=	gas constant
T	=	absolute temperature
Q/K	=	saturation index

The values of η and E_a are determined by regressing data in a plot of log rate versus pH at the various temperatures, if it is assumed that η is independent of temperature and the value of E_a is independent of pH.

The forward glass dissolution rates measured at various temperatures and pH values can be evaluated from the raw data as follows. Dissolution rates, based on steady-state concentrations of elements in the effluent, are normalized to the amount of the element present in the sample by Equation 7.

Equation 7

$$r_i = \frac{(c_i^{out} - c_i^{in}) \cdot q}{f_i \cdot S}$$

where:

r_i	=	the normalized dissolution rate for the i^{th} element [g/(m^2 d)]
c_i^{out}	=	the concentration of element *i* in the effluent (g/m^3)
c_i^{in}	=	the elemental concentration of the influent (g/m^3)
q	=	the flow rate (m^3/s)
f_i	=	the mass fraction of the element in the original material (dimensionless)
S	=	the surface area of the sample (m^2)

The value of *fi* can be calculated from the chemical composition of the sample. However, if a hydrous material is being compared to an anhydrous material the compositions should be compared on the anhydrous basis using an f_i that has been adjusted for the water content of the hydrous material. Flow-

through rates are determined by gravimetric analysis of the fluid collected in each effluent collection vessel upon sampling. The background concentration of the element of interest is determined, as previously discussed, by analyses of the starting input solution and the three blank solutions. Typically, background concentrations of elements are below their respective detection threshold. The detection threshold of any element is defined here as the lowest calibration standard that can be determined reproducibly during an analytical run within 10%. In cases where the analyte is below the detection threshold, the background concentration of the element is set at the value of ½ the detection threshold.

The waste form surface area in ASTM 1662 is recommended to be the geometric surface area for glass waste forms. If a crushed sample is used instead of a monolithic sample, the sample is prepared in the same manner as for PCT analysis, e.g. washed of adhering fines and sieved to -100 and +200 mesh. The recommended elements to be monitored are matrix elements such as aluminum, boron, and silicon rather than alkali metals, as the release rate desired is that of the matrix dissolution.

In order to develop the data needed for Equation 20 one must perform dissolutions at a variety of flow rates, several different constant pH values, and several different temperatures. The constant pH values are achieved by performing the dissolution (glass or mineral) in a variety of pH buffer solutions. The procedure cautions that "buffers should be selected to avoid strong complexants and solutes known to affect the dissolution rate." The buffer solutions recommended in ASTM C1662 are given in Table D - 2, as well as those recently used for SPFT of FBSR product. It should be noted that the buffers used for the SPFT of the FBSR product include oxidizers such as nitric acid, which may alter the dissolution rate of the FBSR products produced under reducing conditions.

Table D - 2. Composition of pH Buffers Used in Various SPFT Tests

ASTM C1662 + McGrail for Na-Ca-Al-B-Si LAW Glass [25]	
Buffer Composition	pH at 90°C
0.005m Potassium hydrogen phthalate + 0.004m LiOH	5.89
0.005m H_3BO_3 + 0.0003m LiOH	7.62
0.005m H_3BO_3 + 0.0020m LiOH	8.59
0.005m H_3BO_3 + 0.0044m LiOH	9.25
0.004m LiCl + 0.001m LiOH	9.39
0.005m LiCl + 0.0107m LiOH	10.39
FBSR Leaching by McGrail [31**] & Lorier [**32,33,34**]**	
0.01m TRIS* + 0.0093 HNO_3	5.50
0.01m TRIS* + 0.0059 HNO_3	6.52
0.05m TRIS* + 0.0079 HNO_3	7.42
0.05m TRIS*	8.52
0.01m LiCl + 0.0107 LiOH	10.12

*TRIS = tris (hydroxymethyl) aminomethane

D1.6 ACCELERATED WEATHERING TESTS

Accelerated tests are used to investigate corrosion behavior that will be important over the regulated service life of a disposal system within a laboratory time frame of a few years or less. Therefore, it is important to know likely site conditions over long times to determine what aspects of the waste form corrosion process need to be considered in the performance assessment (PA). Elevated temperatures and a high S/V are often used to accelerate the reactions and processes occurring during waste form corrosion and, in some cases, lead to enhanced dissolution. It is important to verify that the technique used to

accelerate a reaction or process does not cause a change in the rate-limiting step or mechanism of the process, or if it does, that the change is taken into account. For example, water diffusion, ion exchange, and hydrolysis will be affected to a different degree by changes in the temperature, and the overall temperature dependence of glass corrosion will include contributions from all three processes, although it may be dominated by one process under particular test conditions.

Accelerated test methods that will be used to study the advanced stages of FBSR NAS granular product weathering include the PCT Method B (PCT-B Reference 11) and the pressurized unsaturated flow (PUF) test. Tests will be conducted over a range of conditions to link the dissolution behavior expected to occur in the disposal system with those observed under accelerated test conditions. These tests are also used to provide some indication of the alteration phases expected to form during FBSR NAS granular product weathering.

D1.7 PRODUCT CONSISTENCY TEST-B

Unlike PCT–A, which is conducted under specific test conditions, in PCT–B, the values of the test parameters are not specified. In this water-saturated static (closed-system) test, the reaction products are allowed to accumulate in the aqueous phase, thus altering the solution chemistry in contact with the material. Although information on the solution chemistry is obtained, the changes to the solution chemistry measured in this closed-system test may not be representative of the solution chemistry that is expected in an open-system repository, such as the Integrated Disposal Facility (IDF). For example, PUF test results with LD6-5412 and LAWA33 glasses suggest that in the PUF test, the aging processes are accelerated by as much as 50 times compared with the PCT method run at the same temperature [35]. This observed acceleration in the aging process is probably the result of the differences in the glass–water reaction rate and the solution chemistry, and the rate of alteration phase formation in the PUF test compared with PCT-B.

Because the PCTs are conducted under conditions that are not consistent with the expected disposal system conditions, the results are sensitive to the buildup of waste form components into the solution. This buildup of components provides the best opportunity to calibrate the supporting geochemical data that are required for modeling the dynamic evolution in solution chemistry that occurs as a consequence of glass–water reactions. The term calibration in this context refers to a complex iterative process whereby the evolution in solution composition and secondary phase formation observed in PCT-B experiments is reproduced, with a reasonable level of uncertainty, in modeling the geochemical evolution of the system. The modeling process is complex because during PCT-B tests, changes in the concentrations of dissolved components, the solution pH, and, in some cases, dissolved air components must be modeled simultaneously. Fortunately, the geochemical simulator selected for modeling this system, the EQ3/6 code [36] and/or Geochemist Workbench® [37], both have the capability to handle these complexities.

The calibration process requires, among other things, estimating solubility product values for secondary minerals that are identified in the PCTs, but for which thermodynamic data are not available. These values can be generated by fitting to the PCT data or by using empirical methods, such as a polymer model [38]. However, if a particular phase is found to have an important effect on long-term waste form or mineral corrosion rates, then it is recommended that independent measurements of its solubility product and the kinetics of precipitation and dissolution be performed. Once the geochemical model has been calibrated against the PCT data, the significant aqueous speciation and dissolution-precipitation reactions in the model can be identified. This reaction set and supporting thermodynamic data then make up the reaction network that is used in the reactive transport model to compute radionuclide release from the disposal system [39].

D1.8 PRESSURIZED UNSATURATED FLOW TEST METHOD (References 40,41)

The PUF apparatus (Figure D - 6) allows for accelerated weathering experiments to be conducted under hydraulically unsaturated conditions, thereby mimicking the open-flow-and-transport properties of the disposal system environment while allowing the reacting mineral assemblages to achieve their final weathering state. The final reaction state is reached during long-term weathering that consists of the formation of secondary phases, while the other mechanisms (e.g., network hydrolysis, ion exchange, and network dissolution) occur simultaneously. The PUF apparatus provides the capability to vary the volumetric water content from saturation to 20% or less, minimize the flow rate to increase liquid residence time, and operate at a maximum temperature of 99°C. The PUF column operates under a hydraulically unsaturated condition by (1) creating a steady-state vertical water flow while maintaining uniform water content throughout the column, (2) using gravity to assist in drainage, and (3) maintaining a constant pressure throughout the column. Constant pressure is maintained with a porous Ti plate and gas pressure.

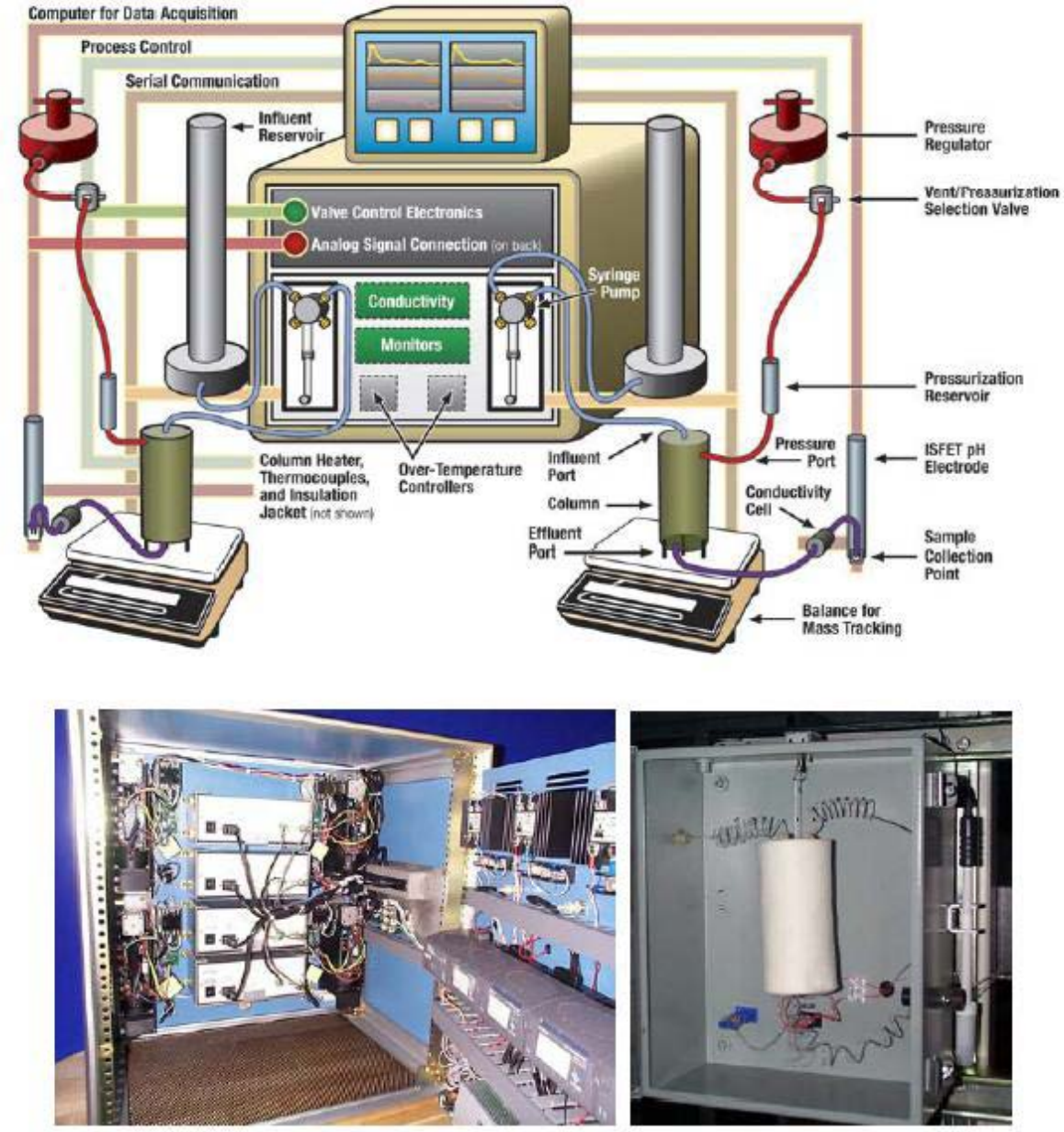

Figure D - 6. Top: Schematic of the second generation PUF Apparatus that has the capability to conduct two simultaneous tests. Bottom left: the third generation PUF apparatus, which has the capability to conduct four simultaneous tests. Bottom right: the PUF box (grey box), insulation wrapped column (center of the box), strain gauge (center of the box above the column), pressure/PUF port Teflon line (top left of the column), influent solution Teflon line (top right of the column), effluent solution Teflon line (bottom of the column), thermocouples (type J [blue connector] and type T [black connector] shown inside the box with black/red wire), pH probe (outside the box shown in white), and collection vial (outside the box connected to the pH probe). The third generation PUF apparatus was used to conduct the LAWAN102 experiment discussed in this manuscript.

The PUF system and test procedure have been described previously by McGrail et al. [42,43] and Pierce et al. [44,45,46,47], so only a general description is provided here. The PUF system contains a 7.62-cm-long and 1.91-cm-diameter column fabricated from a chemically inert material, polyetheretherketone (PEEK) so that dissolution reactions are not influenced by interaction with the column material. A porous Ti plate with a nominal pore size of 0.2 μm is sealed in the bottom of the column to provide an adequate pressure differential for conducting fluid while operating under unsaturated conditions [48]. Titanium is chosen because it is highly resistant to dissolution and has excellent wetting properties. Once the porous Ti plate is water saturated, water, but not air, is allowed to flow through the 0.2-μm pores as long as the applied pressure differential does not exceed the air entry relief pressure, referred to as the bubble or capillary pressure, of the Ti plate. If the pressure differential is exceeded, air will escape through the plate and compromise the capability to maintain unsaturated flow conditions in the column. The PUF test computer control system runs LabVIEW (National Instruments Corporation) software for logging test data from several thermocouples, pressure sensors, inline sensors that measure effluent pH and conductivity, and an electronic strain gauge that measures column weight to accurately track water mass balance and saturation level. The column also includes a PUF port, which is an electronically actuated valve that periodically vents the column gases. The purpose of column venting is to prevent reduction in the partial pressure of important gases—especially O_2 and CO_2—that may be consumed in a variety of chemical reactions.

D1.8.1 Release Rate and Error Calculation

As in any flow-through column experiment, the calculation of kinetic rates from the effluent composition is slightly more involved than in simpler static experiments. The PUF experimental method introduces one additional complication, in that water content is another variable that must be taken into account. A computer macro program was written to perform this calculation directly in the Excel™ spreadsheet used to store the sensor data. Typically, errors in the calculated release rate from the PUF tests range from 55% to 38%. Details of the calculations and error analysis can be found in Reference 1.

D1.9 MODEL VALIDATION EXPERIMENTS

Service condition tests are conducted to verify that the techniques used in accelerated tests do not change the alteration mechanisms. They are designed to approximate, to the extent possible in the laboratory, the physical and chemical environment of the disposal system. Because of the low temperature of the IDF disposal system and the very slow rate of moisture flow expected in the disposal facility, laboratory tests approximating these conditions are unlikely to yield meaningful data in reasonable time periods. Consequently, no specific service condition tests are proposed in this plan. Rather, the parameter values for some tests are selected so as to reflect service conditions. For example, some PUF experiments may be performed at lower temperature or with fractured monoliths instead of ground FBSR product to provide service-condition information on water flow paths and mineral alteration processes in fractures. However, the solution flow rate and the temperature adopted for these tests will likely be higher than the expected conditions. Again, the purpose of the testing program is to demonstrate a scientific understanding of the processes controlling long-term corrosion of the FBSR NAS product so that the models describing these processes can be used with confidence in extrapolating to the expected service conditions.

D1.10 SUMMARY

In summary, this section included a detailed description of each of the test methods that have been used to quantify radionuclide release from a variety of high-level, intermediate-level, and low-level waste forms (glass and ceramic [mineral-based]) by the international community. None of the test methods alone provides all of the information required to predict long-term performance. Each test method represents a

single puzzle piece that is intended to evaluate different aspects of the mineral–water or glass–water reaction (e.g., different mechanism/processes). For example, SPFT experiments are conducted under dilute conditions (low concentration of elements in solution) to monitor the effect of key environmental variables (e.g., pH, chemical affinity, and temperature) on element release. This presumes that the dominant mechanism which leads to elemental release is the result of a surface-mediated hydrolysis mechanism. In the case of the minerals contained in the FBSR matrix, this mechanism is the most plausible process and has been observed in pure phase dissolution experiments. Therefore, to accurately quantify the effect of the key variables on element release, each variable must be isolated and systematically changed. The analysis of these data provide some of the model parameters needed to estimate radionuclide release, which is expected to occur as a result of a breakdown in the structural matrix (via hydrolysis). In ASTM 1308 experiments, the buildup of elements (e.g., saturation state or chemical affinity) changes as a function of time until steady state is achieved.

Unlike SPFT, the PCT-A is a short-term test (7 days) that is designed to ensure a consistent product is produced. It provides little indication of long-term performance of a mineralized waste form. On the other hand, PCT-B is a long-term test that is designed to provide some indication of the long-term release mechanisms of a waste form. In this program we use this test to provide an indication of the alteration phases that can form during the weathering process. To accomplish alteration phase formation in a reasonable time, the weathering process must be accelerated. This acceleration process is accomplished by increasing temperature and/or changing the solid-to-solution ratio.

Similar to PCT-B, the pressurized unsaturated flow experiments are designed to provide equivalent data, but the conditions of the test most represent the open-flow and transport conditions of the IDF. One way to think of the PUF test is to consider it as a PCT-B test with flow. For example, with glass, the S/V ratio for long-term PCT experiments is typically 20,000 m^{-1} (lots of glass very little solution). A PUF test is typically an order of magnitude greater in S/V (200 000 m^{-1}) at steady state conditions when using glass waste forms. To calculate the S/V for PUF experiments, the steady state volumetric water content is used along with the steady-state surface area. The major difference is that the experiment includes water flow. The conditions of the PUF are similar to what should be expected for the Hanford Vadose Zone where the IDF will be located. The environmental situation is such that the mass of waste to volume of water is going to be large for the IDF.

The results from PCT-B and PUF experiments are commonly referred to as providing the chemical reaction network, which consists of a set of mineral phases that are expected to form via a precipitation reaction and control the steady-state concentration of elements in the pore-water of the disposal facility. It is the steady-state concentration of elements (chemical affinity effect or common-ion effect which results in a reduction in the driving potential that can cause dissolution) that can impact how fast elements are released from the waste form, so having accurate time-dependent information on this is critical for calculating accurate estimates of radionuclide release.

In this downselect and the supporting documents a combination of PCT-A, PCT-B, SPFT, PUF, and ASTM C1308 were used to provide the data required to simulate the long-term performance of the FBSR NAS waste form. The afore-mentioned standard test methods, must be augmented with a select number of solid phase characterization approaches to obtain a clear understanding of the processes involved in the element release. Although these measurements provide a large amount of detail on waste form performance mechanisms, additional data may be required to evaluate specific aspects of the weathering process in greater detail. At this stage of the data collection process, these test represent the logical step in obtain the information needed to assessment contaminant release from the FBSR waste form.

The role of FBSR durability testing is also to establish these same types of linkages for the FBSR mineral waste form products. Reference 49 has established the link between “process control ↔ composition

control". The PCT [50,51,52,53], SPFT [31,33,53,54,55] and PUF [31] tests have been performed on multiple FBSR products as documented in those references and summarized in this downselect document. The results of the SPFT and PUF tests have been used in the Hanford RA assessment [31,33] for FBSR. The FBSR mineral dissolution has been compared to glass dissolution (similar mechanisms: surface-mediated hydrolysis mechanism) to establish the remainder of these linkages, e.g. "composition control ↔ dissolution rate control ↔ performance control ↔ accepted performance".

REFERENCES

1 Pierce, E.M., "**Review of Existing Fluidized-Bed Steam Reformer Sodium Aluminosilicate Waste Form Performance Data**". ORNL/TM-2012/19, Rev. 1, Oak Ridge National Laboratory, Oak Ridge, TN (2012; 2014 in revision).

2 Annual Book of ASTM Standards, **"Standard Practice for Prediction of the Long-Term Behavior of Waste Package Materials Including Waste Forms Used in the Geologic Disposal of High-Level Nuclear Waste,"** ASTM Standard C1174, American Society for Testing and Materials, Vol. 12.01, West Conshohocken, PA (2008).

3 DOE, **"Nuclear Waste Materials Handbook: Test Methods,"** US Department of Energy, Washington DC (1982).

4 Annual Book of ASTM Standards , **"Test Method for Static Leaching of Monolithic Waste Forms for Disposal of Radioactive Waste,"** ASTM Standard C1220, American Society for Testing and Materials, , Vol. 12.01, West Conshohocken, PA (2008).

5 Bates, J.K., Ebert, W.L., Mazer, J.J., Bradley, C.R., and Dietz, N., **"The Role of Surface Layers in Glass Leaching Performance,"** In Scientific Basis for Nuclear Waste Management, pp 77-87, Materials Research Society, (1991)

6 Oversby, V., and Phinney, D., **"The Development of Surface Alteration Layers on SRL-165 Nuclear Waste Glass,"** *Journal of Nuclear Materials 190*, 247-268, (1992).

7 Advocat, T., Crovisier, J.L., Vernaz, E., Ehret, G., and Charpentier, H., **"Hydrolysis of R7T7 Nuclear Waste Glass in Dilute Media: Mechanisms and Rate as a Function of pH,"** In *Scientific Basis for Nuclear Waste Management V*, pp 57-64, Material Research Society. (1991)

8 Strachan, D.M., **"Results from Long-term Use of the MCC-1 Static Leach Test Method,"** Nuclear Chemistry and Waste Management 4, 177-188 (1983).

9 MCC. Materials Characterization Center-3 (MCC-3), **"Agitated Powder Leach Test,"** Pacific Northwest Laboratory, Richland Washington, (1984).

10 Shade, J., and Strachan, D.M., **"Effect of High Surface Area to Solution Volume Ratios on Waste Glass Leaching,"** Ceramic Bulletin 65, 1568-1573 (1986).

11 Annual Book of ASTM Standards, **"Standard Test Methods for Determining Chemical Durability of Nuclear Waste Glasses: The Product Consistency Test (PCT) Standard,"** ASTM C1285, Vol. 12.01, American Society for Testing and Materials, West Conshohocken, PA (2014).

12 Ebert, W.L., **"Testing Protocols to Support Waste Form Development, Production, and Acceptance," for GNEP Waste Forms,"** US DOE Report GNEP-WAST-WAST-Al-RT-2008-000302 (September 2008).

13 Barkatt, A., Macedo, P.B., Sousanpour, W., Barkatt, A., Boroomand, M.A., Fisher, C., Shirron, J., Szoke, P., and Rogers, V., **"The Use of a Flow Test and a Flow Model in Evaluating the Durability of Various Nuclear Waste-form Materials,"** Nuclear Chemistry and Waste Management 4, 153-169 (1983).

14 Barkatt, A., Sousanpour, W., Barkatt, A., Boroomand, M. A., and Macedo, P. B., **"Leach Behavior of SRL TDS-131 Defense Waste Glass in Water at High/Low Flow Rates,"** In Scientific Basis for Nuclear Waste Management, pp 643-653 (1984).

15 Tole, M., Lasaga, A., Pantano, C., and White, W., "**The Kinetics of Dissolution of Nepheline ($NaAlSiO_4$),"** *Geochimica et Cosmochimica Acta 50*, 379-392 (1986).

16 Hespe, E., **"Leach Testing of Immobilized Radioactive Waste Solids: A Proposal for a Standard Method,"** In *Atomic Energy Review*, pp 195-207, International Atomic Energy Agency (1971).

17 U.S. Nuclear Regulatory Commission, **"Technical Position on Waste Form (Revision 1)"**, U.S. NRC Low-Level Waste Management Branch Division of Low-Level Waste management and Decommissioning (January 1991).

18 W.L. Ebert, personal communication to C.M. Jantzen, January 2014.

19 Annual Book of ASTM Standards, **"Standard Test Method for Diffusive Releases from Solidified Waste and a Computer Program to Model Diffusive, Fractional Leaching from Cylindrical Waste Forms,"** Standard ASTM C1308, Vol. 12.01, American Society for Testing and Materials, West Conshohocken, PA (2008).

20 Crank, J., **"The Mathematics of Diffusion"**, Oxford University Press, London (1986).

21 Annual Book of ASTM Standards, **"Standard Practice for Measurement of the Glass Dissolution Rate Using the Single-Pass Flow-Through Test Method,"** Standard ASTM C1662, Vol. 12.01, American Society for Testing and Materials, West Conshohocken, PA (2008).

22 Pierce, E.M., Richards, E.L., Davis, A.M., Reed, L.R., and Rodriguez, E.A., "**Aluminoborosilicate Waste Glass Dissolution Under Alkaline Conditions at 40C: Implications for a Chemical Affinity-Based Rate Equation,"** Environmental Chemistry 5, 7-85 (2008).

23 Icenhower, J.P., McGrail, B.P., Shaw, W.J., Pierce, E.M., Nachimuthu, P., Shuh, D.K., Rodriguez, E.A., and Steele, J.L., **"Experimentally Determined Dissolution Kinetics of Na-rich Borosilicate Glasses at Far-From-Equilibrium Conditions: Implications for Transition State Theory,"** Geochimica Cosmochimica Acta 72, 2767-2788 (2008).

24 Pierce, E.M., Reed, L.R., Shaw, W.J., McGrail, B.P., Icenhower, J., Windisch, C., Cordova, E., and Broady, J., **"Experimental Determination of the Effect of the Ratio of B/Al on Glass Dissolution along the Nepheline (NaAlSiO4)-Malinkoite (NaBSiO4) Join,"** Geochimica Cosmochimica Acta 74, 2634-2654 (2010).

25 McGrail, B., Ebert, W., Bakel, A., and Peeler, D., **"Measurement of Kinetic Rate Law Parameters on a Na-Ca-Al Borosilicate Glass for Low-activity Waste,"** Journal of Nuclear Materials 249, 175-189 (1997).

26 Pierce, E.M., Rodriguez, E.A., Calligan, L.J., Shaw, W.J., and McGrail, B.P., **"An Experimental Study of the Dissolution Rates of Simulated Aluminoborosilicate Waste Glasses as a Function of pH and Temperature Under Dilute Conditions,"** Applied Geochemistry, 23 [9], 2559-2573 (2008).

27 Pierce, E.M., Icenhower, J.P., Serne, R.J., and Catalano, J.G., **"Experimental Determination of UO_2(cr) Dissolution Kinetics: Effects of Solution Saturation State and pH,"** Journal of Nuclear Materials, 345, 206-218 (2005).

28 Tole, M.P., **"Factors Controlling the Kinetics of Silicate-Water Interactions,**" Unpublished PhD Thesis, The Pennsylvania State University, University Park, PA (March 1982).

29 Tole, M.P., Lasaga, A.C., Pantano, C., and White, W.B., **"The Kinetics of Dissolution of Nepheline ($NaAlSiO_4$),"** Geochim. Cosmochim. Acta 50, (3), 379-392 (1986).

30 Knauss K.G., and Wolery, T.J., **"Dependence of Albite Dissolution Kinetics on pH and Time at 25°C and 70°C,"** Geochim. Cosmochim. Acta, 50, 2481-2497 (1986).

31 McGrail, B.P., Schaef, H.T., Martin, P.F., Bacon, D.H., Rodriguez, E.A., McCready, D.E., Primak, A.N., and Orr, R.D., **"Initial Evaluation of Steam-Reformed Low Activity Waste for Direct Land Disposal,"** U.S. DOE Report PNWD-3288 (2003).

32 Jantzen, C.M., Lorier, T.H., Marra, J.C., and Pareizs, J.M., **"Durability Testing of Fluidized Bed Steam Reforming (FBSR) Waste Forms,"** Waste Management '06, Paper #6373 (2006).

33 McGrail, B.P., Pierce, E.M., Schaef, H.T., Rodriguez, E.A., Steele, J.L., Owen, A.T., and Wellman, D.M., **"Laboratory Testing of Bulk Vitrified and Steam-Reformed Low-Activity Forms to Support a Preliminary Assessment for an Integrated Disposal Facility,"** U.S. DOE Report PNNL-14414 (2003).

34 Jantzen, C.M., Lorier, T.H., Pareizs, J.M. and Marra, J.C., **"Fluidized Bed Steam Reformed (FBSR) Mineral Waste Forms: Characterization and Durability Testing,"** Scientific Basis for Nuclear Waste Management XXX, D. Dunn (Ed.) 379-386 (2007).

35 McGrail, B.P., Martin, P.F., Lindenmeier, C., and Schaef, H.T., **"Application of the Pressurized Unsaturated Flow (PUF) Test for Accelerated Ageing of Waste Forms,"** In Proceedings of the International Conference on Ageing Studies & Lifetime Extension of Materials (Mallinson, L., Ed.), pp 313-320, Kluwer Academic/Plenum Publishers, Oxford, UK (1999).

36 Wolery, T.J., and Daveler, S.A., **"EQ6, A Computer Program for Reaction Path Modeling of Aqueous Geochemical Systems: Theoretical Manual, User's Guide and Related Documentation (Version 7.0),"** Lawrence Livermore National Laboratory, Livermore, CA. (1992).

37 Bethke, C., **"Geochemical Reaction Modeling,"** Second Edition ed., Oxford University Press, New York (2008).

38 Mattigod, S.V, and McGrail, B.P., **"Estimating the Standard Free Energy of Formation of Zeolites Using the Polymer Model,"** Microporous and Mesoporous Materials, *27*, 41-47 (1999).

39 Bacon, D. H., and McGrail, B. P., **"Source Term Analysis for Hanford Low-Activity Tank Waste Using the STORM Code: A Coupled Unsaturated Flow and Reactive Transport Model,"** In Symposium on Science and Technology for Disposal of Radioactive Tank Wastes (Lombardo, N., and Schulz, W., Eds.), Plenum Publishing, Las Vegas, Nevada (1997).

40. McGrail, B.P., Martin, P.F. and Lindenmeier, C.W., **"Accelerated Testing of Waste Forms Using a Novel Pressurized Unsaturated Flow (PUF) Method,"** Material Research Society Symposium Proceedings, 465, 253-260 (1997).

41 McGrail, B.P., Martin, P.F., and Lindenmeier, C.W., **"Method and Apparatus for Measuring Coupled Flow, Transport, and Reaction Processes Under Liquid Unsaturated Flow Conditions,"** U.S. Patent No. 5974859, Battelle Memorial Institute, USA (1999).

42 McGrail, B. P., Lindenmeier, C., and Martin, P. F., **"Characterization of Pore Structure and Hydraulic Property Alteration in Pressurized Unsaturated Flow Tests,"** In Scientific Basis for Nuclear Waste Management (Wronkiewicz, D. J., and Lee, J., Eds.), pp 421-428, Material Research Society, Warrendale, Pennsylvania (1999).

43 McGrail, B. P., Martin, P. F., Schaef, H. T., Lindenmeier, C., and Owen, A**., "Glass/Ceramic Interactions in the Can-in-canister Configuration for Disposal of Excess Weapons Plutonium,"** In Scientific Basis for Nuclear Waste Management XXIII (Smith, R. W., and Shoesmith, D. W., Eds.), pp 345-352, Material Research Society, Pittsburgh, Pennsylvania (2000).

44 Pierce, E. M., McGrail, B. P., Valenta, M. M., and Strachan, D. M., **"The Accelerated Weathering of a Radioactive Low-activity Waste Glass Under Hydraulically Unsaturated Conditions: Experimental Results from a Pressurized Unsaturated Flow Test,"** Nuclear Technology 155, 149-165 (2006).

45 Pierce, E. M., McGrail, B. P., Martin, P. F., Marra, J., Arey, B. W., Geiszler, K. N., **"Accelerated Weathering of High-level and Plutonium-bearing Lanthanide Borosilicate Waste Glasses Under Hydraulically Unsaturated Conditions,"** Applied Geochemistry *22*, 1841-1859 (2007).

46 Pierce, E. M., McGrail, B. P., Rodriguez, E. A., Schaef, H. T., Saripalli, K. P., Serne, R. J., Krupka, K. M., Martin, P. F., Baum, S. R., Geiszler, K. N., Reed, L. R., and Shaw, W. J., **"Waste Form Release Data Package for the 2005 Integrated Disposal Facility Performance Assessment,"** Pacific Northwest National Laboratory, Richland, WA. (2004).

47 Pierce, E., **"Accelerated Weathering of Fluidized Bed Steam Reformation Material Under Hydraulically Unsaturated Conditions,"** In Material Science and Technology, American Ceramic Society, Detroit, Michigan (2007).

48 Wierenga, P., Young, M., Gee, G., Hills, R., Kincaid, C., Nicholson, T., and Cady, R., **"Soil Characterization Methods for Unsaturated Low-Level Waste Sites,"** Pacific Northwest Laboratory, Richland, WA. (1993).

49 Thor® Treatment Technologies, **"Pilot Plant Report for Treating T48H Simulants Carbonate Flowsheet,"** Document Number 28927-WEC-RPT-00001: Rev.2 (May 2007).

50 Jantzen, C.M., **"Characterization and Performance of Fluidized Bed Steam Reforming (FBSR) Product as a Final Waste Form,"** Ceramic Transactions 155, 319-329 (2004).

51 Pareizs, J.M., Jantzen, C.M., and Lorier, T.H., **"Durability Testing of Fluidized Bed Steam Reformer (FBSR) Waste Forms for High Sodium Wastes at Hanford and Idaho,"** U.S. DOE Report WSRC-TR-2005-00102 (2005).

52 Jantzen, C.M., Pareizs, J.M., Lorier, T.H., and Marra, J.C., **"Durability Testing of Fluidized Bed Steam Reforming (FBSR) Products,"** Ceramic Transactions, 176, 121-137 (2005).

53 Jantzen, C.M., Lorier, T.H., Marra, J.C., and Pareizs, J.P., **"Durability Testing of Fluidized Bed Steam Reforming (FBSR) Waste Forms,"** Waste Management '06, Paper #6373 (2006).

54 Lorier, T.H., Pareizs, J.M., and Jantzen, C.M., **"Single Pass Flow Through (SPFT) Testing of Fluidized Bed Steam Reforming (FBSR) Waste Forms,"** U.S. DOE Report, WSRC-TR-2005-00124 (2005).

55 Jantzen, C.M., Lorier, T.H., Pareizs, J.M., and Marra, J.C., **"Fluidized Bed Steam Reformed (FBSR) Mineral Waste Forms: Characterization and Durability Testing,"** Scientific Basis for Nuclear Waste Management XXX, D. Dunn (Ed.) 379-386 (2007).

Appendix E. X-ray Absorption Spectroscopy Materials and Methods

The Re and ^{99}Tc XAS studies discussed in this report were performed at the National Synchrotron Lightsource (NSLS) at Brookhaven National Laboratory, Stanford Synchrotron Radiation Lightsourse (SSRL) at SLAC National Accelerator Laboratory, and the Advance Photon Source (APS) at Argonne National Laboratory.

Bulk Re L_{II}-edge X-ray Absorption Fine Structure (XAFS) Spectroscopy. Two sample configurations were used for the bulk XAFS analysis and included: (1) sandwiching a thin uniform layer of sample between sheets of Kapton or polypropylene or (2) placing approximately 200-mg of sample in a Teflon holder and sealing with Kapton tape. Bulk Re L_{II}-edge (11 959 eV) XANES and Extended X-ray Absorption Fine Structure (EXAFS) spectra of the FBSR 1125 and BSR Mod B were collected at SSRL, spectra of Hazen P1B were collected at National Synchrotron Light Source (NSLS) and the Advance Photon Source, and spectra of the Re-bearing sodalite (ReZAA and Re sodalite) were collected at APS and NSLS.

The FBSR 1125 and BSR Mod B data spectra were collected at SSRL on beam line 11-2 with a cryogenically cooled Si(220), ϕ = 90°C, double-crystal monochromator. The fluorescence spectra were collected with a 30 element Canberra solid-state germanium detector.

The NSLS and APS were used to collect spectra of Hazen P1B and two rhenium sodalite samples, ReZAA sample produced hydrothermally in 2010 and sodalite04 sample produced hydrothermally in 2004. The NSLS data were collected on microprobe beam line X27A with a water cooled Si(111) monochromator. The fluorescence spectra were collected with a 13 element Germanium detector. The APS data were collected on microprobe beam line 20-BM-B with a Si(111) monochromator. The fluorescence spectra were collected at room temperature with a Vortex Si Drift detector.

Bulk Rhenium L_{II}-edge XAFS Reference Spectra and Data Analysis. Four reference spectra, Re foil [Re(0)], ReO_2 [Re(IV)] ReO_3 [Re(VI)], and $KReO_4$ ([Re(VII)] were used for data fitting [1]. Data were fit using the locally written program "fites," which performs a non-linear least squares fit of the data. Seven parameters were used in the fit: the amplitudes of the four standards, one global energy shift, and slope and offset (linear correction to account for differences in normalization). Data were fit between 11940 and 12040 eV. Data resolution was between ~5 to 7 eV as determined from the white line for each of the measurements performed at the different beam lines. As a result, there were between 14 and 20 independent data (spectral range divided by the resolution) in the spectrum.

In all cases the rhenium EXAFS and XANES spectra fitting were performed as previously described [1,2]. Briefly, the XANES fitting process was done in two stages. First, the XANES spectra were fit including all of the reference spectra. If only one species was found to be present, no further fitting was performed. If more than one species was present, reference spectra within one standard deviation of zero were removed, and the spectra were fit again. The final fit therefore includes only the reference spectra that have non-zero contributions to the fit.

XAFS fitting was performed using Artemis. Theoretical phases and amplitudes were calculated using Feff7 and the structure of nosean with Re replacing S in the sulfate anion (the actual Re-O distance in perrhenate is 0.1 Å shorter than the S-O distance in sulfate).

Bulk Tc K-edge X-ray Absorption Fine Structure (XAFS) Spectroscopy. For bulk XAFS analysis, approximately 200 mg of the as received radioactive sample, Module B and C, was placed in a Teflon sample holder and sealed with Kapton tape. Bulk Tc K-edge XANES and Extended X-ray Absorption Fine Structure (EXAFS) spectra of Module B and C was collected at NSLS and SSRL, respectively.

Analysis of Module B was conducted on beam line X11A at NSLS with a water cooled Si(111) double crystal monochromator. The Si(111) double crystal monochromator was detuned 10% and used to scan the energy range across the Mo and Tc K-edges. Beam dimensions on the sample were 2 × 8-mm. A Mo foil was used as an internal energy calibration standard by scanning across the Mo K-edge in 1eV steps (± 50eV) at the start of each Tc energy scan. The center of the first inflection point of the Mo foil spectrum was assigned to 20,000eV. Tc K-edge spectra were recorded by integrating for 3 seconds at 1eV steps from 50 eV below the edge to 300 eV above the edge (Tc K-edge E_0 was assigned to 21,044eV). Tc fluorescence spectra were acquired with a 13 element solid-state Ge detector (Canberra) set with the single channel analyzer gated on the Tc K-alpha fluorescence emission line.

The Module C sample was analyzed at SSRL on beam line 11-2 with a cryogenically cooled Si(220), ϕ = 90°C, double-crystal monochromator. The fluorescence spectra were collected with a 30 element Canberra solid-state germanium detector with a 0.1-mm Al filter (one sheet of Al cut from a soda can) and a Mo filter with an optical density of 3 at the Mo K-edge. All data were corrected for detector dead time.

Bulk Tc K-edge XAFS Reference Spectra and Data Analysis. Three reference spectra, TcO_4^- on Reillex-HPQ resin [Tc(VII)], technetium sulfide in grout [(Tc_2S_7), Tc(IV)], and $TcO_2 \cdot 2H_2O$ [Tc(IV)] [1,2,3] were used for XANES data fitting. Data were fit using the locally written program "Fites," which performs a non-linear least squares fit of the data. Spectrum processing (calibration, alignment, background subtraction, normalization and averaging) was performed with Athena software. Artemis was used to process the data. All scans were aligned with each other and averaged.

For the NSLS results, the standard spectra for $TcO_2 \cdot 2H_2O$ and TcO_4^- were convolved with a 1.5 eV Gaussian to match the resolution of the spectrum of Tc_2S_7. The NSLS data could not be effectively modeled by further convolving the standard spectra with Gaussians. Rather the resolution of the NSLS data was modeled by making a copy of each standard, shifting the spectrum by 5 eV, then averaging the original and energy shifted spectra. The value of 5 eV was determined by trial and error to be the value that best fit the data. The experimental resolution was assumed to be 10 eV; therefore, each spectrum (21000 to 21150 eV) contains 15 independent data points.

For the SSRL results, the data resolution was significantly better than the reference resolution, so the data were convolved with a 1.6 eV Gaussian such that the convolved energy calibration spectrum (TcO_4^-) matched the TcO_4^- reference spectrum.

In all cases, the technetium EXAFS and XANES spectra were performed as previously described [2,3]. Briefly, the XANES fitting process was done in two stages. First, the XANES spectra were fit including all of the reference spectra. Whenever the contribution of the reference spectrum was within one standard deviation of zero, the spectra were fit again with that reference spectrum excluded. The final fit therefore includes only the reference spectra that have non-zero contributions to the fit.

The EXAFS data analysis the technetium spectra collected at NSLS and SSRL was performed by standard procedures using the program the ifeffit [4] and Athena/Artemis [5]. Theoretical phases and amplitudes were calculated using FEFF7 [6] using $(NH_4)TcO_4$ as the model compound and the structure of Nosean with the sulfur atom replaced by technetium.

F-test for ReL_{II}–edge and Tc K-edge XAFS results. The improvement to the fit due to the inclusion each reference spectrum was determined using the F-test. Briefly, the data was fit using all three or four of the reference spectra to give the best fit. Then, the fit was repeated multiple times with the amplitude of one of the reference spectra set to zero each time, which produced a larger *r*-factor. For each component, *F* was determined using

$$F = \left(\frac{\left(r_q^2 - r_0^2\right)}{r_0^2} \right) \left(\frac{(m-n)}{b} \right) \quad (0.1)$$

where r_q is the *r*-factor of a fit with the amplitude of 1 component set to zero, r_0 is the *r*-factor for the fit including all components, *m* is the number of independent data (14), *n* is the number of parameters in the best fit (7), and *b* is the difference between the number of parameter in the best fit (7) and the number of parameters with one component set to zero (6). The probability that a given value of *F* was due to random error, *p(F)*, was determined using Excel. If *p(F)* <0.05, then the data supports the hypothesis that a given component is present (agreement is > 2σ), and in *p(F)* < 0.01, the data strongly supports the hypothesis (> 3σ).

Beam line micro-XRF and micro-XRD results. The microbeam x-ray fluorescence (μ-XRF) mapping, x-ray absorption spectroscopy (μ-XAS) and x-ray diffraction (μ-XRD) were collected at beamline X26A at the National Synchrotron Light Source (NSLS) located at Brookhaven National Laboratory (BNL). The thin sectioned samples BSR1 and PIB1 were lifted off of the glass slides with acetone and mounted without any backing in the x-ray microprobe x-y-z sample stage at the beamline. Initially, two dimensional XRF maps were recorded by raster-scanning a 1×1 mm region of the sample with the microbeam (beam dimensions 3×5 μm, vertical × horizontal) with a 5μm/pixel spatial resolution. The x-ray energy was fixed at 17.479 keV during the μ-XRF maps and a complete energy spectrum (ca 17-3 keV) of the fluorescence emitted from the sample was recorded for each pixel with a 9-element Canberra germanium detector and two Vortex-EX silicon drift detectors. The XRF maps of rhenium were segmented into three categories based on Re L-edge fluorescence: 1) low or negligible, 2) intermediate, and 3) Re hot-spots. Category 2, intermediate rhenium fluorescence, represented the largest fraction of rhenium in the sample based on spatial extent within the mapped region. Three pixels from different grains of the matrix material within Category 2 segments of each sample were selected for μ-XAS and μ-XRD point analyses to determine rhenium oxidation state and mineralogy of the associated matrix, respectively. The Re L_{II} XANES spectra were conducted with a Si(111) monochromator in fluorescence mode. The μ-XRD diffractograms were collected at the same points at a fixed energy of 17.479 keV. This energy is used to facilitate comparison with powder diffraction database standards collected on benchtop sources using a Molybdenum x-ray source. Two standards (Re-sodalite and Re-ZAA) were also analyzed, but in the powder form sandwiched between two polypropylene windows. The diffracted beam was recorded on a Rayonix SX-165 CCD. The tiff images were processed using FIT2D software to subtract background and convert the data into diffraction intensity versus 2-theta.

1 W. Lukens, **"Dissimilar Behavior of Technetium and Rhenium in Borosilicate Waste Glass as Determined by X-ray Absorption Spectroscopy,"** Chemical Material 19, 559 (2007).

2 W. Lukens, **"Evolution of Technetium Speciation in Reducing Grout,"** Environmental Science & Technology 39, 8064 (2005).

3 I. Almahamid, J. Bryan, J. Bucher, A. Burrell, N. Edelstein, E. Hudson, N. Kaltsoyannis, W. Lukens, D.K. Shuh, H. Nitsche, and T. Reich, **"Electronic and structural investigations of technetium compounds by X-ray absorption spectroscopy,"** Inorg. Chem. 34, 193-198 (1995).

4 M. Newville, **"IFEFFIT, Interactive EXAFS analysis and FEFF fitting**," Journal of Synchrotron Radiation 8, 322-324 (2001).

5 B. Ravel, and M. Newville, and A. Athena, **"Hephaestus: Data Analysis for X-ray Absorption Spectroscopy using IFEFFIT,"** Journal of Synchrotron Radiation 12, 537-541 (2005).

6 J. Rehr, R. Albers, and S. Zabinsky, **"High-order Multiple-scattering Calculations of X-ray Absorption Fine Structure,"** Physical Review Letters 69, 3397 (1992).

Appendix F. Treatment of Unreacted Coal during Durability Testing

In the early durability studies (see Table 3-2 in main text of this document); the unreacted coal was removed from the mineral product in order to study the durability mechanisms by which the mineral species released constituents without the coal present. Once that was determined, the coal has been left in the samples being leached (see Table 3-2 in main text of this document). In 2004 [1], it was shown that carbon content does have an impact on BET surface area (see Figure F - 1) which is used in the denominator of the durability equations for the PCT and SPFT tests in order to express the amount released in g of species "i" released per cm^2 of waste form surface area exposed. Because the carbon is not part of the actual mineral product (i.e., inert in terms of the durability response), a surface area to volume ratio that included carbon may underestimate durability release. Therefore, SA/V results on carbon-free samples are used in calculating durability release rates. Specifically, a sample is sized and meshed and washed in ethanol to remove electrostatic fines to ensure a near Gaussian distribution of particle sizes in the leach test, i.e. particle size control to get a consistent test response. Then a subset of that prepared sample is treated to remove the coal and the BET surface area measured of the roasted product. The remainder of the sample is tested with the coal in it but the roasted BET surface area is used in the calculation to be conservative. Durability testing at SRNL (reference 1) and PNNL (this document) were performed on roasted and non-roasted samples and the durability responses were comparable (see Table 8-40 in main text of this document).

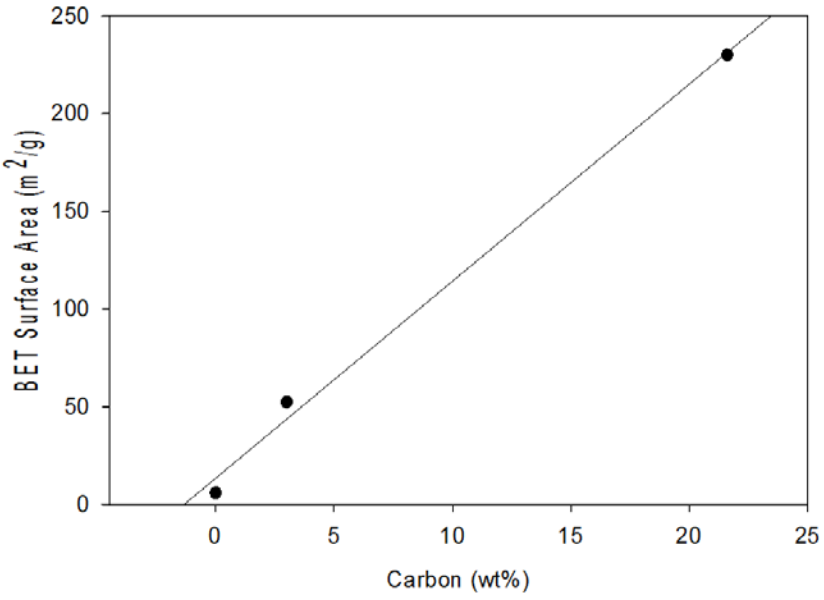

Figure F - 1. BET Surface Area as a Function of Carbon Content for INL SBW Sample Bed 272 (from reference1)

Reference

1 Pareizs, J.M., C.M. Jantzen, and T.H. Lorier, **"Durability Testing of Fluidized Bed Steam Reformer (FBSR) Waste Forms for High Sodium Wastes at Hanford and Idaho"**, U.S. DOE Report, WSRC-TR-2005-00102, Savannah River National Laboratory, Aiken, SC (2005).

Appendix G. Supplementary Data on Monolithing the Granular FBSR Product: Monolith Activities - Historical Through Current

The use of the FBSR process to produce a highly leach resistant mineralized waste form from Hanford LAW has been investigated since 2001 (Table 3-2 in body of document). Initial studies focused on producing and testing the granular mineral product created by processing high sodium waste feeds with clays at ~720°C and understanding the leaching mechanisms. Numerous studies have shown that it is possible to produce a mineral waste form that effectively immobilizes radionuclides and hazardous constituents and these are cited in Table 3-2.

To be accepted for near-surface disposal at Hanford, the waste form is required to meet an acceptance criterion for compressive strength of 500 psi. This requirement is derived from an NRC Branch Technical Position on low level waste (LLW) forms which somewhat arbitrarily specifies 500 psi to preclude subsidence in the waste disposal. It is also noted that a monolithic waste form would reduce the impact to human health for the intruder scenario in the waste site Performance Assessment. While a monolith is desirable, there are other means by which this requirement can be met, e.g. waste stabilization in high integrity containers (HICs).

Using various cements, hydroceramics, Ceramicrete, and geopolymers began in 2005 and continued into 2006.[1,2,3,4] These experiments used the granular FBSR product produced from the SAIC-STAR test program on FBSR product that had the coal roasted out.[5,6] The monolith work began again in the 2008-2009 [7] timeframe and this program used the granular FBSR product produced from the engineering scale HRI/TTT test program [8]. The details of these monolith activities are summarized below.

In 2005-2006, the SRNL performed a monolith feasibility study for granular FBSR product.[1,2] The Work for Others (WFO) with TTT called for monolithing the combined aluminosilicate products from INL's SBW [6,9] and Hanford's LAW [5] from 2003-2004 testing. The composite SBW/LAW granular product consisted by mass of ~32% SBW dynamic and final bed products, ~20% LAW dynamic and final bed products and fines, and ~45% unreacted alumina startup bed that was admixed in the dynamic bed products. The coal residues were roasted out of the composite by heating the samples to 525°C overnight. This temperature was chosen because it is high enough to oxidize (remove) the carbon [10], but not high enough to change the composition or the phase assemblages. Roasting was chosen in order to be able to compare the durability of the granular products with the monolith products in the absence of coal. Monoliths were made out of ordinary portland cement (OPC) at 80-87 wt% FBSR loading, ceramicrete (a blend of MgO and monopotassium phosphate (KH_2PO_4)) at an FBSR loading of 35.7 wt%, and hydroceramics (aluminosilicate zeolite phases formed from metakaolin plus NaOH) at FBSR loadings of 50-80 wt%. The hydroceramics required curing at 70-90°C to ensure that adequate strength developed but performed the best of the monoliths tested, e.g. the hydroceramics possessed the best durability of the monoliths tested and the lowest surface area as measured by BET. In addition, the NAS matrix of the hydroceramics appeared the most compatible with the chemistry of the FBSR granular product. The initial comparisons were made on the following four criteria (1) compressive strength, (2) short term durability testing using the PCT ASTM C1285; (3) X-ray Diffraction (XRD) before and after monolithing, and (4) waste loading.

In 2006-2007, SRNL funded a Laboratory Directed Research & Development (LDRD) project directed at developing geopolymers as low temperature (green technology[f]) waste forms and this provided funding for the SRNL FBSR team to investigate geopolymers for various applications. Geopolymers are ceramic-like, inorganic polymers made from aluminosilicates cross-linked with alkali metal ions. The geopolymers have an amorphous cross-linked three dimensional aluminosilicate structure: geopolymers

[f] The raw material, kaolin, only requires roasting at ~700°C with no off-gas except steam compared to the high temperature kilning of cement raw materials and the formation of greenhouse gases.

remain amorphous because they contain insufficient water to crystallize zeolite phases like the hydroceramics.

During the LDRD project, the roasted SBW/LAW granular products with the coal removed were used for an additional monolith feasibility study in two geopolymer matrices. The two geopolymer matrices (tested in triplicate by ASTM C1285, PCT) performed better than the OPC, Ceramicrete, and hydroceramic binders tested in References 1 and 2. See also Figure G - 1.

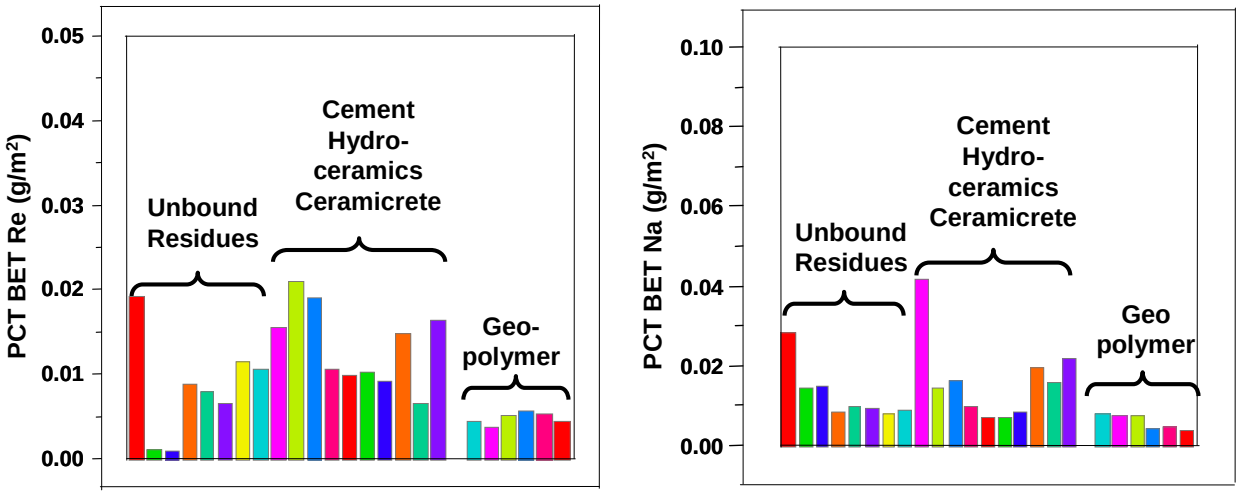

(a) (b)

Figure G - 1. Comparison of Unbound FBSR Products/Residues with The Coal Removed by Roasting to Residues Bound in OPC, Ceramicrete, Hydroceramics and Geopolymer Binders.

The two geopolymer formulations studied during the LDRD project [3,4] were selected in the region of the Na_2O-Al_2O_3-SiO_2 ternary (see Figure G - 2) designated as G1 (parameters from a literature search performed as part of the LDRD study). Geopolymers made in region G1 (atomic Si:Al = 1:1) are often used as applications for bricks, ceramics and fire products, while geopolymers made in region G2 (atomic Si:Al = 2:1) are often used as cements and concretes. Of the two formulations, formulation B from Figure G - 2 exhibited the overall superior performance. The region of formation of hydroceramics is given on Figure G - 2 for reference and it is clear that these formulations lie along a line that crosses the ternary diagram between the kaolin clay compositions and Na_2O, which is added as NaOH and/or sodium silicate solution. In Figure G - 2, the G1 region is defined to be bounded by the following ratios Na_2O/SiO_2 = 0.20-0.48, SiO_2/Al_2O_3 = 3.3-4.5, and H_2O/Na_2O = 10-25 from references by Blackford, et al. (ANSTO), [11] Rowles and O'Connor (Curtin University),[12] Hardjito (Curtin University),[13] Davidos (Geopolymer Institute, France),[14,15] and Kriven (University of Illinois).[16] The LDRD formulations were based on the work of Blackford, et al. but are most similar to those of Kriven (Table G - 1). The LDRD monolith FBSR loadings were in the 33-44 wt% range and used a 16-16-66 and 16-19-64 formulation of Na_2O:Al_2O_3:SiO_2 mol%, which is in the composition region that Kriven [17] maintains is 1:1:4 and the most durable of all geopolymers. The G2 region in Figure G - 2 comes from the work of van Jaarsveld et. al. (University of S. Africa)[18] with Na_2O/SiO_2 = 0.15-0.25, SiO_2/Al_2O_3 = 5.5-6.5, and H_2O/Na_2O = 10-25 (Table G - 1). This range was neither targeted in the LDRD nor subsequent studies and is shown for reference.

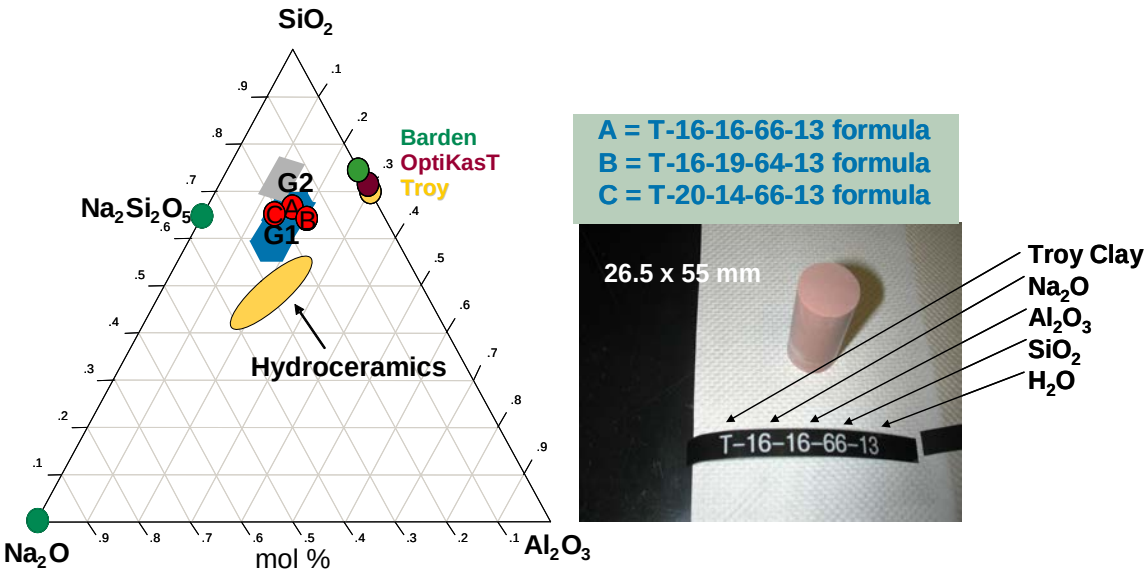

Figure G - 2. Formulation region for geopolymers compared to hydroceramics in the Na_2O-SiO_2-Al_2O_3 (mol%) ternary. Note that the fourth dimension is water content. G1 is the target range. Optimum formulations from LDRD testing are designated as A,B,C and a 1" x 2" cylindrical monolith made with composition A is shown in the photograph.

Table G - 1. Target Geopolymer Compositions from the Literature and Compositions Achieved without FBSR Excess Aluminosilicate Participation in Geopolymerization

Waste Type	Identifier	Identifier	Na_2O/SiO_2	SiO_2/Al_2O_3	H_2O/Na_2O	Na_2O (mol%)	Al_2O_3 (mol%)	SiO_2 (mol%)	FBSR Loading (Wt%)
Targets	Target G1	(Blackford, et.al.,[11], Curtin University,[12,13] Davidos,[14,15]	0.20-0.48	3.3-4.5	10-25	Range	Range	Range	Range
	Target G1	Kriven[16]	0.25-0.3	4	12				
	Target G2	Van Jaarsveld et.al.[18]	0.15-0.25	5.5-6.5	10-25				
STAR Rassat LAW & SBW	LDRD A (Troy clay)	1” x 2”	0.25	3.99	13	16.64	16.71	66.65	33-44
	LDRD B (Troy clay)	1” x 2”	0.25-0.278	3.3-3.55	13	16.09	19.52	64.39	33-44
HRI Rassat LAW	Geo-1 (Troy clay)	2” x 2”	0.396	5.299	17.168	25	12	63	67.44
	Geo-2 (Troy clay)	2” x 2”	0.43	6.205	18.083	27	10	63	72.09
	Geo-3 (Troy clay)	2” x 2”	0.469	7.604	13.973	29	8	63	67.51
	Geo-4 (Troy clay)	2” x 2”	0.537	12.786	13.965	33	5	62	71.72
	Geo-5 (Barden)	2” x 2”	0.418	8.081	13.342	27	8	65	62.72
	Geo-6 (Barden)	2” x 2”	0.391	6.768	17.221	25.5	9.5	65	66.61
	Geo-7 (Fly Ash)	2” x 2”	0.618	4.424	11.223	33.5	12.26	54	67.16
	Geo-1 (Troy clay)	3” x 6”	0.396	5.299	16.048	24.968	11.912	63	67.46
	Geo-7 (Fly Ash)	3” x 6”	0.618	4.425	11.603	33.5	12.26	54	67.17
	Geo-1 (Troy clay)	6” x 12”	0.396	5.304	18.476	24.975	11.902	63	67.44
	Geo-7 (Fly Ash)	6” x 12”	0.618	4.424	11.676	33.511	12.257	54	67.17
BSR Rassat LAW	BSR Geo-7 (Fly Ash)	1” x 2”	0.542	4.445	14.89	30.692	12.73	56.6	67.95
Hanford WTP-SW	Geo-1 (Troy clay)	3” x 6”	0.394	5.284	17.546	24.881	11.954	63	67.45
	Geo-7 (Fly Ash)	3” x 6”	0.62	4.447	11.751	33.616	12.187	54	67.05
	Geo-1 (Troy clay)	6” x 12”	0.396	5.304	16.639	24.977	11.902	63	67.44
	Geo-7 (Fly Ash)	6” x 12”	0.618	4.424	11.676	33.511	12.257	54	67.17
	Geo-7 (Fly Ash)	2” x 4”	0.618	4.424	11.862	33.512	12.257	54	67.16

The LDRD research was followed by a more extensive monolith matrix down selection [7] in 2007-8 where the following matrices were tested with LAW FBSR product known as P1B LAW aggregate, which included 2008 final bed product (no startup bed), HTF fines, and co-mingled coal from the bed and fines that had been processed by TTT at HRI in Golden Colorado:

- Ordinary portland cement (80-87 wt% FBSR loading)
- Three high Alumina Cements (68.6-85.1 wt% FBSR loading)
- Four geopolymers made with Troy clay (67.5-72.1 wt% FBSR loading)
- Two geopolymers made with Barden clay (62.9-66.8 wt% FBSR loading)
- Two geopolymers made with SEFA Class F fly ash (64.1-66.8 wt% FBSR loading)
- One Ceramicrete formulation (50-72.7 wt% FBSR loading)
- One Global Matriarchs NuCap polymer (~45.5 wt% FBSR loading)
- L-TEM™, a proprietary geopolymer formulation by Columbia Energy and Environmental Services (76-82.5 wt% FBSR loading)

It should be noted that while L-TEM™ is marketed as a geopolymer it is a geopolymeric cement and contains heat treated kaolin and/or bentonite clay, microcrystalline silica, calcium and magnesium additives which appear high in sulfate according to SRNL's analyzed composition and cement components such as C_3S ($3CaO \bullet SiO_2$).[19]

The criteria for the monolith binder down selection in Reference 7 were (1) compressive strength, (2) durability measured by the PCT (ASTM C1285), (3) TCLP (EPA Manual SW-846 Method 1311) response at the UTS, and (4) waste loading. XRD of the monoliths before and after fabrication was not a down selection criterion. A schematic of the down selection process to choose between the monolith binders listed above is given in Figure G - 3. Scale up to 6" x 12" size cylinders and measurements of heats of reaction were included during the testing.

The geopolymer formulations used in 2007-8 down select had started with the A and B formulations from the LDRD research (Figure G - 2).[3,4] Of the monoliths tested in Reference 7, the compressive strength was acceptable for OPC up to ~80 wt% FBSR loading, the high alumina cements up to ~74 wt%, the Ceramicrete up to ~50 wt%, and the geopolymers up to ~70 wt% FBSR loading. The short term (7 day) PCT testing had been used as a screening tool. Analyses were performed on the granular LAW and granular WTP-SW containing coal and with the coal roasted out. The FBSR products containing the coal were bound in the high Al_2O_3 containing cements, in OPC, in geopolymers made from Kaolin (Geo-1 to Geo-6) and from fly ash (Geo-7), ceramicrete, NuCap, and a geopolymeric cement (L-TEM). Leachates were analyzed for Al, Si, Na, Cs, Re, I, and S. Bar graphs for each element are given in Figure G - 4 to Figure G - 8. A discussion of each Figure is given below the respective figure.

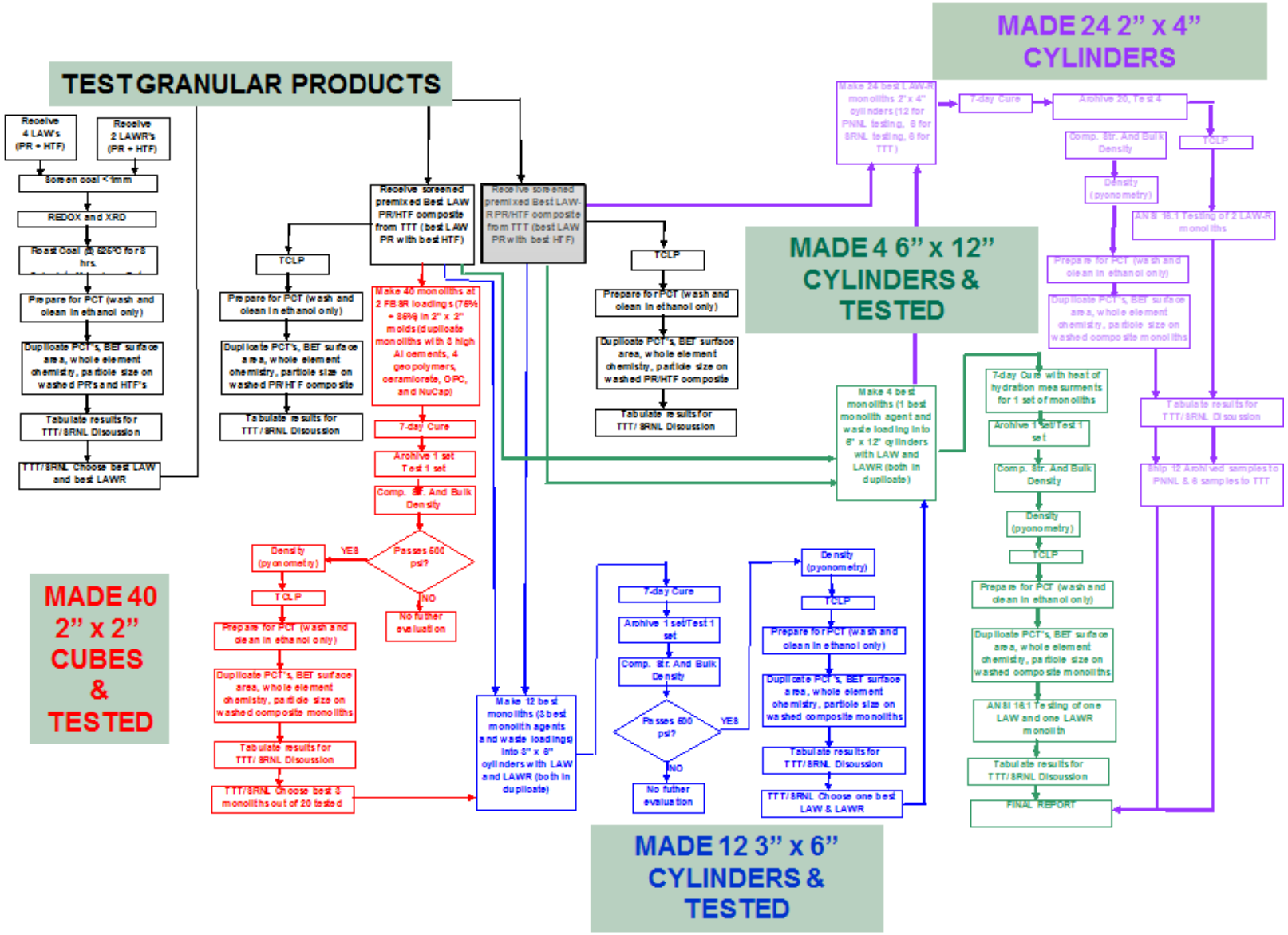

Figure G - 3. Down Selection Logic for Monolith Binder Selection from Reference VII.

The modules depicted in Figure G - 3 are listed below along with key objectives in the chronological order performed, followed by a detailed description of each testing phase.

- Module 1 (black text in Figure G - 3)
  Granular LAW and WTP-SW product bed and fines durability tested with PCT with coal roasted from the product. Granular LAW and WTP-SW blend/aggregates durability tested with PCT with coal present. Note: subsequent durability testing in 2010/2011 allowed for determination of roasted blend/aggregate data for comparison to the roasted product bed and fines data.
  - ► The initial objective of this module was to compare the individual bed products and fines PCT data to select the best LAW and WTP-SW production run from the ESTD testing. Blends from the best production run were then premixed at Hazen and sent to SRNL for further testing (latter phase of Module 1).
- Module 2 (red text in Figure G - 3)
  Granular LAW product with coal is monolithed in 2"cubes (8 binders and 2 FBSR loadings of 75 wt% and 85 wt%)
  - ► The objective of this module was to down-select three different monolith recipes to carry forward into scale-up monolith testing. A fourth monolith recipe using fly ash in geopolymer was also included in the downselect.
- Module 3 (blue text in Figure G - 3)
  Granular LAW product with coal is monolithed in 3" x 6" cylinders (3 best binders and FBSR loadings for LAW and WTP-SW from Module 2 testing)
  - ► The objective of this module was to compare performance data from the scaled up 3"x 6" cylinders versus the previous best 2" cubes. The original intent was to use only the three best monolith recipes, but the fly ash geopolymer was also included.
- Module 4 (green text in Figure G - 3)
  Granular product with coal is monolithed in 6" x 12" cylinders (best binder and FBSR loading for LAW and WTP-SW from Module 3 testing)
  - ► The objective of this module was to compare performance data from the scaled up 6" x 12" cylinders versus the previous 2" cubes and 3" x 6" cylinders. Another objective of this module was to obtain centerline curing temperatures from the monoliths.
- Module 5 (purple text in Figure G - 3)
  WTP-SW granular product with coal is monolithed in 2" x 4" cylinders (best binder and FBSR loading from Modules 3 and 4 testing). Twenty four (24) replicate samples are made of which 12 were shipped to Pacific Northwest National Laboratory (PNNL) for subsequent testing.
  - ► The Objective of this module was to produce a large replicate set of 2"x 4" cylinders made with WTP-SW using the fly ash geopolymer recipe that was judged as one of the best performers (PCT, TCLP and compression testing) from previous modules.

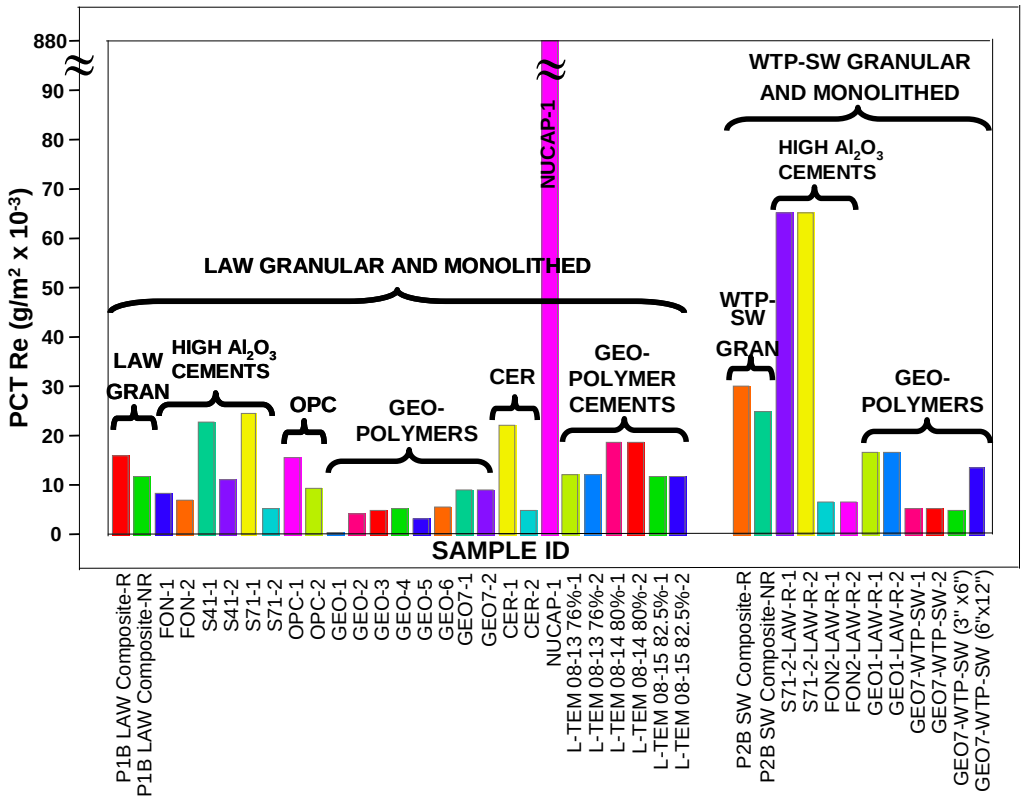

Figure G - 4. Re Release for LAW Granular and Monoliths and for WTP-SW Granular and Monoliths.

Figure G - 4 demonstrates the following for Re release:

- Re release from WTP-SW granular is higher than Re release from LAW granular (note that the WTP-SW sample was more reduced than the LAW granular product);
- Geopolymers based on clay and fly ash had lower Re releases than the high alumina cements, the ordinary portland cements, the Ceramicrete, and the geopolymeric cements known as L-TEM for the LAW granular product;
- Geopolymers and one of the high alumina cements lowered the release of Re from the WTP-SW but not all the same geopolymer formulations that lowered the Re release from the LAW granular product performed as well for the WTP-SW (this included Geo-1 and Geo-7); and
- NuCap performed poorly for Re retention compared to all the other binders tested.

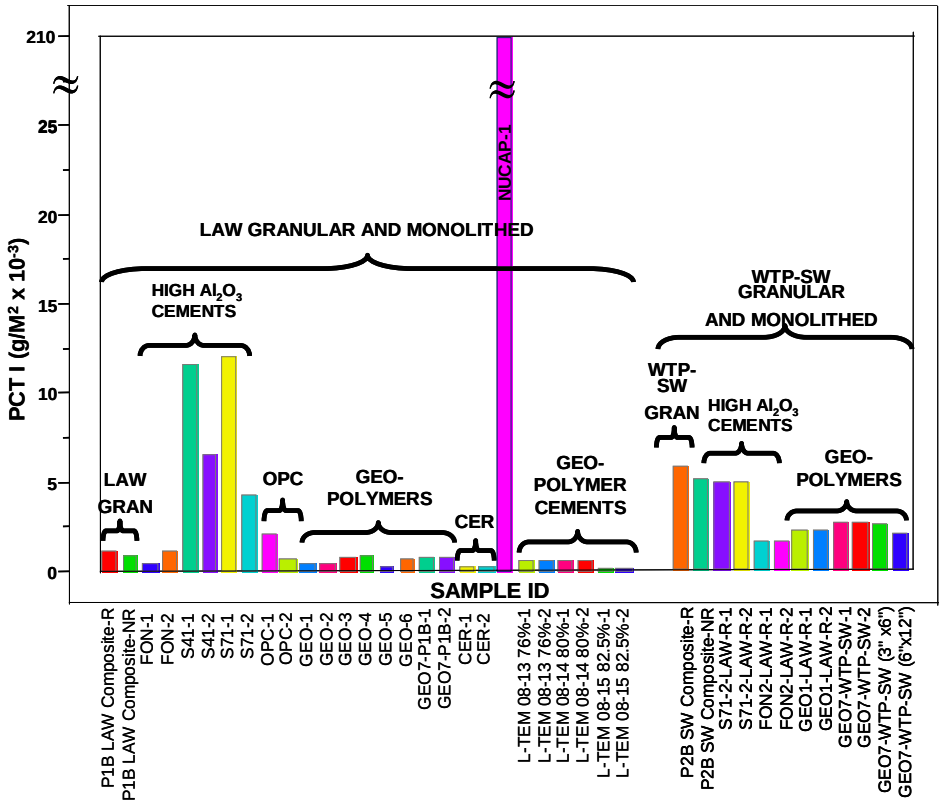

Figure G - 5. I Release for LAW Granular and Monoliths and for WTP-SW Granular and Monoliths.

Figure G - 5 demonstrates the following for I release:

- I release from the WTP-SW was higher than from the LAW granular product (again I release may be impacted by the more reduced condition of the WTP-SW);
- The geopolymers, geopolymeric cements, and Ceramicrete performed better than high alumina and OPC cements for I retention;
- The geopolymers performed better for I retention than the high alumina cements for WTP-SW; AND
- NuCap performed poorly for Re retention compared to all the other binders tested.

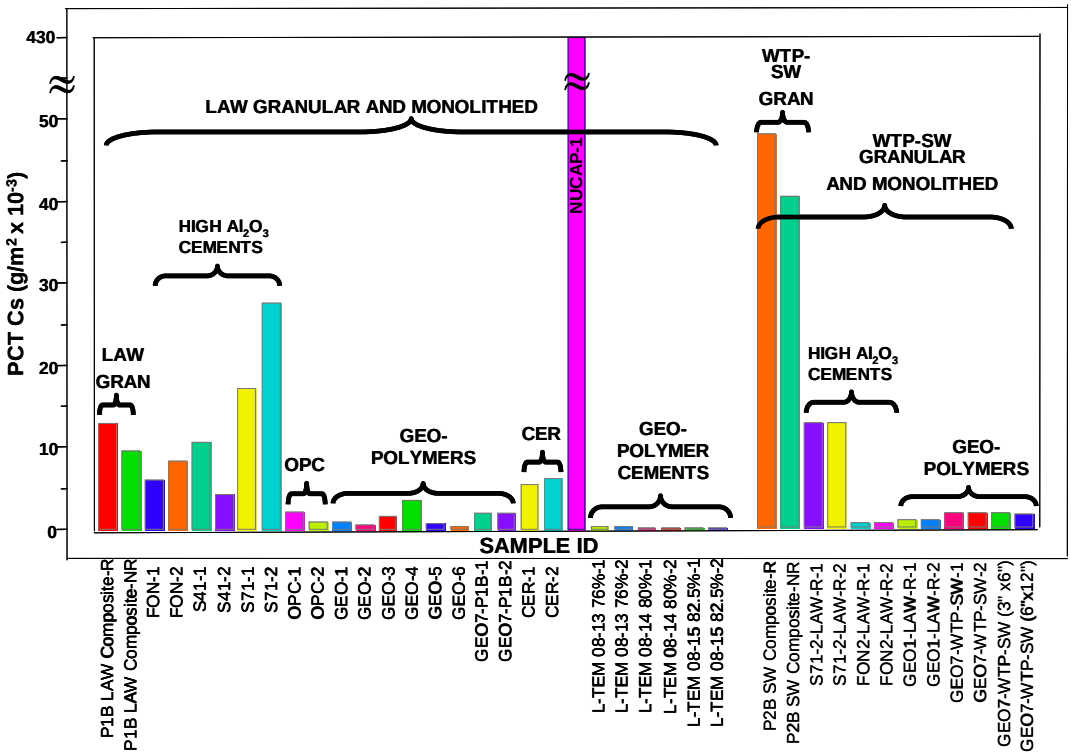

Figure G - 6. Cs Release for LAW Granular and Monoliths and for WTP-SW Granular and Monoliths.

Figure G - 6 demonstrates the following for Cs release:

- Cs release from the WTP-SW was higher than from the LAW granular product;
- For LAW, the Cs release is lowest for the geopolymeric cements followed by the geopolymers and the OPC;
- The high alumina cements, Ceramicrete, and Nu-Cap did not retain Cs very well; and
- The geopolymers and one high alumina cement retained Cs well for the WTP-SW.

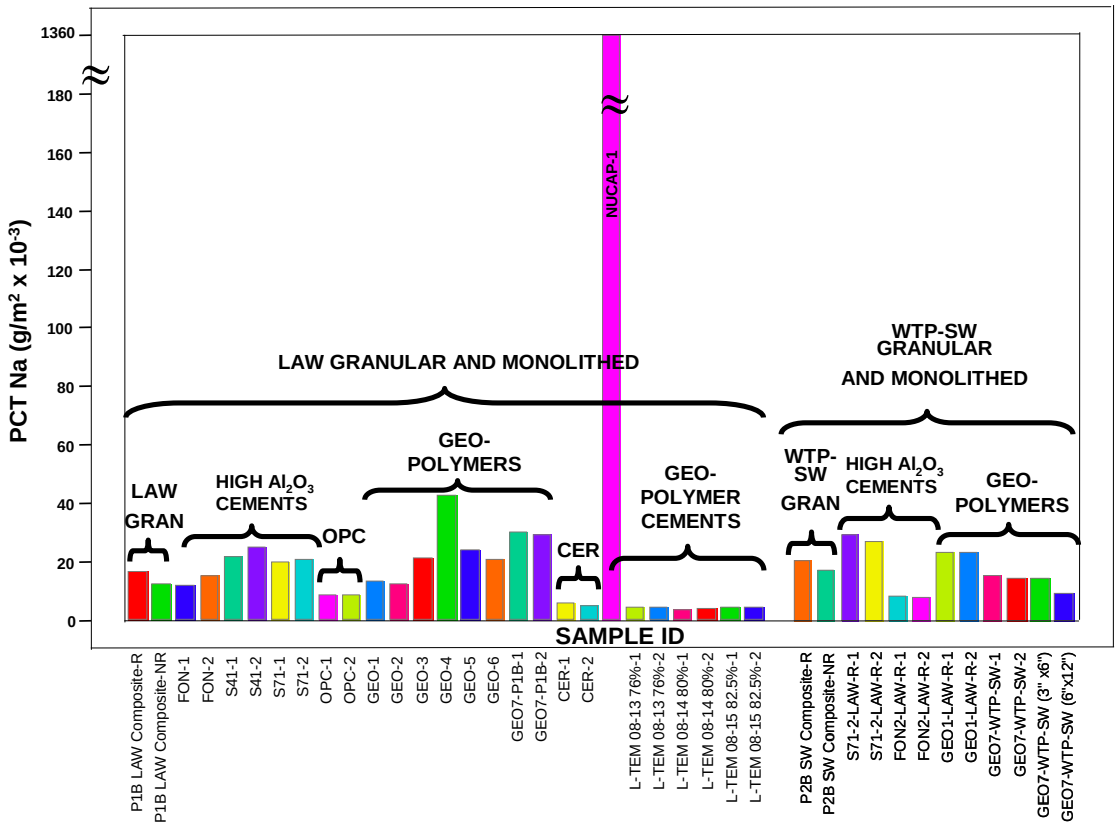

Figure G - 7. Na Release for LAW Granular and Monoliths and for WTP-SW Granular and Monoliths.

Figure G - 7 demonstrates the following for Na release:

- The geopolymeric cements performed the best for Na release, as they are Ca based geopolymeric cements;
- Ceramicrete performed well for Na realease, as it is Mg and P based;
- Geopolymers are made with sodium silicate and sodium hydroxide so it is not unreasonable to find slightly higher concentrations of Na in these binders, however, select geopolymers did not leach any additional Na compared to the granular LAW and WTP-SW;
- Na release from the LAW granular product and the WTP-SW are the about the same: since Na is not a REDOX active element this is another indication that the release of Re and I are impacted by REDOX of the FBSR product; and
- Nu-Cap performed poorly even for Na release.

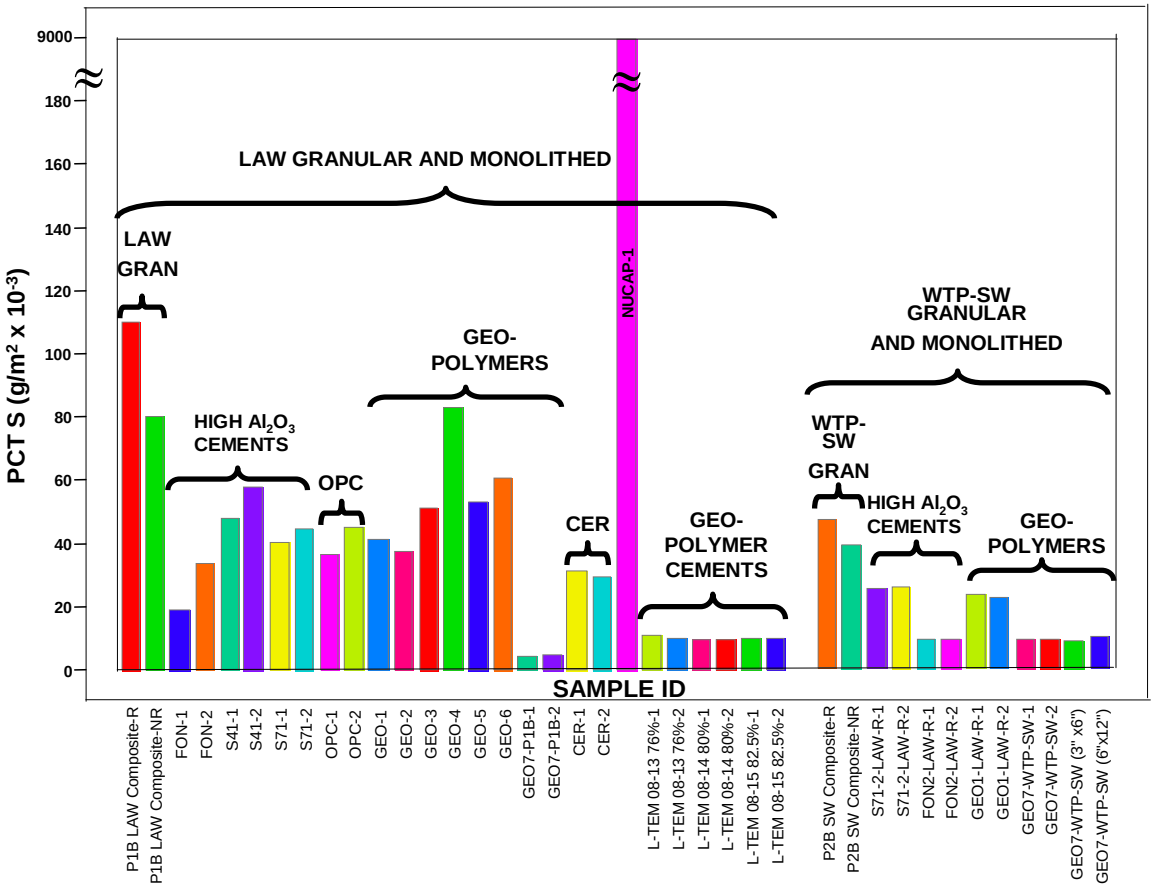

Figure G - 8. S Release for LAW Granular and Monoliths and for WTP-SW Granular and Monoliths

Figure G - 8 demonstrates the following for SO_4 release reported as S release:

- S release from LAW granular was greater than the S release from WTP-SW;
- Geo-7, the only geopolymer made with fly ash instead of kaolin clay, performed the best for S retention of all the monolith binders tested for LAW; and
- Several geopolymer formulations and one high alumina cement performed well with WTP-SW for retention of S.

Overall, the geopolymers appeared to give the lowest leaching for Cs, I, Re, S, and Na of all the monoliths (Figure G - 4 to Figure G - 8) due to the similarity of the NAS chemistry of the binder to that of the FBSR product (Figure G - 10). So geopolymer formulations (Geo-1 and Geo-7) made with fly ash were scaled up to 3" x 6" and 6" x 12" cylindrical forms.

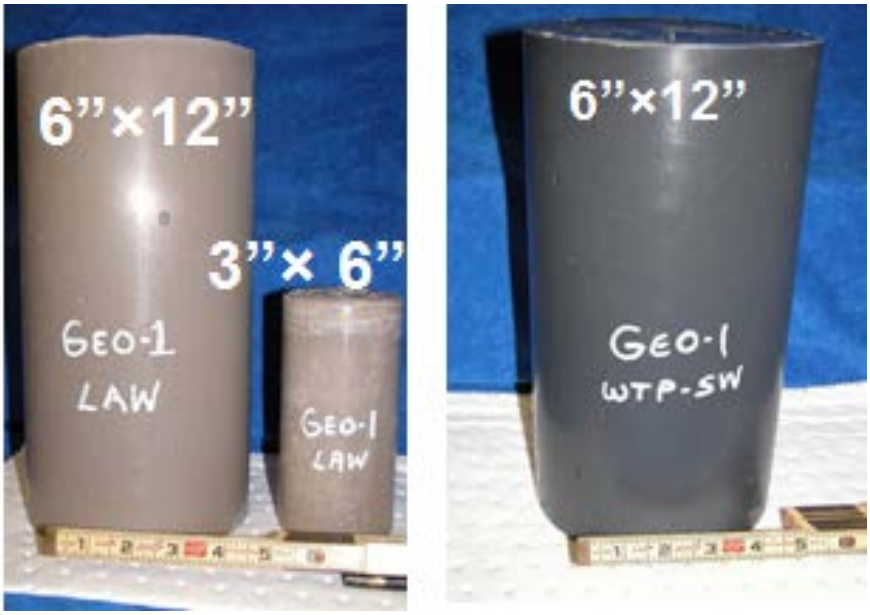

Figure G - 9. ESTD LAW Embedded in Geopolymer Matrix (left) and ESTD WTP-SW Embedded in Geopolymer Matrix. WTP-SW contained more entrained coal in the FBSR fines and so it appears black in the photograph.

Since unreacted clay cores had been observed in all of the FBSR products produced from 2001 to 2004, it was also assumed that ~10% unreacted clay existed in the FBSR product and ~ 20% flyash from the coal that is used during FBSR processing. Geopolymer formulations were targeted close to the LDRD A and B formulations assuming that 30% more free aluminosilicate was available in the FBSR product to participate in the geopolymerization. This also facilitated getting more FBSR product into the monoliths, i.e. higher FBSR loadings. The availability of the excess clay and fly ash was found to be incorrect in 2011 when SEM was performed on the 2008 ESTD LAW and WTP-SW granular samples. The 2008 granular products do not have the unreacted clay cores that were found in the 2001 TTT/HRI samples and the 2003-2004 STAR samples. This is attributed to design and process improvements that were made by TTT/HRI since 2006, which have increased bed reactivity. It was also anticipated based on the previous hydroceramic studies [1,2] that any ash from the Erwin/Bestac® or other coals used in the FBSR process might be available to participate in the alkali reactions.

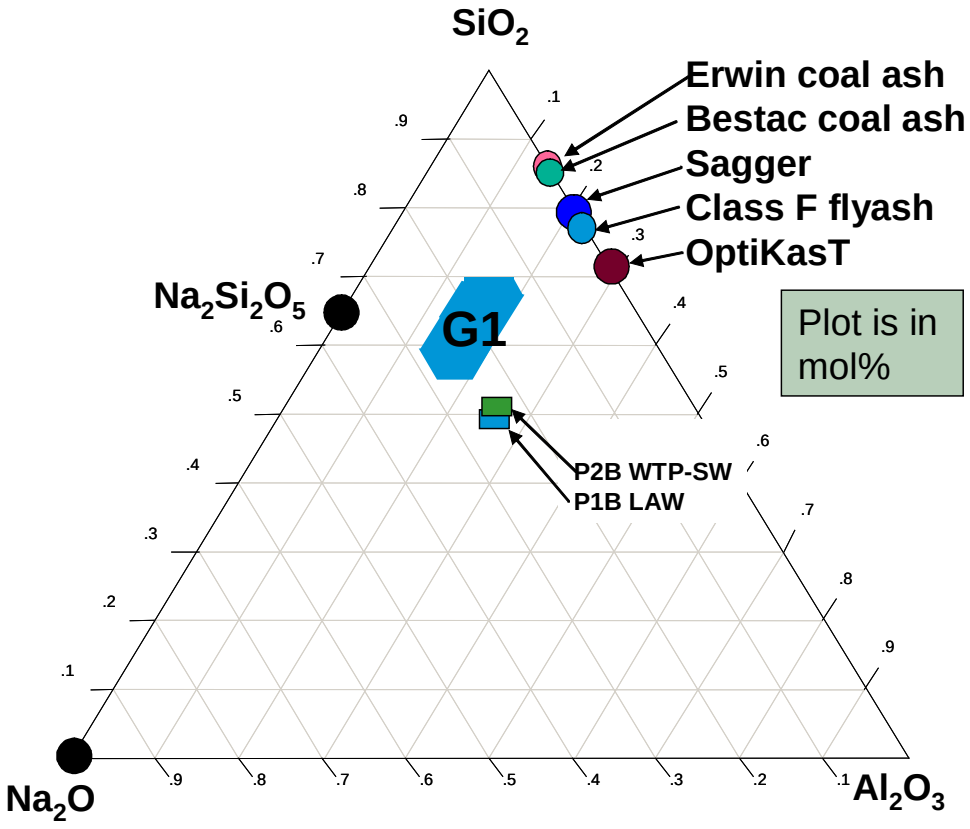

Figure G - 10. Na_2O-SiO_2-Al_2O_3 (mol%) Diagram Showing Region of Geopolymer Formation (G1) and Composition of The WTP-SW and LAW granular FBSR Products.

Since XRD analysis was not a measurement criteria during the down selection [3,4], these analyses were not performed to ensure that the geopolymers remained amorphous after setting. In other words, the monoliths were not checked by XRD to see if they had formed unwanted zeolitic phases which are usually an indication of excess water and/or NaOH.

During testing of the WTP-SW P2B blend cylinders (2" x 4") at PNNL [20], XRD was performed and zeolite phases and excess NaOH in the pore water of the geopolymers were found. These monoliths had been made with the Geo-7 formulation that used fly ash and contained the highest Na_2O of all the geopolymers formulated in 2007-2008 (Table G - 1), which caused a poor durability response for the WTP-SW than for the LAW made with the same binder. It is likely that the high fluoride content in the WTP-SW also preferentially attacked the fly ash that the binder was made from. While the WTP-SW geopolymers performed as well as cast stone and Duralith geopolymers, the NaOH and H_2O content of the formulation should be further optimized toward the silica rich and alkali poor LDRD A and B formulations shown in Figure G - 2 and Table G - 1.

All of the geopolymers made with fly ash (shown by italic print in Table G - 1), the zeolite faujasite or zeolite P or zeolite Y (non-stoichiometric faujasite) formed. These zeolites have the same cage structure as sodalites.[21] Also of note in Table G - 1 is that all of the formulations which were outside the G1 geopolymer quadrilateral shown in Figure G - 2 and Figure G - 10 formed unwanted sodium carbonates such as natrite (Na_2CO_3), thermonatrite ($Na_2CO_3 \bullet H_2O$), and/or trona ($Na_3H(CO_3)_2 \bullet 2H_2O$) from interaction of excess NaOH and CO_2 in the atmosphere. This later observation is attributed to the

geopolymer formulations being outside the targeted region G1 and some of them having been stored as ground powders before the XRD's were completed.

Synchrotron radiation-based infrared microscopy (SR-FTIR) data processed via hierarchical clustering analysis was performed by researchers in Australia on geopolymers made from various fly ash compositions.[22] In general, fly ash was found to be composed of reactive components such as 36.6% amorphous SiO_2 and 15.3% amorphous Al_2O_3 and the remainder is unreactive crystalline mullite, quartz, and iron oxide phases. This was verified for the fly ash used by SRNL, which was found to contain crystalline mullite and quartz.

In the Australian study [22], the formation of higher Si/Al ratio crystals such as faujasite (Zeolite Y) occurred in samples with a slower alumina release rate, e.g. a lower availability of aluminum since the generally accepted reaction sequence of geopolymerization is that the first stage of reaction is the release of aluminate and silicate monomers by alkali attack on the solid aluminosilicate source (clay or fly ash), which is required for the conversion of solid particles to geopolymer gel. Hydrolysis reactions occur on the surface of the solid clay or fly ash particles, followed by the formation of dissolved species that cross-link to form oligomers, and then set and harden by polycondensation and the formation of a three-dimensional aluminosilicate network.

1.1.1.1 *While the formation of faujasite (Zeolite Y) has been well studied in fly ash based geopolymers [22], it is a hydrous phase due to the 7 or 8 waters of hydration bound to its structure that may not be desirable. However, faujasite (Zeolite Y), Zeolite X, and Zeolite P all have the identical cage structures as sodalite.[21] So while the sodalite in the FBSR mineral phases may be attracting structural waters of hydration the sodalite cage structure that retains the COC's appears to remain in tact. Comparisons of the major and minor phases of each granular product in Table G - 2 to the phases that appear after monolith formation show that the major FBSR granular phases are still present. Since the formation of faujasite has been seen in geopolymers without FBSR product, the faujasite is considered to be a reaction product of the geopolymer additives and not reaction with the FBSR product. However, the other zeolites (Table G - 2), such as Zeolite X in the LTEM formulation, could indicate that some of the sodalites have converted to Zeolite X or Zeolite P: these zeolites have the sodalite cage structure [21] and this does not indicate that the COC's could or should be released from these cages.*

The FBSR monolith program after it was discovered that the FBSR ESTD and BSR products did not have unreacted clay cores was two-fold.

1. Formulations made with fly ash were made with less NaOH and in the G1 region
2. Formulations were made with the reactive clays determined from the LDRD program.

Two reasons for preferring kaolin over fly ash are (1) the unreactive nature of some of the components found in fly ash, e.g. the minerals mullite and quartz, and (2) the variable nature of fly ash compositions from various coal production facilities. In addition, fluoride should not attack clay based binders as readily as those made from fly ash. Formulations with clays are preferred since clays are less variable in composition than fly ash and the clays can be chosen, as done in the LDRD study, to have minimal unreactive components such as quartz and muscovite micas. Clays such as Troy®, Barden® and OptiKasT® were found to have good reactivity during the LDRD study. In addition, clays will continue to react with any excess alkali in the formulation as a function of time while this is less likely in fly ash based geopolymers due to unreactive components.

Table G - 2. X-Ray Diffraction Analyses of STAR and ESTD Granular Products and Geopolymer Containing Monoliths

	FBSR Loading (wt%)	Size	Nepheline + K-nepheline+ Carnegeite $(Na,K)AlSiO_4$	Sodalite (Cl)	Nosean/ Hauyne	Al_2O_3 Or Fe_2O_3	SiO_2	$CaCO_3$ and $CaSO_4 \bullet 2H_2O$	Ettring-ite**	Beta-alumina $NaAl_{11}O_{17}$	TiO_2	Sodium Carbon -ates	Zeolite
STAR LAW (RASSAT BLEND) WITH SBW BLEND USED IN LDRD EXPERIMENTATION													
LDRD	0	sphere	Primarily amorphous after 4 years				trace	---	---	---	trace	trace‡	---
	100	granular	Major	Minor	Minor	Major	Minor	---	---	Minor	---		---
LDRD "A"	33	1" x 2"	Major	---	---	Major	Minor	---	---	---	---	trace‡	---
	37		Major	---	---	Major	Minor	---	---	---	---	trace‡	---
	44		Major	---	---	Major	Minor	---	---	Minor	---	trace‡	---
LDRD "B"	33	1" x 2"	Major	---	---	Major	Minor	---	---	Minor	---		---
	37		Major	---	---	Major	Minor	---	---	Minor	---	trace‡	---
	44		Major	---	---	Major	Minor	---	---	Minor	---	trace‡	---
TTT ESTD LAW RASSAT BLEND													
ESTD P1B	100	granular	Major	Minor	---	---	Minor	---	---	---	Minor	---	---
Geo-1 P1B	67	2" x 2"	Major	Minor	---	---	Minor	---	---	---	Minor	Minor	---
		3" x 6"	Major	Minor	---	---	Minor	---	---	---	Minor	Minor‡	---
Geo-7 P1B	68.8	2" x 2"	Major	Minor	---	---	Minor	---	---	---	---	Minor	Faujasite*f*
		3" x 6"	Major	Minor	---	---	Minor	---	---	---	---	Minor‡	Faujasite*f*
		6" x 12"	Major	Minor	---	---	Minor	---	---	---	---	Minor	Faujasite*f*
L-TEM P1A	76	3" x 6"	Major	Minor	---	---	---	Major	Major	Minor	---	---	Zeolite X (Na_2O form)
	82.5	3" x 6"	Major	Minor	---	---	---	Major	Major	Minor	---	---	
SRNL BSR RASSAT LAW													
BSR Geo-7' SIM B	100	granular	Major	---	Major	---	---	---	---	---	Minor	---	---
	67.95	1" x 2"	Major	---	Major	Fe_2O_3	Minor	---	---	---	---	---	Faujasite*f*
TTT ESTD WASTE TREATMENT PLANT SECONDARY WASTE (WTP-SW)													
ESTD P2B	100	granular	Major	Major	---	---	Minor	---	---	---	---	---	---
Geo-1 P2B	67	2" x 2"	Major	Major	---	---	Minor	---	---	---	Minor	Minor‡	---
		3' x 6"	Major	Major	---	---	Minor	---	---	---	Minor	Minor	---
Geo-7 SW	68.8	2" x 2"	*Major*	*Major*	---	---	*Minor*	---	---	---	Minor	Minor	Faujasite*f*
		2" x 4" (PNNL)	Major	Minor (2 types)	---	---	Minor	---	---	---	Minor	---	Zeolite Y*f* Zeolite D_2O
		2" x 4" (SRNL)	Major	Minor	Minor	---	Minor	---	---	---	Minor	---	Faujasite*f*
		3" x 6"	Major	Major	---	---	Minor	---	---	---	Minor	Minor‡	Faujasite*f*
		6" x 12"	Major	Major	---		Minor	---	---	---	Minor	Minor	Faujasite*f*

* sodium carbonates varied between natrite (Na_2CO_3), thermonatrite ($Na_2CO_3 \bullet H_2O$), trona $Na_3H(CO_3)_2 \bullet 2H_2O$), dawsonite $NaAlCO_3(OH)_2$

**$Ca_6Al_2(SO_4)_3(OH)_{12} \bullet 26H_2O$ a hydrated cement phase; *f*Faujasite = $Na_2Al_2Si_4O_{12} \bullet 8H_2O$ or $Na_{1.84}Al_2Si_4O_{11.92} \bullet 7H_2O$ also called Zeolite Y (PDF #38-0238)

References

1 Jantzen, C.M., **"Fluidized Bed Steam Reformer (FBSR) Product: Monolith Formation and Characterization"**, WSRC-STI-2006-00033, Savannah River National Laboratory, Aiken, SC (2006).

2 Jantzen, C.M., "**Fluidized Bed Steam Reformer (FBSR) Monolith Formation**", WM'07, Tucson, AZ, (2007).

3 Jantzen, C.M., A.R. Jurgensen, D.M. Missimer, P.R. Burket, and C.L. Crawford, **"Low Temperature Waste Forms and Containment: Geopolymers"**, U.S. DOE Slide Presentation WSRC-STI-2007-00584S, Savannah River National Laboratory, Aiken, SC (2007).

4 Jantzen, C.M., A.R. Jurgensen, D.M. Missimer, P.R. Burket, and C.L. Crawford, **"Geopolymers: Low Temperature Waste Forms for Hazardous Wastes and Radioactive Thermal Treatment Residues",** SRNL-STI-2008-00127 (in preparation for publication in Jour. Am. Ceramic Society).

5 Olson, A.L., N.R. Soelberg, D.W. Marshall, and G.L. Anderson, **"Fluidized Bed Steam Reforming of Hanford LAW Using THOR™ Mineralizing Technology",** INEEL/EXT-04-02492, Idaho National Laboratory, Idaho Falls, ID (2004).

6 Olson, A.L., N.R. Soelberg, D.W. Marshall, and G.L. Anderson, **"Fluidized Bed Steam Reforming of INEEL SBW Using THOR™ Mineralizing Technology",** INEEL/EXT-04-02564, Idaho National Laboratory, Idaho Falls, ID (2004).

7 Crawford, C.L., and C.M. Jantzen, **"Evaluation of THOR™ Mineralized Waste Forms (Granular and Monolith) for the DOE Advanced Remediation Technologies (ART) Phase 2 Project"**, SRNL-STI-2009-00505, Savannah River National Laboratory, Aiken, SC (in review).

8 THOR® Treatment Technologies, LLC **"Report for Treating Hanford LAW and WTP SW Simulants: Pilot Plant Mineralizing Flowsheet"**, Document Number RT-21-002, Rev. 1, (April 2009).

9 Soleberg, N.R., D.W. Marshall, S.O. Bates, and D.D. Taylor, **"Phase 2 THOR™ Steam Reforming Tests for Sodium Bearing Waste Treatment",** INEEL/EXT-04-01493; Idaho National Engineering & Environmental Laboratory, Idaho Falls, ID (2004).

10 Bullock, Jr., J.H., J.D. Cathcart, and W.J. Betterton, **"Analytical Methods Utilized by the United States Geological Survey for the Analysis of Coal and Coal Combustion By-products",** US Geological Survey, Denver, CO (2002).

11 Blackford, M.G., J.V. Hanna, K.J. Pike, E.R. Vance, and D.S. Perera, "Transmission Electron Microscopy and Nuclear Magnetic Resonance Studies of Geopolymers for Radioactive Waste Immobilization", *J. Am. Ceram. Soc. 90[4]*, 1193-1199 (2007).

12 Rowles, M.R., and B.H. O"Connor, "Chemical and Physical Micro-scale Character of Aluminosilicate Geopolymers Synthesised by Sodium Silicate Activation of Metakaolinite", *J. Am. Ceram. Soc., 92 [10]*, 2354-2361 (2009).

13 Hardjito, D., and B. V. Rangan, **"Development and Properties of Low-Calcium Fly Ash-Based Geopolymer Concrete**", Faculty of Engineering, Curtin University of Technology, Perth, Australia Report (2005).

14 Davidovits, J., "Geopolymers: Man-Made Rock Geosynthesis and Resulting Development of Very Early High Strength Cement", *J. of Materials Education*, 16 [2&3], 91-139 (1994).

15 Davidovits, J., "Geopolymers: Inorganic Polymeric New Materials", *J. Thermal Analysis*, 37, 1633-1656 (1991).

16 Kriven, W.M., M. Gordon, and J.L. Bell, **"Geopolymers: Nanoparticulate, Nanoporous Ceramics Made Under Ambient Conditions",** AFOSR STTR Grant F49620-02 C-010.

17 Kriven, W.M., "Inorganic Polysialates or "Geopolymers", *American Ceramic Society Bulletin*, **89** [4] 31-34 (2010).

18 van Jaaarsveld, J.G.S., J.S.J. van Deventer, and L. Lorenzen, "The Potential Use of Geopolymeric Materials to Immobilise Toxic Metals: Part I. Theory and Applications", *Minerals Engineering*, 10[7], 659-669 (1996).

19 Matthews, J., **"A Proposed Ceramic Encapsulate for Post Process Steam Reformed (e.g. INEEL) Radioactive Waste Products",** (a proposed manuscript).

20 Pires, R.P., J.H. Westsik, R.J. Serene, E.C. Golovich, M.N. Valenta, and K.E. Parker, **"Secondary Waste Form Screening Test Results - THOR® Fluidized Bed Steam Reforming Product in a Geopolymer Matrix",** PNNL- 20551 (July 2011).

21 Depmeier, W., "The Sodalite Family – A Simple but Versatile Framework Structure", in *Reviews in Mineralogy and Geochemistry*, Mineralogical Society of America, Washington, D.C. V. 57, 203-240 (2005).

22 Hajimohammadi, A., J.L. Provis, and J.S.J. van Devente, "Effect of Alumina Release Rate on the Mechanism of Geopolymer Gel Formation", *Chemistry of Materials*, 22, 5199–5208 (2010).

Appendix H. Calculation of Waste Form Volume Reduction

In order to calculate the relative volume increase or volume decrease for a given waste form, the amount of Na_2O achieved in the waste form at a given waste loading was retrieved from published literature values (references are given in Table H - 1) and expressed as an Na_2O concentration in wt% if it was reported in other units.

The calculation proceeds as follows:

$$kg\,wet\,LAW\,waste = gal_{\ LAW} * 3.78L/gal * \rho_{LAW}$$

$$kg\,LAW\,waste oxides = kg\,wet\,LAW\,waste * calcine\,factor\left(\frac{kg\,oxides}{kg\,waste}\right)$$

The calcine factors used for each type of waste are given in Table H - 2.

Next the kilograms of additives needed per kilogram of calcine oxides are calculated. For the sake of the calculation, anything that is not Na_2O (the prime contributor of the waste loading) is assumed to be additives.

$$\frac{kg\,oxides}{kg\,waste} = \frac{100 - Na_2O\,waste loading(wt\%)}{Na_2O\,waste loading(wt\%)}$$

$$kg\,of\,waste\,form = kg\,oxides + \left(\frac{kg\,additives}{kg\,oxides}\right) * kg\,oxides$$

$$Vol\,of\,waste\,form(gal) = \left(\frac{kg\,of\,waste\,form}{\rho_{waste\,form}(kg/m^3)}\right) \div 3.78\left(\frac{m^3}{gal}\right)$$

$$Vol\ \mathrm{Re}duction(\%) = \left(\frac{(gal\,of\,waste\,form) - (gal_{LAW})}{gal\,of\,waste\,form}\right) * 100$$

Table H - 1. Relative Volume Increases and Decreases for Glass, FBSR products (granular and monolith), and Cast Stone

Sample Type	Waste Type	Na_2O (wt%) in Final Waste Form	Volume (gallons Solid Waste Form/gallons LAW)	Volume Reduction (negative) vs. Volume Increase (positive) in %
FBSR HIC	AN-107 (Envelope C)	20.87 [1]	0.776	-22
	Rassatt Simulant (BSR)	21.03 [2]	0.642	-36
	SX-105 (Envelope A)	21.3 [3]	0.648	-35
	AN-103 (Envelope A)	21.16 [3]	0.781	-22
	AZ-101/AZ-102 (Envelope B)	21.98 [3]	0.575	-43
FBSR GEOPOLYMER	AN-107 (Envelope C)	13.57*	0.921	-8
	Rassatt Simulant (rad centroid BSR)	13.67*	0.762	-24
	SX-105 (Envelope A)	13.85*	0.769	-23
	AN-103 (Envelope A)	13.75*	0.927	-7
	AZ-101/AZ-102 (Envelope B)	14.29*	0.682	-32
FBSR OPC	AN-107 (Envelope C)	18.16**	0.812	-19
	Rassatt Simulant (HRI/TTT ESTD)	18.3**	0.672	-33
	SX-105 (Envelope A)	18.53**	0.678	-32
	AN-103 (Envelope A)	18.41**	0.817	-18
	AZ-101/AZ-102 (Envelope B)	19.12**	0.602	-40
FBSR Fondu (High Al Cement)	AN-107 (Envelope C)	14.32[t]	0.937	-6
	Rassatt Simulant (HRI/TTT ESTD)	14.43[t]	0.775	-22
	SX-105 (Envelope A)	14.6[t]	0.783	-22
	AN-103 (Envelope A)	14.52[t]	0.943	-6
	AZ-101/AZ-102 (Envelope B)	15.08[t]	0.694	-31
FBSR Secar 71 (High Al Cement)	AN -107 (Envelope C)	15.44[#]	0.932	-7
	Rassatt Simulant (HRI/TTT ESTD)	15.56[#]	0.771	-23
	SX-105 (Envelope A)	15.76[#]	0.778	-22
	AN-103 (Envelope A)	15.66[#]	0.938	-6
	AZ-101/AZ-102 (Envelope B)	16.27[#]	0.69	-31
LAW GLASS	AN-107 (Envelope C)	10 [4]	0.896	-10
	Rassatt Simulant	14 [4]	0.534	-47
	SX-105 (Envelope A)	10 [4]	0.764	-24
	AN-103 (Envelope A)	14 [4]	0.653	-35
	AZ-101/AZ-102 (Envelope B)	3 [4]	2.33	133
Caststone Baseline	5 Molar Na Caststone	5.63 [5]	1.56	56

* calculated at 65% of HIC granular Na_2O content based on FBSR loading in monoliths in Ref 2
** calculated at 87% of HIC granular Na_2O content based on FBSR loading in monoliths in Ref 1
t calculated at 68.6% of HIC granular Na_2O content based on FBSR loading in monoliths in Ref 6
calculated at 74% of HIC granular Na_2O content based on FBSR loading in monoliths in Ref 6

Table H - 2. Calcine Factors Used for Each Waste Type

Waste Type	Calcine Factors
AN-107 (Envelope C)	0.190
Rassatt Simulant	0.150
SX-105 (Envelope A)	0.160
AN-103 (Envelope A)	0.190
AZ-101/AZ-102 (Envelope B)	0.150

References

1 Jantzen, C.M., "**Fluidized Bed Steam Reformer (FBSR) Product: Monolith Formation and Characterization**", WSRC-STI-2006-00033, Savannah River National Laboratory, Aiken, South Carolina (2006).

2 Jantzen, C.M., C.L. Crawford, C.J. Bannochie, P.R. Burket, A.D. Cozzi, W.E. Daniel, D.M. Missimer, and C.A. Nash, "**Radioactive Demonstration of Mineralized Waste Forms Made from Hanford Low Activity Waste (Tank Farm Blend) by Fluidized Bed Steam Reformation (FBSR)**", SRNL-STI-2011-00383, Savannah River National Laboratory, Aiken, South Carolina (August 2013).

3 Jantzen, C.M., C.L. Crawford, C.J. Bannochie, P.R. Burket, A.D. Cozzi, W.E. Daniel, D.M. Missimer, and C.A. Nash, "**Radioactive Demonstration of Mineralized Waste Forms Made from Hanford Low Activity Waste (Tank SX-105, AN-103, AZ-101/AZ-102) by Fluidized Bed Steam Reformation (FBSR)**", SRNL-STI-2011-00384, Savannah River National Laboratory, Aiken, South Carolina (September 2013).

4 DOE/ORP Contract with Bechtel National, Inc., "**Design, Construction, and Commissioning of the Hanford Tank Waste Treatment and Immobilization Plant"**, Contract Number DE-AC27-01RV14136, U.S. Department of Energy, Office of River Protection, Richland, WA (December 2000).

5 Westsik, J. H. Jr., A.D. Cozzi, W. E. Daniel, R. E. Eibling, E. K. Hansen, P. G. Heasler, M. J. Lindberg, T. M. Mercier, G. F. Piepel, M. M. Reigel, R. L. Russell, and D.J. Swanberg, **"Supplemental Immobilization of Hanford Low-Activity Waste: Cast Stone Screening Tests,"** U.S. DOE Report RPP-RPT-55960, Washington River Protection Solutions, Richland, WA (September 2013).

6 Crawford, C.L., and C.M. Jantzen, "**Evaluation of THOR^{TM} Mineralized Waste Forms (Granular and Monolith) for the DOE Advanced Remediation Technologies (ART) Phase 2 Project**", SRNL-STI-2009-00505, Rev.0, Savannah River Technology Center, Aiken, South Carolina (December 2011).